(200)
R290
no. 83-845

UNITED STATES
DEPARTMENT OF THE INTERIOR
GEOLOGICAL SURVEY

PROCEEDINGS OF CONFERENCE XXII

A WORKSHOP ON "SITE-SPECIFIC EFFECTS OF SOIL AND ROCK ON GROUND MOTION AND THE IMPLICATIONS FOR EARTHQUAKE-RESISTANT DESIGN"

This report is preliminary and has not been edited or reviewed for conformity with U.S. Geological Survey standards and stratigraphic nomenclature. The views and conclusions contained in this document are those of the authors and should not be interpreted as necessarily representing the official policies, either expressed or implied, of the United States Government. Any use of trade names and trademarkes in this publication is for descriptive purposes only and does not constitute endorsement by the U.S. Geological Survey.

Reston, Virginia
1983

USGS LIBRARY-RESTON
3 1818 00071075 4

UNITED STATES
DEPARTMENT OF THE INTERIOR
GEOLOGICAL SURVEY

PROCEEDINGS OF CONFERENCE XXII

A WORKSHOP ON "SITE-SPECIFIC EFFECTS OF SOIL AND ROCK ON GROUND MOTION AND THE IMPLICATIONS FOR EARTHQUAKE-RESISTANT DESIGN"

JULY 25-27, 1983
SANTA FE, NEW MEXICO

Open-file report
Geological Survey
(U.S.)

CONVENED UNDER AUSPICES OF
NATIONAL EARTHQUAKE HAZARDS REDUCTION PROGRAM

SPONSORED BY THE U.S. GEOLOGICAL SURVEY AND THE
NUCLEAR REGULATORY COMMISSION

EDITOR

WALTER W. HAYS
U.S. GEOLOGICAL SURVEY
RESTON, VIRGINIA 22092

U.S. GEOLOGICAL SURVEY
RESTON, VA.
MAR 05 1984
LIBRARY

OPEN FILE REPORT 83-845

COMPILED BY
CARLA KITZMILLER AND DIANA DARNELL

This report is preliminary and has not been edited or reviewed for conformity with U.S. Geological Survey standards and stratigraphic nomenclature. The views and conclusions contained in this document are those of the authors and should not be interpreted as necessarily representing the official policies, either expressed or implied, of the United States Government. Any use of trade names and trademarkes in this publication is for descriptive purposes only and does not constitute endorsement by the U.S. Geological Survey.

Reston, Virginia
1983

351533

Effects of Local Geological Conditions on Strong Ground-Motions in the Vicinity of Coalinga, California
Roger Borcherdt, Charles Mueller, and Leif Wennerberg.....114
Preliminary Analysis of Parkfield Array Recordings of the Coalinga Earthquake (Part 1), and Stability of Empirical Estimates of Site Response (Part 2)
David Boore, Allan Lindh, Brian Tucker, Anthony Shakal, and Richard McJunkin.....144
Spatial Variability of Earthquake Intensity from the SMART 1 Array, Tiwan
Bruce Bolt.....167
The Effect of Site Response on High Frequency Ground Motions; Analysis of the Aftershocks of the New Brunswick Earthquake
John Boatwright and Mary Astrue.....172
The September 4, 1981, Santa Barbara Island, California Earthquake: Interpretation of Strong Motion Data
John Anderson.....191

THEME II: AMPLIFICATION MODELS

Site Amplification Models
Geoffrey Martin.....227
Site Effects: Two-Dimensional Modeling and Earthquake Engineering
Pierre-Yves Bard.....231
Estimating Site Effects on Strong-Ground Motion Using Local Shear-Wave Velocity
William Joyner, Thomas Fumal, and John Tinsley.....251
Ground Motions and Response Spectra at Soil Sites from Seismological Models of Radiated Spectra
David Boore and William Joyner.....261

THEME III: PREDICTING SITE-SPECIFIC ATTENUATION OF GROUND MOTION

The Effects of Site Characteristics on Near-Source Recordings of Strong-Ground Motion
Kenneth Campbell.....280

Predicting Site-Specific Attenuation of Ground Motion: Comments, Concerns, and Controversy
Joseph Fischer.....310
Perspectives on Properties of Attenuation Function Variabilities Using a Naive Rupture Model
David Perkins.....319

THEME IV: UNCERTAINTY AND POSSIBLE ERRORS

Uncertainty in Ground Motion Predictions
Martin McCann.....331
Soil-Structure Interaction Effects at Accelerograph Stations
C. B. Crouse.....354
Some Possible Errors in Recorded Free-Field Ground Motions
Robert McNeill.....357

THEME V: GENERATION OF SITE-DEPENDENT SPECTRA

The Use of Site-Dependent Spectra
Jeffrey Kimball.....361
Considerations in the Development of Site-Specific Spectra
Khrosrow Sadigh.....423
Theoretical and Empirical Studies of Strong Ground Motion
David Hadley and Randy Apsel.....459
Empirical Resolution of Ground Motion Effects
Gerald Frazier.....463
A Model for the Shape of the Fourier Amplitude Spectrum of Acceleration at High Frequencies
John Anderson and Sue Hough.....466

HIGHLIGHTS OF THE WORKSHOP ON "SITE-SPECIFIC EFFECTS OF SOIL AND ROCK ON GROUND MOTION AND THE IMPLICATIONS FOR EARTHQUAKE-RESISTANT DESIGN"

by

Walter W. Hays
U.S. Geological Survey,
Reston, Virginia 22092

INTRODUCTION

The U.S. Geological Survey (USGS) and the U.S. Nuclear Regulatory Commission (NRC) sponsored a 3-day workshop in Santa Fe, New Mexico, on July 25-27, 1983. The objectives were to review the state-of-knowledge about the effects of soil and rock on ground motion and to discuss methods for incorporating site-specific effects in the earthquake-resistant design of nuclear power plants and other important facilities. This workshop brought together forty-three scientists and engineers representing: academia, industry, architectural and engineering firms, State and Federal Governments, and representatives of agencies of three foreign governments. These participants, listed below, represent a large percentage of those who are actively involved in research on the site-specific effects of soil and rock on ground motion.

Ted Algermissen	U.S. Geological Survey
Boualem Ameur	CTC (Algeria)
John Anderson	University of California, San Diego
Pierre-Yves Bard	IRIGM (France)
(Unabled to attend, but submitted a paper)	
John Boatwright	U.S. Geological Survey
Bruce Bolt	University of California, Berkeley
David Boore	U.S. Geological Survey
Roger Borcherdt	U.S. Geological Survey
Kenneth Campbell	Lawrence Livermore National Laboratory
C. B. Crouse	Ertec, Inc.
Neville Donovan	Dames and Moore
Djamel El Foul	CTC (Algeria)
Joseph Fischer	Geoscience Associates, Inc.
Gerald Frazier	Science Applications, Inc.
Asadour Hadjian	Bechtel Power Corporation
David Hadley	Sierra Geophysics
Gene Hawkins	Southern California Edison

Walter Hays	U.S. Geological Survey
Lyman Heller	U.S. Nuclear Regulatory Commission
Joe Hunt	Tennessee Valley Authority
Izzat Idriss	Woodward Clyde Consultants
Robert Jackson	U.S. Nuclear Regulatory Commission
William Joyner	U.S. Geological Survey
Jeffrey Kimball	U.S. Nuclear Regulatory Commission
Jerry King	U.S. Nuclear Regulatory Commission
Kenneth King	U.S. Geological Survey
William Kovacs	National Bureau of Standards
Geoffrey Martin	Ertec, Inc.
Martin McCann	Jack R. Benjamin and Associates
Robert McNeill	Consulting Engineer
(Unabled to attend, but submitted a paper)	
Charles Mueller	U.S. Geological Survey
John Murphy	S-Cubed
Stephen Obermeier	U.S. Geological Survey
David Perkins	U.S. Geological Survey
Antonio Pugliese	ENEAC (Italy)
Leon Reiter	U.S. Nuclear Regulatory Commission
Al Rogers	U.S. Geological Survey
Khrosrow Sadigh	Woodward Clyde Consultants
Jogeshwar Singh	Harding Lawson Associates
M'hamed Slimani	CTC (Algeria)
John Tinsley	U.S. Geological Survey
Brian Tucker	California Division of Mines & Geology
Leif Wennerberg	U.S. Geological Survey

This workshop is the twenty-second in a series of conferences and workshops USGS has sponsored with other agencies since 1977. Each conference and workshop has the general goal of improving knowledge utilization and is designed to foster a process that will counteract the well known fact that much of the knowledge produced through research is not always fully utilized. Experience has shown that conferences and workshops provide a forum where knowledge producers and knowledge users are willing to come together to discuss areas of agreement and disagreement then work to create a process that will sharpen the focus of the research and improve the utilization of the results. The subject of this workshop is an example of an area where such a forum was needed. Although more than fifty years have passed since the effects of soil and rock on earthquake ground motion were noted by Japanese researchers, certain aspects of this research problem still cause a high degree of controversy among scientists and engineers.

STATEMENT OF THE PROBLEM

Knowledge of the nature and severity of ground motion induced at a site is fundamental to sound earthquake-resistant design. The present understanding of the effects of soil and rock on earthquake ground motions has come from two sources: 1) accelerograms recorded from past earthquakes, especially since the 1971 San Fernando earthquake, and 2) theoretical considerations and analytical modeling based on research in the past twenty years. It is well known that the amplitude, temporal, and spectral characteristics of earthquake ground motion at a site are complicated functions of the earthquake source mechanism, the epicentral distance, and the geometry and physical properties of the geologic structures traversed by the body and surface waves as they propagate from the source to the site. Researchers have recognized and documented since the early 1900's that the physical properties of the soil and rock underlying the recording site can have profound effects on earthquake ground motions. Generally, the more deformable the site (because of either the softness of the soil or its thickness), the greater the difference in the characteristics of ground shaking. The soil can either increase or decrease the response of a structure depending on the type of the structure and the dimensions and physical properties of the soil. These complex phenomena were not understood well enough to be incorporated into building codes and earthquake-resistant design procedures until the 1970's.

When the unconsolidated materials underlying a recording site modify the ground-motion input, the amplitude of the modified ground motion is a function of many parameters including the level of shear strain, the shear-wave velocity, the density and material damping, the thickness, water content, and the surface and subsurface geometry of the unconsolidated deposits and underlying rock. The period range that is modified depends strongly on the thickness of the soil and the contrast in shear-wave velocity between the soil and bedrock.

Evaluation of the effects of soil and rock on ground motion is complicated by the fact that soils behave nonlinearly. Laboratory tests have demonstrated that soils have shear modulus and damping characteristics that depend on the level of strain, suggesting that, under certain conditions, nonlinearities and

inelasticities in the soil may attenuate rather than amplify the surface ground motions observed at sites underlain by soil. Unfortunately, empirical ground-motion data representing the high levels of strain produced in the laboratory have not been recorded. The current strong ground-motion data sample represents strain levels up to about 0.5 percent.

It is becoming more common to generate site-specific ground motions for use in designing or verifying the design of important facilities such as nuclear power plants. When necessary, a major effort is made to determine and model the response of the local site to earthquake ground motions for nuclear power plants. A number of methods are used to achieve this goal. However, scientists and engineers debate the technical issues associated with each method. Siting issues encountered in the Eastern United States provide a good example of the problem. Because of the lack of adequate strong ground-motion records in the Eastern United States, seismic design parameters are typically generated by extrapolating earthquake ground-motion data recorded in the Western United States, guided and supplemented by theory and analytical models. The problem is that, depending upon the location of the site, some or all of the physical conditions of the source, path, and local site are different in the Eastern and Western United States. In terms of site conditions, the primary differences are:

1) A lower amount of material attenuation (higher values of Q) in the Eastern United States, relative to the Western United States, which causes high-frequency energy to be propagated to much greater distances in the East.

2) The soil and rock column in the East (typically consisting of alluvium, saprolites, and stiff, overconsolidated glacial tills overlying competent crystalline rock having a very high value of shear-wave velocity) has a larger contrast in acoustic impedance than the typical soil and rock column in the West. In many cases, the physical properties of sites in the East indicate that high-frequency ground motions will be amplified, a matter of concern for securing equipment in a nuclear power plant. No empirical data are available to quantify soil amplification in the East.

Although scientists and engineers attempt to account for these differences, a final verification of assumptions awaits actual recordings of strong ground motions in the Eastern United States at sites underlain by soil and rock.

WORKSHOP PROCEDURES

The procedures used in the workshop were designed to enhance the interaction between scientists and engineers and to clarify the technical issues from the perspective of each discipline. Each participant was asked to follow the basic guideline; **"It is okay to disagree as long as you seek to clarify the reasons for disagreement and work together to define experiments to resolve the technical issues causing disagreement."**

In order to stimulate vigorous discussion, five procedures were followed throughout the workshop:

Procedure 1: Two to four scientists and engineers gave presentations of 30 to 45 minutes each at the beginning of the five technical sessions. The role of each speaker was: a) to define the problem indicated by the session theme, b) to identify the most important technical issues needing resolution, and c) to summarize the state-of-knowledge and establish a broad framework for group discussion.

Procedure 2: A panel of two to four scientists and engineers responded to the presentations of the speakers. The role of each panelist was: a) to agree or disagree with the speakers' assertions about the state-of-knowledge and technical issues, b) to present information to illustrate a particular point of view, and c) to present and discuss empirical data showing site-specific effects.

Procedure 3: Following the presentation of the speakers and panelists, all participants responded to the questions that were posed to determine the range of views of the participants and to clarify technical issues.

Procedure 4: Three Special Study Groups composed of scientists and engineers were formed informally on the first day of the workshop and met formally after the fifth technical session to discuss: a) the high strain versus low strain issue, b) generation of site-dependent spectra, and c) uncertainty.

Each group suggested specific experiments to resolve technical issues associated with these problems and recommended specific actions. The report of each Special Study Group is included at the end of Part 1 of this publication.

Procedure 5: Ample time was provided for ad hoc discussions to probe topics of interest more deeply.

The technical papers forming the basis for the five technical sessions and the interactive discussions are contained in Part II of this publication. The papers were prepared in advance and distributed as "draft" papers at the workshop. All the papers were finalized after the workshop. Many of the papers addressed more than one session theme.

TECHNICAL SESSIONS

The overall theme of the workshop was developed in five technical sessions. The themes, objectives, speakers, panelists, and discussion questions posed for each session are described below.

SESSION I: EMPIRICAL DATA SHOWING SITE-SPECIFIC EFFECTS OF SOIL AND ROCK ON GROUND MOTION

OBJECTIVE: Presentations to establish a framework for discussion in all five technical sessions of the workshop and to give the perspectives of earth scientists and engineers concerning the evaluation of site-specific effects of soil and rock on ground motion. The presentations focused mainly on the effects of the site on ground motion (rather than on the source or path) and gave a summary of the state-of-knowledge and state-of-

practice, emphasizing: a) the results of analyses of specific ground motion data, b) important conclusions regarding site-specific effects of soil and rock on ground motion, and c) important technical issues needing resolution.

SPEAKERS: Albert Rogers, Neville Donovan, John Murphy, and Jogeshwar Singh

PANELISTS: Bruce Bolt, Izzat Idriss, Roger Borcherdt, David Boore, John Boatwright, and Brian Tucker

QUESTIONS FOR DISCUSSION

1) Should design ground motions be modified for site response?

2) Are the geologic and ground motion data bases adequate for modeling site response and incorporating site response in earthquake-resistant design in the Western United States?--In the Eastern United States?

3) Can existing data be further analyzed to quantify and model site effects better? How?

4) Does nonlinear soil behavior invalidate empirical methods of modeling site response that are based on low-strain level ground motions? (i.e., do low-strain level ground motions have any value in earthquake-resistant design?)

5) Are instrument arrays in place that would provide data to test the importance of non-linear soil behavior? Is it possible to record high-strain level ground motions?

6) What experiments might be performed to resolve the technical issues associated with site-specific effects of soil and rock on ground motion?

SESSION II: AMPLIFICATION MODELS

OBJECTIVE: Presentation and discussion of procedures for the characterization of soil and rock properties and their use in 2- and 3-dimensional analytical models to predict site-specific effects on body and surface waves.

SPEAKER: Geoffrey Martin

PANELISTS: Izzat Idriss and William Joyner

QUESTIONS FOR DISCUSSION:

1) Is there anything better than SHAKE?

2) Can 2- and 3-dimensional variations in soil and rock properties and subsurface topography be dealt with realistically?

SESSION III: PREDECTING SITE-SPECIFIC ATTENUATION OF GROUND MOTION

OBJECTIVE: Presentation and discussion of technical issues associated with seismic wave attenuation laws.

SPEAKERS: Kenneth Campbell and David Boore

PANELISTS: Joseph Fischer, Jogeshwar Singh, and Izzat Idriss

QUESTIONS FOR DISCUSSION:

1) Are the data bases adequate for describing seismic wave attenuation for rock sites?--For soil sites?

2) Do peak ground motion saturate with magnitude?

3) Can peak ground motions and spectral ordinates be scaled accurately in the near field?--In the far field?

4) Can the uncertainty associated with median values of ground motion described by attenuation laws be quantified accurately? What causes the uncertainty? How can the uncertainty be reduced?

5) Can uncertainty in attenuation laws used for deterministic and probabilistic hazard maps be treated adequately?

SESSION IV: UNCERTAINTY AND POSSIBLE ERRORS

OBJECTIVE: Presentation and discussion of the various factors that contribute to scatter in ground motion data and possible errors in recorded free-field ground motion.

SPEAKERS: Martin McCann and C. B. Crouse

PANELISTS: David Perkins, John Anderson

QUESTIONS FOR DISCUSSION:

1) Are the data bases adequate for quantifying uncertainty in the median values of ground motion variables? If not, what should be done to obtain the proper data base? Can present estimates of uncertainty be reduced? How much?

2) Does the existing strong motion data sample have errors? If so, what should be done?

SESSION V: GENERATION OF SITE-DEPENDENT SPECTRA

OBJECTIVE: Presentation and discussion of the current procedures for calculating site-specific spectra for use in earthquake-resistant design in the United States and their appropriateness.

SPEAKERS: Jeffrey Kimball and Khrosrow Sadigh

PANELISTS: John Tinsley, David Hadley, Jogeshwar Singh, William Joyner, and Gerald Frazier

QUESTIONS FOR DISCUSSION:

1) Are present methods used for generating site-dependent spectra adequate? If not, how can they be improved?

VIEWS OF THE PARTICIPANTS

Ballots were taken during the workshop to define the areas of agreement and disagreement of the participants and to sharpen the focus of the discussions. The results, which are summarized below, give the views of the participants.

1) Ninety-eight percent of the participants stated that earthquake-resistant design of important structures should incorporate site effects.

2) Sixty-two percent of the participants indicated that, in their opinion, the existing geologic, geotechnical, and ground-motion data bases are adequate for modeling site response and incorporating its effects in earthquake-resistant design in the Western United States, but inadequate in the Eastern United States.

3) Sixty-two percent of the participants noted that, in their opinion, the existing ground-motion data base, consisting almost totally of data recorded at low-strain levels, could be used in earthquake-resistant design.

4) Eighty-six percent of the participants expressed the belief that it is possible to record high-strain ground motions, but fifty-five percent indicated that, in their opinion, existing strong-motion arrays will not be able to provide data that would test the importance of non-linear behavior.

5) Fifty-five percent of the participants expressed the view that existing geologic and geotechnical data and analytical models can be

used to model 2- and 3-dimensional variations in site properties in a realistic manner.

6) Fifty-five percent of the paticipants indicated that, in their view, the current geologic, geotechnical, and ground-motion data bases are adequate for describing seismic wave attenuation for sites underlain by rock, but only forty percent expressed this opinion for sites underlain by various types of soils.

7) Ninety percent of the participants expressed the opinion that peak ground acceleration saturates with increase in magnitude.

RECOMMENDATIONS

The recommendations of the Special Study Groups are described later in Part I of this document. Several general recommendations are given below:

1) The participants recommended that the USGS provide the leadership needed to create, establish, and foster the use of a comprehensive national strong ground-motion data base, collaborating with NRC, National Science Foundation (NSF), California Division of Mines and Geology (CDMG), and others to define goals and to obtain funding. The strong ground-motion data base should be a national resource that is readily available to all researchers.

2) The participants called for carefully planned experiments to seek solutions to specific technical issues concerning site-specific effects of soil and rock on ground motion. The experiments should have both scientific and engineering objectives. Several types of experiments should be considered: a) use of existing methodologies and data, b) acquisition of new data, and c) computer simulation. The experiments should be integrated so as to produce both short- and long-term results with regard to: a) the low-strain vs high-strain issue, b) uncertainty in earthquake-resistant design parameters incorporating site response, and c) generating site-dependent response spectra.

3) The participants recommended establishing 2- and 3-dimensional strong-motion instrument arrays to capture ground motion records at locations in the United States having the greatest potential for experiencing a large earthquake. Although such arrays are expensive, they are realizable. One array (funded by NSF) now exists in Yugoslavia. Japan also has such arrays.

4) The participants recommended additional multidisciplinary meetings, similar in format to this workshop, to examine in greater detail a number of important ground motion problems. They recommended using a format that will encourage detailed discussion of the differences in views of scientists and engineers and foster cooperative problem solving.

ACKNOWLEDGEMENTS

A special note of appreciation is extended to each of the following individuals for their contributions to the workshop:

1) The Steering Committee of Jerry King [1] (NRC), Gene Hawkins (Southern California Edison Company), and Walter Hays (USGS) planned and organized the workshop.

2) Leon Reiter (NRC), Larry Wight (TERA Corp.), Brian Tucker (CDMG), and Robert McNeill (Consulting Engineer) provided advice and encouragement at critical times to transform the workshop from an idea into reality.

3) The participants who vigorously joined in the technical sessions and the Special Study Groups were the key to the success of the workshop. The candid exchange of ideas made the workshop practical and stimulating.

4) Carla Kitzmiller, Paula Gori, Wanda Seiders, Cheryl Miles, Joyce Costello, Susan Kibler, Peggy Randalow, Lynne Downer, and Diana Darnell of U.S. Geological Survey provided strong and capable administrative support.

---

[1] Now working with Electric Power Research Institute, Palo Alto, CA

REPORT AND RECOMMENDATIONS OF SPECIAL STUDY GROUP ONE

by

Rogert D. Borcherdt
U.S. Geological Survey
and
Jogeshwar P. Singh
Harding Lawson Associates

FOREWORD

This report gives a summary of the recommendations proposed by members of Special Study Group 1 at the workshop on "Site-specific effects of soil and rock on ground motion and the implications for earthquake-resistant design," held in Santa Fe, New Mexico, July 25-27, 1983. Participants included:

Boualem Ameur, CTC, (Algeria)
John Anderson, University of California, San Diego
Roger Borcherdt, **(Moderator)**, U.S. Geological Survey
Djamel El Foul, CTC, (Algeria)
Gerald Frazier, Science Applications, Inc.
Gene Hawkins, Southern California Edison
Joe Hunt, Tennessee Valley Authority
Izzat Idriss, Woodward Clyde Consultants
Robert Jackson, U.S. Nuclear Regulatory Commission
Jerry King, U.S. Nuclear Regulatory Commission
Jogeshwar Singh, **(Recorder)**, Harding Lawson Associates
M'hamed Slimani, CTC, (Algeria)

The objective of the group was to discuss experiments for: 1) resolving the high-strain versus low-strain issue, and 2) improving site-dependent spectra.

After a lengthy discussion of the two subject topics, the following recommendations were made by the Special Study Group I:

High Strain vs. Low Strain Issue (non-linear material behavior)

A. It was recommended that two adhoc committees be formed:

1. to interact with USGS and CDMG programs to assist in experiment design and data interpretation, and

2. to evaluate data such as that available from the Nevada Test Site (NTS) or SMART 1 Array, etc.

B. Downhole experiments were recommended to resolve the high strain vs. low strain issue. It was also reocmmended that the experiments be performed in at least three different sites in a given location. The suggestions for different locations included Imperial Valley, Parkfield, and other areas with likely soft soil sites.

C. Installation of soil-rock pairs of strong motion instruments in the free-field was recommended in areas where soil profile changes over short distances (i.e., rock to soft soil or rock to deep cohesionless soil, etc.).

Site Dependent Spectra

The site dependent spectra studies were divided into three groups: A) source spectra; B) distance effects; and C) site corrected spectra.

A. Source Spectra - It was recommended that theoretical and empirical studies be performed to develop source spectra for seismic sources in the Eastern and Western United States. The theoretical studies should use existing modeling techniques with any required modifications.

The empirical studies should include:

1. Development of adequate strong motion arrays in the Eastern United States

2. Development of additional source arrays in the Western United States

3. Development of supporting data in terms of soil profiles and geological structure

B. Distance Effects - It was recommended that studies on distance effects be performed to account for differences in attenuation characteristics of the Eastern and Western United States.

C. Site Corrected Spectra - It was recommended that all data on spectra be compiled and average site effects on spectra be estimated in light of other factors that are known to influence ground motions.

In addition to the two topics for discussion, the following general recommendations were made by the group:

A. Develop a national strong motion data base.

B. Install more strong motion instrument arrays.

C. Develop supporting geotechnical information at strong motion instrument sites.

D. Perform extensive analytical/empirical studies for sites with strong motion records.

REPORT AND RECOMMENDATIONS OF SPECIAL STUDY GROUP TWO

by

Joseph Fischer
Geoscience Associates, Inc.
and
C. B. Crouse
ERTEC, Inc.

FOREWORD

This report gives a summary of the recommendations proposed by members of Special Study Group 2 at the workshop on "Site-specific effects of soil and rock on ground motion and the implications for earthquake-resistant design," held in Santa Fe, New Mexico, July 25-27, 1983. Participants included:

Ted Algermissen, U.S. Geological Survey
John Boatwright, U.S. Geological Survey
David Boore, U.S. Geological Survey
C. B. Crouse, **(Recorder)**, Ertec, Inc.
Neville Donovan, Dames and Moore
Joseph Fischer, **(Moderator)**, Geoscience Associates, Inc.
Lyman Heller, U.S. Nuclear Regulatory Commission
Jeffrey Kimball, U.S. Nuclear Regulatory Commission
John Tinsley, U.S. Geological Survey
Brian Tucker, California Division of Mines & Geology

The objective of the group was to discuss experiments for: 1) improving site-dependent spectra, and 2) quantifying and reducing uncertainty in earthquake-resistant design parameters that incorporate site response.

SUMMARY OF GROUP DISCUSSION

On the basis of the vigorous discussions during and following the five technical sessions, members of Special Study Group 2 urged that steps be taken to improve communication and understanding between seismologists and geotechnical engineers. One way to improve the dialogue between these two disciplines is to create multidisciplinary steering committees involving seismologists, geologists and engineers. For example, one committee, composed of about 5 to 7 people, could propose specific experiments, and another committee could review, approve

or suggest modifications to them. Liasion groups, representing potential funding agencies who have an interest in these committee activities, might also participate as observers. Potential liasion groups include the NSF, USGS, CDMG, and National Academy of Sciences.

The members of Special Study Group 2 proposed specific recommendations addressing the objectives of special Study Group 2. These included:

1) The existing data bases that are relevant to the problems of site-dependent spectra and uncertainty need to be collected, synthesized and ultimately organized, using the concept of a data-base management and retrieval system.

2) Strong-motion instrument arrays should be carefully planned and deployed as soon as possible in earthquake-prone regions, selecting as top priority those regions having the best chance of providing useful data quickly.

   One option to consider is that of supplementing existing free-field and structural arrays with, for example, downhole instruments and instruments that are closely spaced (i.e. spacing on the order of the foundation dimensions of typical structures). Two concepts were discussed; one would deploy such "three dimensional" arrays in areas where earthquakes were expected; the other would involve a "Rapid Development Team" ready to monitor aftershock sequences immediately after a major earthquake. Aftershocks offer an excellent opportunity for a quick payoff in data acquisition. However, an extremely well planned and coordinated effort, perhaps utilizing one of the multidisciplinary steering committees, noted above, is necessary before instruments can be successfully and expeditiously positioned in the aftershock zone. Expedient placement immediately after the main shock by the responsible agency, university, or institution is still encouraged. However, the location of some instruments could be modified as a result of the multidisciplinary committee's recommendations after the initial placement.

3) Smaller workshops, focusing on ground motion problems that need to be solved to accomplish the objectives of the Special Study Group, should be organized.

(4) Consideration should be given to the potential use of the centrifuge, a machine that is becoming more widely recognized among geotechnical engineers as a valuable tool for providing insight into the dynamic response of a variety of soil-structure systems. The centrifuge has potential application to many soil and wave-propagation problems.

REPORT AND RECOMMENDATIONS OF SPECIAL STUDY GROUP THREE

by

Kenneth W. Campbell

Lawrence Livermore National Laboratory

and

John R. Murphy

S-Cubed

FOREWORD

This report gives a summary of the recommendations proposed by members of Special Study Group 3 at the workshop on "Site-specific effects of soil and rock on ground motion and the implications for earthquake-resistant design," held in Santa Fe, New Mexico, July 25-27, 1983. Participants included:

Kenneth Campbell, **(Moderator)**, Lawrence Livermore Laboratory
David Hadley, Sierra Geophysics
Walter Hays, U.S. Geological Survey
William Joyner, U.S. Geological Survey
Kenneth King, U.S. Geological Survey
Geoffrey Martin, Ertec, Inc.
Martin McCann, J. R. Benjamin and Associates
John Murphy, **(Recorder)**, S-Cubed
David Perkins, U.S. Geological Survey
Leon Reiter, U.S. Nuclear Regulatory Commission
Albert Rogers, U.S. Geological Survey
Khrosrow Sadigh, Woodward Clyde Consultants

The objective of the group was to discuss experiments for: 1) quantifying and reducing uncertainty in earthquake-resistant design paramenters that incorporate site response, and 2) resolving the high-strain versus low-strain issue.

SUMMARY OF GROUP DISCUSSION

The primary objective of this group was to recommend experiments directed toward quantifying and reducing uncertainty in the specification of the effects of local site geology on strong ground motion, including experiments specifically designed to help resolve the high strain versus low strain

issue. Preliminary discussions were wide-ranging and served to generate a rough concensus concerning both the current status of the empirical data base and a general recommended course of action for addressing some of the most important outstanding problems. These preliminary discussions served as a foundation for the following conclusions and recommendations:

1) It is concluded that peak acceleration, by itself, is not an adequate parameter for defining the effects of local geology on strong ground motion.

2) There is an urgent need to establish a computerized strong motion data base in which all source, propagation path and local site parameters of interest are assigned on a uniform basis. A single group (or Agency) should be assigned responsibility to work with the geotechnical and seismological communities to assemble and maintain this data base and to ensure that all relevant data are readily available to all interested investigators. A high priority should be assigned to ensuring continuity of funding for this project, so that the data base can be promptly updated and revised in the future as additional information becomes available.

3) The available geotechnical characterizations of sites at which strong ground motions have been measured is not adequate for research needs. Existing data should be compiled and presented in a uniform manner. Additional sites should be identified and studied to compliment the existing data. A new program should be initiated to measure systematically all of the physical properties of interest at these sites, using uniform data acquisition and reduction procedures. The final design of this program should be arrived at through the cooperative efforts of both the geotechnical engineering and seismological communities.

4) There are currently very few sites at which strong ground motions have been measured under both low- and high-strain conditions. Therefore, in order to assess the potential importance of nonlinear soil response on local site effects, it is important that these few sites be

examined in great detail. In particular, the soils at these sites should be characterized using both insite and laboratory procedures and the results should be compared and contrasted and critically assessed with respect to their ability to explain the observed strong motion characteristics. New experimental procedures, such as the use of the Boeing centrifuge, should also be evaluated under this program in an attempt to define the procedures which are most appropriate for defining the response of various soil types under strong, dynamic loading conditions.

5) The strong motion instrumentation in place in the United States at the present time can only be expected, in the near future, to provide more of the same limited data which have been slowly accumulating over the past few decades. Therefore, a long term (i.e., 5-10 year) program must be initiated to establish and maintain one or more national strong-motion laboratories designed to improve significantly our understanding of local site effects. A key feature of these proposed experimental facilities would be the deployment of three-dimensional instrumentation arrays which could be used to define precisely the incoming wave fields and to monitor their progression up through the soil column to the surface. It is envisioned that these facilities would be flexible enough to accommodate a variety of research investigations and would be calibrated well enough to serve as test beds for the evaluation of different geotechnical site characterization and ground motion prediction procedures. The details of the experimental configurations should be defined by a working group composed of both geotechnical engineers and seismologists. However, the following preliminary list indicates some of the fundamental design criteria which should be considered.

   a) The sites should be situated such that there is a high probility of recording strong earthquake ground motions during the life of the project.

   b) The selected sites should sample the widest possible range of near-surface geologic environments, and the sites should have available or readily attainable geotechnical characteristics.

c) Priority should be given to sites at which strong motion measurements have already been made.

d) Priority should be given to sites where explosive tests can be conducted.

e) The instrumentation selected for deployment should be digital, broadband and have a wide dynamic range so that regional and teleseismic data, as well as strong motion data, can be recorded.

Criteria (d) and (e) are important because they enable the laboratories to produce short-term as well as long-term results. That is, they assure that useful data can be collected and analyzed on a nearly continuous basis while awaiting the occurrence of the infrequent, large local earthquake.

EVALUATION OF THE WORKSHOP ON "SITE-SPECIFIC EFFECTS OF SOIL AND ROCK ON GROUND MOTION AND THE IMPLICATIONS FOR EARTHQUAKE-RESISTANT DESIGN"

by

Paula Gori and Carla Kitzmiller
U. S. Geological Survey
Reston, VA 22092

INTRODUCTION

At the conclusion of the workshop in Santa Fe, New Mexico, the participants were asked to evaluate the two-and-a-half day meeting, using a questionnaire (Figure 1). They were asked to evaluate the success of the workshop in reaching its goals and to rate the various activities of the workshop. Responses to the evaluation questions were elicited on a five-point scale, 1 and 2 representing the lowest level of agreement, 3 and 4 moderate agreement, and 5 highest agreement, or a "yes" response (see Figure 1). Because not all participants returned the questionnaire, percentages were based only on the 29 participants who submitted the evaluations (see Figure 2).

WORKSHOP MEETS GOALS

Evaluations returned by 29 participants indicate that the meeting was highly successful in meeting its goals. Ninety-three percent of the respondents thought that the workshop did a good to excellent job in defining the state-of-knowledge of the site-specific effects of soil and rock ground motion and clarifying the differences in perspectives of earth scientists and engineers. Over three-quarters (79%) of the evaluators felt that the workshop was successful in defining the technical issues. Some of these issues were:

1) Should design ground motions be modified for site response?

2) Are the geologic and ground motion data bases adequate for modeling site reponse and incorporating site response in earthquake-resistant design in the Western United States? - In the Eastern United States?

FIGURE 1

EVALUATIONS OF THE WORKSHOP ON "SITE-SPECIFIC EFFECTS OF SOIL AND ROCK ON GROUND MOTION AND THE IMPLICATIONS FOR EARTHQUAKE-RESISTANT DESIGN" BY INDIVIDUAL PARTICIPANTS

The numbers shown represent the number of participants who rated the workshop in terms of the questions below. Number 5 represents the highest rating and number 1, the lowest.

	Scale Low 1	2	3	4	High 5
1. Did you find the workshop to be useful for:					
a. defining the state-of-knowledge?	1	1	10	15	2
b. defining the technical issues?	0	6	8	11	4
c. clarifying differences in perspectives of earth scientists and engineers?	1	1	8	16	3
d. describing the current state-of-practice for incorporating site-specific effects into earthquake-resistant design?	2	7	13	5	2
e. developing experiments to resolve important technical issues	1	7	10	7	3
f. recommending future research?	1	2	13	8	4
2. Did the conference benefit you or your organization by:					
a. providing new information, ideas, and perspectives?	0	3	6	14	6
b. establishing better understanding of ways to resolve the technical issues?	1	4	12	8	3
3. Did you find the following activities useful:					
a. presentations by the speakers?		1	11	11	6
b. response by the panelists to stimulate discussions?	2	5	5	12	5
c. group discussions?	1	0	4	17	6
d. special study groups	2	2	9	10	6
e. informal discussions during coffee breaks, lunches, and after hours?	2	1	7	11	8
f. notebook containing expanded abstracts and papers?	1	1	8	10	9

	Yes	No
4. If the clock were turned back and the decision to attend the workshop were given you again, would you want to attend?	29	
5. Are you willing to participate in future workshops to continue the work initiated at this meeting?	28	

FIGURE 2

EVALUATIONS OF THE WORKSHOP ON "SITE-SPECIFIC EFFECTS OF SOIL AND ROCK ON GROUND MOTION AND THE IMPLICATIONS FOR EARTHQUAKE-RESISTANT DESIGN" BY PERCENTAGES OF PARTICIPANTS

Please circle the number which best represents your response to the following questions Number 5 represents the highest rating and number 1, the lowest.

	Fair Low 1 & 2	Good 3 & 4	Excellent High 5
1. Did you find the conference to be useful for:			
a. defining the state-of-knowledge?	7%	85%	8%
b. defining the technical issues?	21%	68%	11%
c. clarifying differences in perspectives of earth scientists and engineers?	7%	83%	10%
d. describing the current state-of-practice for incorporating site-specific effects into earthquake-resistant design?	31%	66%	3%
e. developing experiments to resolve important technical issues?	29%	61%	10%
f. recommending future research?	10%	76%	14%
2. Did the conference benefit you or your organization by:			
a. providing new information, ideas, and perspectives	10%	70%	20%
b. establishing better understanding of ways to resolve the technical issues?	18%	71%	11%
3. How effective were the following workshop procedures:			
a. presentations by the speakers?	4%	75%	21%
b. response by the panelists to stimulate discussions?	22%	59%	19%
c. interactive group discussions?	10%	69%	21%
d. special study groups	13%	66%	21%
e. informal ad hoc discussions	10%	62%	28%
f. preprints of papers?	6%	65%	29%
		Yes	No
4. If the clock were turned back and the decision to attend the workshop were given you again, would you want to attend?		100%	
5. Are you willing to participate in future workshops to continue the work initiated at this meeting?		97%	

3) Can existing data be further analyzed to quantify and model site effects better? How?

4) Does nonlinear soil behavior invalidate empirical methods of modeling site response that are based on low-strain level ground motions? (i.e., do low-strain level ground motions have any value in earthquake-resistant design?)

5) Are instrument arrays in place that would provide data to test the importance of non-linear soil behavior? Is it possible to record high-strain level ground motions?

Eight-two percent of the respondents felt that the workshop established better understanding of the ways to resolve the specific technical issues described above. Respondents were somewhat less enthusiastic about the workshop's success with developing experiments to resolve the technical issues (70% of the respondents answered good to excellent). However, the participants did establish guidelines for future experiments. They recommended that experiments be based on: 1) use of existing methodologies and data, 2) acquisition of new data, and 3) use of computer simulation. They also recommended that the experiments be integrated so as to produce both short- and long-term results with regard to: 1) the low strain vs high strain issue, 2) reducing uncertainty in earthquake-resistant design parameters that incorporate site response, and 3) improving site dependent response spectra.

Describing the current state-of-practice for incorporating site-specific effects into earthquake-resistant design was rated as good to excellent by over two-thirds of the evaluators (69%). Rated very high was the workshop's success in recommending future research (90%) and providing new ideas, and perspectives on site-specific effects of soil and rock on ground motion and the implications for earthquake-resistant design (90%). Specifically, participants encouraged the U.S. Geological Survey to take the lead in establishing a comprehensive national strong-motion data base which would be a national resource readily available to all researchers. The National Science Foundation and Nuclear Regulatory Commission, which share interests in such a data base, should also provide resources for achieving this objective.

One individual's comment regarding the effectiveness of the workshop sums up well the feeling of the participants who rated the workshop.

> Overall, I found the workshop very stimulating and feel that the subsequent planned follow up [experiments] should achieve the objectives. The most satisfying feature [of the workshop] was the recognition that seismologists and engineers need to work together to resolve their differences and plan future experiments to address technical issues.

The fact that over two-thirds (69%) of the respondents rated the workshop very high in providing new information, ideas, and perspectives emphasizes the success of the workshop in giving seismologists and engineers a better understanding of each others' disciplines and concerns.

WORKSHOP COMBINES FORMAL AND INFORMAL PRESENTATIONS AND DISCUSSIONS

To indicate which activities were viewed as the most useful, participants were asked to rate formal presentations, panel discussions, special study groups, and informal discussions. Formal presentations by speakers received the highest rating with 96% of the respondents judging them as good to excellent. The evaluation reflects the high quality of the speakers at this meeting. A large percentage of those who are involved in research on the site-specific effects of soil and rock on ground motion spoke at Santa Fe. The panel response to the formal presentations was viewed as valuable by the respondents (78%); however, not as valuable as the formal presentations possibly because of the time constraints imposed on these sessions. Both the interactive group discussions, which took place in small group meetings, and the ad hoc discussions, which took place during coffee breaks, lunches, and after hours, were rated as useful with 90% of the respondents rating these activities as good to excellent. The study groups, which met to discuss and suggest specific experiements regarding the technical issues of high strain versus low strain, generation of site-dependent spectra, and uncertainty, were rated by 87% of the respondents as useful to very useful. Clearly, the format of the meeting received high marks as expressed by one of the participants.

> The best thing about the meeting was to put together not only scientists of different but complementary fields but also scientists having different approaches concerning the same issues; this made the debate very interesting.

The next best thing was the way the workshop was organized including:

a) Presentations by speakers involved with the day to day specific problems exposing the different approaches.

b) Discussions stimulated by the panelists to focus on the main outcomes or differences still existing.

c) Group discussion to finalize the whole thing, and in the light of the newly acquired idea on the state-of-knowledge, try to come out with recommendations.

The importance and success of this workshop is shown in the response of all of those submitting evaluations that they would, knowing what to expect, attend similar workshops. In fact, all but one respondent stated that they would be willing to participate in future workshops to continue the work initiated at the meeting.

SUMMARY

Workshops are generally designed to do more than provide a forum for the exchange of information. Workshops should be a catalyst for further action. Because this workshop stimulated interest in resolving the technical and policy issues involved in site-specific effects of soil and rock on ground motions and in earthquake-resistant design, recommended further research and experiments, received the commitment of a large percentage of the participants to continue the work discussed and initiated there, the workshop met its goals and will be viewed as an important force in resolving the issues confronting earth scientists and engineers.

PARTICIPANTS

WORKSHOP ON "SITE-SPECIFIC EFFECTS OF SOIL AND ROCK ON GROUND MOTION AND THE IMPLICATIONS FOR EARTHQUAKE-RESISTANT DESIGN, SANTA FE, NEW MEXICO, JULY 26-28, 1983

Dr. Ted Algermissen
U.S. Geological Survey
Denver Federal Center
Denver, Colorado 80225

Mr. A. Ameur
Engineer at the Soil Mechanics Department
Control Technique de La Construction
Rue Kaddour Rahim Prologee
Hussein-dey
Algiers, Algeria

Dr. John Anderson
IGPP - 8025
University of California
San Diego, California 92092

Dr. Pierre-Yves Bard
Universite Scientifique et Medicale de Grenoble
Laboratorie De Geophysique Interne
Boite Postal N° 68
38402 St Martin D'Heres Cedes
France

Dr. Jack Boatwright
U.S. Geological Survey
345 Middlefield Road, MS 77
Menlo Park, California 94025

Dr. Bruce Bolt
Professor of Seismology and Director of the Seismographic Stations
475 Earth Science Building
University of California
Berkeley, California 94720

Dr. David Boore
U.S. Geological Survey
345 Middlefield Road
Menlo Park, California 90425

Dr. Roger D. Borcherdt
U.S. Geological Survey
345 Middlefield Road, MS 77
Menlo Park, California 94025

Dr. Kenneth W. Campbell
U.S. Geological Survey
Denver Federal Center
Denver, Colorado 80225

Mr. C. B. Crouse
Senior Engineer
ERTEC Western Inc.
P.O. Box 7765
3777 Long Beach Boulevard
Long Beach, California 90807

Dr. Neville Donovan
Principal Engineer
Dames and Moore
500 Sansome Street
San Francisco, California 94111

Mr. Djamol El Foul
Engineer at the Soil Mechanics Department
Control Technique de La Construction
Rue Kaddour Rahim Prologee
Hussein-dey
Algiers, Algeria

Mr. Joseph A. Fischer
President
Geoscience Associates, Inc.
50 Division Avenue
Millington, New Jersey 07946

Dr. Gerald Frazier
Science Applications, Inc.
P.O. Box 2351
La Jolla, CA 92038

Dr. David Hadley
Sr. Vice President
Sierra Geophysics, Inc.
15446 Bell-Red Road #400
Redmont, Washington 98025

Mr. Asadour H. Hadjian
Principal Engineer
Bechtel Power Corporation
12400 East Imperial Highway
Norwalk, California 90650

Mr. Gene Hawkins
Geologist
Southern California Edison Company
P.O. Box 800
2244 Walnut Grove Ave.
Rosemead, California 91711

Dr. Walter W. Hays
U.S. Geological Survey
905 National Center
Reston, Virginia 22092

Dr. Lyman Heller
U.S. Nuclear Regulatory Commission
P-214
Washington, D.C. 20555

Mr. Joe Hunt
Geology and Geotechnical Engineering
Group Head
Tennessee Valley Authority
400 West Summit Hill Drive, 179 LB
Knoxville, Tennessee 37902

Dr. I.M. Idriss, Principal
Woodward-Clyde Consultants
203 North Golden Circle Drive
Santa Ana, California 92705

Dr. Robert Jackson
Chief, Geosciences Branch
U.S. Nuclear Regulatory Commission
Washington, D.C. 20555

Dr. Bill Joyner
Geophysicist
U.S. Geological Survey
345 Middlefield Road
Menlo Park, California 94025

Mr. Jeff Kimball
Seismologist
U.S. Nuclear Regulatory Commission,
P-514
Washington, D.C. 20555

Dr. Jerry King
Electric Power Research Institute
3412 Hillview Avenue
Palo Alto, California 94303

Mr. Ken King
U.S. Geological Survey MS 966
Denver Federal Center
Denver, Colorado 80225

Dr. William D. Kovacs
Geotechnical Engineering Group
Structures Division
National Bureau of Standards
Washington, D.C. 20234

Dr. Geoffrey Martin
Vice President
ERTEC Western, Inc.
PO Box 7765
3777 Long Beach Boulevard
Long Beach, California 90807

Dr. Martin McCann
Jack R. Benjamin & Associates, Inc.
Consulting Engineers
444 Castro Street, Suite 501
Mountain View, California 94041

Dr. Robert McNeill
Consulting Engineer
3936 Garcia, N.E.
Albuquerque, New Mexico 87111

Mr. John R. Murphy
S-Cubed
11800 Sunrise Valley Drive
Suite 112
Reston, Virginia 22091

Mr. Stephen F. Obermeir
U.S. Geological Survey
926 National Center
Reston, Virginia 22092

Mr. David Perkins
U.S. Geological Survey
MS 966
Denver Federal Center
Denver, Colorado 80225

Mr. Antonio Pugliese
Viale America 111
Roma, Italy 00100

Dr. Leon Reiter
U.S. Nuclear Regulatory Commission
P-514
Bethesda, Maryland 20014

Dr. Al Rogers
U.S. Geological Survey
MS 966
Denver Federal Center
Denver, Colorado 80225

Dr. Khrosrow Sadigh
Woodward Clyde Consultants
100 Pringle Avenue
Walnut Creek, California 94596

Dr. Jogeshwar P. Singh
Harding-Lawson Associates
7655 Redwood Boulevard
Novato, California 94947

Mr. M. Slimani
Engineer at the Soil Mechanics
Department
Control Technique de La Construction
Rue Kaddour Rahim Prologee
Hussein-dey
Algiers, Algeria

Dr. John Tinsley
U.S. Geological Survey,
345 Middlefield Road, MS 77
Menlo Park, California 94025

Dr. Brian Tucker
California Division of Mines
and Geology
1416 9th Street
Sacramento, California 95814

Mr. Leif G. Wennerberg
U.S. Geological Survey
345 Middlefield Road, MS 77
Menlo Park, California 94025

The Issues Surrounding the Effects of Geologic Conditions on the Intensity of Ground Shaking

by

A. M. Rogers, USGS, Golden, Colorado

J. C. Tinsley, USGS, Menlo Park, California, and

W. W. Hays, USGS, Reston, Virginia

Introduction

This paper will outline the issues related to site response effects and expand some of these topics based on data principally from the Los Angeles region. In some cases we will review and reevaluate old and new data from the perspectives provided by comparison of these data sets. In spite of fairly strong evidence showing the significance of site conditions on the level of ground shaking, questions continue to be raised about either the importance of site effects or whether they can be accurately predicted. We outline many of these questions and address some of them in the following discussion.

The Issues

A. What do we know about site response?

a. What is the range and nature of site effects in the time and frequency domain?

i.) What are the effects of site conditions on peak ground motion parameters?

ii.) Is the influence of site effects minimal in peak acceleration data sets?

iii.) If site effects do not significantly contribute to peak acceleration variability, are these effects important to consider in design?

iv.) What are the effects of site conditions on the ground motion spectrum? How important is site resonance and under what conditions does it occur?

v.) What is the evidence for non-linear soil behavior?

vi.) When non-linear soil behavior occurs, how important is it, and is its effect on the site transfer function significant?

vii.) Will all soils in the zone of non-linearity have the same level of ground shaking?

b. How great is the variability in site effects?

i.) Are site effects at a given location reproducible within useful statistical bounds?

ii.) Is site response too variable geographically to accurately predict without unreasonable quantities of geotechnical information?

iii.) Is the rate of geographical variability in site response a function of the period band of interest?

iv.) Do surface topography and lateral subsurface heterogeneity produce important changes in site

response, particularly as epicentral distance or source-receiver azimuth changes?

B. Can site response effects be predicted?

a. What theoretical methods exist?

i.) Are linear or non-linear methods most appropriate?

ii.) How well do theoretical models predict observed site response?

b. What empirical methods exist?

i.) Does non-linear soil behavior invalidate empirical methods of prediction that have been based on low-level ground motions?

ii.) Do low-level, ground-motion measurements of site response significantly overestimate site effects during strong shaking?

iii.) How well do empirical models predict observed site response?

c. Are prediction methods available that will work in any region and that reconcile to some degree the diverse site response observations from many regions into a unified picture?

C. Do we need to perform additional experiments?

a. Are the geologic and ground motion data bases adequate to study site response effects?

i.) Are they of high quality, sufficient quantity, and appropriately collected?

ii.) Has soil-structure interaction significantly modified the strong motion data base?

b. What experiments might be performed to resolve the issues?

i.) Are instrument arrays in place that would provide data to further test the importance of non-linear soil behavior?

ii.) Are instrument arrays in place that would provide data to test various prediction schemes?

iii.) What geotechnical data are needed, and how will the data be collected?

iv.) How can existing data be further analyzed to study site effects?

D. How can site response predictions and data best be utilized?

a. Should design ground motions be modified for site response?

i.) Are the currently employed mean spectral shapes adequate to describe changes in site response as a function of geologic conditions?

ii.) Do we know how to modify design coefficients or synthethic seismograms to account for site response in a realistic way?

iii.) How will imbedment modify the design motion?

iv.) How will soil-structure interaction modify the design motion?

b. How should site response predictions be used for urban planning, disaster planning, and loss estimation?

i.) Are site response maps the most useful form of input to these studies?

The Existence of Site Shaking Effects

A reasonable starting point is to address a more basic question than those listed above. That is, is site response an important phenomena that significantly affects the level of strong shaking at ground periods of engineering interest. This question has been frequently addressed in the literature with responses ranging from "very significant" to "not important in this region" to "important, but impossible to predict." The preponderance of data, however, including damage statistics, intensities, strong motion measurements, and low-level ground-motion measurements indicates that site response effects are significant. The Japanese and Russians have examined numerous case studies showing that the geographic distribution of damage and intensity is in some way related to the thickness and/or other physical properties of the near-surface sediments (Kanai, 1952; Ooba, 1957; Minakami and Sakuma, 1948; Medvedev, 1962). Using recordings of low-level ground motions produced by distant nuclear explosions, Borcherdt and Gibbs (1976) found a high correlation between geographic changes in intensities in the 1906 San Francisco earthquake and geographic changes in mean spectral amplification. This correlation exists up to the highest shaking

levels that occurred in that earthquake (Modified Mercalli $\geq$ X). Site effects have recently been isolated in the strong motion data from the 1979 Imperial Valley earthquake (Mueller and others, 1982) and are also observed in the strong motion data recorded during the Fruili and Ancona, Italy earthquakes (Chiaruttini and Siro, 1981). Analysis of the San Fernando earthquake data set by Rogers and others (1983a) shows that site effects occur at the 28 strong-motion sites they studied. For these sites mean spectral amplification on soil ranged as high as a factor of 5. Data at other Los Angeles sites, employing recordings of Nevada Test Site nuclear explosions, indicated that at some alluvium sites mean spectral amplifications as large as 11 are observed. Many other examples of ground motion studies could be cited that demonstrate the importance of geologic conditions on strong ground shaking.

A Discussion of the Importance of Non-Linear Soil Behavior

Although laboratory data suggest that soils behave in a non-linear fashion when strain levels exceed 10^{-5} (Seed and Idriss, 1970) or 10^{-4} (Turner and Stokoe, 1982), field data have been collected suggesting that high- and low-amplitude soil response are similar, perhaps for strains up to 10^{-3}. Rogers and others (1983a) compare site shaking effects measured using distant nuclear explosions (strains near 10^{-5}) with site effects at the same locations measured with data from the 1971 San Fernando earthquake (strains near 10^{-3}) and find that the two data sets

are equivalent within the expected variability of the statistics. Rogers and Hays (1978) using strong ground motion recordings of nuclear explosions on the Nevada Test Site, find that site response measured at strains of 10^{-3} and 10^{-4} are approximately equal. Joyner and others (1981) find that site response can be predicted using linear theory for strains up to 10^{-4}. Several recently collected strong motion data sets also indicate that if non-linear soil behavior is a factor limiting the magnitude of ground motions on soils, the limiting values may still be quite high (Mueller and others, 1982; Chiaruttini and Siro, 1981). The Borcherdt and Gibbs (1976) comparison of intensity increments and mean spectral ratio, cited above, may also be evidence that non-linear soil behavior is of secondary importance.

The effect of non-linear soil response may also be restricted to a small area surrounding the causative fault (Hays and Algermissen, 1982). For instance, a magnitude 7-7.5 earthquake develops velocities on soil sites exceeding 100 cm/s at distances less than 7-13 km (50 percentile, Joyner and Boore, 1981). For soil sites with 200 m/s shear velocities, strains of $5x10^{-3}$ will be developed within this zone. Based on the observations discussed above this strain level may still be below the level of significant non-linear behavior. Because damaging motions on soils IMM>VI occur to distances of 60-100 km (50 percentile) for a 30 km rupture, the area of damage susceptible to non-linear soil response is about 2-9% of the total area of damage. In cases where the fault passes through developed

regions, however, the zone of non-linear behavior may be the zone of greatest life loss, although a high percentage (as much as 90%) of the economic loss occurs outside this zone (Algermissen and others ,1972). In other cases where the fault passes outside the urban zone or the earthquake is too small to induce non-linear soil response, this behavior will not be a factor at all. The 1967, M = 6.4, Caracas, Venezuela earthquake is a good example that demonstrated strong site effects within a city that experienced numerous building failures and several hundred lives lost for an earthquake 50 km away (Seed and others, 1972). The 1977 Romania earthquake (M = 7.2; ISC, 1977) was centered about 120 km from Bucharest, where 1387 people were killed. Bucharest is underlain by alluvium, some of Holocene age (Carte des Sols, 1964), that we infer had a role in the damaging ground motions that occurred there, but because of the distance (120 km) from the earthquake fault, the alluvium is unlikely to have behaved non-linearly (the peak velocities in Bucharest are estimated to be about 50 cm/s (Skinner, 1977)).

Prediction of Site Response Effects

Prediction of site response has frequently been attempted by several empirical techniques. In one empirical method, low-strain measurements of small earthquakes or distant nuclear explosions are obtained over a region at rock and soil sites in a pattern dense enough to essentially measure relative site-response (Hays and Algermissen, 1982; Murphy and Hewlett, 1975).

Another empirical technique compares limited measurements of site-response, relating response to known geological data, and predicting relative shaking effects, over a broad region or to a specific site, based on mapped geologic units having distinctive seismic behavior. This technique, using Nevada Test Site nuclear explosions, was first examined by Borcherdt (1970) using recordings in the San Francisco region and by Murphy and others (1971) in the Las Vegas region. These studies demonstrated that mean spectral amplification from nuclear explosions is correlated with changes in earthquake shaking intensity and that, in cases where geologic structure and shear velocities are well known, the measured site response can be predicted from theory with fair success. Borcherdt and Gibbs (1976) also established a correlation between age of surficial deposits and mean spectral amplification that enabled them to produce a regional map showing the predicted relative geographic changes in shaking intensity. These studies in addition to studies by Rogers and others (1983a), Mueller and others (1982), and King (1982) suggest that in many cases differences in wave types, angles of incidence, and source azimuth have a second order importance relative to site response and do not mask the underlying character of the site shaking effect.

In this study we extend the technique developed by Borcherdt and Gibbs (1976) to the Los Angeles region and recast the technique to include the effects of geologic structure and near-surface site properties. In order to determine relations between

local geologic factors and shaking amplification, nineteen nuclear explosions were recorded at 98 sites throughout the Los Angeles region (Figure 1). Sites for the study were chosen to obtain as complete a sample of underlying geologic conditions and as broad a geographic coverage as possible. Because the seismic source lies between 400 and 450 km from the recording sites, effects of azimuthal variations in the energy radiated by the nuclear source and major portions of the crustal propagation paths are similar for all sites. Estimation of each site's response characteristics over the period band 0.2 to 10 seconds was accomplished by computing Fourier spectra and alluvium-to-crystalline rock spectral ratios (Rogers and others, 1980). The site CIT, underlain by crystalline rock, was occupied for every recorded nuclear explosion and served as the base rock site.

In the case of ground motions from distant nuclear explosions, the effects of site conditions predominate on the recorded time histories. For example, Figure 2 shows time histories recorded simultaneously at eight sites from a single Nevada Test Site nuclear explosion. The example illustrates several effects local site conditions commonly have on the recorded time histories from distant sources of shaking. For instance, maximum amplitudes of motion recorded on the alluvial sites are several times larger than those recorded on the sedimentary or the crystalline rock sites. The degree of amplification occurring in the long-period peak amplitudes of these records is greatest at sites underlain by the thickest

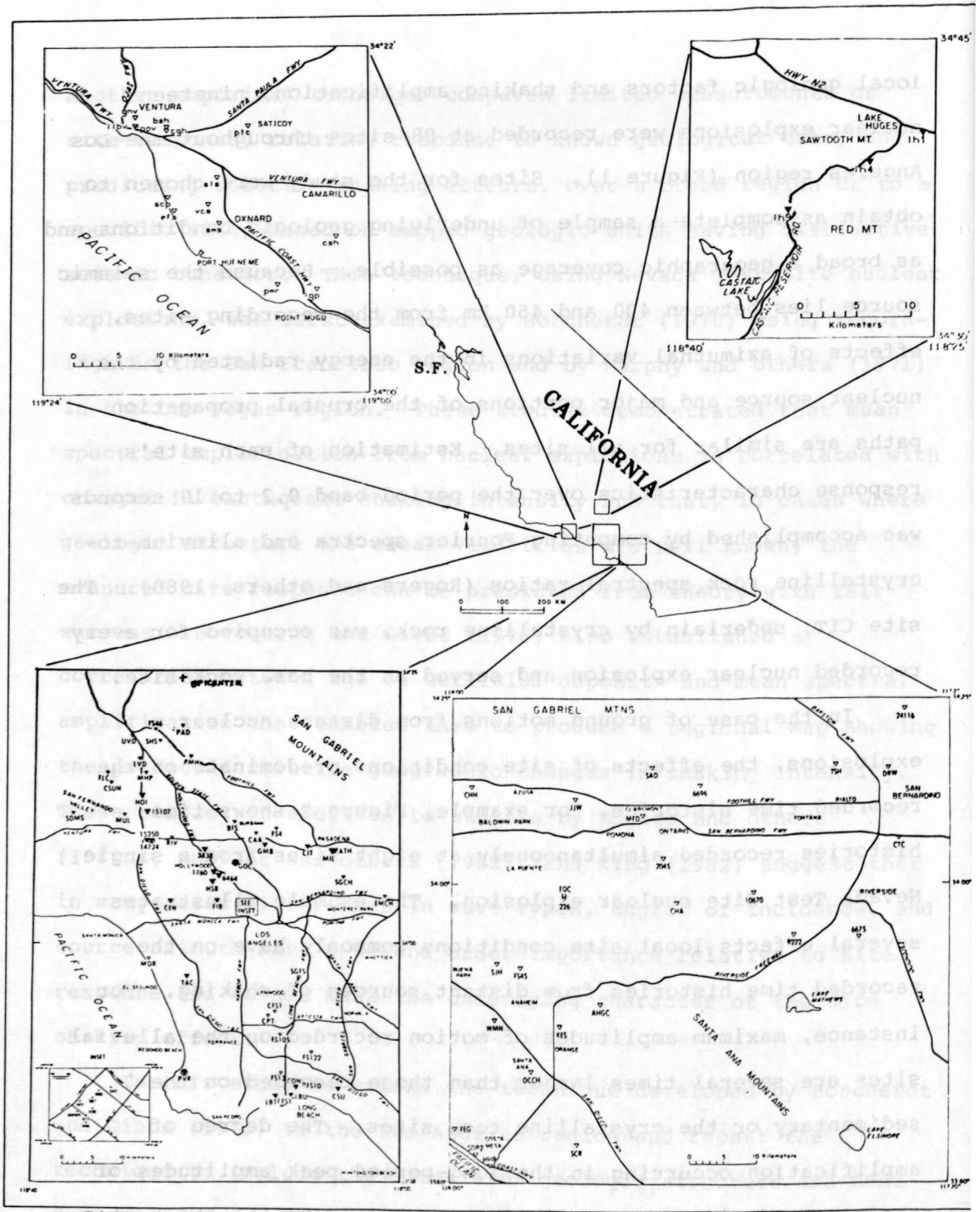

Figure 1. Locations of sites in the Los Angeles region at which ground motion recordings of nuclear explosions at the Nevada Test Site were obtained. Strong motion recordings of the 1971 San Fernando earthquake were also available at some of these locations. The epicenter of the 1971 earthquake is shown by +.

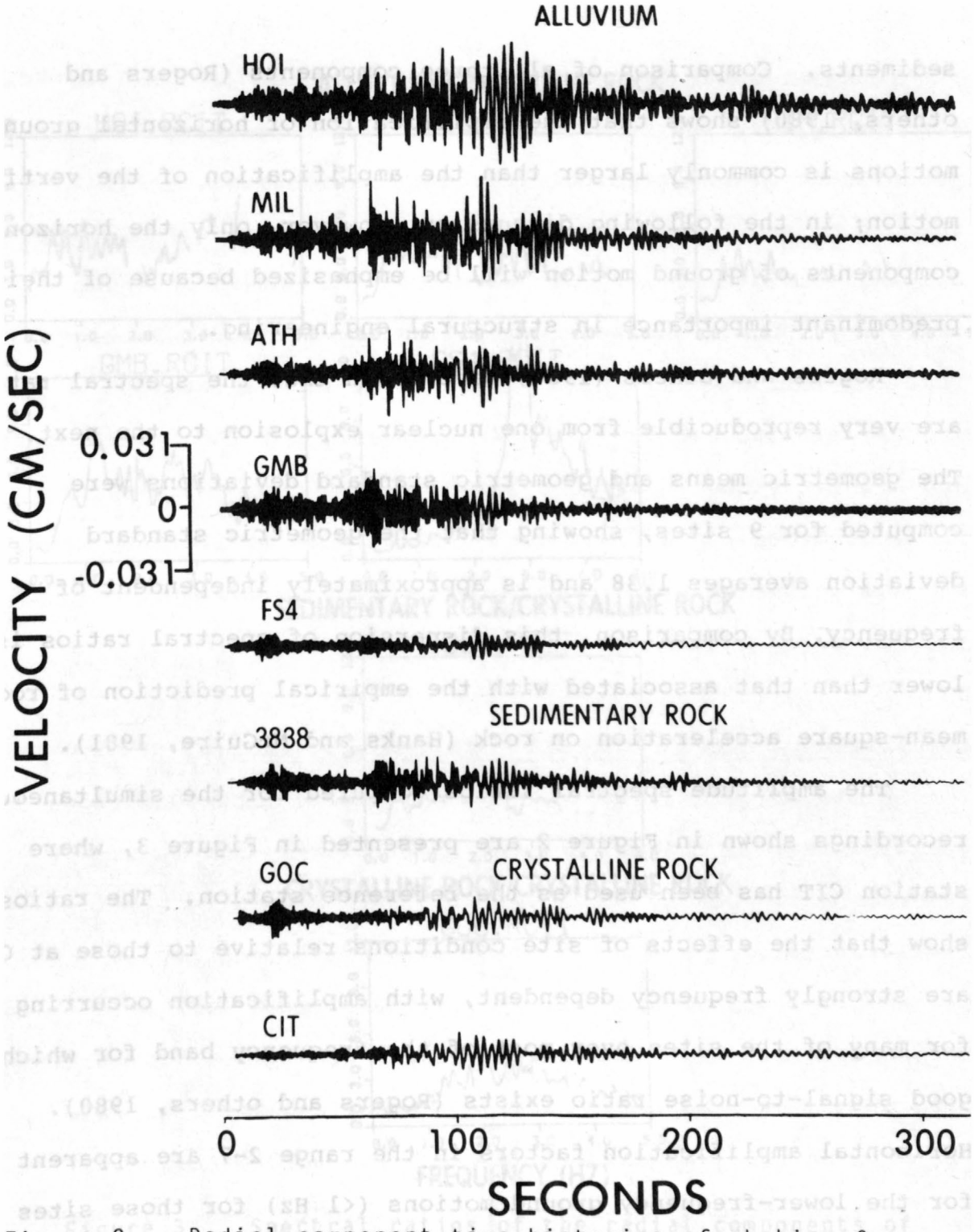

Figure 2. Radial component time histories of shaking from a distant underground nuclear explosion in Nevada recorded simultaneously at eight sites, in the Los Angeles region, grouped according to type of geologic materials immediately beneath each recording station. The ground motions are clearly amplified at locations underlain by alluvium compared to locations underlain by rock. The degree of amplification also appears to be related to the thickness of underlying alluvium (HOI: 300 m; 372 m: ATH: 372 m; GMB: 120 m; FS4: 15 m).

sediments. Comparison of all three components (Rogers and others, 1980) shows that the amplification of horizontal ground motions is commonly larger than the amplification of the vertical motion; in the following discussion, however, only the horizontal components of ground motion will be emphasized because of their predominant importance in structural engineering.

Rogers and others (1980) have shown that the spectral ratios are very reproducible from one nuclear explosion to the next. The geometric means and geometric standard deviations were computed for 9 sites, showing that the geometric standard deviation averages 1.38 and is approximately independent of frequency. By comparison, this dispersion of spectral ratios is lower than that associated with the empirical prediction of root-mean-square acceleration on rock (Hanks and McGuire, 1981).

The amplitude spectral ratios computed for the simultaneous recordings shown in Figure 2 are presented in Figure 3, where station CIT has been used as the reference station. The ratios show that the effects of site conditions relative to those at CIT are strongly frequency dependent, with amplification occurring for many of the sites over most of the frequency band for which a good signal-to-noise ratio exists (Rogers and others, 1980). Horizontal amplification factors in the range 2-7 are apparent for the lower-frequency ground motions (<1 Hz) for those sites on thick sections of alluvium, with lower amplifications being apparent at these frequencies for the site underlain by a thin section of alluvium. Considerable amplification at intermediate

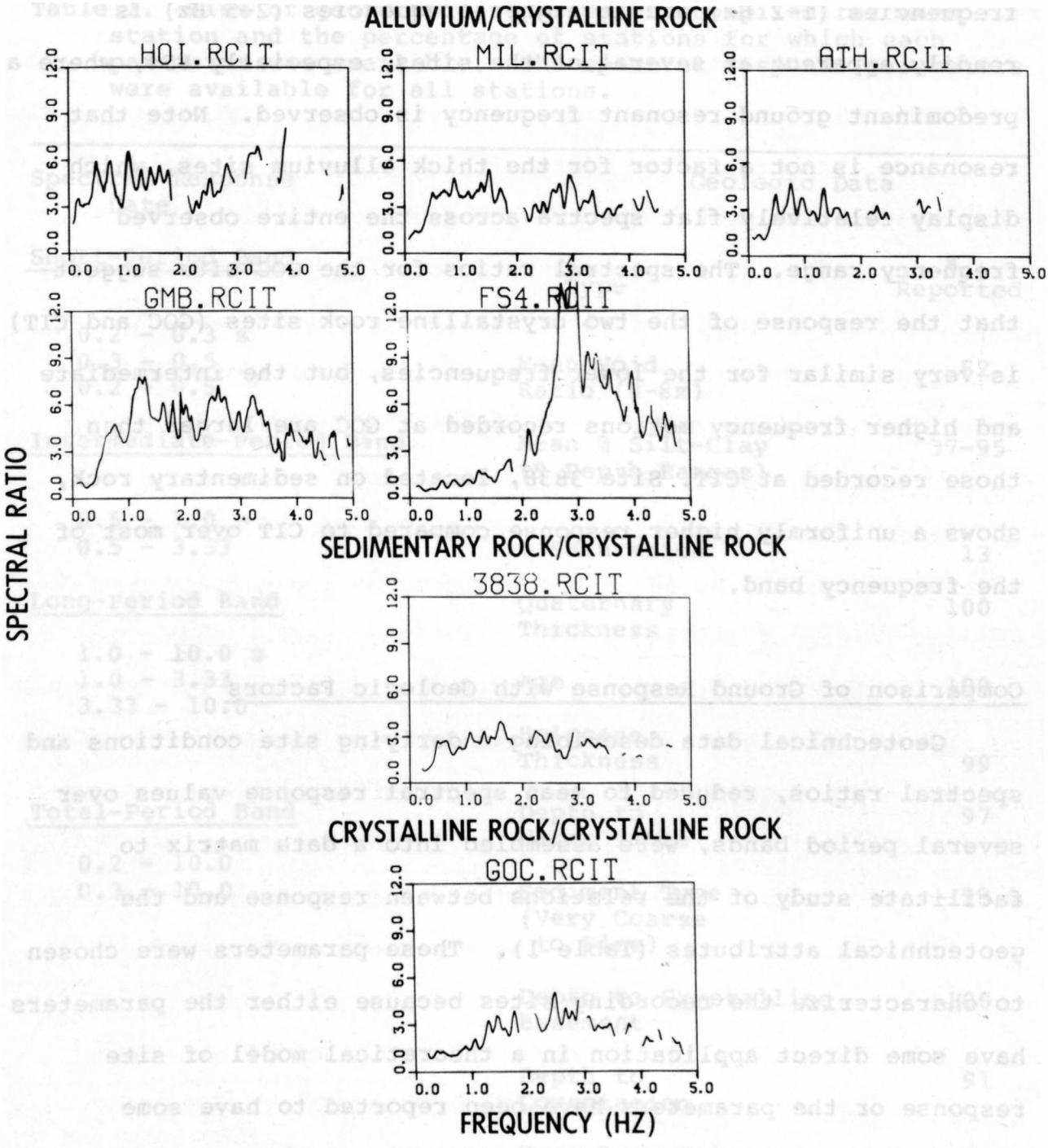

Figure 3. Spectral ratios of the radial components of ground motion recorded on sites of varied geology (see Figure 3) relative to the crystalline rock site (CIT). These diagrams show that spectral site amplification ranges from about 1 to greater than 12, with the highest ratios occurring at sites underlain by alluvium. Site FS4 displays a resonant frequency between 2 and 3 Hz, whereas other sites have more uniform amplification, averaging as much as 6 in some frequency bands.

frequencies (1-2 Hz) and at higher frequencies (2-5 Hz) is readily apparent at several of the sites, especially FS4, where a predominant ground resonant frequency is observed. Note that resonance is not a factor for the thick alluvium sites, which display relatively flat spectra across the entire observed frequency range. The spectral ratios for the GOC site suggest that the response of the two crystalline rock sites (GOC and CIT) is very similar for the lower frequencies, but the intermediate and higher frequency motions recorded at GOC are larger than those recorded at CIT. Site 3838, located on sedimentary rock, shows a uniformly higher response compared to CIT over most of the frequency band.

Comparison of Ground Response with Geologic Factors

Geotechnical data describing underlying site conditions and spectral ratios, reduced to mean spectral response values over several period bands, were assembled into a data matrix to facilitate study of the relations between response and the geotechnical attributes (Table 1). These parameters were chosen to characterize the recording sites because either the parameters have some direct application in a theoretical model of site response or the parameters have been reported to have some influence on ground shaking in past studies. Thus, parameters such as % silt-clay, % saturation, and depth-to-water table have been reported to influence site response, while shear velocity (or void ratio, which strongly influences the shear modulus),

Table 1. List of geotechnical parameters compiled for each station and the percentage of stations for which each parameter was available. The spectral response parameters were available for all stations.

Spectral Response Date	Geologic Data Type	% Reported
Short-Period Band		
0.2 - 0.3 s		
0.3 - 0.5	Mean Void Ratio (0-8m)	82
0.2 - 0.5		
Intermediate-Period Band	Mean % Silt-Clay (9 Depth Ranges)	37-95
0.5 - 1.0 s		
0.5 - 3.33	% Saturation	13
Long-Period Band	Quaternary Thickness	100
1.0 - 10.0 s		
1.0 - 3.33	Age	100
3.33 - 10.0		
	Holocene Thickness	99
Total-Period Band	Depth to Water Table	97
0.2 - 10.0		
0.3 - 10.0	Sediment Type (Very Coarse to Fine)	99
	Depth to Crystalline Basement	100
	Depth to Comentation	91
	Mean Bore-Hole Shear Velocity (4 intervals)	51

Holocene thickness, Quaternary thickness, and depth-to-basement are all parameters that might be used directly in a model of site response. Most of these data are obtainable from geologic maps, well logs, and city files containing engineering boreholes for construction projects. The data, therefore, would be of great value if related to site response in some quantifiable manner.

To examine the relation between site response and the geological parameters, the most straightforward approach is to group the sites according to variations in one of the geologic factors and to compute mean response for each group. Table 2 indicates the following ground response characteristics: 1.) Sites underlain by Holocene and Pleistocene sedimentary deposits undergo levels of shaking 2.6 to 3.4 times greater than those underlain by crystalline rock for all period bands; 2.) The void ratio has a strong influence on short-period response, with void ratios in the 0.8-0.9 range indicating a mean response on soil 6 times greater than on crystalline rock and 3 times greater than on low-void-ratio soils; 3.) Amplitudes in the long-period band generally increase with increasing thickness of Quaternary deposits and/or depth to basement.

More detailed examination of the influence of all the geologic parameters using the methods of exploratory data analysis (Mosteller and Tukey, 1977; Velleman and Hoaglin, 1981) indicate that the strongest changes in site response were correlated with changes in void ratio, Holocene thickness, depth to basement, and Quaternary thickness. Applying the smoothing

Table 2. Comparison of Shaking Response (relative to crystalline rock) from distant nuclear explosions recorded at sites within the Los Angeles region.

A) Response in three period bands compared with age of materials.

Age	Short-period (0.3 - 0.5s)	Intermediate Period (0.5 - 3.3s)	Long-period (3.3 - 10.0s)
Holocene	3.4	3.3	2.6
Pleistocene	3.2	3.1	2.6
Pliocene	1.4	1.6	2.0
Miocene	2.5 [1.9]	2.2 [1.8]	1.4 [1.3]
Mesozoic	1.7	1.1	0.8

B) Short-period response compared with average void ratio in the uppermost 8 m.

Void Ratio	Short-period Mean Response (0.3 - 0.5s)
0.2 - 0.4	2.3
0.4 - 0.6	3.1
0.6 - 0.7	3.0
0.7 - 0.8	4.2
0.8 - 0.9	6.2

C) Intermediate- and long-period response compared with thickness of Quaternary deposits.

Quaternary Thickness (M)	Intermediate Period Mean Response (0.5 - 3.3s)	Long-period Mean Response (3.3 - 10.0s)
0	1.6	1.3
0-75	2.3	1.4
75-200	3.6	2.9
200-500	3.6	3.1
500-1000	4.1	5.9
>1000	3.4	3.1

D) Intermediate- and long-period response compared with depth to basement rocks.

Depth to Basement (km)	Intermediate Period Mean Response (0.5 - 3.3s)	Long-period Mean Response (3.3 - 10.0s)
0	1.1	0.8
0-2	2.6	1.3
2-4	2.8	2.5
4-6	3.8	4.1
>6	3.8	3.9

techniques of exploratory data analysis, it is frequently possible to extract the influence of one factor on the response variable given a body of data in which several factors are changing simultaneously. Figure 4, for instance, shows the smoothed short-period ratio plotted against Holocene deposit thickness (A) and void ratio (B). The peak in short-period response for Holocene thicknesses near 15 m is due to the shift through this period band of the fundamental resonance period of the Holocene layer. The general increase in the short-period response as void ratio increases is principally due to the increasing shear-wave velocity contrast at the Holocene-Pleistocene boundary. For comparative purposes, theoretical spectral ratios were computed using a horizontally layered SH-body-wave model and assuming constant Q. The physical properties of the geologic column used in this modelling were generated by computer from the geologic data matrix with variable surface layer velocities, fixed lower layer velocities, and depths to velocity contrasts determined by Holocene deposit thickness, Quaternary thickness, and depth to basement (Figure 5). Surface layer velocities were either measured borehole shear velocities (Fumal and others, 1983) or were computed from void ratios. The theoretical spectral ratios and mean spectral values were processed in exactly the same fashion as the observed quantities. The concordance between the observed data and the theory supports our interpretation of the observed behavior. While similar analysis of other factors indicates that variables

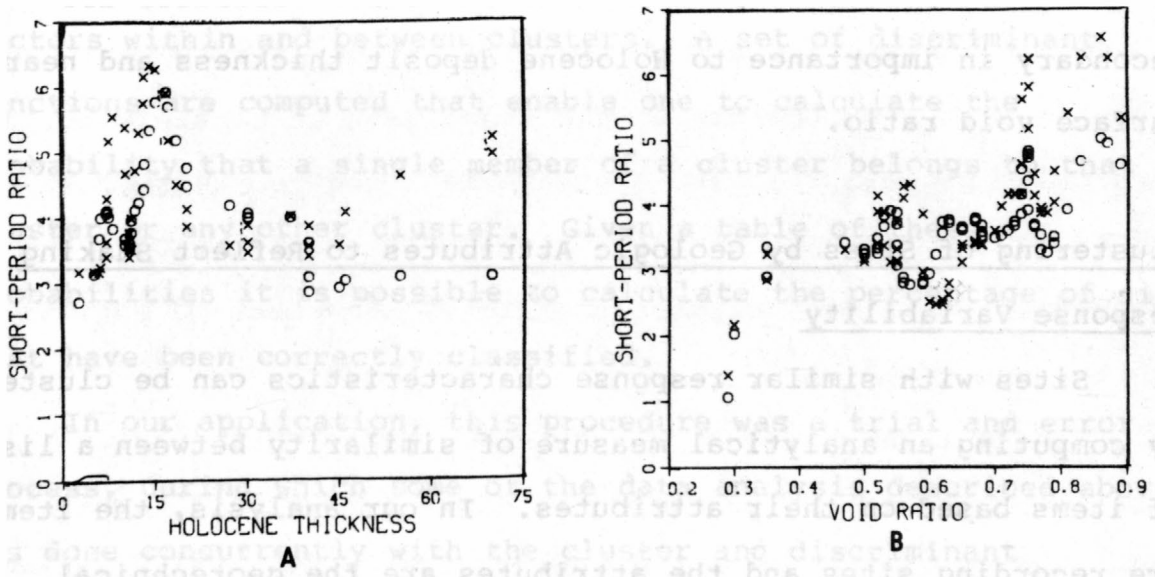

Figure 4. Smoothed short-period response at sites on Holocene deposits in comparison with Holocene thickness (A) and void ratio (B). In order to minimize the influence of void ratio in (A), only sites with void ratios greater than 0.65 were included. A circle or X indicates theoretical or observed values, respectively.

		SHEAR VELOCITY (m/s)	DENSITY (gm/c³)	Q	REMARKS
HOLOCENE	t_H	V_m / V_c	1.46 g/cm³	50	V_c=42.9+94.1/e²
PLEISTOCENE 1	tp_1 = QTHK − t_H	350m/s	2.10	200	tp_1 NOT ALLOWED TO EXCEED 100m
PLEISTOCENE 2	tp_2 = QTHK − tp_1 − t_H	600m/s	2.10	200	ONLY PRESENT WHEN QTHK-t_H>100m
TERTIARY ROCK	T_t=dtb − QTHK	1500m/s	2.35	500	ONLY PRESENT WHEN dtb>QTHK
CRYSTALLINE BASEMENT		3000m/s	2.50		

QTHK=THICKNESS OF QUATERNARY DEPOSITS
dtb=DEPTH TO CRYSTALLINE ROCK

Figure 5. Shear-wave velocity model used to compute theoretical damped SH-wave response.

such as depth to basement and Quaternary thickness have an effect on the short-period response, these and other variables are secondary in importance to Holocene deposit thickness and near-surface void ratio.

Clustering of Sites by Geologic Attributes to Reflect Shaking Response Variability

Sites with similar response characteristics can be clustered by computing an analytical measure of similarity between a list of items based on their attributes. In our analysis, the items are recording sites and the attributes are the geotechnical properties of each site. (Note that we do not use the response factor as an attribute because we are attempting to predict response as a function of the geologic properties of the site.) The clustering algorithm (Anderberg, 1973; Hartigan, 1975; IMSL, 1982) uses a computing rule to establish those items most nearly alike and the similarity level at which clusters of similar items are alike. The results can be plotted as an inverted hierarchical tree of similarity nodes. The choice of a similarity level below which clusters form is a subjective judgment and in practice may change across the cluster diagram.

Once a set of clusters is formed by this procedure on a chosen set of factors it is possible to analyze the degree to which these factors define unique groups using discriminant analysis (Morrison, 1969; Morrison, 1974; Cooley and Lohnes, 1971; Nie and others, 1975), which determines the significance of

each factor's discriminating power using the statistics of factors within and between clusters. A set of discriminant functions are computed that enable one to calculate the probability that a single member of a cluster belongs to that cluster or any other cluster. Given a table of these probabilities it is possible to calculate the percentage of sites that have been correctly classified.

In our application, this procedure was a trial and error process, during which some of the data analysis described above was done concurrently with the cluster and discriminant analysis. At the start, the site response data were first divided into rock and alluvium groups, and then clusters were examined in which many or all of the measured factors were part of the clustering model. This approach, however, produces too many clusters, with too few station members. The number of factors in the clustering process was reduced iteratively by gradually discarding factors having low statistical significance in the discriminant analysis.

Comparison of the mean response values in each cluster set for the three period bands revealed that some clustering parameters reduced the response variance in each cluster better than others, in accord with the results of the preliminary data analysis showing that the most important factors in each period band should be different. Ultimately, the cluster sets selected were chosen because they had the lowest dispersion in the defining variables while employing those factors having the

strongest effect in a given period band; in addition, we required that the probability of misclassification be low, and that each cluster in the set had a sufficient amount of data to estimate the mean cluster properties. The final sets of clusters are a compromise between the many clusters required to preserve the complexity in the site response as a function of geology, and the requirement that each cluster contain enough cases to estimate its average response.

Figure 6 shows the set of two rock and eight alluvium clusters that were derived for the short-period band. This figure is can be understood by using cluster 4A as an example; that cluster includes sites with depth to basement rocks greater than 0.5 km, Holocene deposit thickness greater than 20 m, void ratios in the range 0.6-0.7, and a geometric mean response of about 3.6. Using these clusters to predict response preserves the important features of site behavior noted above. For instance, for a fixed Holocene deposit thickness, response increases as void ratio increases (i.e., compare clusters 1A, 3A, and 6A, for example). Response also increases, for a constant void ratio, as the Holocene deposit thickness increases to the critical range (i.e., compare clusters 6A, 7A, and 8A, for example). Note that the clusters with thin Holocene cover also contain most of the Pleistocene sites; those Pleistocene sites in the thickness range 11 to 20 m, however, are grouped with the Holocene sites in this range. The rock sites 1R and 2R indicate a geometric mean response that is typically lower than that of the alluvium

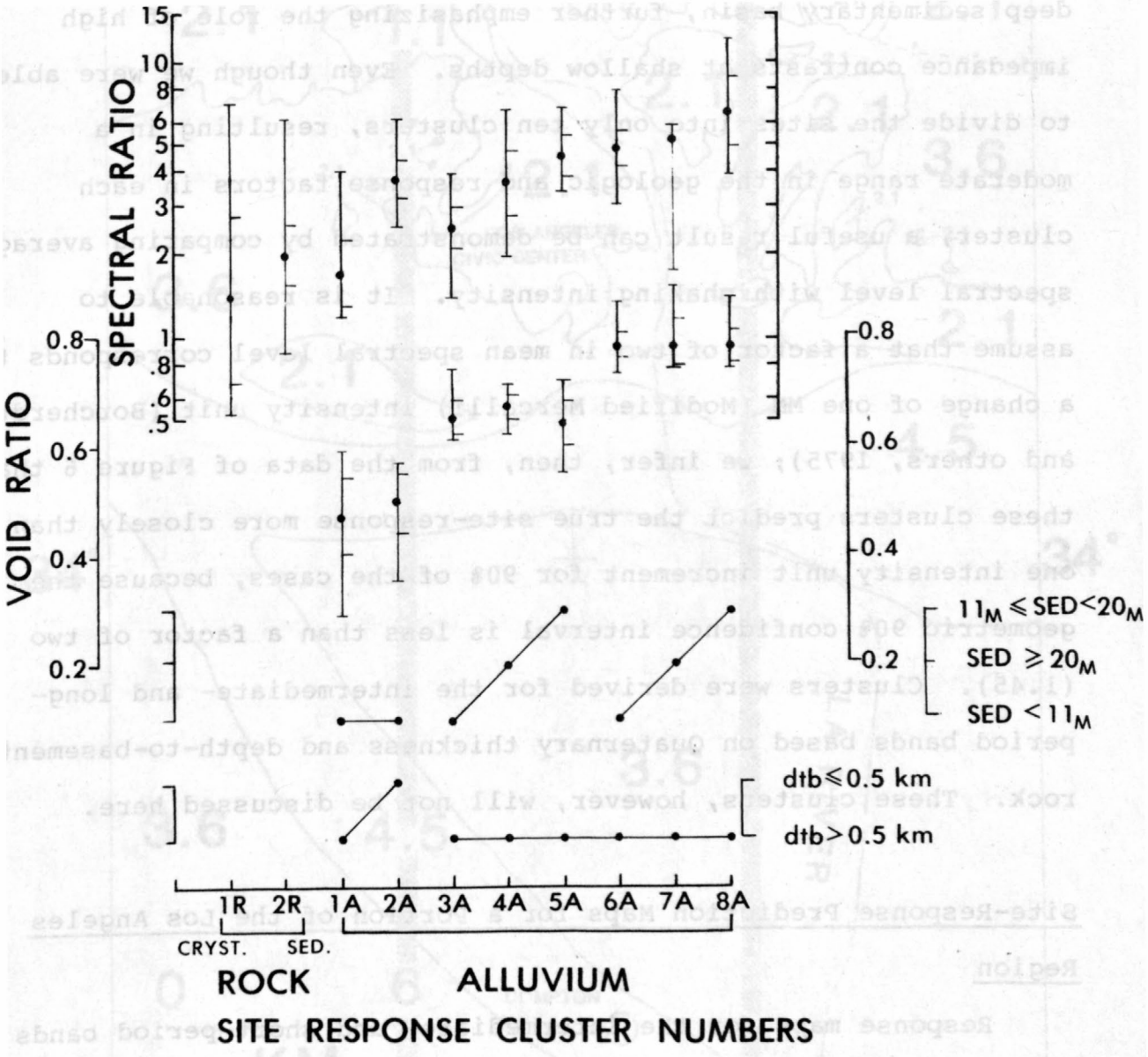

Figure 6. Site clusters for short-period ground motions in the Los Angeles region. Solid dots indicate the mean of the short-period spectral ratios for a given cluster, mean void ratio Holocene thickness and depth to basement rock groups, as appropriate. Vertical bars indicate the range in the variable for a given cluster, and side ticks indicate the 90% confidence intervals.

clusters, as might be predicted on the basis of surface velocities. A comparison of clusters 1A and 2A shows that sites underlain by shallow alluvium over crystalline rock (2A) have a response two times higher than the same type of site overlying a deep sedimentary basin, further emphasizing the role of high impedance contrasts at shallow depths. Even though we were able to divide the sites into only ten clusters, resulting in a moderate range in the geologic and response factors in each cluster, a useful result can be demonstrated by comparing average spectral level with shaking intensity. It is reasonable to assume that a factor of two in mean spectral level corresponds to a change of one MM (Modified Mercalli) intensity unit (Borcherdt and others, 1975); we infer, then, from the data of Figure 6 that these clusters predict the true site-response more closely than one intensity unit increment for 90% of the cases, because the geometric 90% confidence interval is less than a factor of two (1.45). Clusters were derived for the intermediate- and long-period bands based on Quaternary thickness and depth-to-basement rock. These clusters, however, will not be discussed here.

Site-Response Prediction Maps for a Portion of the Los Angeles Region

Response maps for the intermediate- and short-period bands for a small area approximately centered on the Los Angeles Civic Center are shown in figures 7a and 7b, which are based on the clusters discussed above and on a set of maps delineating the

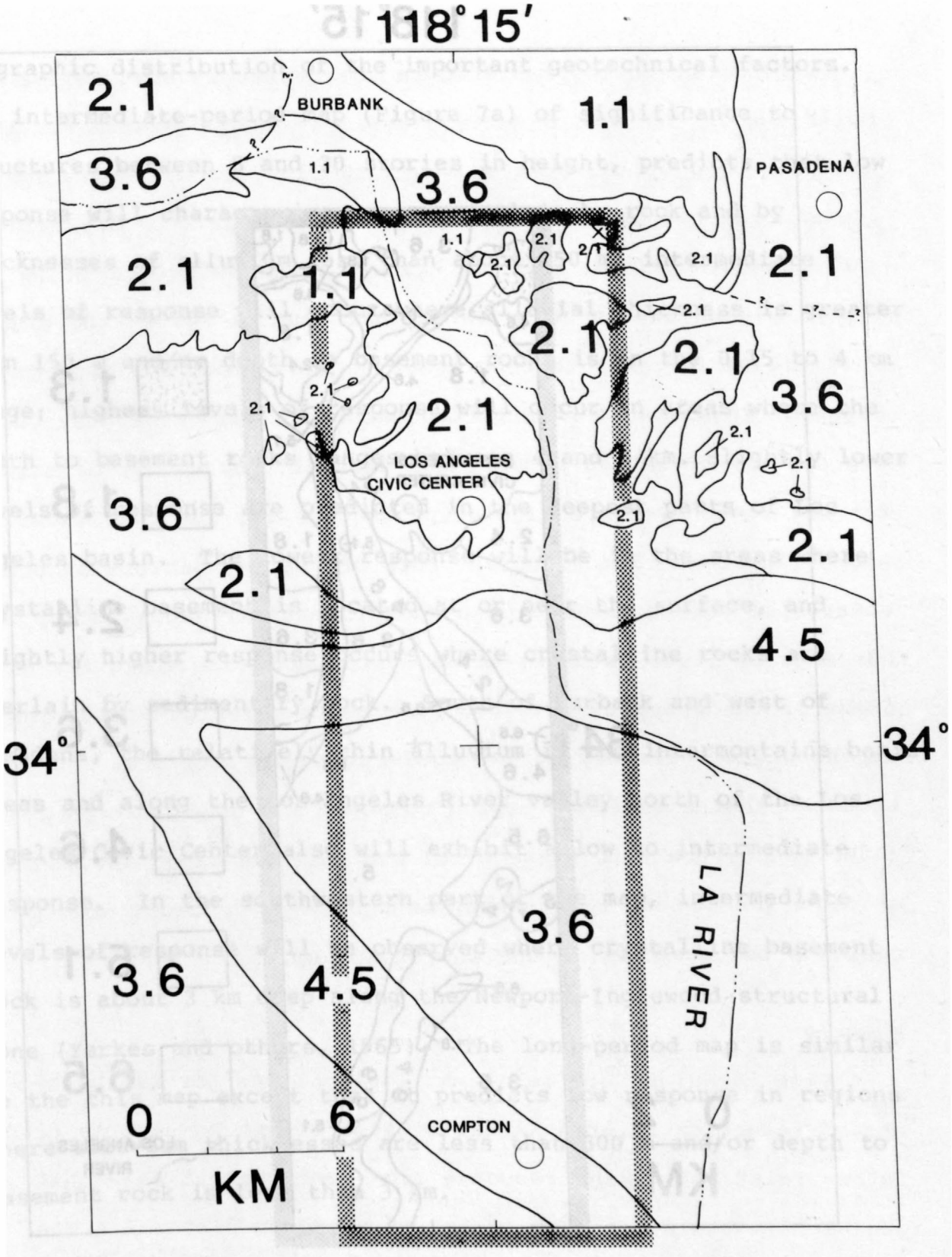

Figure 7 (a & b). Maps of predicted relative shaking response for part of the Los Angeles basin. Numbers are mean amplification factors, comparing levels of shaking to sites on crystalline basement rock.

a. Map for intermediate-periods (0.5-3.3 seconds) a band of significance to buildings 5 to 30 stories in height. Stippling outlines area of Figure 7b.

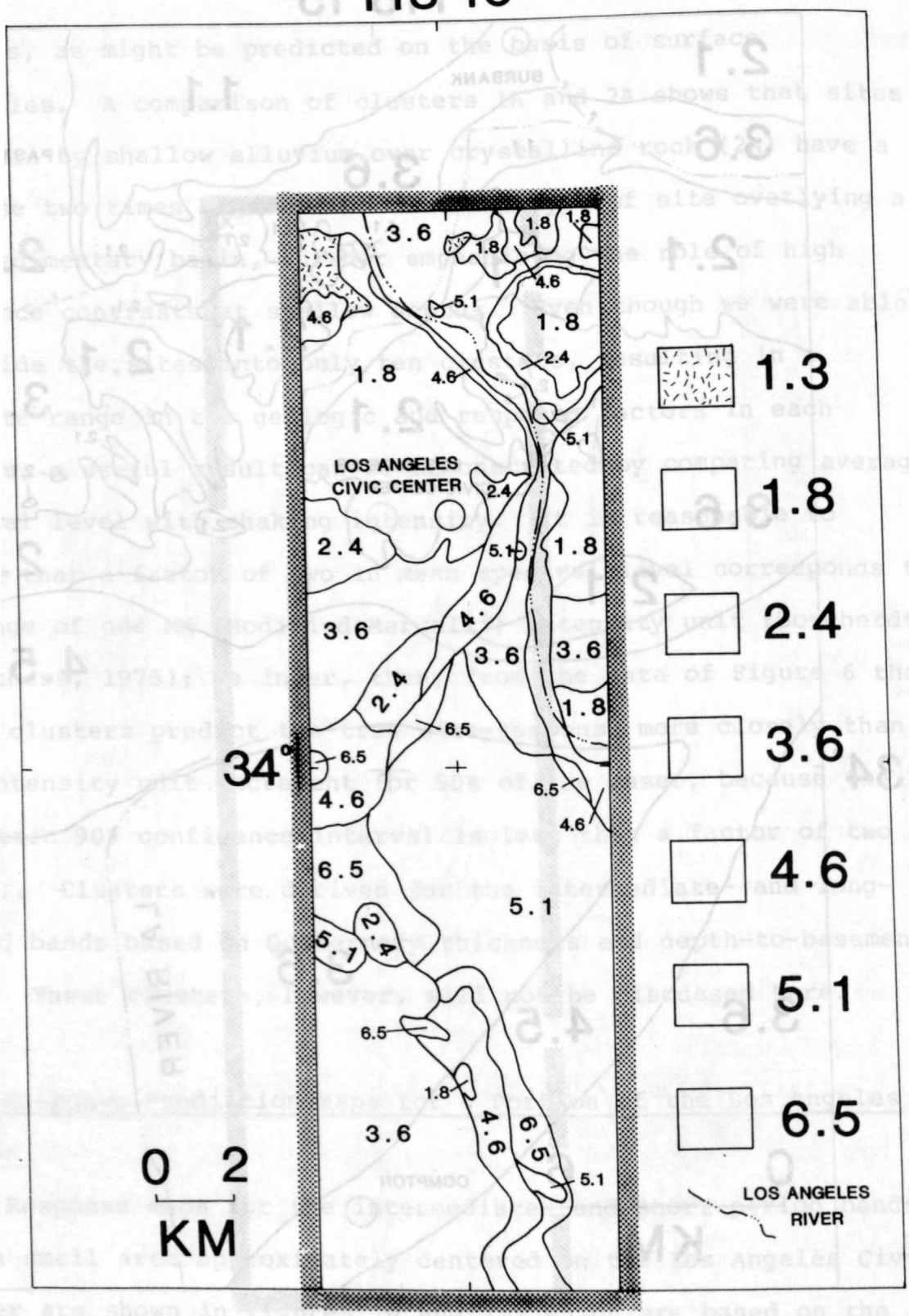

Figure 7 (a & b). Maps of predicted relative shaking response for part of the Los Angeles basin. Numbers are mean amplification factors, comparing levels of shaking to sites on crystalline basement rock.

b. Map for short-periods (0.2-0.5 seconds), a band of significance to buildings 2 to 5 stories in height.

geographic distribution of the important geotechnical factors. The intermediate-period map (Figure 7a) of significance to structures between 5 and 30 stories in height, predicts that low response will characterize areas underlain by rock and by thicknesses of alluvium less than about 150 m; intermediate levels of response will occur where alluvial thickness is greater than 150 m and/or depth to basement rocks is in the 0.15 to 4 km range; highest levels of response will occur in areas where the depth to basement rocks ranges between 4 and 6 km. Slightly lower levels of response are predicted in the deepest parts of Los Angeles basin. The lowest response will be in the areas where crystalline basement is located at or near the surface, and slightly higher response occurs where crystalline rocks are overlain by sedimentary rock. South of Burbank and west of Pasadena, the relatively thin alluvium in the intermontaine basin areas and along the Los Angeles River valley north of the Los Angeles Civic Center also will exhibit a low to intermediate response. In the southwestern part of the map, intermediate levels of response will be observed where crystalline basement rock is about 3 km deep along the Newport-Inglewood structural zone (Yerkes and others, 1965). The long-period map is similar to the this map except that it predicts low response in regions where alluvium thicknesses are less than 300 m and/or depth to basement rock is less than 3 km.

The short-period map (Figure 7b), which is most relevant to buildings in the 2 to 5 story class, has been prepared for the central third of the area shown in the long-period map. The lowest response is predicted for areas underlain by crystalline and sedimentary rock, and the highest response occurs in regions where thicknesses of near-surface alluvium (11-20 m) and high void ratios (greater than or equal to 0.7) produce significant resonant response in this period band. In some respects, this map closely resembles a surficial geologic map; thus, details of the alluviated valleys, including that of the Los Angeles River, are delineated. The southwest part of the map depicts an area where silt (characterized by high-void-ratios) deposited by the Los Angeles River thin to the west and wedge out along the east flank of the Newport-Inglewood zone where deformed Pleistocene deposits characterized by low-void-ratios are exposed. It should be noted that high short-period response may occur at sites underlain by rock, if these sites are near the crest of a ridge or other pronounced topography, as shown by the range of high response for clusters 1R and 2R (Figure 6).

Summary

This technique has important implications for earthquake-hazard reduction in urban areas because it can be used to predict future relative shaking response from geotechnical data that are ordinarily obtained in the course of urban development. The ability of this technique to provide estimates of shaking

response for period bands pertinent to structures of varied size suggest that the mapping procedure could be used for seismic zonation in many earthquake-prone urban areas, provided that the specific geologic framework of the regions being studied fit the clustering scheme developed here.

References

Algermissen, S. T., W. A. Rinehart, and J. C. Stepp (1972). A technique for seismic zoning: Economic considerations, Proc. Int'l. Conf. on Microzonation for Safer Construction, 1st, Seattle, Washington, 943-956.

Anderberg, M. R. (1973). Cluster analysis for applications, Academic Press, New York.

Borcherdt, R. D. and J. F. Gibbs (1976). Effects of local geologic conditions in the San Francisco Bay region on ground motions and the intensities of the 1906 earthquake, Bull. Seism. Soc. Am. 66, 467-500.

Borcherdt, R. D., W. B. Joyner, R. E. Warrick, and J. F. Gibbs (1975). Response of local geologic units to ground shaking, in Studies for Seismic Zonation of the San Francisco Bay Region, U.S. Geol. Surv. Prof. Paper 941A, 52-67.

Borcherdt, R. D. (1970). Effects of local geology on ground motion near San Francisco Bay, Bull. Seism. Soc. Am., 60, 29-61.

Borcherdt, R. D. and J. F. Gibbs (1976). Effects of local geologic conditions in the San Francisco Bay region on ground motions and the intensities of the 1906 earthquake, Bull. Seism. Soc. Am. 66, 467-500.

Borcherdt, R. D., W. B. Joyner, R. E. Warrick, and J. F. Gibbs (1975). Response of local geologic units to ground shaking, in Studies for Seismic Zonation of the San Francisco Bay Region, U.S. Geol. Surv. Prof. Paper 941A, 52-67.

Carte Des Sols (1964). Map of the Republique Populaire Roumaine, 1:1,000,000.

Chiaruttini, C. and L. Siro (1981). The correlation of peak ground horizontal acceleration with magnitude, distance, and seismic intensity for Friuli and Ancona, Italy, and the Alpide Belt, Bull. Seism. Soc. Am. 71, 1993-2009.

Cooley, W. W. and P. R. Lohnes (1971). Multivariate data analysis, John Wiley and Sons, New York.

Fumal, T. E., J. F. Gibbs, and E. F. Roth (1983). In-situ measurements of seismic velocity at 22 locations in the Los Angeles, California region, U.S. Geol. Surv. Open-File Report, (in press).

Gutenberg, B. (1957). Effects of ground on earthquake motion, Bull. Seism. Soc. Am. 47, 221-250.

Hanks, T. C. and R. K. McGuire (1981). The character of high-frequency strong Ground Motion, Bull. Seism. Soc. Am., 21, 2071-2095.

Hardin, B. O. and V. P. Drnevich (1972). Shear modulus and damping in soils: Measurement and parameter effects, Journal of the Soil Mechanics and Foundations Div., ASCE, 98, 603-624.

Hartigan, J. A. (1975). Clustering algorithims, John Wiley and Sons, New York.

Hays, W. W. and S. T. Algermissen (1982). Problems in the construction of a map to zone the earthquake ground shaking hazard, Third Int'l. Earthquake Microzonation Conf. Proc., Seattle, Wash., I, 145-156.

IMSL (1982). IMSL computer programs, IMSL Inc., Houston, Texas.

ISC (1977). Felt and damaging earthquakes, International Seismological Centre, Berkshire, U.K.

Joyner, W. B., R. E. Warrick, and T. E. Fumal (1981). The effect of quaternary alluvium on strong ground motion in the Coyote Lake, California Earthquake of 1979, Bull. Seism. Soc. Am., 71, 1333-1349.

Joyner, W. B. and D. M. Boore (1981). Peak horizontal accelerations and velocity from strong motion records including records from the 1979 Imperial Valley, California Earthquake, Bull. Seism. Soc. Am.II, 2011-2038.

Kanai, K. (1952). Relation between the nature of surface layer and the amplitude of earthquake motion, Tokyo, Univ. Earthquake Research Inst. Bull., 30, pt.1, 31-37.

King, K. W. (1982). A study of surface and subsurface ground motions at Calico Hills, Nevada, Test Site, U.S. Geol. Surv. Report, USGS-OFR-82-1044, 19 pp.

Medvedev, J. V. (1962). Engineering Seismology, Moscow, Academia Nauk Press, Translated into English by Israel Program for Scientific Translations, Jerusalem 1965, 260 pp.

Minakami, T. and S. Sakuma (1948). The earthquake-motions on various formations of the earth's surface (I). Observations at Koti City, Tokyo Univ. Earthquake Res. Inst. Bull, 26, 61-66.

Morrison, D. G. (1969). On the interpretation of discriminant analysis, Journal of Marketing Research, 6, 156-163.

_____(1974). Discriminant analysis, in R. Ferber, Handbook of Marketing Research, N.Y., McGraw-Hill.

Mosteller, F. and J. W. Tukey (1977). Data analysis and regression, Addison-Wesley Publ. Co. Reading, Mass., 588 pp.

Mueller, C. S., D. M. Boore, and R. L. Porcella (1982). Detailed study of site amplification at El Centro strong-motion array station No. 6, Third Int'l. Earthquake Microzonation Conf. Proc., Seattle, Wash., I, 413-424.

Murphy, J. R. and R. A. Hewlett (1975). Analysis of seismic response in the city of Las Vegas, Nevada: A preliminary microzonation, Bull. Seism. Soc. Am., 65, 1575-1597.

Murphy, J. R., N. L. Weaver, and G. B. Lamers (1970). Effects of local geology on the amplitudes of seismic waves, U.S. Atomic Energy Comm. Report NVO-1163-205, vols. I, II, and III (available from NTIS).

Nie, N. H., C. H. Hull, J. G. Jenkins, K. Steinbrenner, and D. H. Bent (1975). SPSS statistical package for the social sciences, McGraw-Hill, New York.

Ooba, S. (1957). Study of the relation between subsoil conditions and the distribution of the damage percentage of wooden dwelling houses in the province of Totomi in the case of the Tonankai earthquake of December 7, 1944, Tokyo Univ. Earthquake Res. Inst. Bull., 36, 201-295.

Rogers, A. M., R. D. Borcherdt, P. A. Covington, and D. M. Perkins (1983a). A comparative ground response study using nuclear explosions and the 1971 San Fernando earthquake (in preparation).

Rogers, A. M., J. C. Tinsley, and R. D. Borcherdt (1983b). Predicting relative shaking response from local geologic factors (in prep.), U.S. Geol. Surv. Prof. Paper.

Rogers, A. M., P. A. Covington, R. B. Park, R. D. Borcherdt, and D. M. Perkins (1980). Nuclear event time histories and computed site transfer functions for locations in the Los Angeles region, U.S. Geol. Surv. Open-File Report 80-1173, 207 pp.

Rogers, A. M. and W. W. Hays (1978). Preliminary evaluation of site transfer functions developed from earthquake and nuclear explosions, Proc. Second Int'l. Conf. Microzonation, San Francisco, Calif., 2, 753-764.

Seed, H. B. and I. M. Idriss (1970). Soil moduli and damping factors for dynamic response analysis, Univ. Calif., Berkeley, Report EERC 70-10, 15 pp.

Seed, H. B., R. V. Whitman, H. Dezfulian, R. Dorey, and I. M. Idriss (1972). Soil conditions and building damage in 1967 Caracas earthquake, J. Soil Mech. and Found. Div., ASCE, 98, 787-806.

Skinner, R. I. (1977). Romanian earthquake March 1977, Summary report on a study of earthquake damage in Bucharest, Romania, 4th March 1977, Bull. N.Z. Natn. Soc. Eq. Eng., 10, 106-108.

Turner, E. and K. H. Stokoe (1982). Static and dynamic properties of clayey soils subjected to 1979 Imperial Valley earthquake, Geotech. Eng. Report GR82-26, Geotech. Eng. Center, Univ. of Texas, Austin, 208 pp.

Velleman, P. and D. Hoaglin (1981). ABC's of EDA, Duxbury Press.

Wood, H. D. (1983). Preliminary report on the Long Beach earthquake, Bull. Seism. Soc. Am. 23, 42-56.

Yerkes, R. F., T. H. McCulloh, J. E. Schcellhamer, and J. G. Vedder (1965). Geology of the Los Angeles Basin, California--An Introduction, U.S. Geological Survey Professional Paper 420-A, 57 pp.

A PRACTITIONER'S VIEW OF SITE EFFECTS ON STRONG GROUND MOTION

by

Neville Donovan
Dames & Moore
San Francisco, California

INTRODUCTION

The perspective of a practicing engineer towards the effects of different site conditions on the characteristics of ground motion is different from others engaged primarily in research. Where those in research are primarily engaged in examination of specific aspects of individual events, the practicing engineer involved in earthquake engineering is concerned with attempts to characterize possible future events as they may affect the hazard exposure for a site where engineered construction is planned. This viewpoint encourages a more intense interest in the general characteristics of earthquakes that show similar effects consistently rather than a specific event characteristics such as the demonstrated directivity of the Livermore earthquakes of January 1980. The future threat to most sites could come from many directions so special effect considerations have only limited application.

One approach for this workshop might be to first examine some of the areas where there seems to be agreement and how this agreement can be used before contemplating new areas of research. The following compares the development of how site effects have

been considered in attenuation relationships by various researchers and practitioners, and proposes relationships for site dependent v/a ratios. A straightforward method by which site effects can be included in design response spectra is also presented.

ATTENUATION OF GROUND MOTION

Attenuation of ground motion is considered to be a topic with continuing diverse views. A more careful examination shows that this is not so. Two distinct changes have occurred following the increased data base that followed the 1979 and 1980 California earthquakes. The divergence of results among different investigators is becoming smaller and the reaction whereby higher values are urged after each event is also being stilled. The ability of recently developed attenuation equations to estimate the values obtained during the Coalinga earthquake within reasonable error bounds confirms that a consensus is being reached with respect to the attenuation of peak acceleration values measured in moderately strong earthquakes.

If we consider the example source to site configuration on Figure 1 which was first used by Idriss (1978), the consensus of values which would be obtained today would not be the same as Idriss obtained in 1978. The values he gave for Site A (which emphasizes differences in the near-field interpretation) ranged from 0.4g to 0.56g after the lowest and highest values had been discarded; more recent equations (Campbell, 1981, Joyner and

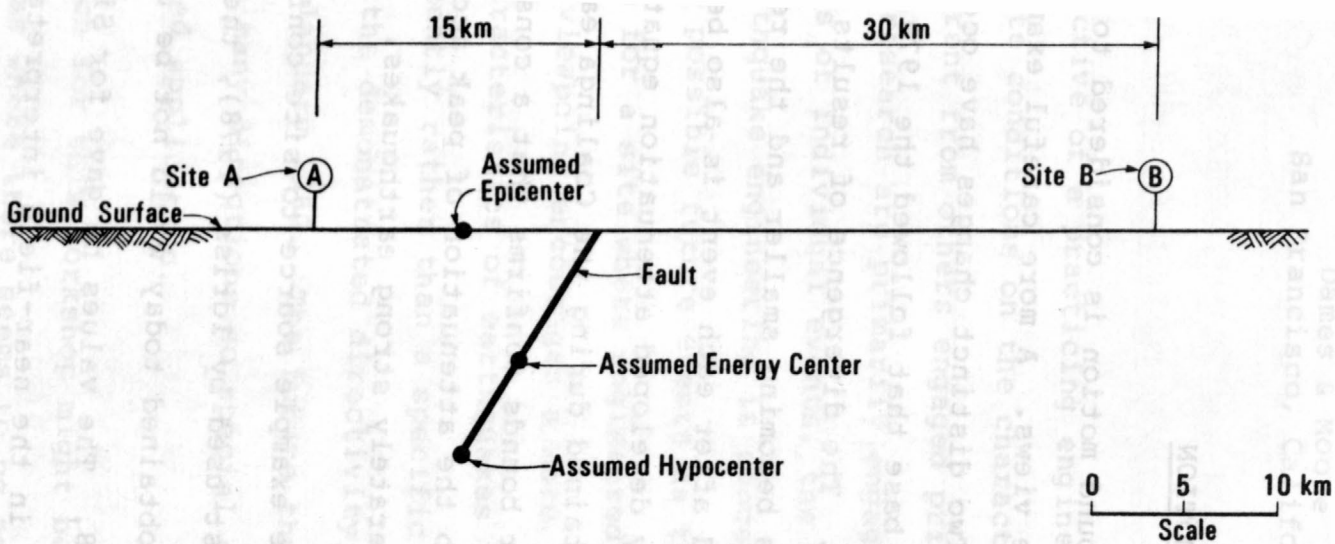

Fig. 1. LOCATION OF SITES AND CONFIGURATION OF ASSUMED SOURCE after Idriss (1978)

Boore, 1982, Bolt and Abrahamson, 1982 and Idriss, 1983) range between 0.19g and 0.33g. (The lowest value considered in the 1978 Idriss study (Donovan and Bornstein, 1975) fell substantially below the range of other investigations at 0.26g and was therefore discounted. It is interesting to note that the recent equations envelop the "low" value very nicely.) For Site B the recent equations give values between 0.09g and 0.14g compared with values between 0.12g and 0.18g given by Idriss.

The Coalinga earthquake provided an additional set of data points, shown together with the recent attenuation curves on Figure 2. The comparison is quite favorable. Because the Coalinga event had no surface rupture, the source-to-site distances used are the horizontal distances to the edge of the aftershock area using a preliminary plot of aftershock locations. The two shaded zones on Figure 2 represent the zone within which 50 percent of the data values would be expected to lie if their scatter followed a lognormal distribution with deviations of either 0.35 (Idriss, 1983) or 0.64 (Joyner and Boore, 1982) about the mean of each of the 4 attenuation equations. For the Coalinga earthquake the smaller error term is sufficient to contain close to 50 percent of the Coalinga data points, but the bounds represented by the larger error term contain more than 70 percent of the data points. It would appear from this result that the error term applied to intermediate magnitude earthquakes may be too large.

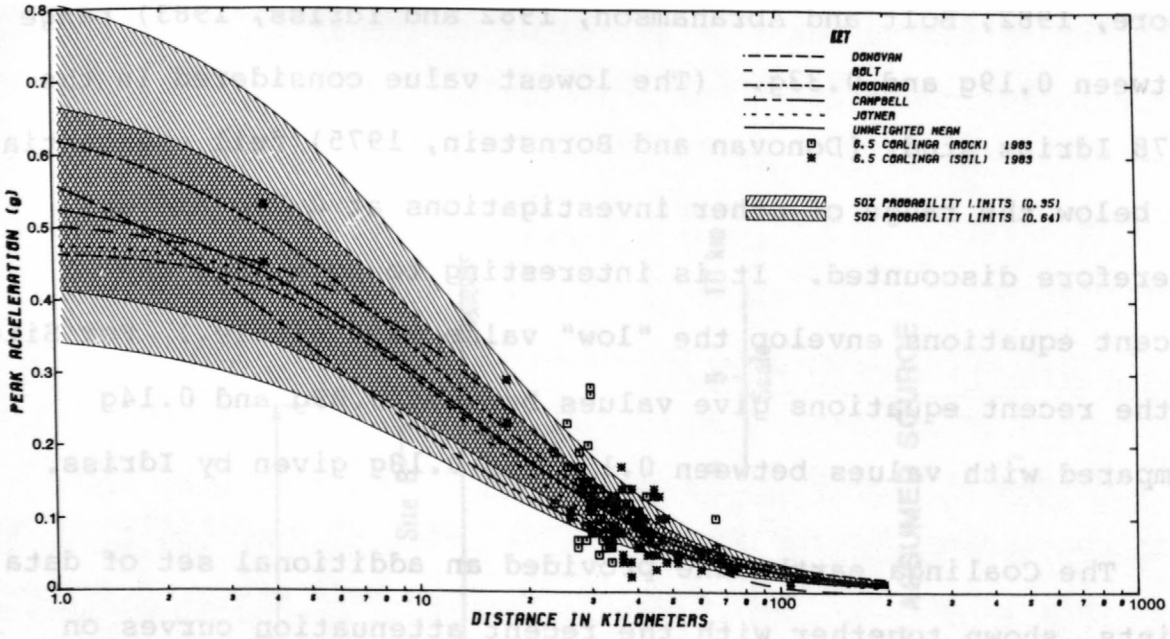

Figure 2. Acceleration attenuation relationships for magnitude 6.5 event compared with data recorded during the May 2, 1983 Coalinga earthquake.

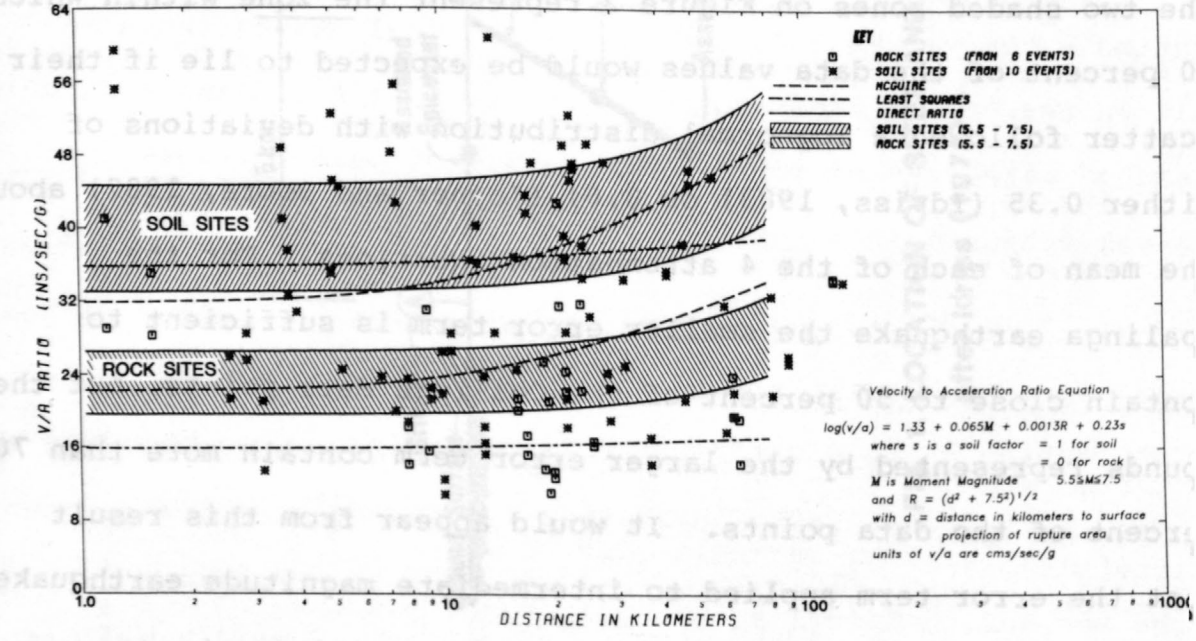

Figure 3. Measured velocity/acceleration (V/A) ratios and derived V/A equations. Shaded areas show range of values obtained using equation for rock and soil sites.

For design purposes an agreement on a peak acceleration value is but one step in the approach to the selection of suitable ground motions. Other parameters such as duration, velocity and the spectral content must be considered. Attenuation equations for velocity have been proposed but the data base for these has been much smaller than for studies of acceleration. Deriving attenuation equations for spectral parameters directly has also been attempted (Joyner and Boore, 1982). At the present time a more direct approach to estimation of design spectra is believed to be preferable. Joyner and Boore in their spectral studies showed that the NRC recommended spectra, based on Newmark, Blume and Kapur (1973), had major shortcomings. The Joyner and Boore studies did show, however, that if the acceleration and velocity values upon which the spectra are based were carefully chosen the Hall, et al. (1976) criteria for constructing a response spectrum can give excellent results.

VELOCITY TO ACCELERATION RATIO

The velocity to acceleration ratio (v/a) has been widely used by those responsible for developing design spectra. In contrast, little attention has been given to the effect of both event magnitude and distance on this parameter. Where distance effects have been treated equally in developing an attenuation equation, it is possible to obtain a magnitude and distance dependent v/a relationship in equation form by dividing the velocity attenuation equation by the acceleration attenuation equation. The results of two relationships obtained in this way

are shown on Figure 3. McGuire's (1978) relationships were used together with velocity and acceleration equations derived using an expansion of the Joyner and Boore data set (Donovan, 1982) to produce the two relationships. Also shown on Figure 3 are the measured v/a ratios for rock and soil sites. An equation relating distance and magnitude to the measured v/a ratios was obtained directly using the same equation fitting process followed by Joyner and Boore. While the scatter in the v/a ratio value is considerable, the end results confirm a strong site dependent relationship. The shaded areas on Figure 3 represent the range between magnitudes 5.5 and 7.5 for soil sites and rock sites. Magnitude appears to have a larger effect on the ratio than distance. These effects have been expected. Of more concern is the introduction of errors by the use of spectral construction procedures which have not considered these effects.

SITE DEPENDENT RESPONSE SPECTRA

Joyner and Boore (1982) capably demonstrated the inapplicability of the NRC response spectra for all but a narrow range of conditions. Of the various methods for preparing design response spectra which have met with a favorable reception by the design profession, none have considered the effect of distance and magnitude on the spectral design parameters (Newmark and Hall, 1969, Mohraz, 1976, Seed et al., 1976). It is imperative that these efficient ways of constructing design response spectra be made capable of considering the differences associated with event size and distance and the local site conditions. The results of

direct spectral regression by Joyner and Boore are one attempt in this direction. The control of their results in areas where the equations must be extrapolated is difficult, however.

An alternative approach is suggested here, consisting of three distinct steps. The first is to estimate the mean peak acceleration using a choice of attenuation relationships such as those referenced earlier and shown graphically in Figure 2. The second step is to compute the v/a ratio for the appropriate site conditions and the event characteristics using the relationship for v/a shown on Figure 3. The final step is to compute the response spectra using the construction procedure described by Hall et al. (1976) and spectral amplification factors given by Newmark and Hall (1982) with the one exception that the ground velocity value be maintained compatible with the v/a ratio computed in the second step. Figures 4 and 5 demonstrate examples of response spectra developed in this way. The events are assumed to be of magnitude 5.5, 6.5 and 7.5 at distances of 0, 10, 20 and 40 kilometers in all figures. Figure 4 is for a rock site and Figure 5 is for a site with a considerable soil profile. In addition to the familiar spectra shapes drawn using the Newmark-Hall construction procedure, each figure shows additional curves from Joyner and Boore (1982). These two curves are based on regression of the average response of the two components.

Magnitude has a strong effect on the response spectra shapes shown in Figures 4 and 5. This should serve as a cautionary

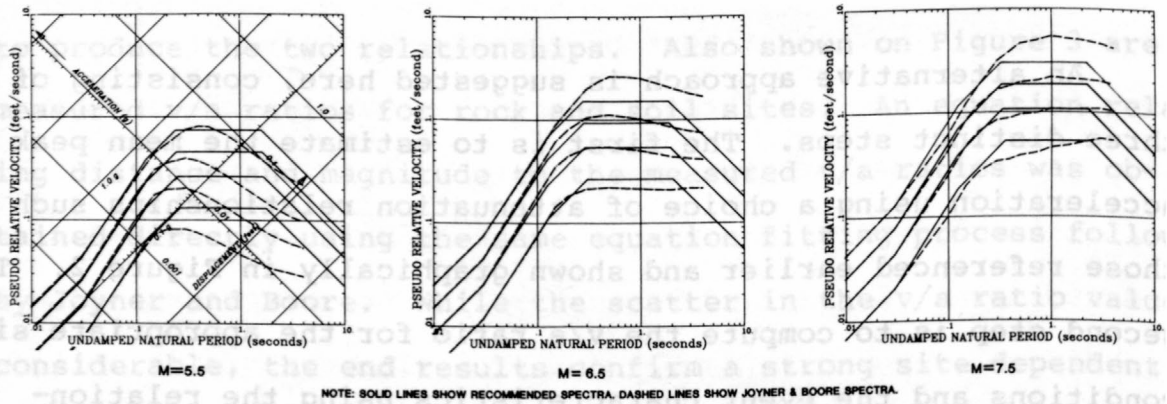

Figure 4. Comparison of recommended spectra construction with Joyner-Boore response spectra. All spectra are 50th percentile values for a damping of 5 percent. Values at each magnitude level are for distances at 0, 10, 20 and 4 kilometers.

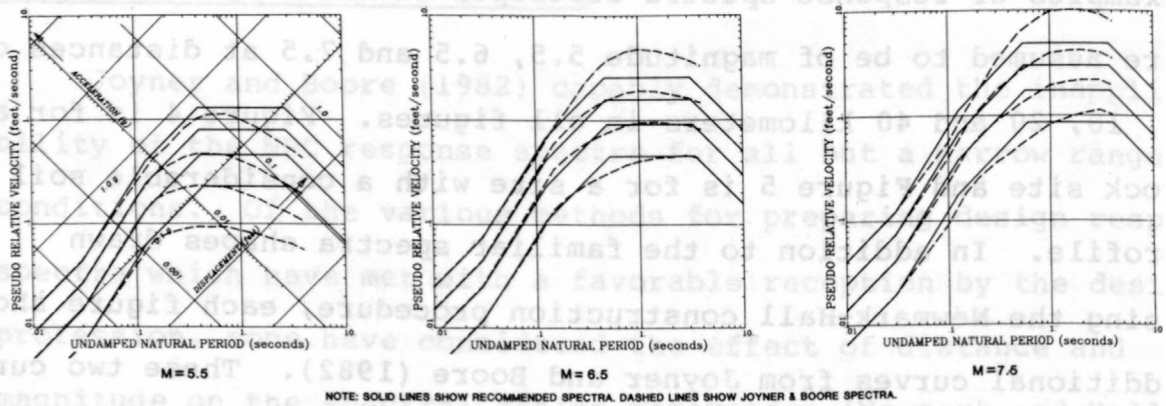

Figure 5. Comparison of recommended spectra construction with Joyner-Boore response spectra. All spectra are 50th percentile values for a damping of 5 percent. Values at each magnitude level are for distances at 0, 10, 20 and 40 kilometers.

warning that ground motion recorded at low strain amplitudes should not be linearly extrapolated to other ground motion levels.

It has been suggested that the ground acceleration and velocity values could be considered separately rather than by the use of a v/a ratio. This is not recommended here for two related reasons. The recommended procedure is a step by step operation which can be easily followed and, because the necessary parameters are not derived independently, is less susceptible to possible misuse. It can be readily seen that the simple modification to an already familiar procedure allows a very effective representation of site effects.

CONCLUSIONS

A straightforward procedure has been demonstrated for the development of design response spectra. The procedure is based on the widely familiar Newmark-Hall response spectra construction with the incorporation of a velocity to acceleration ratio based on direct strong motion data with consideration of site effects, distance from the source and the event magnitude.

The strong motion data base is dominated by data from moderate sized earthquakes ($6.0 \leq M \leq 6.7$) recorded at distances of between 20 and 50 kilometers. The comparisons of attenuation equations on Figure 2 show closest agreement in the intermediate distances and the response spectra comparisons on Figures 4 and 5 are closest for magnitude 6.5. The divergence of values at

other magnitudes and distances results from extrapolation to and beyond the data base and all values should be used with care. Additional research using near field data perhaps augmented by theoretical studies is sorely needed at this time.

LIST OF REFERENCES

Bolt, B.A. and N.A. Abrahamson (1982), "New Attenuation Relations for Peak and Expected Accelerations of Strong Ground Motion," Bulletin of the Seismological Society of America, Volume 72, Number 6 (Part A), pp. 2307-2322, December.

Campbell, K.W. (1981), "Near-Source Attenuation of Peak Horizontal Acceleration," Bulletin of the Seismological Society of America. Vol. 71, No. 6, December, pp. 2039-2070.

Donovan, N.C. and A.M. Becker (1983), "Some Aspects of Seismic Hazard Studies in Western Canada," Fourth Canadian Conference on Earthquake Engineering, Vancouver, June 15-17, pp. 19-29.

Donovan, N.C. and A.E. Bornstein (1975), "A Review of Seismic Risk Applications," Second International Conference on Applications of Statistics and Probability in Soil and Structural Engineering, Aachen, Sept., Vol. III, pp. 287-300.

Donovan, N.C. and A.E. Bornstein (1978), "Uncertainties in Seismic Risk Procedures," Journal of the Geotechnical Engineering Division, ASCE, Vol. 104, No. GT7, Paper 13896, pp. 869-887.

Donovan, N. C. (1982), "Attenuation of Vertical Acceleration and a Review of Attenuation Equation Processes," U.S.G.S. Workshop on Near Field Seismology, Lake Tahoe, Nevada, October 21-23, 1981, Open File Report 82-591, pp. 185-202.

Hall, W.J., B. Mohraz and N.M. Newmark (1976), "Statistical Studies of Vertical and Horizontal Earthquake Spectra," prepared for the United States Nuclear Regulatory Commission, NUREG-003, January.

Idriss, I.M. (1978), "Characteristics of Earthquake Ground Motions," Proceedings of ASCE Geotechnical Engineering Division Specialty Conference on Earthquake Engineering and Soil Dynamics, Pasadena, California, June 19-21, Volume III, pp. 1151-1266.

Idriss, I.M. (1983), "Site Response and Design Ground Motions," notes prepared for EERI Annual Meeting Seminar, Reno, Nevada, February 10, 1983.

Joyner, W.B. and D.M. Boore (1982), "Prediction of Earthquake Response Spectra," Proceedings of the 51st Annual Convention of the Structural Engineers Association of California, October 1982.

McGuire, R.K. (1978), "Seismic Ground Motion Parameter Relations," Proceedings of the Geotechnical Engineering Division, A.S.C.E., Vol. 104, No. GT4, April, pp. 481-492.

Mohraz, B. (1976), "A Study of Earthquake Response Spectra for Different Geological Conditions," Bulletin of the Seismological Society of America, Vol. 66, No. 3, pp. 915-935.

Newmark, N.M., J.A. Blume and K.K. Kapur (1973), "Seismic Design Spectra for Nuclear Power Plants," Journal of Power Division, ASCE, Vol. 99, 902.

Newmark, N.M. and W.J. Hall (1969), "Seismic Design Criteria for Nuclear Reactor Facilities," Proceedings of the Fourth World Conference on Earthquake Engineering, Santiago, Chile, Volume II, pp. B4 37-50.

Newmark, N.M. and W.J. Hall (1982), "Earthquake Spectra and Design," Earthquake Engineering Research Institute Monograph Series, M.S. Agbabian, editor.

Seed, H.B., C. Ugas and J. Lysmer (1976), "Site Dependent Spectra for Earthquake-Resistant Design," Bulletin of the Seismological Society of America, Vol. 66, No. 1, February, pp. 221-244.

SITE EFFECTS ON STRONG GROUND MOTION OBSERVED FROM UNDERGROUND NUCLEAR EXPLOSIONS

by

John R. Murphy

S-CUBED

Reston Geophysics Office

11800 Sunrise Valley Drive

Reston, Virginia 22091

INTRODUCTION

It has long been recognized that the near-surface geologic conditions at a recording site can have a significant effect on the amplitude level and spectral composition of the ground motions recorded at that site. However, because earthquake strong motion instrumentation is not generally deployed with the purpose of studying these effects, it has proven to be difficult to perform detailed empirical studies using the few available earthquake observations. On the other hand, the ongoing underground testing program at the Nevada Test Site (NTS) provides a unique opportunity to document ground motion variability in that it provides a relatively repeatable and predictable source of strong ground motion which can be monitored using seismic networks specifically deployed for that purpose. In particular, it offers the opportunity to design experimental tests of various hypotheses concerning the effects of the propagation path and local site geology on recorded ground motion. A number of such experiments have been conducted at NTS over the past 20 years

and the objective of this paper is to provide a brief overview of some of the results of these studies which appear to be pertinent to the evaluation of site-specific effects on ground motion.

EMPIRICAL EVIDENCE OF SITE EFFECTS FROM NTS EXPERIENCE

A number of examples illustrating the effects of local site geology on observed ground motion have been carefully documented using both body and surface waves recorded at near-regional distances from NTS explosions. For example, one of the best illustrations of the effects of low-velocity surface layers on body waves is provided by the recordings at a pair of adjacent stations in Tonopah, Nevada, located about 100 km northwest of NTS. Although these two instrument locations are separated by less than 200 m, one (Tonopah Church) is situated on hardrock, while the other (Tonopah Motel) has been placed on a thin layer of fill overlying the same hardrock base. As a result, they consistently record very different ground motions. This is illustrated in Figure 1 which shows comparisons of the particle velocity time histories and response spectra for a particular explosion recorded at these two sites. The ratio of the alluvium to the hardrock spectrum is shown at the bottom of this figure and demonstrates that the site effect is frequency dependent and produces a magnification of the spectral amplitude level at the fill site which is as much as a factor of six for frequencies near 7.0 Hz. These observations have been repeated for a large number of NTS explosions and it has been found that this frequency dependent amplification effect is quite consistent for

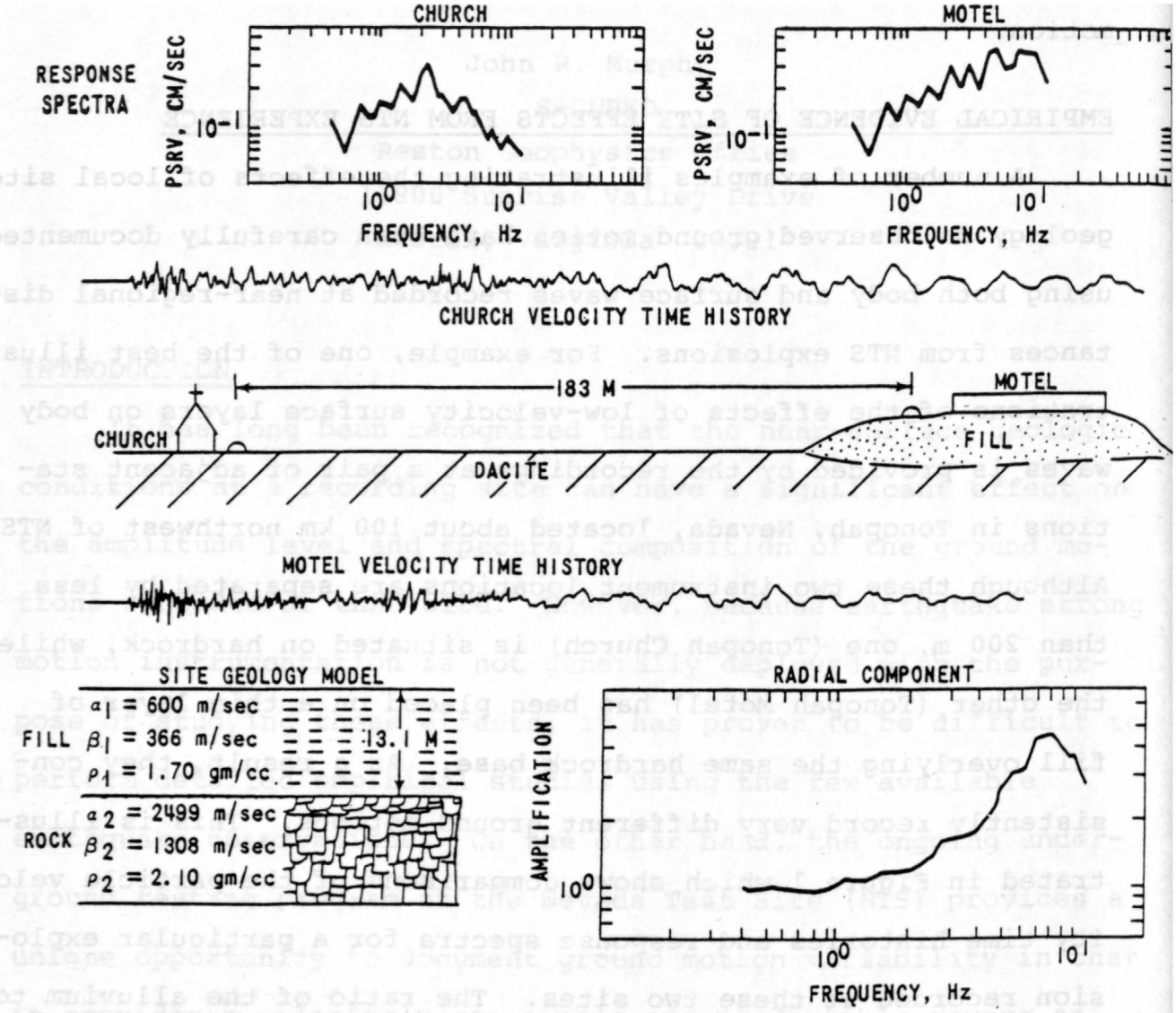

Figure 1. An Example of the Frequency Dependent Effect of Local Site Geology on Ground Motion, Tonopah, Nevada.

input motions corresponding to peak accelerations in the 10^{-5} to 10^{-2} g range. In addition, some earthquake data have also been simultaneously recorded at these two stations and it has been found that they provide evidence of the local site effect which is entirely consistent with that inferred from the explosion data. For example, Figure 2 shows a comparison of the alluvium/hardrock spectral ratio computed from data recorded from the southern Nevada Massachusetts Mountain earthquake (8/5/71) with the average spectral ratio determined from a large sample of explosion data. It can be seen that the observed earthquake spectral ratio quite consistently falls within the $\pm$ 1 σ bounds on the explosion mean, indicating that the site effect on the response spectrum is essentially independent of source type. That is, the site effect on earthquake recordings can be reliably inferred from explosion data, at least in this case.

Another example representative of stronger motion excitation is presented in Figure 3, which shows the spectral ratios computed from recordings made at an adjacent alluvium/hardrock pair of stations located on NTS, at a distance of only 17 km from the explosion source. The solid lines on this figure show the spectral ratios computed from the ground motions observed from two different explosions and provide a measure of the consistency of the local site effect. The dotted lines correspond to the theoretical spectral ratios computed using a simple, linear elastic model of the site response to incident S waves. It can be seen that the simple linear model provides a reasonable description of the observed data in this case, even though the

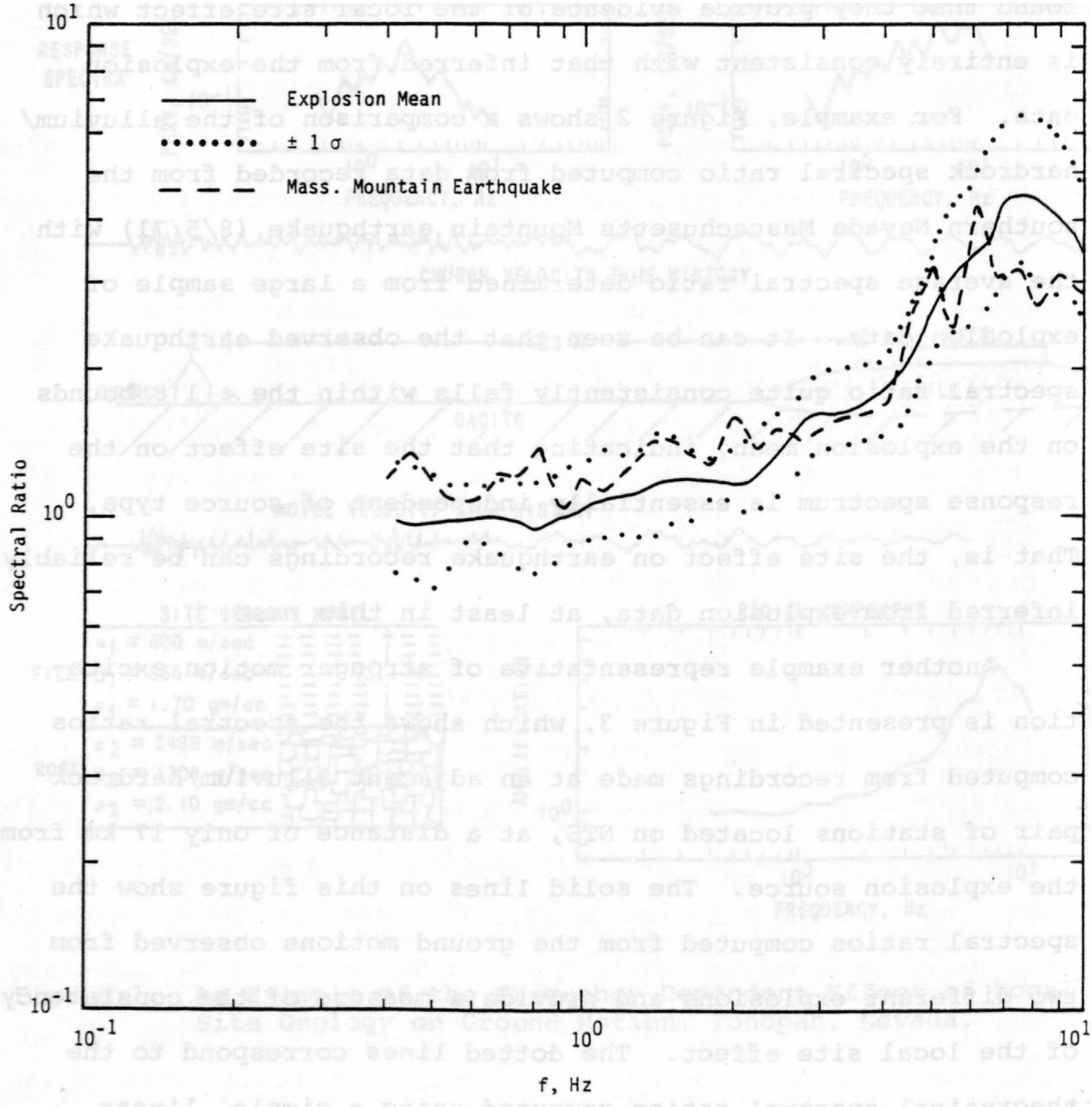

Figure 2. Comparison of Alluvium/Hardrock (Tonopah Motel/Tonopah Church) Spectral Ratio Computed From Massachusetts Mountain Earthquake Data With the Mean Spectral Ratio Determined From a Large Sample of Explosion Data. The Dotted Lines Indicate the ± 1 σ Bounds on the Explosion Mean.

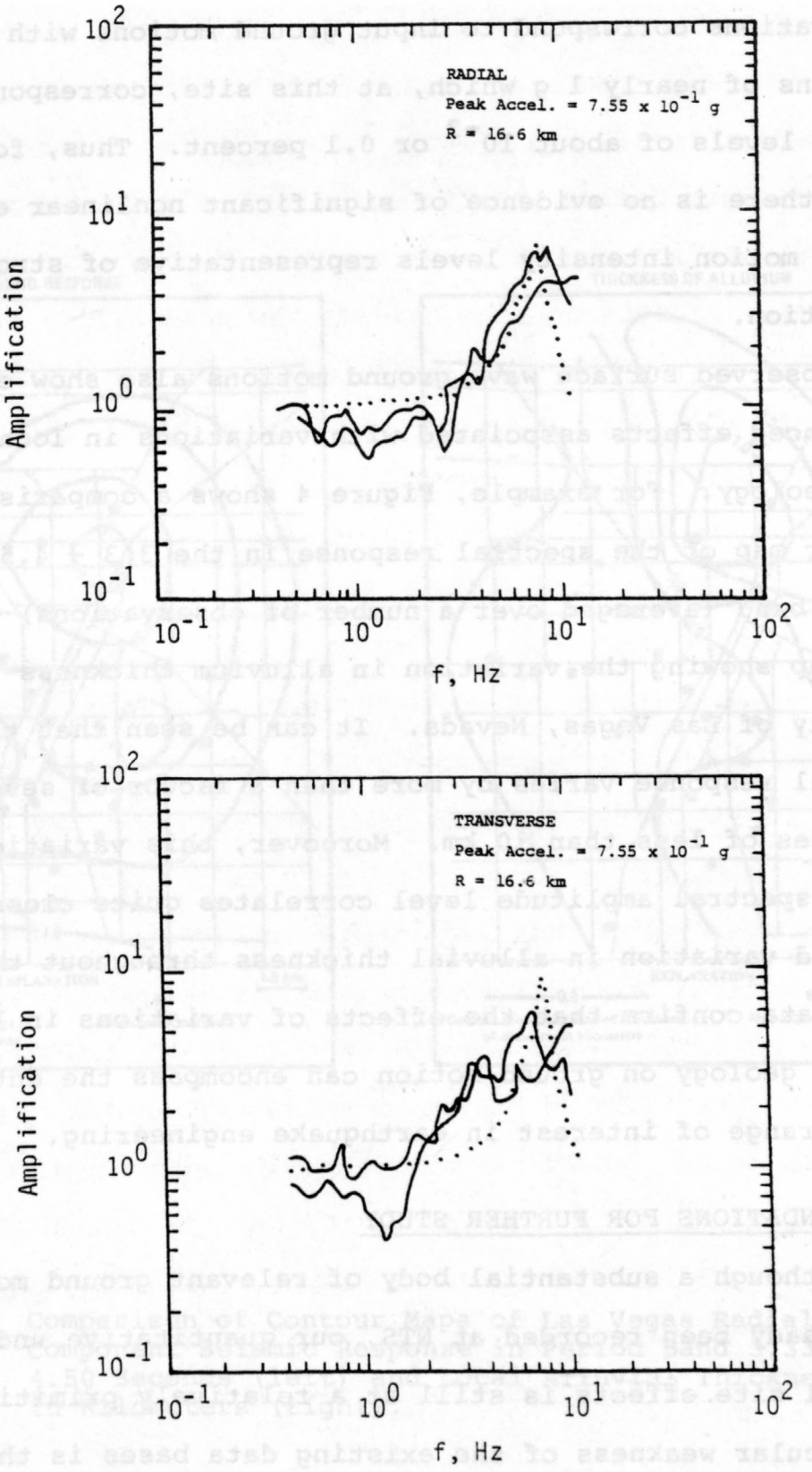

Figure 3. Comparison of Linear Theoretical (dotted) Alluvium/Hardrock Spectral Ratios With Observed Spectral Ratios (solid) Computed From Strong Motion (~ 1 g) Recordings.

observations correspond to input ground motions with peak accelerations of nearly 1 g which, at this site, correspond to peak strain levels of about 10^{-3} or 0.1 percent. Thus, for this soil type, there is no evidence of significant nonlinear effects at ground motion intensity levels representative of strong motion excitation.

Observed surface wave ground motions also show evidence of pronounced effects associated with variations in local subsurface geology. For example, Figure 4 shows a comparison of a contour map of the spectral response in the 3.3 - 4.5 second period band (averaged over a number of observations) with a contour map showing the variation in alluvium thickness throughout the city of Las Vegas, Nevada. It can be seen that the observed spectral response varies by more than a factor of seven over distances of less than 10 km. Moreover, this variation in ground motion spectral amplitude level correlates quite closely with the inferred variation in alluvial thickness throughout the city. These data confirm that the effects of variations in local subsurface geology on ground motion can encompass the entire frequency range of interest in earthquake engineering.

RECOMMENDATIONS FOR FURTHER STUDY

Although a substantial body of relevant ground motion data has already been recorded at NTS, our quantitative understanding of local site effects is still at a relatively primitive level. A particular weakness of the existing data bases is that few direct measures of the physical properties of the near-surface materials are available and, consequently, uncertainty remains

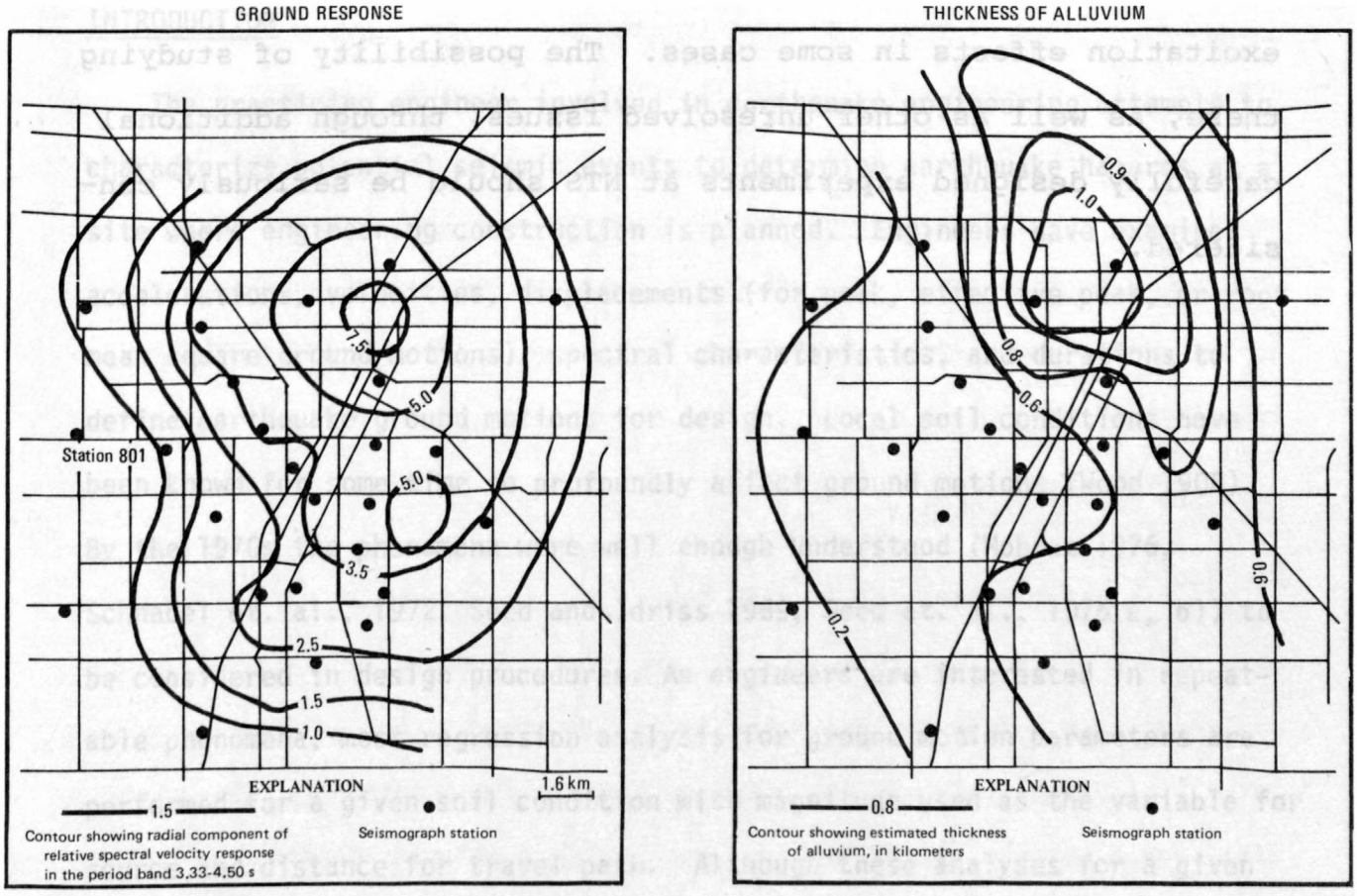

Figure 4. Comparison of Contour Maps of Las Vegas Radial Component Seismic Response in Period Band 3.33 - 4.50 Seconds (left) and Local Alluvial Thickness in Kilometers (right).

concerning the actual predictive capability of various simplified theoretical models which appear to fit the data. On a more fundamental level, the effects of realistic, three-dimensional incident wave fields on site response has received little attention to date and may be important in defining strong motion excitation effects in some cases. The possibility of studying these, as well as other unresolved issues, through additional carefully designed experiments at NTS should be seriously considered.

CAUSES OF VARIATION IN STRONG GROUND MOTION IN THE NEAR-FIELD FOR A GIVEN SOIL CONDITION

by

J. P. Singh
Harding Lawson Associates
Novato, California

INTRODUCTION

The practicing engineer involved in earthquake engineering attempts to characterize potential seismic events to determine earthquake hazards at a site where engineering construction is planned. Engineers have examined accelerations, velocities, displacements (for peak, effective peak, or root mean square ground motions), spectral characteristics, and durations to define earthquake ground motions for design. Local soil conditions have been known for some time to profoundly affect ground motions (Wood 1908). By the 1970s the phenomena were well enough understood (Mohraz 1976, Schnabel et. al., 1972, Seed and Idriss 1969, Seed et. al., 1976 a, b)) to be considered in design procedures. As engineers are interested in repeatable phenomena, most regression analysis for ground motion parameters are performed for a given soil condition with magnitude used as the variable for source and distance for travel path. Although these analyses for a given seismic region such as Japan or the western United States result in a reasonable average, there is large scatter in the data. Recent studies (Idriss 1978, Nuttli 1981, Singh 1981, Singh 1982 a, b) that address the generic strong ground motion problem have recognized that the basic characteristics of strong ground motions are significantly influenced by the source and travel path characteristics and modified by the local soil conditions.

Studies conducted as early as 1955 postulated that for near-fault sites, the direction in which an earthquake source propagates (directivity) has a strong influence on the maximum amplitude of ground shaking at a given site. Not until the late 1970s, however, was the strong ground motion problem studied extensively. The purpose of this paper is to 1) address the impact on ground motions of moving sources (source directivity) and geological conditions along the major faults (fault seams); 2) develop a better understanding of how these factors may impact ground motions of interest to engineering and structural design; and 3) recommend areas of further research. The interpretation of strong motion records obtained during two California earthquakes, i.e., 1940 El Centro and 1979 Imperial Valley, are used for illustration.

OVERVIEW OF THE PROBLEM

A stationary seismic fault slip source can be modeled as a double couple at a point. It follows that there is an azimuthal radiation pattern in wave amplitude even before rupture velocity is introduced. For a simple right lateral strike slip fault, for example, the radiation pattern in the near-field for S waves will involve four lobes with a maximum amplitude occurring in the direction of the fault and at right angles to it. In real earthquakes, a rupturing fault relates to the progression of the dislocation along the fault, i.e., a moving source. The moving source introduces effects on the generated seismic waves and produces deformations of the

radiation lobes with asymetrical effects in front of and behind the moving dislocation (see Figure 1). Brune (1978) states, "The concept of focusing or directivity is important in strong motion seismology because in addition to the effect of radiation pattern, it can introduce large azimuthal variation in ground motion."

The terms "directivity" and "focusing" are synonymous in Brune's usage. As used in this paper, the terms have the following definitions. Wave focusing means the concentration of wave energy by variations in the refraction indices of the transmitting media, as in focusing of light by an optical lens or focusing of P- and S-waves by changes in elastic moduli at structural boundaries. Directivity or source directivity describes the azimuthal change in wave energy around the source due to moving rupture. This azimuthal dependence is a function of the direction and speed of rupture and hence is defined as a directivity effect.

Strong azimuthal patterns in seismic wave radiation have been observed instrumentally both locally and teleseismically for many years. The first strong evidence for the effect of a moving source in seismology was discussed by Benioff (1955) in his explanation of the intensity patterns observed in the 1952 Kern County, California, earthquake. He argued that the moving source (propagation of dislocation along the fault) would cause different signals to be received at opposite ends of the fault, with larger intensities of higher frequency in the direction of propagation and smaller intensities and lower frequencies at the opposite end. The kinematics or geometrical effects in the case of a source moving along a straight line are

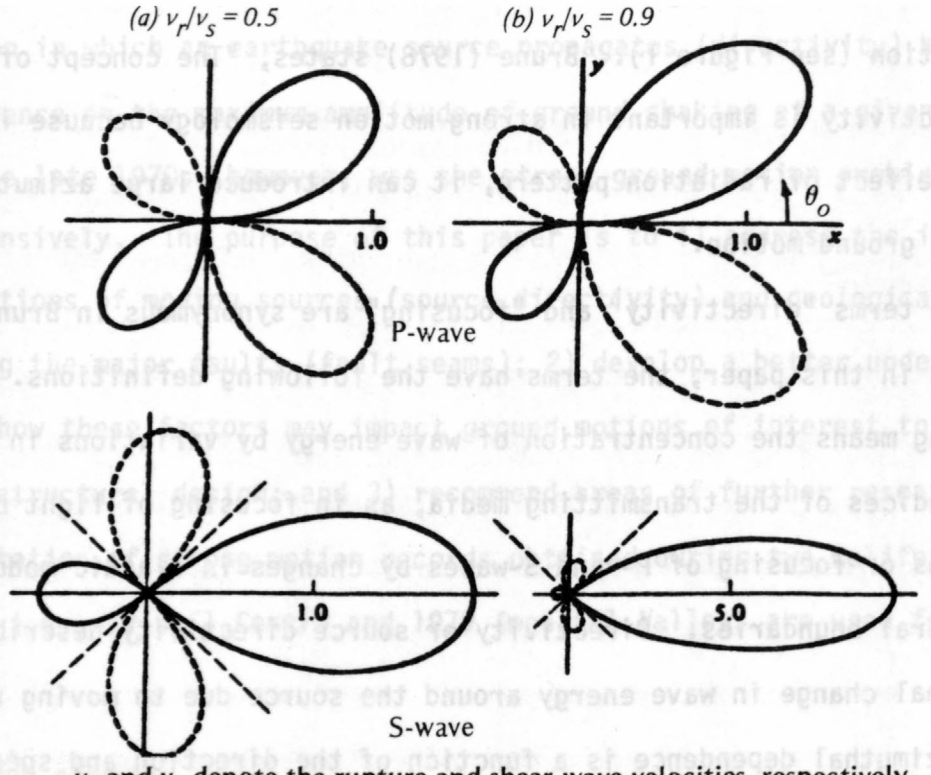

v_r and v_s denote the rupture and shear wave velocities, respectively.

Figure 1 Radiation patterns of the P-waves and S-waves from sources with unilateral rupture propagation :

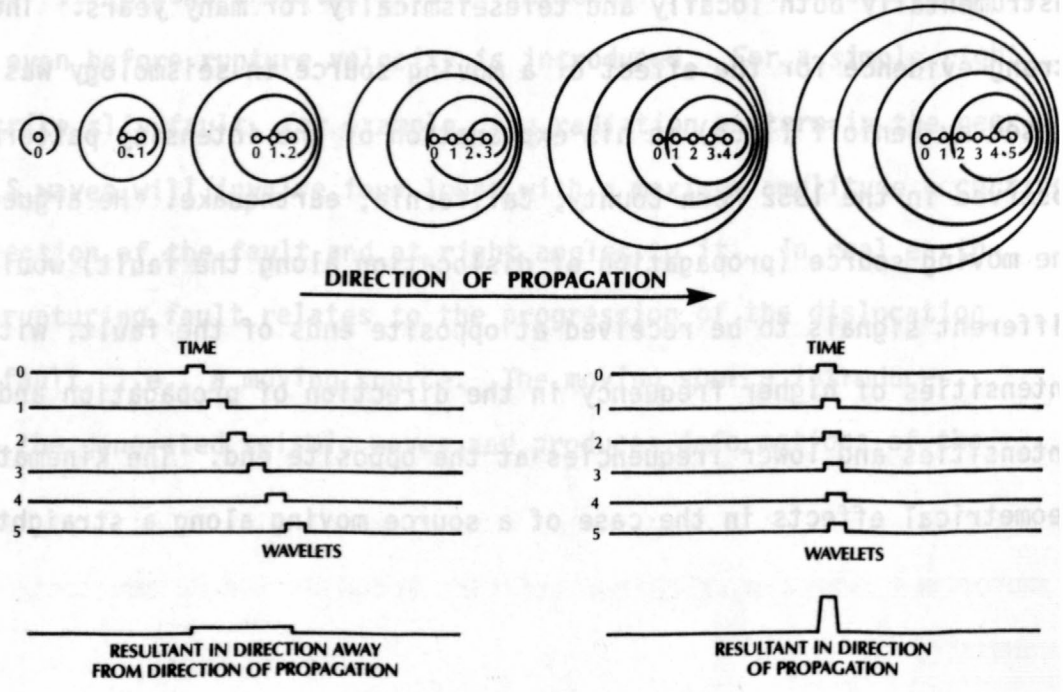

Figure 2 Schematic Representation of a Moving Radiating Source and Its Effect on Wave Amplitudes and Shapes (Modified from Benioff, 1955).

demonstrated simply by means of circular wavefronts which are emitted at equal intervals of time (see Figure 2).

Ben Meneham (1961) used results for a moving source in acoustics to determine source parameters such as fault length and average rupture velocity. Only recently has the problem of seismic wave generation by a moving source been studied from the point of view of the effects on ground motion, which is of interest to engineering and structural design. The theoretical estimates using simple directivity factors from moving sources in acoustics indicate that the amplitudes of seismic waves travelling ahead of the moving dislocation might be greater by an order of magnitude than those propagating in the opposite direction of the dislocation. The models are based on a finite line source traveling at uniform speed in a fixed plane and must be interpreted with caution in terms of the frequencies of waves and rupture conditions.

First of all, the assumption of uniform speed in a fixed plane (i.e., a smooth rupture) is equivalent to having phase coherence throughout the source path. In actual earthquakes, there will be "chattering" of the rupture through patches of roughness in the fault plane, which will cause variations of speed and intensity along the dislocation front and result in degradation of phase coherence. Secondly, the fault zones are seldom simple planes separating elastic media. Particularly in the case of large magnitude earthquakes, the moving source of the earthquake progresses within a definite fracture zone produced by previous faulting. That is, new dislocation in this case occurs in a zone which may resemble a seam of lower velocity and higher attenuating material within the surrounding country rock. For

example, geological conditions along major faults like the San Andreas and its subsidiaries show a rather broad zone (up to 500 meters or more in horizontal width) of crushed and sheared rock often containing bands of gouge extending to considerable depth.

The question arises as to what extent theoretical prediction for models with a single fault plane separating perfectly elastic media is relevant to predicting strong ground motion in a very large earthquake very close to a causative fault zone.

There would be two effects of the fault zone. First is the effect of the fault zone structure itself; geometrically it resembles a slab or "seam" like a coal seam through country rock. For clarity in describing this structure, the term "fault seam" will be used. Secondly, the fault seam would have lower seismic velocity and a higher attentuation than the unfractured rocks outside the seam.

As seismic waves are generated by the moving dislocations at depth, it is expected that some of the energy would be channeled within the seam. Some channel waves would be refracted out of the seam and leak seismic wave energy into the country rock depending on the lengths and types of waves in question; the effect would be to modify both body waves and surface waves. In addition, interaction with seam boundaries would cause partitioning in the wave energy between the various types of waves. This may result in special types of trapped waves with appropriate wave lengths (analogous to Stoneley waves which are known to travel under certain circumstances along boundaries between rocks of different properties at depth in the earth). On the other hand, there would be enhanced attenuation of waves trapped within

the seam as compared to the attentuation of wave energy diffracted out of the seam channel. These effects would modify the wave fields considerably from those which are predicted by a finite line source traveling with a uniform speed along a fixed plane.

In geotechnical work which endeavors to predict ground motions at a site by determining strong ground motion parameters, questions on directivity have been raised seriously only in the last few years. Strong arguments have been made that, for near-fault sites, unless the effects of directivity are included in ground motion estimation, the actual maximum amplitudes of the ground shaking may be underestimated. To address this issue, convincing evidence must be available from strong motion records in the near-field rather than from theorectical models or from sensitive seismographs remote from the source that record small ground motions.

At present, instrumental evidence is available on the question of directivity effects close to the source for only a few California earthquakes. Subsequent sections of this paper describe the available evidence and other factors that need to be considered in determining directivity effects on strong ground motions for specific sites.

EVIDENCE FROM CALIFORNIA EARTHQUAKES

Strong motion data recorded during several earthquakes have shown that for a given soil condition the ground motions obtained at stations equidistant from the source can vary widely in peak ground acceleration (PGA), peak ground velocity (PGV), peak ground displacement (PGD), durations, spectral content, and time histories. To illustrate this variation, the 1940 El Centro, and 1979 Imperial Valley, California, earthquakes will be discussed.

Both earthquakes occurred on the Imperial fault (see Figure 3). The epicenter of the El Centro earthquake was located approximately 15 km north of the United States/Mexico border; the epicenter of the Imperial Valley earthquake was about 1 km south of the border. The magnitude of both earthquakes was about 6.5. The major difference in these two earthquakes is that their ruptures propagated in opposite directions; the 1979 earthquake propagated northward, whereas the 1940 earthquake propagated southward.

The 1979 earthquake was recorded by over 40 strong motion stations. Approximately two-thirds of these instruments were located within about 30 km of the zone of rupture; 13 of these instruments belong to a 45-km-long array called the "El Centro Array" that straddles both the Imperial and the Brawley faults approximately 24 km from the international border (see Figure 3). All recording stations are located on deep sediments of the Imperial Valley, except for the Superstition Mountain (in the U.S.) and the Cerro Prieto (in Mexico) stations, which are located on rock. The 1940 earthquake was recorded in the town of El Centro by a single instrument underlain by deep sediment. The strong ground motion records from the 1979 earthquake illustrate the spatial variations in ground motion for a given source. The records obtained at a common site in El Centro for the 1940 and 1979 earthquakes show the influence on strong ground motions of comparable earthquakes occurring at the same source and propagating in opposite directions.

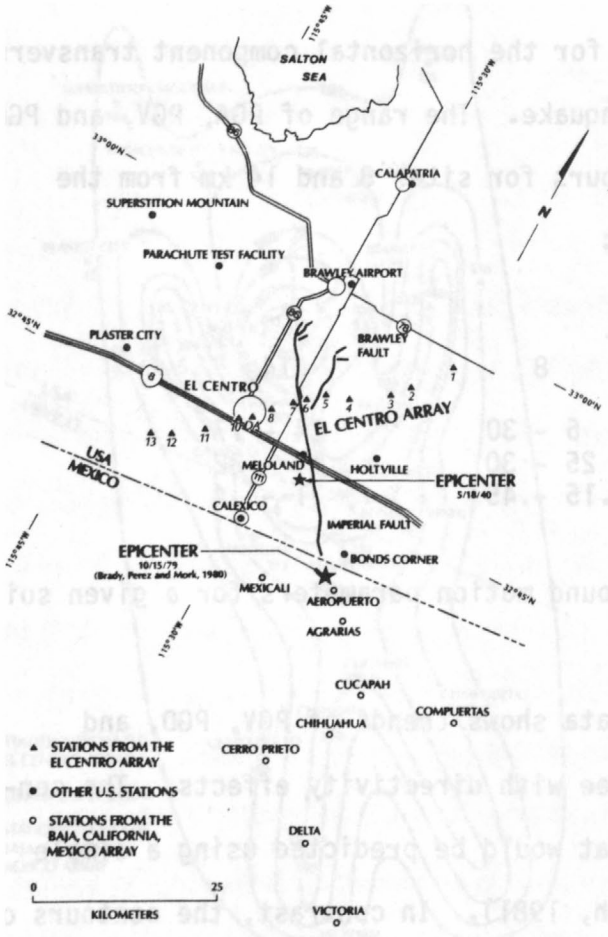

Figure 3
Location Map of Strong Motion Instruments

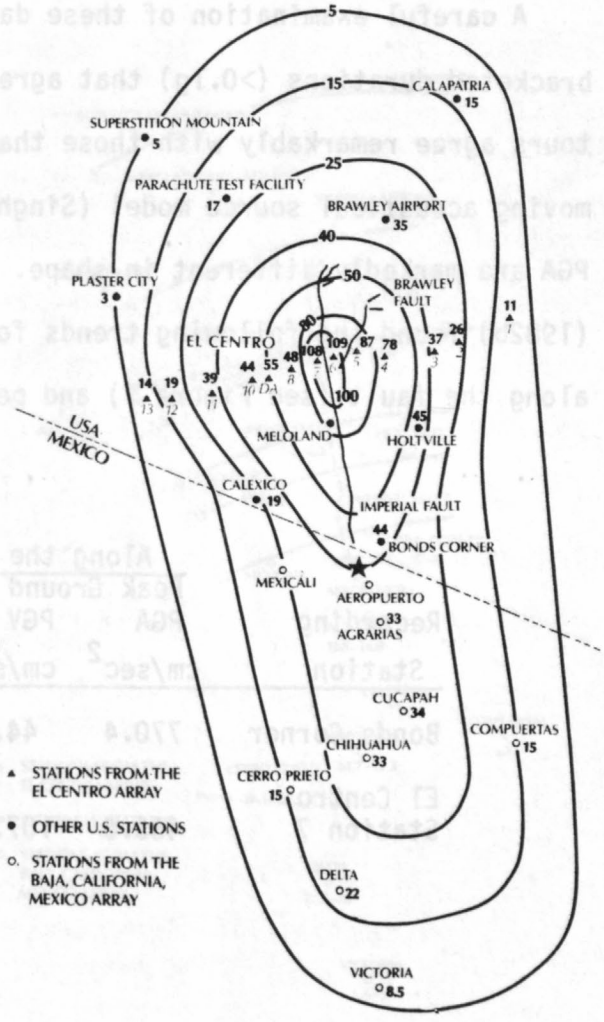

Figure 4 **Contours of Peak Ground Velocity (PGV) in cm/sec (230° Component)**

Figures 4, 5, and 6 show respectively the idealized contours of PGV, PGA, and bracketed durations (>0.1g) for the horizontal component transverse to the fault (230°) of the 1979 earthquake. The range of PGA, PGV, and PGD (not shown), estimated from the contours for sites 8 and 14 km from the causative fault, is summarized below:

Distance to Causative Fault (km)	8	14
PGD (cm)	6 - 30	14 - 17
PGV (cm/sec)	25 - 30	14 - 32
PGA (g)	.15 -.45	.1 - .4

As can be seen, the variations in ground motion parameters for a given soil condition are very large.

A careful examination of these data shows trends of PGV, PGD, and bracketed durations (>0.1g) that agree with directivity effects. The contours agree remarkably with those that would be predicted using a simple moving acoustical source model (Singh, 1981). In contrast, the contours of PGA are markedly different in shape. From examination of the data, Singh (1982b) found the following trends for the 230° horizontal component both along the fault (see Figure 7) and perpendicular to the fault (see Figure 8).

	Along the Fault			
	Peak Ground Motions			Bracketed
Recording Station	PGA cm/sec^2	PGV cm/sec	PGD cm	Duration >0.1g(sec)
Bonds Corner	770.4	44.1	14.6	13.2
El Centro Station 7	453.6	107.8	41.4	4.9

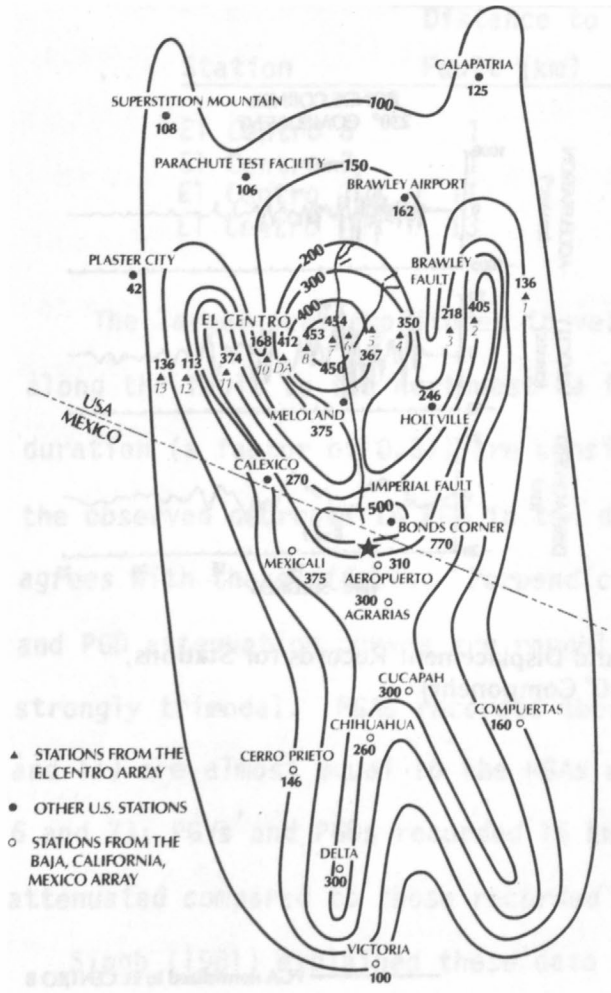

Figure 5
Contours of Peak Ground Acceleration (PGA) in cm/sec^2 (230° Component)

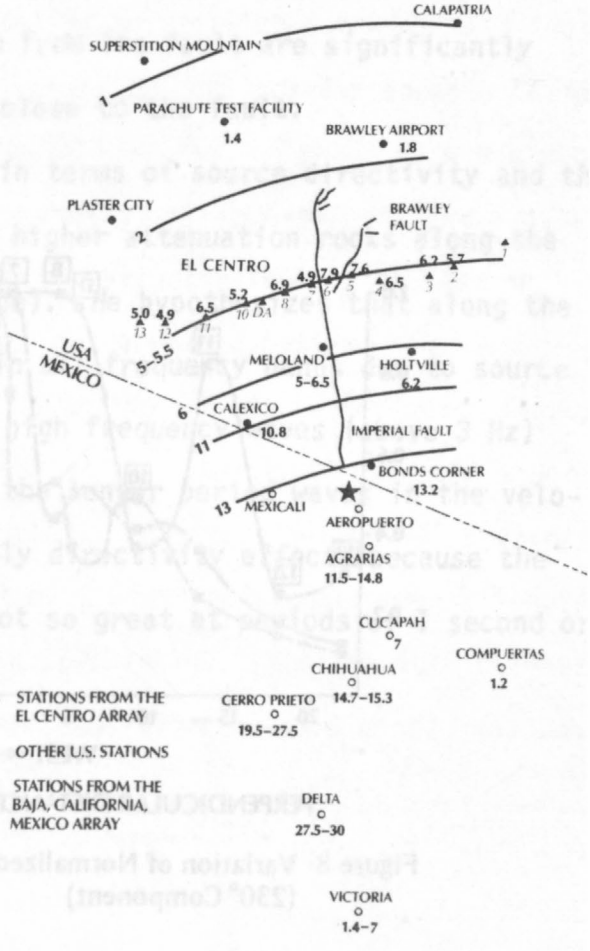

Figure 6 **Contours of Bracketed Durations (> 0.1g) in seconds (230° Component)**

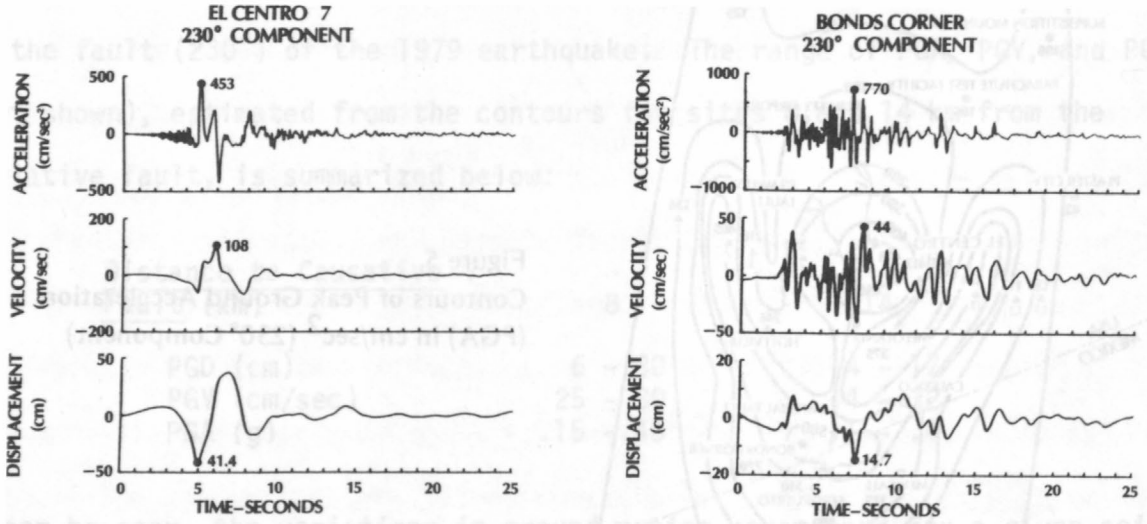

Figure 7 Corrected Acceleration, Velocity and Displacement Records for Stations, Bonds Corner and El Centro 7 (230° Component)

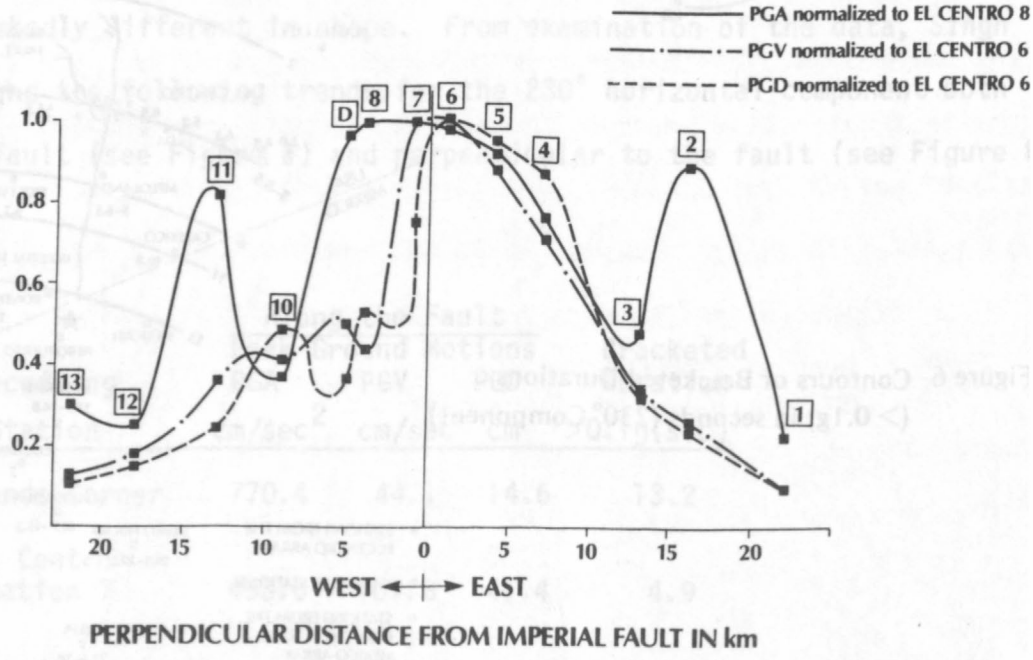

Figure 8 Variation of Normalized PGA, PGV and PGD along the El Centro Array (230° Component)

Perpendicular to the Fault				
Station	Distance to Fault (km)	PGA cm/sec^2	PGV cm/sec	PGD cm
El Centro 6	1	428	109	55
El Centro 7	1	454	108	41
El Centro 2	11	405	26	13
El Centro 11	13	375	39	13

The larger peak amplitudes in velocity and displacement ground motions along the fault to the northwest (a factor of about 3) and the decrease in duration (a factor of 0.37) are consistent with the directivity model, but the observed decrease in PGA in the direction of rupture propagation disagrees with these effects. Perpendicular to the fault (see Figure 8), PGV and PGD attenuation curves are roughly unimodal and the PGA curves are strongly trimodal. PGAs recorded about 16 km from the fault (El Centro 2 and 11) are almost equal to the PGAs recorded 1 km from the fault (El Centro 6 and 7); PGVs and PGDs recorded 16 km from the fault are significantly attenuated compared to those recorded close to the fault.

Singh (1981) explained these data in terms of source directivity and the presence of a zone of low velocity and higher attenuation rocks along the fault zone (approximately 1 to 2 km wide). He hypothesizes that along the path of rupture, the larger increases in all frequency bands due to source directivity are damped markedly in the high frequency waves (above 3 Hz) recorded in the accelerograms, whereas the longer period waves in the velocity and displacement records show mainly directivity effects because the damping effects of the fault seam are not so great at periods of 1 second or longer.

With respect to Stations 6 and 7, which are closest to the fault, a significant increase in PGV and PGD would result with little to no increase (or possibly a reduction) in the value of PGA. A similar hypothesis for stations at some distance from the fault would mean a moderate increase in all frequency bands due to directivity and a moderate decrease in high frequencies due to attenuation of high frequency energy diffracting into the country rock from the fault seam. For stations 2 and 11 a moderate increase in PGV and PGD with minor effects on PGA would occur. The actual variation of PGA (i.e., the location of peaks and troughs) may result from factors such as radiation patterns and the refraction or scattering of the high frequency energy leaking from the fault seam into the surrounding intact country rock. In explaining the spatial variations of PGAs, Singh (1981) has drawn attention to their resemblance to the effect of an aperture on a light beam in which diffraction patterns are set up. He has also shown a correspondence between the amplitude patterns on the far side of a light aperture with those he observed in the variation of PGAs at various sections taken along the Imperial fault (see Figure 9).

An example of redistribution of spectral energy resulting from these phenomena can be seen by comparing spectral amplitudes for the 230° horizontal component of the El Centro 7 and Bonds Corner stations shown in Figure 10. The spectral envelope for El Centro 7 exceeds the spectral envelope for Bonds Corner for a frequency less than 1 Hz and is less for higher frequencies. This result is in line with the above argument. In terms of V/A and AD/V^2 ratios that are used to develop the design response spectra, the V/A ratio increases from a value of about 22 for Bonds Corner

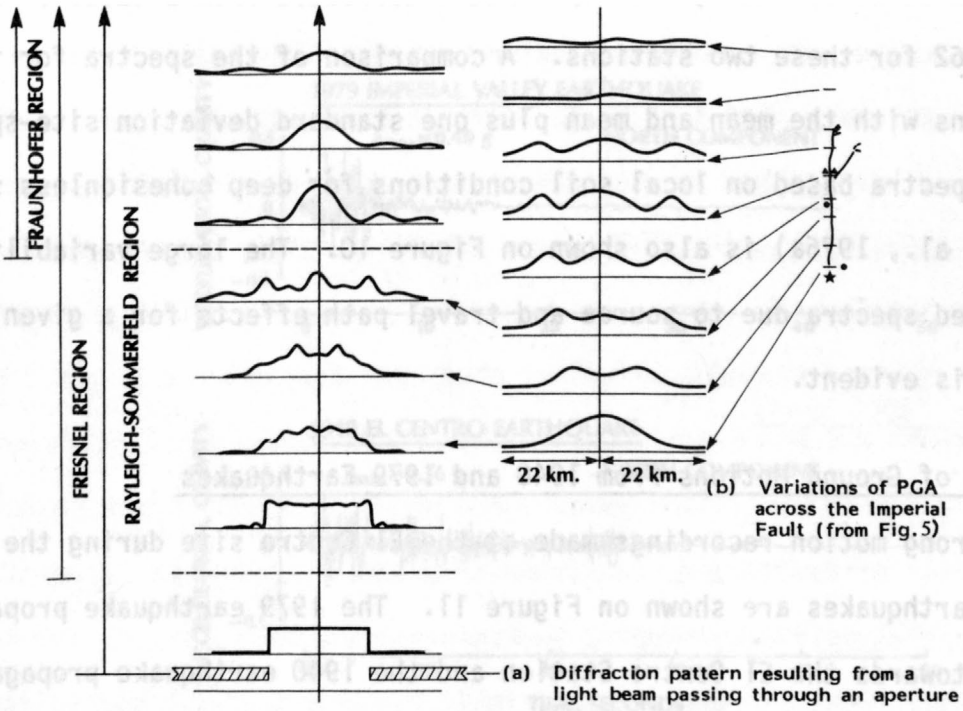

Figure 9 Comparison of PGA Variation across the Imperial Fault with Rayleigh-Sommerfeld Diffraction Patterns Resulting from a Light Beam passing through an Aperture (Singh 1981)

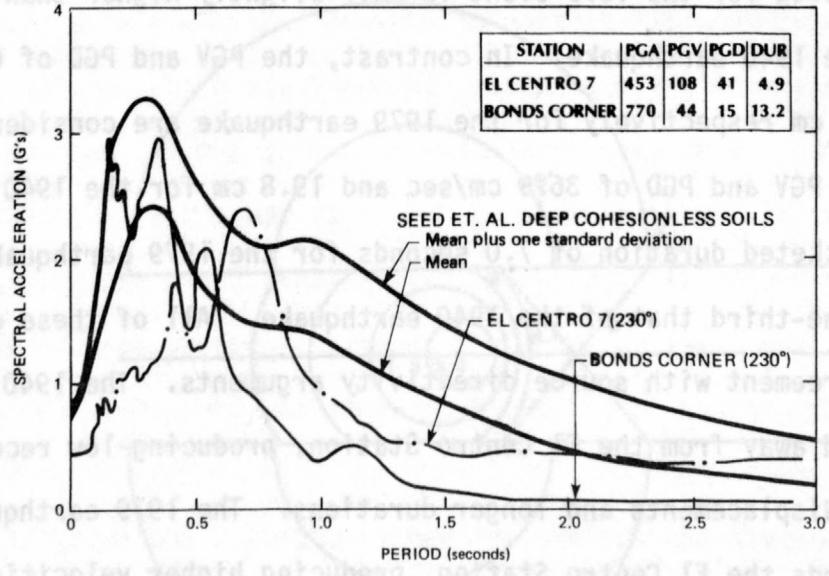

Figure 10 A Comparison of Response Spectra for Stations El Centro 7 and Bonds Corner with Site Dependent Spectra for Deep Cohesionless Soils

to about 92 at El Centro 7; the AD/V^2 ratio decreases from a value of about 5.78 to 1.62 for these two stations. A comparison of the spectra for the two stations with the mean and mean plus one standard deviation site-specific response spectra based on local soil conditions for deep cohesionless soils (Seed, et. al., 1976a) is also shown on Figure 10. The large variability of the recorded spectra due to source and travel path effects for a given soil condition is evident.

Comparison of Ground Motions From 1940 and 1979 Earthquakes

The strong motion recordings made at the El Centro site during the 1940 and 1979 earthquakes are shown on Figure 11. The 1979 earthquake propagated northward towards the El Centro Station and the 1940 earthquake propagated away from it. A comparison of the peak ground motions (PGA, PGV, and PGD) and the bracketed durations recorded at El Centro during these two events are summarized below:

The PGA of 0.4g for the 1979 event is only slightly higher than the PGA of 0.36g for the 1940 earthquake. In contrast, the PGV and PGD of 67.8 cm/sec and 33.8 cm respectively for the 1979 earthquake are considerably higher than the PGV and PGD of 36.9 cm/sec and 19.8 cm for the 1940 earthquake. The bracketed duration of 7.0 seconds for the 1979 earthquake is approximately one-third that of the 1940 earthquake. All of these observations are in agreement with source directivity arguments. The 1940 earthquake propagated away from the El Centro Station, producing low recorded velocities and displacements and longer durations. The 1979 earthquake propagated towards the El Centro Station, producing higher velocities and displacements and shorter durations.

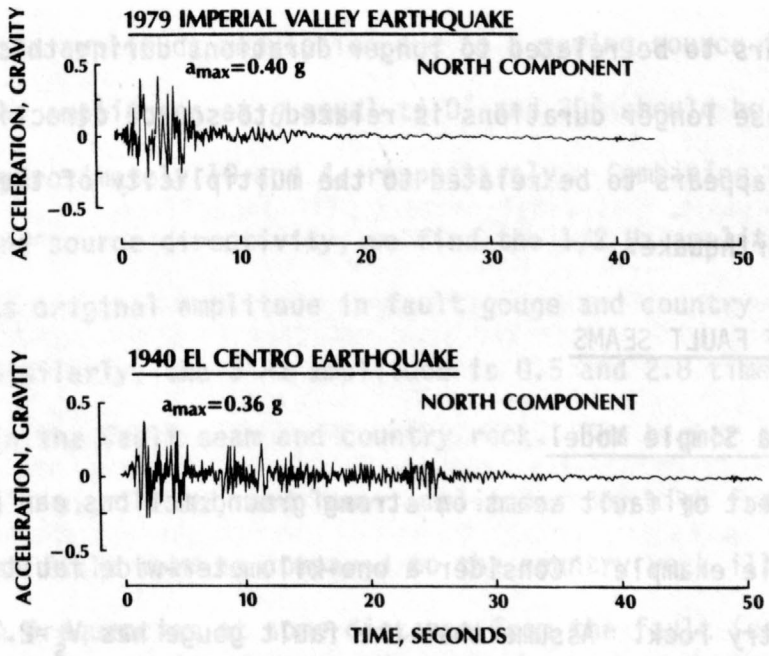

Figure 11 A Comparison of Strong Motion Records Obtained at the El Centro Station (North Component) during May 18, 1940, and October 15, 1979, Earthquakes.

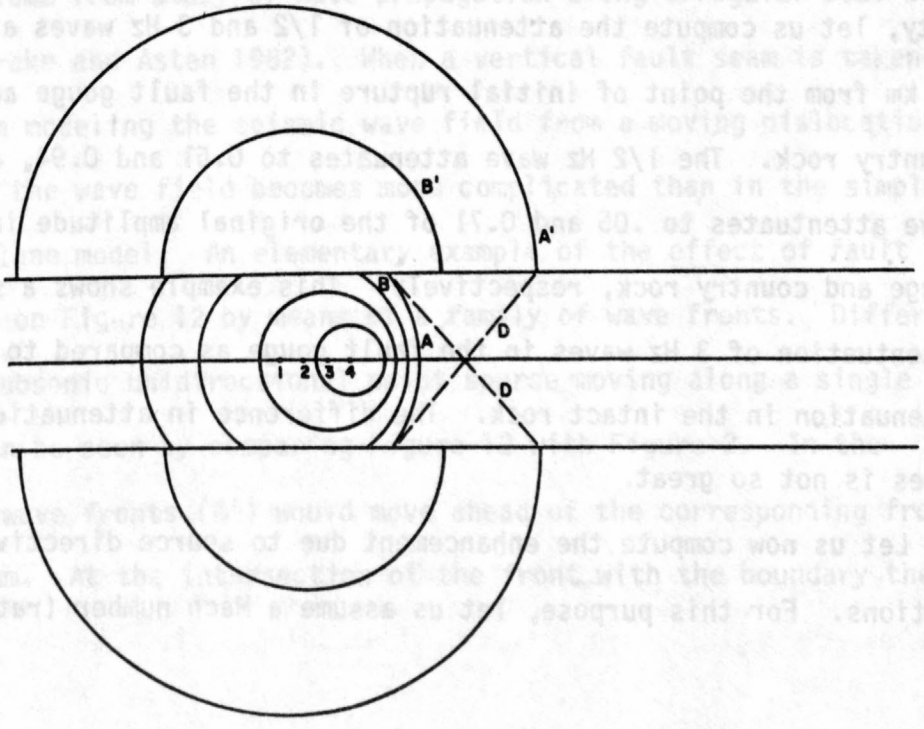

Figure 12 Wave Fronts for a Moving Source in a Low-Velocity Channel

The maximum intensity of IX felt in the town of El Centro during the 1940 earthquake as compared to the intensity of VII during the 1979 earthquake appears to be related to longer durations during this event. A large part of these longer durations is related to source directivity and only a small part appears to be related to the multiplicity of the source during the 1940 earthquake.

MODELING OF FAULT SEAMS

Results of a Simple Model

The effect of fault seams on strong ground motions can be illustrated with a simple example. Consider a one-kilometer-wide fault zone bounded by intact country rock. Assume that the fault gouge has V_s=2.1 km/sec and Q = 30 and that the surrounding intact rock has a V_s = 3.1 km/sec and Q = 175. Using the relationship for frictional attenuation, i.e, $A\, e^{-\omega R/2cQ}$ where ω is the angular frequency, R is the distance, and c is the wave velocity, let us compute the attenuation of 1/2 and 3 Hz waves at a distance of 20 km from the point of initial rupture in the fault gouge and the intact country rock. The 1/2 Hz wave attenuates to 0.61 and 0.94, and the 3 Hz wave attentuates to .05 and 0.71 of the original amplitude in the fault gouge and country rock, respectively. This example shows a significant attentuation of 3 Hz waves in the fault gouge as compared to only moderate attenuation in the intact rock. The difference in attenuation for 1/2 Hz waves is not so great.

Let us now compute the enhancement due to source directivity at these stations. For this purpose, let us assume a Mach number (ratio of rupture

velocity to shear wave velocity) of 0.7 and that the station in the fault seam is located at θ=0° and the station in country rock is located at θ = 30°. Using the amplitude modulation due to a moving source i.e., $1/(1-M\cos\theta)^2$, the amplitudes at θ equal to 0° and 30° should be enhanced by a factor of approximately 10 and 4, respectively. Combining the effects of attenuation and source directivity, we find the 1/2 Hz amplitude to be 6 and 3.7 times its original amplitude in fault gouge and country rock, respectively. Similarly, the 3 Hz amplitude is 0.5 and 2.8 times its original amplitude in the fault seam and country rock. The higher amplitude for low frequencies, i.e., 1/2 Hz, and lower amplitudes for high frequencies, i.e., 3 Hz in the fault seam as compared to the country rock illustrates the presence of high frequencies at some distance from the fault (see Figure 8).

Results of Studies of Wave Propagation Along Coal Seams

Bolt (1983) has drawn attention to other numerical analogies to the problem which come from study of wave propagation along irregular coal seams (Krey, 1963; Drake and Asten 1982). When a vertical fault seam is taken into account in modeling the seismic wave field from a moving dislocation, computation of the wave field becomes more complicated than in the simple single fault-plane model. An elementary example of the effect of fault seams is shown on Figure 12 by means of a family of wave fronts. Differences from a subsonic unidirectional point source moving along a single fault plane can be seen by comparing Figure 12 with Figure 2. In the country rock, wave fronts (A') would move ahead of the corresponding fronts (A) in the seam. At the intersection of the front with the boundary there

would be a conical head wave of diffracted type (shown as dashed line D for initial front only) propagating in the seam as a leading fringe of energy.

A few inferences on the likely modifications to the effects of directivity by the fault seam are:

a. A simple quadrantal pattern with lobes (see Figure 1) would no longer describe the wave amplitude in all the near-field.

b. Enhanced damping of the waves in the seam would reduce the wave amplitudes within the seam relative to waves refracted out of the seam.

c. The diffraction, multiple reflection, and progressive interference effects within the seam would be a function of the effective seam width relative to the wave lengths. The higher frequency (above 5 Hz) waves are likely to be most attenuated by the multiple interference and damping within the seam.

Recent detailed finite element modeling of waves channeling along coal seams have been carried out by Drake and Asten. Although these models do not include any damping terms in the finite element computation, they do show that the presence of a fault zone with significantly different seismic parameters could have significant consequences as far as directivity focusing properties are concerned.

CONCLUSIONS

From the seismological point of view, the effect of the moving source has been clearly demonstrated in numerous studies using seismographs located at moderate to greater distances (i.e., far-field) from the source. Such studies, however, usually concern long-period seismic waves with periods above 2 to 5 seconds. When the seismic waves in the near-field with a range of wave frequencies characteristic of engineered structures are considered,

there is only limited definite evidence available. Based on the California data set, it can be concluded that in developing upper bounds of spectral content at high frequencies and amplitudes of PGA near the earthquake source, it becomes very important to consider the effects on high frequency waves of the damping characteristics of the fault seam and the bounding intact country rock. The evidence from the California data set is that PGAs tend to saturate and have much less dependence on magnitude in the near field than in the intermediate and far fields. In contrast, PGVs and PGDs show a somewhat stronger dependence on magnitude and source directivity in the near field and do not appear to be influenced as much by the damping characteristics of the material in the fault zone. The ratio of peak horizontal ground motions in the forward direction of fault rupture to the peak motion in the backward direction is probably greatest for displacements and velocities and least for accelerations.

Because directivity is a special near-field effect which may be experienced at a site toward which fracture propagations progress, local amplification of ground motion might arise. This effect should, therefore, be considered in shaking estimates for critical structures such as dams, bridges, power plants, etc., because directivity can significantly increase the spectral components of ground motion employed as input into seismic design.

From Figure 10, it is clear that the longer period parts of response spectra in the near-field are realistically energetic due to the enhancement of a single unidirectional long period pulse. In contrast, long period parts of the spectra at a soft soil site for a large distant earthquake may

be due to amplification of the long period harmonics with several cycles depending upon the duration the earthquake. Although both conditions may produce energetic long period motions in the spectra, the actual characteristics of the ground motion producing these motions will be different and they should be properly considered in design of different structural systems.

Time histories close to the fault in a given earthquake (see Figure 7), and from two comparable magnitude earthquakes on the same source (see Figure 11) vary widely in character, depending upon the direction of rupture propagation. Furthermore, near-source records contain a long period pulse (see Figure 7) corresponding to the "fling" along the fault as the dislocation passes by the site and must properly be considered in design. For example, the failure of the Olive View Hospital structure during the 1971 San Fernando earthquake apparently occurred during the long duration pulse (which can be seen about 3 seconds after the instrument triggered) rather than during the high frequency peak acceleration (greater than 1.0g) which occurred about 8 seconds after the pulse.

RECOMMENDATIONS FOR FUTURE RESEARCH

1. Geological and geophysical studies are required to study the crustal structure. The studies should be devoted to identifying the physical properties and extent of materials contained in the fault zone and the nature of the contact with bounding intact rock.
2. The results of the geological and geophysical studies should be used in analytical models to improve the understanding of near-field ground

motions. Appropriate two-dimensional or preferably three-dimensional finite element models should be used to simulate low velocity and low Q fault seams bounded by high velocity and high Q intact rock. These models would examine the quantitative effect of directivity in the frequency range of interest in hazard assessments.

3. Significant advance in knowledge of directivity focusing effects depends on the installation and maintenance of strong-motion accelerometers along active faults where large earthquakes might be generated. There are still only a handful of accelerograms from moderate to large earthquakes that allow comparisons at the front and back of a moving source dislocation. In order to achieve the instrumental requirements, specially designed digital instrument arrays must be installed along active fault zones. These arrays can be designed to give the quantitative detail necessary to model properly the intricacies of strong ground motion near a source moving through a geologically realistic medium.

4. There are several factors that influence the seismic intensity of the ground motion at a given point. Therefore, it is recommended that more measurements of strong motions from different seismic regions be made to address the issue of site-specific ground motion. It is also recommended that strong motion arrays be installed and custom-designed to fit the local conditions.

5. To reduce the dispersion estimates of the ground motion parameters for a given site, the effect of local soil conditions should be

further refined in light of the significant effect of source and travel path on ground motion. Such refinement will involve the introduction of additional parameters to describe the details of earthquake source mechanism and transmission path and the development of accurate information on local soil and geological conditions at an accelerograph site.

6. The earthquake source and the local soil conditions have a profound effect on the long period component of the ground motions. Therefore, in order to properly separate the effects of source and soil, it is important to evaluate the non-linear effects of deep alluvial and soft sediments on the earthquake ground motions. Evaluation of such long period motions becomes particularly important for structures such as high rise buildings, offshore platforms, large tanks, and high dams.

REFERENCES

1. Bolt, B. A. The Contribution of Directivity Focusing to Earthquake Intensities. State-of-the-art for Assessing Earthquake Hazards in the United States, U.S. Army Engineer Waterway Experiment Station, Misc. Paper S-73-1, Report 20, 1983.

2. Bolt, B. A. Interpretation of Strong Ground Motion Records. State-of-the-art for Assessing Earthquake Hazards in the United States, U.S. Army Engineer Waterway Experiment Station, Misc. Paper S-73-1, Report 17, 1981.

3. Benioff, H. (1955). Mechanism and strain characteristics of the White Wolf fault as indicated by the aftershock sequence, Earthquakes in Kern County, California during 1955 (G.B. Oakeshott, ed.), Cal. Div. Mines Bull. 171, 199-202.

4. Ben-Manahem, A. (1961). Radiation patterns of seismic surface waves from finite moving sources, Bull. Seism. Soc. Am., 51, 401-435.

5. Brune, J. N. (1978). Contention 3 Ground Motion, Testimony on behalf of Intervenors before USNRC Atomic Safety and Licensing Board in matter of Diablo Canyon Nuclear Power Plants, Units 1 and 2, Docket Nos. STN 50-275, 50-323.

6. Drake, L. A., and M. W. Asten (1982). Wave Propagationin Irregular Coal Seams, private communication with B.A. Bolt.

7. Idriss, I. M. Characteristics of Earthquake Ground Motion, State-of-the-Art Report, ASCE Geotechnical Engineering Division Specialty Conference, June 19-21, Pasadena, California, Proc. Vol. III, 1978, pp. 1151-1265.

8. Krey, T. C. (1963). Channel waves as a tool of applied geophysics in coal mining, Geophysics, 28, 701-714.

9. Mohraz, B. A Study of Earthquake Response Spectra for Different Geological Conditions, Bulletin of the Seismological Society of America, Vol. 66, No. 3, June, 1976, pp. 915-936.

10. Morse, P. M., and K. V. Ingard (1968). Theoretical Acoustics, McGraw-Hill Book Company, New York.

11. Nuttli, O. W. Similarities and Differences Between Western and Eastern United States Earthquakes, and their Consequences for Earthquake Engineering: Proc. Conference on Earthquakes and Earthquake Engineering: "The Eastern U.S.," Sept. 14-17, Knoxville, Tennessee, 1981.

12. Schnabel, P., Seed, H. B., and Lysmer, J. Modification of Seismograph Records for Effects of Local Soil Conditions. Bulletin of Seismological Society of America, Vol. 62, 1972, pp. 1649-1664.

13. Seed, H. B. and Idriss, I. M. Influence of Soil Conditions on Ground Motions during Earthquakes, Journal of the Soil Mechanics and Foundations Division, ASCE, Vol. 95, No. SM1, January, 1969, pp. 99-137.

14. Seed, H. B., Ugas, C. and Lysmer, J. Site-Dependent Spectra for Earthquake-Resistant design, Bulletin of the Seismological Society of America, Vol. 66, No. 1, February, 1976a, pp. 221-243.

15. Seed, H. B., Murarka, R., Lysmer, J. and Idriss, I. M. Relationships of Maximum Accelerations, Maximum Velocity, Distance from Source and Local Site Conditions for Moderately Strong Earthquakes, Bulletin of the Seismological Society of America, Vol. 66, No. 4, August, 1976b, pp. 1323-1342.

16. Singh, J. P. The Influence of Seismic Source Directivity on Strong Ground Motions. Ph.D. dissertation, University of California, Berkeley, 1981.

17. Singh, J. P. Seismic Source Directivity Evidence from the August 6, 1979 Coyote Lake Earthquake, Proceedings, Conference on Earthquake Hazards of the Eastern San Francisco Bay Area, Hayward, California, California Division of Mines and Geology, 1982.

18. Singh, J. P. Importance of Local Structure and Source Characteristics in Estimation of Nearfield Strong Ground Motions, Proceedings, Third International Earthquake Microzonation Conference, Seattle, Washington, 1982.

19. Wood, H. O. Distribution of Apparent Intensity in San Francisco, the California Earthquake of April 18, 1906, Report of the State Earthquake Investigation Commission, A. C. Lawson, Chairman Carnegie Institution of Washington, Washington, D.C., 1908, pp. 220-245.

EFFECTS OF LOCAL GEOLOGICAL CONDITIONS ON STRONG-GROUND MOTIONS IN THE VICINITY OF COALINGA, CALIFORNIA

by

R. D. Borcherdt, C. S. Mueller, and L. G. Wennerberg

U.S. Geological Survey

345 Middlefield Road, MS 77

Menlo Park, California

ABSTRACT

An array of six portable digital event recorders (GEOS) recorded eighteen aftershocks (M 1-4.3) during a three-day deployment to investigate the effects of local site conditions on earthquake-generated ground motions in the community of Coalinga. Large frequency-dependent amplitude variations due to local site conditions were observed over distances less than 1.5 km. The sites underlain by alluvium, including two sites in the community of Coalinga, show site resonances with inferred amplifications of horizontal motion exceeding a factor of 10 in some cases. In general, the wide dynamic range signals recorded on the array show considerable amplification of the higher frequency components of shaking (5-15 Hz), suggesting that the alluvial deposits underlying the community of Coalinga could have contributed to the damage sustained by the older masonry structures during the May 2, 1983 Coalinga earthquake.

INTRODUCTION

The moderate earthquake (M_L 6.5), which occurred on May 2, 1983 (23h 42m 37.85s GMT) approximately 10 km northeast of Coalinga, California, caused more than 30 million dollars in damage. A majority of the damage was associated with older unreinforced-masonry structures located in Coalinga (C. Rojahn, oral commun.). As the community of Coalinga is underlain by a thick section of alluvium, a significant question for evaluation of earthquake-induced damage concerns the influence of local geological conditions. This paper provides a preliminary interpretation of ground motions generated by aftershocks of the main event as recorded on wide-dynamic range, broad-bandwidth instrumentation (GEOS) located along a profile through the community of Coalinga.

GEOLOGIC SETTING AND STRONG MOTION DATA

The community of Coalinga is located in a northwest trending alluvial basin which is the surface expression of the Coalinga syncline. The basin is bounded on the northeast and southwest by sedimentary rocks of Tertiary and Cretaceous age which in turn are underlain by rocks of the Franciscan assemblage, comprising the core of the Coalinga anticline. The damaging earthquake of May 2, 1983 occurred approximately 10 km northeast of Coalinga at a depth of 10.5 km (Eaton, 1983) beneath the surface axis of the Coalinga anticline.

To investigate the effects of the alluvial section underlying Coalinga on strong ground shaking, six recording stations were established along a profile extending from the heavily damaged area of Coalinga across the basin margin to a competent rock outcrop, approximately 4 km southwest of Coalinga (figure 1). The array was installed on May 19 and 20 and operated through May 23 as

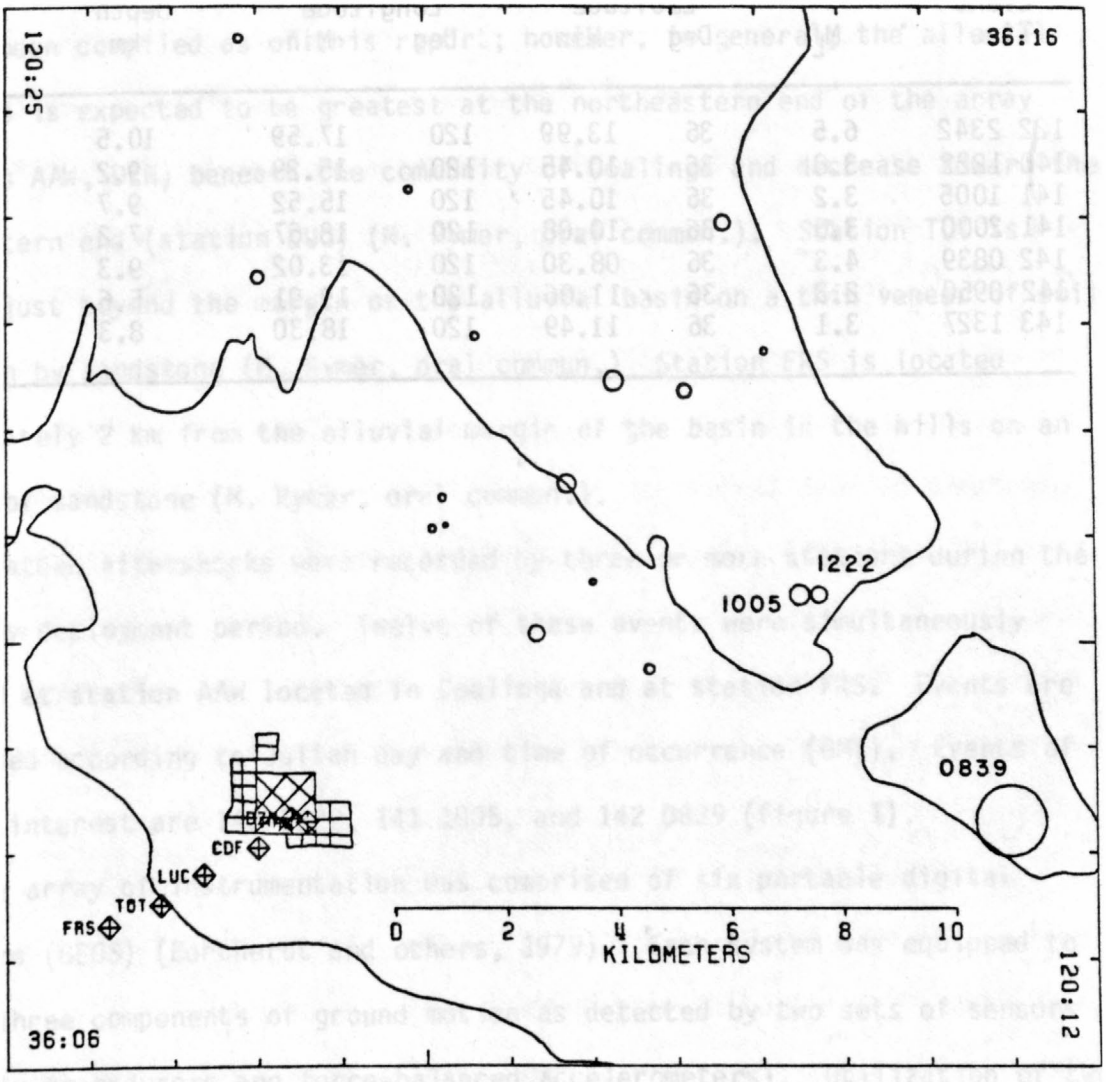

Figure 1. Location map for aftershocks recorded on a broad-band, digital array of six stations extending from the community of Coalinga to a nearby bedrock outcrop.

Table 1. Main event and some of the aftershocks recorded on the Coalinga array.

Event Time	M_L	Latitude Deg	Latitude Min	Longitude Deg	Longitude Min	Depth km	Dist AAW km
122 2342	6.5	36	13.99	120	17.59	10.5	12.1
140 1222	3.0	36	10.45	120	15.29	9.2	13.6
141 1005	3.2	36	10.45	120	15.52	9.7	13.7
141 2000	3.0	36	10.08	120	18.67	7.2	9.0
142 0839	4.3	36	08.30	120	13.02	9.3	15.7
142 0950	2.3	36	11.06	120	19.91	5.6	7.9
143 1327	3.1	36	11.49	120	18.30	8.3	11.2

part of a larger strong-motion seismological study of the Coalinga aftershock sequence (Borcherdt and others, 1983).

Detailed information on alluvial thickness and seismic velocity structure had not been compiled as of this report; however, in general, the alluvial thickness is expected to be greatest at the northeastern end of the array (stations AAW, DZN) beneath the community of Coalinga and decrease toward the southwestern end (station LUC) (M. Rymer, oral commun.). Station TOT is located just beyond the margin of the alluvial basin on a thin veneer of soil underlain by sandstone (M. Rymer, oral commun.) Station FRS is located approximately 2 km from the alluvial margin of the basin in the hills on an outcrop of sandstone (M. Rymer, oral commun.).

Eighteen aftershocks were recorded by three or more stations during the three day deployment period. Twelve of these events were simultaneously recorded at station AAW located in Coalinga and at station FRS. Events are identified according to Julian day and time of occurrence (GMT). Events of special interest are 140 1222, 141 1005, and 142 0839 (figure 1).

The array of instrumentation was comprised of six portable digital recorders (GEOS) (Borcherdt and others, 1979). Each system was equipped to record three components of ground motion as detected by two sets of sensors (velocity transducers and force-balanced accelerometers). Utilization of two sets of sensors permits the microcomputer-based recording system to record on-scale seismic signals ranging from that of the seismic background noise to the upper limit of the accelerometers (> 1g) with 16 BIT (96 dB) signal resolution without change in gain settings. The wide dynamic range and broad frequency bandwidth of the recorded signals provides a unique opportunity to investigate the high-frequency response of an alluvial basin.

ANALOG AMPLIFICATIONS

Three components of ground velocity generated by the largest aftershock recorded on the array (142 0839, M_L 4.3) are shown for five of the array stations (figures 2a, 2b, and 2c). Visual comparison of the time histories shows that, in general, the amplitudes and durations of the velocity time histories are greater for the sites underlain by alluvium (AAW, DZN, LUC) than those for sandstone (FRS). The apparent soil amplification effects are greater for the horizontal components of motion than for the vertical components. Station TOT near the margin of the basin shows vertical amplitudes greater than those on the alluvial sites, but horizontal amplitudes comparable or less than those at the alluvial sites. It should be pointed out that the horizontal velocity recordings for stations LUC and TOT are "clipped" due to gain settings inappropriate for the dyamic range and sensitivity of the velocity transducers. Calculation of soil responses for this event will be based on recordings of the force-balance accelerometers to be discussed in a later section.

A similar set of recordings for a smaller event (141 1005 M_L 3.2) located more inline with the array profile (figure 1) is shown in figures 3a, 3b, and 3c. These time histories also suggest that the ground velocities recorded on the alluvial sites are several times larger than those observed on the sandstone site with the largest time-history amplitudes occurring for the horizontal components of ground velocity recorded at the sites AAW and DZN located in Coalinga. The maximum peak-to-peak amplitudes observed for events of magnitude greater than 2.5 are tabulated (table 2). Corresponding ratios with respect to station FRS and scaled to account for geometrical spreading are also tabulated (table 2, cols. 3-6). Events 140 1222 and 141 1005 are of similar magnitude, depth, and azimuth with respect to the array (see table 1

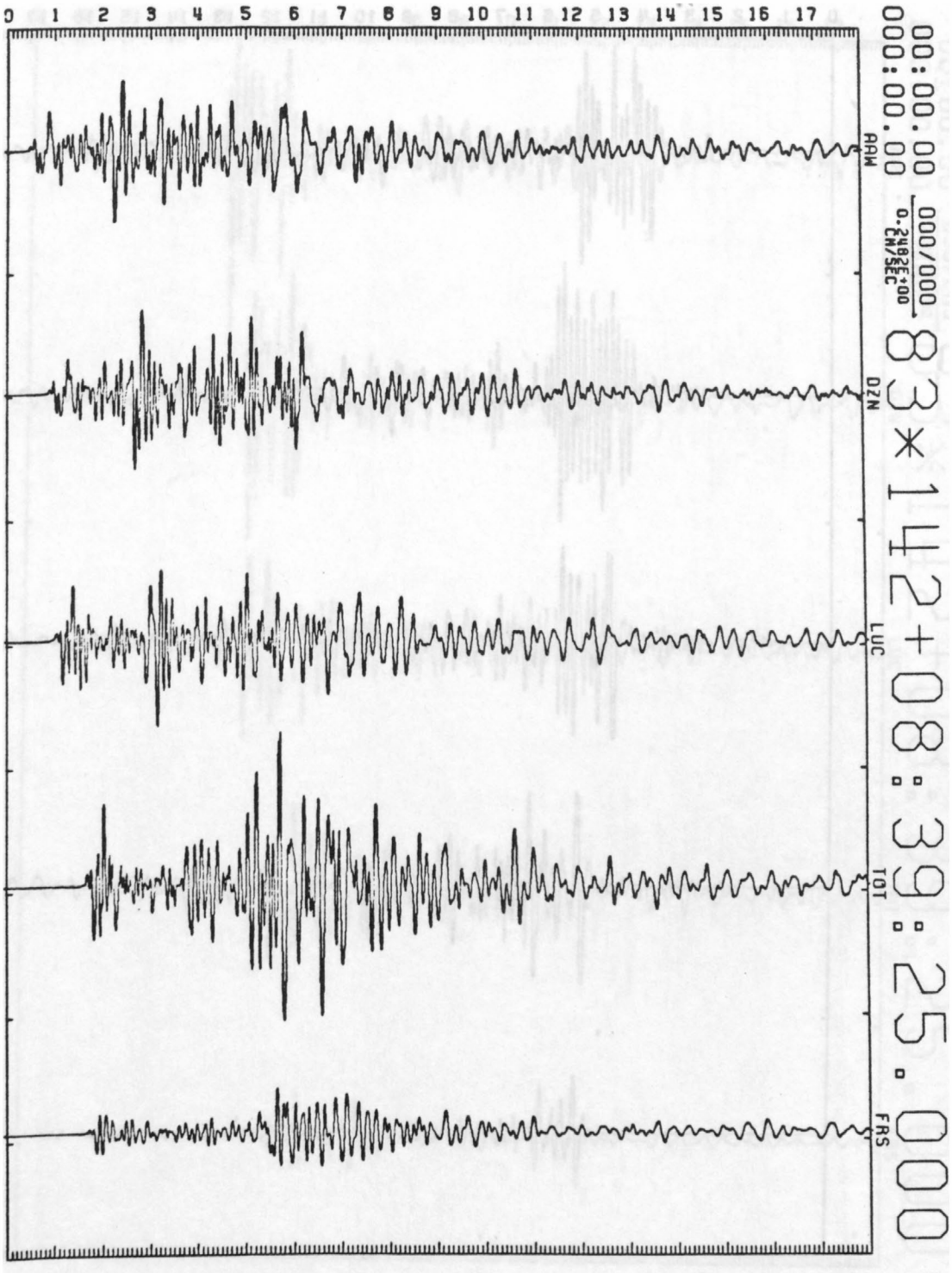

Figure 2a. Vertical component of ground velocity recorded at five stations for event 142 0839 (M = 4.3).

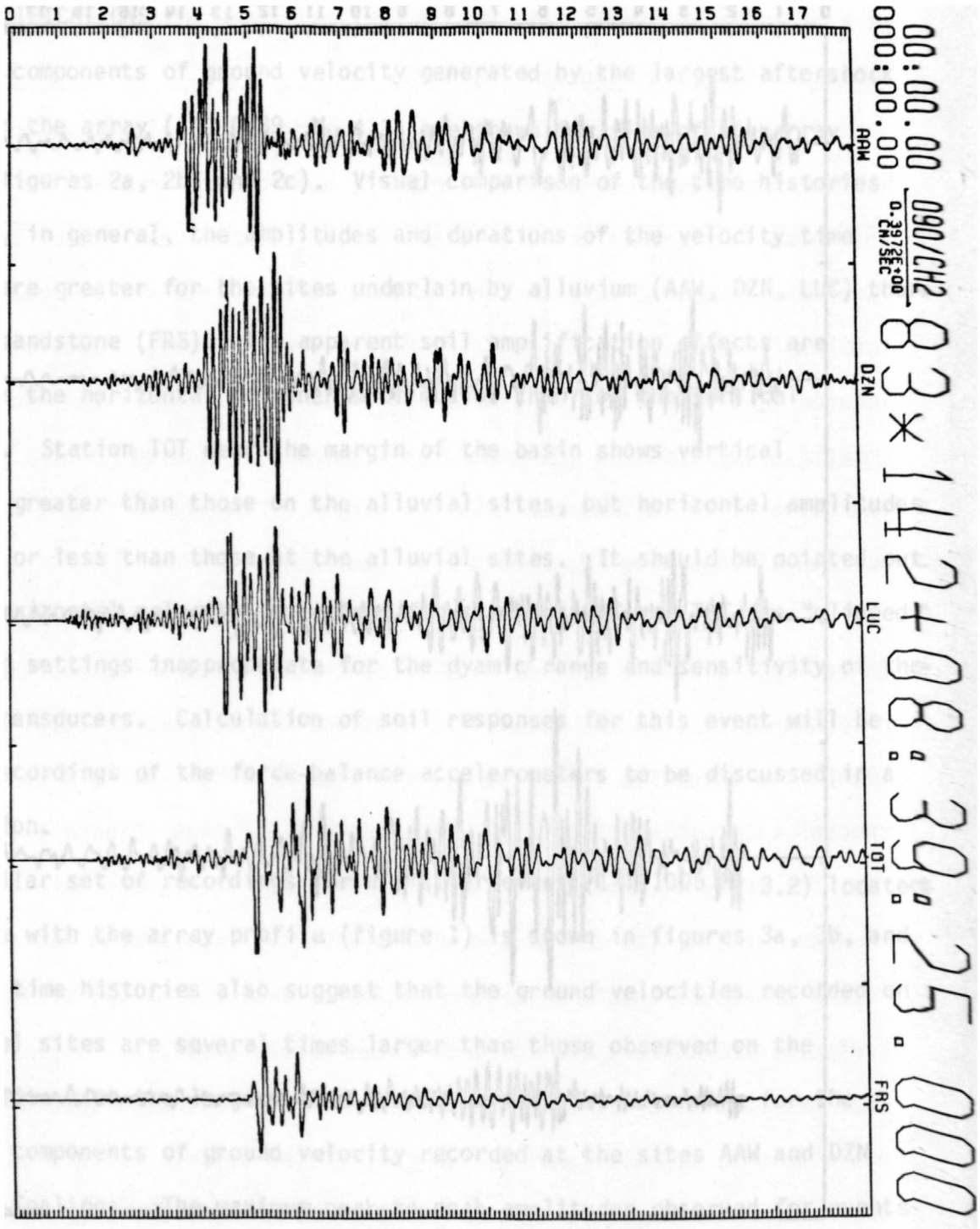

Figure 2b. East-west component of ground velocity recorded at five stations for event 142 0839.

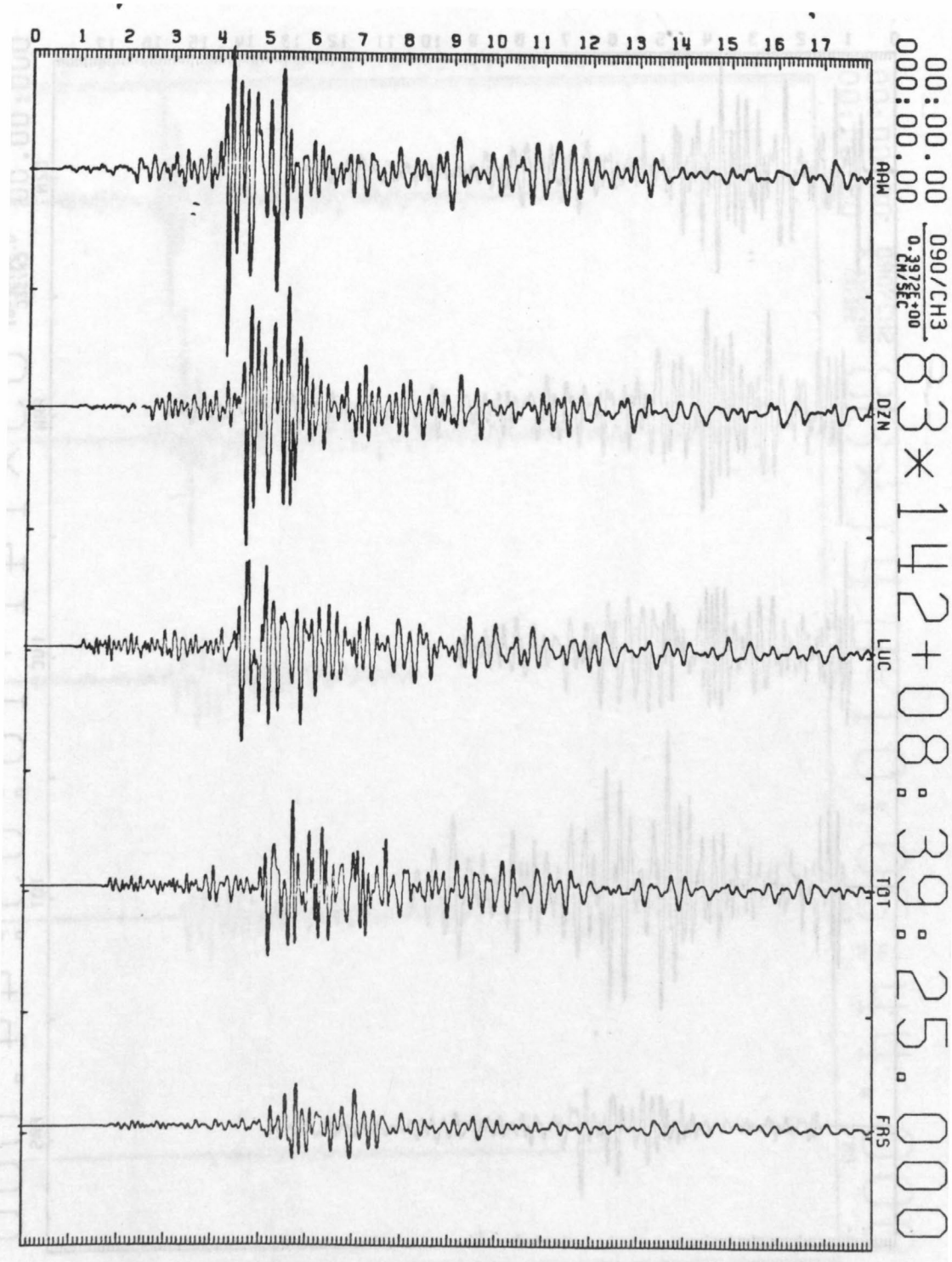

Figure 2c. North-south component of ground velocity recorded at five stations for event 142 0839.

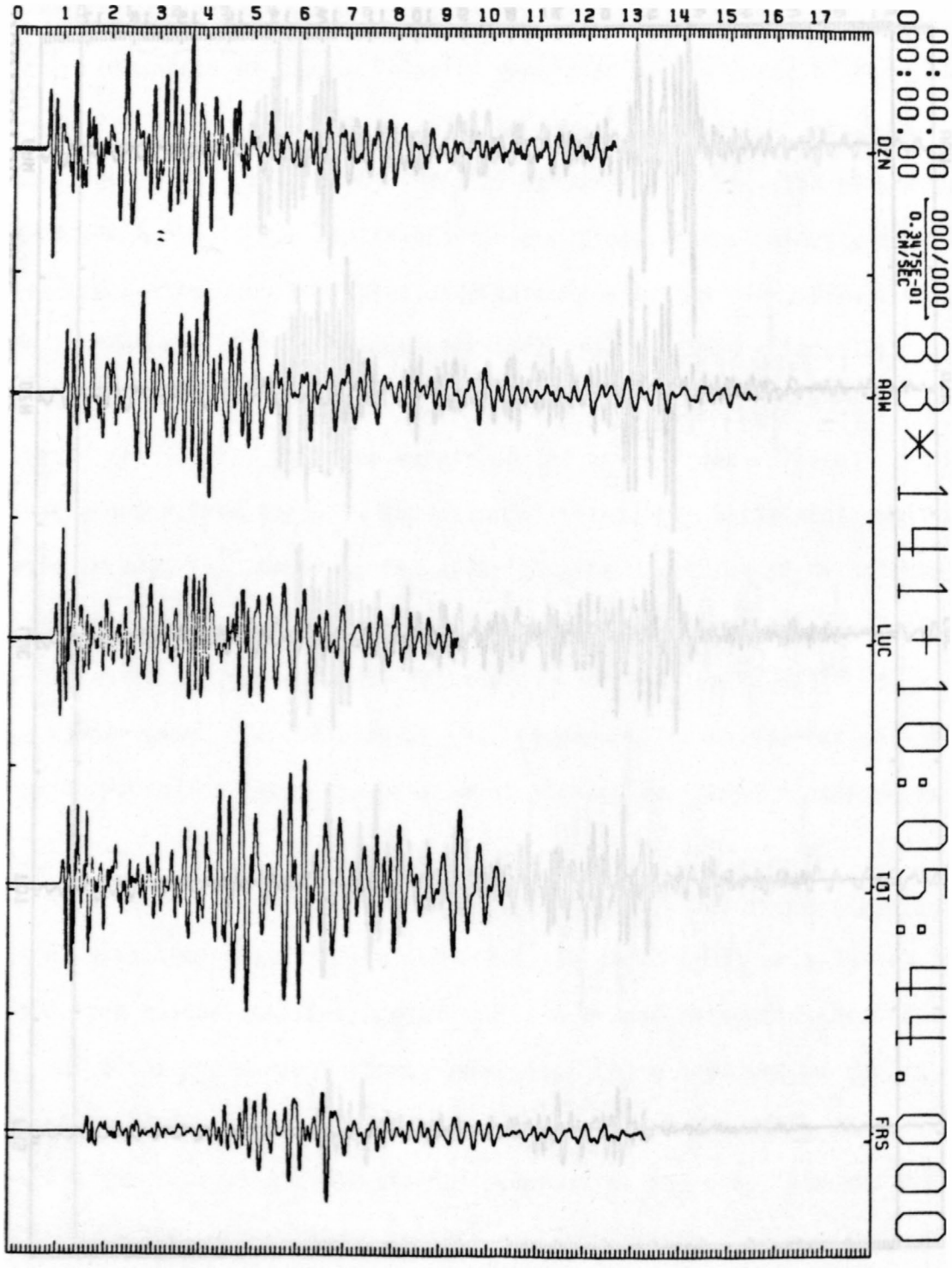

Figure 3a. Vertical component of ground velocity recorded at five stations for event 141 1005 (M = 3.2).

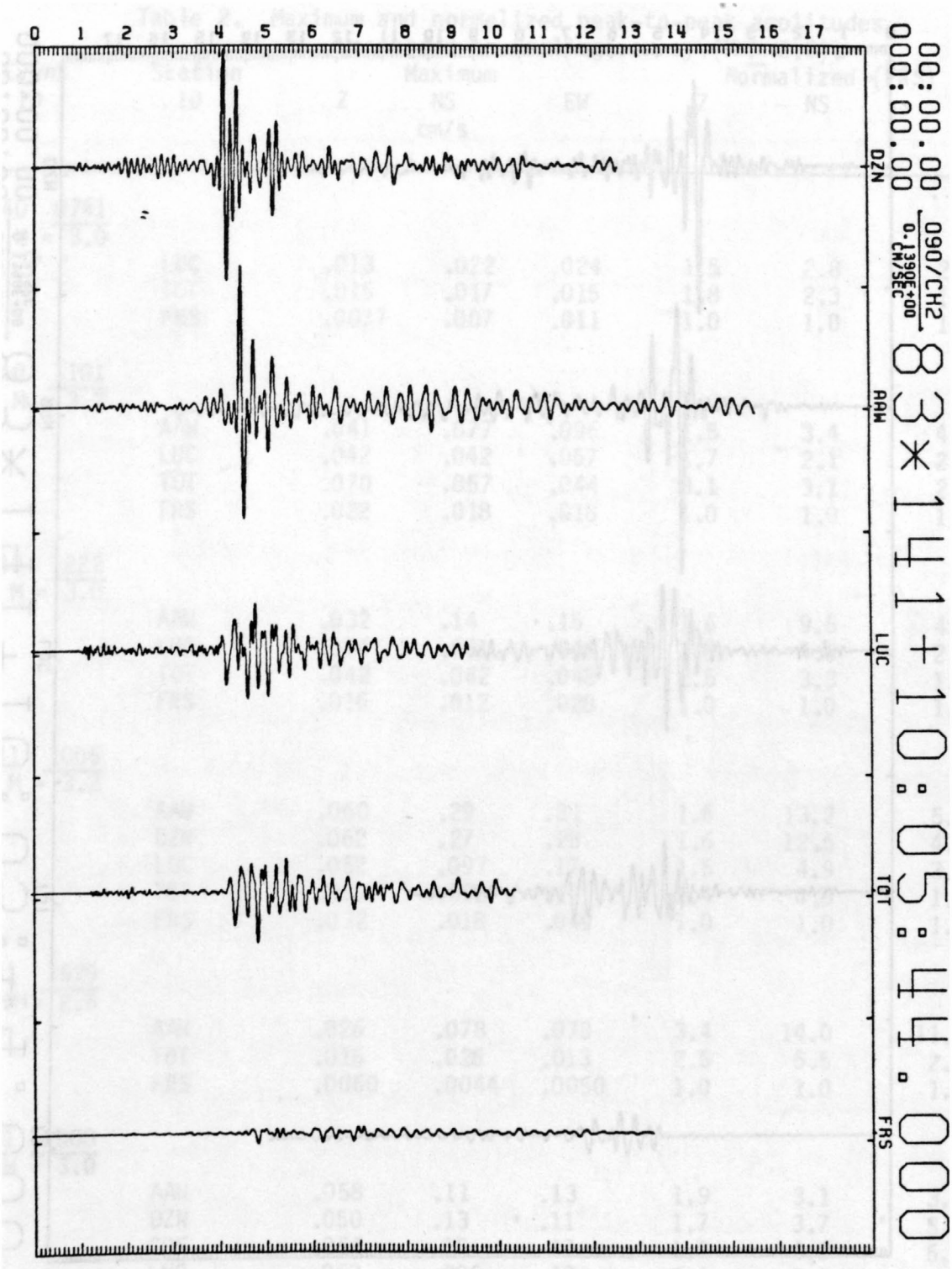

Figure 3b. East-west component of ground velocity recorded at five stations for event 141 1005.

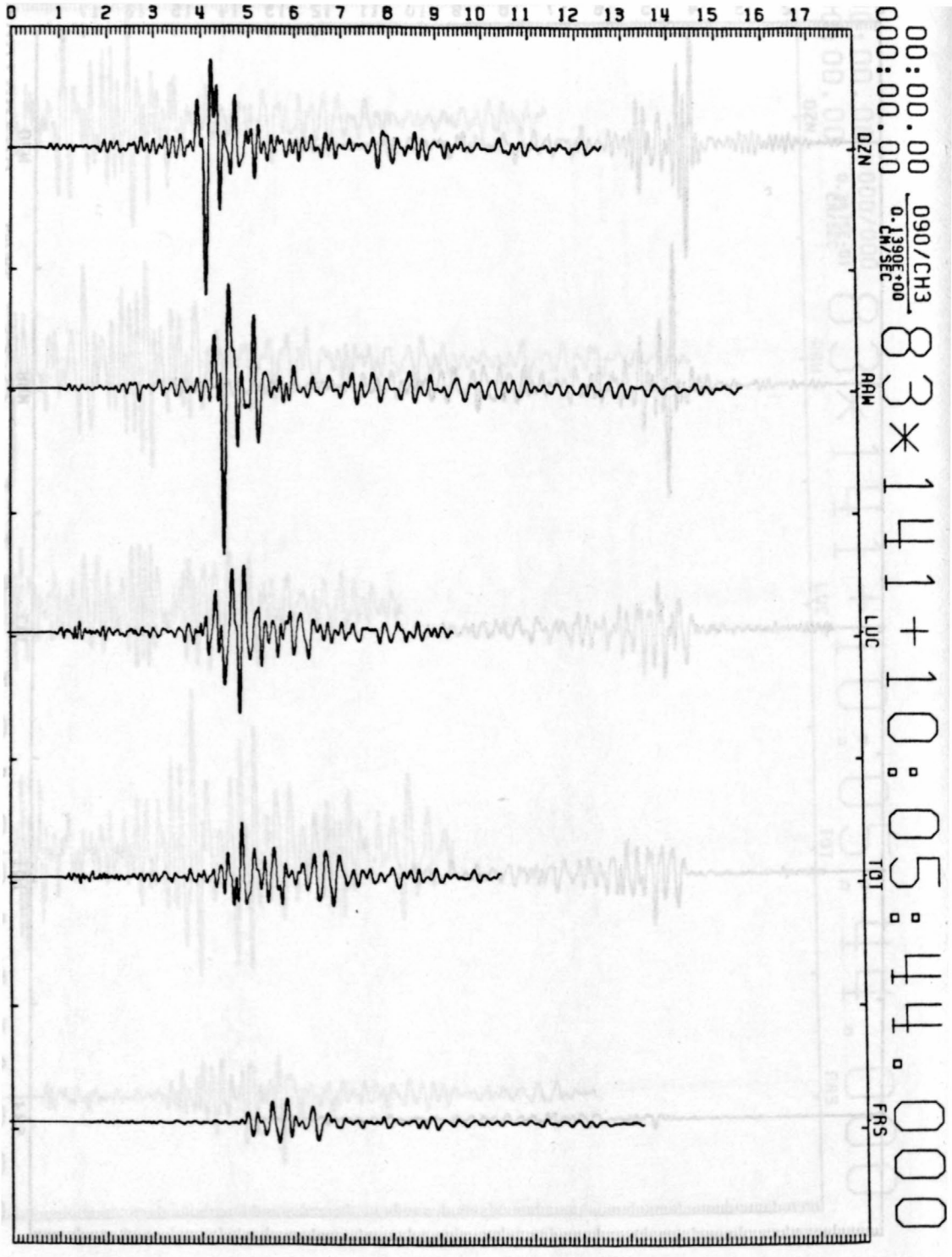

Figure 3c. North-south component of ground velocity recorded at five stations for event 141 1005.

Table 2. Maximum and normalized peak-to-peak amplitudes recorded on Coalinga array ($M \geq 2.5$).

Event ID	Station ID	Maximum cm/s Z	Maximum cm/s NS	Maximum cm/s EW	Normalized (FRS) Z	Normalized (FRS) NS	Normalized (FRS) EW
140 0741 M = 3.0							
	LUC	.013	.022	.024	1.5	2.8	2.0
	TOT	.015	.017	.015	1.8	2.3	1.3
	FRS	.0077	.007	.011	1.0	1.0	1.0
140 1101 M = 3.2							
	AAW	.041	.077	.095	1.5	3.4	4.2
	LUC	.042	.042	.057	1.7	2.1	2.9
	TOT	.070	.057	.044	3.1	3.1	2.3
	FRS	.022	.018	.018	1.0	1.0	1.0
140 1222 M = 3.0							
	AAW	.032	.14	.15	1.6	9.6	4.4
	LUC	.034	.061	.090	1.9	4.6	2.9
	TOT	.042	.042	.048	2.5	3.3	1.6
	FRS	.016	.012	.028	1.0	1.0	1.0
141 1005 M = 3.2							
	AAW	.060	.29	.31	1.6	13.2	5.2
	DZN	.062	.27	.28	1.6	12.5	4.7
	LUC	.052	.097	.17	1.5	4.9	3.2
	TOT	.081	.092	.10	2.4	4.8	1.9
	FRS	.032	.018	.049	1.0	1.0	1.0
141 1629 M = 2.6							
	AAW	.026	.078	.073	3.4	14.0	11.5
	TOT	.016	.026	.013	2.5	5.5	2.4
	FRS	.0060	.0044	.0050	1.0	1.0	1.0
141 2000 M = 3.0							
	AAW	.058	.11	.13	1.9	3.1	3.6
	DZN	.050	.13	.11	1.7	3.7	3.2
	CDF	.054	.15	.17	1.9	4.5	5.1
	LUC	.063	.086	.13	2.4	2.8	4.2
	TOT	.056	.073	.070	2.2	2.5	2.4
	FRS	.023	.027	.027	1.0	1.0	1.0

Table 2. (Continued)

Event ID	Station ID	Maximum Z	Maximum NS cm/s	Maximum EW	Normalized (FRS) Z	Normalized (FRS) NS	Normalized (FRS) EW
142 0839 M = 4.3							
	AAW	.30	.70	.98	1.6	1.4	3.0
	DZN	.33	.75	.82	1.8	1.5	2.6
	LUC	.32	.94	.78	1.9	2.1	2.7
	TOT	.44	.96	.52	2.7	2.2	1.8
	FRS	.16	.41	.27	1.0	1.0	1.0
142 2103 M = 2.8							
	DZN	.050	.049	.076	6.3	5.4	7.5
	CDF	.039	.032	.063	5.2	3.7	6.4
	LUC	.035	.026	.047	4.7	3.1	4.9
	TOT	.044	.028	.055	6.1	3.4	5.9
	FRS	.0070	.0080	.0090	1.0	1.0	1.0
143 0925 M = 3.1							
	AAW	.013	.023	.013	1.3	3.8	2.4
	TOT	.036	.016	.015	4.3	3.1	3.2
	FRS	.0080	.0050	.0045	1.0	1.0	1.0
Average							
	AAW				1.8±0.7	6.9±5.2	4.9±3.0
	DZN				2.9±2.3	5.8±4.8	4.5±2.2
	CDF				3.6±2.3	4.1±0.6	5.8±0.4
	LUC				2.2±1.1	3.2±1.1	3.3±1.4
	TOT				3.1±1.3	3.4±1.1	2.5±1.4

and figure 1). Event 142 0839 is of larger magnitude (M_L 4.3 vs 3), comparable depth, comparable distance, and along a more easterly azimuth more in line with the long axis of the alluvial basin. In the case of the magnitude 4.3 event (142 0839), the variations in normalized amplitudes from those for events 140 1222 and 141 1005 suggest that source location with respect to syncline axis may be a significant factor in relative ground response observed on the array.

Averages computed at each site for the nine events with $M_L \geq 2.5$ (table 2) suggest the amplifications of vertical motion increase with decreasing thickness of alluvium with the largest amplifications occurring at the margin of the basin. Inversely, the horizontal amplifications increase with increasing thickness and are largest for the sites in Coalinga.

Examples of the Fourier amplitude spectra scaled to the hypocentral distance of station FRS are shown for three components of acceleration generated by the magnitude 4.3 event for station AAW (downtown Coalinga) (figure 4a) and station FRS (figure 4b). Inspection of the amplitude spectra computed for all of the recorded time histories suggests that a seismic signal level significantly above the seismic noise level can be expected in the frequency bandwidth of 0.5-25 Hz.

Instrumentation response curves computed from calibration signals automatically recorded at each of the stations provide an accurate means of estimating variations in observed amplitude due to variations in instrumentation response at the time events are recorded. Examples of the instrumentation response to a step function in acceleration applied to the velocity transducers for stations AAW and FRS are illustrated in figures 5a and 5b. Comparison of the curves shows that the amplitude response for the systems are similar, but subtle variations suggest that instrument calibration

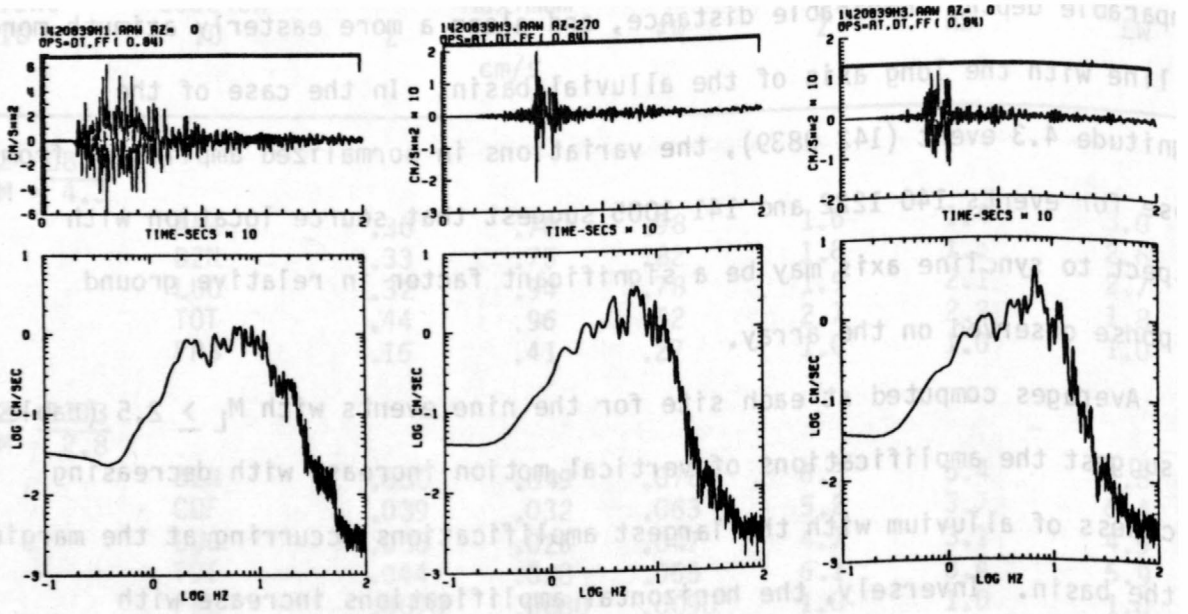

Figure 4a. Fourier amplitude and acceleration time histories for the three components of ground acceleration recorded at site AAW in Coalinga (figure 4a) and at the rock site FRS (figure 4b).

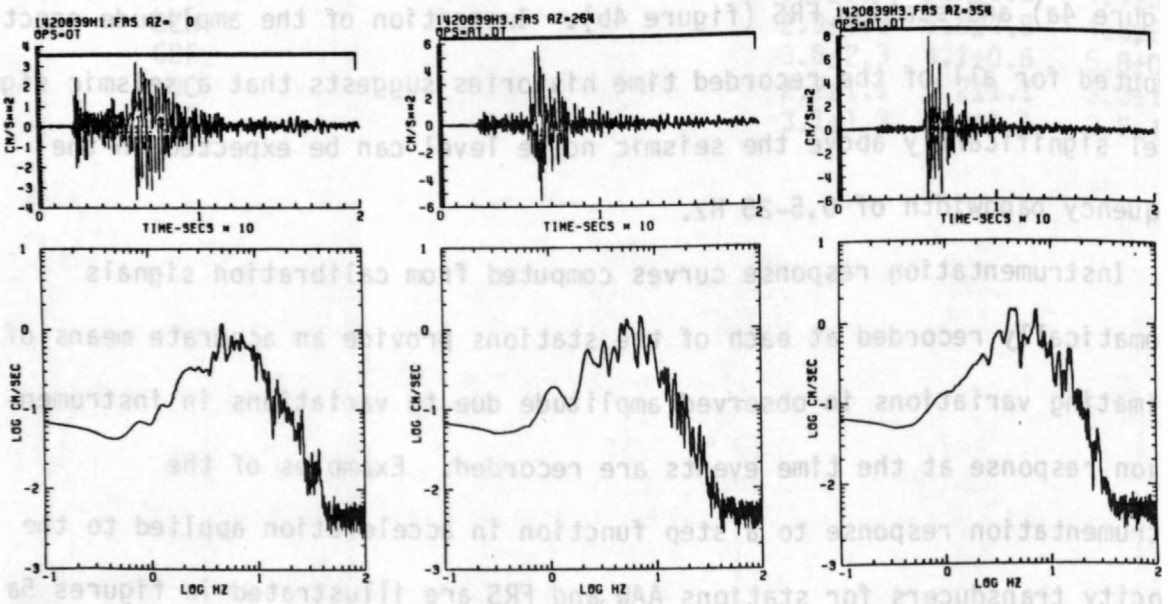

Figure 4b. Fourier amplitude and acceleration time histories for the three components of ground acceleration recorded at site AAW in Coalinga (figure 4a) and at the rock site FRS (figure 4b).

at the time of data recovery is useful for comparative ground motion measurements. Previous comparative studies by Borcherdt (1970) using analog instrumentation have shown a similar result.

SPECTRAL AMPLIFICATIONS

To better isolate the effects of local site conditions from those of sensor, recording instrument, seismic source, and propagation path, Fourier amplitude spectral ratios (slightly smoothed) were computed with respect to station FRS underlain by sandstone. To account for variations in amplitude due to geometrical spreading the amplitude spectra were scaled to correspond to the hypocentral distance of station FRS. Examples of the vertical component spectral ratios are shown for two magnitude 3 events (140 1222 and 141 1005) and the magnitude 4.3 event (142 0839) (in figure 6). The radial and transverse component spectral ratios for these events are shown in figures 7 and 8, respectively.

The spectral ratios for the two magnitude 3 events (140 1222 and 141 1005) which occurred in about the same location (see figure 1) are very nearly the same for each of the sites, especially for frequencies less than 15 Hz (compare figures 6a and 6b, 7a and 7b, and 8a and 8b). However, the spectral ratios for the magnitude 4.3 event (142 0839) when compared to those for the magnitude 3 events show significant variations as a function of frequency with evidence for possible resonances, especially for frequencies greater than 5 Hz (compare figures 6b and 6c, 7b and 7c, and 8b and 8c). The variations in the spectral ratios shown for the three events suggests that the high-frequency response (> 5 Hz) of the soil sites is strongly dependent on both source location and near-surface velocity structure pertinent to various propagation paths. A more detailed interpretation of the spectral ratios must await

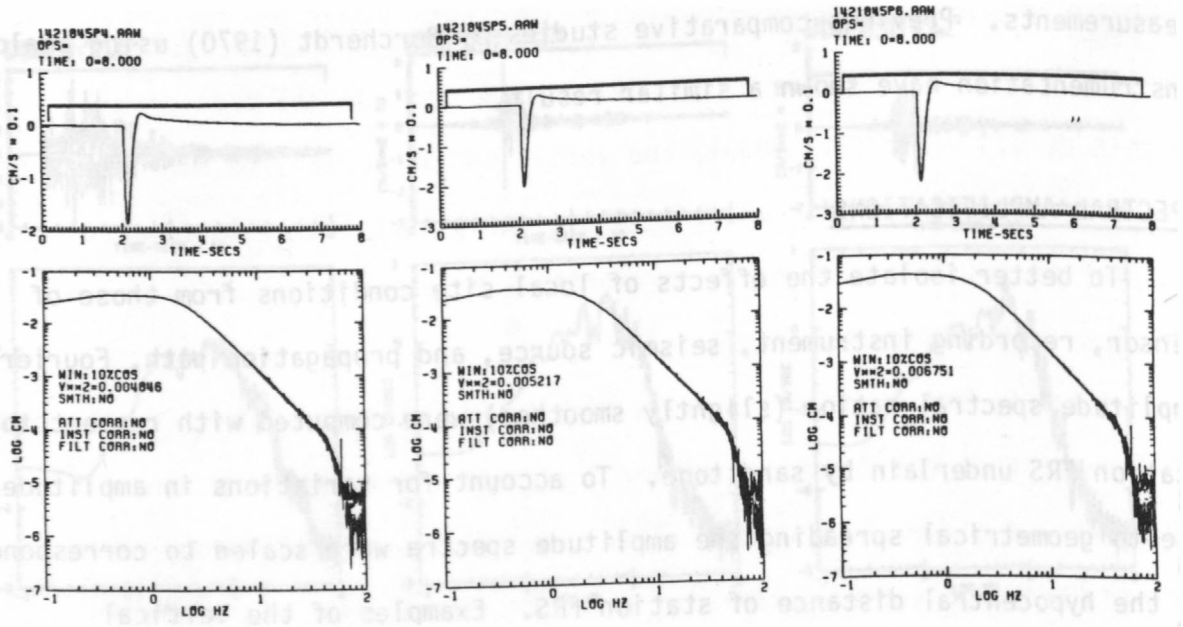

Figure 5a. Time history and Fourier amplitude response of GEOS recording system to step function in acceleration applied to velocity transducer automatically in the field at stations AAW (figure 5a) and FRS (figure 5b).

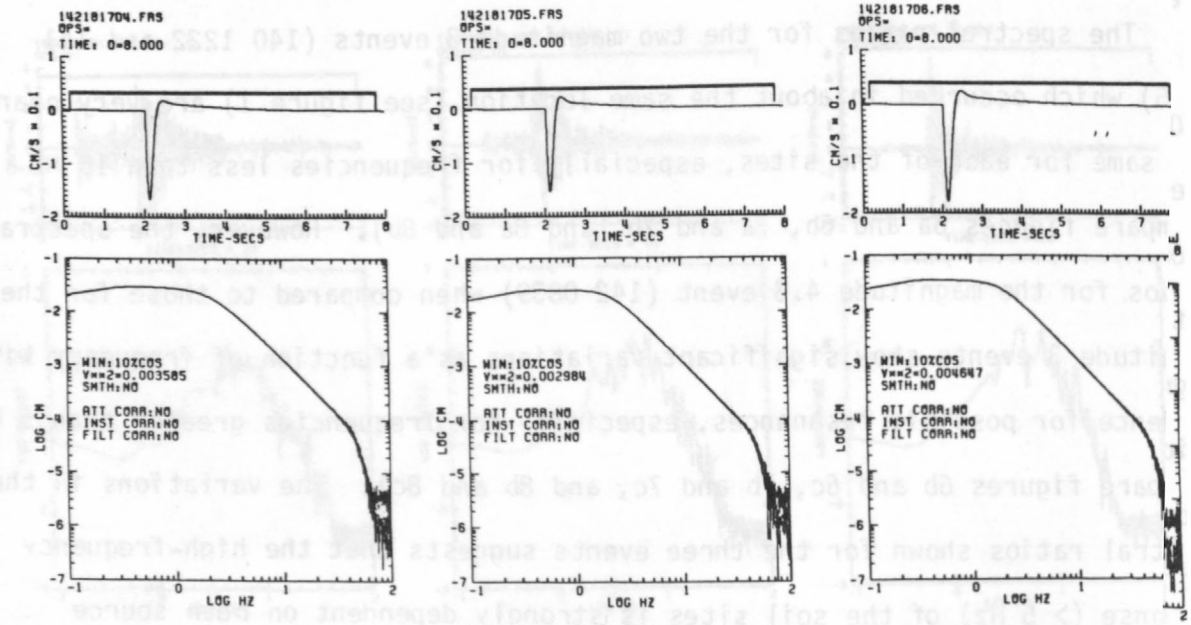

Figure 5b. Time history and Fourier amplitude response of GEOS recording system to step function in acceleration applied to velocity transducer automatically in the field at stations AAW (figure 5a) and FRS (figure 5b).

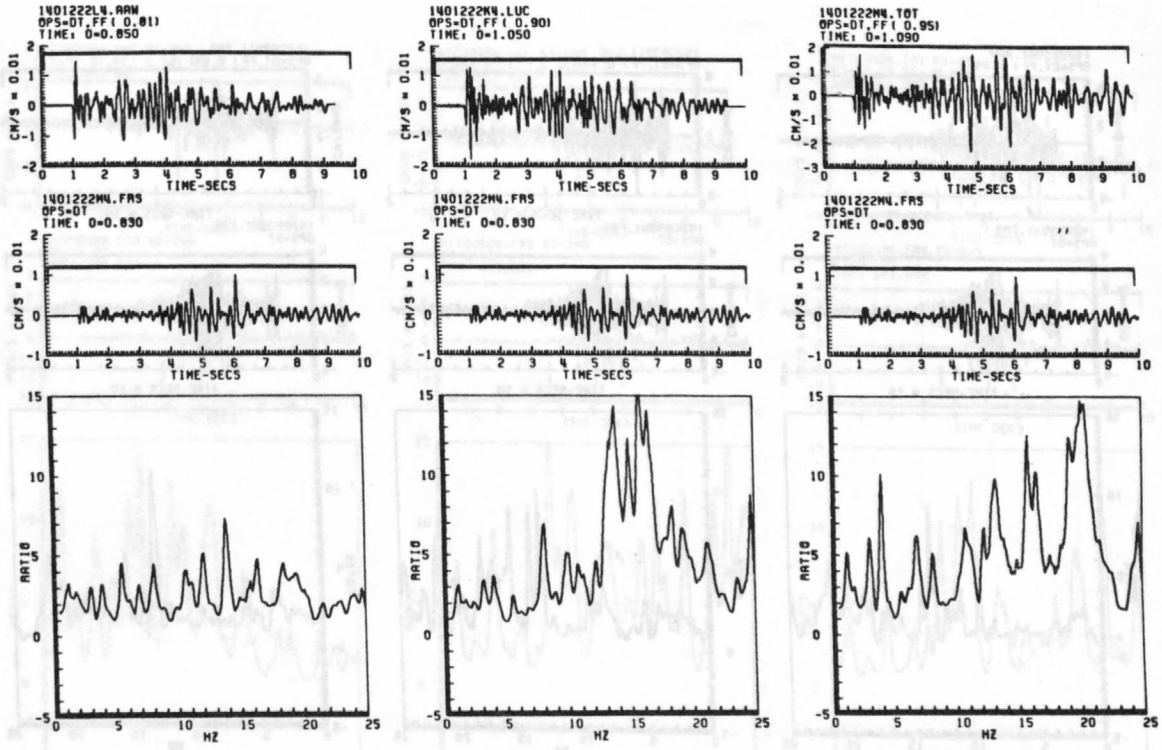

Figure 6a. Time histories and amplitude spectral ratios computed for vertical component of motion at sites AAW, LUC, and TOT generated by event 1222 (figure 6a), event 1005 (figure 6b) and event 0839 (figure 6c).

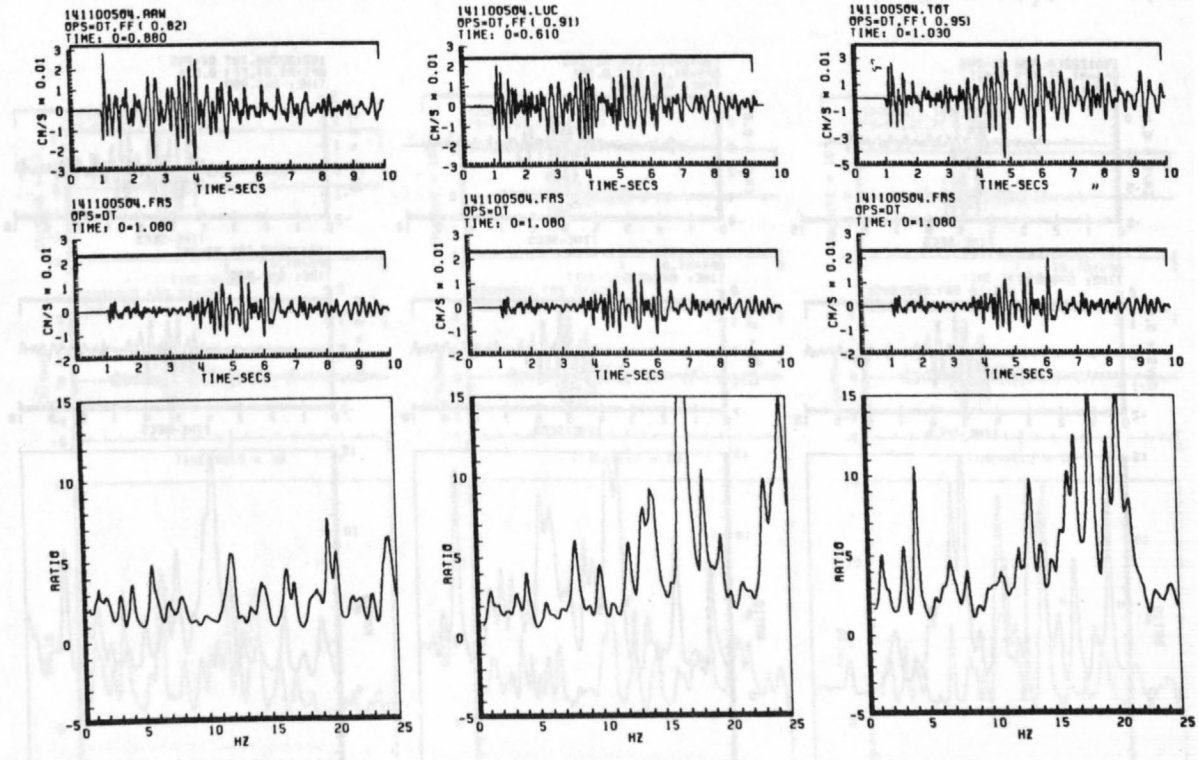

Figure 6b. Time histories and amplitude spectral ratios computed for vertical component of motion at sites AAW, LUC, and TOT generated by event 1222 (figure 6a), event 1005 (figure 6b) and event 0839 (figure 6c).

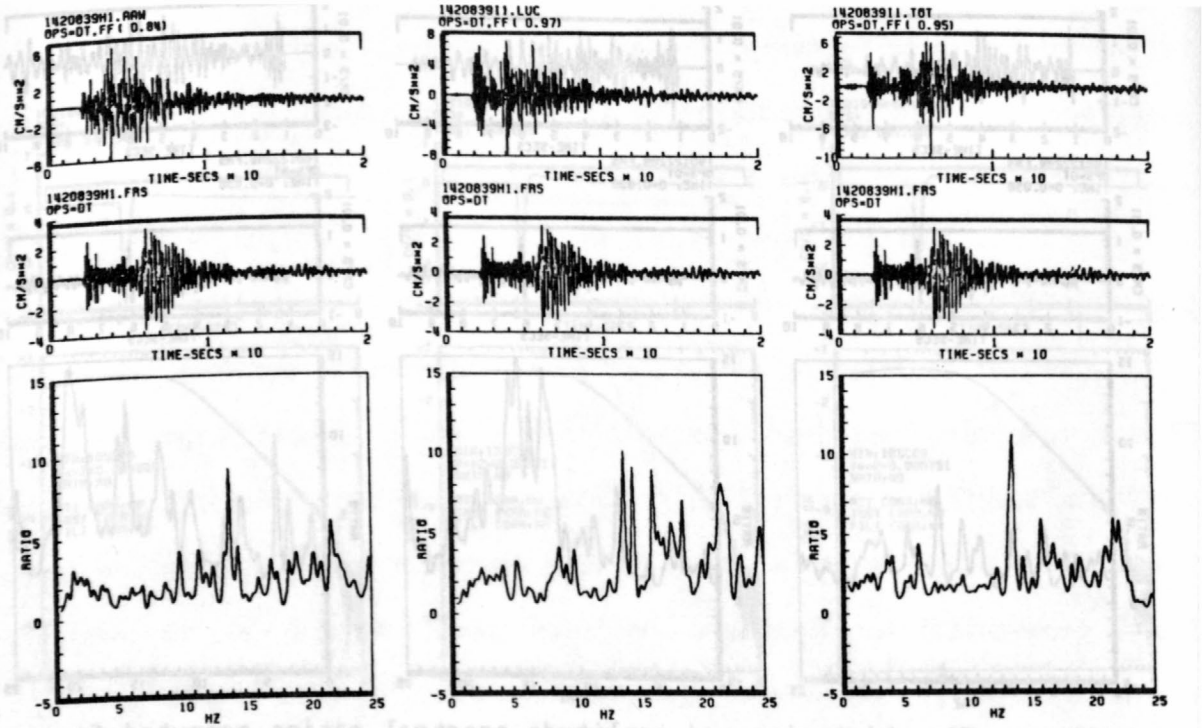

Figure 6c. Time histories and amplitude spectral ratios computed for vertical component of motion at sites AAW, LUC, and TOT generated by event 1222 (figure 6a), event 1005 (figure 6b) and event 0839 (figure 6c).

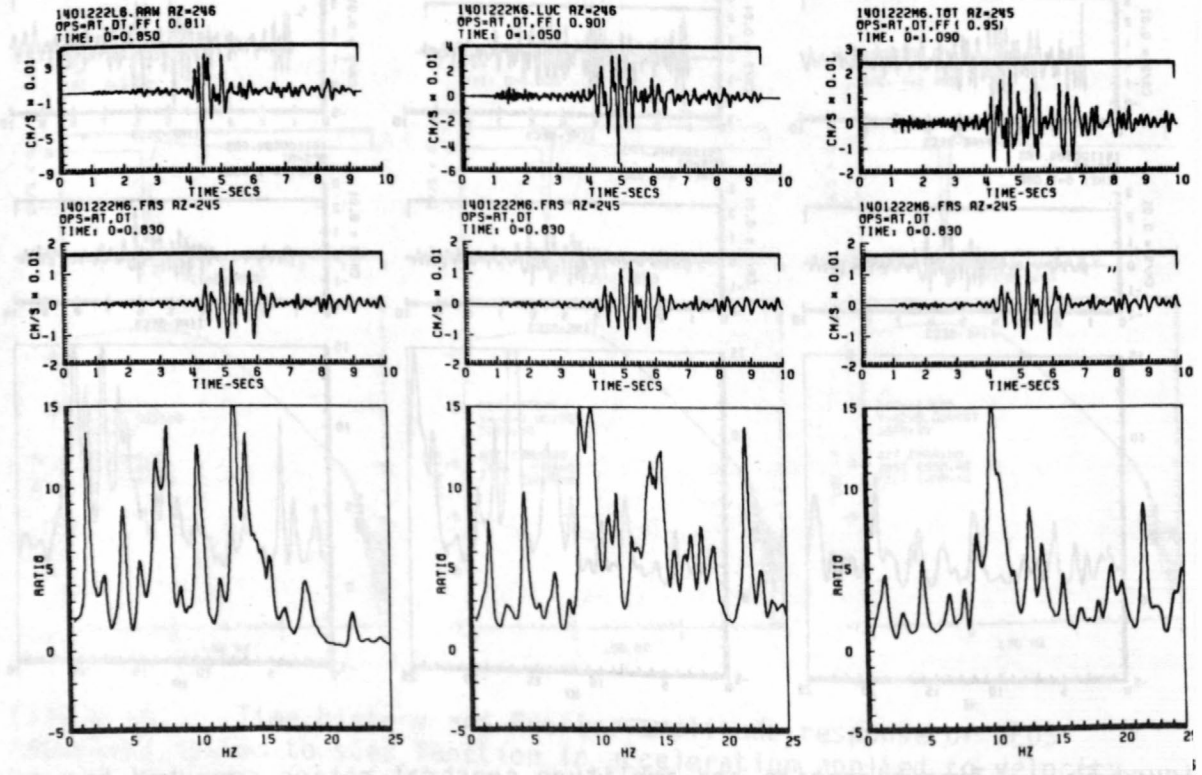

Figure 7a. Time histories and amplitude spectral ratios computed for radial component of motion at sites AAW, LUC, and TOT generated by event 1222 (figure 7a), event 1005 (figure 7b) and event 0839 (figure 7c).

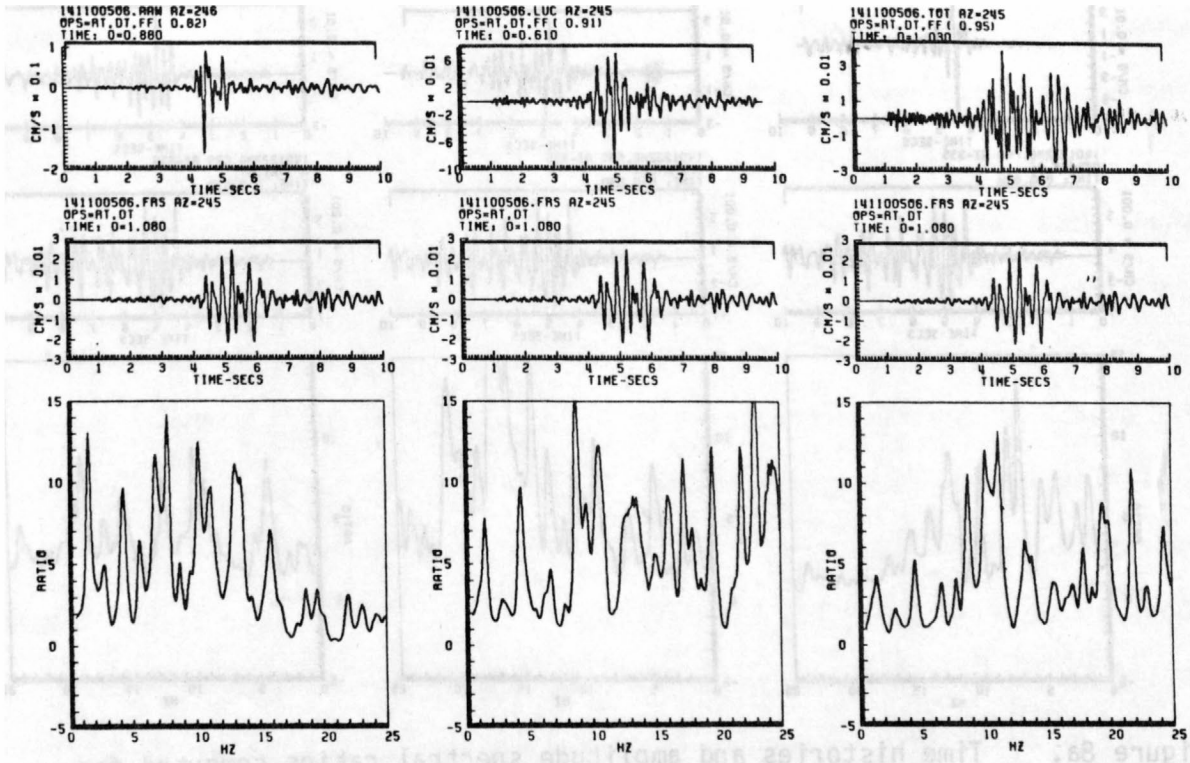

Figure 7b. Time histories and amplitude spectral ratios computed for radial component of motion at sites AAW, LUC, and TOT generated by event 1222 (figure 7a), event 1005 (figure 7b) and event 0839 (figure 7c).

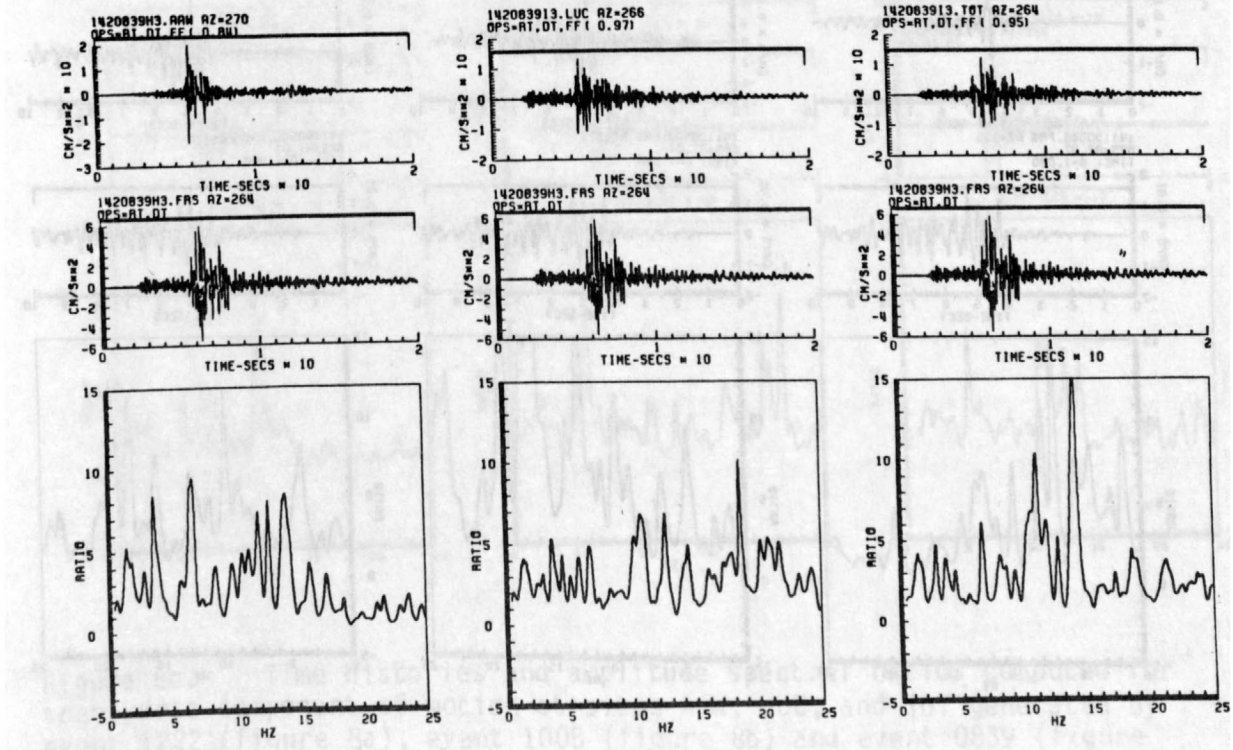

Figure 7c. Time histories and amplitude spectral ratios computed for radial component of motion at sites AAW, LUC, and TOT generated by event 1222 (figure 7a), event 1005 (figure 7b) and event 0839 (figure 7c).

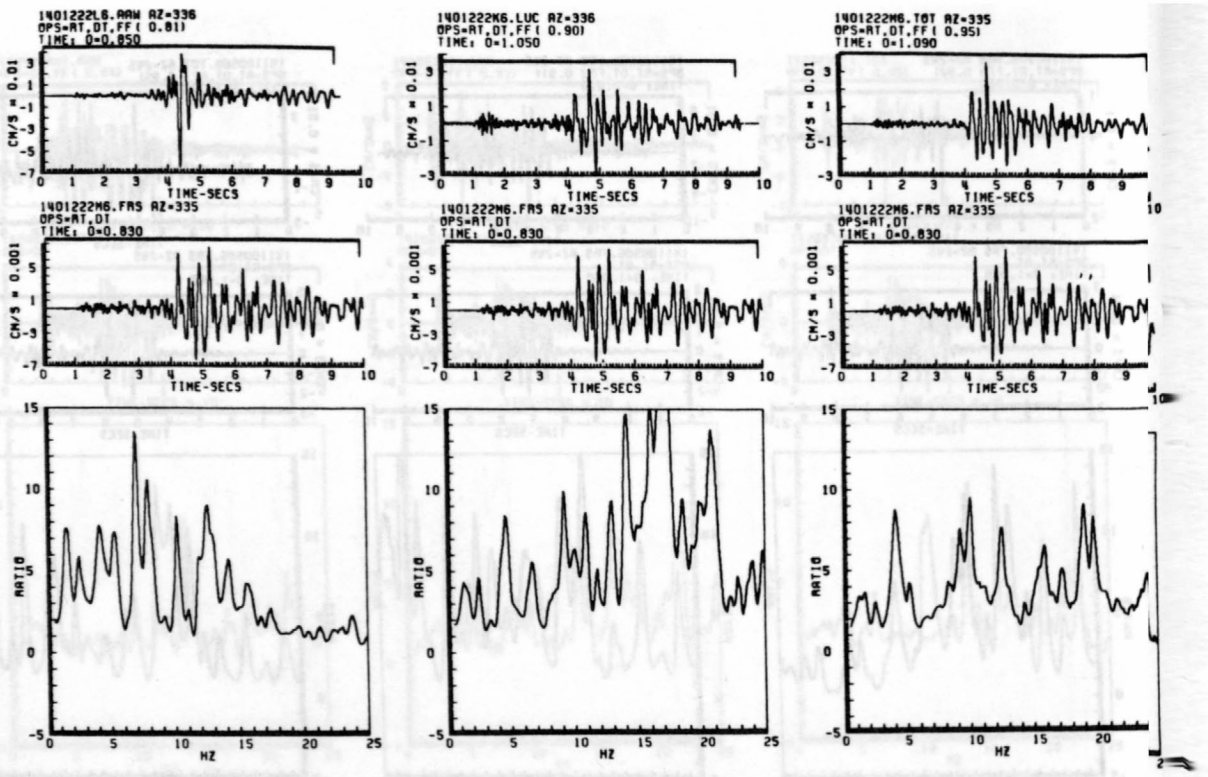

Figure 8a. Time histories and amplitude spectral ratios computed for transverse component of motion at sites AAW, LUC, and TOT generated by event 1222 (figure 8a), event 1005 (figure 8b) and event 0839 (figure 8c).

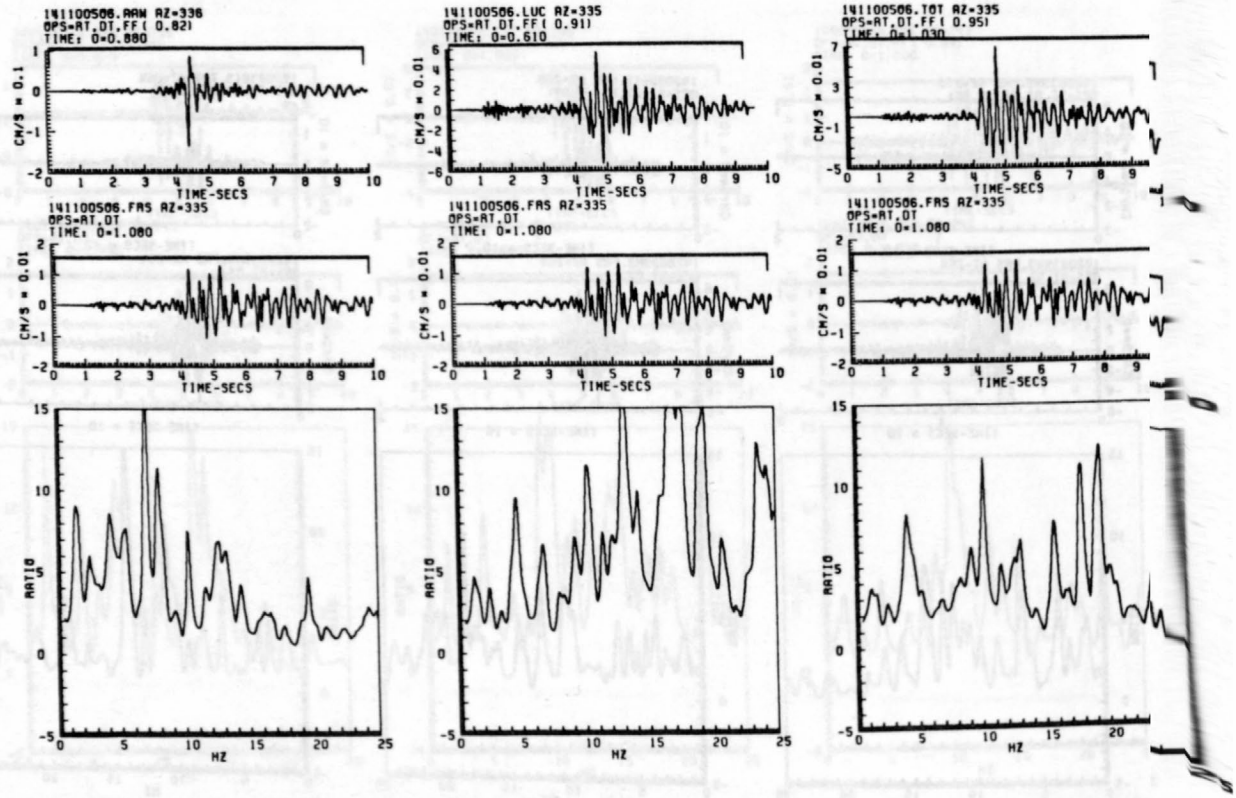

Figure 8b. Time histories and amplitude spetral ratios computed for transverse component of motion at sites AAW, LUC, and TOT generated by event 1222 (figure 8a), event 1005 (figure 8b) and event 0839 (figure 8c).

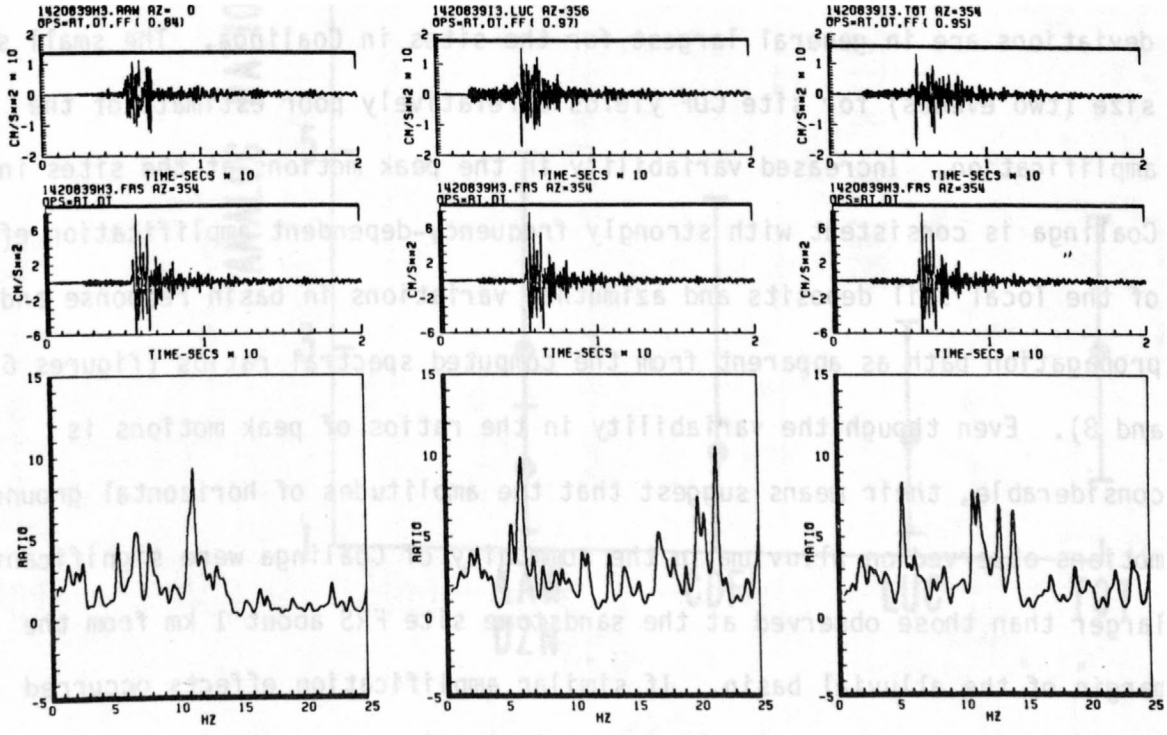

Figure 8c. Time histories and amplitude spectral ratios computed for transverse component of motion at sites AAW, LUC, and TOT generated by event 1222 (figure 8a), event 1005 (figure 8b) and event 0839 (figure 8c).

compilation of information on near-surface velocity structure, basin geometry and estimates of source radiation characteristics.

To summarize the amplifications observed for a larger sample of events than those for which spectral ratios were computed, means and standard deviations (of the observations about the mean) are plotted for the analog ratios of peak ground motions (table 2) determined relative to station FRS for all events of magnitude greater than 2.5 (figures 9a, 9b, and 9c). The mean amplification ratios suggest that in general the mean horizontal response of the soil sites decreases from about a factor of 5 for the sites in Coalinga to about a factor of 3 for the site TOT on the margin of the basin. Mean analog amplifications of the vertical motion show an inverse relation with the largest amplifications occurring for site TOT.

Uncertainty in the estimates as measured by the computed standard deviations are in general largest for the sites in Coalinga. The small sample size (two events) for site CDF yields a relatively poor estimate of the amplification. Increased variability in the peak motions at the sites in Coalinga is consistent with strongly frequency-dependent amplification effects of the local soil deposits and azimuthal variations in basin response and propagation path as apparent from the computed spectral ratios (figures 6, 7, and 8). Even though the variability in the ratios of peak motions is considerable, their means suggest that the amplitudes of horizontal ground motions observed on alluvium in the community of Coalinga were significantly larger than those observed at the sandstone site FRS about 1 km from the margin of the alluvial basin. If similar amplification effects occurred during the May 2 event, then analog amplifications observed from the aftershocks suggest that the local site conditions beneath Coalinga could have been a contributory factor in the amounts of resultant damage.

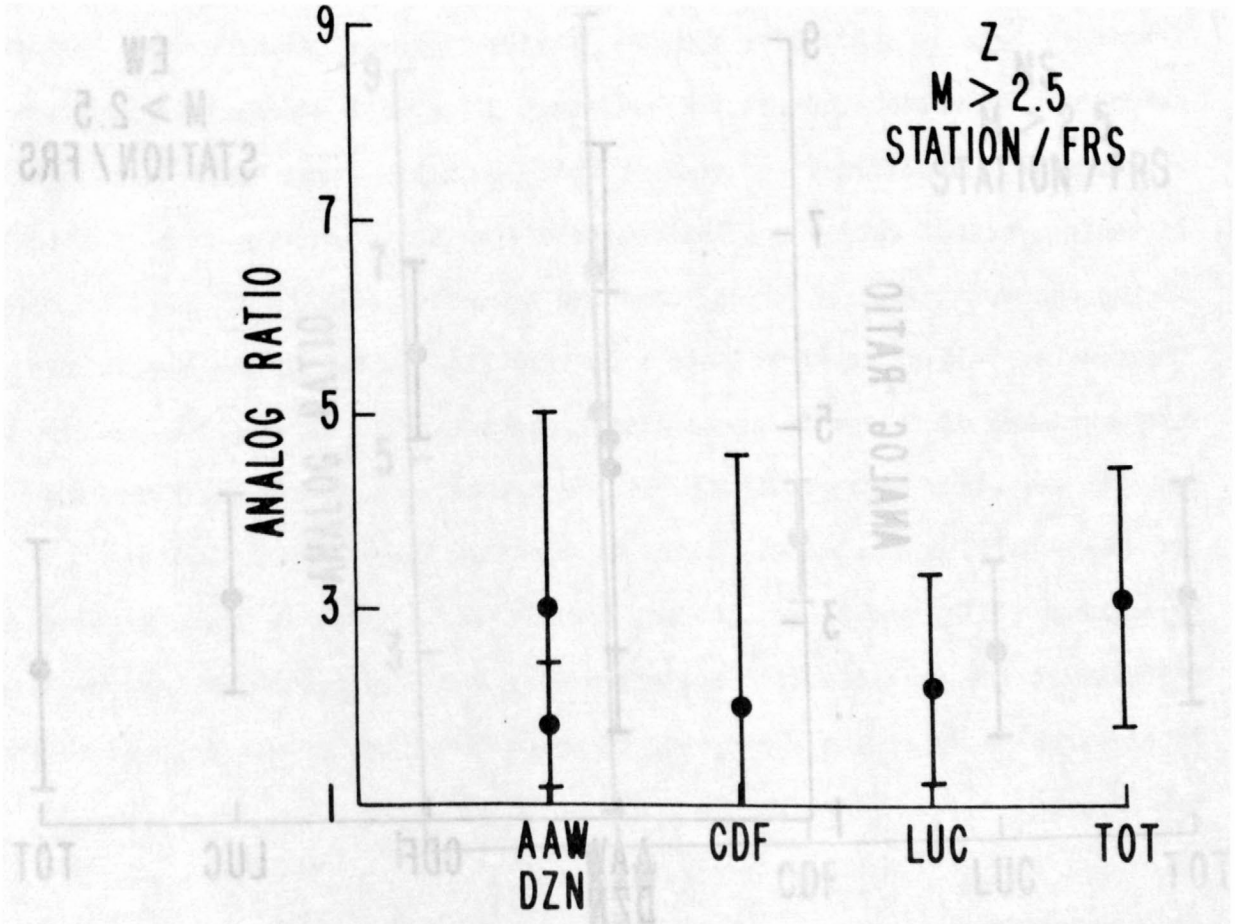

Figure 9a. Mean and standard deviation computed for analog ratios determined from recording of the vertical component of ground motion for events of magnitude greater than 2.5 (table 2). The analog ratios are computed with respect to station FRS with corresponding corrections for geometrical attenuation.

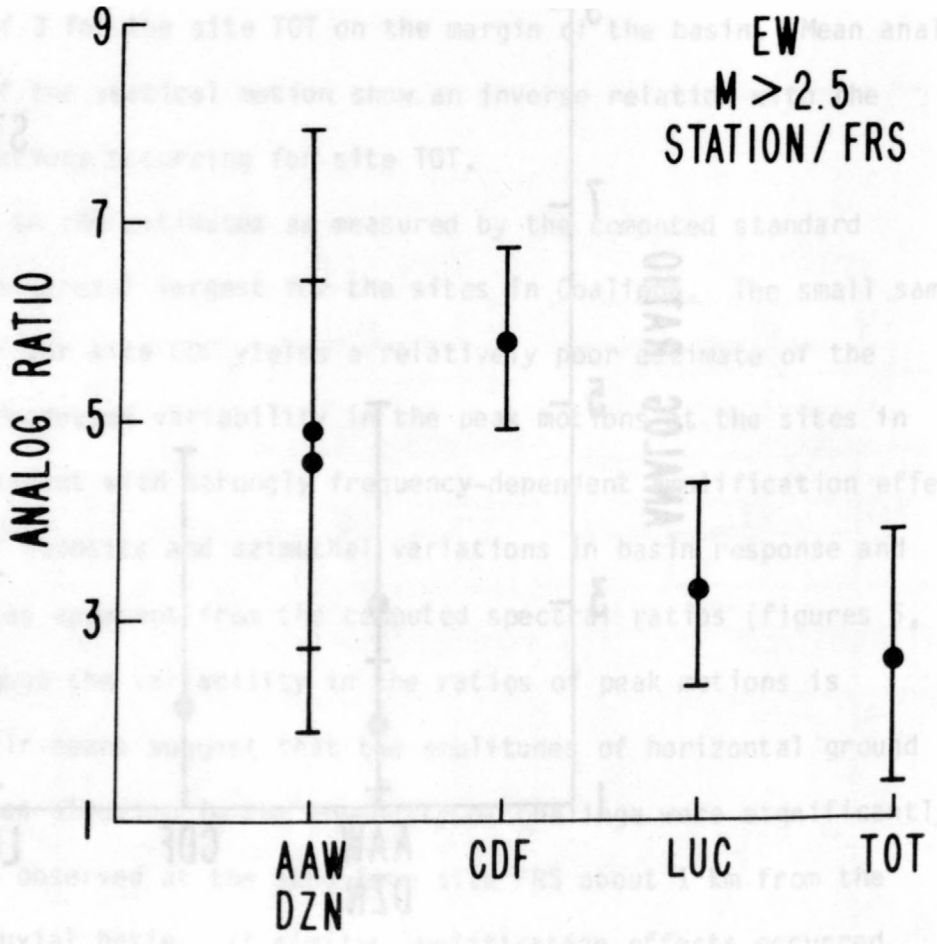

Figure 9b. Mean and standard deviation computed for analog ratios determined from recordings of the east-west horizontal component of ground motion for events of magnitude greater than 2.5 (table 2). The analog ratios are computed with respect to station FRS with corresponding corrections for geometrical attenuation.

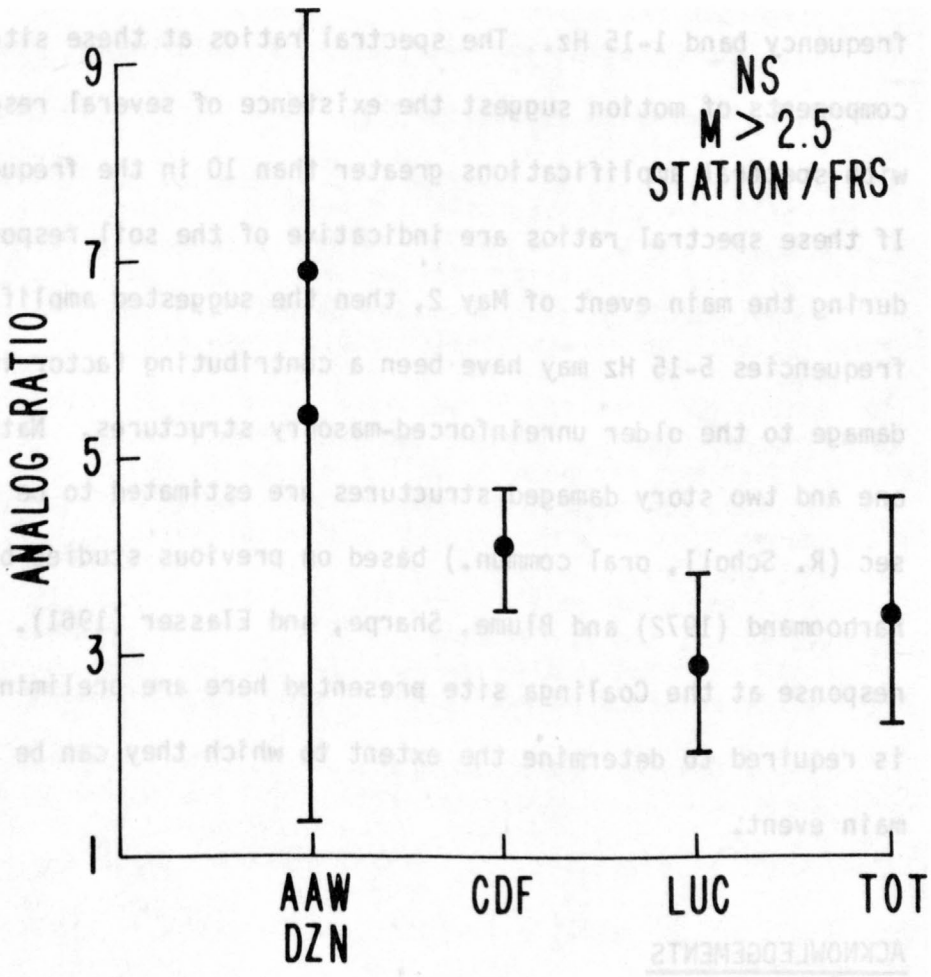

Figure 9c. Mean and standard deviation computed for analog ratios determined from recording of the north-south horizontal component of ground motion for events of magnitude greater than 2.5 (table 2). The analog ratios are computed with respect to station FRS with corresponding corrections for geometrical attenuation.

The spectral ratios computed for three events (figures 6, 7, and 8) suggest that the calculated ground-motion spectra are strongly site and path dependent with large frequency-dependent amplitude variations occurring over relatively short distances (< 1.5 km). Considerable amplification of the higher-frequency part of the spectrum (> 5 Hz) is apparent for the three components of motion at each of the sites.

The spectral ratios for the sites in Coalinga suggest average amplifications over the frequency band, 0.5-25 Hz, of about 2 (vertical), 4 (radial), and 3 (transverse) with larger average amplifications for the frequency band 1-15 Hz. The spectral ratios at these sites for the horizontal components of motion suggest the existence of several resonant frequencies with spectral amplifications greater than 10 in the frequency band 1-15 Hz. If these spectral ratios are indicative of the soil response at this site during the main event of May 2, then the suggested amplification at the higher frequencies 5-15 Hz may have been a contributing factor in the resulting damage to the older unreinforced-masonry structures. Natural periods for the one and two story damaged structures are estimated to be in the range 0.05-0.2 sec (R. Scholl, oral commun.) based on previous studies by Scholl and Farhoomand (1972) and Blume, Sharpe, and Elasser (1961). The estimates of soil response at the Coalinga site presented here are preliminary and further study is required to determine the extent to which they can be extrapolated to the main event.

ACKNOWLEDGEMENTS

The acquisition and analysis of this data set has been made possible by the dedicated efforts of a number of individuals. To mention only a few, G. Maxwell and G. Jensen have made outstanding contributions to the development

of the GEOS system and E. Cranswick has developed analysis procedures without which the timely analysis of this data set would not have been feasible. E. Sembera provided field deployment and data recording expertise. J. Boatwright and D. Boore provided helpful review comments.

REFERENCES

Blume, J. A., R. L. Sharpe, E. Elsasser (1961). A structural dynamic investigation of fifteen school buildings subjected to simulated earthquake motions, Division of Architecture, California.

Borcherdt, R. D. (1970). Effects of local geology on ground motion near San Francisco Bay: Bulletin of the Seismological Society of America, vol. 60, no. 1, pp. 29-61, February 1970.

Borcherdt, R. D., E. Cranswick, G. Maxwell, C. Mueller, R. McClearn, G. Sembera, and L. Wennerberg (1983). Digital strong motion data recorded by U.S. Geological Survey near Coalinga, California, in U.S. Geological Survey Open-File Report 83-511.

Borcherdt, R. D., J. B. Fletcher, C. W. Eckels, R. C. Brodine, J. R. Van Schaack, and R. E. Warrick (1979). A General Earthquake Observation System (GEOS-I), EOS, American Geophysical Union Transactions, v. 60, p. 889.

Eaton, J. P. (1983). Seismic setting, location and focal mechanism of the May 2, 1983, Coalinga earthquake in U.S. Geological Survey Open-File Report 83-511.

Scholl, R. E., and I. Farhoomand (1972). Observed dynamic response characteristics of residential structures: Project Trinidad, Report JAB-99-89, John A. Blume Associates, Engineers, San Francisco, California.

SOME STUDIES CONCERNING SITE RESPONSE:

PART 1. PRELIMINARY ANALYSIS OF PARKFIELD ARRAY RECORDINGS OF THE COALINGA EARTHQUAKE

PART 2. STABILITY OF EMPIRICAL ESTIMATES OF SITE RESPONSE

by

David M. Boore
Allan G. Lindh
U.S. Geological Survey
Menlo Park, California

Brian E. Tucker
Anthony F. Shakal
Richard D. McJunkin
California Division of Mines and Geology
Sacramento, California

INTRODUCTION

This paper has two purposes: to give a preliminary interpretation of accelerograms recorded during the recent Coalinga earthquake, with special emphasis on those recorded on the Parkfield accelerograph array, and to comment on the empirical determination of local site amplification using sources of varying location and strength. There is a link between the two parts of the paper, for sensitive seismometers have been co-located with accelerographs in the Parkfield array with the intent that site variations observed from small aftershocks and other earthquakes can be compared with those from the main shock.

While it is widely recognized that local site effects can be large, the degree to which they are stable from earthquake to earthquake is controversial. They may vary as a result of many factors, including differing amplitudes of motion, wave types, approach azimuth, and angle of incidence. It is important to settle this controversy concerning the stability of empirically-determined site response because this would tell us to what extent measurements of site effects based on observations of weak motions can be used to predict site

effects which will be present during future strong motions. The present paper summarizes two studies which have attempted to measure the stability of site effects (one in the Imperial Valley of California and the other near Garm, USSR) and describes a third such experiment which we are presently conducting on the dense Parkfield array.

PRELIMINARY ANALYSIS OF PARKFIELD ARRAY RECORDINGS

The Parkfield Strong-Motion array, described in McJunkin and Shakal (1983), consists of 47 SMA-1 accelerographs deployed along and perpendicular to the San Andreas fault, within a radius of about 20 km of the town of Parkfield in central California (Figure 1). The instruments are grouped into 4 more or less linear arrays called "limbs" that are perpendicular to the San Andreas fault and into several linear groups of instruments within or near the fault zone (termed, appropriately enough, "fault zone stations"). The purpose of this array is to aid in the study of ground motion attenuation, local site effects, and earthquake source mechanics. Parkfield is a good setting for such studies because site conditions are variable and moderate-sized earthquakes have occurred there every 15-30 years over the last century.

The general geologic setting of the array is shown in Figure 1. The key thing to remember is that the array straddles a geologically complex region. Mesozoic rocks predominate to the east of the fault zone and younger Cenozoic rocks predominate to the west. The fault zone itself is probably bounded on the west by an unnamed fault (dashed in Figure 1, as is another fault farther to the west with over 1 km of relief in the crystalline basement). Quaternary deposits occur within the fault zone and along the western profile of the Cholame Limb. The depths may vary substantially. Slivers of Mesozoic rocks

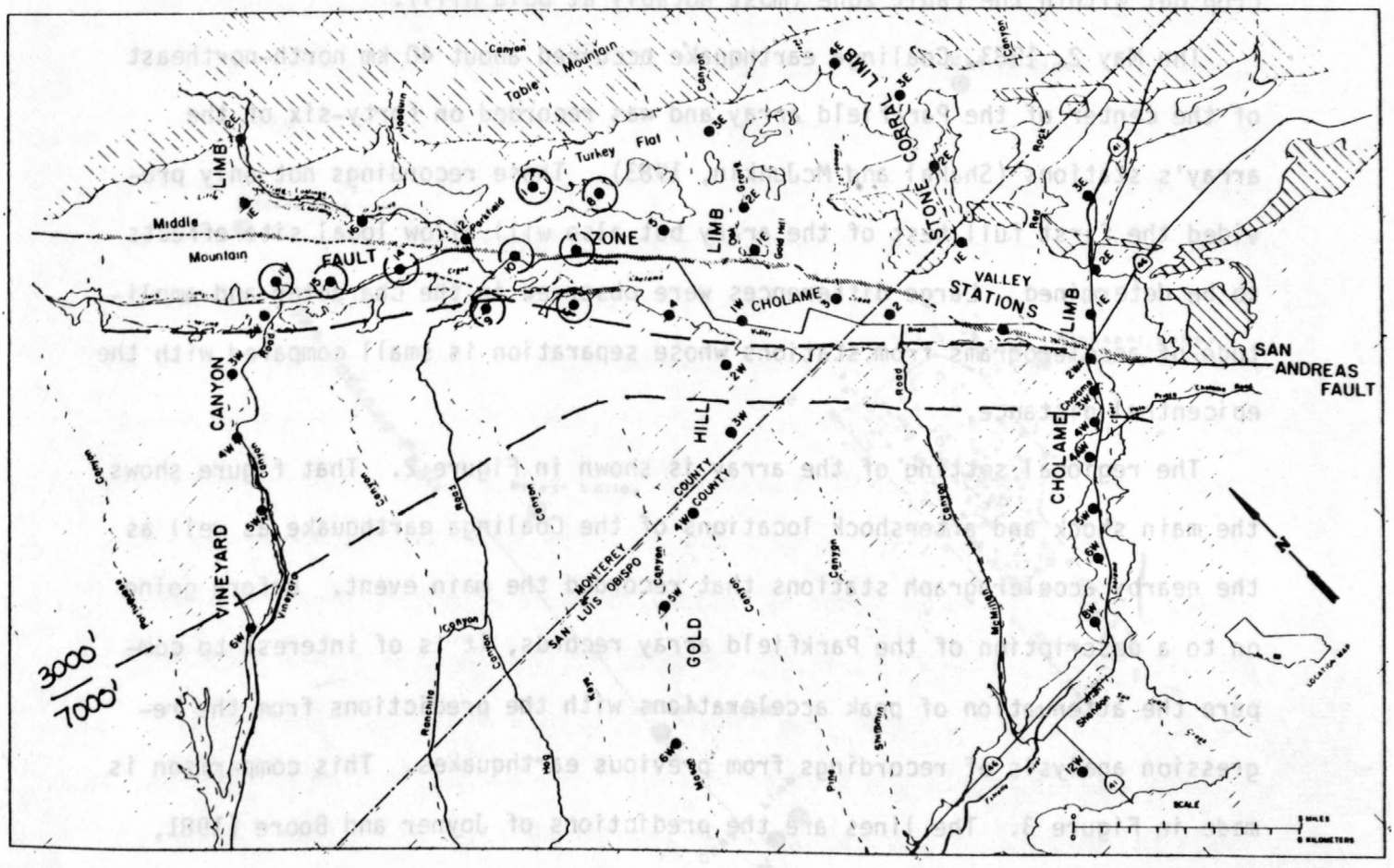

Figure 1.--Generalized geology along the San Andreas fault and CDGM Parkfield strong-motion array. The array consists of one profile of stations parallel to the San Andreas fault zone and four profiles (Cholame, Stone Corral, Gold Hill, and Vineyard Canyon) perpendictular to the fault. The trace of the 1966 Parkfield earthquake is indicated (after Brown and Vedder, 1967; Brown, 1970). Geological data are modified after Jennings (1958), Dickenson (1966a,b), Hanna et al., (1972), and Dibblee (1973). Accelerograms of the Coalinga earthquake which were recorded at the stations that are circled are presented in Figures 6-8. This Figure is from Shakal and McJunkin (1983) and McJunkin and Shakal (1983).

crop out within the fault zone (most notably at Gold Hill).

The May 2, 1983, Coalinga earthquake occurred about 40 km north-northeast of the center of the Parkfield array and was recorded on forty-six of the array's stations (Shakal and McJunkin, 1983). These recordings not only provided the first full test of the array but also will allow local site effects to be determined. Large differences were observed in the character and amplitude of accelerograms from stations whose separation is small compared with the epicentral distance.

The regional setting of the array is shown in Figure 2. That figure shows the main shock and aftershock locations of the Coalinga earthquake as well as the nearby accelerograph stations that recorded the main event. Before going on to a description of the Parkfield array records, it is of interest to compare the attenuation of peak accelerations with the predictions from the regression analysis of recordings from previous earthquakes. This comparison is made in Figure 3. The lines are the predictions of Joyner and Boore (1981, 1982). In general the data fall within the bounds expected from previous experience. There is a tendency for the Coalinga data to be somewhat higher than the predicted mean. This is not at all surprising, for the predicted mean is based on data from many earthquakes; the data from any one earthquake would be expected to be systematically above (or below) the mean curve. The results in Figure 3 are preliminary for several reasons: first, the moment magnitude, used as an independent variable by Joyner and Boore, was not available for the Coalinga earthquake at the time of writing. Second, the surface projection of the rupture surface, needed in measuring distances from source to recording station, was not known when the figure was prepared. Based largely on the aftershock distribution, the dashed outline in Figure 2 was assumed to corre-

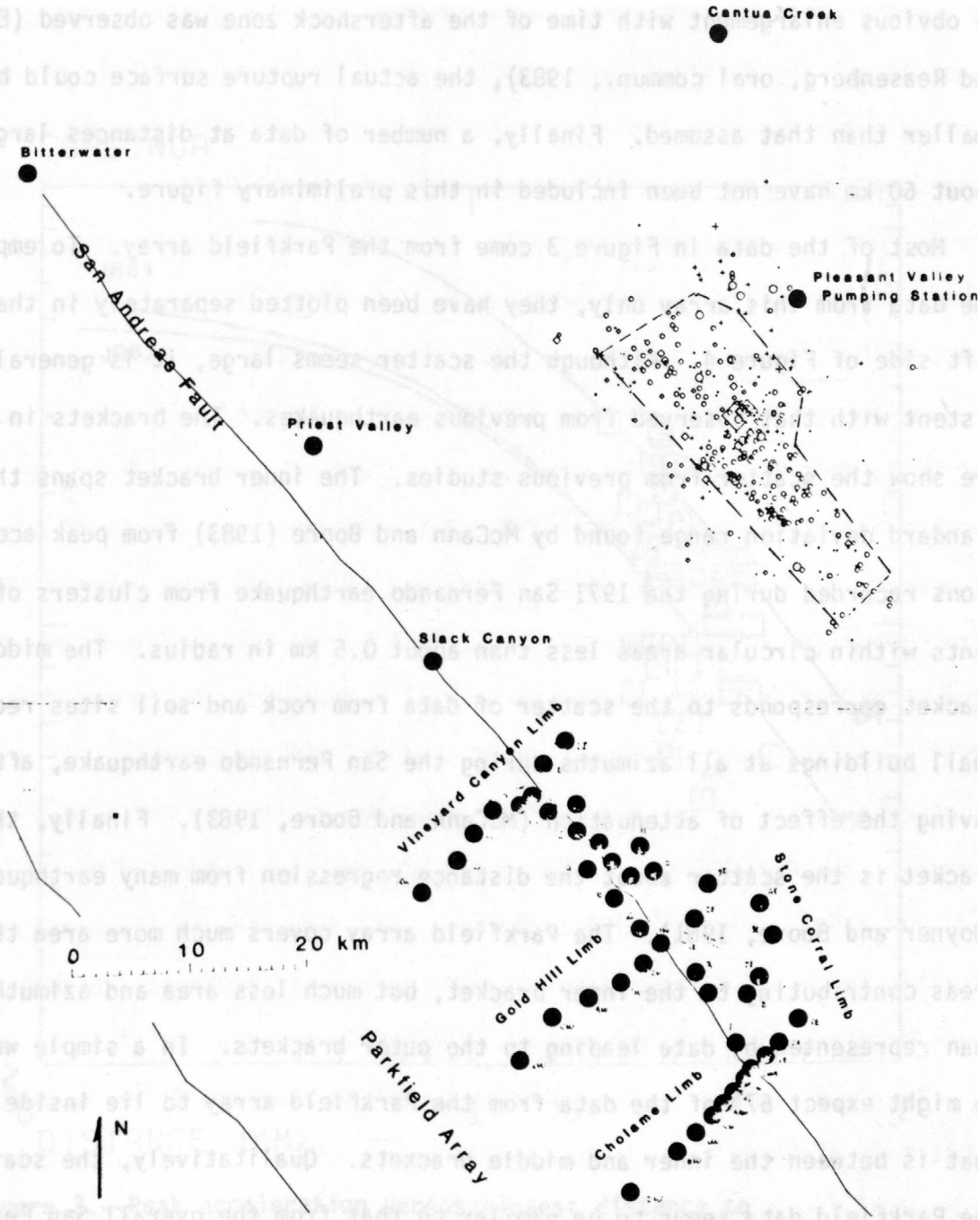

Figure 2.--Accelerograph sites (solid dots) and aftershocks of the Coalinga earthquake (open symbols). The epicenter of the main shock is shown by the large diamond. The dashed line is the postulated surface projection of the rupture surface.

spond to the surface projection. Although, in contrast to many earthquakes, no obvious enlargement with time of the aftershock zone was observed (Eaton and Reasenberg, oral commun., 1983), the actual rupture surface could be smaller than that assumed. Finally, a number of data at distances larger than about 60 km have not been included in this preliminary figure.

Most of the data in Figure 3 come from the Parkfield array. To emphasize the data from this array only, they have been plotted separately in the upper left side of Figure 4. Although the scatter seems large, it is generally consistent with that observed from previous earthquakes. The brackets in the figure show the scatter from previous studies. The inner bracket spans the $\pm$ 1 standard deviation range found by McCann and Boore (1983) from peak accelerations recorded during the 1971 San Fernando earthquake from clusters of instruments within circular areas less than about 0.5 km in radius. The middle bracket corresponds to the scatter of data from rock and soil sites recorded in small buildings at all azimuths during the San Fernando earthquake, after removing the effect of attenuation (McCann and Boore, 1983). Finally, the outer bracket is the scatter about the distance regression from many earthquakes (Joyner and Boore, 1981). The Parkfield array covers much more area than those areas contributing to the inner bracket, but much less area and azimuthal range than represented by data leading to the outer brackets. In a simple way, then, we might expect 67% of the data from the Parkfield array to lie inside a bound that is between the inner and middle brackets. Qualitatively, the scatter from the Parkfield data seems to be similar to that from the overall San Fernando data set. For this reason, the scatter in the Parkfield data may be somewhat larger than expected from previous experience (it should be noted, however, that the contribution of distance attenuation to the variance has not been re-

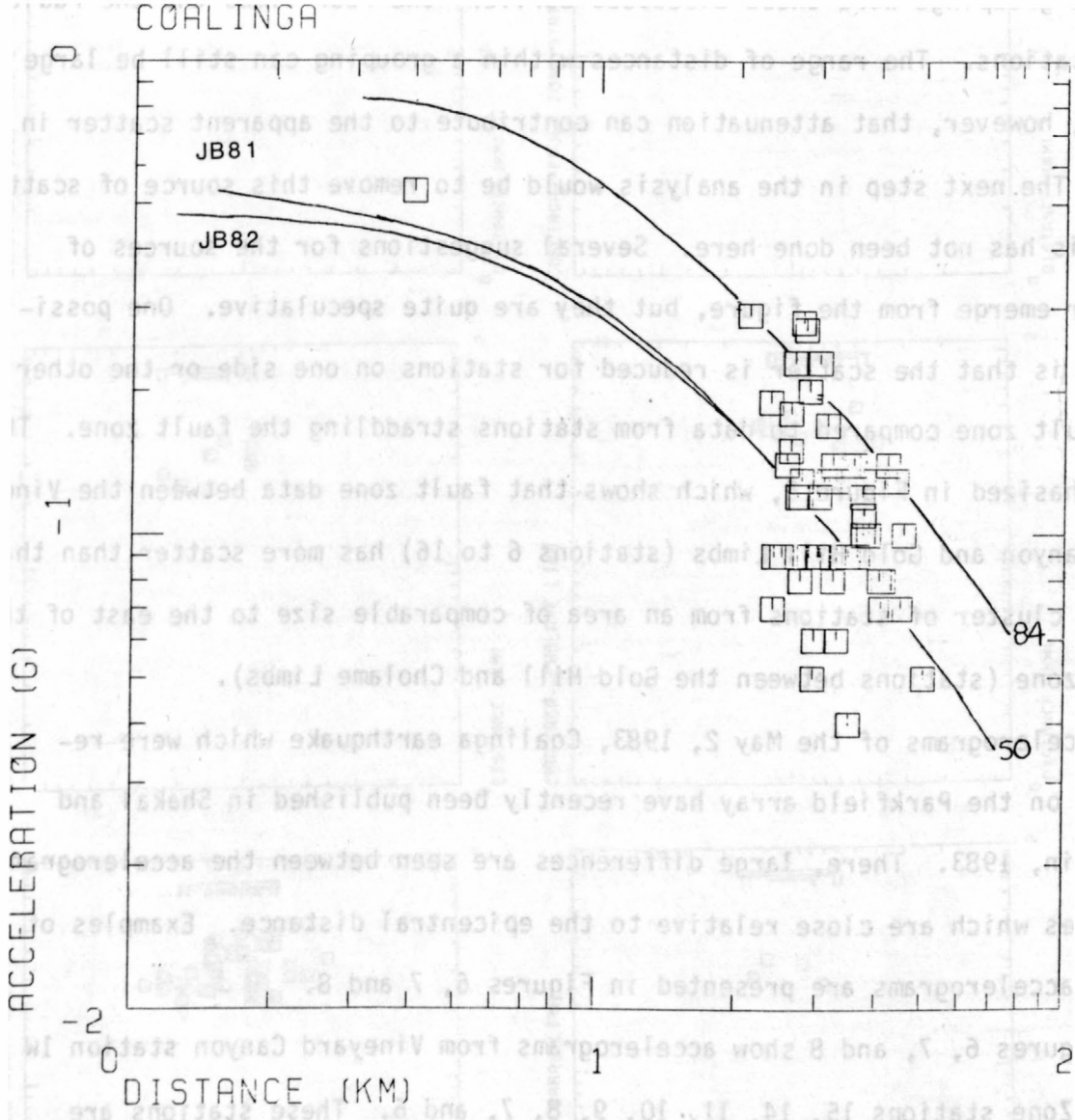

Figure 3.--Peak acceleration versus closest distance to surface projection of the rupture surface. Lines are from the regression studies of data from previous earthquakes (JB81: Joyner and Boore, 1981; JB82: Joyner and Boore 1982). The 50% and 84% confidence limits are shown.

moved from the Parkfield array data in this study).

In a preliminary effort to understand the sources of the scatter, various subgroups of the Parkfield array data were plotted separately (Figure 4). The station groupings were those discussed earlier--the four limbs and the fault zone stations. The range of distances within a grouping can still be large enough, however, that attenuation can contribute to the apparent scatter in the data. The next step in the analysis would be to remove this source of scatter, but this has not been done here. Several suggestions for the sources of scatter emerge from the figure, but they are quite speculative. One possibility is that the scatter is reduced for stations on one side or the other of the fault zone compared to data from stations straddling the fault zone. This is emphasized in Figure 5, which shows that fault zone data between the Vineyard Canyon and Gold Hill Limbs (stations 6 to 16) has more scatter than that from a cluster of stations from an area of comparable size to the east of the fault zone (stations between the Gold Hill and Cholame Limbs).

Accelerograms of the May 2, 1983, Coalinga earthquake which were recorded on the Parkfield array have recently been published in Shakal and McJunkin, 1983. There, large differences are seen between the accelerograms of sites which are close relative to the epicentral distance. Examples of these accelerograms are presented in Figures 6, 7 and 8.

Figures 6, 7, and 8 show accelerograms from Vineyard Canyon station 1W and Fault Zone stations 15, 14, 11, 10, 9, 8, 7, and 6. These stations are circled in Figure 1. The typical epicentral distance of these stations to the Coalinga event is 40 km, whereas the typical separation of adjacent stations is 3 km. The peak accelerations range from 0.03g at the Fault Zone stations 6 and 9, to 0.28g at the Fault Zone station 14.

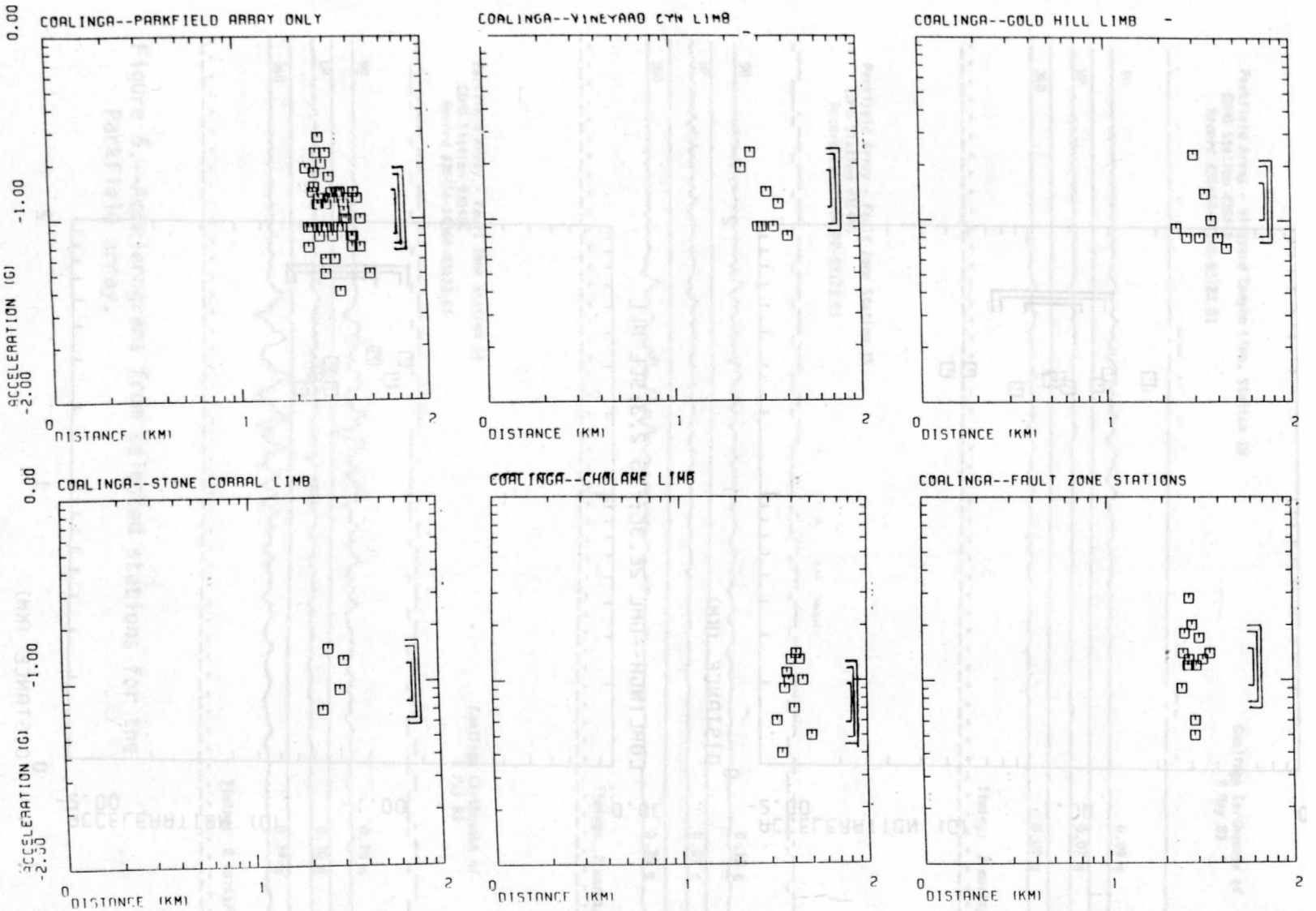

Figure 4.--Peak acceleration versus distance for the Parkfield array and various subgroups of the array.

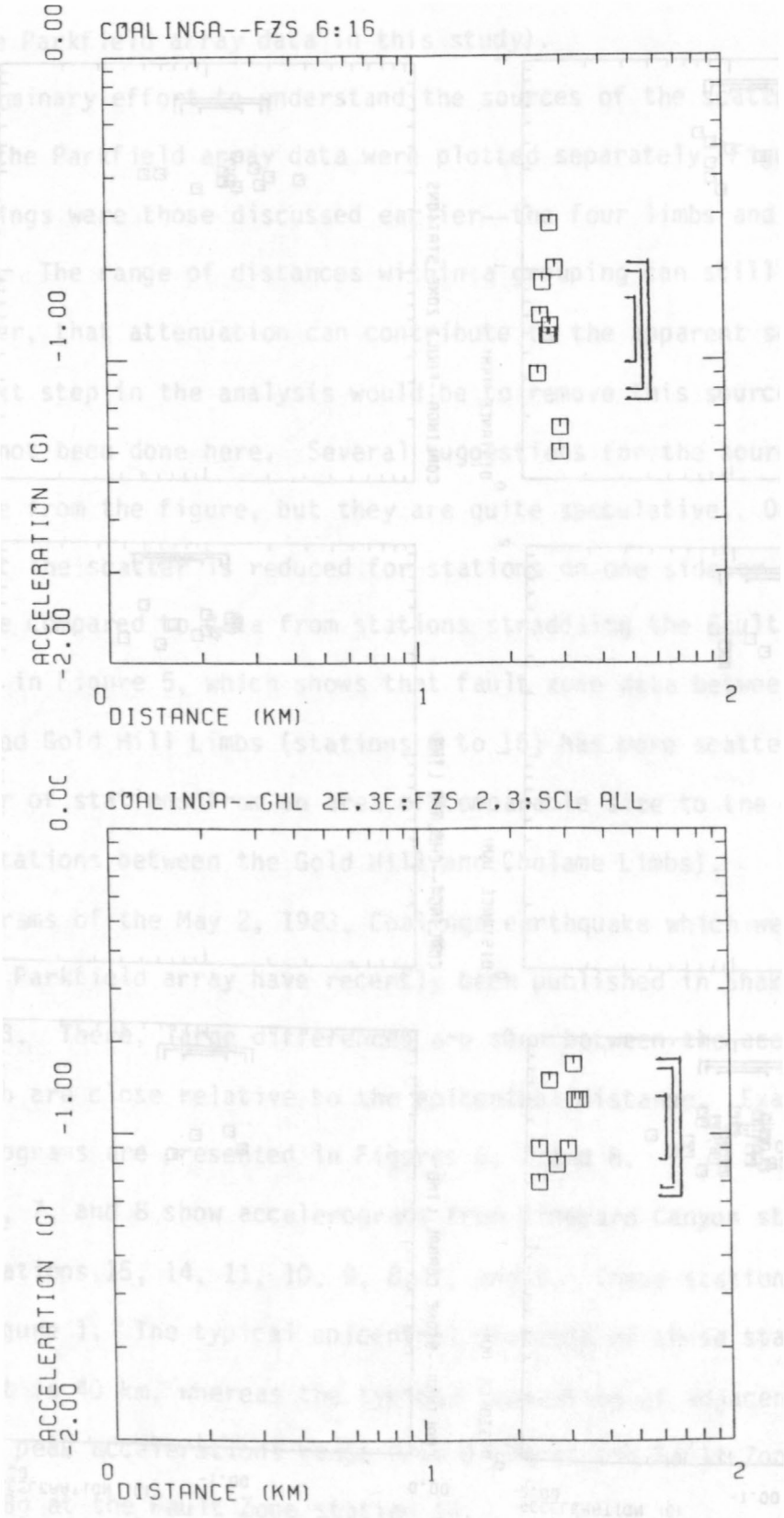

Figure 5.--Peak acceleration for two subgroups of the Parkfield array.

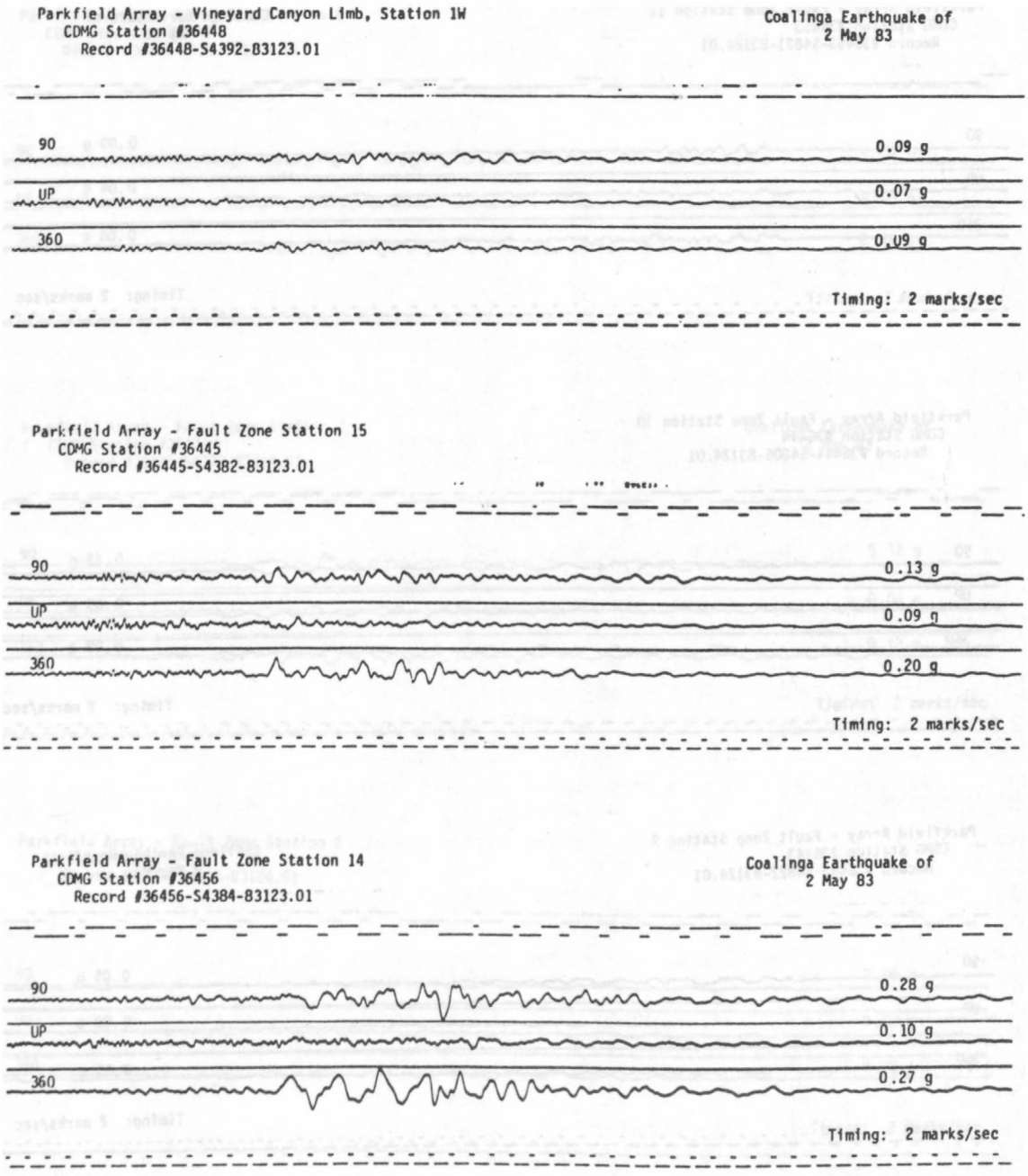

Figure 6.--Accelerograms from selected stations for the Parkfield array.

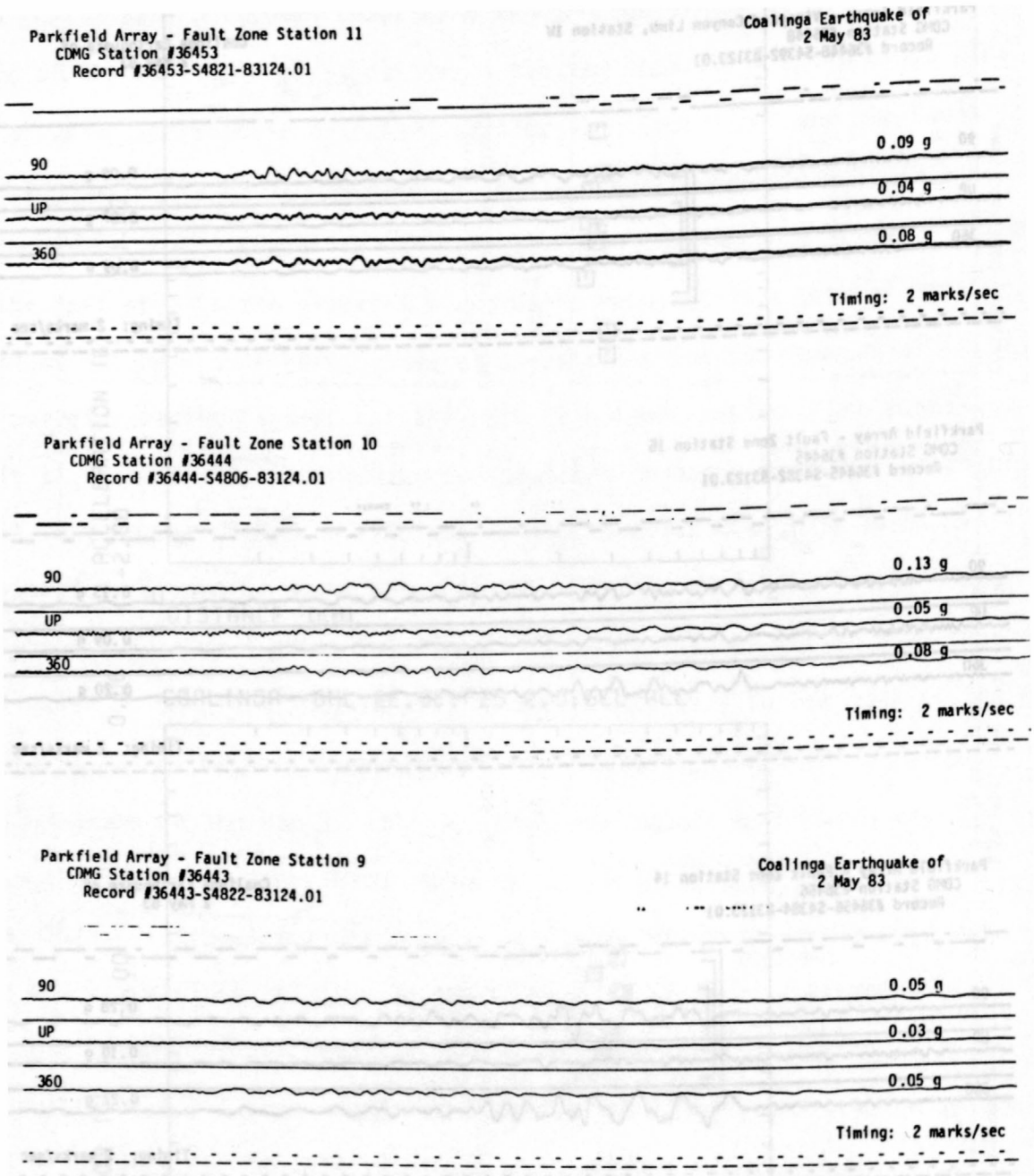

Figure 7.--Accelerograms from selected stations for the Parkfield array.

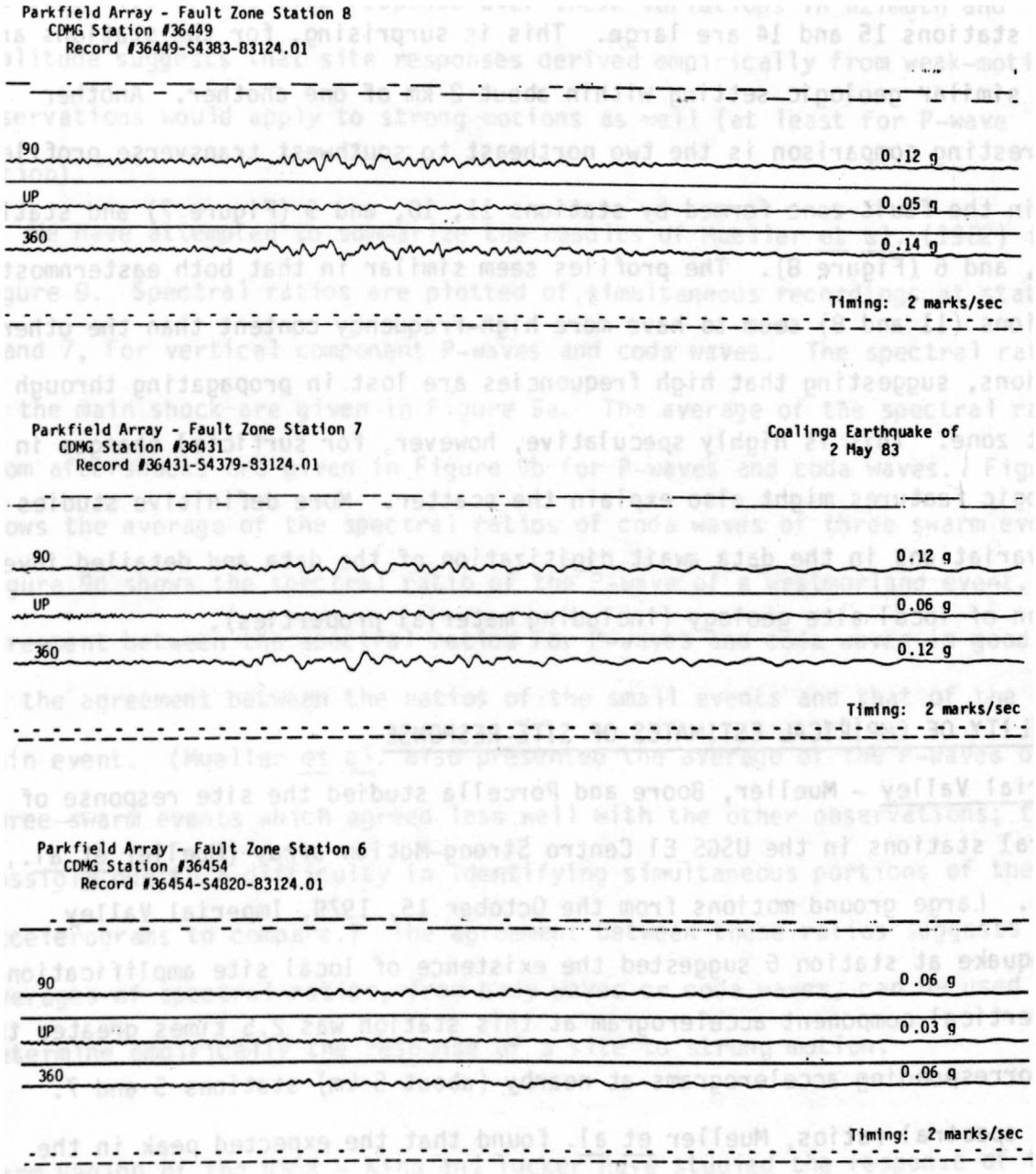

Figure 8.--Accelerograms from selected stations for the Parkfield array.

The differences in accelerograms from adjacent stations cannot be easily characterized. The differences between Vineyard Canyon station 1W and Fault Zone stations 15 and 14 are large. This is surprising, for the stations are in a similar geologic setting within about 2 km of one another. Another interesting comparison is the two northeast to southwest transverse profiles within the fault zone formed by stations 11, 10, and 9 (Figure 7) and stations 8, 7, and 6 (Figure 8). The profiles seem similar in that both easternmost stations (11 and 8) seem to have more high-frequency content than the other stations, suggesting that high frequencies are lost in propagating through the fault zone. This is highly speculative, however, for surficial changes in geologic features might also explain the scatter. More definitive studies of the variations in the data await digitization of the data and detailed investigation of local site geology (including material properties).

STABILITY OF EMPIRICAL ESTIMATES OF SITE RESPONSE

Imperial Valley - Mueller, Boore and Porcella studied the site response of several stations in the USGS El Centro Strong-Motion array (Mueller et al., 1982). Large ground motions from the October 15, 1979, Imperial Valley earthquake at station 6 suggested the existence of local site amplification. The vertical component accelerogram at this station was 2.5 times greater than the corresponding accelerograms at nearby (about 5 km) stations 5 and 7. Using spectral ratios, Mueller et al. found that the expected peak in the ratios for the main shock was also found in the ratios for eight other Imperial Valley earthquakes, having different amplitudes and azimuths. The dominant spectral peak was at about 10 Hz and corresponded to an amplification at station 6 relative to stations 5 and 7 of 2 to 5. The range of peak

accelerations was large: 1.74g to 0.03g at site 6, 0.65 to 0.01g at site 7. The stability of the site response over these variations in azimuth and amplitude suggests that site responses derived empirically from weak-motion observations would apply to strong motions as well (at least for P-wave motion).

We have attempted to summarize the results of Mueller et al. (1982) in Figure 9. Spectral ratios are plotted of simultaneous recordings at stations 6 and 7, for vertical component P-waves and coda waves. The spectral ratios of the main shock are given in Figure 9a. The average of the spectral ratios from aftershocks are given in Figure 9b for P-waves and coda waves. Figure 9c shows the average of the spectral ratios of coda waves of three swarm events. Figure 9d shows the spectral ratio of the P-wave of a Westmorland event. The agreement between the spectral ratios for P-waves and coda waves is good, as is the agreement between the ratios of the small events and that of the large, main event. (Mueller et al. also presented the average of the P-waves of the three swarm events which agreed less well with the other observations; this is possibly due to a difficulty in identifying simultaneous portions of the accelerograms to compare.) The agreement between these ratios suggests that averages of spectral ratios, from body waves or coda waves, can be used to determine empirically the response of a site to strong motion.

Garm Region of the USSR - King and Tucker have studied the response of three sediment-filled valleys in the Garm region of the USSR (Tucker et al., 1983); King and Tucker, 1983; and Tucker and King, 1983). The average site responses were experimentally determined and found to apply, to within $\pm$ 0.25 log units, to earthquakes of any azimuth, to S-waves and coda waves, and for ground

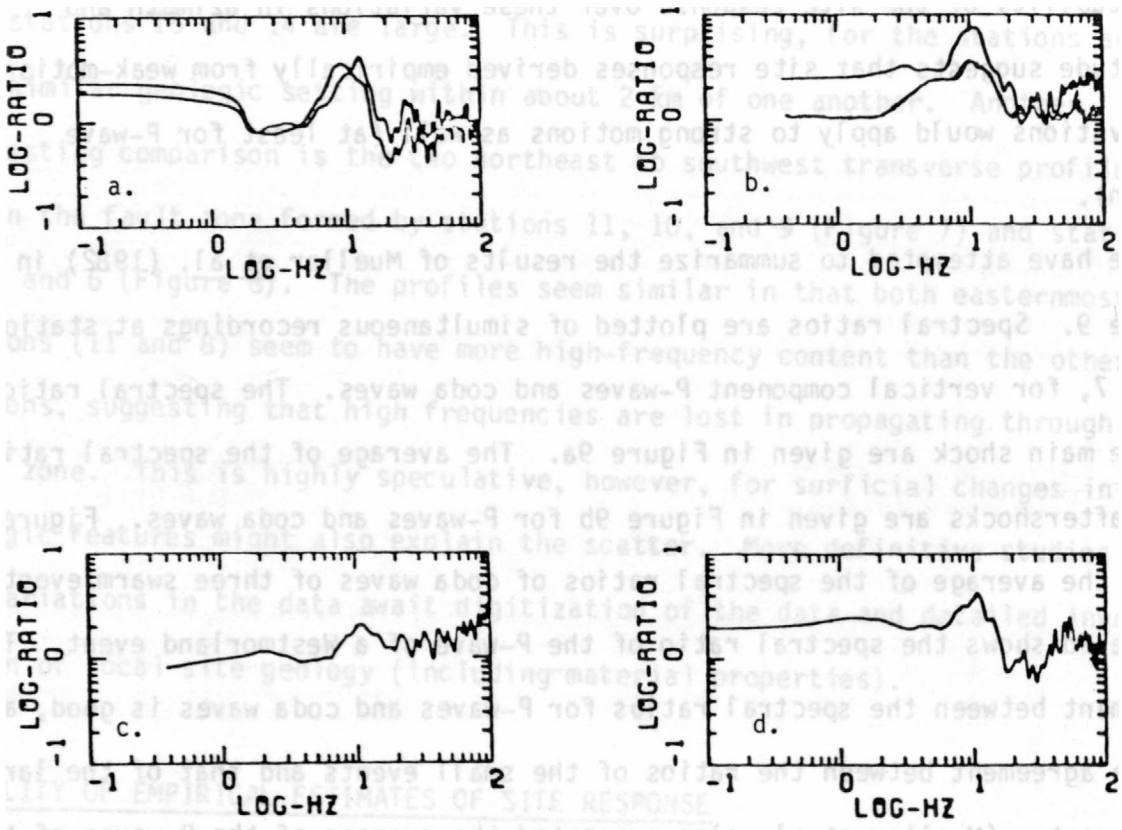

Figure 9.--Observations of site response in Imperial Valley for different input azimuths and amplitudes for vertical component recordings. Smooth spectral ratios of the vertical recordings at at the USGS El Centro Station 6 and the simultaneous vertical recording at Station 7 are plotted. (a) Spectral ratios of sites 6/7 for the P-waves and coda waves of the October 15, 1979, main shock (peak acceleration 1.74 g). (b) The average spectral ratios of sites 6/7 for the P-waves and coda waves of four aftershocks (typical peak acceleration 0.08 g). (c) The average spectral ratio of 6/7 for the coda waves of three swarm events (typical peak acceleration 0.1 g). (d) The spectral ratio of 6/7 for the P-wave of a Westmorland event (peak acceleration 0.03 g).

accelerations ranging from 10^{-5} to 0.2g. In two valleys with sediment-basement impedance contrasts of about 5:1, average site amplification was as much as a factor of five in certain frequency bands. In another valley, with a sediment-basement impedance contrast of 3:1, sediment amplification was about a factor of two.

Figure 10 shows an example of King and Tucker's observations, which indicates the degree of stability of site response for the Yasman Valley for variations of the input signals' azimuth and incidence. The spectral ratios of four events are plotted. Three events (8, 9, and 16) are local events which have very different azimuths with respect to the recording stations; the other event (14) is a distant event (in Afghanistan) with still another azimuth angle and a much steeper incidence angle. Spectral ratios were formed for the first eight seconds of the S-waves, as recorded in the middle of the valley (site 2), the edge of the valley (site 4), and a rock outcrop (site R) which bordered the valley. Spectral ratios are shown for two horizontal components of motion: one parallel to the valley's sides and one perpendicular to the valley sides.

Figure 10 shows that the largest variations are for the middle-to-rock ratios, where the average maximum difference between curves is about a factor of three. This means that a spectral ratio value can be specified $\pm$ 50% and apply to any azimuth.

Figure 11 shows Tucker and King's observations of the dependence of a sedimentary site's response on the input signal amplitude. The spectral ratios plotted here are of S-wave recordings from the middle (site 2) of Chusal Valley and those from the edge (site 11) of Chusal Valley. The observations are grouped according to the input signal's amplitude: weak-motion recordings (10^{-5} - 10^{-3}g) and strong-motion recordings (.04 - 0.2g). Three components

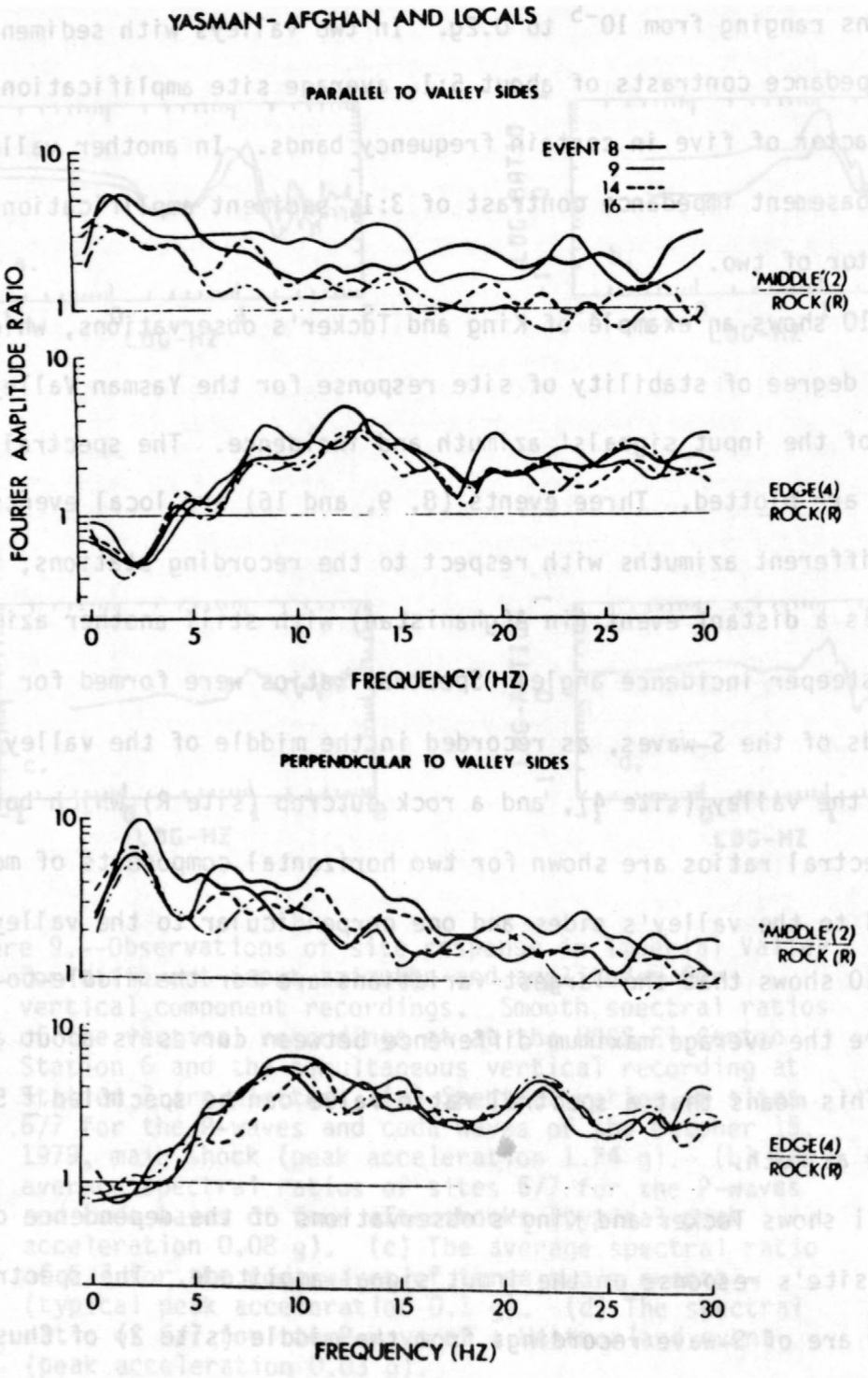

Figure 10.--Observations of site response in Garm for different input azimuths. Spectral ratios of recordings in the middle and edge of Yasman Valley with respect to recordings on a rock outcrop bordering the valley are plotted for three local events (8, 9, and 16) and one Afghanistan event (14). The spectral ratios were for the first eight seconds of the P-waves, recorded on horizontal seismometers oriented parallel to the perpendicular to the valley's edges. These four events had very different azimuths with respect to the recording sites.

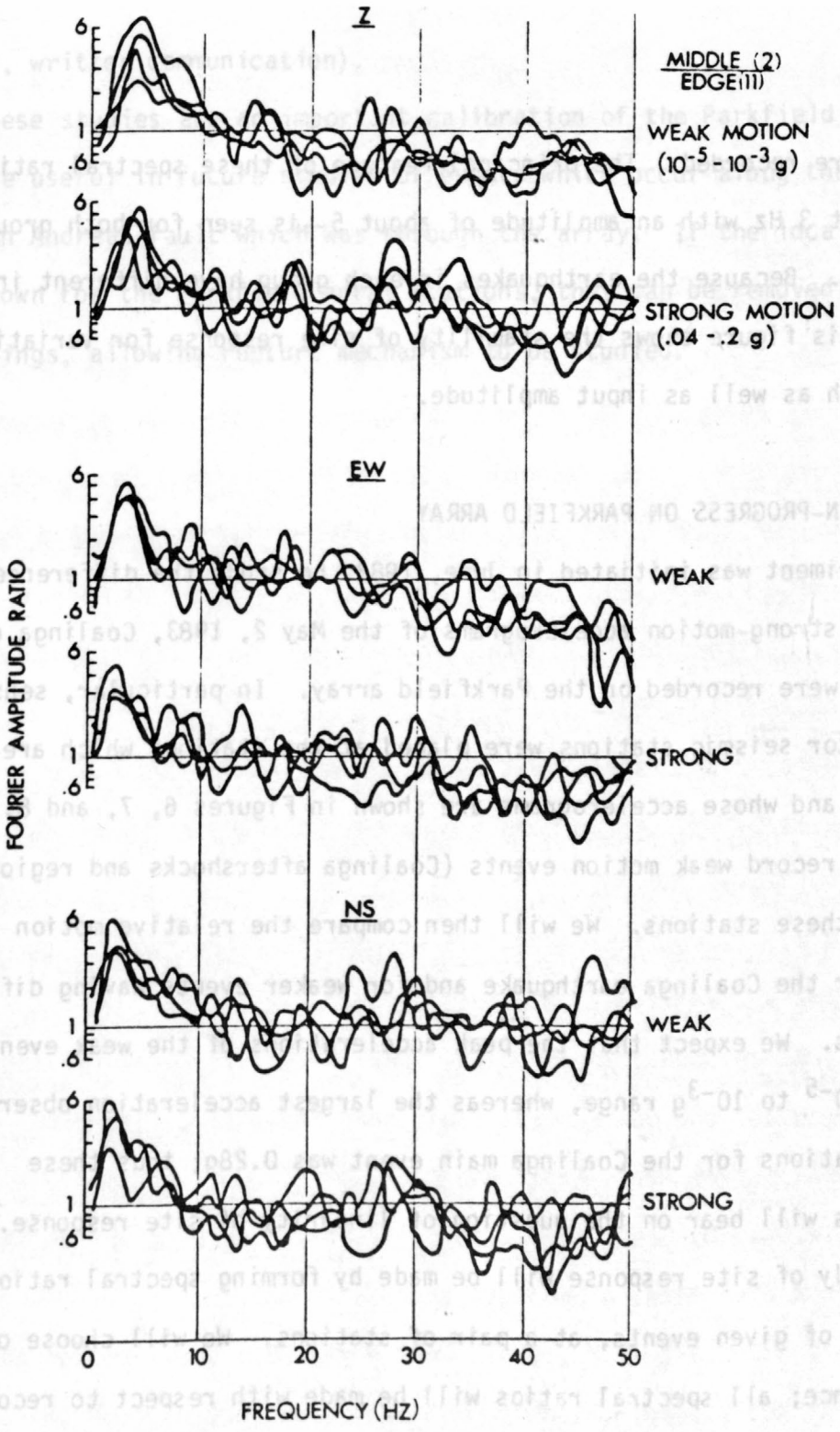

Figure 11.--Observations of site response in Garm for different input amplitudes. Mid-Valley/valley-edge spectral ratios for P-waves of four small events, having peak accelerations ranging from 10^{-5} to 10^{-3} g, and from larger events having peak acclerations ranging from 0.04 to 0.2 g, for three components of motion in Chusal Valley. Since these events are at widely-different azimuths with respect to Chusal, these curves test the dependence of the response on both input azimuth and amplitude. No significant differences between the weak-motion and stong-motion groups are evident.

of motion were recorded. The principal feature of these spectral ratios--the peak at about 3 Hz with an amplitude of about 5--is seen for both groups of observations. Because the earthquakes in each group have different input azimuths, this figure shows the stability of site response for variations in input azimuth as well as input amplitude.

EXPERIMENT IN-PROGRESS ON PARKFIELD ARRAY

An experiment was initiated in June, 1983, to study the differences observed in strong-motion accelerograms of the May 2, 1983, Coalinga earthquake which were recorded on the Parkfield array. In particular, sensitive event-detector seismic stations were placed at the stations which are circled in Figure 1 and whose accelerograms are shown in Figures 6, 7, and 8.

We will record weak motion events (Coalinga aftershocks and regional events) on these stations. We will then compare the relative motion at these stations for the Coalinga earthquake and for weaker events having different azimuths. We expect that the peak accelerations of the weak events will be in the 10^{-5} to 10^{-3}g range, whereas the largest acceleration observed on these stations for the Coalinga main event was 0.28g; thus these measurements will bear on the question of linearity of site response.

Our study of site response will be made by forming spectral ratios of recordings, of given events, at a pair of stations. We will choose one site as a reference; all spectral ratios will be made with respect to recordings at this reference site.

Another study we will attempt will use ratios, for a given event, of S-wave spectra and coda-wave spectra of that event's recording at a given station. Such ratios should measure propagation-path effects (S. Phillips and

K. Aki, written communication).

These studies are an important calibration of the Parkfield array. They will be useful in future studies of events which occur along that portion of the San Andreas fault which was through the array. If the local site effects are known for the Parkfield array stations, they can be removed from future recordings, allowing rupture mechanism to be studied.

REFERENCES

Brown, R.D., Jr., 1970, Map showing recently active breaks along the San Andreas and related faults between the northern Gabilan Range and Cholame Valley, California: U.S. Geological Survey Misc. Geologic Investigations Map I-575, scale 1:62,500.

Brown, R.D., Jr., and Vedder, J.G., 1967, Surface tectonic features along the San Andreas fault, in The Parkfield-Cholame, California, earthquakes of June-August 1966: U.S. Geological Survey Professional Paper 579, p. 2-23.

Dibblee, T.W., Jr., 1973, Regional geologic map of San Andreas and related faults in Carrizo Plain, Temblor, Caliente, and La Panza Ranges and vicinity, California: U.S. Geological Survey Misc. Investigations Map I-757, scale 1:125,000.

Dickenson, W.R., 1966a, Structural relations of San Andreas fault system, Cholame Valley and Castle Mountain Range, California: Geol. Soc. Am. Bull., v. 77, p. 707-725.

Dickenson, W.R., 1966b, Table Mountain serpentine extrusion in California Coast Ranges: Geol. Soc. Am. Bull., v. 77, p. 451-472.

Hanna, W.F., Burch, S.H., and Dibblee, T.W., Jr., 1972, Gravity, magnetics, and geology of the San Andreas fault near Cholame, California: U.S. Geological Survey Prof. Paper 646-C, 29 p.

Jennings, C.W., 1958, Geologic map of California, San Luis Obispo Sheet: California Div. Mines a Geology, scale 1:250,000.

Joyner, W.B., and Boore, D.M., 1981, Peak horizontal acceleration and velocity from strong motion records including records from the 1979 Imperial Valley, California, earthquake, Bull. Seismol. Soc. Am., v. 71, p. 2011-2038.

Joyner, W.B., and Boore, D.M., 1982, Prediction of earthquake response spectra, U.S. Geol. Surv. Open-File Rep. 82-977, 16 p.

King, J.L., and Tucker, B.E., 1983, Observed variations of earthquake motion across a sediment-filled valley, submitted to Bull. Seism. Soc. Am.

McCann, M.W., Jr., and Boore, D.M., Variability in ground motions: root mean square acceleration and peak acceleration for the 1971 San Fernando, California earthquake, Bull. Seism. Soc. Am., v. 73, p. 615-632.

McJunkin, R.D., and Shakal, A.F., 1983, The Parkfield strong-motion array, California Geology, v. 36, n. 2, p. 27-34.

Mueller, C.S., D.M. Boore, and Porcella, R.L., 1982, Detailed study of site amplification at El Centro strong-motion array station 6, Proc. of the Third Conf. on Earthquake Microzonation, 1, Convened Seattle, Wash., June 28-July 1, 1982, 413-424, 1982.

Shakal, A.F., and McJunkin, R.D., 1983b, "Preliminary Summary of CDMG Strong-Motion Records from the 2 May 1983 Coalinga, California, Earthquake," 27 May 1983, California Div. Mines a Geology, OSMS Report 83-5.2, 49 p.

Tucker, B.E., and King, J.L., 1983, Dependence of sediment-filled valley response on input amplitude and valley properties, submitted to Bull. Seism. Soc. Am.

Tucker, B.E., King, J.L., Hatzfeld, D., Nasesov, I.L., 1983, Variations of earthquake motion on hard rock, submitted to Bull. Seism. Soc. Am.

SPATIAL VARIABILITY OF EARTHQUAKE INTENSITY FROM THE SMART 1 ARRAY, TAIWAN

by

Bruce A. Bolt
Seismographic Station
University of California
Berkeley, California

SCOPE

Array measurements allow quantitative assessment of the amount of variation in time and space of large amplitude seismic waves in a region around a specific site. Estimation problems that must be addressed include the types, speeds, evolution, and direction of propagation of wave components, together with power spectra variations and phase relations. Correlations of ground acceleration across an appropriately scaled seismic array provide a method to study these quantities. Consecutive time intervals can be lagged so that wave orbitals, for example, can be identified; coherency spectra even promise that the seismic dislocation may be followed along the rupturing fault. The key practical seismological questions asked by engineers involve the variability over short distances of seismic wave intensity in amplitude and frequency, the measurement of in-phase and out-of-phase wave components over distances comparable to the base dimensions of engineered structures, the measurement of torsional components of ground motion, and the effect of rigid structural foundations on spatial averaging.

THE STRONG MOTION INSTRUMENT ARRAY IN TAIWAN

The SMART 1 strong motion array near Lotung, Taiwan, consists of a central station (C00) and thirty-six stations located on three concentric rings of radii 200 meters (I-ring), 1 km (M-ring) and 2 km (O-ring), respectively. The triaxial

digital strong motion accelerometers have a common time base and delay memories of approximately 2.5 seconds. Signals are digitized as 12 bit words at 100 samples per second. By June 1983, over twenty earthquakes have been recorded with significant ground motion by part or all of the array. Of particular importance for theoretical work and array calibrations, the earthquakes range from focal depth of 7 to 70 km. The three largest are 14 November 1980 (local magnitude 5.9, epicentral distance 10 km), 29 January 1981 (local magnitude 6.9, epicentral distance 30 km), and 17 December 1982 (local magnitude 6.3, epicentral distance 100 km). The January 1981 earthquake has been studied most to date. The maximum horizontal and vertical accelerations were 0.24g and 0.09g, respectively, and 27 array stations recorded the seismic waves. The acceleration, velocity, and displacement seismograms of the three components of motion from this earthquake are very suitable records for the study of spatial wave variability. The December 1982 earthquake recorded on all thirty-six operational instruments of the array with a peak acceleration of 0.07g.

WAVE FORMS AND FOURIER SPECTRA. SPATIAL VARIATIONS

For the larger earthquakes, wave forms of individual components of acceleration vary markedly across the array, but certain wave packets, especially in the S wave train, are coherent across the rings. In the case of spectra, in the January 1981 earthquake, the N-S component had, in general, the highest Fourier spectral levels and the vertical component had the lowest. For sites C00 and M06, the overall spectral level at M06 is lower for all three components and the vertical component has significantly more energy for frequencies less than 4 Hz. Variations in Fourier spectra across SMART 1 in the vertical components were found to be greater than the variations in the horizontal components for this magnitude 6.9 earthquake. For response spectra also, the N-S component in this earthquake had more energy for periods greater than 0.5 sec than the E-W

component. The results indicate that over even 200 m distance shapes of response spectra differ for vertical and horizontal components and between different earthquakes. Simultaneous inversion of array station spectra should eventually provide individual site anomalies.

Pseudo-acceleration response spectra have shapes which fall most closely along previously published averages for hard site conditions. The observation is somewhat inconsistent with the relatively soft site conditions of the SMART 1 array. Recent reflection surveys show flat surficial alluvial layers of depths 10 and 50 meters with P wave propagation velocities of 600 and 1500 mps. This softer material is underlain by dipping alluvial layers with velocities from 1800 to 2000 meters per second.

Wood-Anderson seismograms computed from the broadband digital accelerograms provide measures of peak amplitude. Hence, Richter magnitude can be calculated as a function of position across the SMART 1 area. The results indicate that the Richter magnitude estimates are subject to significant changes due to local structural variations within the linear dimension of 2 km. For example, the equivalent Richter magnitude for the January 1981 earthquake ranged between 6.0 and 6.4 across the array with a mean of 6.24 ± 0.08. The scatter about the mean is not random, but there is a systematic azimuthal trend.

IN- AND OUT-OF-PHASE MOTIONS AND MULTI-SUPPORT SYSTEMS

If $a_{ri}(t)$ and $b_{si}(t)$ are the recorded ground accelerations at stations r and s, respectively, in the ith coordinate direction (i = x, y, z) at time t, the in-phase and out-of-phase components are given by

$$a_{ri}(t) = \{\frac{a_{ri}(t) + a_{si}(t)}{2}\} + \{\frac{a_{ri}(t) - a_{si}(t)}{2}\}$$

and

$$a_{si}(t) = \{ \text{"} + \text{"} \} - \{ \text{"} - \text{"} \} .$$

Comparisons for the two earthquakes of November 1980 and January 1981 between station pairs show that the in-phase component for the first (near array source) is much stronger than the out-of-phase component, except for frequencies in the approximate range of 5-6 Hz. In the 29 January 1981 earthquake (more distant source), the in-phase and out-of-phase components are approximately equal in intensity over the frequency bands 1-7 Hz. More generally, the relative variation in the phase components changes from earthquake to earthquake and from site to site across the array. Dynamic analysis of frames, beams, and other structures with two or more supports is now possible, given such ground phase measurements.

STRAIN AND ROTATION MEASUREMENT

Free field motion on the ground surface can be represented in terms of a strain tensor defined by the space derivatives (array station spacing) of the recorded motions specified as $a_{ri}(t)$ above.

The precise timing between array elements allows components e_{ij} and Σ_{ij} (rotation) to be computed as a function of time. Eventually, variations in such time histories over distances of a few hundred meters may be obtained. A preliminary estimate yields a maximum ground strain varying between 2.4 and 3.3×10^{-5} across the array for the January 1981 earthquake.

FUTURE WORK

Seismologically, array measurements have already been demonstrated to provide valuable information on (frequency-dependent) wave attenuation, wave identification, mode conversion, seismic phase evolution, energy scattering, and source properties. Both soil-structure interaction and inputs for large structures are matters of some debate in engineering. Advances in predicting appropriate site ground motions for use in such treatments require further analysis of suites of

observations by array configurations such as SMART 1. In other words, for important engineering studies, a single (three-component) "time history", with an associated response spectrum, is not sufficient as site specific input. In the future, "site-distributed" time histories will be required, effectively giving components of the strain tensor and its time derivatives. Information of an appropriate mix of horizontally and vertically propagating waves will also be needed; such time histories require measurements from arrays with down-hole accelerometers.

THE EFFECT OF SITE RESPONSE ON HIGH FREQUENCY GROUND MOTIONS; ANALYSIS OF THE AFTERSHOCKS OF THE NEW BRUNSWICK EARTHQUAKE

by

John Boatwright and Mary Astrue

U.S. Geological Survey

345 Middlefield Road

Menlo Park, California 94025

Abstract

The recordings of 29 aftershocks, recorded at three different sites, are analyzed to determine the frequency-dependent response of the sites. These sites are approximately characterized as shallow alluvial sites, that is, 5-7 m of glacial till overlying granitic bedrock. Because there was no "hard-rock" or unamplified recording site, the response of the sites must be determined through assumptions on the character of the earthquake source spectra. We assume that the average source spectra of the five best recorded events is flat above the average corner frequency of the events. Specific amplifications as much as a factor of three are determined at frequencies from 15 to 30 Hz at the sites. Analysis of four SMA-1 recordings of a M_L = 4.8 aftershock indicate that the frequencies above 10 Hz are amplified by a factor of two relative to frequencies below 10 Hz at these shallow alluvial sites.

Introduction

One week after the New Brunswick earthquake of January 9, 1982, the U.S. Geological Survey, in co-operation with the Earth Physics Branch of the Canadian Department of Energy, Mines and Resourses, deployed six three-component digital seismographs (DR-100) in the epicentral area. Forty aftershocks ($m_{bLG} < 3.5$) were recorded in the following week; their moments ranged from 10^{18} to 10^{21} dyne-cm and their hypocentral depths ranged from 1.0 km to 7.5 km. The digital seismographs were removed on January 22. In the first week in Febuary, the Canadians installed an array of five strong motion accelerographs (SMA-1's). Three of the accelerographs were deployed at the seismograph sites. A large aftershock ($m_{bLG} = 4.8$) occurred on the 31st of March, and was recorded by all the accelerographs. Four of the accelerograms were digitized at the U.S. Strong Motion Data Center at Menlo Park.

In order to analyze the Dr-100 and SMA-1 recordings for the relevant source parameters of the earthquakes, it was necessary to estimate the high-frequency response of the various sites. A new method for determining site response was derived, which depends on the essential randomness of the accelerations radiated by crustal earthquakes. The results determined using this method are of sufficient importance to warrant this separate presentation.

The DR-100 Recordings

The epicenters of the forty located aftershocks are shown in Figure 1, along with the four sites occupied by the DR-100 and SMA-1 instruments. The

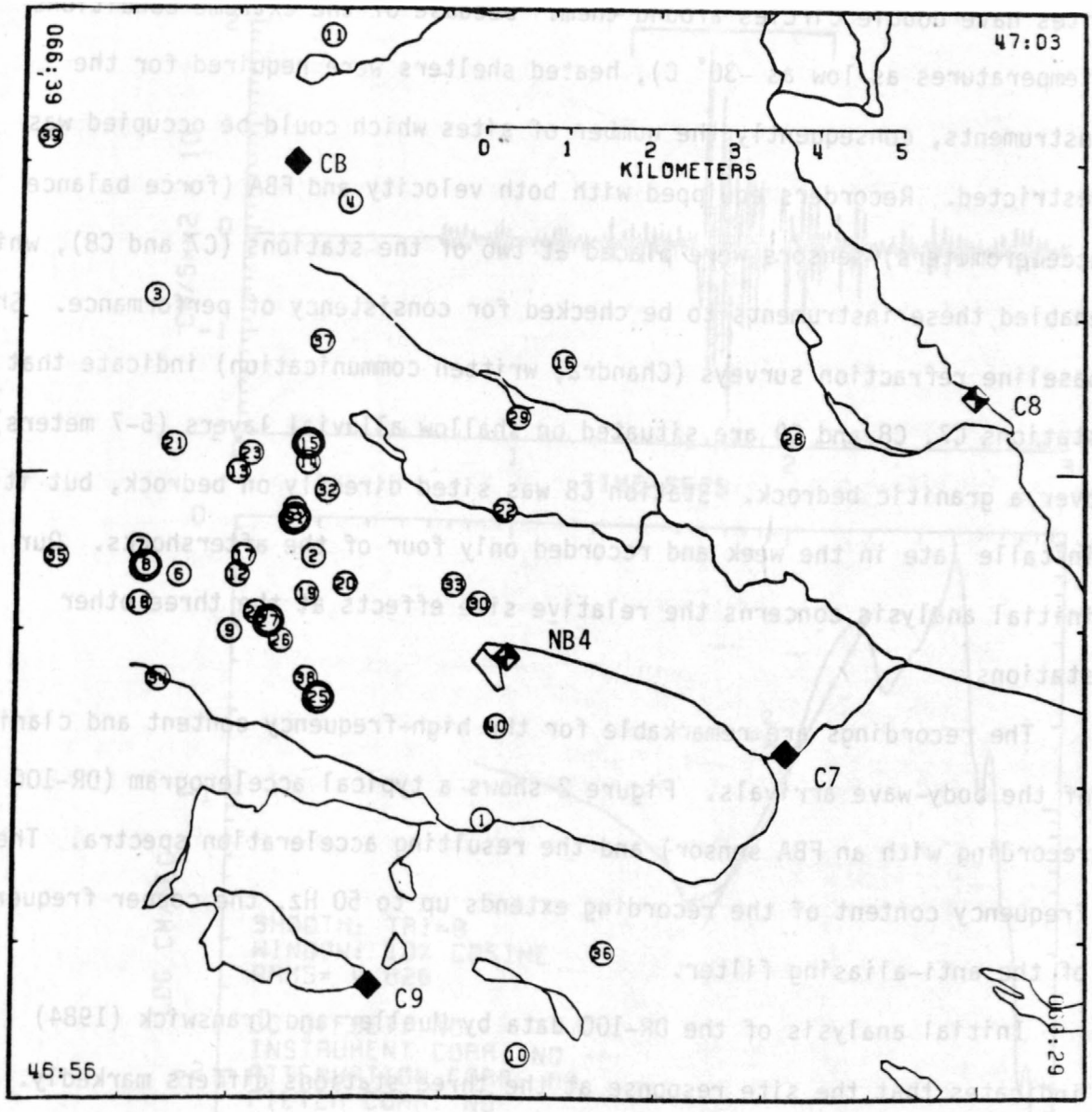

Figure 1. Epicentral locations for the 40 locatable aftershocks of the New Brunswick earthquake which were recorded by the DR-100 array. The four DR-100 sites are the diamonds labelled C7, C8, C9 and CB. The five aftershocks used to compare the response of sites C7, C8 and C9 have double circles around them. Sites C7, C9 and CB were reoccupied by the Canadian SMA-1 array, along with the site labelled NB4.

epicenters of the five events used to estimate the response of the DR-100 sites have double circles around them. Because of the extreme conditions (temperatures as low as -30° C), heated shelters were required for the instruments, consequently the number of sites which could be occupied was restricted. Recorders equipped with both velocity and FBA (force balance accelerometers) sensors were placed at two of the stations (C7 and C8), which enabled these instruments to be checked for consistency of performance. Short baseline refraction surveys (Chandra, written communication) indicate that stations C7, C8 and C9 are situated on shallow alluvial layers (5-7 meters) over a granitic bedrock. Station CB was sited directly on bedrock, but it was installe late in the week and recorded only four of the aftershocks. Our initial analysis concerns the relative site effects at the three other stations.

The recordings are remarkable for the high-frequency content and clarity of the body-wave arrivals. Figure 2 shows a typical accelerogram (DR-100 recording with an FBA sensor) and the resulting acceleration spectra. The frequency content of the recording extends up to 50 Hz, the corner frequency of the anti-aliasing filter.

Initial analysis of the DR-100 data by Mueller and Cranswick (1984) indicates that the site response at the three stations differs markedly. To standardize the source-parameter analysis for aftershocks which were recorded by different groups of stations, it was necessary to determine the frequency-dependent site response for each station. Because each of the DR-100 stations recorded very similar acceleration spectra for all events, regardless of the size or the azimuth of the event, there is no reference station to which we could compare them. It was therefore necessary to estimate the site response

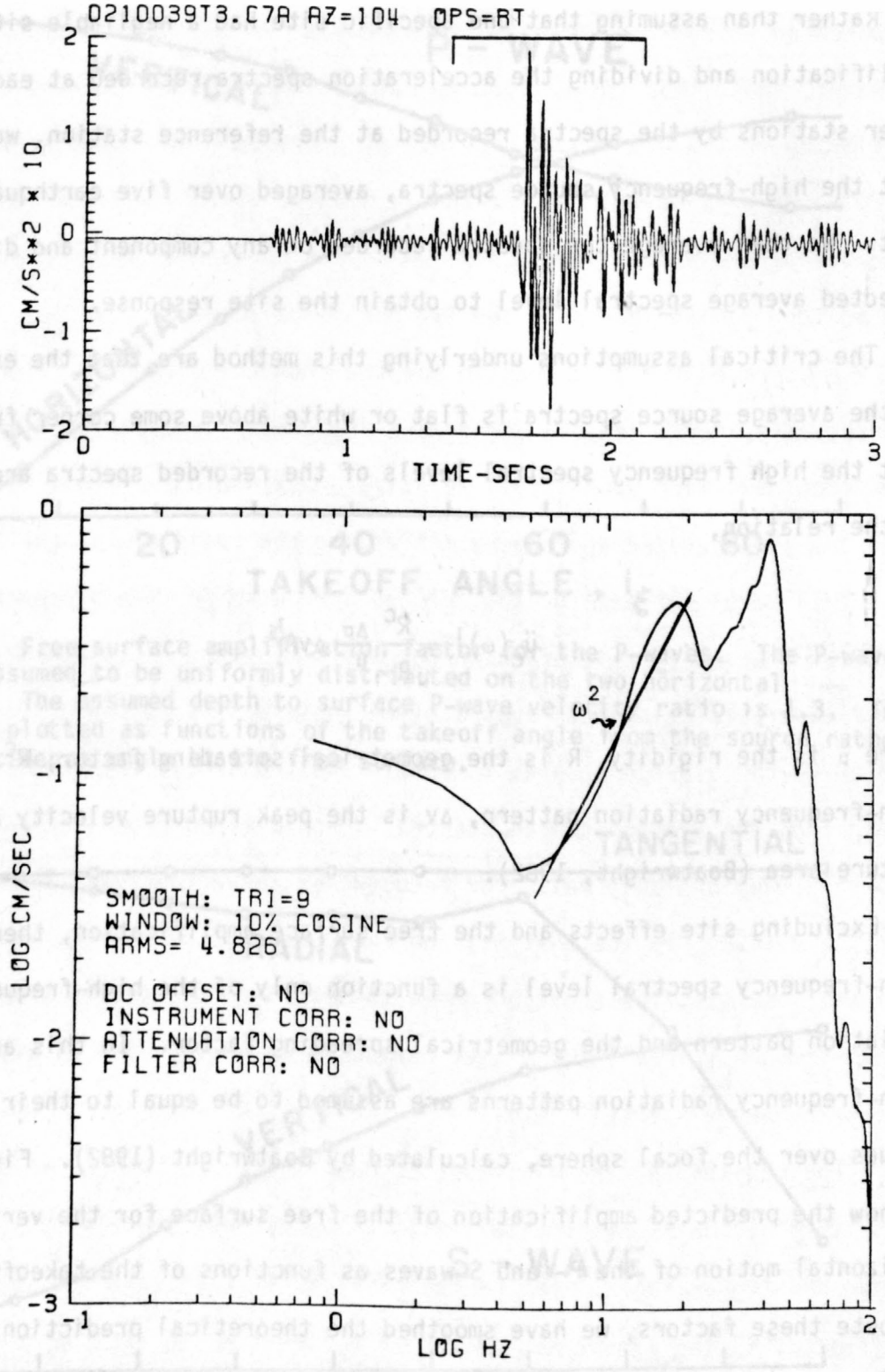

Figure 2. Typical horizontal accelerogram (FBA sensor) from the DR-100 recordings. Note the clarity and impulsive character of the S-wave arrival and the significant frequency content above 10 Hz. The line drawn on the acceleration spectra has a slope of ω^2, corresponding to a flat asymptote in the displacement spectra, and can be used to estimate the moment of the event.

at these stations without using the standard spectral division approach.

Rather than assuming that one specific site had a negliable site amplification and dividing the acceleration spectra recorded at each of the other stations by the spectra recorded at the reference station, we assume that the high-frequency source spectra, averaged over five earthquakes, is flat. We then average the spectra recorded on any component and divide by the expected average spectral level to obtain the site response.

The critical assumptions underlying this method are that the expectation of the average source spectra is flat or white above some corner frequency and that the high frequency spectral levels of the recorded spectra are predicted by the relation,

$$\ddot{u}_c(\omega)| = \frac{R^c}{R} \frac{\Delta\sigma}{\mu} \Delta v A^{\frac{1}{2}} \quad ,$$

where μ is the rigidity, R is the geometrical spreading factor, R^c is the high-frequency radiation pattern, Δv is the peak rupture velocity and A is the rupture area (Boatwright, 1982).

Excluding site effects and the free surface amplification, then, the high-frequency spectral level is a function only of the high-frequency radiation pattern and the geometrical spreading factor. In this analysis, the high-frequency radiation patterns are assumed to be equal to their average values over the focal sphere, calculated by Boatwright (1982). Figures 3 and 4 show the predicted amplification of the free surface for the vertical and horizontal motion of the P- and S-waves as functions of the takeoff angle. To compute these factors, we have smoothed the theoretical predictions for a half-space (Aki and Richards, 1980, p. 190) and then corrected the takeoff

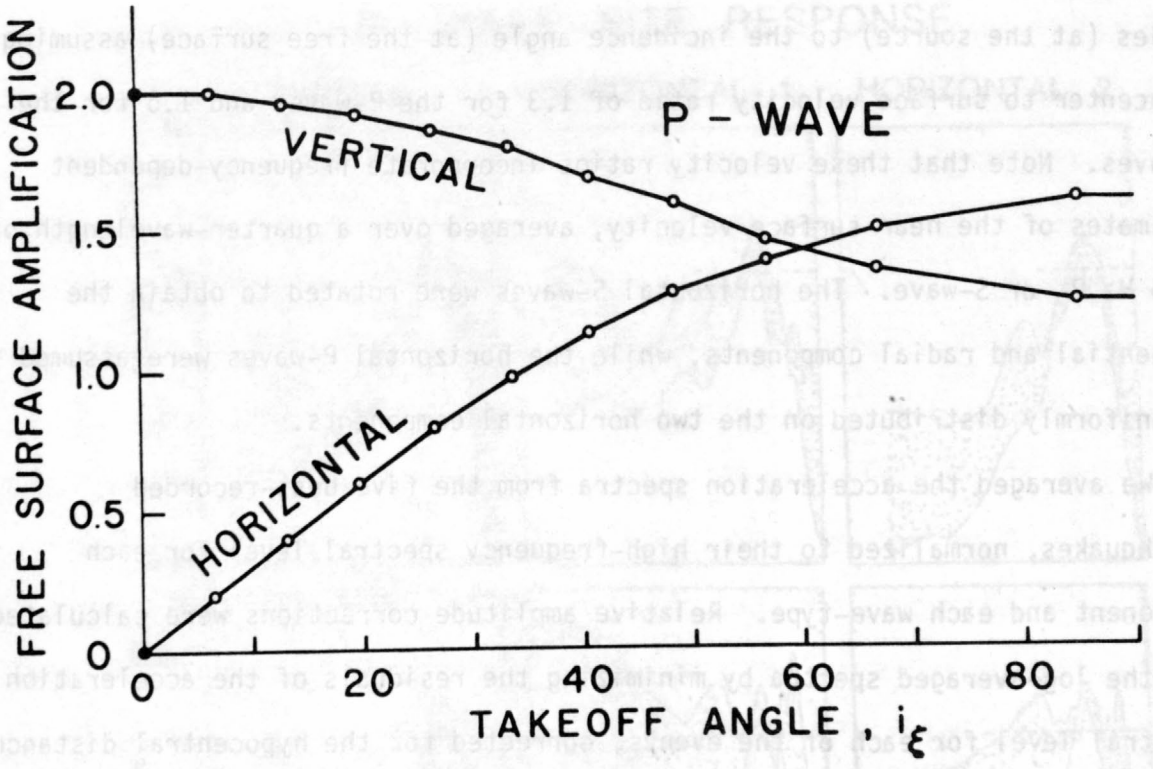

Figure 3. Free surface amplification factor for the P-waves. The P-wave motion is assumed to be uniformly distributed on the two horizontal components. The assumed depth to surface P-wave velocity ratio is 1.3. The factors are plotted as functions of the takeoff angle from the source rather than the incidence angle at the free surface.

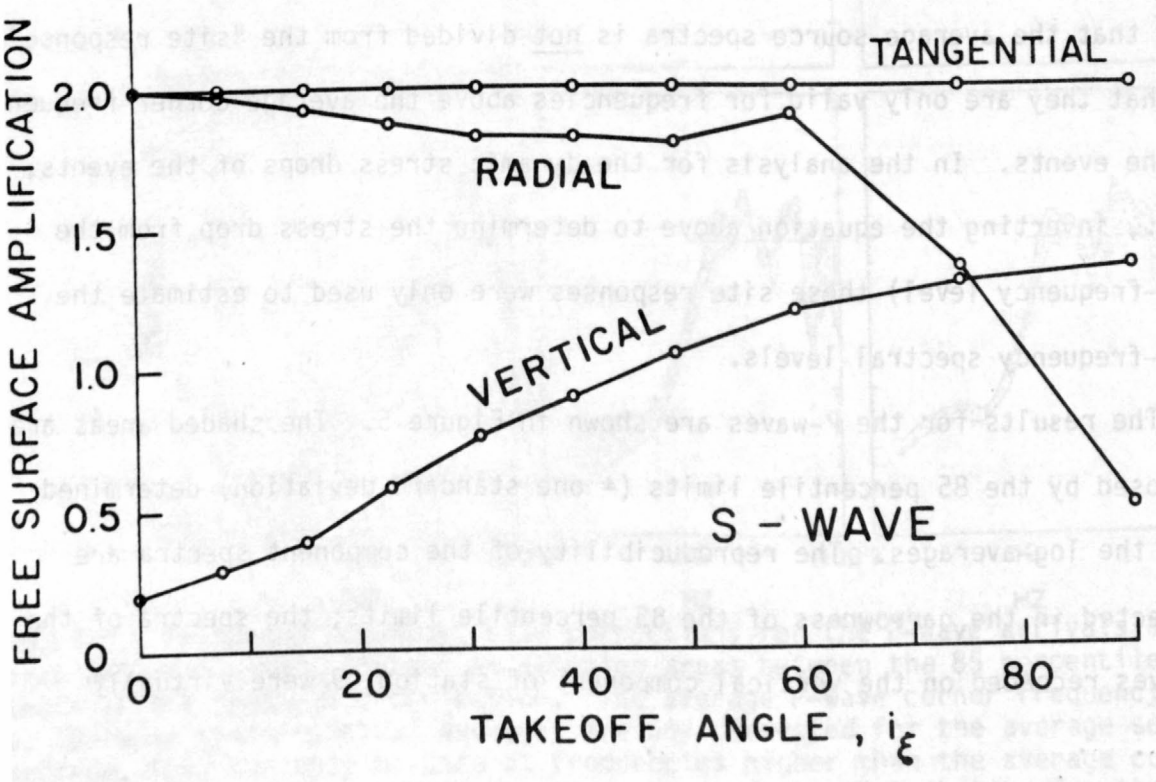

Figure 4. Free surface amplification factors for the S-waves. The assumed depth to surface S-wave velocity ratio is 1.5.

angles (at the source) to the incidence angle (at the free surface) assuming a hypocenter to surface velocity ratio of 1.3 for the P-waves and 1.5 for the S-waves. Note that these velocity ratios incorporate frequency-dependent estimates of the near-surface velocity, averaged over a quarter-wavelength of a 25 Hz P- or S-wave. The horizontal S-waves were rotated to obtain the tangential and radial components, while the horizontal P-waves were assumed to be uniformly distributed on the two horizontal components.

We averaged the acceleration spectra from the five best-recorded earthquakes, normalized to their high-frequency spectral level for each component and each wave-type. Relative amplitude corrections were calculated for the log-averaged spectra by minimizing the residuals of the acceleration spectral level for each of the events, corrected for the hypocentral distance and the free-surface interaction for the components. The corrections for each wave-type were calculated separately. These amplitude corrections are then added to the average spectra to obtain the frequency-dependent site response. Note that the average source spectra is <u>not</u> divided from the "site response" so that they are only valid for frequencies above the average corner frequency of the events. In the analysis for the dynamic stress drops of the events, (i.e., inverting the equation above to determine the stress drop from the high-frequency level) these site responses were only used to estimate the high-frequency spectral levels.

The results for the P-waves are shown in Figure 5. The shaded areas are enclosed by the 85 percentile limits (± one standard deviation) determined from the log-averages. The reproducibility of the component spectra are reflected in the narrowness of the 85 percentile limits; the spectra of the P-waves recorded on the vertical component of station C9 were virtually

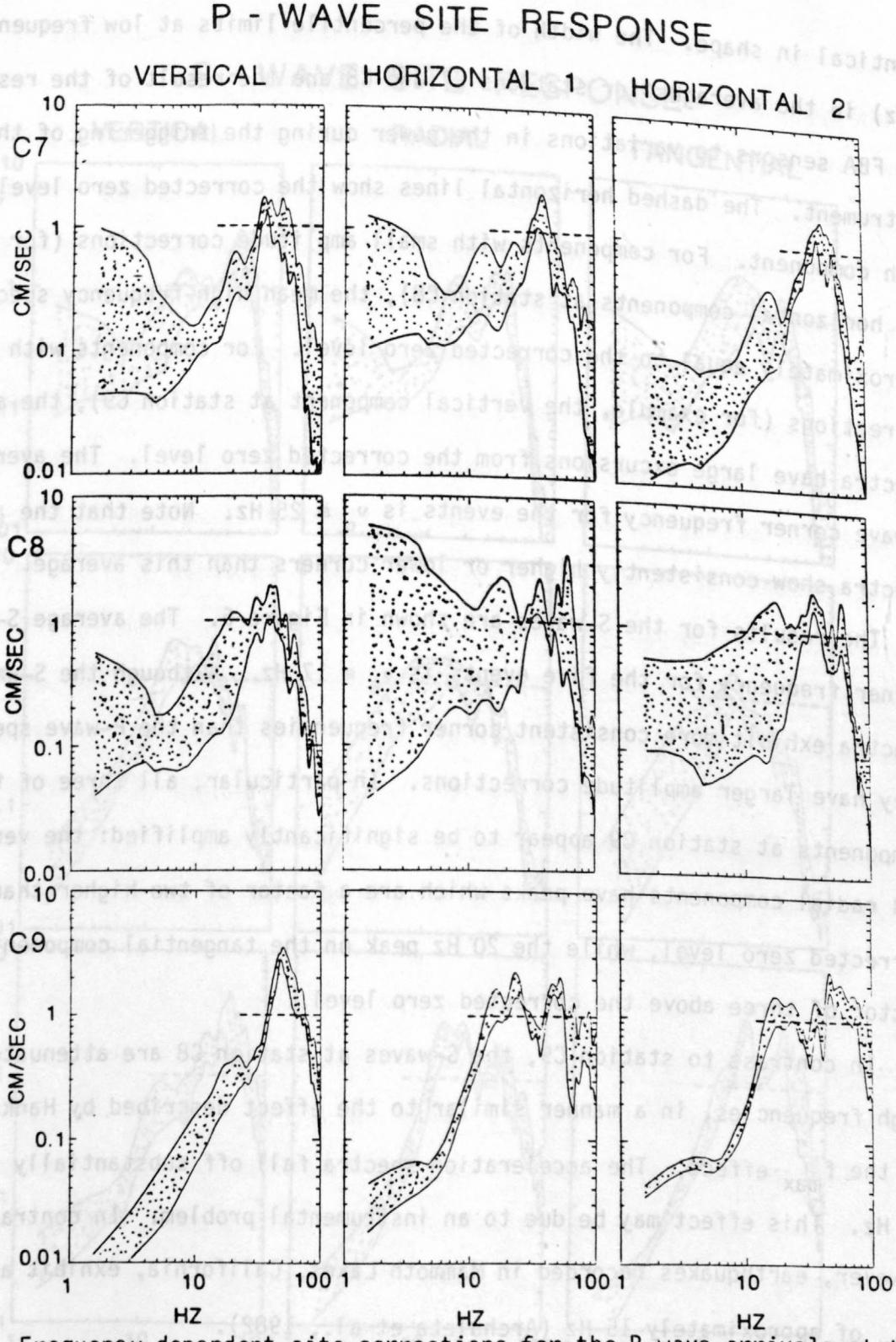

Figure 5. Frequency dependent site corrections for the P-wave arrivals at the three alluvial sites, plotted as stippled areas between the 85 percentile limits of the spectral distribution. The average P-wave corner frequencyis 25 Hz. Because these spectral averages are not corrected for the average source spectrum, they can only be used at frequencies higher than the average corner frequency of the events. Note the narrowness of the distribution for the vertical component at station C9; the spectra from this component were identical in shape over the set of five events.

identical in shape. The width of the percentile limits at low frequencies (< 4 Hz) in the averages for stations C7 and C8 are the result of the response of the FBA sensors to variations in the power during the triggering of the instrument. The dashed horizontal lines show the corrected zero level for each component. For components with small amplitude corrections (for example, the horizontal components at station C8), the mean high-frequency spectra are approximately equal to the corrected zero level. For components with large corrections (for example, the vertical component at station C9), the average spectra have large excursions from the corrected zero level. The average P-wave corner frequency for the events is $\nu_\alpha \cong 25$ Hz. Note that the average spectra show consistently higher or lower corners than this average.

The results for the S-waves are shown in Figure 6. The average S-wave corner frequency for the five events is $\nu_\beta \cong 17$ Hz. Although the S-wave spectra exhibit more consistent corner frequencies than the P-wave spectra, they have larger amplitude corrections. In particular, all three of the components at station C9 appear to be significantly amplified: the vertical and radial components have peaks which are a factor of two higher than the corrected zero level, while the 20 Hz peak on the tangential component is a factor of three above the corrected zero level.

In contrast to station C9, the S-waves at station C8 are attenuated at high frequencies, in a manner similar to the effect described by Hanks (1982) as the f_{max} effect. The acceleration spectra fall off substantially above 30 Hz. This effect may be due to an instrumental problem. In contrast, however, earthquakes recorded in Mammoth Lakes, California, exhibit an average f_{max} of approximately 15 Hz (Archuleta et al., 1982).

Because the events used to determine the station corrections occurred in a

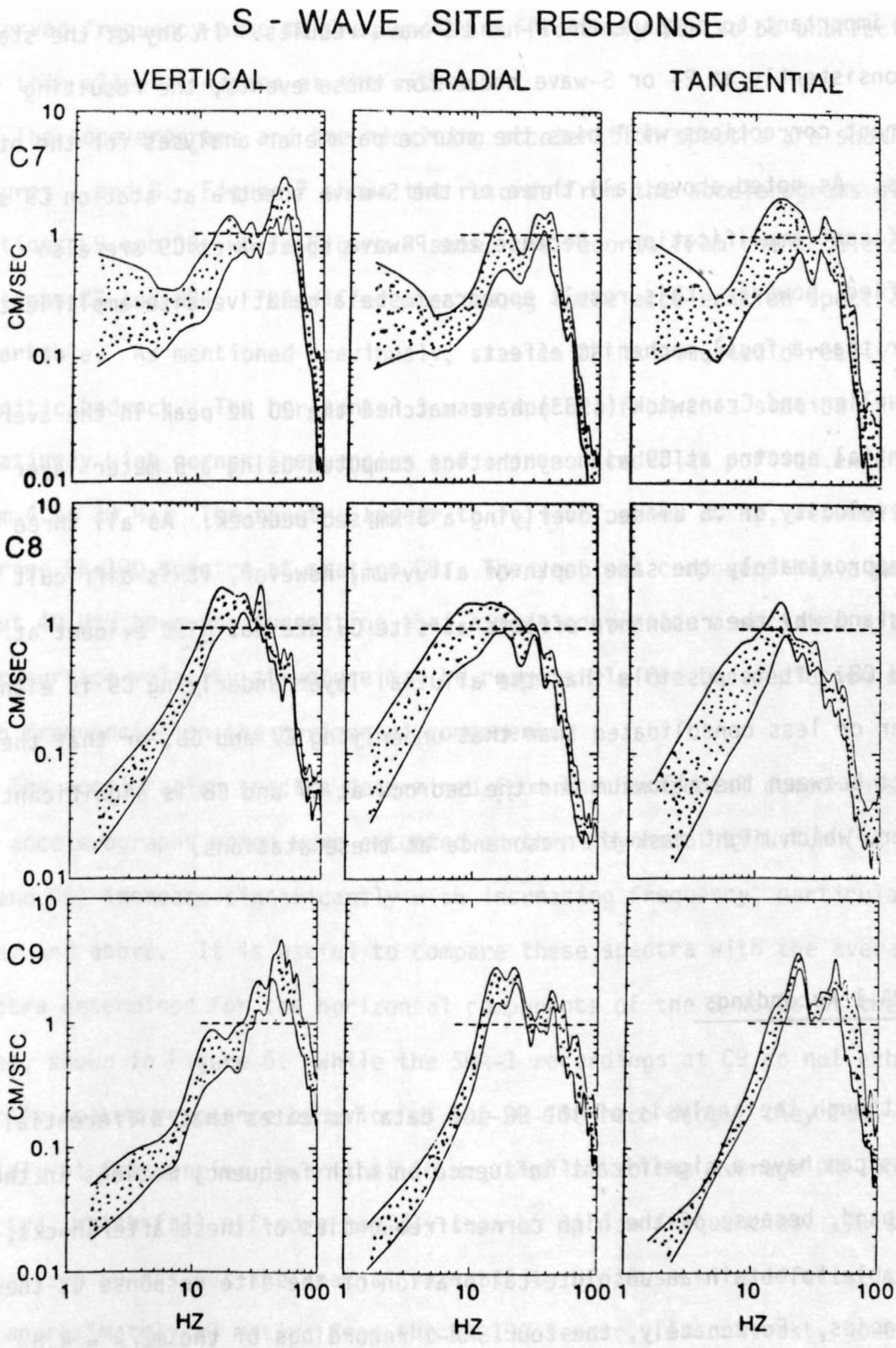

Figure 6. Frequency dependent site corrections for the S-waves arrivals at the DR-100 stations. The average corner frequency for these events is 17 Hz. Note the amplification at 20 Hz on the horizontal components of station C9.

relatively small source volume and may have shared the same focal mechanism, it is important to compare the P- and S-wave results. If any of the stations are consistently at P- or S-wave nodes for these events, the resulting component corrections will bias the source parameter analyses for the other events. As noted above, all three of the S-wave spectra at station C9 show significant amplification. Because the P-wave spectra at C9 are also amplified, however, this result appears to be a relative site amplification rather than a focal mechanism effect.

Mueller and Cranswick (1983) have matched the 20 Hz peak in the average tangential spectra at C9 with synthetics computed using a 5 meter layer with a shear velocity of .5 km/sec overlying a 3 km/sec bedrock. As all three sites have approximately the same depth of alluvium, however, it is difficult to understand why the resonance effects at site C9 are not also evident at sites C7 and C8. It is possible that the alluvial layer underlying C9 is either thicker or less consolidated than that underlying C7 and C8, or that the contact between the alluvium and the bedrock at C7 and C8 is significantly rougher, which might mask the resonance at these stations.

The SMA-1 Recordings

Although the analysis of the DR-100 data indicates that differential site effects can have a significant influence on high frequency motions in the 25-50 Hz band, because of the high corner frequencies of these aftershocks, we are unable to obtain an absolute calibration of the site response at these frequencies. Fortunately, the four SMA-1 recordings of the $m_{bLG} = 4.8$

aftershock which occurred on March 31, 1982, can be used to extend the observed frequency band to frequencies sufficiently low to be unaffected by the thin alluvial layers at the sites.

The accelerograms and the resulting acceleration spectra are shown in Figures 7 and 8. Figure 7 shows the records from the accelerograms at stations C9 and CB, while Figure 8 shows the records from the accelerograms at stations C7 and NB4. The differences among these acceleration spectra are remarkable. As mentioned previously, station CB is situated directly on the granitic bedrock. The horizontal S-wave spectra from this station exhibit relatively high corner frequencies and a pronounced flat portion extending from 4 to 30 Hz. The spectra appear to fall off above 30 Hz, resembling the average DR-100 spectra at station C8. The vertical component has a peak at about 40 Hz, however, suggesting that a mode conversion associated with the near-surface velocity structure may be responsible for the depletion of the high frequencies on the horizontal components.

The acceleration spectra determined from the horizontal components of the two accelerographs which were situated on thin layers of alluvium (at stations C7 and C9) increase significantly with increasing frequency, particularly at 10 Hz and above. It is useful to compare these spectra with the average spectra determined for the horizontal components of the S-waves at these sites, shown in Figure 6. While the SMA-1 recordings at C9 do not exhibit the sharply peaked resonance behavior of the DR-100 recordings, they fall off rapidly at frequencies lower that 10 Hz, similar to the average DR-100 spectra, which fall off more rapidly than ω^2 at low frequencies. This comparison points out the spatial variability of these site effects; the SMA-1 was approximately 10 meters from the DR-100 sensor. In contrast, however, the

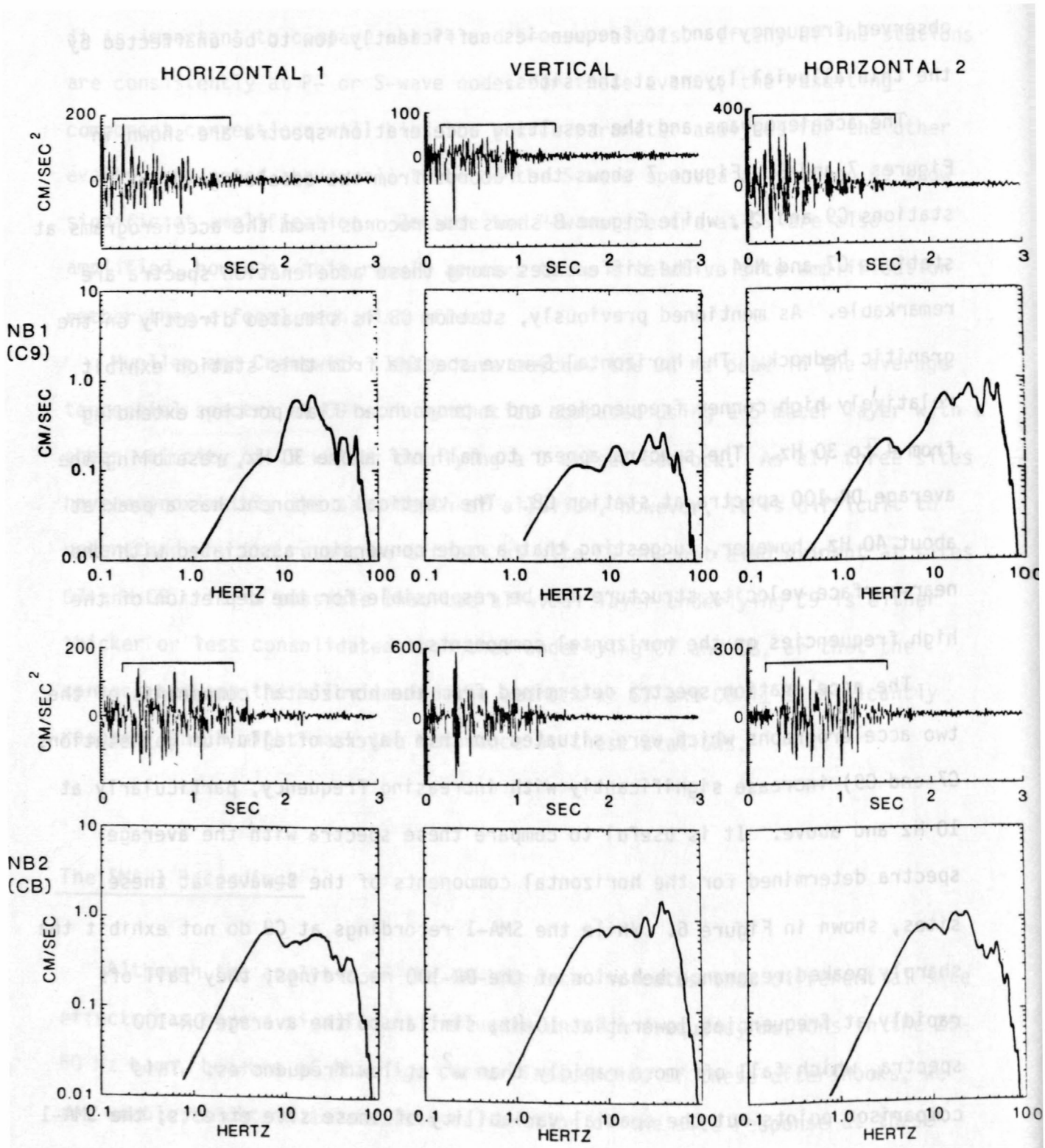

Figure 7. Accelerograms and spectra from the March 31 aftershock. The horizontal bars show the samples used to calculate the spectra. Note the relative high-frequency character of the vertical component at station CB (NB2).

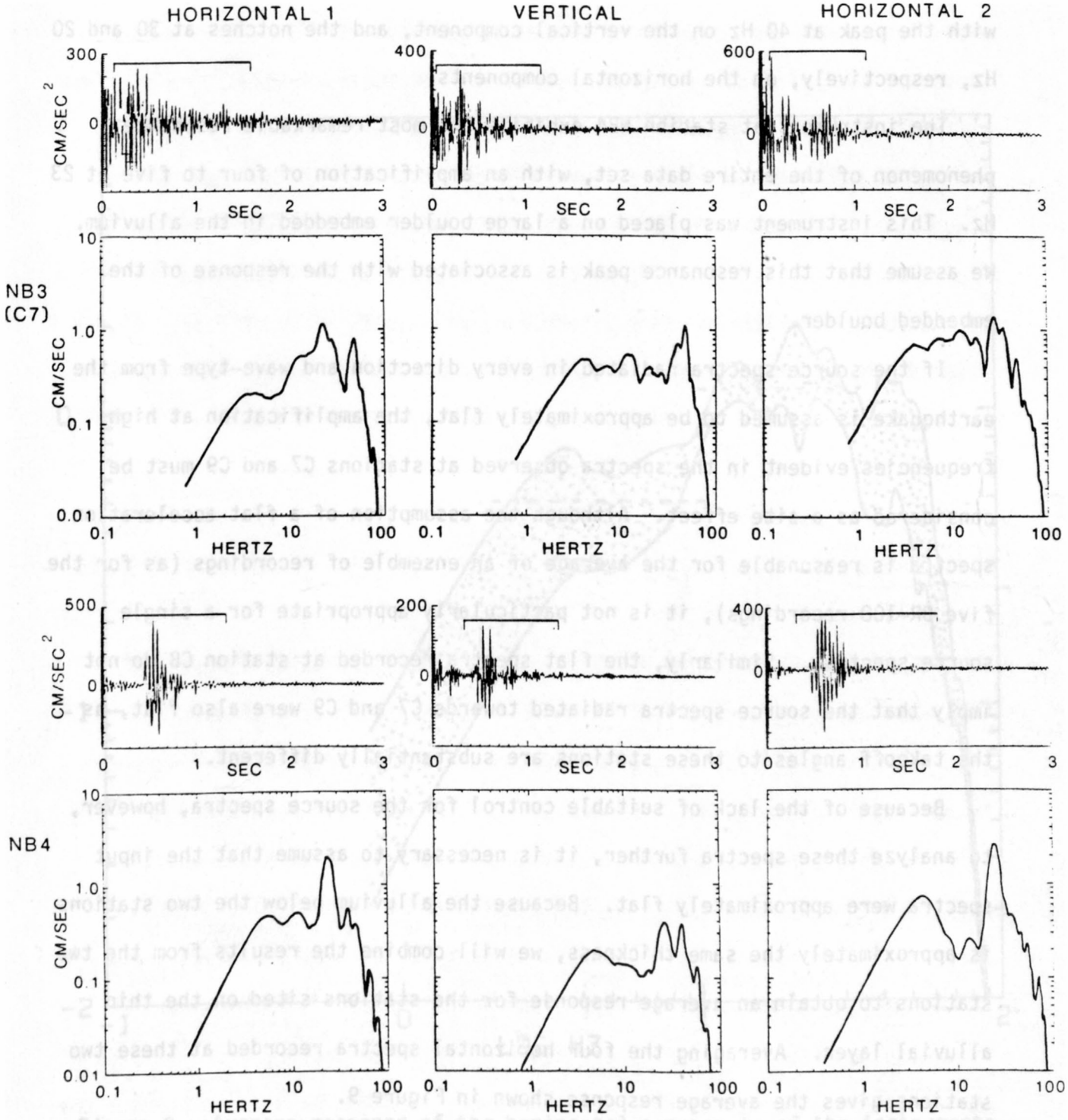

Figure 8. Accelerograms and spectra from the March 31 aftershock. The spectra at station C7 can be compared directly to the spectra shown in Figure 6, as the two horizontal components are closest to the tangential and the radial directions, respectively. The NB4 instrument was sited directly on a large boulded embedded in the alluvium, which may account for the marked resonance peak at 20 Hz.

SMA-1 recordings at station C7 strongly resemble the average DR-100 spectra, with the peak at 40 Hz on the vertical component, and the notches at 30 and 20 Hz, respectively, on the horizontal components.

The instrument at station NB4 exhibits the most remarkable resonance phenomenon of the entire data set, with an amplification of four to five at 23 Hz. This instrument was placed on a large boulder embedded in the alluvium. We assume that this resonance peak is associated with the response of the embedded boulder.

If the source spectra radiated in every direction and wave-type from the earthquake is assumed to be approximately flat, the amplification at high frequencies evident in the spectra observed at stations C7 and C9 must be considered as a site effect. Although the assumption of a flat acceleration spectra is reasonable for the average of an ensemble of recordings (as for the five DR-100 recordings), it is not particularly appropriate for a single source spectrum. Similarly, the flat spectra recorded at station CB do not imply that the source spectra radiated towards C7 and C9 were also flat, as the takeoff angles to these stations are substantially different.

Because of the lack of suitable control for the source spectra, however, to analyze these spectra further, it is necessary to assume that the input spectra were approximately flat. Because the alluvium below the two stations is approximately the same thickness, we will combine the results from the two stations to obtain an average response for the stations sited on the thin alluvial layer. Averaging the four horizontal spectra recorded at these two stations gives the average response shown in Figure 9.

Shear waves with periods of .3 seconds can be expected to have a quarter-wavelengths significantly longer than the depth of the alluvial layer, and

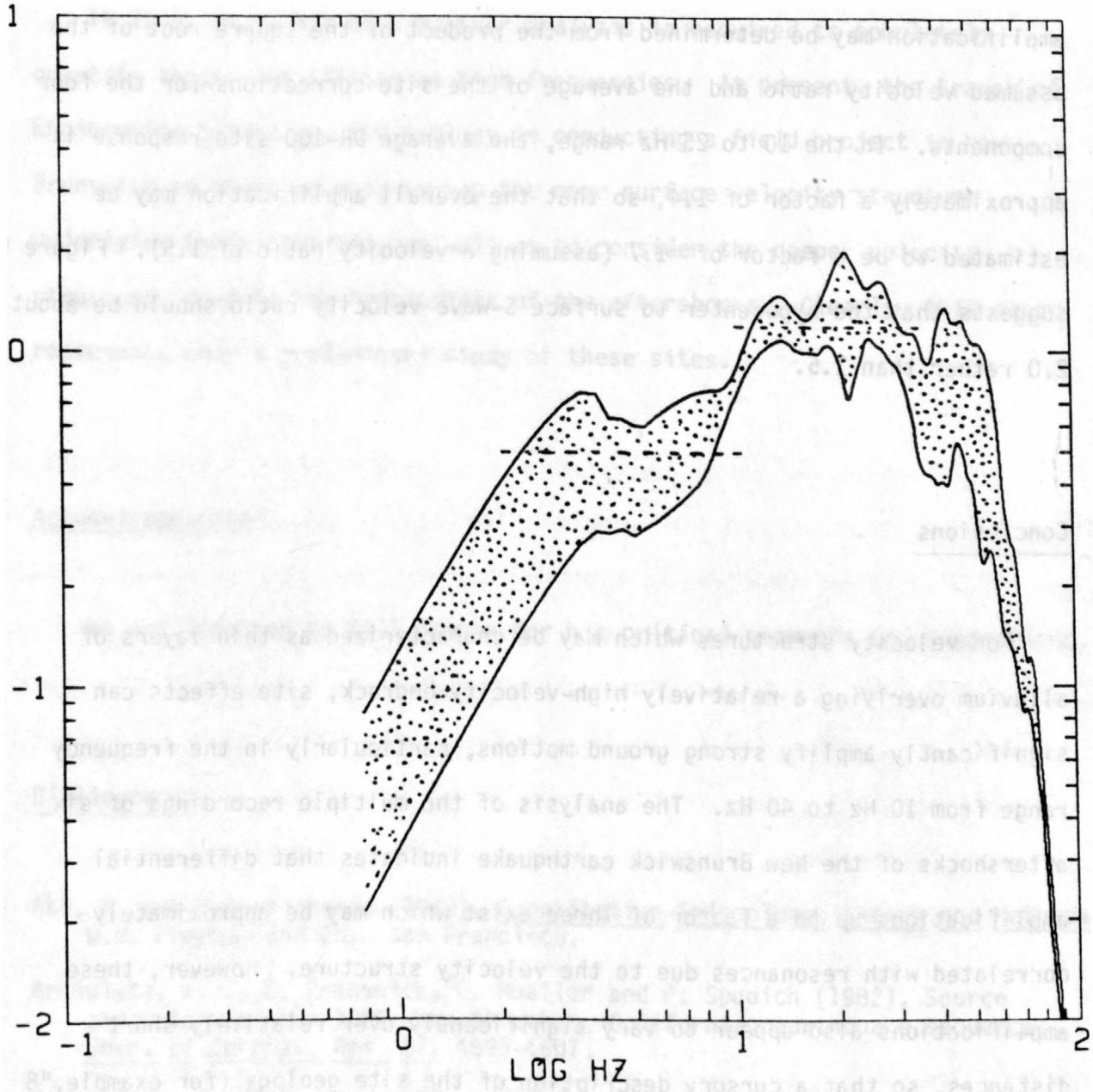

Figure 9. Average response of the horizontal components of the instruments sited at station C7 and C9. The dashed lines are approximate averages over the 3-8 Hz and 10-25 Hz frequency bands. The stippled area lies between the 85 percentile limits of the distribution of the four spectra.

should therefore be unaffected by the near-surface velocity structure. The amplification of the 10 to 25 Hz frequency band over the 3 to 8 Hz band is a factor of two. Following the analysis of the DR-100 recordings, the absolute amplification may be determined from the product of the square root of the assumed velocity ratio and the average of the site corrections for the four components. In the 10 to 25 Hz range, the average DR-100 site response is approximately a factor of 1.4, so that the overall amplification may be estimated to be a factor of ~1.7 (assuming a velocity ratio of 1.5). Figure 9 suggests that the hypocenter to surface S-wave velocity ratio should be about 2.0 rather than 1.5.

Conclusions

For velocity structures which may be characterized as thin layers of alluvium overlying a relatively high-velocity bedrock, site effects can significantly amplify strong ground motions, particularly in the frequency range from 10 Hz to 40 Hz. The analysis of the multiple recordings of six aftershocks of the New Brunswick earthquake indicates that differential amplifications up to a factor of three exist which may be approximately correlated with resonances due to the velocity structure. However, these amplifications also appear to vary significantly over relatively short distances, so that a cursory description of the site geology (for example,"8 meters of alluvium overlying granitic bedrock") cannot be used to predict the either the approximate amplitude or frequency dependance of the site response.

These results have been determined using a new approach which does not

require a specific "transparent" or hard-rock recording of the earthquakes, but incorporates the available information in an objective fashion without assuming one station is correct.

It is evident that much further analysis is required to completely quantify these site effects at high frequencies. At present, the Branch of Engineering Seismology and Geology is conducting a field project in New Brunswick in which we hope to map the near surface velocity structure underlying these stations, as well as to consider the deeper velocity structure, down to the hypocenters of the aftershocks. Clearly, this paper represents only a preliminary study of these sites.

Acknowledgements

We are indebted to Bill Joyner for his critical comments and suggestions.

Bibliography

Aki, K. and P.G. Richards (1980), Quantitative Seismology, Theory and Methods, W.H. Freeman and Co., San Francisco.

Archuleta, R.J., E. Cranswick, C. Mueller and P. Spudich (1982), Source parameters of the 1980 Mammoth Lakes, California, earthquake sequence, Jour. of Geophys. Res. 87, 4595-4607.

Boatwright, J (1982), A dynamic model for far-field acceleration, Bull. Seism. Soc. Am. 72, 1049-1068.

Hanks, T.C. (1982), f_{max}, Bull. Seism. Soc. Am. 72, 1867-1880.

Mueller, C. and E. Cranswick (1983), Processing and interpretation of the Miramimichi aftershock data, submitted to Bull. Seism. Soc. Am. 73.

THE SEPTEMBER 4, 1981, SANTA BARBARA ISLAND CALIFORNIA, EARTHQUAKE: INTERPRETATION OF STRONG MOTION DATA

by

John G. Anderson

University of California, San Diego

La Jolla, California 92093

ABSTRACT

Seven timed strong motion accelerograms were recorded between the distances of 45 km and 80 km from the Santa Barbara Island earthquake. Accelerograms at these distances are not normally digitized for earthquakes with magnitude less than 6. From the accelerograms, the average estimate for M_L is 6.0, compared to an average of M_L = 5.5 from more distant recordings. When M_L is estimated from accelerograph data using the distance correction to the M_L scale proposed by Luco (1982), an average of 5.3 is obtained. This suggests that the correction slightly over-compensate in this magnitude and distance range, in which Luco lacked data, at least for this earthquake.

S-wave spectra, from three accelerograms which recorded the complete S-wave, imply a seismic moment of 1.5×10^{24} dyne-cm and, by the method of Brune (1970), a source radius of 2 km and a stress drop of 90 bars. If the displacement spectrum is assumed to be approximated by two asymptotes, f^0 at frequencies less than the corner frequency and f^{-2} at frequencies greater than the corner frequency, the level of the f^{-2} asymptote can be constrained by RMS

acceleration (Hanks, 1979). This leads to a smaller estimated source radius and a higher stress drop.

In the process of matching these spectra, an average value of Q can be inferred to be consistent with the spectra at high frequencies. This value is between 300 and 500 for the assumed spectral shapes.

One accelerograph, located on a ridge, recorded an anomalously high amplitude ringing at 2 Hz on the transverse component only. Subsurface geological structure is the most likely cause of the amplification.

INTRODUCTION

On September 4, 1981, at about 8:51 AM local time (Pacific Daylight Time), an earthquake occurred southeast of Santa Monica, and was felt through most of the western part of southern California, from San Luis Obispo to San Diego. Because the epicenter was at sea (Figure 1), there was little damage. However, ground motions were strong enough to trigger perhaps 50 percent of the accelerographs in the nearest on-land locations. Locations of accelerographs from Los Angeles accelerograph network (Anderson et al., 1981) which recorded the earthquake are shown in Figure 1.

The peak accelerations which were recorded in the earthquake are all less than 50cm/sec^2 (.05g). Accelerograms at this level are not normally digitized or studied in any detail. However, accelerograms from the Santa Barbara Island earthquake have been digitized. This paper reports on an anlaysis of these accelerograms.

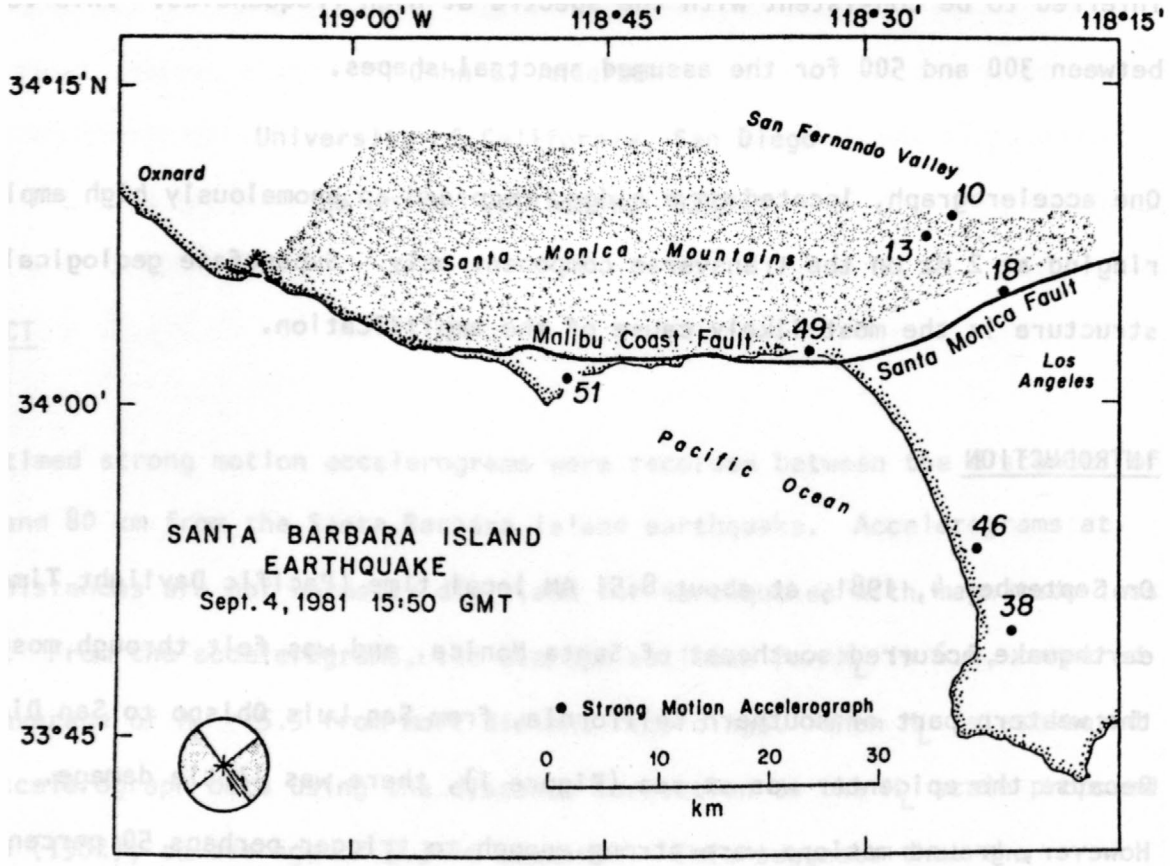

Figure 1. Map showing epicenter of the September 4, 1982 earthquake and strong-motion stations which recorded the shaking. The focal mechanism (with preferred slip plane) of Corbett and Piper (1981), is plotted at the epicentral location of Henyey (personal communication): 33°48.57'N, 119°7.08'W. Geological data on this map is after Jennings and Strand (1969).

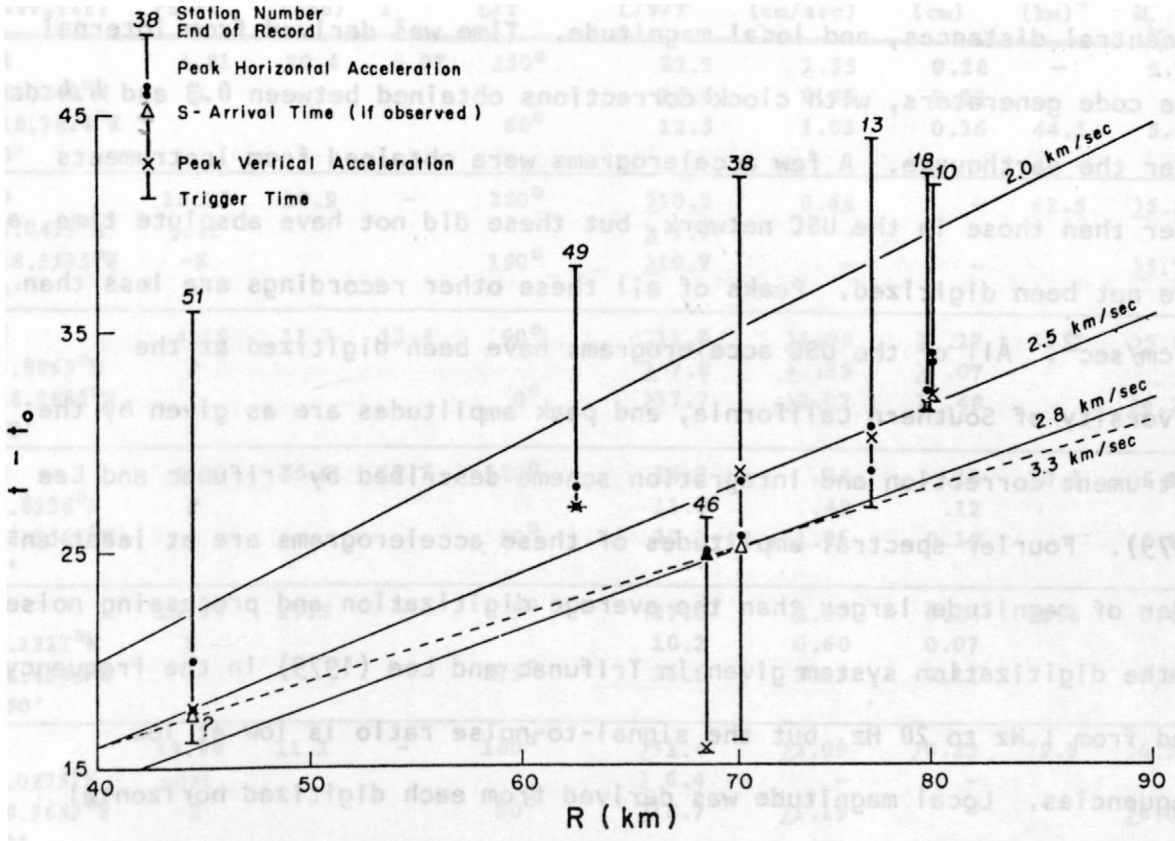

Figure 2. Times at which each accelerograph recorded strong shaking. Each vertical line applies to one site (number is given above), and is plotted as a function of distance between epicenter and site. Time scale is in seconds after origin time of earthquake, taken as 15 hrs 50 min 43.57 sec, GMT (Henyey, personal communication). Solid lines for constant group velocity, originate at the epicenter at $t - t_0 = 0$; light dashed line has intercept at $t - t_0 = 4.0$.

DATA

The accelerograms which are discussed in this paper are listed in Table 1. The sites are part of the Los Angeles vicinity accelerograph network which was installed by the University of Southern California (USC) (Anderson et al., 1981). Table 1 also gives the instrument trigger time, the S-wave arrival time if the instrument triggered before the S-wave, inferred peak amplitudes, epicentral distances, and local magnitude. Time was derived from internal time code generators, with clock corrections obtained between 0.3 and 4.4 days after the earthquake. A few accelerograms were obtained from instruments other than those in the USC network, but these did not have absolute time, and have not been digitized. Peaks of all these other recordings are less than 50 cm/sec^2. All of the USC accelerograms have been digitized at the University of Southern California, and peak amplitudes are as given by the instrument correction and integration scheme described by Trifunac and Lee (1979). Fourier spectral amplitudes of these accelerograms are at least an order of magnitude larger than the average digitization and processing noise of the digitization system given in Trifunac and Lee (1979) in the frequency band from 1 Hz to 20 Hz, but the signal-to-noise ratio is low at low frequencies. Local magnitude was derived from each digitized horizontal component as in Kanamori and Jennings (1978).

Figure 2 shows when each of the USC accelerographs was operating during the earthquake. Based on the S-wave arrival times at stations 46 and 38, the S-wave arrived at these stations with an average velocity of 2.8 km/sec. This in turn implies that sites 51 and 13 were triggered near the time of the S-wave arrival, and that stations 49, 18, and 10 triggered 3 or more seconds

Table 1 - Summary of Accelerograph Data from the Sept. 4, 1981 Santa Barbara Island Earthquake.

Site No. Lat/Long. Elev.(ft)	Trigger Time,[1] Phase[2]	Record Dur. (sec)	T_s [1]	Orientation L/T	Peak Accel.[2] (cm/sec^2) L/V/T	Peak Vel.[3] (cm/sec)	Peak Displ.[3] (cm)	Epic. Dist.[4] (km)	M_L	M_L^{L} [5]
51	4.81	20.4	6.07	150°	22.3	1.35	0.28	-	5.76	5.02
34.0240°N	S				15.4	0.86	0.21			
118.7874°W				60°	12.5	1.03	0.26	44.5	5.57	4.75
30'										
49	15.59	10.9	-	280°	≥10.2	0.64	-	62.5	≥5.57	≥4.78
34.0419°N	post				≥ 7.3	-	-			
118.5535°W	-S			190°	≥10.7	-	-		≥5.75	≥5.03
90'										
46	4.16	11.1	13.4	90°	≥11.3	≥1.08	≥ .17	68.7	≥5.89	≥4.93
33.8869°N	P				≥ 7.8	≥ .39	≥ .07			
118.3885°W				0°	≥17.7	≥2.07	≥ .48		≥6.25	≥5.45
150'										
38	4.80	25.9	13.7	180°	16.3	.88	.13	70.3	5.83	4.86
33.8228°N	P				11.0	.48	.12			
118.3561°W				90°	20.1	1.06	0.19		5.87	4.92
75'										
13	15.64	17.5	-	9°	27.6	2.09	0.24	76.6	6.45	6.02
34.1317°N	S				10.2	0.60	0.07			
118.4395°W				279°	26.6	2.13	0.17		6.36	5.89
1250'										
18	19.99	11.1	-	180°	≥31.4	≥2.09	≥0.23	79.3	≥6.36	≥5.53
34.0875°N	post				≥ 6.4	-	-			
118.3653°W	-S			90°	≥18.7	≥1.19	-		≥6.00	≥5.02
240'										
10	20.46	10.4	-	182°	≥21.9	≥2.18	≥ .39	79.4	≥6.39	≥5.58
34.1460°N	post				≥10.1	-	-			
118.4125°W	-S			92°	≥17.6	≥1.17	≥0.22		≥6.15	≥5.23
634'										

[1] Trigger time and S-arrival times (T_s) are in seconds. The day, hour, and minute are 4 September, 1981 (Julian 247), 15 hours, 51 minutes UTC.

[2] Phase which caused accelerograph to trigger.

[3] Where blank, unreliable because signal-to-noise ratio is small.

[4] Based on epicentral location of 33°43.57'N, 119°07.08'W

[5] $M_L^L = 1.43[M_L - C(d) - 0.23S]$ (Luco, 1982) s = 0, sites 49,13; s = 1 otherwise; C(d) given by Luco (1982).

after the first S-wave arrival. Station 46 turned off in the midst of the S-wave arrivals. One interpretation of the accelerogram at station 51 is that the S-wave arrives about 1.2 second after the trigger time. Although this interpretation is uncertain, it is shown in Figure 2, and if correct, implies that the phase velocity across the region was about 3.3/ km/sec. In the S-wave velocity model for the western United States obtained by Lee and Solomon (1978) the shallowest resolvable layer has a velocity of 3.3 $\pm$ 0.1 km/sec.

Corbett and Piper (1981) find that the focal mechanism for this earthquake is predominantly right-lateral strike slip, and infer that the fault plane is oriented N37^{o}W, as shown in Figure 1. This implies that stations in the direction of station 13 and 10 would have nodal P-wave arrivals and that SH radiation is at a maximum. Stations 38 and 46 are nearest to the maximum in the P-wave radiation pattern, consistent with the observation that only these sites were triggered by the P-wave. Station 38 is closest to a node for SH arrivals, but is 15^{o} away from the predicted node. The classical radiation pattern for a strike slip double couple source implies SH amplitudes at station 38 equal to 0.5 times the amplitudes at stations near the radiation maximum (stations 49, 13, 18, 10), and SV amplitudes at station 38 equal to 0.87 times the amplitudes at stations near the radiation maximum (Aki and Richards, 1980). This radiation pattern does not seem to be a conspicuous influence on observed peak acceleration.

Accelerograms are shown in Figures 3, 4, and 5. Figure 3 shows the vertical component, Figure 4 the radial component, and Figure 5 the transverse component of acceleration at each site. Accelerograms are plotted in reduced

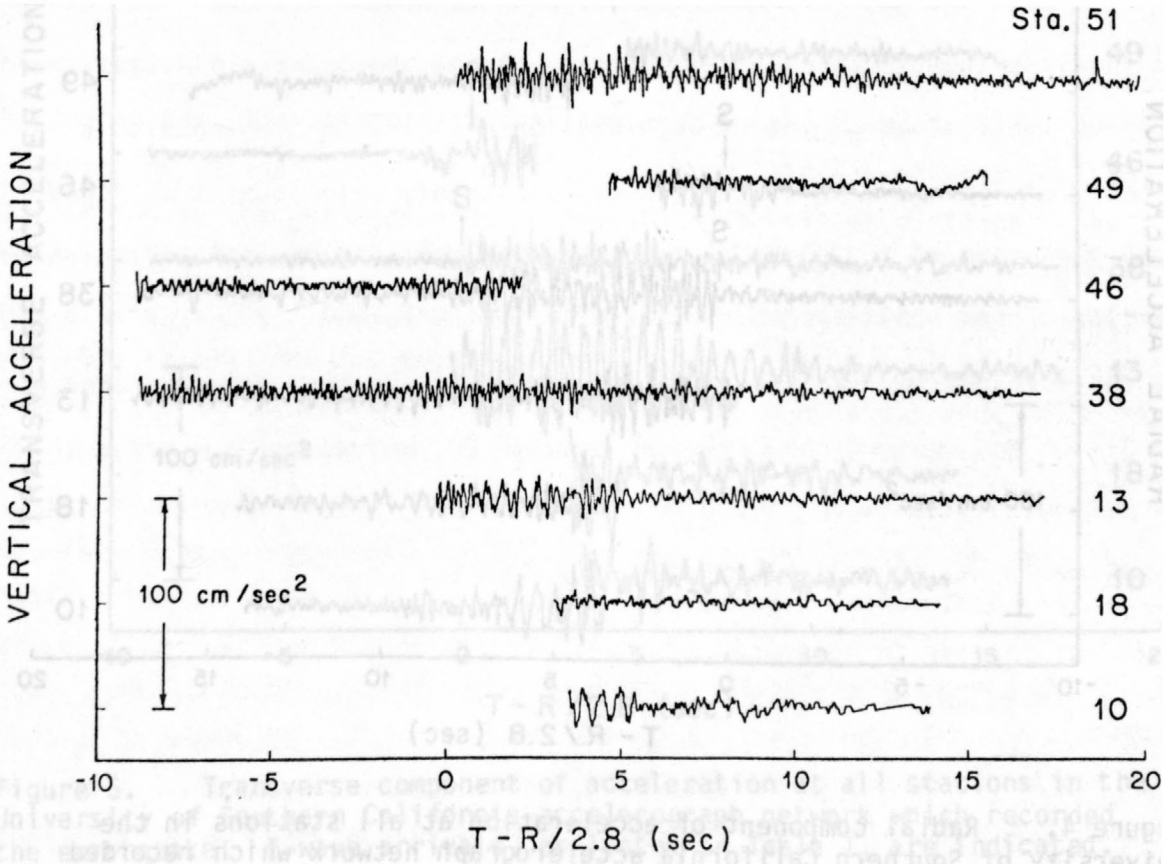

Figure 3. Vertical acceleration at all stations in the University of Southern California accelerograph network which recorded the earthquake.

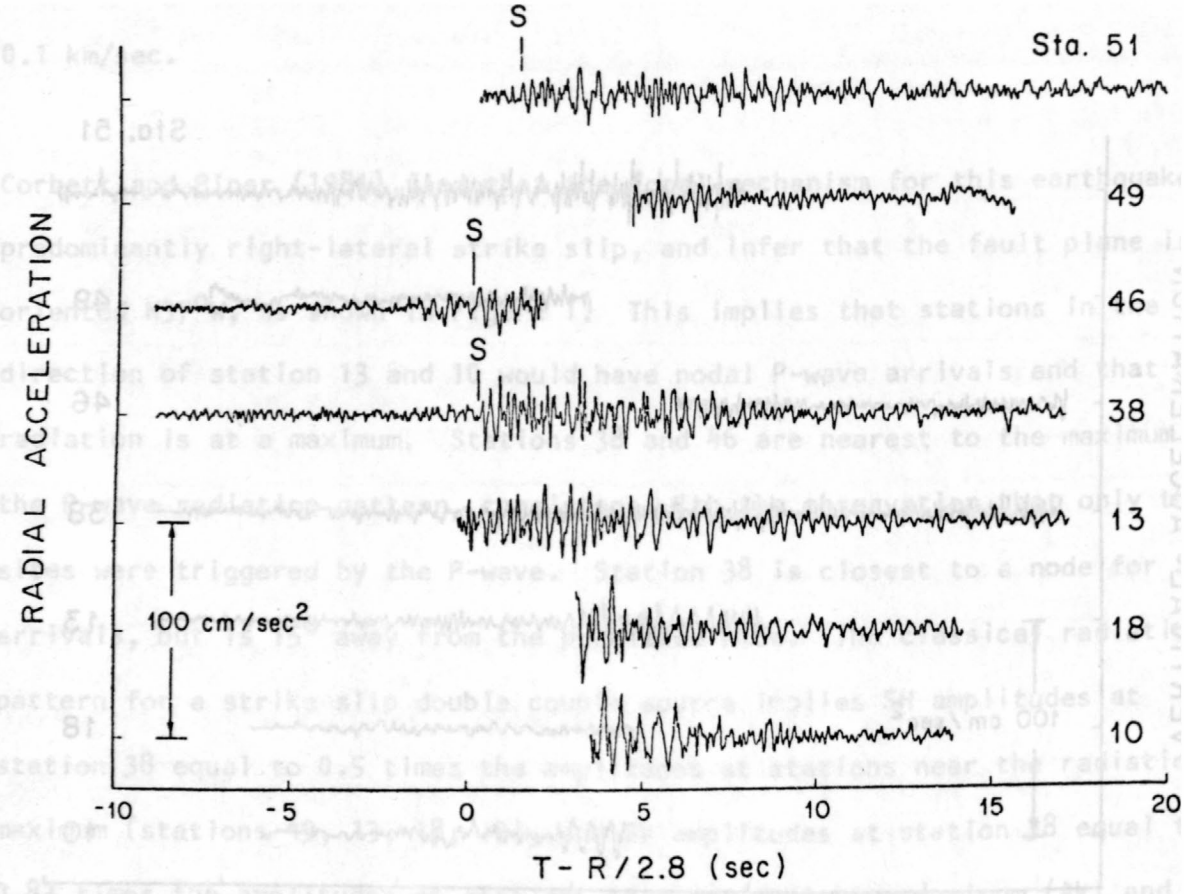

Figure 4. Radial component of acceleration at all stations in the University of Southern California accelerograph network which recorded the earthquake. S-wave arrivals, as listed in Table 1, are indicated.

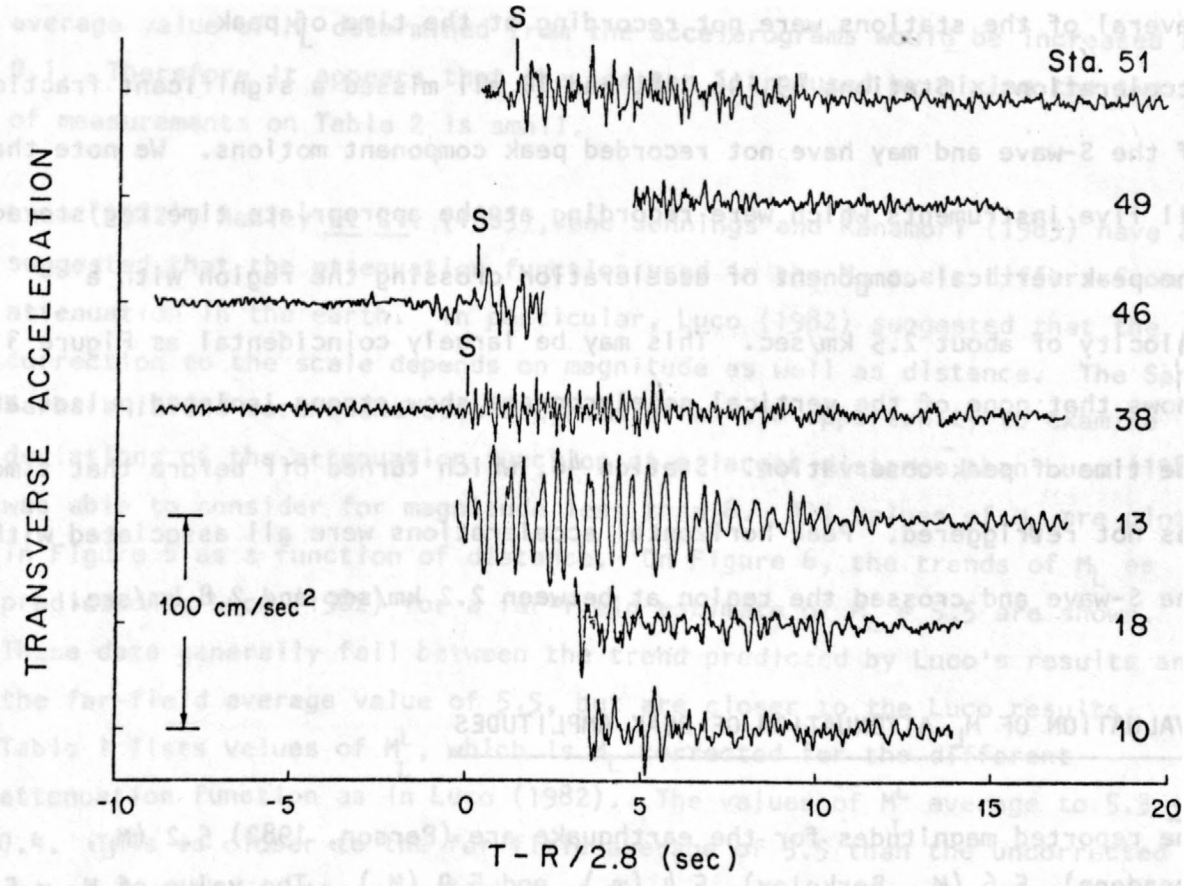

Figure 5. Transverse component of acceleration at all stations in the University of Southern California accelerograph network which recorded the earthquake. S-wave arrivals, as listed in Table 1, are indicated.

time t - $\frac{R}{2.8 \text{ km sec}}$ where t is time in seconds after the origin time of the earthquake and R is distance between the epicenter and the accelerograph.

Times of peak accelerations on each component are shown on Figure 2. Peaks on the vertical component are indicated by an "x", and on the horizontal component by a dot. There appears to be a significant probability that several of the stations were not recording at the time of peak accelerations. Stations 49, 46, 18, and 10 all missed a significant fraction of the S-wave and may have not recorded peak component motions. We note that all five instruments which were recording at the appropriate time registered the peak vertical component of acceleration crossing the region with a velocity of about 2.5 km/sec. This may be largely coincidental as Figure 3 shows that none of the vertical accelerograms show strong isolated pulses at the time of peak observation. Station 46, which turned off before that time, was not retriggered. Peak horizontal accelerations were all associated with the S-wave and crossed the region at between 2.2 km/sec and 2.8 km/sec.

EVALUATION OF M_L ATTENUATION OF PEAK AMPLITUDES

The reported magnitudes for the earthquake are (Person, 1982) 5.2 (M_L, Pasadena), 5.6 (M_L, Berkeley), 5.4 (m_b), and 5.9 (M_s). The value of M_L = 5.2 (PAS) has been revised to 5.3 (R. Geary, personal communication). Wood-Anderson stations which recorded the earthquake are summarized in Table 2; the average value of M_L based on all Wood-Anderson recordings is 5.5. This value is much less than the average value of $M_L = 6.0 \pm 0.3$, based on the strong motion stations, as listed in Table 1.

Table 2 indicates two ways in which amplitudes have been measured from the Wood-Anderson records to determine magnitude. The procedure which is preferred by the Seismological Laboratory at the California Institute of

Technology (CalTech) and by Kanamori and Jennings (1978) is to use half the maximum peak-to-peak displacement of the Wood-Anderson trace. The measurements by the Seismological Laboratory at Berkeley are the maximum zero-to-peak displacements. Some of the measurements in Table 2 from the records at CalTech are also made this way, as the photographic recordings are off-scale in one direction. On the synthetic Wood-Anderson records derived from the accelerograms, the procedure of Kanamori and Jennings (1978) has been used. If the maximum zero-to-peak measurements had been used instead, the average value of M_L determined from the accelerograms would be increased by 0.1. Therefore it appears that the scatter introduced by mixing the two types of measurements on Table 2 is small.

Luco (1982), Hadley *et al.* (1983), and Jennings and Kanamori (1983) have all suggested that the attenuation function used in the M_L scale differs from attenuation in the earth. In particular, Luco (1982) suggested that the correction to the scale depends on magnitude as well as distance. The Santa Barbara Island earthquake accelerograms offer the opportunity to examine deviations of the attenuation function at a larger distance than Luco (1982) was able to consider for magnitude less than 6. All values of M_L are plotted in Figure 6 as a function of distance. On Figure 6, the trends of M_L as predicted by Luco (1982) for a far-field estimate of $M_L = 5.5$ are shown. These data generally fall between the trend predicted by Luco's results and the far-field average value of 5.5, but are closer to the Luco results. Table 1 lists values of M_L^L, which is M_L corrected for the different attenuation function as in Luco (1982). The values of M_L^L average to 5.3 ± 0.4. This is closer to the far field average of 5.5 than the uncorrected values, but the scatter is slightly increased. Thus for this particular magnitude and distance range, which is outside the scope of the data used by Luco, a literal interpretation of these data suggests that the correction to the M_L scale extrapolated from Luco's results may slightly overcompensate for inaccuracy in Richter's attenuation curve, at least for this earthquake. My judgement is that this conclusion is not modified by incomplete recordings or by site effects. These two factors will tend to have small, but opposing effects on M_L estimates.

Table 2 - Wood-Anderson Stations which Recorded the September 4, 1981 Santa Monica, Basin Earthquake, and Interpretation for M_L.

Station	Comp.	Epicentral Distance	Peak Amplitude	Station Correction	M_L	Source
PASADENA	N	101.8	>124.0*	0.1	>5.21	1
	E		>134.0*	0.1	>5.25	1
RIVERSIDE	N	164.6	102.8†	0.0	5.46	1
	E		69.8†	0.0	5.29	1
PALOMAR	N	211.9	145.5*	0.0	5.77	1
	E		100.5*	0.0	5.61	1
ISABELLA	N	228.6	18.0†	+0.2	5.15	1
COTTONWOOD	N	321.4	12.7†	0.0	5.22	1
	E		14.4†	0.0	5.27	1
TINEMAJA	N	383.9	69.0*	-0.2	6.04	1
	E		44.6*	-0.2	5.85	1
MT. HAMILTON	N	467.7	5.4*	0.1	5.51	2
	E		4.5*	+0.1	5.43	2
BERKELEY	N	546.3	6.1*	0.0	5.59	2
	E		9.8*	0.0	5.79	2

Source

1 R. Geary, Personal Communication.

2 R. Miller, Personal Communication.

* Maximum 0 - peak values.

† Half of maximum peak-to-peak recordings.

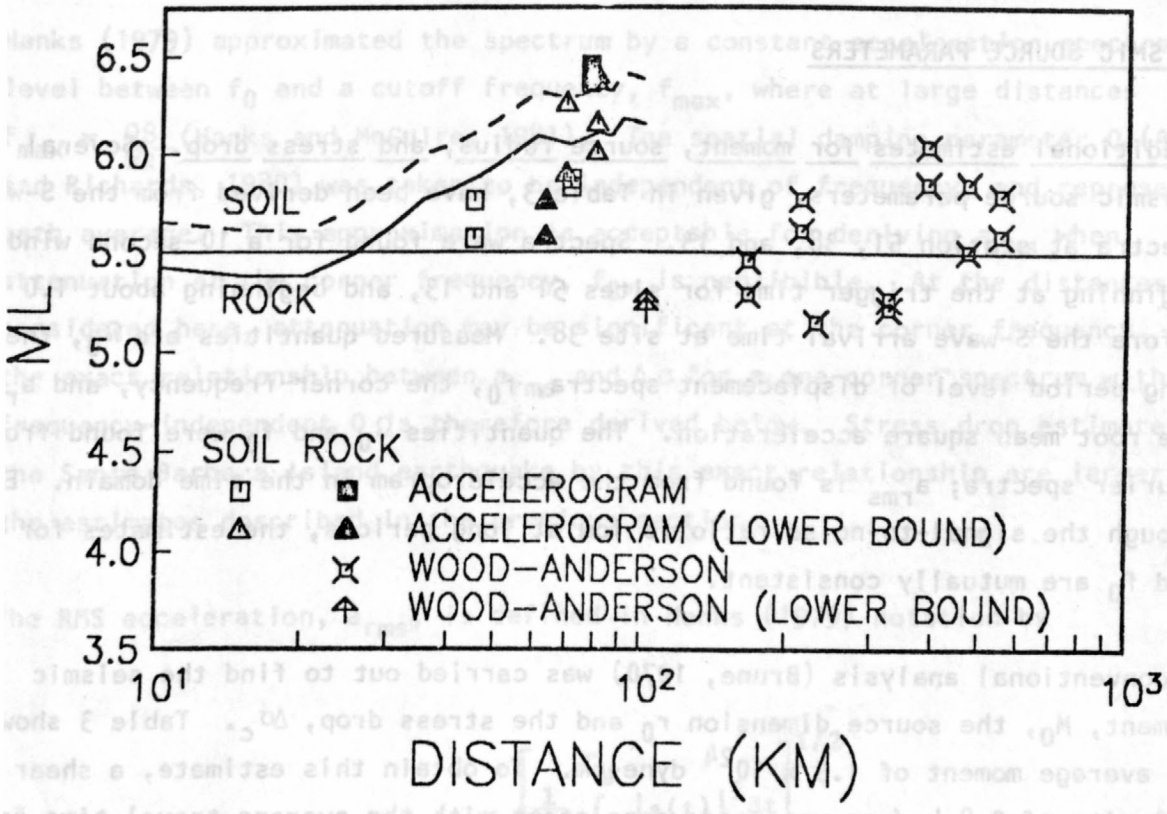

Figure 6. Estimates of M_L from several instruments. Instruments of R less than 100 km are accelerographs; instruments at R greater than 100 km are standard Wood-Anderson stations. Curves show expected values of M_L (Luco, 1982) at accelerograph sites based on large-distance average M_L of 5.5.

Peak recorded accelerations were predictable. For example, the larger horizontal peak at each station (Table 1) is within one standard deviation of the regression curve obtained by Joyner and Boore (1981), except at station 49, which triggered late. Only station 51 is within the magnitude and distance range employed by Joyner and Boore. Thus this data verifies the extrapolation of their regression to distances of 50 to 80 km for magnitudes 5.5 to 6.0. In testing the extrapolation of the results by Campbell (1981), it was found that Eq. (3), was more consistent with these data than Eq. (5) of his paper.

SEISMIC SOURCE PARAMETERS

Traditional estimates for moment, source radius, and stress drop. Several seismic source parameters, given in Table 3, have been derived from the S-wave spectra at station 51, 38, and 13. Spectra were found for a 10-second window beginning at the trigger time for sites 51 and 13, and beginning about 1.0 sec before the S-wave arrival time at site 38. Measured quantities are Ω_0, the long period level of displacement spectra, f_0, the corner frequency, and a_{rms}, the root mean square acceleration. The quantities Ω_0 and f_0 were found from Fourier spectra; a_{rms} is found from the accelerogram in the time domain. Even though the signal-to-noise ratio is low at long periods, the estimates for Ω_0 and f_0 are mutually consistent.

A conventional analysis (Brune, 1970) was carried out to find the seismic moment, M_0, the source dimension r_0 and the stress drop, $\Delta\sigma_c$. Table 3 shows an average moment of 1.5×10^{24} dyne-cm. To obtain this estimate, a shear velocity of 2.8 km/sec was used, consistent with the average travel time from the source. This value was used for consistency with entire-path Q estimates to be shown subsequently. If a shear velocity of 3.2 km/sec had been used as in Thatcher and Hanks (1973), the average moment would be 2.3×10^{24} dyne-cm. By Hanks and Kanamori (1979) the value of M_S (5.9) implies a moment of 7×10^{24} dyne-cm; the cause of the discrepancy is unknown. Modiano and Hatzfeld (1982) have independently checked the assumed R^{-1} dependence of M_0 in the Brune (1970) model for $R \leq 50$ km, and find it supported. The average estimate for the source radius is 2.0 or 2.3 km, depending on which shear

velocity is used, and the average estimate for the Brune (1970) stress drop is 90 bars.

Source parameters constrained by RMS acceleration. Hanks (1979), McGuire and Hanks (1980), and Hanks and McGuire (1981) have studied some consequences of the additional assumption that the spectral fall-off at frequencies above f_0 is proportional to f^{-2}. In particular, the root mean square acceleration, a_{rms}, is then simply related to the stress drop. In this section, a study of these consequences is continued.

Hanks (1979) approximated the spectrum by a constant acceleration spectral level between f_0 and a cutoff frequency, f_{max}, where at large distances $f_{max} = \frac{Q\beta}{\pi R}$ (Hanks and McGuire, 1981). The spatial damping parameter Q (Aki and Richards, 1980) was taken to be independent of frequency, and represents a path average. This approximation is acceptable for deriving a_{rms} when attenuation at the corner frequency, f_0, is neglibible. At the distances considered here, attenuation may be significant at the corner frequency, and the exact relationship between a_{rms} and $\Delta\sigma$ for a one-corner spectrum with a frequency-independent Q is therefore derived below. Stress drop estimates of the Santa Barbara Island earthquake by this exact relationship are larger than the estimates described in the previous section.

The RMS acceleration, a_{rms}, is defined in Hanks (1979) notation by

$$a_{rms} = \left[\frac{1}{T_\omega}\int_0^{T_\omega} |a(t)|^2 dt\right]^{1/2} \qquad (1)$$

in which T_ω is the length of the time window and a(t) represents the accelerogram. Hanks chose $T_\omega = T_d = 1/f_0$, where T_d is approximately the duration of faulting. The equations are kept general in this derivation. By Parseval's theorem, a_{rms} is related to the spectrum by

$$a_{rms} = \left[\frac{2}{T_\omega}\int_0^{\infty} |\tilde{a}(f)|^2 \, df\right]^{1/2} \qquad (2)$$

In Eq. (2), a(f) represents the Fourier transform of a(t). The spectrum is assumed to have the shape:

$$\tilde{a}(f) = \begin{cases} (2\pi f)^2 \Omega_0 \exp\left(\frac{-\pi R f}{Q\beta}\right) & 0 < f \leq f_0 \\ (2\pi f_0)^2 \Omega_0 \exp\left(\frac{-\pi R f}{Q\beta}\right) & f_0 < f \end{cases} . \quad (3)$$

For this $\tilde{a}(f)$, which approximates the shape proposed by Brune (1970) by its asymptotic limits and adds attenuation, the integral in Eq. (2) can be evaluated exactly, and yields

$$a_{rms} = (2\pi) \frac{2R_{\theta\phi}}{106} \left(\frac{T_d}{T_\omega}\right)^{1/2} \frac{\Delta\sigma}{\rho R} \left[\frac{Q\beta}{\pi R f_0}\right]^{1/2} (f_0 T_d)^{-1/2} \exp\left(-\frac{\pi R f_0}{Q\beta}\right) \cdot \left\{1 + 4! \sum_{k=5}^{\infty} \frac{\left|\frac{2\pi R f_0}{Q\beta}\right|^{k-4}}{k!}\right\}^{1/2} \quad (4)$$

where we have used, from the Brune (1970) model,

$$\Omega_0 f_0^3 = \frac{2R_{\theta\phi}}{106} \frac{\Delta\sigma}{\rho R} \quad (5)$$

In these equations, $R_{\Theta\phi}$ is a radiation pattern and is the density. Eq. (4) differs from the expression in Hanks and McGuire (1981) by the ratio

$$\left(\frac{T_d}{T_\omega}^{1/2}\right)$$

which corrects for an arbitrary window length, by the factor $(f_0 T_d)^{-1/2}$, which they assumed to be 1, by the exponential term, and by the error team represented by the infinite series. For low corner frequencies, short distances, or high Q, the exponential and error terms are close to unity.

Hanks and McGuire (1981) have shown that when T_ω is chosen as close as possible to T_d and the correction term $(T_d/T_\omega)^{1/2}$ is assumed to equal 1.0, then a_{rms} is generally consistent with a stress drop of about 100 bars. On the other hand, a_{rms} is not sensitive to reasonable choices of window length T_ω (McCann and Boore, 1983); this insensitivity of a_{rms} to T_ω may contribute to the good predictive capability of Eq. (4) after the simplifying assumptions have been made.

Table 3 lists stress drop estimates based on the formulation of Hanks and McGuire (1981) for this earthquake ($\Delta\sigma_{HM}$). These employ Q = 300 for all records. As observed by Hanks and McGuire for other earthquakes, the median observed value of this stress drop parameter is in the vicinity of 100 bars.

It is a useful check to go backwards and superimpose the spectra implied by the parameters derived by the Hanks and McGuire formulation on the observed spectra. When that was done using the parameters given in Table 3, the agreement was generally rather poor. Contributions to the misfit came from incompatibility of a_{rms} and the seismic moment obtained from the Brune (1970)

Table 3 – Evaluation of source paramaters for the September 4, 1981 Santa Barbara Island earthquake.

Record[1]	Ω_0 cm-sec	f_0 Hz	a_{rms} cm/sec^2	M_L	Brune Method[2] $M_0 \times 10^{24}$ dyne-cm	Brune Method[2] $\mathfrak{M}^3$	Brune Method[2] r km	Brune Method[2] $\Delta\sigma_c$ bars	$\Delta\sigma_{HM}$	Eq. 7 Q	Eq. 7 f_0 Hz	Eq. 7 $\Delta\sigma_7$ bars
51-R	0.36	0.47	4.16	5.57	1.4	5.43	2.2	56	44	300	.63	137
-T	0.46	0.69	5.48	5.74	1.8	5.50	1.5	227	70	300	.64	183
38-R	0.47	0.43	5.47	5.95	2.9	5.64	2.4	88	110	500	.63	273
-T	0.18	0.60	4.60	5.87	1.1	5.36	1.7	92	110	500	.94	356
13-R	0.20	0.49	5.58	6.17	1.3	5.41	2.1	61	137	500	1.0	535
-T	0.13	2.74*	13.42*	6.51*	0.87	5.29	0.38*	6925*	777*	500	2.1*	2886*

[1] R is radial component, T is transverse component.

[2] $M_0 = 4\pi\rho\beta^3\Omega_0 R/0.85$ (Thatcher and Hanks, 1973); ρ = 2.7 gm/cm^3, β = 2.8 km/sec.

$\mathfrak{M} = \frac{2}{3} \log M_0 - 10.7$ (Hanks and Kanamori, 1979)

$r = 2.34\beta/2\pi f_0$ (Thatcher and Hanks, 1973).

$\Delta\sigma_c = \frac{7}{16} M_0/r^3$ (Thatcher and Hanks, 1973).

* These values regarded as unreliable, introduced by unusual site conditions.

analysis with the selected corner frequency, from the difference between T_ω and T_d $(=1/f_0)$, and from the choice of Q.

Here we abandon the original estimate for the corner frequency in favor of a new estimate which is consistent with M_0 and a_{rms}. Combining relations from the Brune (1970) model, one obtains

$$f_0 = k_2 \beta \left(\frac{\Delta\sigma}{M_0} \right)^{\frac{1}{3}} \tag{6}$$

$$\text{in which } k_2 = \frac{2.34}{2\pi} \left(\frac{16}{7} \right)^{\frac{1}{3}}.$$

Substituting (6) into (4), one obtains

$$a_{rms} = \frac{2\pi^2 R_{\theta\phi}}{106} \left(\frac{T_d}{T_\omega} \right)^{1/2} \left(\frac{Q}{\pi k_2} \right)^{1/2} \frac{M_0^{\frac{1}{6}} \Delta\sigma^{\frac{5}{6}}}{\rho^{\frac{3}{2}} R^2} \left(f_0 T_d \right)^{-1/2} \exp \left\{ - \frac{k_2 \pi R}{Q} \left(\frac{\Delta\sigma}{M_0} \right)^{\frac{1}{3}} \right\}$$

$$\cdot \left\{ 1 + 4! \sum_{k=5}^{\infty} \left[\frac{\left(\frac{2\pi k_2 R}{Q} \left(\frac{\Delta\sigma}{M_0} \right)^{\frac{1}{3}} \right)^{k-4}}{k!} \right] \right\}^{1/2} \tag{7}$$

Eq. (7) can not be solved for $\Delta\sigma$ explicitly, except under the approximation that attenuation is not important near the corner frequency. Hanks and McGuire (1981) obtained the same dependence of a_{rms} on M_0 and $\Delta\sigma$.

The stress drop, obtained from Eq. (7), and designated as $\Delta\sigma_7$, was found by a numerical procedure, for Q = 100, 300, and 500. The observed spectra, and the implied theoretical spectra are plotted in Figure 7. The theoretical spectra match the observations at high frequencies and low frequencies but tend to overestimate the amplitudes of the observed spectra near the corner frequency. Specifically, high frequencies from station 51 appear to be fit reasonably well by the theoretical spectra with Q = 300, although a slightly larger value of Q may be better. Station 38 spectra are better fit by the theoretical spectra with Q = 500. The radial component at station 13 may be better fit by Q = 500 than by Q = 300. The transverse component of station 13 is affected by the strong site effect and in fact, for Q = 100, there is no spectral shape (Eq. 3) consistent with a_{rms} and M_0 as given in Table 3 because of the dominant role of attenuation at and below the apparent corner frequency; the shape which is shown for Q = 100 has an infinite corner frequency, but does not have the correct value of a_{rms}. Table 3 lists estimates for revised corner frequency and the corresponding stress drop for Q = 300 at station 51, and Q = 500 at stations 38 and 13. In this solution, the median stress drop is about 270 bars. The scatter in log $(\Delta\sigma_7)$ is about the same as the scatter in log $(\Delta\sigma_c)$. Because only three stations are used, and because the moment is somewhat uncertain, this high stress drop is not highly reliable, and the procedure suggested here needs to be tested on additional earthquakes.

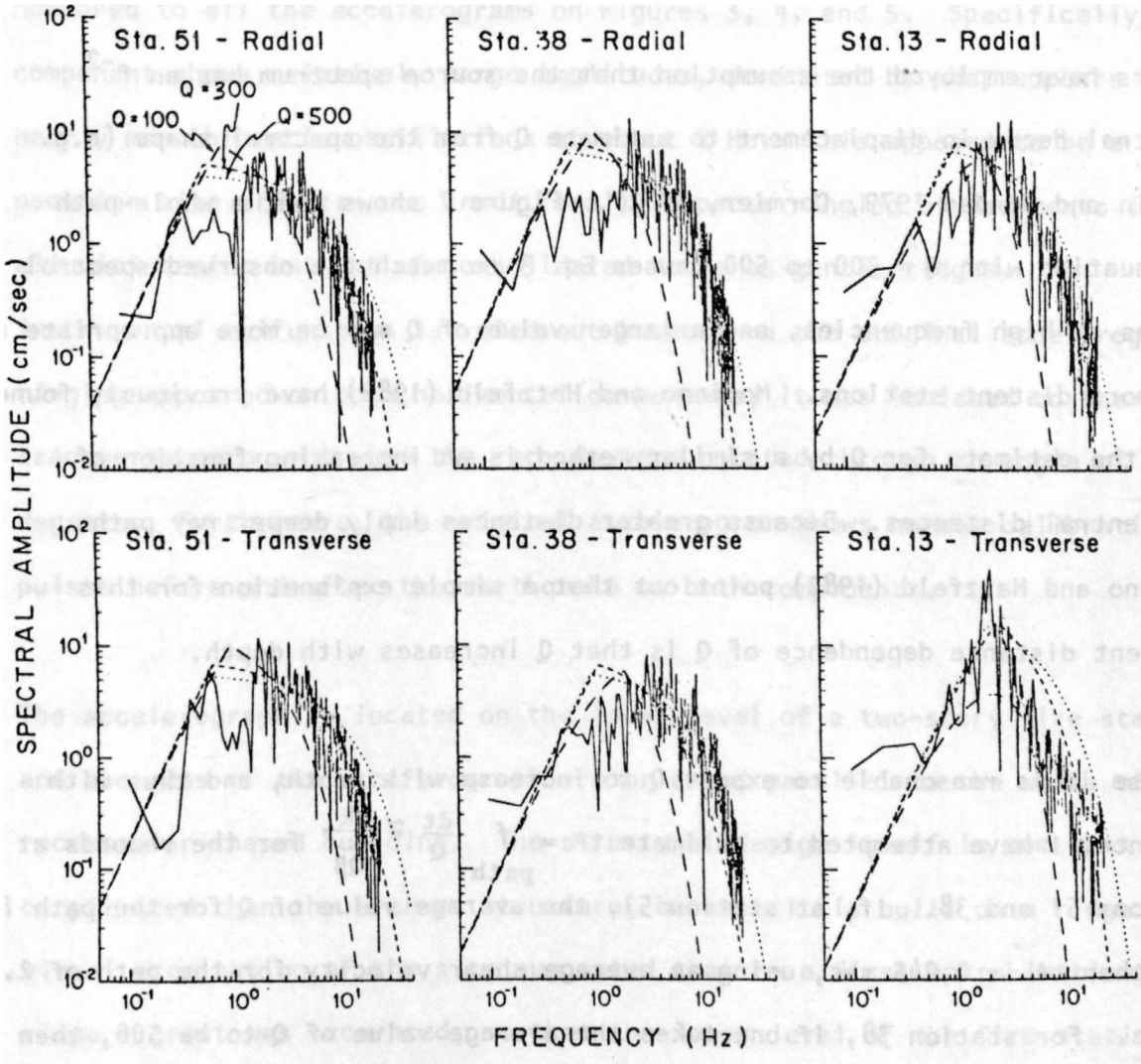

Figure 7. Fourier amplitude spectra of all S-wave accelerograms, radial and transverse components. Curves show acceleration Fourier amplitude spectra corresponding to assumed f_0 behavior at the source for frequencies above corner frequency, constrained by both a_{rms} and M_0, for three values of Q.

To alleviate problems introduced by the low signal-to-noise ratio, one could use an alternative fitting procedure in which all the spectra are constrained to be consistent with a single moment estimate. Under this procedure, if M_0 is constrained to be consistent with M_S (5.9) the stress drop estimate is lowered.

Others have employed the assumption that the source spectrum has an f^{-2} spectral decay in displacement to estimate Q from the spectral shape (e.g. Sipkin and Jordan 1979, Cormier, 1982). Figure 7 shows that a whole-path attenuation with $Q \tilde{=} 300$ to 500 causes Eq. 3 to match the observed spectral shapes at high frequencies, and a larger value of Q may be more appropriate at the more distant stations. Modiano and Hatzfeld (1982) have previously found that the estimate for Q by a similar method is an increasing function of hypocentral distances. Because greater distances imply deeper ray paths, Modiano and Hatzfeld (1982) point out that a simple explanation for this apparent distance dependence of Q is that Q increases with depth.

Because it is reasonable to expect Q to increase with depth, and thus with distance, I have attempted to estimate $t^* = \int_{path} \frac{dt}{Q} \cong \frac{R}{Q\beta}$ for the records at stations 51 and 38. If, at station 51, the average value of Q for the path is 350, then t* is 0.045 sec, using an average shear velocity for the path of 2.8 km/sec. For station 38, if one takes the average value of Q to be 500, then one obtains t* = 0.050 sec. By assuming an f^{-2} behavior above the corner frequency, Singh et al. (1982) estimated that the upper 3.75 km in Imperial Valley contribute 0.048 to t*. A larger set of spectral measurements, such as those from the San Fernando earthquake accelerograms, together with a more rigorous form of this procedure might be a productive way to study

attenuation.

DISCUSSION OF STATION 13 ACCELEROGRAM

The transverse component of acceleration at station 13 appears anomalous when compared to all the accelerograms on Figures 3, 4, and 5. Specifically, that component shows relatively large amplitudes, dominated by what appears to be nearly monochromatic oscillations at about 2 Hz. This appears to be a peculiar site effect: one traditionally expects ringing of sediments in alluvial basins but not of consolidated rocks on gentle ridges. An instrumental malfunction is ruled out because on the original accelerogram the ringing appeared on both horizontal components; it was isolated to the transverse component when the records were rotated through an angle of 45 degrees. Furthermore, the original accelerogram shows normal calibration pulses before and after the earthquake on both components.

The accelerograph is located on the lower level of a two-story fire station and the axes of the accelerograph are oriented parallel to the walls of the rectangular-shaped building. The structural design itself is somewhat more complicated than the average structure, because it is built on a ridge. A visual examination of the site suggested that to a first approximation, the ridge - crest was excavated, so that the lower level of the fire station is below the original grade, and the upper level is about even with the original grade. On a local scale ($\sim$200 m) the station is oriented with walls parallel to, and perpendicular to the ridge crest. The ringing is isolated on a component which is oriented approximately 45_o to the structural and local ridge orientation; this seems to rule out a structural cause for ringing.

Furthermore, at 2 Hz, the predominant frequency is somewhat lower than one would expect for a two-story structure.

Figure 8 shows the Fourier amplitude spectrum of acceleration for the transverse components of acceleration at sites 13 and 38. Since these two stations are nearly equidistant from the epicenter, no distance corrections are applied. Between frequencies of about 1.3 Hz and 3.6 Hz, the Fourier amplitude of acceleration at station 13 is larger by a factor of about 5, on the average, than the Fourier amplitude at station 38. Conceivably, half of this difference could be the result of the radiation pattern, as described earlier. However, Hanks and McGuire (1981) and Boatwright and Boore (1982) have argued that the excitation of high frequency motion is far more isotropic than double-couple point source models allow. Modiano and Hatzfeld (1982) were unable to find an experimental relationship between long period S-wave spectral amplitudes and radiation pattern amplitudes. The spectra in Figure 8 are similar for frequencies less than 1.3 Hz and greater than 3.6 Hz. Thus no radiation pattern correction has been applied.

The result of a very simple experiment to attempt to simulate this amplification is shown in Figures 8 and 9. For this experiment which will be called "Model A," it was hypothesized that the amplification could be modeled as if the acceleration at station 38 has been affected by a single-degree of freedom oscillator, with low damping, to obtain the acceleration at site 13. Figure 9 compares the raw accelerograms and the Model A output for an oscillator with natural frequency of 2 Hz and damping of 2 percent. The spectrum of the accelerogram Model A is shown in Figure 8.

The spectrum of Model A on Figure 8 shows two somewhat larger peaks at about 2 Hz than the peaks associated with the accelerogram from site 13. Between 2.5 Hz and 3.6 Hz, the spectrum in Model A is still not large enough. We note that the impulse response of a single degree of freedom oscillator shows only a single peak; the twin peaks in the model are a result of the input spectrum. Figure 9 illustrates more shortcomings of the model. During the first 8 seconds, the shaking at site 13 looks more monochromatic, and has larger amplitudes than predicated by Model A. Later in the Model A accelerograms, the 2 Hz energy is much larger than what was actually observed. One plausible explanation is that the amplification is sensitive to the mode of propagation of the incident waves. For example, a consistent hypothesis is that the first 8 sec of the S-wave arrives with a steep angle of incidence and is amplified, the next 7 seconds consists of Love waves, with horizontal incidence, and are not amplified and the last 2 seconds consist of coda arrivals, which again are amplified slightly. Amplification of ground motion in the presence of irregular topography (e.g. Wong and Jennings, 1975) is expected to depend on the angle of incidence of the incoming waves. These considerations suggest that the large amplitudes at site 13 are not highly local site effects.

Figure 10 shows the topography in the vicinity of sites 13 and 10. Topographic relief is much greater in the vicinity of station 13 than in the vicinity of any other site. It is situated on the east-west trending central ridge of the Santa Monica Mountains. Streams flowing north and south from this central ridge cut deeply into the hillside. The station is located at the head of one of these valleys, and the elevation decreases most rapidly to the north.

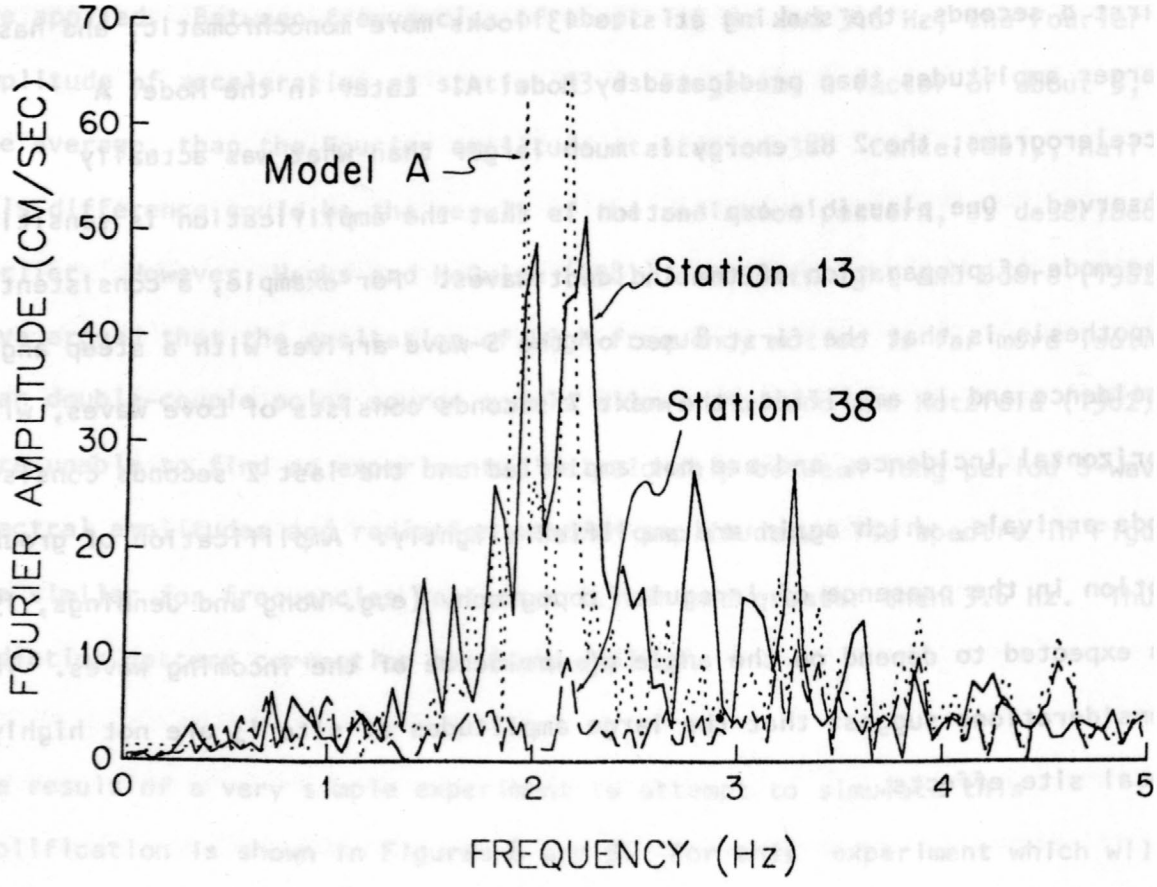

Figure 8. Fourier amplitude spectra of the transverse component of acceleration from sites 38 and 13. Dotted lines shows result of an attempt to duplicate site 13 accelerations by a simplified model applied to site 38 recording.

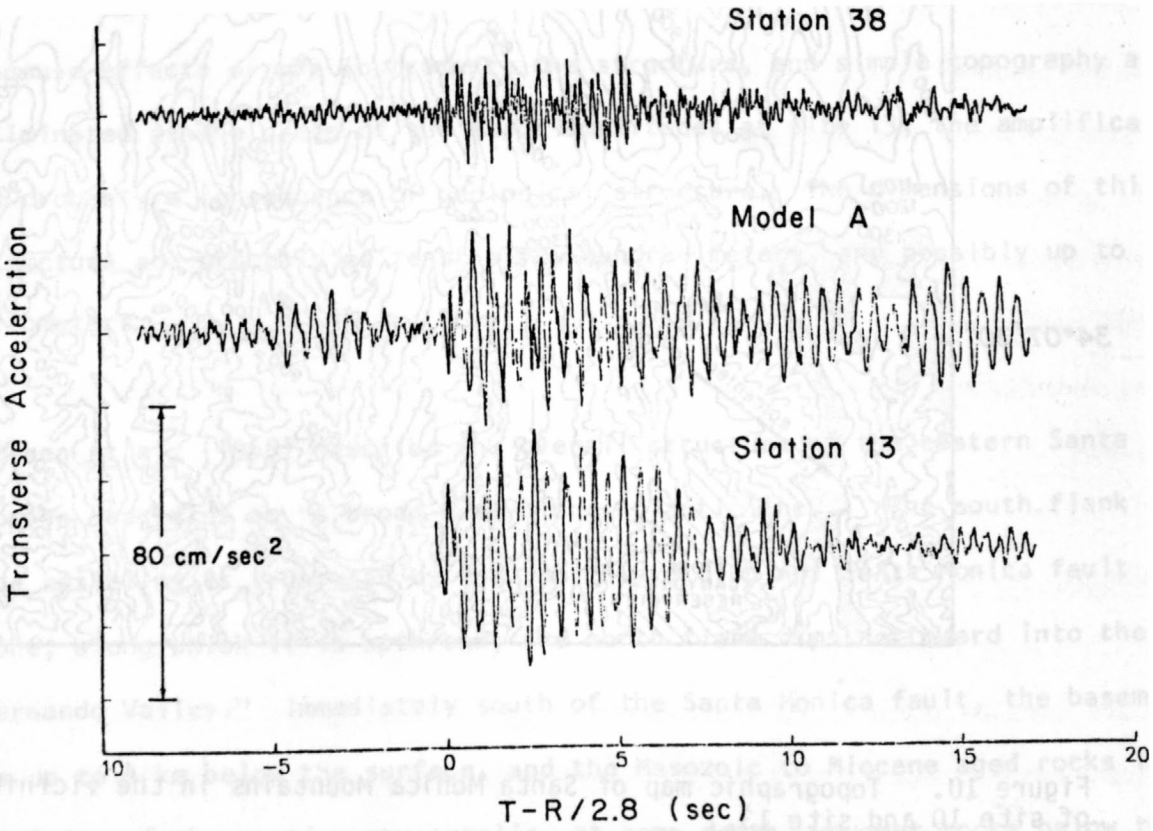

Figure 9. Transverse component of acceleration at sites 38 (Top) and 13 (bottom). Central trace is accleration response of a single-degree of freedom oscillator with natural frequency of 2 Hz and damping of 2% to site 38 accelerogram as input.

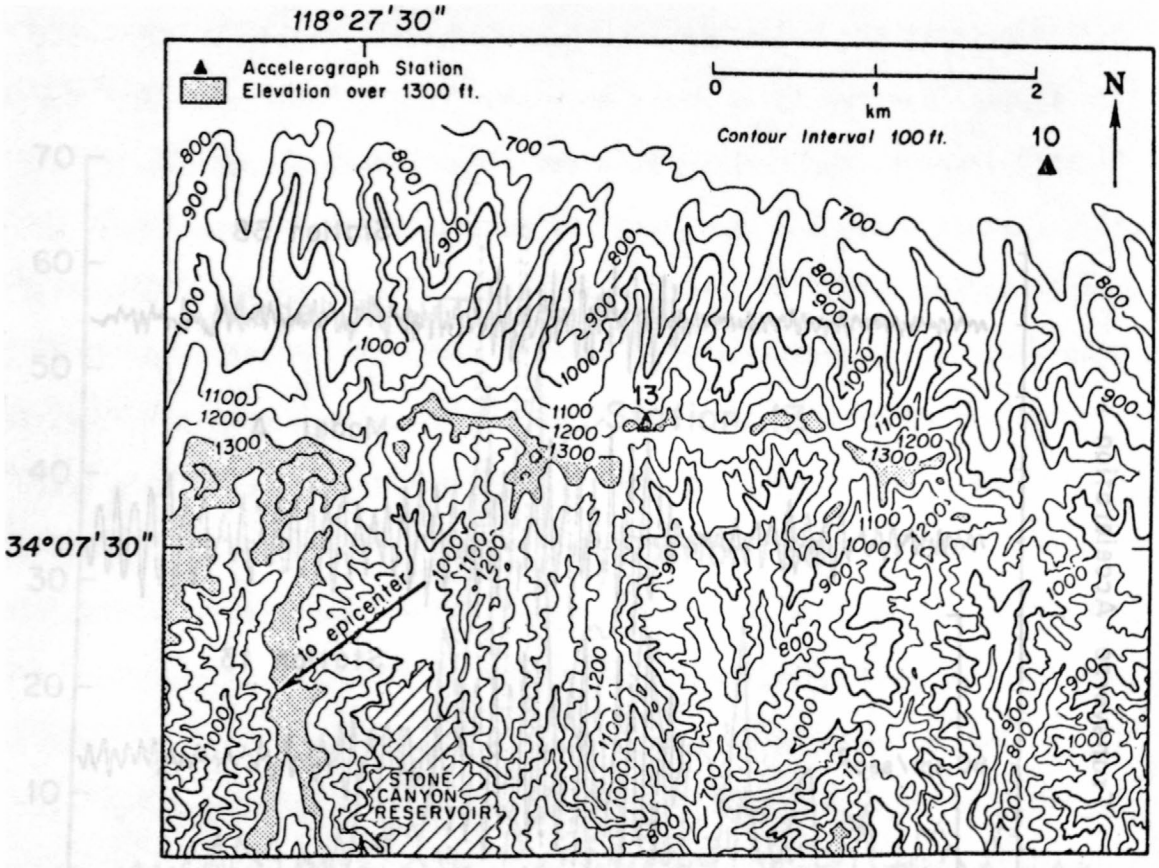

Figure 10. Topographic map of Santa Monica Mountains in the vicinity of site 10 and site 13.

The ringing at site 13 cannot be explained by simple topographic amplification, based on two-dimensional approximations of the topography (Figure 10), scaled to results of Boore (1972), Bouchon (1976), and Brune (1982). There is uncertainty in the choice of scaling parameters, but several estimates indicate that amplitudes on a two-dimensional topographic ridge of uniform material, shaped by the maximum gradient from the station, would be less than 1.6 times the amplitudes on the surface of a half space.

Because effects of the instrument, the structure, and simple topography are eliminated as the cause of the large amplitudes at site 13, the amplification is probably a consequence of geological structure. The dimensions of this structure are probably at least a few hundred meters, and possibly up to a few kilometers.

Yerkes et al. (1965) describe the overall structure of the eastern Santa Monica Mountains as "a broad west-plunging anticline... The south flank of the anticline is truncated by the (northward dipping) Santa Monica fault zone, along which it is upthrown; the north flank dips northward into the San Fernando Valley." Immediately south of the Santa Monica fault, the basement is up to 4 km below the surface, and the Mesozoic to Miocene aged rocks in the vicinity of the station may overlie, at some depth, younger rocks below the thrust fault.

If the regional geology near station 13 is the cause for this anomalous record, sites 10 and 18 also might be affected. We note that these stations triggered late in the S-wave arrivals, but still yield above-average peaks in acceleration. In the time interval when all three of these stations were

operating, the radial components at sites 10 and 18 show larger amplitudes than the radial component at station 13 (Figure 4). The transverse components do not show any prominent ringing, however (Figure 5).

CONCLUSION

Analog accelerograms with small amplitudes such as those considered in this paper are not routinely digitized. However, these records were used to examine several problems of interest to geophysicists and engineering seismologists. The accurate internal time codes which were recorded on the film greatly facilitated this work. Results include verification of the local magnitude scale M_L) and attenuation relations in a magnitude and distance range not covered by previously digitized data sets, seismological data about wave velocities, source mechanism and Q, and evaluation of possible site effects.

ACKNOWLEDGEMENTS

I have benefited from discussions with James Brune, J. Enrique Luco, Allen Olson, and Michael Reichle at the University of California, San Diego and S. K. Singh at U.N.A.M. The strong motion accelerograph network in the Los Angeles vicinity was established in 1978-1980 with support of the National Science Foundation, and continued operation is supported by the National Science Foundation. K. Moslem and A. Amini at the University of Southern California carried out necessary preparatory work for this study, and M. D. Trifunac and V. W. Lee at the University of Southern California participated in the digitization of the accelerograms. Mr. Roy Miller

(University of California at Berkeley) and Mr. Riley Geary (California Institute of Technology) provided raw amplitude data from the Wood-Anderson recordings which formed the basis for M_L calculations at their respective stations. This research was supported by National Science Foundation Grant CEE 81-20096.

REFERENCES

Aki, K. and P. G. Richards (1980). Quantitative Seismology Theory and Methods, W. H. Freeman and Company, San Francisco.

Anderson, J. G., M. D. Trifunac, T. L. Teng, A. Amini, and K. Moslem (1981). Los Angeles vicinity accelerograph network, Report No. CE 81-04, Dept. of Civil Engineering, University of Southern California, Los Angeles.

Boatwright, J. and D. M. Boore (1982). Analysis of the ground accelerations radiated by the 1980 Livermore Valley earthquake for directivity and dynamic source characteristics, Proceedings of Workshop XVI, The Dynamic Characteristics of Faulting Inferred From Recordings of Strong Ground Motion, Open File Report 82-591, United States Geological Survey, Menlo Park, California, 238-275.

Boore, D. M. (1972). A note on the effect of simple topography on sesismic SH waves, Bull. Seism. Soc. Am., 62, 275-284.

Bouchon, M. (1976). Discrete wavenumber representation of seismic wave fields with application to various scattering problems, Ph.D. Thesis, Massachusetts Institute of Technology, Cambridge.

Brune, J. N. (1970). Tectonic stress and the spectra of seismic shear waves from earthquake, J. Geophys. Res., 75, 4997-5009.

Brune, J. N. (1982). Preliminary results on topographic seismic amplification effects on a foam rubber model of the topography near Pacoima Dam, EOS, Trans of AGU, (abstract).

Campbell, K. W. (1981). Near source attenuation of peak horizontal acceleration, Bull. Seism. Soc. Am., 71, 2039-2070.

Corbett, E. J. and K. A. Piper (1981). Santa Barbara Island, California earthquake, September 4, 1981 (abstract), Trans., Am. Geophys. Union, Nov. 11, 1981.

Cormier, V. F. (1982). The effect of attenuation on seismic body waves, Bull. Seism. Soc. Am., 72, S169-S200.

Hadley, D. M., D. V. Helmberger, and J. A. Orcutt (1982). Peak acceleration scaling studies, Bull. Seism. Soc. Am., 72, 959-979.

Hanks, T. C. (1979). b-values and w seismic source models: implications for tectonic stress variations along active crustal fault zones and the estimation of high-frequency strong ground motion, J. Geophys. Res., 84, 2235-2242.

Hanks, T. C. (1982). f_{max}, Bull. Seism. Soc. Am., 72, 1867-1879.

Hanks, T. C. and H. Kanamori (1979). A moment magnitude scale, J. Geophys. Res., 84, 2348-2350.

Hanks, T. C. and R. K. McGuire (1981). The character of high-frequency strong ground motion, Bull. Seism. Soc. Am., 71, 2071-2095.

Jennings, C. W. and R. G. Strand (1969). Geologic map of California, Los Angeles Sheet, California Div. of Mines and Geology, Sacramento.

Jennings, P. C. and H. Kanamori (1983). Effect of distance on local magnitudes found from strong-motion records, Bull. Seism. Soc. Am., 73, 265-280.

Joyner, W. B. and D. M. Boore (1981). Peak horizontal acceleration and velocity from strong-motion records including records from the 1979 Imperial Valley, California, earthquake, Bull. Seism. Soc. Am., 71, 2011-2038.

Kanamori, H. and P. C. Jennings (1978). Determination of local magnitude M_L, from strong motion accelerograms, Bull. Seism. Soc. Am., 68, 471-485.

Lee, W. B. and S. C. Solomon (1978). Simultaneous inversion of surface wave phase velocity and attenuation: Loves waves in western North America, J. Geophys. Res., 83, 3389-3400.

Luco, J. E. (1982). A note on near-source estimates of local magnitude, Bull. Seism. Soc. Am., 72, 941-958.

McGann, M. W. and D. M. Boore (1983). Variability in ground motions: root mean square acceleration and peak acceleration for the 1971 San Fernando, California, earthquake, Bull. Seism. Soc. Am., 73, 615-632.

McGarr, A. (1981). Analysis of peak ground motion in terms of a model of inhomogenous faulting, J. Geophys. Res., 86, 3901-3912.

McGuire, R. K. and T. C. Hanks (1980). RMS accelerations and spectral amplitudes of strong ground motion during the San Fernando, California earthquake, Bull. Seism. Soc. Am., 70, 1907-1919.

Modiano, T. and D. Hatzfeld (1982). Experimental study of the spectral content for shallow earthquake, Bull. Seism. Soc. Am., 72, 1739-1758.

Person, W. J. (1982). Seismological Notes - September-October 1981, Bull. Seism. Soc. Am., 72, 1449-1452.

Singh, S. K., R. J. Apsel, J. Fried, and J. N. Brune (1982). Spectral attenuation of SH-waves along the Imperial fault, Bull. Seism. Soc. Am., 72, 2003-2016.

Sipkin, S. A. and T. H. Jordan (1979). Frequency dependence of Q ses, Bull. Seism. Soc. Am., 69 1055-1079.

Thatcher, W. and T. C. Hanks (1973). Source paramters of southern California earthquakes, J. Geophys. Res., 78, 8547-8576.

Trifunac, M. D. and V. W. Lee (1979). Automatic digtitization and processing of strong-motion accelerograms, Report No. 79-15, Dept. of Civil Enigneering, University of Southern California, Los Angeles.

Wong, H. L. and P. C. Jennings (1975). Effects of canyon topography on strong ground motion, Bull. Seism. Soc. Am., 65, 1239-1257.

Yerkes, R. F., T. H. McCulloh, J. E. Schrellhamer, and J. G. Vedder (1965). Geology of the Los Angeles Basin - An Introduction, Prof. Paper 420-A, U.S. Geological Survey, Washington, D.C.

AMPLIFICATION MODELS

by

Geoffrey R. Martin
Ertec, Inc.
3777 Long Beach Boulevard
Long Beach, California 90807

The presentation will present an overview of:

- Methods and uncertainties associated with characterization of soil and rock properties for use in the site amplification models;
- The complexities related to defining the boundary conditions needed for analytical modeling;
- Various analytical models used to evaluate local site and topographic effects on earthquake ground response.

Characterization of soil and rock properties for use in dynamic site response models is generally achieved through a combination of in-situ geophysical tests and dynamic laboratory tests on undisturbed samples. A brief review of the methods used and the uncertainties in identifying in-situ parameters from laboratory tests will be provided. Research priorities and recommendations focus primarily on:

- Improved high amplitude in-situ test methods;
- Improved techniques for extrapolating lab test data to equivalent in-situ parameters; and
- Continued development of laboratory test tanks for "miniature" geophysical tests.

Problems related to site characterization in terms of spatial variations in soil properties, stratigraphy, and boundary conditions will be discussed with reference to selected power plant and offshore platform sites. The relationships between regional and site specific characterization will be discussed to provide a perspective on the problem of site specific modeling. The simplifications needed to transform site specific characterization to simplified models amenable to analytical treatment provide considerable challenge and uncertainty. Improved and more cost effective means for defining spatial variation of soil properties and boundary conditions are required. New developments with Cone Penetrometer Tests (CPT) and recent modifications of CPT equipment for downhole geophysical tests appear to be providing improved tools for site profiling and characterization.

An overview of methods of analysis for evaluating local site and topographic effects on earthquake ground response will discuss the important conclusions from representative research studies encompassing (see attached figure):

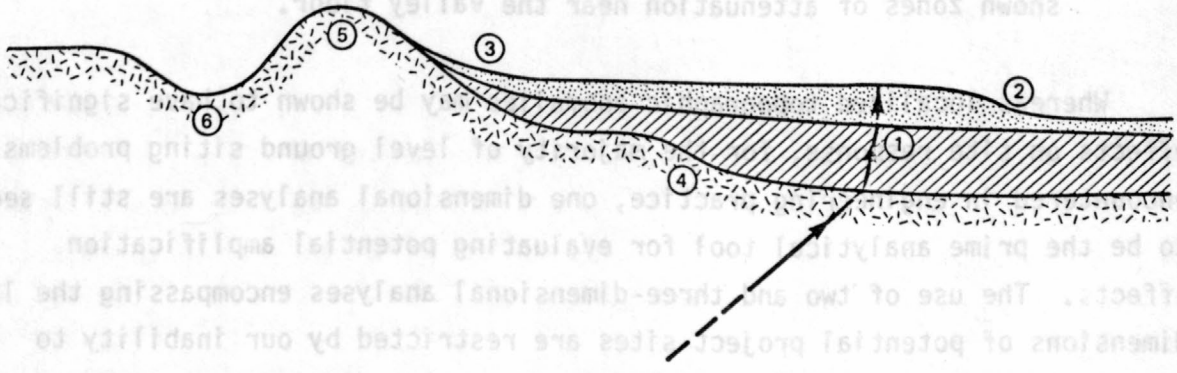

LOCAL SITE AND TOPOGRAPHIC EFFECTS ON EARTHQUAKE GROUND RESPONSE

1. Analyses evaluating the effects of reflection and transmission of elastic waves in multilayered media, including a discussion of shear and surface waves and the simplification to the case of vertically propagating SH waves as encompassed in the program SHAKE. The relative merits of nonlinear versus equivalent linear one-dimensional analyses will be briefly reviewed.

2. Results of two-dimensional finite element analyses indicating the influence of changes in surface topography on ground response.

3. Two-dimensional analyses reflecting the effects of "wedge" type soil topography defined by a downdipping rock interface. Field observations and numerical results have shown that such near surface features may have a strong effect on ground response during earthquakes.

4. Two-dimensional analyses for ground motion modifications arising from underlying downdipping rock layers and focusing effects from underlying basin type interfaces.

5. Analyses evaluating the effects of SH waves incident on ridge structures. Results have shown significant amplification at high frequencies.

6. Analyses for rock valleys, similar to those for ridges. Results have shown zones of attenuation near the valley floor.

Whereas localized topographic anomalies may be shown to have significant effects on site response, for the majority of level ground siting problems encountered in engineering practice, one dimensional analyses are still seen to be the prime analytical tool for evaluating potential amplification effects. The use of two and three-dimensional analyses encompassing the large dimensions of potential project sites are restricted by our inability to adequately define spatial variations in soil properties, geometric boundary conditions, and spatial variations in earthquake ground motions incident at the site boundary, as well as economic considerations.

With respect to analysis methods and associated research needs, it is recommended that priorities be given to:

- Centrifuge studies of wave propagation from fault or explosive sources and centrifuge studies evaluating site response analyses using a shake table;

- A continued emphasis on the development of accelerometer arrays (surface and borehole) at selected highly seismic sites to clarify uncertainties surrounding site response characteristics and separation of wave types.

SITE EFFECTS: TWO-DIMENSIONAL MODELLING AND EARTHQUAKE ENGINEERING

BY

Pierre-Yves Bard

I.R.I.G.M., Universite Scientifique et Medicale de Grenoble,
Grenoble, France

INTRODUCTION

Most of the calculations currently performed in earthquake engineering to estimate the effects of local site conditions make use of well-known one-dimensional (1-D) models, such as SHAKE. These models often provide valuable insight into what can occur at the surface of the ground.

One-dimensional models, although very sophisticated as to the soil rheological behavior, are extremely simple with regard to the incident wavefield and the geological structure. The most recent experimental data (Tucker and King, 1983) suggest two facts: 1) a realistic modelling of site effects should include a sophistication of the models in two directions, and 2) use of the two-dimensional (2-D) models allows one to take into account the lateral variations of the surficial geological structure and to consider obliquely incident body waves and surface waves.

The goal of this paper is to summarize the results obtained during the last few years using one of the now numerous 2-D methods for the two main kinds of 2-D structures (surface topography and sediment-filled valleys). By doing this, the importance of 2-D effects for earthquake engineering purposes and the limitation of the widely used 1-D approach can be shown.

SUMMARY OF THEORETICAL RESULTS; COMPARISON WITH EXPERIMENTAL DATA

Many theoretical methods have been developed during the last decade: finite difference, finite elements, glorified optics, boundary methods,

analytical methods, discrete wave-number representation. As long as they deal with the same geometrical model and the same mechanical behavior (i.e. in general, linear, homogeneous, isotropic elasticity), all these methods provide very similar results, as shown by Bard and Bouchon (1980a). We will therefore summarize here the results obtained with one of them, the Aki-Larner model, which in spite of some drawbacks, is computationally very cheap and very tractable.

These results are detailed in Bard (1982) for the topographical features and in Bard (1983) for the sediment-filled valleys. We have summarized the results in Table I, indicating in each case the main physical bases, the spectral characteristics of their surface effects, and finally the engineering consequences. We will comment briefly on this Table, and compare the theoretical results with the presently available experimental data.

1. Effects of surface topography

a) Theoretical results

The characteristics of the computed response spectra, as illustrated on Figure 1a, are basically related to the diffraction scheme on the topography. The incident waves are reflected with different angles according to the local surface slope, which mainly has two consequences: first there is some kind of energy focusing within the mountain, near its top, and secondly it produces two outward propagating surface waves, the interference of which with the primary wave induces the oscillatory pattern of the response spectra at mid-slope and mountain base (Figure 1).

b) Comparison with the experimental results

The agreement between the theoretical predictions and the experimental data is illustrated in Figure 1 and is generally much better qualitatively than quantitatively:

Table 1. Summary of basic phenomena, spectral characteristics and applications to earthquake engineering for various 2-D structures.

Effects / 2D Structure	Basic phenomena	Spectral characteristics	Application to Earthquake Engineering
Surface topography 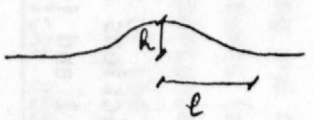	Diffraction of outward propagating surface waves Energy focusing in convex parts (such as moutain top)	Broad band effects centered on the frequency for which the wavelength is comparable to the width of the topographic feature ($\lambda = 5l$ to $\lambda = l/4$)	- Amplification on top, deamplification at mountain base differential motion on slopes - Effects much larger on the horizontal components than on the vertical component.
Plane layer (Haskell mode) 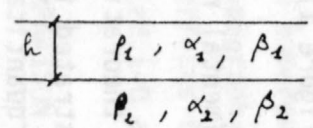	Vertical resonance	Narrow band effects Resonant frequencies : $f_n = (2n+1)\ c/4h$ with $c = \beta_1$ for S waves $c = \alpha_1$ " P "	- Large amplifications at resonant frequencies
Shallow sediment-filled valley 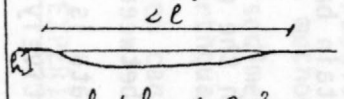	Vertical resonance and generation and propagation within the sediment cover of large amplitude surface waves	Narrow band peaks, but much more numerous and near to each other than in the 1D approximation. Fundamental frequency : $f_0 = c/4h$ (see above)	- Very large amplifications (up to twice those predicted with the 1D approximation) - Strong prolongation of motion duration - Large differential motion, especially over abrupt changes in sediment thickness
Deep sediment-filled valley 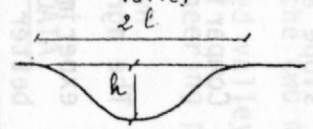	"Global" 2D resonance	Narrow band and well-separated peaks Fundamental frequency: $f_0 = c/4h\ (1 + ah/w)^{0.5}$ with a = 1 in the SH case 1.7 " SV " 0.5 " P "	- Very large amplifications (up to four times those predicted with 1D models - Frequencies very different from 1D predictions (up to 80-100%) - The resonant frequencies are the same for each valley site (center and edges) - Very strong prolongation - Large differential motion

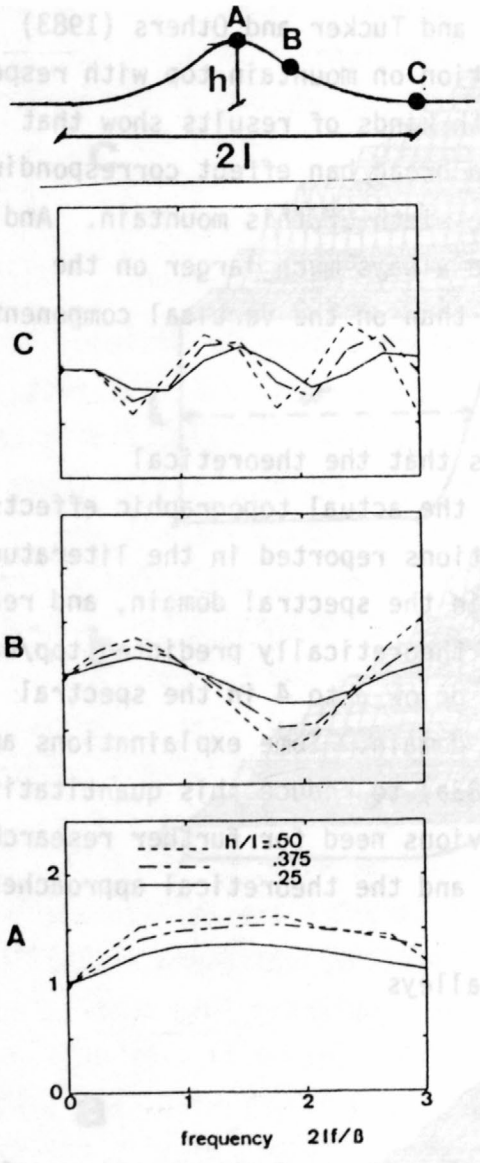

a

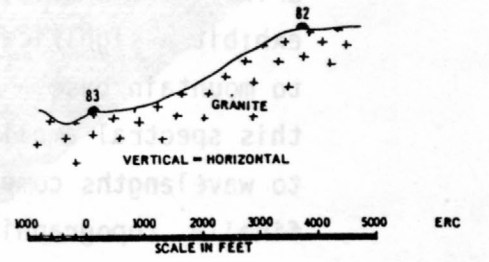

Topography, geology and station locations, Kagel Mountain.

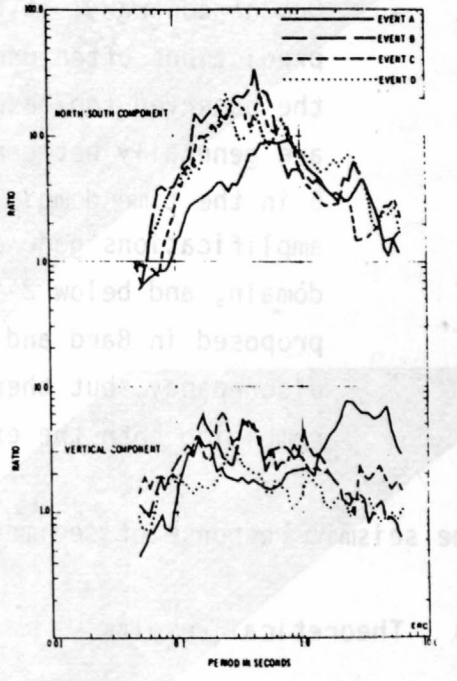

Ratios of *PSRV* Spectra at Kagel Mountain (Station 82, crest to Station 83, base).

b

Figure 1.--Examples of theoretically predicted (a) and observed topographic effects. A cross section of the topographic feature is shown at the top; the corresponding effects in the frequency domain are shown at the bottom of each figure.

(a) denotes SH response spectra at three sites located, respectively, on the top, mid-slope, and base for three different mountain heights (from Bard, 1982).

(b) denotes ratios of PSRB spectra (crest to base) for four different events and two components of motion (from Davis and West, 1973).

- As predicted by the theory, the experimental observations reported in Davis and West (1973), Rogers and Others (1974), Griffiths and Bollinger (1979), and Tucker and Others (1983) exhibit a significant amplification on mountain top with respect to mountain base. Moreover, both kinds of results show that this spectral amplification is a broad ban effect corresponding to wavelengths comparable to the width of this mountain. And finally, topographic effects are always much larger on the horizontal components (S waves) than on the vertical component (P waves).

- On the contrary, it also appears that the theoretical predictions often underestimate the actual topographic effects; the observed top/base amplifications reported in the literature are generally between 5 and 20 in the spectral domain, and reach 5 in the time domain, while the theoretically predicted top/base amplifications generally remain below 3 to 4 in the spectral domain, and below 2 in the time domain. Some explainations are proposed in Bard and Tucker (1983a) to reduce this quantitative discrepancy, but there is an obvious need for further research, combining both the experimental and the theoretical approaches.

2. The seismic response of sediment-filled valleys

a) Theoretical results

As for the surface topography, the main effect of the curvature of the sediment-basement interface is to generate surface waves which propagate within the sediment cover, where the ground motion is therefore significantly amplified and prolongated. Sediment-filled valleys, thus, exhibit essentially two main behaviors, according to their shape ratio (ratio of their maximum thickness h to their half-width 1) in shallow (wide) valleys (Figure 2b), these surface waves induce significant lateral interferences which superpose to the "vertical" interferences (the same as predicted by the classifical 1-D theories, Figure 2a), and significantly alter the surface motion.

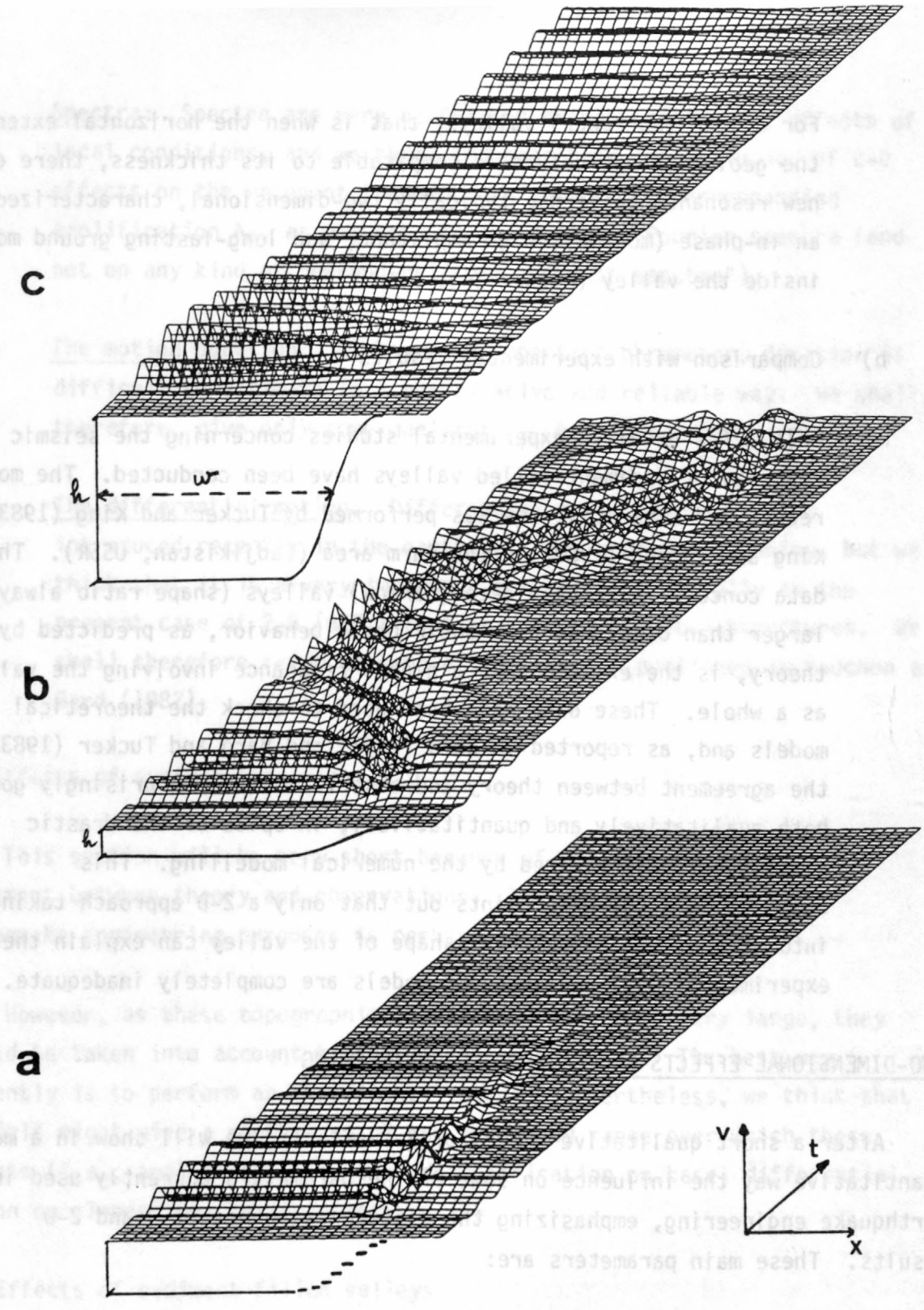

Figure 2.--Diagrams showing the spatial (x) and temporal (t) evolution of the surface displacement of a sediment-filled valley excited by an SH wave having a chracteristic frequency f_p = 1/4 h where h is the sediment thickness.

(a) 1-D approximation considering only the sediment thickness.
(b) 2-D modelling for a shallow valley (h/w = 0.06).
(c) 2-D modelling for a deep valley (h/w = 0.7).

For deeper (narrower) valleys, that is when the horizontal extent of the geological structure is comparable to its thickness, there exists new resonance patterns, typically two-dimensional, characterized by an in-phase (module), high amplitude, and long-lasting ground motion inside the valley (Figure 2c).

b) Comparison with experimental results

Only a few detailed experimental studies concerning the seismic response of sediment-filled valleys have been conducted. The most recent and exhaustive one was performed by Tucker and King (1983) and King and Tucker (1983) in the Garm area (Tadjikistan, USSR). These data concern relatively deep (narrow) valleys (shape ratio always larger than 0.25), so that their basic behavior, as predicted by the theory, is the existence of a global resonance involving the valley as a whole. These data have been used to check the theoretical models and, as reported in Bard (1983) and Bard and Tucker (1983), the agreement between theory and observations is surprisingly good, both qualitatively and quantitatively, in spite of the drastic simplifications required by the numerical modelling. This comparative study also points out that only a 2-D approach taking into account the geometrical shape of the valley can explain the experimental data and that 1-D models are completely inadequate.

TWO-DIMENSIONAL EFFECTS AND EARTHQUAKE ENGINEERING

After a short qualitative survey of 2-D effects, we will show in a more quantitative way the influence on some of the parameters currently used in earthquake engineering, emphasizing the difference between 1-D and 2-D results. These main parameters are:

The peak amplitude: As the prediction of a peak amplitude also requires the prediction of the input motion, trying to find out the modulation of the peak amplitude due to site effects is possible only in some very rare and very well-defined cases.

- Spectra: Spectra are very useful for characterizing the effects of local conditions, and we shall indicate here the influence of 2-D effects on the resonant frequency f_0 and on the corresponding amplification A_0, as measured on the computed Fourier spectra (and not on any kind of "pseudo-relative response spectra").

- The motion duration: Although an important parameter, duration is difficult to estimate in a quantitative and reliable way. We shall, therefore, give only some qualitative, but interesting, results.

- The differential motion: Differential motion has only been introduced recently in the earthquake engineering community, but we think that it is a very important parameter, especially in the present case of 2-D (and a fortiori 3-D) geological structures. We shall therefore refer to some of the results published in Bouchon and Bard (1982).

1. Effects of surface topography

This section will be very short because of the lack of quantitative agreement between theory and observations. The use of 2-D models for earthquake engineering purposes is perhaps still premature.

However, as these topographical effects prove to be very large, they should be taken into account by engineers and builders. The best way presently is to perform an experimental study. Nevertheless, we think that 2-D models might give a rough idea of the frequency range over which these effects (i.e., amplification on top, deamplification on base, differential motion on slopes) may be important.

2. Effects of sediment-filled valleys

a) Spectra

As may be seen on Figure 3, there are strong differences between spectra obtained with 1-D and 2-D models.

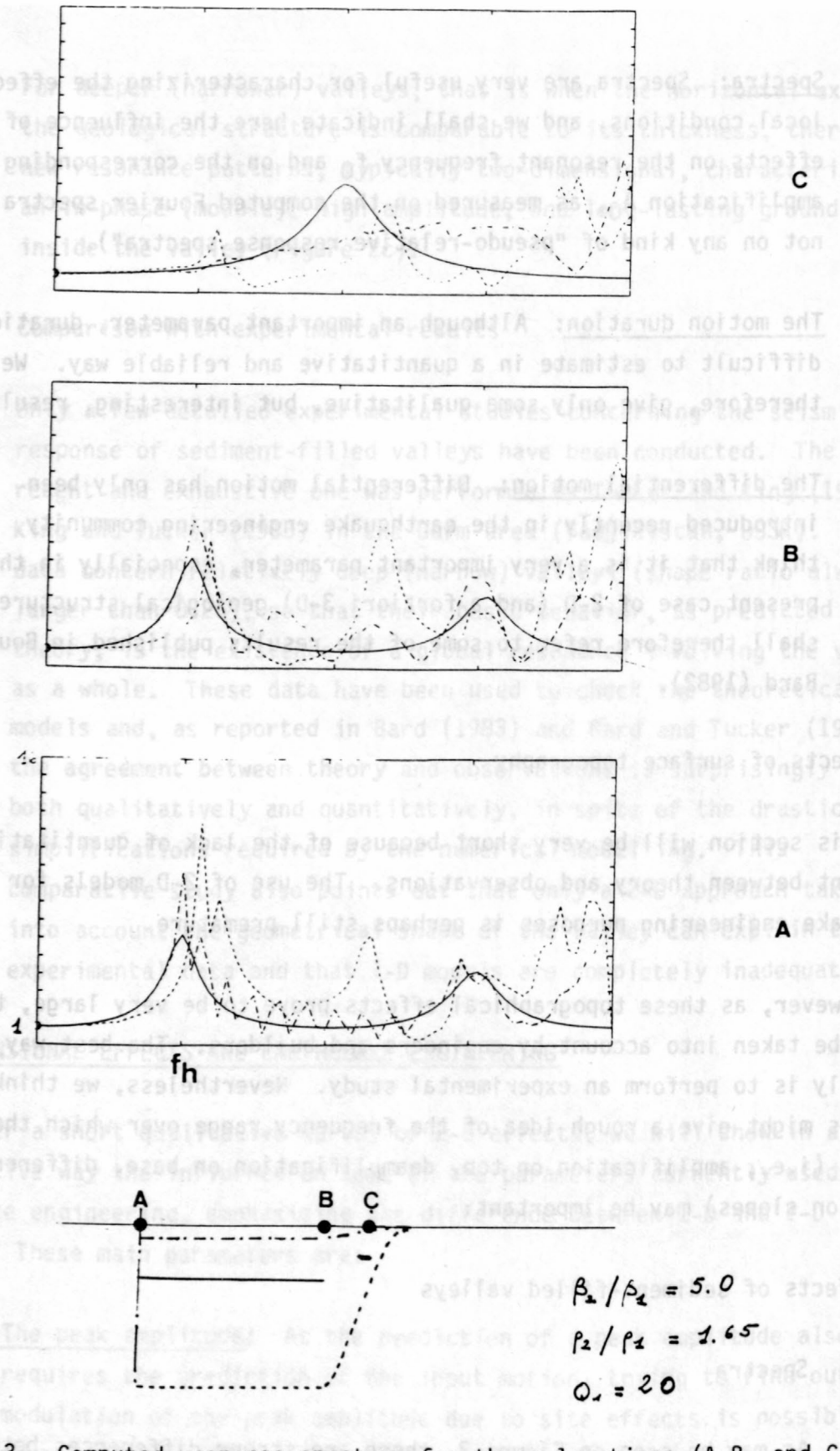

Figure 3.--Computed response spectrum for three locations (A,B, and C) on the valley surface. The continuous line represents the 1-D approximation; the chain-dotted line shows the shallow valley; and the dotted line represents the deep valley illustrated in Figure 2.

For 1-D models, we observe the classical resonance spectrum, with a main peak associated to the fundamental mode, and secondary peaks associated with the harmonics. The frequency of these peaks is related to both the sediment velocity and thickness.

For shallow (wide) valleys, the fundamental frequency remains almost the same (1/4h), but many secondary peaks, very near to one another, are present. These peaks correspond to the lateral interferences between the primary wave and the surface waves generated on the edges, and their spectral spacing is therefore related to the valley width.

For deep (narrow) valleys, the 2-D resonances imply that the frequencies of the spectral peaks are the same over the whole width of the valley. For the largest peak (generally the most important because of the damping within the sediments), the frequency at valley center is significantly larger (up to 100 percent in extreme cases) than what is predicted by 1-D models, while on the edges this frequency is significantly smaller than the 1-D value corresponding to the local sediment thickness.

Bard (1983) shows that the dimensionless fundamental frequency $f_o = 1/4$ does not depend on incidence angle nor on the impedance contrast between sediments and bedrock. However, it does depend on both the valley shape ratio and on the type of input motion (P, in-plane SV or out-of-plane SH waves). This dependency is illustrated in Figure 4.

As for the spectral amplifications, we shall make several observations. If one considers only the valley center, the maximum amplification generally corresponds to the largest peak. The value of amplification obviously depends on the sediment-basement impedance contrast, but it also depends on the valley shape ratio. This is shown very clearly on Figure 5, where one can see that the geometrical amplification due to the curvature of the interface may induce strong differences with 1-D predicted values, up to 200 percent in extreme cases. For purposes of clarity, the values illustrated in Figure 5 have been obtained with no attenuation within the sediments, but Figure 6 shows that the

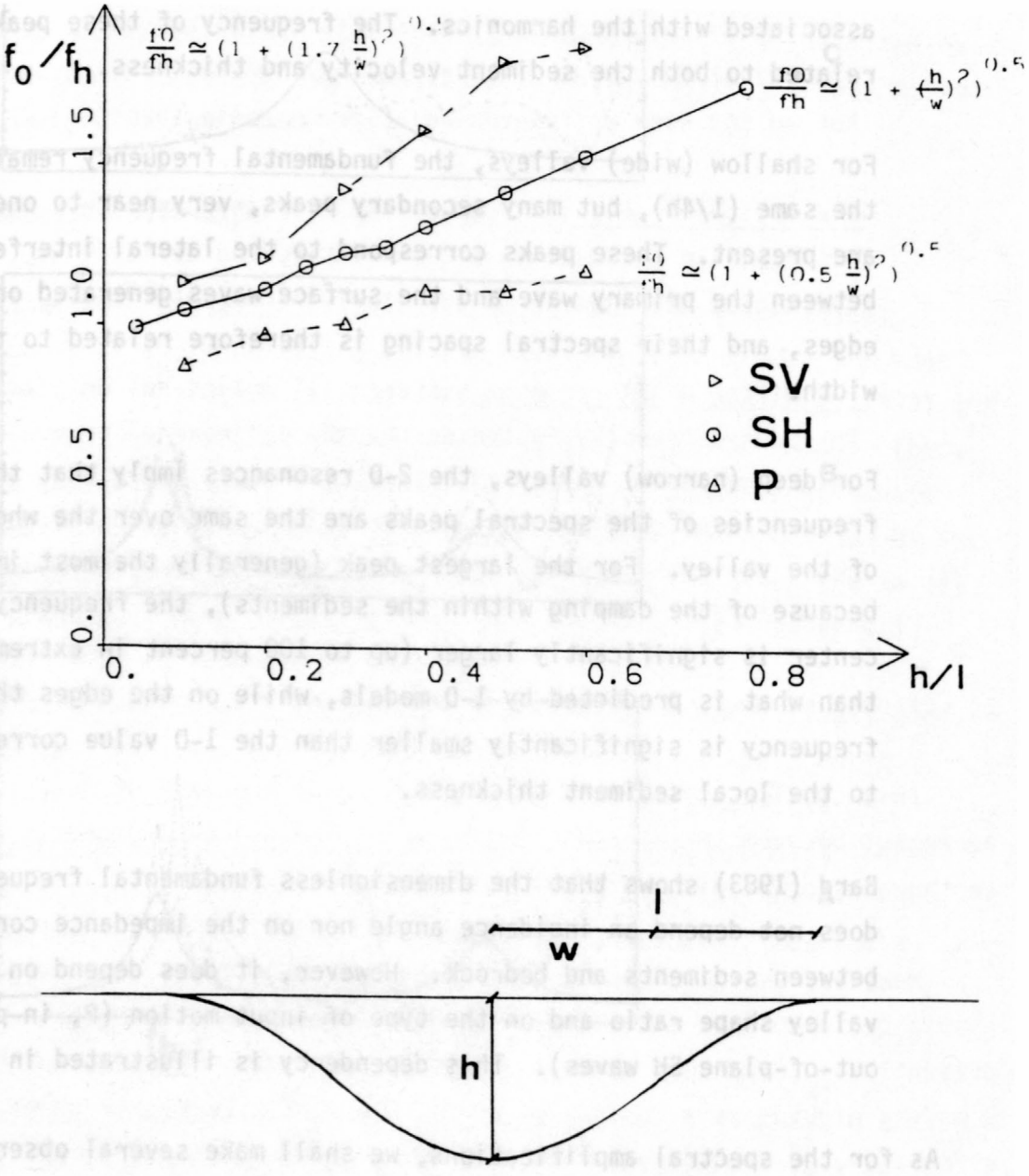

Figure 4.--Influence of the valley shape ratio (h/l) and the incident wave type on the dimensionless fundamental frequency for P and S waves.

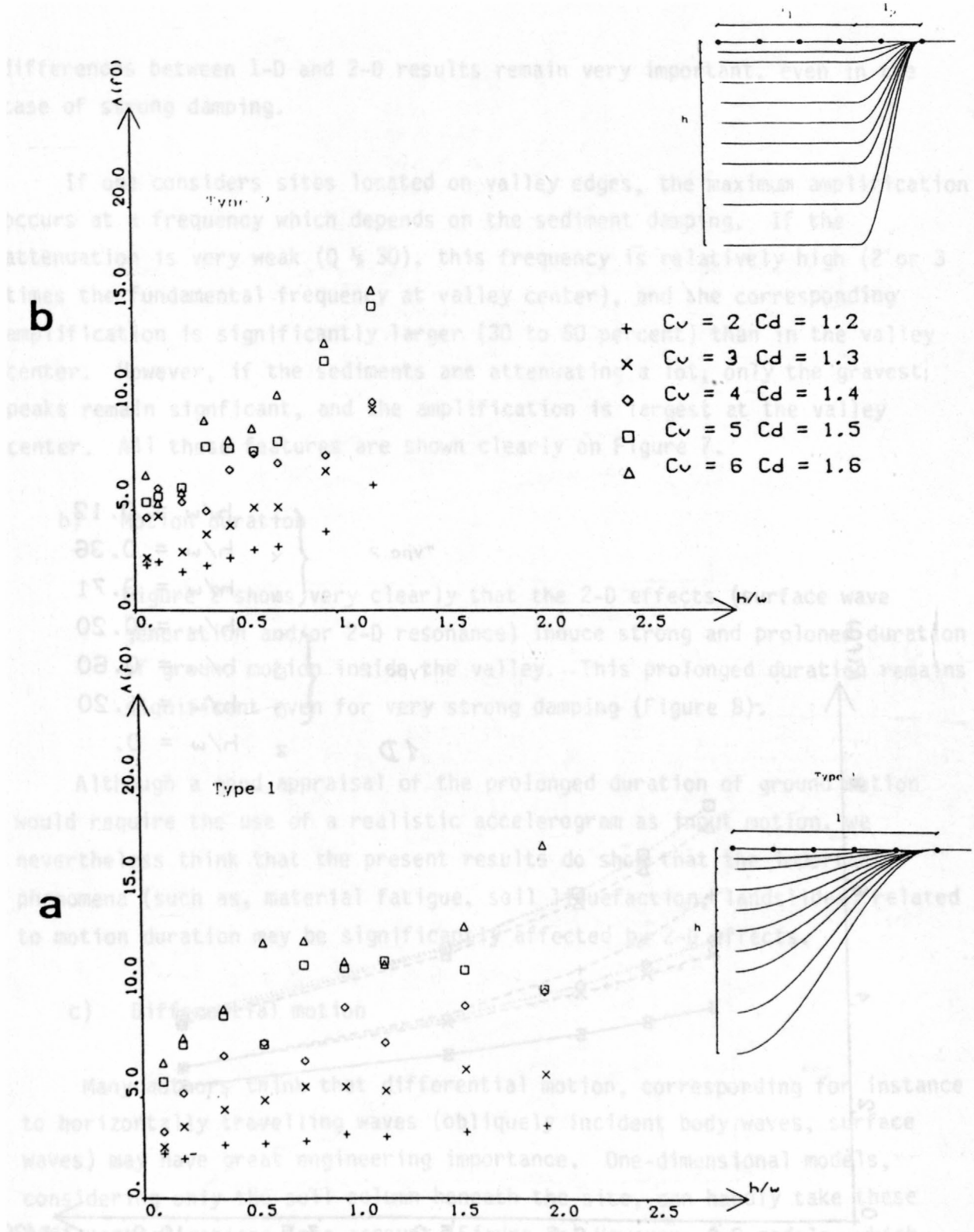

Figure 5.--Influence of the valley shape ratio (h/l) and the acoustic impedience constrast of the sediment/basement on the maximum spectral amplification at the center of the valley. C_v represents the velocity contrast; C_d the density contrast. W is the "equivalent width", the width over which the local sediment thickness is greater than half the valley thickness.
(a) Results for sine-shaped valley ("type 1 valley").
(b) Results for a valley having a wide central part ("type 2 valley").

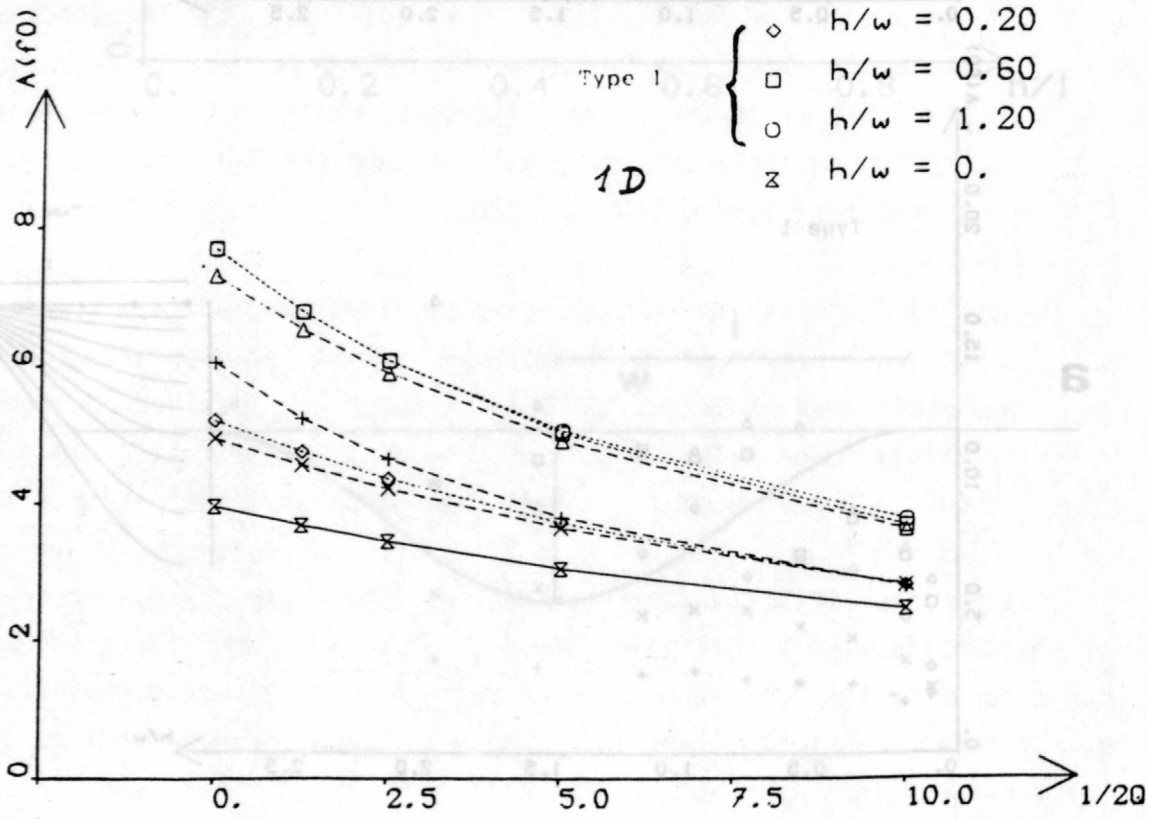

Figure 6.--Influence of attenuation within the sediments on the maximum spectral amplification at the center of the valley. These curves correspond to six sediment-filled valleys having the same impedience contrast (C_v = 4 and C_d = 1.4) but different shapes. The 1-D approximation is shown by the continuous line.

differences between 1-D and 2-D results remain very important, even in the case of strong damping.

If one considers sites located on valley edges, the maximum amplification occurs at a frequency which depends on the sediment damping. If the attenuation is very weak (Q ½ 30), this frequency is relatively high (2 or 3 times the fundamental frequency at valley center), and the corresponding amplification is significantly larger (30 to 50 percent) than in the valley center. However, if the sediments are attenuating a lot, only the gravest peaks remain signficant, and the amplification is largest at the valley center. All these features are shown clearly on Figure 7.

b) Motion duration

Figure 2 shows very clearly that the 2-D effects (surface wave generation and/or 2-D resonance) induce strong and proloned duration of ground motion inside the valley. This prolonged duration remains significant even for very strong damping (Figure 8).

Although a good appraisal of the prolonged duration of ground motion would require the use of a realistic accelerogram as input motion, we nevertheless think that the present results do show that the important phenomena (such as, material fatigue, soil liquefaction, landslides) related to motion duration may be significantly affected by 2-D effects.

c) Differential motion

Many authors think that differential motion, corresponding for instance to horizontally travelling waves (obliquely incident body waves, surface waves) may have great engineering importance. One-dimensional models, considering only the soil column beneath the site, can hardly take these differential motions into account (Figure 2a).However, 2-D models, which consider the geological structure as a whole, are much better suited to estimate these differential motions in a satisfactory way. Such a study was reported in Bouchon and Bard (1982), and shows that in shallow valleys the differential motion is essentially related to the surface waves; whereas, in

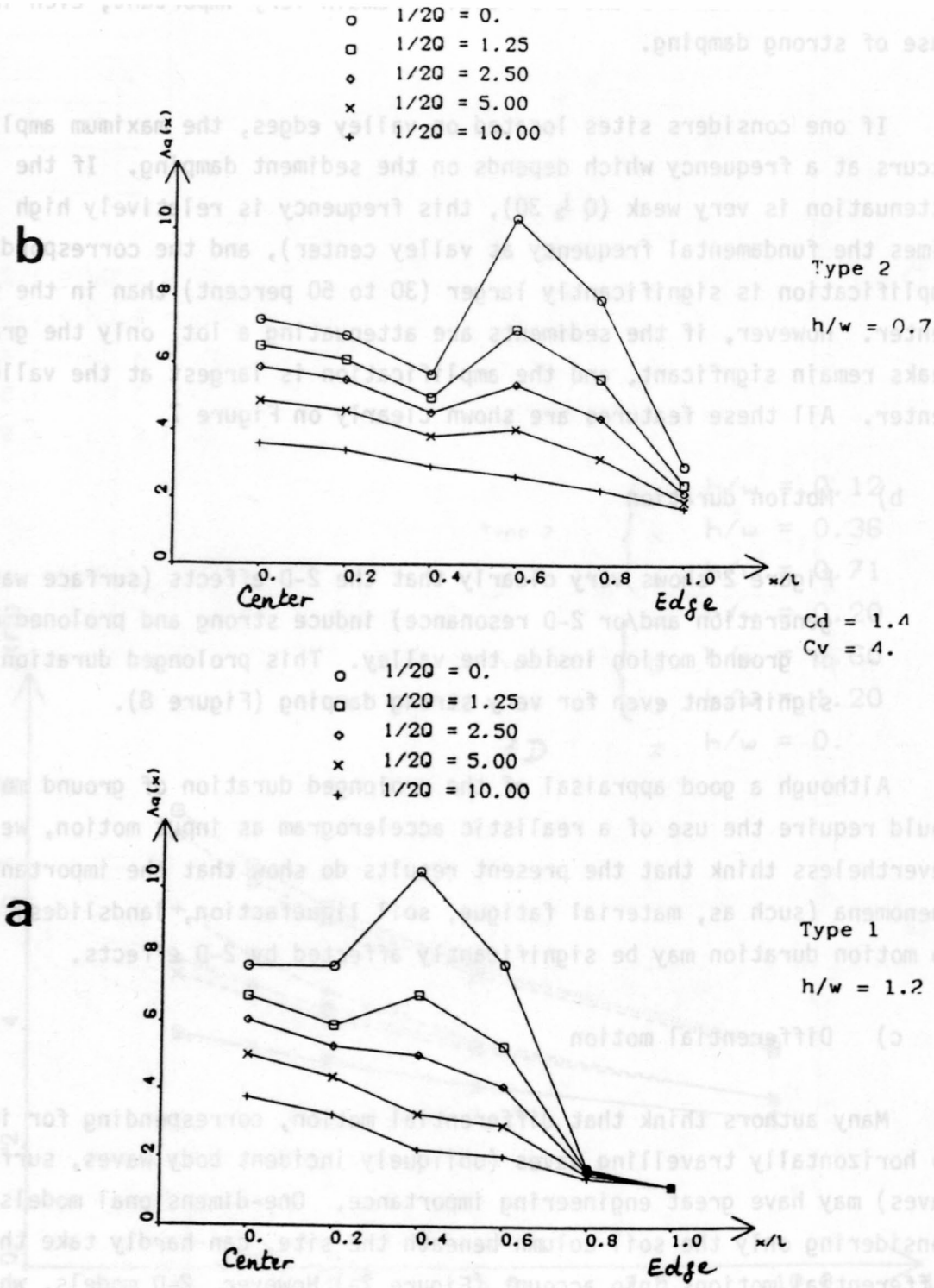

Figure 7.--Influence of the damping of the sediments on the spatial distribution of the maximum spectral amplification for two valleys having an impedience contrast of 5.6 (C_v = 4; C_d = 1.4) and two different shapes.

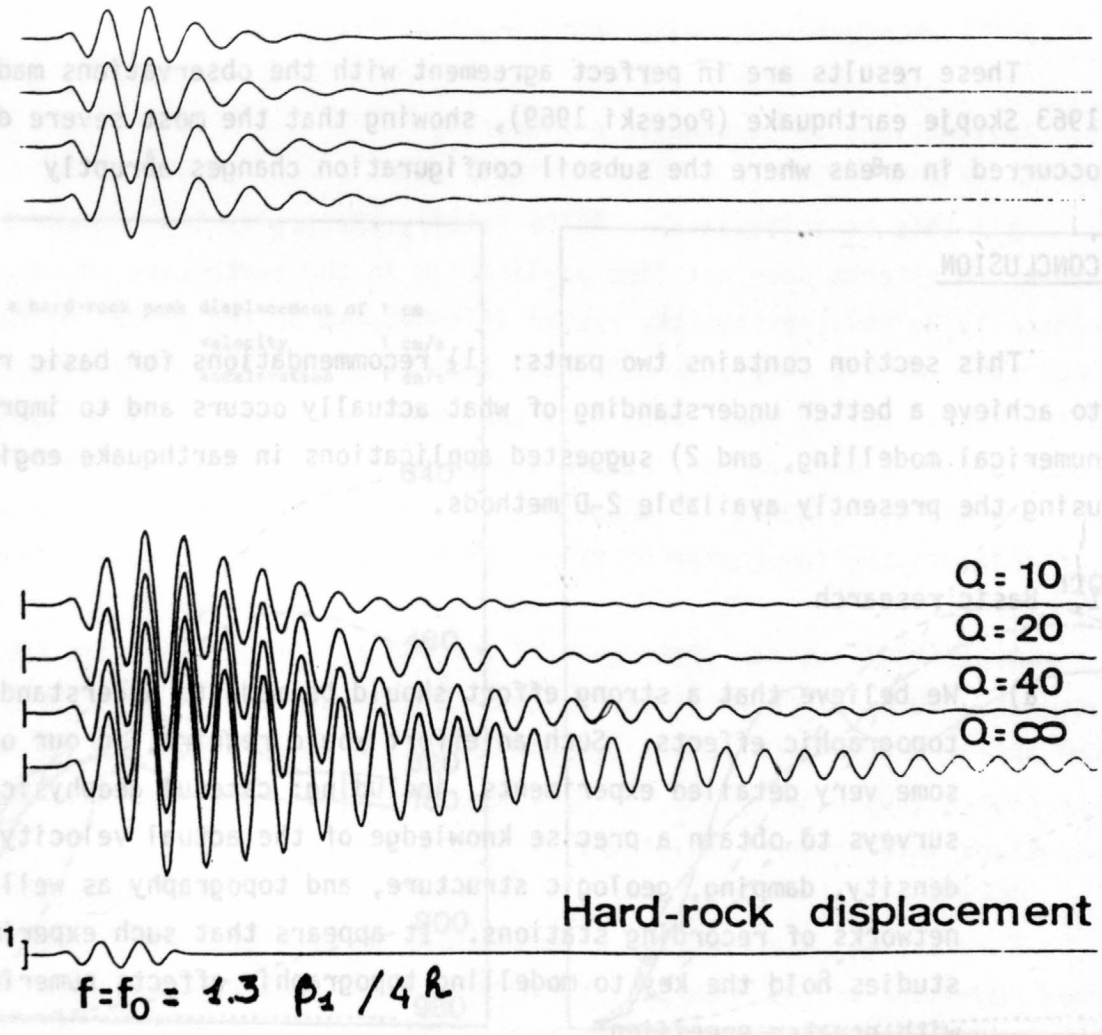

Figure 8.--Influence of damping of the sediments on the duration of ground motion within the valley. The bottom trace represents the surface displacement when sediments are absent and is twice the incident signal. The four middle traces represent the computed seismograms at the center of a sine-shaped valley having a shape ratio (h/l = 0.4) and an impedience contrast of 8, excited by an incident SH wave.

deep valleys, it is mainly associated with the harmonic modes of the 2-D resonance. In both cases, however, these differential motions are systematically larger on valley edges than in valley center, as may be seen in Figure 9.

These results are in perfect agreement with the observations made for the 1963 Skopje earthquake (Poceski 1969), showing that the most severe damage occurred in areas where the subsoil configuration changes abruptly

CONCLUSION

This section contains two parts: 1) recommendations for basic research to achieve a better understanding of what actually occurs and to improve numerical modelling, and 2) suggested applications in earthquake engineering using the presently available 2-D methods.

1. Basic research

a) We believe that a strong effort should be made to understand topographic effects. Such an effort would require, in our opinion, some very detailed experiments, including: careful geophysical surveys to obtain a precise knowledge of the actual velocity, density, damping, geologic structure, and topography as well as dense networks of recording stations. It appears that such experimental studies hold the key to modelling topographic effects numerically with greater precision.

b) As to sediment-filled valleys, we also believe that a need exists for good empirical data, such as those of Tucker and King (1983), and Tucker, King, Hatzfeld, and Nersesov (1983); this requires the installation of dense networks over well-known structures. In particular, it would be very interesting to know how these two-dimensional effects are modified, if at all, in the high-strain domain (strong motion).

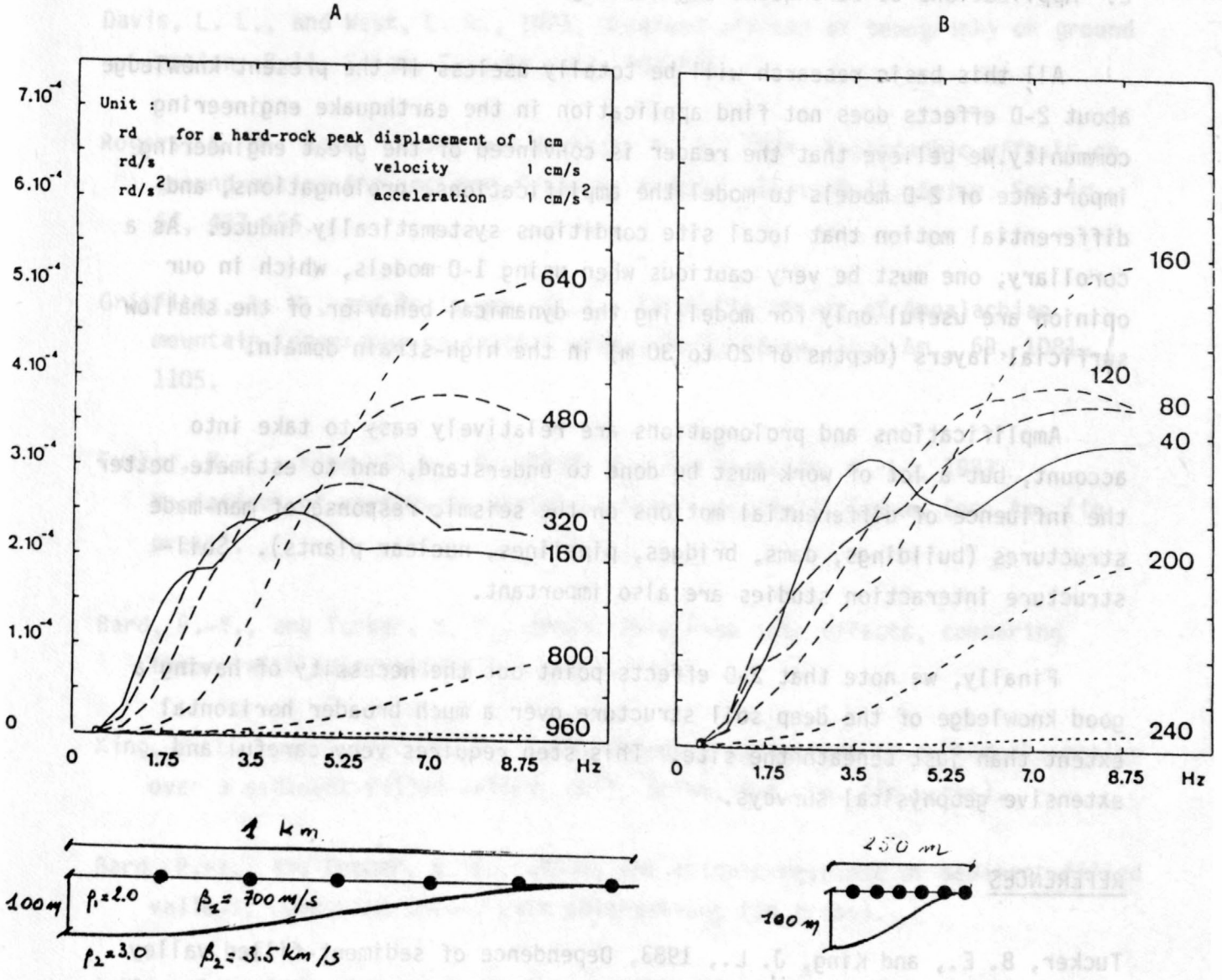

Figure 9.--Differential-motion spectra for a shallow (left) and a deep (right) sediment-filled valley. Each curve represents the maximum rotation, (i.e., half the spatial derivative of the SH motion; r = 0.5 dv/dx) recorded at different surface sites illustrated schematically on the bottom of the figure as a function of frequency (from Bouchon and Bard, 1982).

In addition to these experimental studies, a lot of theoretical work should be done to improve the present 2-D models, especially regarding their extension to 3-D structures as well as to more realistic rheological behaviors for the surficial soils (including inhomogeneity, anisotropy, non-linearity, water).

2. Applications to earthquake engineering

All this basic research will be totally useless if the present knowledge about 2-D effects does not find application in the earthquake engineering community.We believe that the reader is convinced of the great engineering importance of 2-D models to model the amplifications, prolongations, and differential motion that local site conditions systematically induce. As a corollary, one must be very cautious when using 1-D models, which in our opinion are useful only for modelling the dynamical behavior of the shallow surficial layers (depths of 20 to 30 m) in the high-strain domain.

Amplifications and prolongations are relatively easy to take into account, but a lot of work must be done to understand, and to estimate better the influence of differential motions on the seismic response of man-made structures (buildings, dams, bridges, pipelines, nuclear plants). Soil-structure interaction studies are also important.

Finally, we note that 2-D effects point out the necessity of having a good knowledge of the deep soil structure over a much broader horizontal extent than just beneath the site. This step requires very careful and extensive geophysical surveys.

REFERENCES

Tucker, B. E., and King, J. L., 1983, Dependence of sediment-filled valley response on input amplitude and valley properties, Bull. Seism. Soc. Am. (in press).

Bard, P.-Y, and Bouchon, M., 1980a, The seismic response of sediment-filled valleys, Part 1: The case of incident SH waves, Bull. Seism. Soc Am., 70, 1263-1286.

Bard, P.-Y., 1982, Diffracted waves and displacement field over two-dimensional elevated topographies, Geophys. J. R. Astr. Soc., 71, 731-760.

Bard, P.-Y., 1983, Les effets de site d'origine structurale en sismologie, Modelisation et interpretation, Application au risque sismique, These de Doctorat d'Etat, IRIGM-USMG, Grenoble, June 1983 (in French).

Davis, L. L., and West, L. R., 1973, Observed effects of topography on ground motion, Bull. Seism. Soc. Am., 63, 283-298.

Rogers, A. M., Katz, L. J., and Bennett, T. J., 1974, Topographic effects on ground motion for incident P waves: A model study, Bull. Seism. Soc Am., 64, 437-456.

Griffiths, D. W., and Bollinger, G. A., 1979, The effect of Appalachian mountain topography on seismic waves, Bull. Seism. Soc. Am., 69, 1081-1105.

Tucker, B. E., King, J. L., Hatzfeld, D., and Nersesov, I. L., 1983, Variations of earthquake motion on hard rock, Bull. Seism. Soc. Am. (in press).

Bard, P.-Y., and Tucker, B. E., 1983a, Hard rock site effects, comparing theory with observations (in press).

King, J. L., and Tucker, B. E., 1983. Observed variations of earthquake motion over a sediment-filled valley, Bull. Seism. Soc. Am. (in press).

Bard, P.-Y., and Tucker, B. E., 1983b, The seismic response of sediment-filled valleys, comparing theory with observations (in press).

Bouchon, M., Aki, K., and Bard, P.-Y., 1982, Theoretical evaluation of differential ground motions produced by earthquakes, Proceedings of the Third International Conference on Microzonation, Seattle, June 1982.

Poceski, A., 1969, The ground effects of the Skopje July 26, 1963, earthquake, Bull. Seism. Soc. Am., 59, 1-22.

ESTIMATING SITE EFFECTS ON STRONG GROUND MOTION USING LOCAL SHEAR-WAVE VELOCITY

by

William B. Joyner

Thomas E. Fumal

and

John C. Tinsley

U. S. Geological Survey

345 Middlefield Road

Menlo Park, California 94025

INTRODUCTION

We present here estimates of the site effects on strong ground motion as functions of local shear-wave velocity. The estimates are made for peak horizontal acceleration, velocity, and response spectra at 5 percent damping. The method makes use of the ground-motion predictive equations of Joyner and Boore (1981; 1982a; 1982b) and down-hole shear velocity measurements made to depths generally equal to or greater than 20 m at 33 of the strong motion sites where data used in deriving the predictive equations were recorded. The method and results are presented briefly here; a fuller discussion will be published elsewhere.

There is a basis in traditional seismological theory (Bullen, 1965; Aki and Richards, 1980) for the use of local shear-wave velocity in estimating the site effect on ground motion amplitude. If we neglect losses due to reflection, scattering, and anelastic attenuation, the energy along a tube of rays is constant and the amplitude is inversely proportional to the square root of the product of the density and the propagation velocity. (This product is commonly referred to as the seismic impedance.) If we include a correction for the change in cross-sectional area of the ray tube due to refraction in a medium where velocity is a function of depth, the amplitude of ground motion is proportional to

$$(\cos i)^{-1/2} (\rho V)^{-1/2}$$

where ρ is the density, V the propagation velocity and i is the angle of incidence measured from the vertical. The variations in density are relatively small and tend to correlate with the shear-velocity. Because of the tendency for propagation velocity to increase with depth, incidence angles are small near the surface and the factor in cos i can be neglected. Thus amplitude is approximately proportional to the reciprocal of the square root of the propagation velocity. As proposed by Joyner and others (1981) in analyzing strong-motion data from the 1979 Coyote Lake earthquake, we use shear velocity, measured over a depth of one quarter wave length of the period of concern, for predicting the site effect on ground motion. This method of predicting site effects does not account for resonance effects, involving reinforcing multiple reflections. Narrow band measures of ground motion such as Fourier spectra or undamped response spectra are certainly affected significantly at some sites by resonance. Broader band measures such as we

propose to predict, however, will in general be less affected. Resonance effects appear in undamped response spectra as sharp peaks at the resonant frequency. Such peaks are substantially reduced in the 5 percent damped spectral values we propose to predict, as is demonstrated in studies by Boore and Joyner (1983).

ESTIMATING THE SITE EFFECTS

To estimate the site effects we start with the predictive equations of Joyner and Boore (1981; 1982a; 1982b), which have the form

$$\log y = c_0 + c_1 (M-6) + c_2 (M-6)^2 + c_3 \log r + c_4 r + S \qquad (1)$$

$$5.0 \leq M \leq 7.7$$

$$r = (d^2 + h^2)^{1/2}$$

$$S = 0 \text{ at rock sites}$$

$$= c_5 \text{ at soil sites}$$

where y is the ground motion parameter to be predicted, M is moment magnitude (Hanks and Kanamori, 1979) and d is the closest distance from the site where ground motion is being predicted to the vertical projection on the earth's surface of the rupture surface for the earthquake. The parameters c_0 through c_5 and h have been determined from strong-motion data by regression analysis. At the strong-motion sites where shear-wave velocity data are available we take the residuals of log y with respect to the values predicted by equation (1) for rock sites. We then do a linear regression between those residuals and the logarithm of the shear-wave velocity averaged over a depth of one-quarter wavelength of the period of interest. This in many cases requires us to extend the downhole shear-wave velocity profile to depths

substantially greater than the deepest measurement, using whatever geologic data is available. To decouple the site-effects variation from the earthquake-to-earthquake variation, we do the regression using the following equation:

$$\log R_{ij} = p_i + c_6 V_j \qquad (2)$$

where R_{ij} is the residual for earthquake i at site j, V_j is the average shear velocity to the appropriate depth at site j, and p_i and c_6 are parameters determined by the regression. Figure 1 shows a log-log plot of the residuals against shear-wave velocity for peak horizontal ground velocity. The regression using equation (2) gives us the slope of the straight line relating the logarithm of ground motion residual to the logarithm of site shear velocity, but it does not give us a unique intercept. We obtain the intercept by requiring that the average site effect term calculated using the shear-wave velocity be the same as the average calculated for the same group of stations using the simple rock versus soil classification. The resulting site effect term can be cast in the form

$$S = c_6 \log \left(\frac{V}{V_o}\right) \qquad (3)$$

where V is the local shear-wave velocity and V_o is a reference velocity. Values of c_6 and V_o are given in Table 1 for the various ground-motion quantities to be predicted, except for peak acceleration and a few of the short period response values for which the correlation between the logarithm of ground motion residual and the logarithm of shear velocity is not statistically significant at the 90 percent level. The values of c_6 given in Table 1 are generally close to the 0.5 value derived be requiring conservation

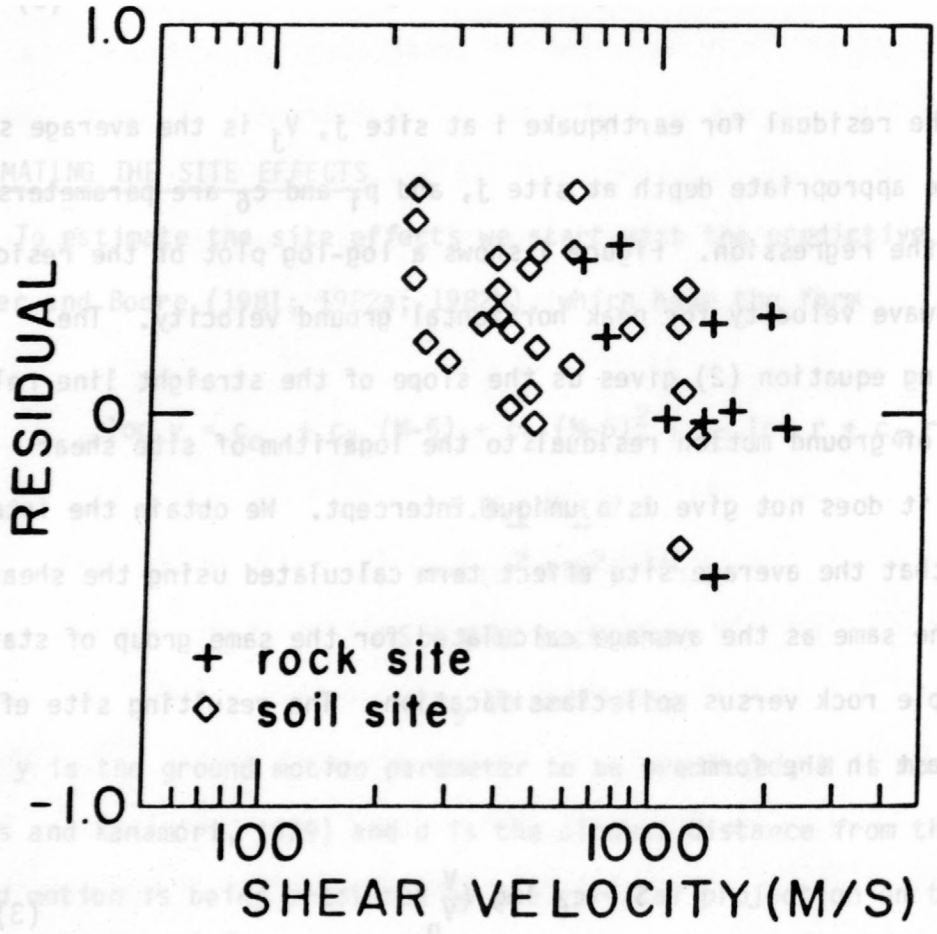

Figure 1. Residuals of the logarithm of peak horizontal velocity with respect to the values predicted by equation (1) for rock sites, plotted against the average shear-wave velocity to a depth of a one-quarter wavelength of a one-second wave.

Table 1. Parameters for predicting the site effect on peak horizontal acceleration, velocity, and pseudo-velocity response at 5 percent damping (Asterisks indicate that the correlation with shear-wave velocity is not statistically significant at the 90 percent level.)

	Period	V_o	c_6
	s	m/s	
Peak Acceleration		*	*
Peak Velocity		1190	-0.45
Pseudo-Velocity Response	0.1	*	*
	0.15	*	*
	0.2	*	*
	0.3	590	-0.28
	0.4	830	-0.33
	0.5	1020	-0.38
	0.75	1410	-0.46
	1.0	1580	-0.51
	1.5	1620	-0.59
	2.0	1620	-0.64
	3.0	1550	-0.72
	4.0	1450	-0.78

of energy along tubes of rays. It is not clear why the values are less than 0.5 for response spectra at periods less than 1.0 s or why there is no statistically significant correlation with shear wave velocity for peak acceleration or for response spectra at periods less than 0.3 s. There are at least two possible reasons for values greater than 0.5. If we take account of density differences and if density correlates positively with shear velocity, as one would expect, then the coefficient of the logarithm of the velocity ratio would exceed 0.5. Resonance effects could also contribute to a larger coefficient. One should also bear in mind that the argument involving energy conservation along ray tubes is essentially a body-wave argument, and may not adequately describe the amplification, particularly at long periods, if surface-wave propagation is significantly involved.

In an attempt to understand why peak horizontal acceleration and response spectra at periods less than 0.3 s did not show a statistically significant correlation with local shear wave velocity, we also tried a linear regression against two independent variables, local shear-wave velocity to a depth of one-quarter wavelength and depth to overlying rock. The idea was to see if two mutually cancelling effects were present. The analysis was performed using two alternative definitions of rock: (1) material characterized by shear-wave velocity in excess of 750 m/s; (2) material characterized by shear-wave velocity in excess of 1500 m/s. The first value corresponds generally to soft sedimentary rock and the second to hard crystalline rock. In the case of peak acceleration and short-period response, the results showed no statistically significant correlation with either shear-wave velocity or depth to rock, for the 750 m/s definition of rock. Peak acceleration was analyzed using the 1500 m/s definition of rock, and the results in that case also showed no correlation with either variable. For peak velocity and longer-

period response spectra, the results showed significant correlation with both shear wave velocity and depth to rock for the 750 m/s definition of rock. For the 1500 m/s definition an analysis of peak velocity showed correlation only with shear-wave velocity. The correlation with depth to rock noted for the 750 m/s definition was in the sense of decreasing ground motion with increasing depth. The coefficient relating ground motion to depth was relatively small, and, although formal tests indicated statistical significance at better than the 90 percent level, we frankly doubt the validity of the correlation. For reasonable values of Q, anelastic attenuation is not large enough to account for the correlation. Moreover, if the strong-motion data from the 1971 San Fernando earthquake are analyzed separately, the results do not show significant correlation. All things considered, we do not believe it appropriate with the present data set to use depth to rock in predicting site effects. Figure 2 shows the residuals of peak horizontal velocity corrected for site effects with equation (3) plotted against depth to rock using the 750 m/s definition of rock. It seems clear that we are not losing much by not using depth to rock in our prediction scheme.

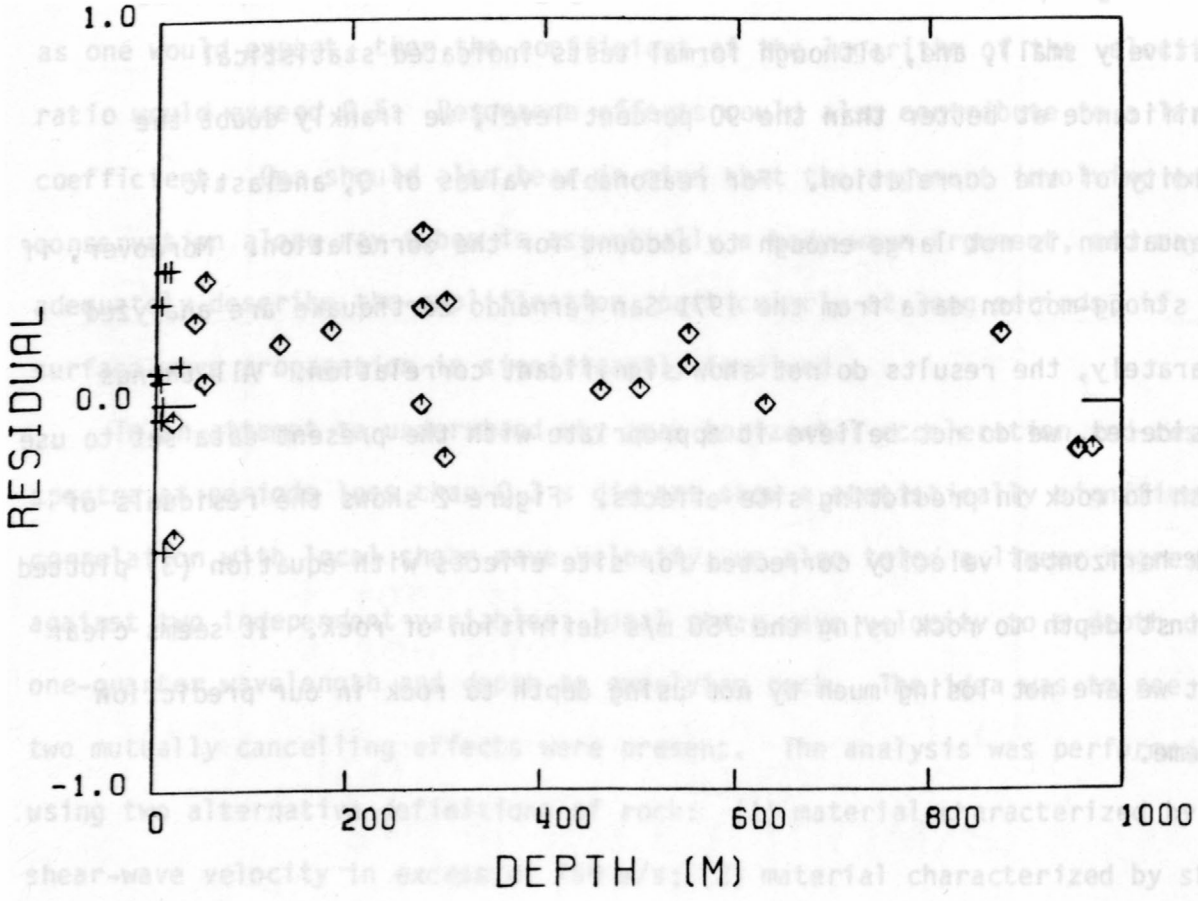

Figure 2. Residuals of the logarithm of peak horizontal velocity with respect to the values predicted by equation (1) for rock sites corrected for site effects using equation (3) and plotted against depth to rock. The definition of rock in this case is material with a shear wave velocity greater than 750 m/s.

REFERENCES

Aki, K., and Richards, P. G., 1980, Quantitative seismology: W. H. Freeman, San Francisco, v. 1, 557 p.

Boore, D. M., and Joyner, W. B., 1983, Ground motions and response spectra at soil sites from seismological models of radiated spectra (this volume).

Bullen, K. E., 1965, An introduction to the theory of seismology: Cambridge University Press, Cambridge, 381 p.

Hanks, T. C., and Kamamori, H., 1979, A moment magnitude scale: Journal Geophysical Research, v. 84, p. 2348-2350.

Joyner, W. B., and Boore, D. M., 1981, Peak horizontal acceleration and velocity from strong-motion records including records from the 1979 Imperial Valley, California, Earthquake: Bulletin, Seismological Society of America, v. 71, p. 2011-2038.

Joyner, W. B., and Boore, D. M., 1982a, Estimation of response-spectral values as functions of magnitude, distance, and site conditions: U. S. Geological Survey Open-File Report No. 82-881, 14 p.

Joyner, W. B., and Boore, D. M., 1982b, Prediction of earthquake response spectra: U. S. Geological Survey Open-File Report No. 82-977, 16 p.

Joyner, W. B., Warrick, R. E., and Fumal, T. E., 1981, The effect of Quaternary alluvium on strong ground motion in the Coyote Lake, California, earthquake of 1979: Bulletin, Seismological Society of America, v. 71, p. 1333-1349.

GROUND MOTIONS AND RESPONSE SPECTRA AT SOIL SITES FROM SEISMOLOGICAL MODELS OF RADIATED SPECTRA

by

David M. Boore
William B. Joyner

U.S. Geological Survey
345 Middlefield Road
Menlo Park, California 94025

INTRODUCTION

It is straightforward to compute site response in the form of Fourier spectral ratios between the surface motion and the equivalent motion recorded in the absence of soil layers, at least for cases where nonlinear response is not expected. As we will show in this paper, however, the Fourier spectral ratios can give a misleading impression of the effect of the site response on structures. More useful for seismic design is the computation of response spectra at the surface of a soil column. This requires specification of the input time series. To do this, we use a recently developed technique based on seismological source models for generating a suite of accelerograms for arbitrary magnitudes and distances (Boore, 1983); using these as input motions with any of the available methods for computing soil response enables us to compute ground motions and response spectra at soil sites.

METHOD

Input Motion. The specification of the input motion lies at the heart of the method. Discussed in detail by Boore (1983), only a brief description is given here. The essence of the method is to filter windowed, Gaussian white noise so that the amplitude spectrum is equal, on the average, to a target

spectrum obtained from seismological considerations. An ω-squared spectrum with a magnitude-independent high-frequency cutoff and a constant stress parameter has been used for the target or model spectrum. At a given distance, the change of spectral shape and level with earthquake size is controlled by only one parameter: moment magnitude. Figure 1 shows acceleration spectra for magnitudes ranging from 4 to 7 at a distance of 10 km. The target spectrum for a magnitude 5 event and the actual spectrum from one realization of the stochastic process are shown in the upper part of Figure 2. The lower part is similar, except the average spectrum from 20 time series is shown. As emphasized by this example, the target spectrum is met only on the average; we think this is a more realistic procedure than demanding that one time series reproduce the target spectrum exactly.

Some of the justification for this simple procedure for generating strong motion is shown in Figure 3, in which peak acceleration and peak velocity are compared with the regression results of Joyner and Boore (1981; 1982). As shown in more detail in Boore (1983), the model agrees with predictions of most important measures of strong ground motion, predictions based on the analysis of hundreds of recordings from earthquakes in western North America.

Soil Response. For illustration, all soil responses in this paper were computed by Haskell's method for propagating SH-waves through a stack of constant velocity layers (Haskell, 1960). The method allows for anelastic attenuation by using complex rigidities in each layer (Joyner and Chen, 1975), but assumes linearity. We don't believe that the assumption of linearity is a severe restriction, but the justification for this statement is beyond the scope of this paper (see, e.g., Joyner and others, 1981). Because an input time series is derived, nonlinear soil response calculations could be made if

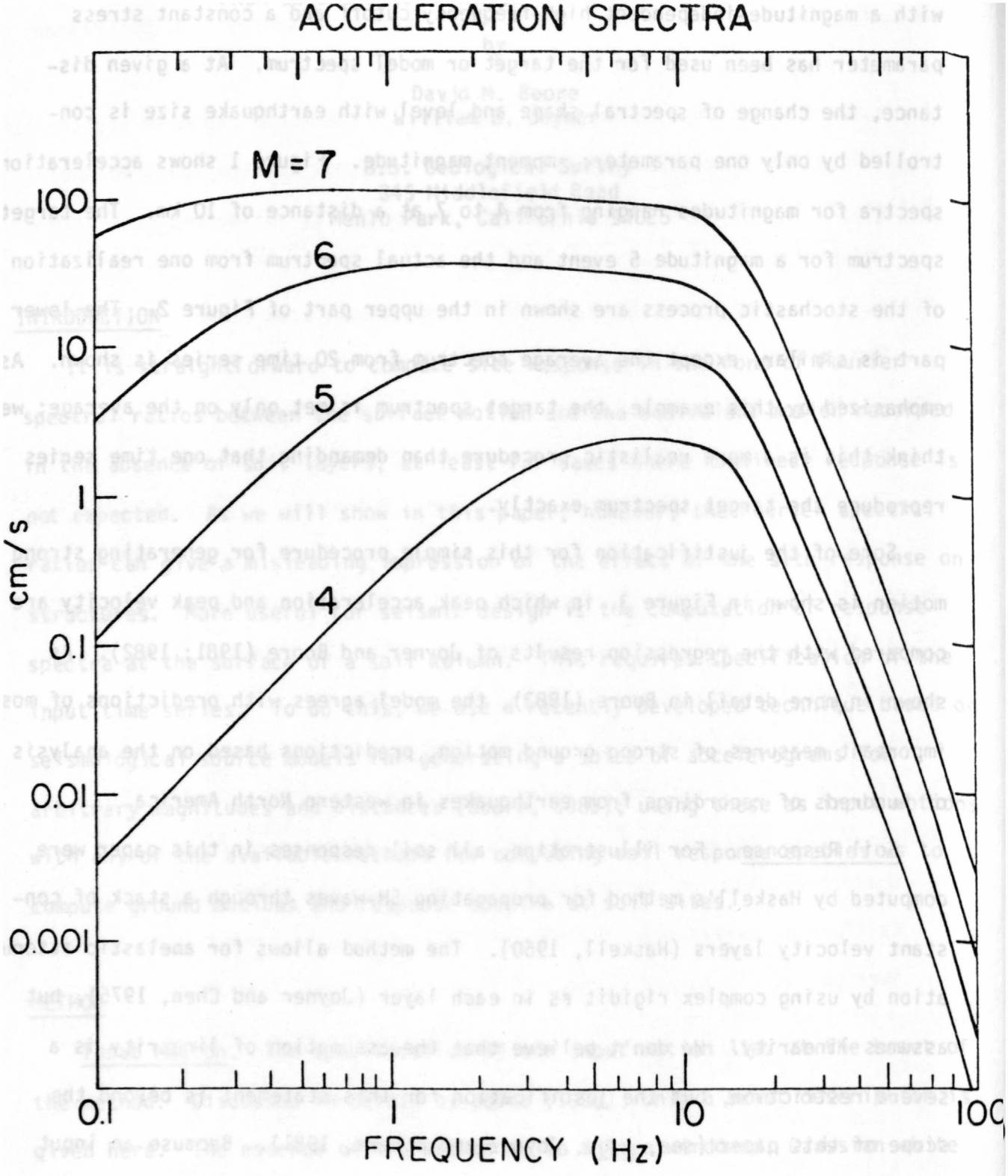

Figure 1. Acceleration Fourier spectra at 10 km for a model with a stress parameter equal to 100 bars and a high-frequency corner of 15 Hz.

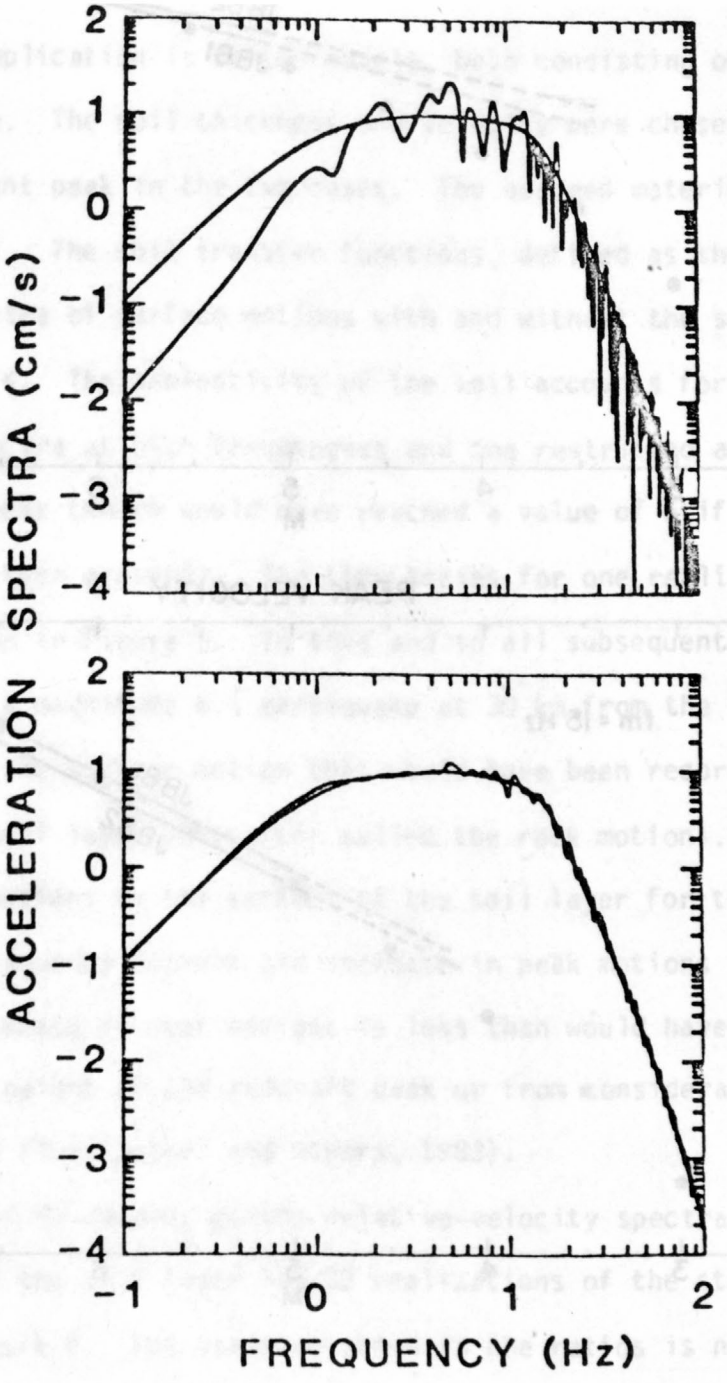

Figure 2. Acceleration Fourier spectra at 10 km from a magnitude 5 earthquake. Smooth curves: model spectra. Jagged curves: spectra from 1 simulation (top) and average of 20 simulations (bottom).

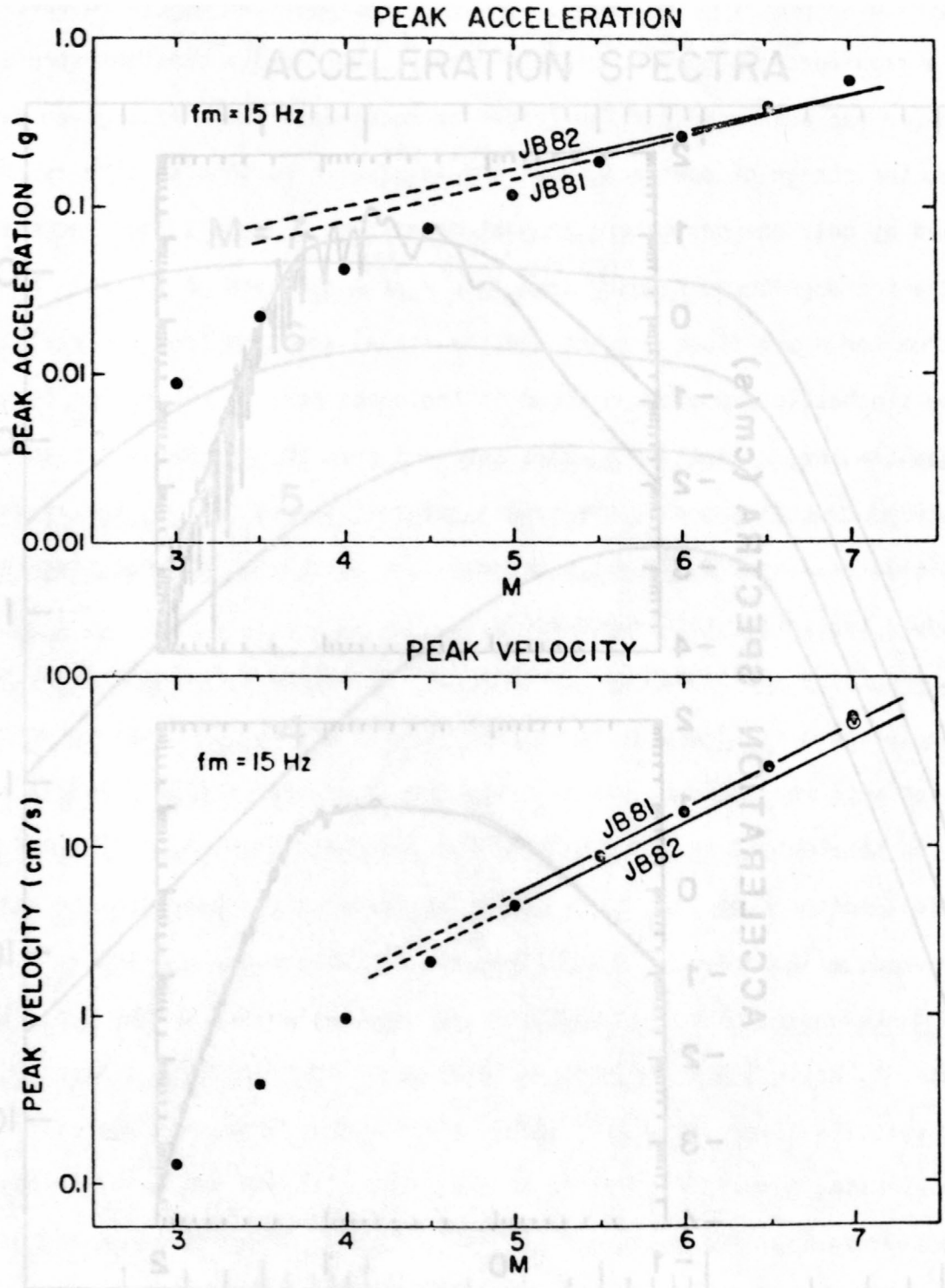

Figure 3. Comparison of mean peak acceleration and peak velocity, derived from 20 simulations (circles), and curves determined from regression studies of data (JB81: Joyner and Boore, 1981; JB82: Joyner and Boore, 1982). No data from earthquakes less than magnitude 5 were used in the regression analyses, and therefore the curves have been dashed for M < 5.

necessary.

APPLICATIONS

The first application is to two models, both consisting of a single layer over a halfspace. The soil thickness and velocity were chosen to give a 1-Hz and 10-Hz resonant peak in the two cases. The assumed material properties are given in Table 1. The soil transfer functions, defined as the ratio between the Fourier spectra of surface motions with and without the soil layer, are shown in Figure 4. The anelasticity of the soil accounts for both the gradual decay of the spectra at high frequencies and the restricted amplitude of the first resonant peak (which would have reached a value of 5 if no anelastic attenuation had been present). The time series for one realization of the process are shown in Figure 5. In this and in all subsequent examples the motions are for a magnitude 6.5 earthquake at 30 km from the source. The bottom trace is the surface motion that would have been recorded in the absence of the soil layer (hereafter called the rock motion). The other two traces are the motions on the surface of the soil layer for the two models. The change in frequency content and increase in peak motions is clear. On the average, the increase in peak motions is less than would have been predicted either from the height of the resonant peak or from considerations of conservation of energy flux (Joyner and others, 1983).

The ratios of 5%-damped, pseudo relative-velocity spectra at the surface with and without the soil layer for 20 realizations of the stochastic process are shown in Figure 6. The variance shown in the ratios is not simply related to the variance in the spectra of the input motions. This is most easily seen for the model with a 10-Hz fundamental frequency; at lower frequency the soil

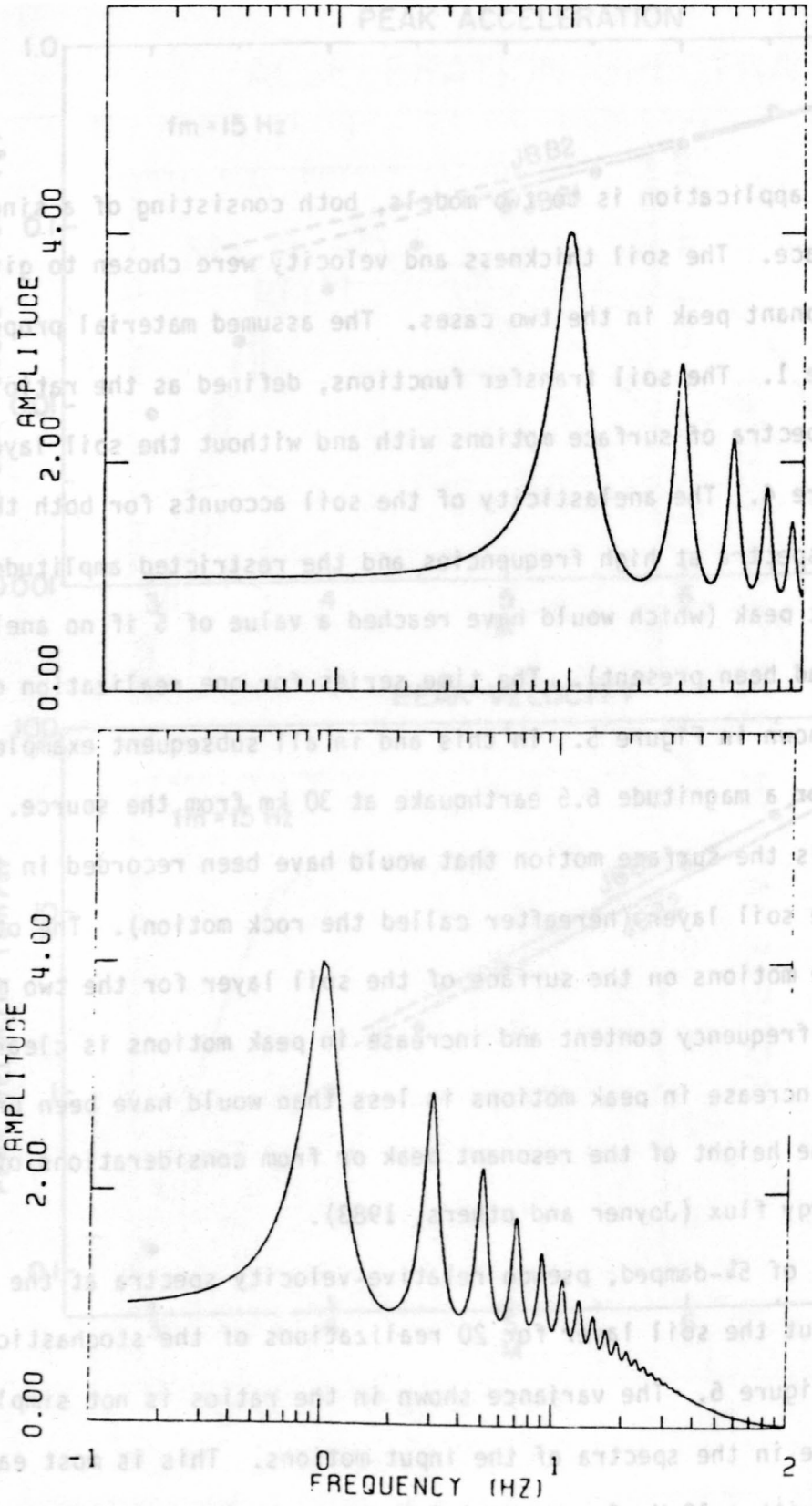

Figure 4. Soil transfer functions for the two single-layer models.

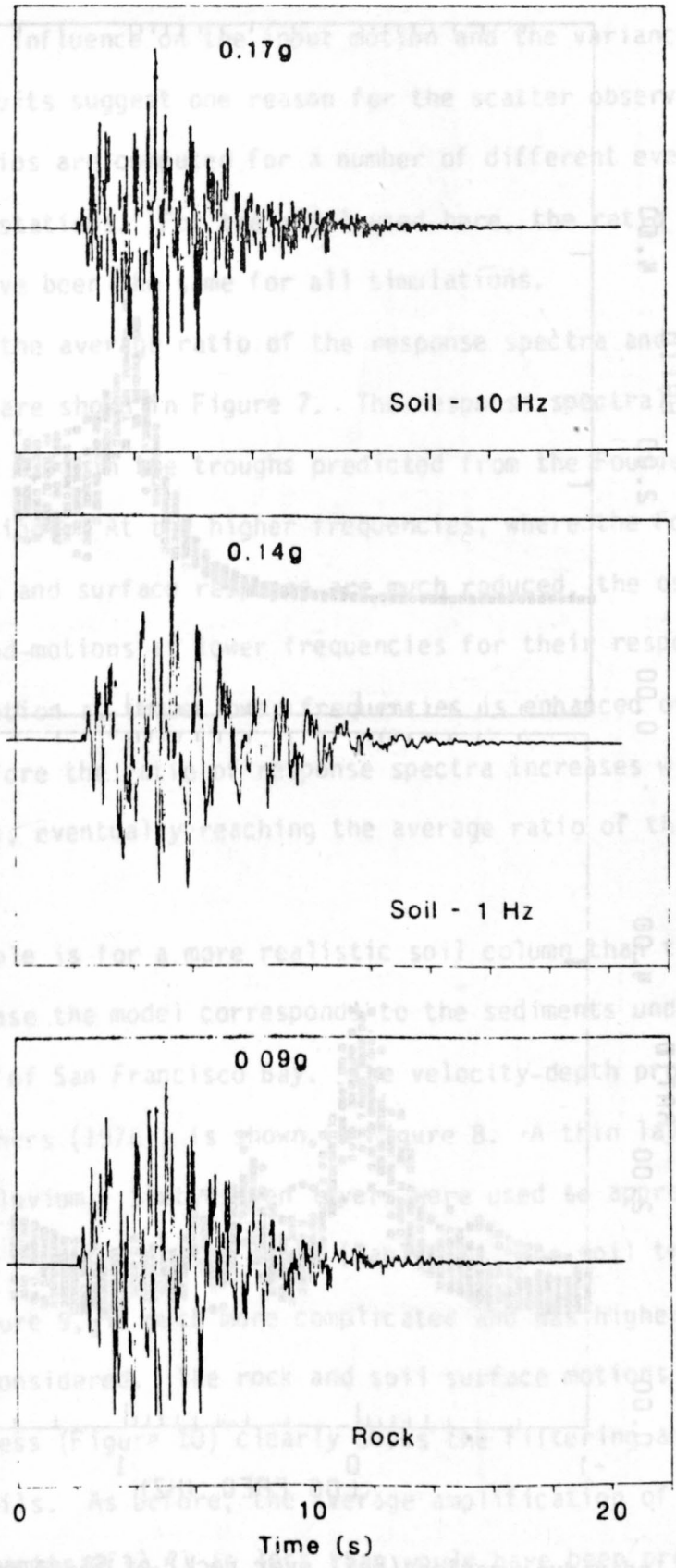

Figure 5. Accelerograms for magnitude 6.5 earthquake at 30 km at rock site (bottom) and two single-layer soil sites. Average peak accelerations from 20 simulations are shown.

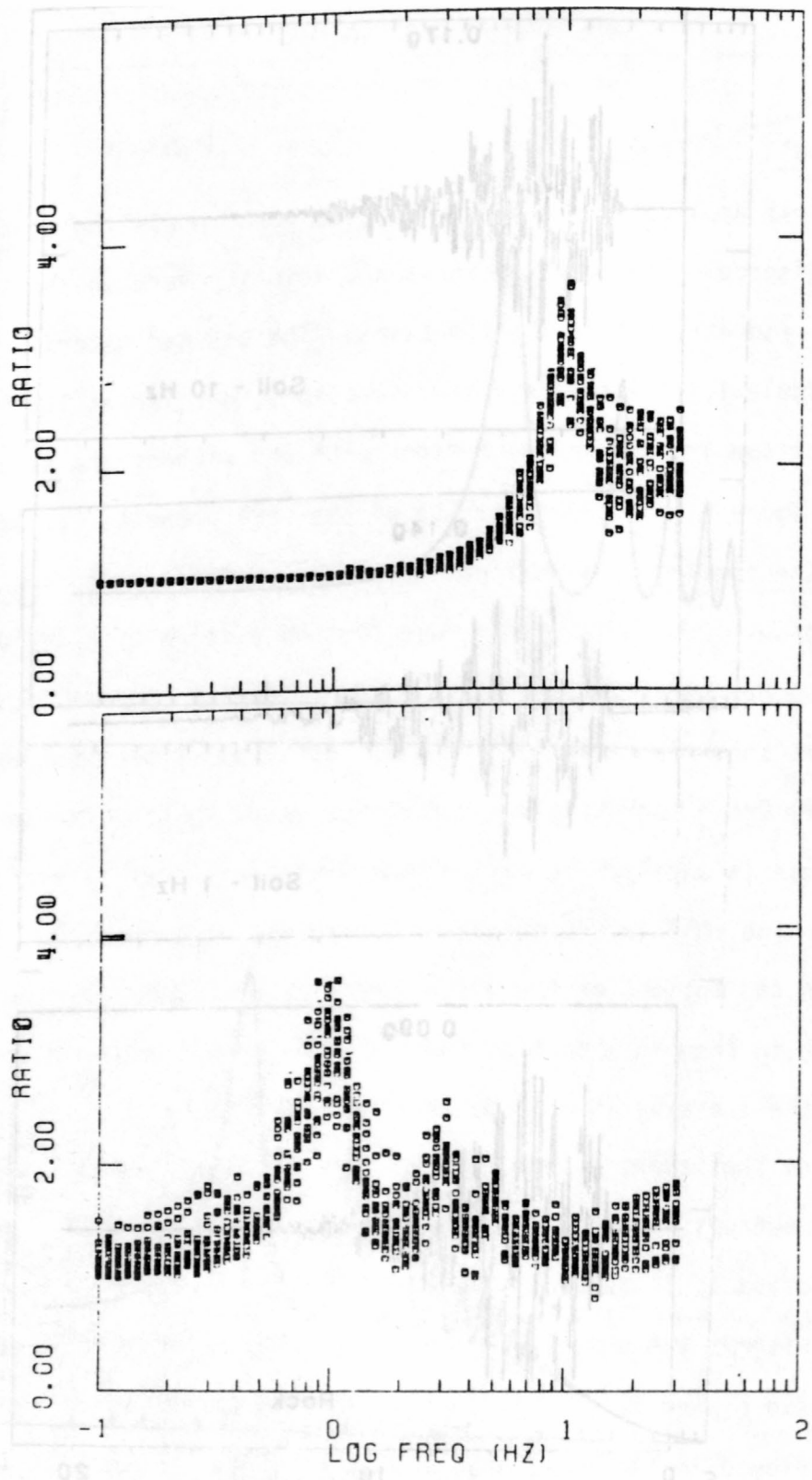

Figure 6. Individual ratios (soil over rock) of 5%-damped pseudo relative-velocity response spectra for the two single-layer models from 20 simulations of a magnitude 6.5 earthquake. FMAX = 15 and R = 30 km.

layer exerts little influence on the input motion and the variance in the ratio decreases. The results suggest one reason for the scatter observed when response spectral ratios are computed for a number of different events recorded at a given pair of stations. For the model used here, the ratio of Fourier transforms would have been the same for all simulations.

Comparisons of the average ratio of the response spectra and the soil transfer functions are shown in Figure 7. The response spectral ratios tend to lower the peaks and fill in the troughs predicted from the Fourier-spectral soil transfer functions. At the higher frequencies, where the Fourier spectra of the input motion and surface response are much reduced, the oscillators must reach back to ground-motions at lower frequencies for their response. On the average the soil motion at these lower frequencies is enhanced over the rock motions, and therefore the ratio of response spectra increases with frequency at high frequencies, eventually reaching the average ratio of the peak accelerations.

The final example is for a more realistic soil column than the previous examples. In this case the model corresponds to the sediments underlying a portion of the margin of San Francisco Bay. The velocity-depth profile, taken from Joyner and others (1976), is shown in Figure 8. A thin layer of bay mud is underlain by alluvium. Sixty-seven layers were used to approximate the velocity-gradients expected in the soils (Table 1). The soil transfer function, shown in Figure 9, is much more complicated and has higher peaks than those previously considered. The rock and soil surface motions for one realization of the process (Figure 10) clearly shows the filtering and amplification produced by the soils. As before, the average amplification of the peak accelerations (a factor of 3.4) is less than would have been predicted from

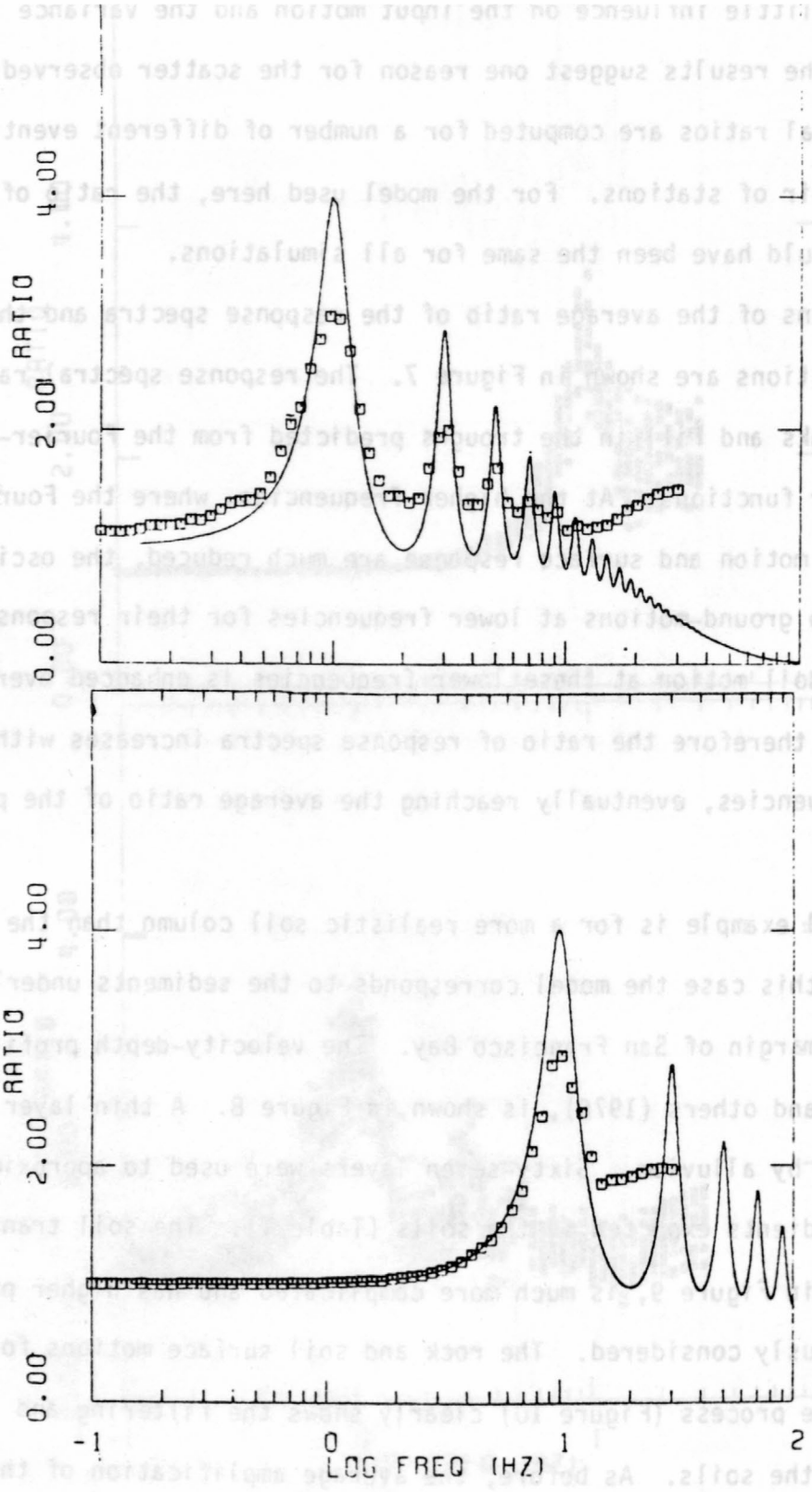

Figure 7. Comparison of mean Fourier soil transfer functions (solid lines) and averaged ratios of response spectra (symbols) for the two single-layer soil models. FMAX = 15 and R = 30.

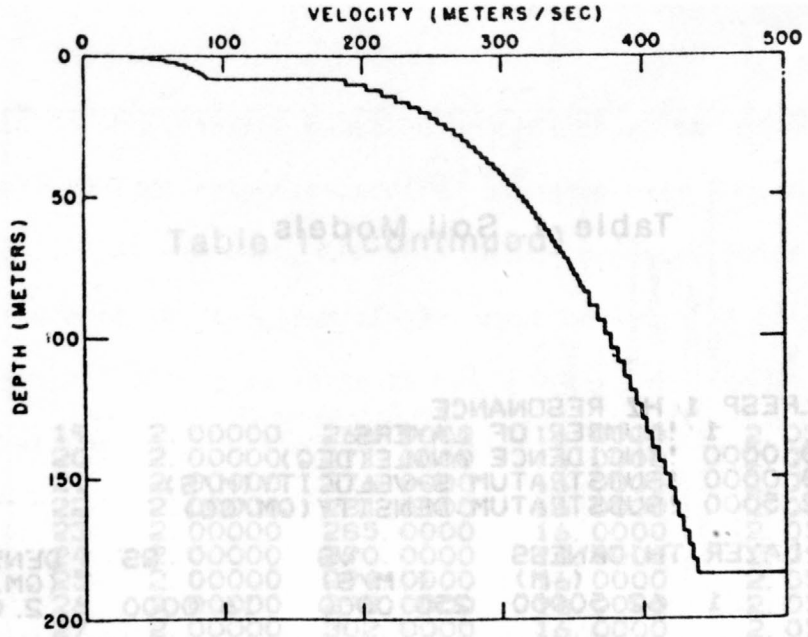

Figure 8. Shear velocity-depth function (from Joyner and others, 1976).

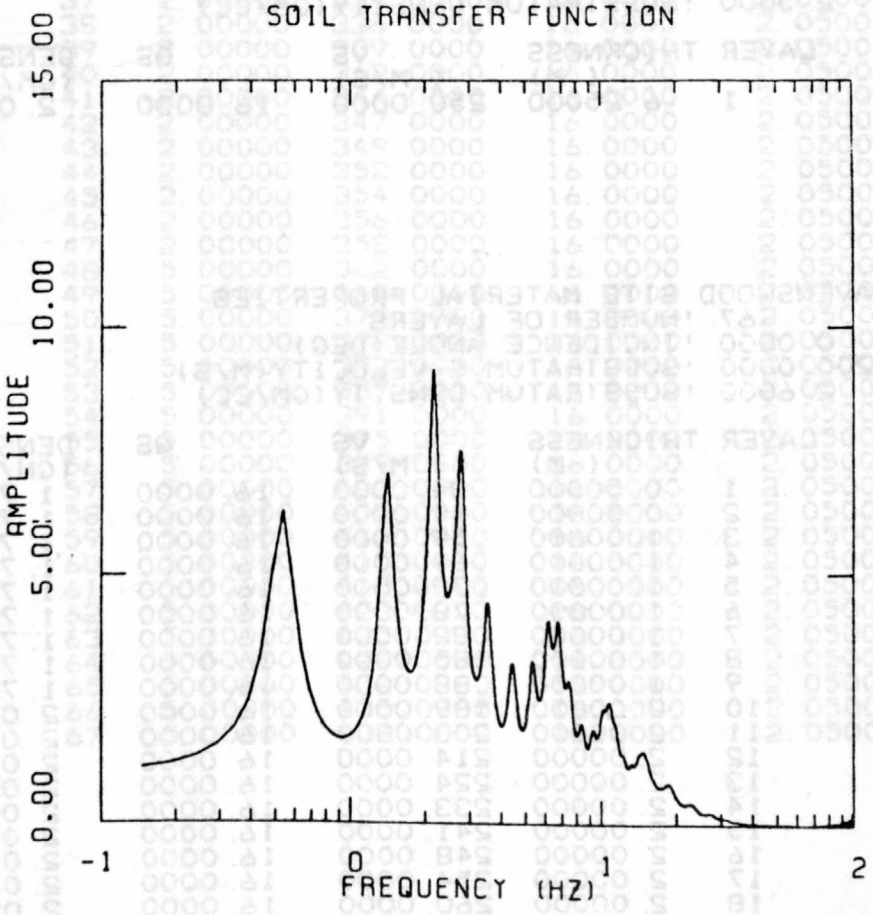

Figure 9. Soil transfer function for model of bay sediments.

Table 1. Soil Models

SOILRESP 1 HZ RESONANCE

1	!NUMBER OF LAYERS
0.0000	!INCIDENCE ANGLE(DEG)
1000.0000	!SUBSTRATUM S-VELOCITY(M/S)
2.5000	!SUBSTRATUM DENSITY(GM/CC)

LAYER	THICKNESS (M)	VS (M/S)	QS	DENSITY (GM/CC)
1	62.50000	250.0000	16.0000	2.0000

SOILRESP 10 HZ RESONANCE

1	!NUMBER OF LAYERS
0.0000	!INCIDENCE ANGLE(DEG)
1000.0000	!SUBSTRATUM S-VELOCITY(M/S)
2.5000	!SUBSTRATUM DENSITY(GM/CC)

LAYER	THICKNESS (M)	VS (M/S)	QS	DENSITY (GM/CC)
1	6.25000	250.0000	16.0000	2.0000

RAVENSWOOD SITE MATERIAL PROPERTIES

67	!NUMBER OF LAYERS
0.0000	!INCIDENCE ANGLE(DEG)
2200.0000	!SUBSTRATUM S-VELOCITY(M/S)
2.6000	!SUBSTRATUM DENSITY(GM/CC)

LAYER	THICKNESS (M)	VS (M/S)	QS	DENSITY (GM/CC)
1	0.50000	34.0000	16.0000	1.7000
2	0.50000	49.0000	16.0000	1.7000
3	1.00000	59.0000	16.0000	1.7000
4	1.00000	67.0000	16.0000	1.7000
5	1.00000	73.0000	16.0000	1.7000
6	1.00000	78.0000	16.0000	1.7000
7	1.00000	82.0000	16.0000	1.7000
8	1.00000	85.0000	16.0000	1.7000
9	1.00000	88.0000	16.0000	1.7000
10	2.00000	189.0000	16.0000	2.0500
11	2.00000	203.0000	16.0000	2.0500
12	2.00000	214.0000	16.0000	2.0500
13	2.00000	224.0000	16.0000	2.0500
14	2.00000	233.0000	16.0000	2.0500
15	2.00000	241.0000	16.0000	2.0500
16	2.00000	248.0000	16.0000	2.0500
17	2.00000	254.0000	16.0000	2.0500
18	2.00000	260.0000	16.0000	2.0500

Table 1. (continued)

19	2.00000	266.0000	16.0000	2.0500
20	2.00000	271.0000	16.0000	2.0500
21	2.00000	276.0000	16.0000	2.0500
22	2.00000	281.0000	16.0000	2.0500
23	2.00000	285.0000	16.0000	2.0500
24	2.00000	290.0000	16.0000	2.0500
25	2.00000	294.0000	16.0000	2.0500
26	2.00000	298.0000	16.0000	2.0500
27	2.00000	302.0000	16.0000	2.0500
28	2.00000	305.0000	16.0000	2.0500
29	2.00000	309.0000	16.0000	2.0500
30	2.00000	312.0000	16.0000	2.0500
31	2.00000	316.0000	16.0000	2.0500
32	2.00000	319.0000	16.0000	2.0500
33	2.00000	322.0000	16.0000	2.0500
34	2.00000	325.0000	16.0000	2.0500
35	2.00000	328.0000	16.0000	2.0500
36	2.00000	331.0000	16.0000	2.0500
37	2.00000	334.0000	16.0000	2.0500
38	2.00000	336.0000	16.0000	2.0500
39	2.00000	339.0000	16.0000	2.0500
40	2.00000	342.0000	16.0000	2.0500
41	2.00000	344.0000	16.0000	2.0500
42	2.00000	347.0000	16.0000	2.0500
43	2.00000	349.0000	16.0000	2.0500
44	2.00000	352.0000	16.0000	2.0500
45	2.00000	354.0000	16.0000	2.0500
46	2.00000	356.0000	16.0000	2.0500
47	2.00000	358.0000	16.0000	2.0500
48	5.00000	362.0000	16.0000	2.0500
49	5.00000	368.0000	16.0000	2.0500
50	5.00000	373.0000	16.0000	2.0500
51	5.00000	378.0000	16.0000	2.0500
52	5.00000	382.0000	16.0000	2.0500
53	5.00000	387.0000	16.0000	2.0500
54	5.00000	391.0000	16.0000	2.0500
55	5.00000	395.0000	16.0000	2.0500
56	5.00000	399.0000	16.0000	2.0500
57	5.00000	403.0000	16.0000	2.0500
58	5.00000	407.0000	16.0000	2.0500
59	5.00000	411.0000	16.0000	2.0500
60	5.00000	415.0000	16.0000	2.0500
61	5.00000	418.0000	16.0000	2.0500
62	5.00000	422.0000	16.0000	2.0500
63	5.00000	425.0000	16.0000	2.0500
64	5.00000	428.0000	16.0000	2.0500
65	5.00000	432.0000	16.0000	2.0500
66	5.00000	435.0000	16.0000	2.0500
67	5.00000	438.0000	16.0000	2.0500

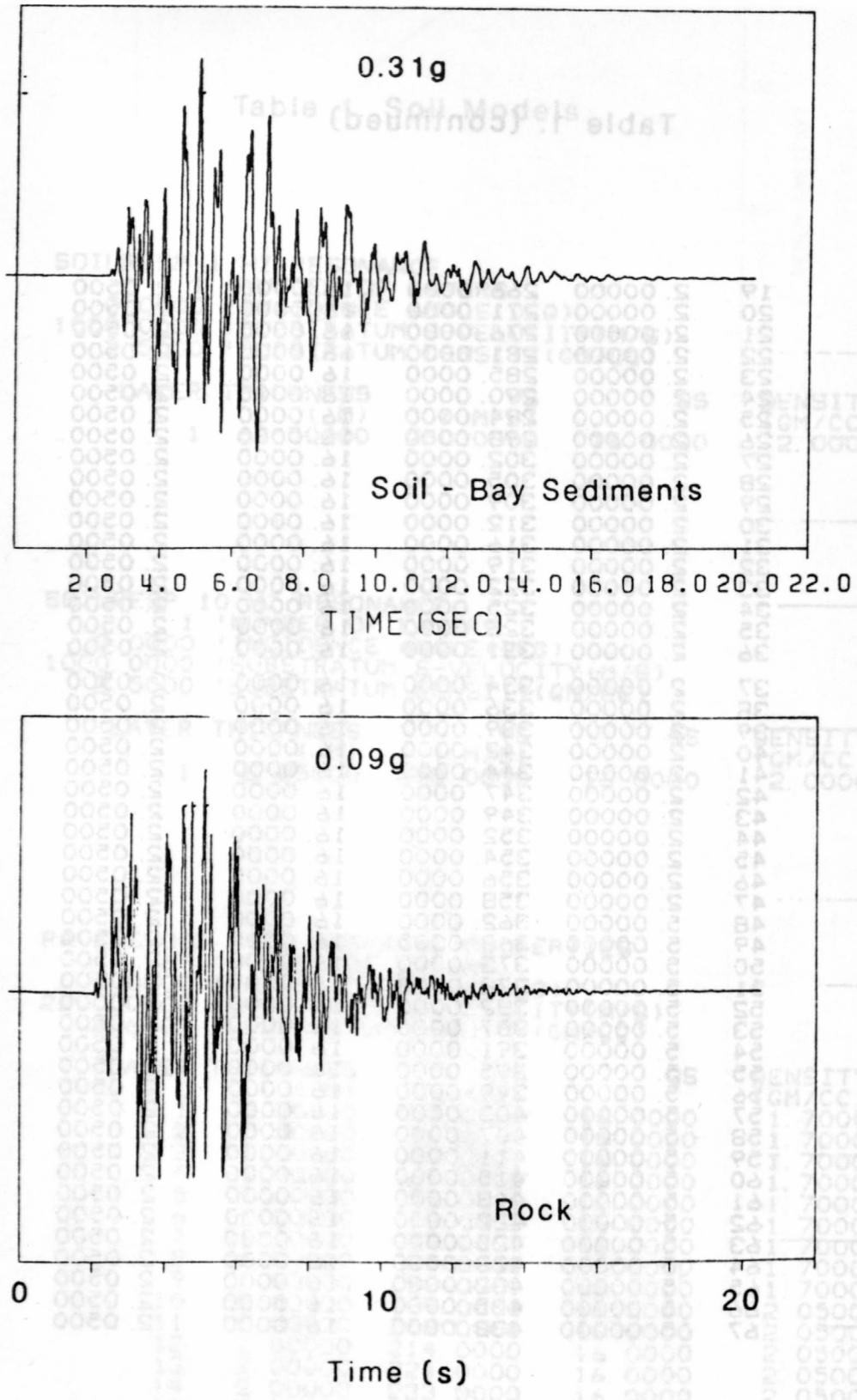

Figure 10. Accelerograms for magnitude 6.5 earthquake at 30 km at rock site (bottom) and bay sediment site (top). Peak accelerations shown are averages for 20 simulations.

either the peaks in the transfer function or considerations of energy flux. The rock and soil surface response-spectra, averaged over 20 simulations, are shown in Figure 11. As expected, the soil column produces major changes in shape and amplitude of the spectrum of the input motion. As before, however, these changes are not nearly as large as would have been expected from considerations of the Fourier spectral transfer function (Figure 12).

CONCLUSIONS

A simple, yet powerful, method for constructing ground motions and response spectra at the surface of soil sites underlain by sediments has been presented. The method uses, as input to a sediment column, stochastic simulations of time series whose amplitude spectra and duration are controlled by seismological considerations. Applications to simple and complex soil profiles suggest the following conclusions:

- The amplification of peak acceleration on soil sites is less than expected from considerations of peaks in soil transfer functions and from energy conservation arguments.

- The large variations expected in Fourier spectral transfer functions are subdued when damped response spectra are considered. This suggests caution in either using Fourier spectra to characterize site response for engineering purposes, or in using ratios of response spectra to infer the properties of the underlying sediments.

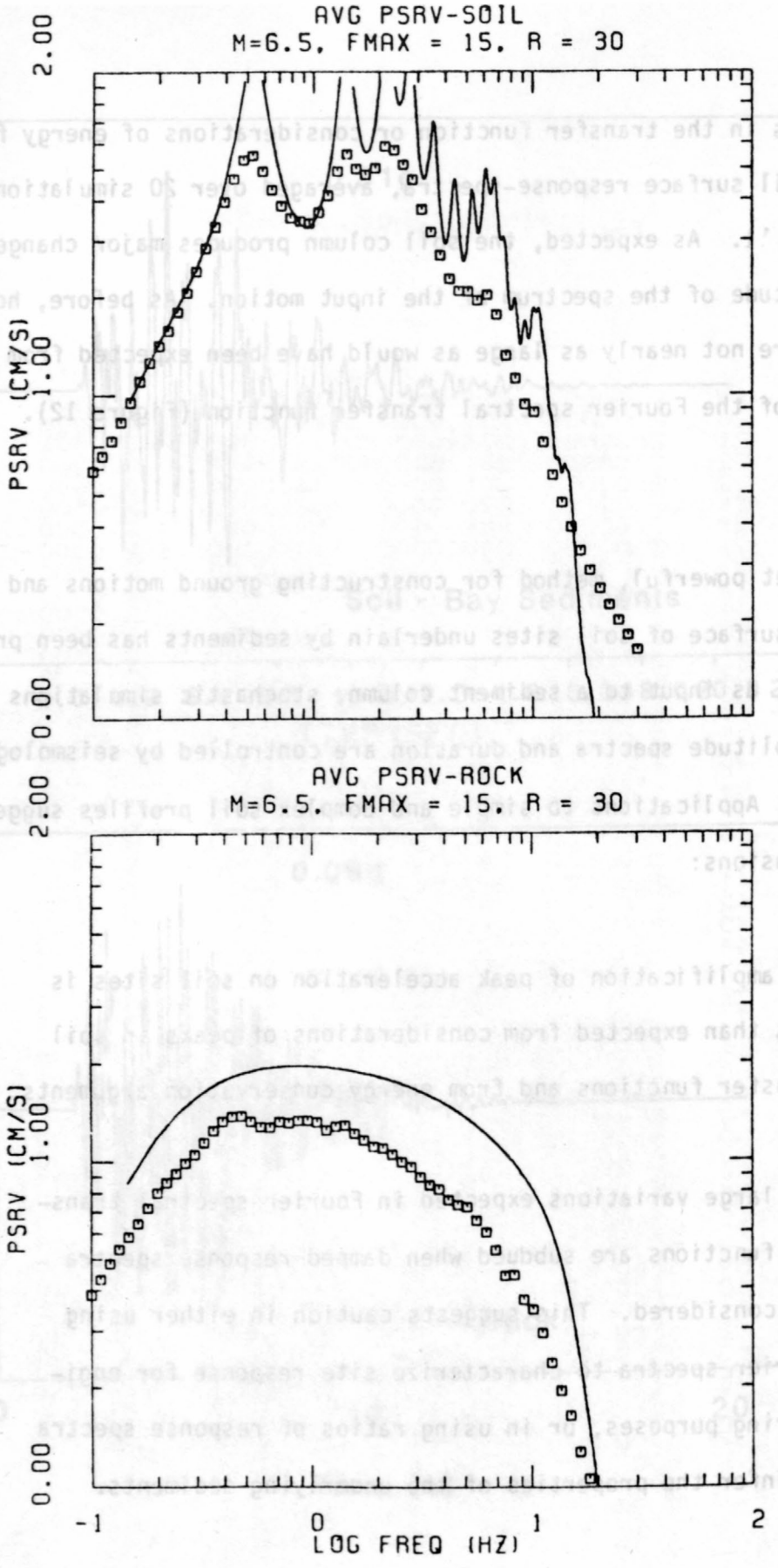

Figure 11. 5%-damped pseudo relative-velocity response spectra at rock and soil sites, averaged over 20 simulations of a magnitude 6.5 earthquake at 30 km (symbols) and Fourier amplitude spectra (lines) for the same event.

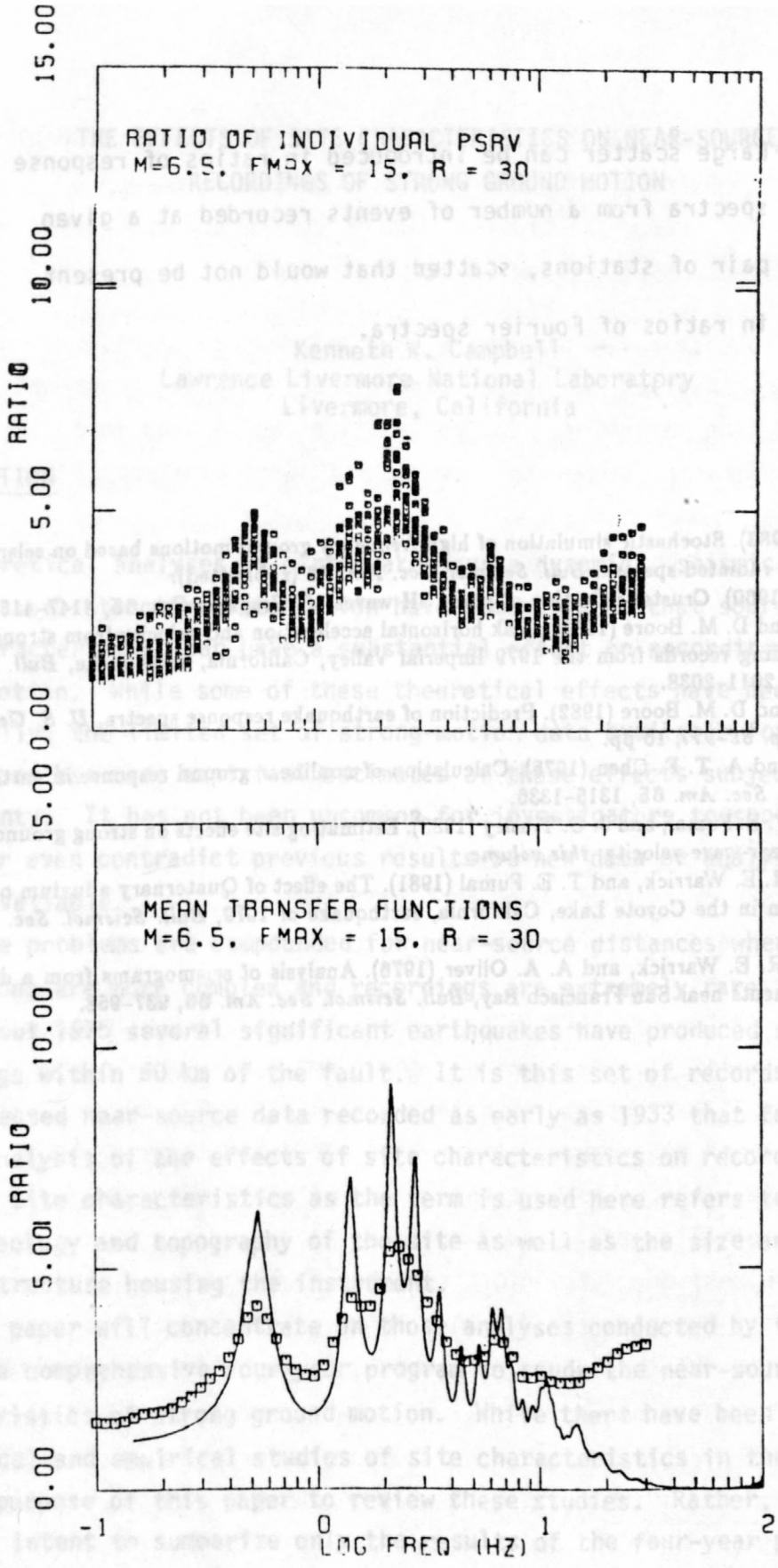

Figure 12. Ratios of response spectra (top) individual ratios; (bottom) averaged ratios (symbols) and Fourier transfer function (line).

- Large scatter can be introduced in ratios of response spectra from a number of events recorded at a given pair of stations, scatter that would not be present in ratios of Fourier spectra.

REFERENCES

Boore, D. M. (1983). Stochastic simulation of high-frequency ground motions based on seismological models of the radiated spectra, *Bull. Seismol. Soc. Am.* **73** (submitted).

Haskell, N. A. (1960). Crustal reflection of plane SH waves, *J. Geophys. Res.* **65**, 4147–4150.

Joyner, W. B. and D. M. Boore (1981). Peak horizontal acceleration and velocity from strong motion records including records from the 1979 Imperial Valley, California, earthquake, *Bull. Seismol. Soc. Am.* **71**, 2011–2038.

Joyner, W. B. and D. M. Boore (1982). Prediction of earthquake response spectra, *U. S. Geol. Surv. Open-File Rep. 82–977*, 16 pp.

Joyner, W. B. and A. T. F. Chen (1975). Calculation of nonlinear ground response in earthquakes, *Bull. Seismol. Soc. Am.* **65**, 1315–1336.

Joyner, W. B., T. E. Fumal, and J. C. Tinsley (1983). Estimating site effects on strong ground motion using local shear-wave velocity, *this volume*.

Joyner, W. B., R. E. Warrick, and T. E. Fumal (1981). The effect of Quaternary alluvium on strong ground motion in the Coyote Lake, California, earthquake of 1979, *Bull. Seismol. Soc. Am.* **71**, 1333–1349.

Joyner, W. B., R. E. Warrick, and A. A. Oliver (1976). Analysis of seismograms from a downhole array in sediments near San Francisco Bay, *Bull. Seismol. Soc. Am.* **66**, 937–958.

THE EFFECTS OF SITE CHARACTERISTICS ON NEAR-SOURCE RECORDINGS OF STRONG GROUND MOTION

by

Kenneth W. Campbell
Lawrence Livermore National Laboratory
Livermore, California

INTRODUCTION

Theoretical analyses of earthquake source dynamics, seismic wave propagation and soil-structure interaction have demonstrated that source, path and site characteristics can have a substantial effect on recordings of strong ground motion. While some of these theoretical effects have been confirmed empirically, the limited set of strong-motion data available for such comparisons has made empirical estimates of these effects subject to large uncertainty. It has not been uncommon for investigators to substantially revise or even contradict previous results as new data or analyses have become available.

These problems are compounded for near-source distances where theoretical predictions are more complex and recordings are extremely rare. However, since about 1975 several significant earthquakes have produced strong-motion recordings within 50 km of the fault. It is this set of records together with selected near-source data recorded as early as 1933 that form the basis for an analysis of the effects of site characteristics on recorded ground motion. Site characteristics as the term is used here refers to such factors as the geology and topography of the site as well as the size and embedment of the structure housing the instrument.

This paper will concentrate on those analyses conducted by the writer as part of a comprehensive four-year program to study the near-source characteristics of strong ground motion. While there have been numerous theoretical and empirical studies of site characteristics in the past, it is not the purpose of this paper to review these studies. Rather, it is the writer's intent to summarize only the results of the four-year program.

Other recent studies are referred to only when they can be meaningfully compared to the current results.

METHOD OF ANALYSIS

Several statistical methods were used to identify significant site effects. Most involved regression analysis of relevant strong-motion data to establish scaling variables. The mathematical model used to define this scaling relationship is expressed by the following equation,

$$\text{Ln GP} = a + bM - d \ln [R + C_1 \exp(C_2 M)] \pm \varepsilon \quad (1)$$

where GP is the ground-motion parameter of concern, R is the closest distance to the fault rupture plane (hereafter referred to as fault distance), and M is a magnitude scale consistent with both the moment-magnitude and Richter-magnitude scales, defined as surface-wave magnitude (M_s) when both local magnitude (M_L) and surface-wave magnitude are greater than or equal to 6.0 and defined as local magnitude when both M_L and M_s are below this value. The ε parameter is an error term represented by a random variable with a mean of zero and a standard deviation of σ, the standard error of estimate for the regression.

The form of Equation (1) is that commonly used in engineering studies of strong ground motion. The magnitude-dependent term involving the coefficient C_1 and C_2 was first proposed by Esteva (1970) and has been successfully used to model the near-source attenuation characteristics of both recorded (Campbell, 1981, 1982a) and synthetically generated (Hadley and Helmberger, 1980; Hadley et al., 1982) ground motions.

If the expression on the right side of Equation (1), excluding ε, is replaced by the function f(R,M), then the equation used to establish additional site-related scaling variables may be represented by the following expression,

$$\text{Ln GP} = f(R,M) + \sum_i (e_i F_i) \pm \varepsilon \quad (2)$$

where e_i represents the scaling variables as determined from the regression analyses and F_i is a "dummy variable" which takes on values of either 0 or

1 depending on the classification of the data. For example, if one were to classify data as representing either rock or soil, then such a geologic classification could be identified by the variable F_1, where F_1 = 1 for rock and F_1 = 0 for soil. More sophisiticated analyses can involve multivariate classifications and "dummy variables" involving both M and R, if more complicated scaling relationships are required.

Because of the functional form of f(M,R), a nonlinear regression analysis was necessary to establish the values of the scaling variables in Equations (1) and (2). Furthermore, in order to control the influence and possible bias associated with a few earthquakes that contribute a large number of recordings to the analysis, a weighted regression was performed, where weights were assigned to give each earthquake an equal contribution to the analysis within each of nine distance intervals. Justification for this weighting scheme is discussed by Campbell (1981, 1982a). Because of the possible nonlinear distribution of scaling variables, standard tests that assume normal distributions for these variables could not be used to determine whether the variables established from the regression analyses were statistically significant. Therefore, alternate methods were used which relied on empirical distributions of the variables and on the distribution of the residuals of each classification. Empirical distributions were developed from Monte Carlo simulation procedures suggested by Gallant (1975). Statistical tests on the residuals were accomplished by performing the regression analysis omitting the scaling variable of interest, then analyzing the residuals of the data representing the particular site classification for significant differences.

Residuals were simply defined as the difference between the observed and predicted values of the natural logarithm of GP. Before analysis, each residual was transformed into a normalized weighted residual (NWR). The weighting was required to make each residual consistent with that used in the weighted least-squares analyses employed in the regression. Weighted residuals were then normalized to have a mean of 0 and a variance of 1 for the sake of consistency and ease of computation and plotting. Letting n equal the total number of observations used in the regression, the normalized weighted residual for the ith observation was computed from the equation

$$NWR_i = \frac{[w_i (\ln GP_i - \overline{\ln GP_i})] - MWR}{\sigma} \quad (3)$$

where,

$$MWR = \frac{1}{n} \sum_{i=1}^{n} w_i (\ln GP_i - \overline{\ln GP_i})$$

$$\sum_{i=1}^{n} w_i = n.$$

In these expressions, w is the weight used in the regression analysis, ln GP is the natural logarithm of the observed value of GP, $\overline{\ln GP}$ is the predicted value of the natural logarithm of GP, σ is the standard error of the regression, and MWR is the mean weighted residual.

Three types of analyses were used to test the effect of various site parameters on GP. In the first analysis, the mean normalized weighted residual (MNWR) for each subset, selected on the basis of the parameter under study, was compared to either a value of 0 appropriate for the entire population or the MNWR of another subset when appropriate, where MNWR is given by the expression

$$MNWR = \frac{1}{n_j} \sum_{i=1}^{n_j} NWR_i \quad (4)$$

and n_j represents the number of observations in subset j. In the second analysis, the variance of each subset was compared to either the population variance of 1 or the variance of another subset when appropriate. The third analysis consisted of visual inspection of the normalized weighted residuals plotted as a function of distance, magnitude, and predicted value together with an accompanying correlation analysis to determine possible trends between the residuals and these three variables. Standard hypothesis testing techniques were used to test the significance of observed variations (e.g., Bowker and Liebermann, 1972).

For the purpose of this study, differences in the residuals were neglected if they were not found to be significant at a level of confidence

of 90% or greater. Those parameter subsets found to be significantly different from the population or from one another were then parameterized and a regression analysis performed to establish the appropriate scaling variable. Since the addition of a parameter to the equation could change the other coefficients in the expression, thereby affecting the significance of the variable being added, verification of significance was confirmed by several methods. In addition to simple inspection, the scaling variable determined from the regression analysis was compared to the difference in the mean normalized weighted residuals of each subclass determined from the previous analysis of residuals. As a third verification, the function f(M,R) determined from the nonlinear regression was substituted into a linear regression analysis and the significance of additional scaling variables tested using standard t-tests. A scaling variable was only considered statistically significant if all three tests gave consistent results.

Many of the statistical tests used in the analysis of residuals required the assumption that the residuals be distributed normally. Since the regression analysis was performed on the logarithm of the ground motion parameter, this requires that GP be lognormally distributed. A statistical validation was obtained from a normal probability plot where the normal score, an estimate of the cumulative distribution function of the normalized weighted residuals, is plotted against the observed residuals. A linear trend of this plot suggests that the residuals are normally distributed. A Kolmogorov- Smirnov test is used to confirm that the assumed normal distribution falls within the 90% confidence limits of the actual distribution, a criterion commonly used in engineering applications.

When available, adjacent pairs of recordings representing two subclasses of data for a given earthquake and distance are used to establish scaling variables for various site classifications. This eliminates the need for enough data to perform regression analyses and, unlike regression analyses, isolates local site characteristics from source and path effects. When applicable, simple statistical analyses or linear regressions on these observed scaling variables are used to establish means and standard deviations for these variables.

As has been noted by other investigators (e.g., Boore et al., 1980; Crouse, 1978), the potential effects of the various site characteristics are subject to biases in the distribution of data among the various site

classifications. For instance, most of the available near-source recordings are obtained in buildings sited on soil. Furthermore, the larger the building the more likely it has a basement. For those buildings with basements, there is a tendancy for the larger buildings to be more deeply embedded, and large embedded buildings are generally associated with earthquakes having reverse or reverse-oblique faulting mechanisms. For rock sites, most tend to be located on the tops or sides of steep mountains and ridges. Thus, the effects of site geology, building size, embedment depth, topography and fault mechanism are extensively interrelated.

We segregate these effects by isolating one classification from the others when analyzing the residuals or by selecting a subset of data for use in the regression analyses when possible. When there is not enough data for such a segregation, then regressions are performed on several variables simultane- ously, with those determined to be significant being retained and the least significant being eliminated. This sequence is repeated in a backwards- stepwise fashion until only those scaling variables found to be significant at the required 90% level of confidence are included.

DATA BASES

Several data bases have been used to study the near-source characteristics of strong ground motion. The first was compiled by Campbell (1981, 1982a) in a study of peak horizontal acceleration (PHA) for earthquakes of magnitude 5.0 M_L or larger recorded within 50 km of the fault. Weighted nonlinear least squares techniques were used to establish two scaling relations. The first was an unconstrained relationship whose coefficients were determined solely from the regression analysis. However, because of the limited amount of data within 3 to 5 km of the rupture zone and because a restriction to the near-source region excluded data beyond 50 km, a second relationship having specified near-field and far-field properties was developed and compared to the unconstrained model. As a result, two boundary conditions were applied in the second analysis. First, the far-field attenuation of PHA was constrained to $R^{-1.75}$ based upon the studies of other investigators, and second, PHA at the fault rupture surface was constrained to be independent of magnitude, consistent with the results of some recent earthquake modeling studies.

The unconstrained analysis led to the following expression for the median (50th percentile)value of PHA,

$$PHA = 0.0159 \exp(0.868M)[R + 0.0606 \exp(0.700M)]^{-1.09} \quad (5)$$

where PHA is the mean of the peak values from the two horizontal components and the other parameters are as defined in the preceding section. All the coefficients were found to be statistically significant at levels of confidence exceeding 95%, based on empirical distributions of the coefficients developed using procedures set forth by Gallant (1975). The 84th percentile value of PHA is obtained by multiplying the median value by a factor of 1.45, which represents a standard error of 0.372 on the natural logarithm of PHA. The goodness-of-fit is represented by an r^2 value of 0.81.

The constrained regression analysis resulted in the following expression for the median value of peak acceleration,

$$PHA = 0.0185 \exp(1.28M)[R + 0.147 \exp(0.732M)]^{-1.75} \quad (6)$$

Application of the empirical procedure of Gallant (1975) found the unconstrained coefficients of this expression to be statistically significant at levels of confidence exceeding 99%. The 84th percentile value of PHA is obtained by multiplying the median value by a factor of 1.47, which represents a standard error of 0.384 on the natural logarithm of PHA. The goodness-of- fit is represented by an r^2 value of 0.79.

In a second study, a multiple regression analysis similar to that performed by Campbell (1981, 1982a) was used to develop near-source ground motion scaling relationships for both peak horizontal acceleration and horizontal pseudo-relative velocity response spectra (S_v) at four selected periods and three values of damping (TERA Corp., 1982; Campbell, 1983). The periods selected were 0.10, 0.12, 0.15 and 0.20 sec., representing frequencies of 5 to 10 Hz. The selected damping values were 2, 5, and 10 percent of critical. S_v was defined as the mean of the response spectral values selected from the two horizontal components in cm/sec. Magnitude and distance were defined as previously.

The data base was essentially the same as that of Campbell (1981, 1982a). Some revision of the data was necessary as a result of new information which had become available since the previous studies. Furthermore, in order that the predictions would represent as closely as possible "freefield" conditions, neither recordings obtained in large buildings (greater than two stories) nor those obtained on either the abutments or toes of dams were included. Other- wise, the selection criteria were the same as those applied to the previously referenced study on peak acceleration. Because they had not as yet been digitized, some of the recordings in the original data base could not be used in the analysis of S_v. These undigitized records amounted to about 20% of the total number of original records and primarily represented the more distant recordings from the smaller earthquakes.

Equations (1) and (2) were used to model the scaling characteristics of both PHA and S_v. Peak acceleration relationships developed for both the complete PHA data base and the more limited spectral data base indicated that results based on the reduced data base were not substantially biased. The results of the regression analyses are summarized in Table 1. These analyses indicate a significant systematic bias associated with reverse/reverse-oblique fault mechanisms and instrument embedment. Therefore, scaling variables were included to account for these biases. This was accomplished through the parameters F and E (Table 1), which take on values of 0 or 1 depending upon the classification; that is, F = 0 for strike-slip, normal and normal-oblique fault types, F = 1 for reverse and reverse-oblique fault types, E = 0 for ground-level instruments, and E = 1 for buried instruments or instruments in the basement of small buildings (1-2 stories).

The data base used to study the scaling characteristics of S_v was also used to establish the near-source behavior of peak vertical acceleration by extending the study of Campbell (1982b). Weighted nonlinear regression analysis was used to establish the following scaling relationship,

$$PVA = 0.279 \exp(0.687M) [R + 9.15]^{-1.68} \exp(0.35F) \exp(-0.31E) \quad (7)$$

where PVA is peak vertical acceleration in g and M and R are as defined previously. The parameters F and E represent classifications by fault type

TABLE 1

Summary of Multiple Regression Analyses
for Pseudo-Relative Velocity

$$\ln S_v = a + bM + d \ln(R + c_1 e^{c_2 M}) + eF + fE$$

Period (sec)	Damping (%)	Regression Coefficients a	b	c_1	c_2	d	e	f	Statistics σ	r^2	n
0.10	2	5.440	.569	16.07	.055	-2.03	.404	-.340	.396	.77	62
	5	4.215	.612	7.57	.148	-1.88	.440	-.305	.356	.79	62
	10	2.020	.606	3.39	.195	-1.41	.374	-.255	.346	.80	62
0.12	2	7.282	.792	17.68	.110	-2.64	.383	-.319	.418	.75	62
	5	3.686	.623	9.25	.098	-1.71	.404	-.265	.375	.78	62
	10	2.360	.625	4.27	.169	-1.46	.386	-.237	.357	.79	62
0.15	2	4.559	.502	17.24	.000	-1.56	.398	-.234	.436	.70	62
	5	3.662	.451	12.22	.000	-1.35	.407	-.264	.411	.73	62
	10	2.819	.455	8.63	.016	-1.22	.378	-.259	.392	.75	62
0.20	2	4.593	.613	16.45	.033	-1.64	.326	-.205	.427	.71	62
	5	3.566	.550	11.36	.038	-1.38	.324	-.219	.410	.72	62
	10	2.790	.483	9.62	.000	-1.16	.312	-.198	.407	.72	62
PHA(g) (Spectra Data Set)		-2.633	.640	0.137	.575	-1.11	.421	-.146	.347	.80	62
PHA(g) (Entire Data Set)		-2.829	.827	0.177	.595	-1.39	.335	-.119	.378	.82	84

Notes: (1) S_v is pseudo-relative velocity in cm/sec.
(2) F=0 for normal, normal-oblique and strike-slip faults; F=1 for reverse and reverse-oblique faults.
(3) E=0 for ground level recordings; E=1 for embedded recordings.

and embedment as defined above. The standard error of estimate for the natural logarithm of PVA was determined to be 0.413, representing an 84th percentile value of PVA that is 1.51 times the median value. The r^2 value was 0.85.

One can see by comparing Eq. (7) to that representing peak horizontal acceleration in Table 1 that there are considerable differences between the scaling characteristics of PVA and PHA. Most notable are differences in the rate of attenuation. Peak vertical acceleration not only decays much more rapidly with distance than its horizontal counterpart, its rate of decay is virtually independent of magnitude. In contrast, peak horizontal acceleration exhibits very little magnitude scaling at small distances, becoming independent of magnitude at R = 0. While the scaling for fault type is very similar for the two parameters, the scaling of PVA with embedment is similar to that obtained for 5-10 Hz S_v.

The same data base used to analyze S_v and PVA has also been used to develop a preliminary scaling relationship for peak horizontal velocity (PHV). The only difference is that all recordings have been used in the regression, including those from shallow soil sites, soft soil sites, and large structures. Consistent with peak acceleration, PHV was defined as the mean of the peak values from the two horizontal components in cm/sec. As before, a weighted nonlinear regression analysis was used to establish the scaling relationship

$$PHV = 0.283 \exp(1.01\ M)\ [R + 0.0068 \exp(0.880M)]^{-0.919} \qquad (8)$$

The standard error of estimate of the natural logarithm of PHV is 0.522, representing an 84th percentile value that is 1.68 times the median value. The r^2 value was 0.74. While no selection criteria regarding site characteristics were applied, inspection of the residuals indicated that rock recordings, especially those on hard rock, are substantially overestimated by this expression. It was also observed that large buildings tend to be associated with higher than average velocities. These characteristics will be discussed in more detail in the discussion presented in the remainder of this paper.

Several other data bases have been compiled to extend the near-source analyses of peak horizontal acceleration to magnitudes as small as 3.5 M_L.

The first of these was reported by Campbell (1979). This original analysis has been revised several times by applying various selection criteria to the data and using various definitions of distance. Most notable among these criteria are the inclusion or exclusion of large buildings, embedded instruments, and earthquakes of $M_L > 5.0$. Events for which fault distance was not available were defined in terms of epicentral or hypocentral distance, depending on the purpose of the relationship.

A data base composed of nearby recordings of strong ground motion from the same earthquake has been compiled by TERA Corp. (1980) and later revised by Darragh and Campbell (1981). It serves as a case study of the effects of building size and embedment on recorded ground motion. Such a study essentially removes certain inherent biases that exist in the regression analyses. For example, the use of nearby recordings from the same earthquake removes the potential effects of source and path differences leaving only local site conditions as a possible bias.

In the original study by TERA Corp (1980) the only criterion applied to the selection of nearby recordings was that they be no further than 1300 m apart. In the revision by Darragh and Campbell (1981) more strict criteria were applied. In addition to a station separation of 1300 m or less, they selected recordings only if the magnitude of the earthquake was larger than 3.4 M_L and the epicentral distance was 75 km or less. A subsequent unpublished revision has additionally excluded data having peak accelerations less than 0.02g because of the potential unreliability and large round off errors associated with such low recordings.

In both studies nearby recordings were classified into four groups. Type IA compared freefield recordings (small shelters) with those obtained in the basement of buildings; Type IB compared freefield recordings with those obtained in buildings without basements; Type II compared recordings from buildings without basements with those from buildings with basements; and Type III compared buildings of different height using recordings obtained in pairs of embedded or non-embedded buildings. Reductions in percent were computed with respect to the freefield, non-embedded, or smaller building (GP_2) using the expression

$$100\left[1 - \frac{GP_1}{GP_2}\right].$$

This definition is consistent with reductions determined from the regression analyses.

FAULT TYPE

While fault type is not a site characteristic, it was found to be extensively interrelated with building size and embedment. Therefore, it was found that a scaling variable for fault type was required in order to appropriately account for these other site effects. The potential bias associated with large buildings was minimized by restricting the analyses to instrument shelters and small buildings (hereafter referred to as freefield data).

In the first study earthquakes were identified as having either reverse, oblique, strike slip, or normal mechanisms. Two analyses were conducted, one comparing reverse to strike-slip data and another comparing reverse to non-reverse data. These analyses found PHA from reverse faults to be 32% higher than those from strike-slip faults and 28% higher than those from non-reverse faults (Campbell and Davis, 1980; Campbell, 1981, 1982a). It should be noted, however, that the non-reverse data were predominantly from strike-slip faults, which accounts for the small difference between the two values of the scaling variable.

The revised study (TERA Corp., 1982; Campbell, 1983) demonstrated that two other factors were biasing the potential effects of fault type. First, earthquakes originally classified as having oblique faulting mechanisms were found to be more accurately classified as reverse-oblique and more appropriately grouped together with reverse faults in the analysis of fault type. Second, it was found that the scaling variable for fault type was being affected by recordings obtained from embedded instruments, even when the analysis was confined to freefield data. By using only freefield recordings and including a scaling variable for embedment, the revised analysis indicated that recordings from reverse and reverse-oblique faults are about 40% higher than those from non-reverse faults for PHA and 38% to 55% higher for 5%-damped, 5-10 Hz S_v (Table 1). The factor for S_v may be somewhat inflated due to the reduced data set available for the spectral regressions as suggested from a comparison of factors determined separately for PHA using the entire data set and the more limited spectral data set. In a subsequent

analysis, the vertical components of peak acceleration were found to exhibit a similar reverse and reverse-oblique fault bias as that associated with the horizontal components. Although preliminary, the analysis of peak velocity suggests that PHV is not as strongly affected by fault type as acceleration and pseudo-relative velocity.

An independent justification of the effect of fault type on strong ground motion has recently appeared in the literature. McGarr (1982) used stress conditions appropriate for pure reverse, pure strike-slip, and pure normal mechanisms together with an asperity model to estimate upper bounds of peak acceleration that can be expected on the free surface directly above the asperity. His analysis indicated upper bounds of 2g, 0.7g, and 0.4g for reverse, strike-slip, and normal faults, respectively. A modeling study by Luco and Anderson (1983) indicates that the dip associated with most reverse faults can also result in higher ground motions near the fault.

GEOLOGY

Sites were initially classified into the six groups described in Table 2 based on geotechnical and geological descriptions available in the literature or from geology maps. Those sites originally classified as rock sites (types C and D) or suspected of being shallow soil deposits were further subjected to a field visit by an engineering geologist who obtained an accurate description of the site geology, topography, and instrument location for each of these sites. This investigation revealed that about one-half of the sites originally determined to be rock either by us or other investigators were actually found to be overlain by shallow soil or fill.

To study the significance of these findings, regression analyses were first performed on freefield data from all geologic classifications (types A through F) to test the potential bias of the shallow soil sites (Campbell, 1981, 1982a). For this purpose, the shallow soil sites were separated into those having soil depths of 5 m or less and those whose soil depths were between 5 and 10 m. Both groups were found to have a mean weighted residual that was significantly higher than the average for all geology types. Their combined effect represented on the average an 84% higher PHA when compared to predictions based on the other geologic classifications. This factor was found to decrease to a value of 63% when a reverse-fault variable was

TABLE 2

Geological Classification Scheme

Site Geology	Description	Classification
Recent Alluvium	Holocene Age soil deposits with rock $\geq$ 10 m deep	A
Pleistocene Deposits	Pleistocene Age soil deposits with rock $\geq$ 10 m deep	B
Soft Rock	Sedimentary rock, soft volcanics and soft metasedimentary rock	C
Hard Rock	Crystalline rock, hard volcanics and hard metasedimentary rock	D
Shallow Soil Deposits	Holocene or Pleistocene Age soil deposits < 10 m deep overlying Soft or Hard Rock	E
Soft Soil Deposits	Extremely soft or loose Holocene Age soils such as beach sand or recent floodplain, lake, swamp, estuarine, and delta deposits	F

included. These results are consistent with studies of Chiaruttini and Siro (1981) and Faccioli (1981) who found average amplifications of 100% for shallow soil sites (soil depths < 20 m) that recorded aftershocks of the 1976 Friuli, Italy earthquake.

Although predictions of PHA were found to be essentially unaffected by the presence of shallow soil deposits in the data base due to the small number of such recordings, the real bias in these data came from their influence on the standard error of regression and on conclusions regarding the effect of site conditions on recorded ground motion. In the past, investigators have included sites having as much as 5 to 10 m of soil or fill as rock sites in their analyses of site effects. To test the significance of this bias, sites were divided into soil and rock and two regression analyses performed: one including shallow soil deposits as rock and one excluding them altogether. When they were included as rock, PHA recorded on rock sites were found to be an average of 26% higher than those recorded on soil sites, significant at a 90% level of confidence. When shallow soil sites were excluded, differences in accelerations recorded on soil and rock were not found to be statistically significant, consistent with the finding of Boore et al. (1980) and Joyner and Boore (1981). We did find, however, that soft rock sites had a tendency to have lower than average peak accelerations when compared to hard rock and soil sites. This observation, while not statistically significant, was found to be closely interrelated with the potential effects of topography, fault type, and embedment depth as discovered in the second study of TERA Corp. (1982) and Campbell (1983).

In this second study, records associated with large structures including dams were removed from the data set to reduce the potential bias associated with these records. This differed from the original study on geology effects only in the removal of recordings associated with dams. These records, located primarily on rock abutments, were found to have accelerations among the largest of those obtained on rock, most likely resulting from the combined effects of topographic amplification and response of the dam. The additional inclusion of scaling variables for fault type and embedment resulted in PHA and 5-10 Hz S_v being significantly lower for soft rock sites than for other geological classifications. Similar results were found for peak vertical acceleration. As will be discussed in the next section, this was significantly affected by the topography of the immediate site area. An

inspection of the residuals associated with those sites not believed to be associated with topographic amplification found all (both soft rock and hard rock sites) to be below their median predictions. While this is based on a relatively small number of recordings, it does suggest that the traditional view that accelerations on rock are greater than those on soil in the near-source region may have been biased by several other factors including topography, building size and embedment, fault type, and the presence of shallow soil deposits.

The preliminary analysis of peak horizontal velocity suggests that PHV is substantially influenced by site geology. Most notable is the effect of hard rock, where peak recordings of PHV were found to be approximately 50% lower than those on soil. In contrast, soft rock sites were only found to be about 10% lower than soil sites. As will be discussed in a later section, these results are probably influenced by the inclusion of large buildings. Such buildings were found to have larger than average values of peak velocity, whether sited on soil or rock. Because of the substantial number of large buildings on soft rock, the 10% reduction associated with these sites is no doubt considerably underestimated. Its true value is expected to be somewhere between that of soil and hard rock.

TOPOGRAPHY

In the Campbell (1981, 1982a) study, a site investigation by an engineering geologist identified seven stations in the data base considered to be located within an area of steep topographic relief, defined as the top or side of a steep ridge, hill, or slope. In addition, four stations classified as shallow soil deposits and the Pacoima Dam station were also found to be located in areas of steep topographic relief.

A statistical analysis of the seven stations used in the regression revealed that their mean residual was significantly higher than that for the entire data set. Due to the small number of stations, however, the magnitude of this bias is probably not reliable and was not reported. Similar results were obtained for the 11 topographically affected stations when shallow soil sites were included in the regression analysis. When the topographically affected stations were excluded from the analysis, predictions of PHA were

found to be essentially unaffected, a result of the relatively small number of such records.

Although this bias could be the result of factors other than topography, such an explanation for the above results is not considered reasonable. Of the seven stations used in the analyses, three are located on abutments of dams, two are located in small buildings, and two are located in large buildings. Of the five earthquakes represented, two of them had reverse or thrust mechanisms and three of them had strike-slip mechanisms. While all of the stations are located on rock, four are situated on hard rock and three on soft rock.

The Pacoima Dam recording from the 1971 San Fernando earthquake has been the subject of much investigation in the past. The strong-motion station is located on a narrow rocky ridge near the south abutment of a 113-m-high thin concrete arch dam. Boore (1973) used a simple topographic model together with finite difference techniques to estimate the effect of the instrument location on the recorded accelerations. He found that the peak acceleration from the S16^{o}E component of the accelerogram may have been amplified by as much as 50% due to the effect of topography.

Mickey et al. (1973) empirically studied the combined effects of topography, response of the dam, and local geological conditions on the Pacoima Dam recording. They simultaneously recorded eight aftershocks (M_L = 2.7 to 3.7) at three stations: the dam crest, the existing abutment strong-motion station, and a freefield site located on rock on the valley floor downstream from the dam. Their results indicated an average amplification of 75% in the peak motion recorded at the strong-motion station as compared to the freefield site for the S16^{o}E component and an average amplification of 190% for the S74^{o}W component. The large amplification for the S74^{o}W component was thought to be due in part to the response of the dam, as interpreted from the recordings obtained on the crest of the dam and studies by Reimer et al. (1973).

In order to explore the effect of topography in more detail, the second study (TERA Corp., 1982; Campbell, 1983) classified all rock sites into four categories based on the topography of the region: (I) Sites located on the tops of hills, ridges or steep slopes, (II) Sites located on the sides of such features, (III) Sites located at the bottom of such features, and (IV) Sites located on relatively flat terrain. Analysis of 5-10 Hz S_v, PHA and PVA

indicated that recordings obtained on the tops and sides of hills or slopes (Classes I and II) were higher than those obtained at the bottom of slopes or on relatively flat ground (Classes III and IV). Although at present there are very little data for the last two categories, this indicates that the topography of the site should be considered in both the analysis and prediction of these strong-motion parameters. Preliminary analysis of peak horizontal velocity, however, indicates that this parameter may not be as strongly affected by topography as the other parameters investigated.

STRUCTURE

In order to isolate the effects of building size and embedment from geologic effects, the data base of Campbell (1981, 1982a) was divided into four subgroups, all situated on soil (types A and B), represented by embeddded or ground-level recordings at either freefield stations or in large buildings. The effects of both embedment and building size were studied by regression analysis of the above selected data. Due to limitations in these data, valid comparisons could only be made between freefield recordings (including small buildings without basements) and recordings obtained in the lowest basement of large buildings. This comparison indicated that PHA recorded in the basement of large buildings was 24% lower on the average than those recorded at ground level.

While large structures were excluded from the study of TERA Corp. (1982) and Campbell (1983), they did attempt to investigate a possible bias that may be associated with so-called "freefield" recordings obtained in small shelters. These recordings were obtained from instruments located in light weight instrument shelters attached to small concrete pads. Bycroft (1978), McNeill (1983), and Crouse (1983) have indicated that such installations located on relatively soft soil deposits can substantially amplify the true ground motions, especially at the higher frequencies. However, an analysis of residuals indicated that there were no systematic differences in the mean weighted residuals for recordings obtained in small shelters, standard one- and two-story buildings, or massive one- and two-story buildings once the effects of fault type and embedment were accounted for through the inclusion of scaling variables. However, it should be noted that only a few of these recordings were obtained at sites situated on soft soil.

Recordings obtained at the Differential Array during the 1979 Imperial Valley earthquake (M_S = 6.9) may, however, lend support to Bycroft's and others hypothesis. Adjacent recordings obtained from instruments of similar dynamic characteristics were found to give significantly different amplitudes, expecially at high frequencies. The larger recordings were obtained in a small instrument shed attached to a concrete pad (Dogwood Road). The smaller recordings were obtained in an instrument buried approximately 4 ft in a 5-inch diameter hole (Differential Array No. 1). Bycroft and others indicate that this latter installation should approximate freefield conditions. The soils are relatively soft, having a shear-wave velocity of approximately 300-400 ft/sec near the surface.

The ratios of the pseudo-relative velocity response spectra (5% damping) for the two stations appear in Figure 1. Substantial amplification of S_V is found to occur at frequences of about 5 to 15 Hz for the horizontal components. This is consistent with simple soil-structure interaction calculations which predict that the peak horizontal amplification of the Dogwood Road installation should occur at a frequency of about 10 Hz. These calculations assume that the shallow embedment of the Differential Array No. 1 instrument does not substantially effect the true ground motion. This is confirmed by simple response calculations that suggest the shallow embedment of this instrument should not effectively alter the surface motion for frequencies within the dynamic range of the instrument ($\leq$25 Hz). It is also apparently confirmed by the similarity of the vertical components for frequencies of 25 Hz and less (Fig. 1).

The case study performed by Darragh and Campbell (1981) augmented the statistical analyses described earlier in this section. The mean reduction in peak acceleration due to the size and embedment of buildings as given in their study appears in Table 3. This table confirms the results of the statistical analyses, indicating that embedded buildings have peak horizontal accelerations some 33% lower than ground level buildings and freefield stations. Note that the largest reductions are found for the freefield vs. embedded building comparisons as is expected. While the reduction in vertical accelerations are similar to those for PHA for the Type I comparisons, they are found to be substantially less for the Type II comparisons. This suggests that ground level buildings tend to reduce peak vertical accelerations to a greater extent than the horizontal components. This may be a result of the higher

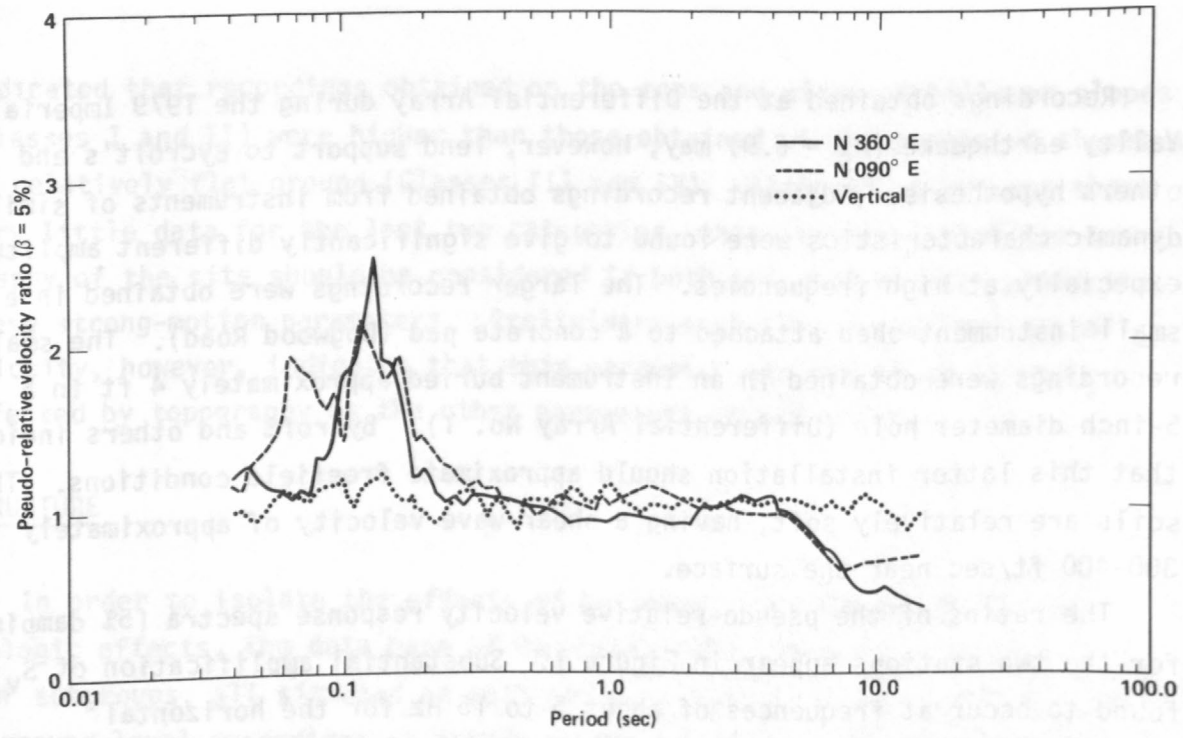

Figure 1. Ratio of 5%-damped Psuedo-Relative Velocity Spectra between Dogwood Road Instrument Shed and Differential Array No. 1 for the 15 October 1979 Imperial Valley Earthquake.

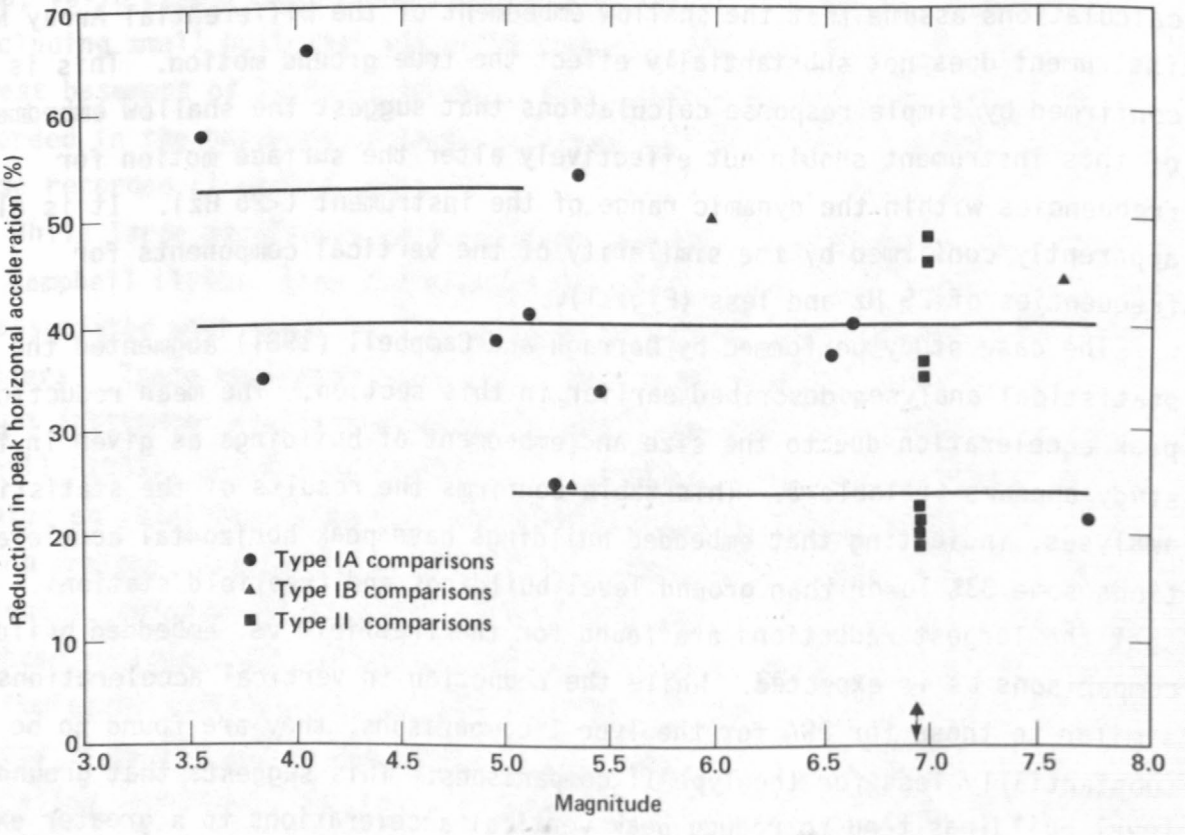

Figure 2. Reduction in peak horizontal acceleration for Types IA, IB, and II comparisons. The horizontal bars represent the reductions resulting from regression analyses of all near-source data as a function of magnitude and distance for the magnitude ranges shown.

TABLE 3

Results of Case Studies

Type	Description	Reduction in Peak Acceleration (%) Horiz.	No.	Vert.	No.
IA	Embedded Building vs. Freefield	39	7	44	5
IB	Non-embedded Building vs Freefield	29	4	29	2
II	Embedded Building vs. Non-embedded Building	33	7	19	7
IA,IB	Building vs. Freefield	35	11	40	7
IA,IB,II	Building vs. Non-embedded Instruments	34	18	29	14

characteristic frequencies and shorter wave lengths typical of the vertical components of acceleration.

Inspection of the case studies of Darragh and Campbell (1981) and TERA Corp. (1980) indicates that the reduction in peak horizontal acceleration observed for Type I and Type II comparisons are apparently related to earthquake magnitude. This is demonstated in Figure 2, where the reduction in peak horizontal acceleration is plotted as a function of magnitude. There appears to be a tendancy for smaller reductions at the higher magnitudes. Superimposed as the solid bars on this figure are the results of regression analyses and analyses of residuals on three data sets selected on the basis of magnitude. All reductions for these analyses were based on combined Type IA and Type II comparisons. These results also show a distinct trend towards smaller reductions at larger magnitudes and are found to be consistent with the observed reductions observed in the case studies.

The case studies also investigated the effect of building size on the amplitudes of peak horizontal acceleration. Pairs of buildings, either both at ground level or both embedded, were investigated for systematic differences in recorded accelerations due to differences in height, determined on the basis of differences in the number of stories. The taller buildings were consistently found to have smaller accelerations, the difference being larger for greater differences in the heights of the buldings. A simple regression analysis indicated that this reduction in percent was equivalent to 1.2 ΔS (Fig. 3), where ΔS is the difference in the number of stories. The standard error of this estimate is rather large, representing a $\pm$ 29% variation in the percent reduction calculated by this expression.

McCann and Boore (1983) have given evidence in support of a decrease in peak acceleration with increasing depth of embedment for buildings that recorded the San Fernando earthquake. However, as they indicate there is a strong correlation between depth of embedment and building height which makes the separation of these two effects extremely difficult. The case study by Darragh and Campbell (1981) attempted to minimize embedment effects by comparing only ground-level or basement-level recordings, but embedment is probabily still a factor. Both studies no doubt include the effects of both building size and embedment in their analyses.

Preliminary analyses on peak horizontal velocity indicate that large buildings, whether embedded or not, tend to be associated with higher

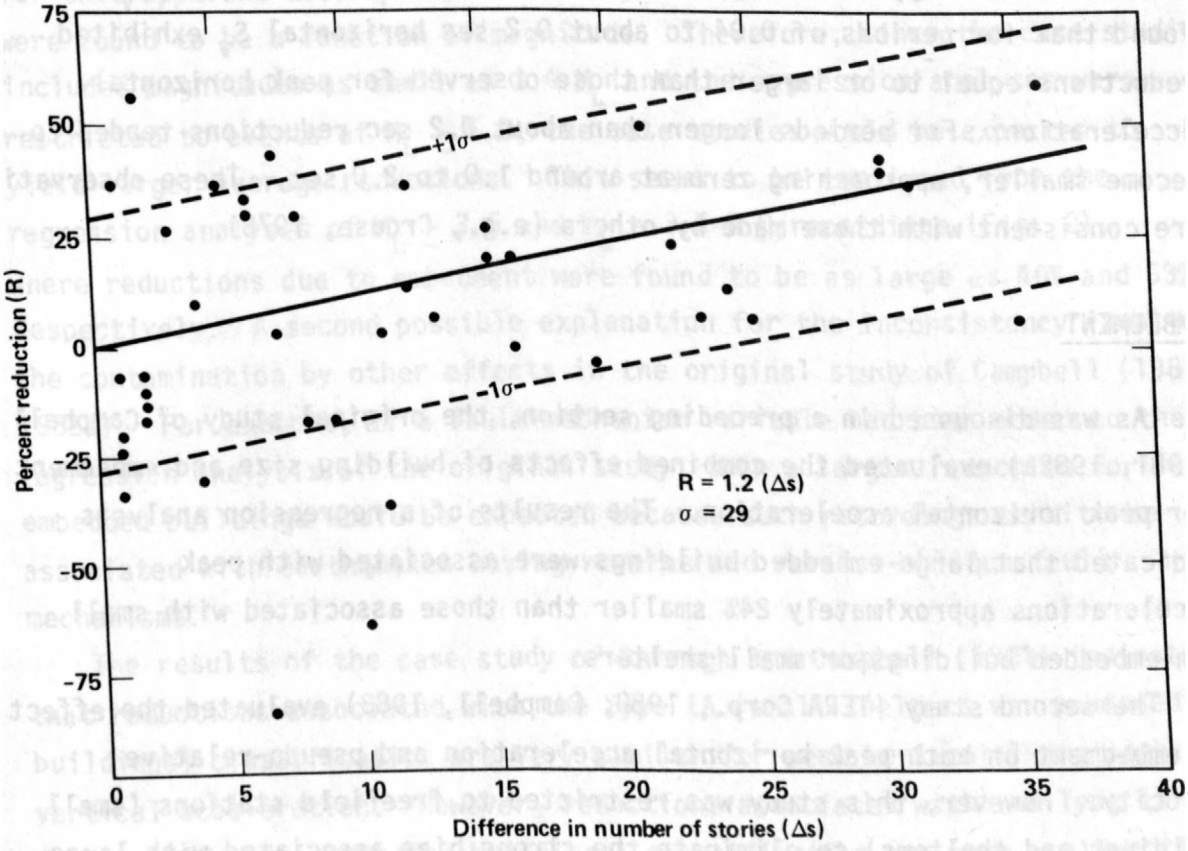

Figure 3. Reduction in peak horizontal acceleration for Type II comparisons. The solid line represents the results of a linear regression between the two variables plotted and the dashed lines represent the one standard error bounds.

velocities than small buildings or freefield stations; this increase being approximately 20%. This would indicate that the response of the building tends to amplify the motion at the base of the building at the mid-range frequencies associated with peak velocity. On the other hand the relatively long wave lengths associated with velocity renders the relatively shallow embedment depths associated with buildings ineffective in modifying peak velocity.

The case study of TERA Corp. (1980) also investigated the reductions associated with Type I and Type II classifications for 5%-damped S_v. They found that for periods of 0.04 to about 0.2 sec horizontal S_v exhibited reductions equal to or larger than those observed for peak horizontal acceleration. For periods longer than about 0.2 sec reductions tended to become smaller, approaching zero at around 1.0 to 2.0 sec. These observations are consistent with those made by others (e.g., Crouse, 1978).

EMBEDMENT

As was discussed in a preceding section, the original study of Campbell (1981, 1982a) evaluated the combined effects of building size and embedment for peak horizontal acceleration. The results of a regression analysis indicated that large embedded buildings were associated with peak accelerations approximately 24% smaller than those associated with small non-embedded buildings or small shelters.

The second study (TERA Corp., 1980; Campbell, 1983) evaluated the effect of embedment on both peak horizontal acceleration and pseudo-relative velocity. However, this study was restricted to freefield stations (small buildings and shelters) to eliminate the strong bias associated with large embedded buildings. The results of the regression analysis indicated that small embedded buildings on the average were associated with peak accelerations that are 11% smaller than those associated with freefield stations (Table 1). Similar analyses on peak vertical acceleration and high-frequency ordinates of S_v indicated a much stronger dependence on embedment, with reductions in PVA of about 27% and reductions in 5%-damped S_v ranging from 25% to 35% at frequencies of 5 to 10 Hz.

The reductions in peak vertical acceleration and pseudo-relative velocity are similar in amplitude to those found for PVA and high-frequency ordinates

of S_v in the case studies of Darragh and Campbell (1981) and TERA Corp. (1980). Comparisons of S_v in the case studies were restricted to recordings from the 1971 San Fernando earthquake (M_s = 6.6) because that was the only earthquake studied that had digitized strong-motion data available. The reductions in PHA from the regression analyses (11%-24%) are considerably smaller than the reductions for non-embedded versus embedded recordings of the case studies, where reductions of 39% and 33% were found for Type IA and Type II classifications, respectively (Table 3). Two possible explanations exist for this apparent discrepancy. For one, the reductions in the case studies were found to be a function of magnitude. Therefore, since the case studies included magnitudes as small as 3.4 M_L and the regression analyses were restricted to events of $M_L \geq 5.0$, the case studies would be expected to yield larger average reductions. This seems to be confirmed from the regression analyses of $M_L \geq 3.5$ and M_L = 3.5-5.0 recordings (Fig. 2), where reductions due to embedment were found to be as large as 40% and 53%, respectively. A second possible explanation for the inconsistency involves the contamination by other effects in the original study of Campbell (1981, 1982a). For example, if a fault-mechanism variable had been added to the regression analysis of the original study, then a larger reduction for large embedded buildings would be expected because such recordings tend to be associated with earthquakes having reverse and reverse-oblique fault mechanisms.

The results of the case study of Darragh and Campbell (1981) indicates that reductions associated with the Type IA (small shelters vs. embedded buildings) classification are very similar for peak horizontal and peak vertical acceleration. However, reductions associated with the Type II (non-embedded vs. embedded buildings) classification are much smaller for peak vertical than for peak horizontal accelerations. This may indicate a greater effect of base size on the reduction of the higher-frequency vertical component of ground motion, with PVA being reduced more effectively by non-embedded foundations than PHA. This hypothesis has yet to be confirmed by regression analyses.

Preliminary regression analyses of peak horizontal velocity ($M_L \geq 5.0$) indicates that this index is insensitive to the shallow embedment depths associated with standard buildings. This results from the relatively long wave lengths associated with partical velocity ground motions which are an

order of magnitude longer than the maximum depths associated with normal buildings.

CONCLUSIONS

A comprehensive near-source data base has been used to study the effects of site characteristics on recorded ground motion. Various statistical methods, including regression analyses and hypothesis testing techniques, have been used to establish scaling variables for these characteristics. This has been complicated by various biases in these data, most notable being the interrelationship of several of the characteristics. These interrelationships cause many characteristics to be highly correlated making the separation of their effects difficult. However, the adherence to a strict set of data selection criteria and appropriate analysis techniques has minimized these problems and allowed a reasonable separation of the major effects.

Site effects associated with several ground motion parameters were studied; these parameters include peak horizontal acceleration, peak vertical acceleration, peak horizontal velocity, and several high- frequency ordinates of horizontal pseudo-relative velocity. We have found that all of the ground motion parameters investigated were significantly influenced by one or more of the following characteristics: the geology and topography of the site, the size and embedment of the structure housing the instrument, and the fault mechanism of the earthquake. While the last characteristic is related to the source rather than the site, it was included because of its significant effect on the other site characteristics. We conclude that these characteristics should be considered in the analysis and prediction of strong ground motion.

REFERENCES

Anderson, J. G. and J. E. Luco (1983), "Parametric Study of Near-Field Ground Motions for Oblique-Slip and Dip-Slip Dislocation Models," Bull. Seism. Soc. Am., 73:45-57.

Boore, D. M. (1973), "The Effect of Simple Topography on Seismic Waves: Implications for the Accelerations Recorded at Pacoima Dam, San Fernando Valley, California," Bull. Seism. Soc. Am., 63:1603-1609.

Boore, D. M., W. B. Joyner, A. A. Oliver III and R. A. Page (1980), "Peak Acceleration, Velocity, and Displacement from Strong-Motion Records," Bull. Seism. Soc. Am., 70:305-321.

Bowker, A. H. and G. J. Liebermann (1972), "Engineering Statistics," Prentice-Hall, Inc., Englewood Cliffs, New Jersey.

Bycroft, G. N. (1978), "The Effect of Soil-Structure Interaction on Seismometer Readings," Bull. Seism. Soc. Am., 68:828-843.

Campbell, K. W. (1979), "Preliminary Evaluation of Near-Source Attenuation of Peak Acceleration in the United States," (Abstract), Program and Abstracts, Eastern Section of Seism. Soc. Am.

Campbell, K. W. (1981), "Near-Source Attenuation of Peak Horizontal Acceleration," Bull. Seism. Soc. Am., 71:2039-2070.

Campbell, K. W. (1982a), "Near-Source Scaling Characteristics of Peak Horizontal Acceleration for Moderate-to-Large Earthquakes," Proceedings of Workshop XVI: The Dynamic Characteristics of Faulting Inferred from Recordings of Strong Ground Motion, U.S. Geological Survey Open-File Report 82-591, Vol. I, pp. 120-184.

Campbell, K. W. (1982b), "A Study of the Near-Source Behavior of Peak Vertical Acceleration," (Abstract), EOS, 63:1037.

Campbell, K. W. (1983), "Preliminary Analysis of the Near-Source Scaling Characteristics of 5 to 10 Hz Pseudo-Relative Velocity," (Abstract), Earthquake Notes, 54:55-56.

Campbell, K. W., and B. J. Davis (1980), "The Effect of Fault Type on Recorded Peak Ground Acceleration," (Abstract), Program and Abstracts, Eastern Section of Seism. Soc. Am., p. 8.

Chiaruttini, C. and L. Siro (1981), "The Correlation of Peak Ground Horizontal Acceleration with Magnitude, Distance, and Seismic Intensity for Friuli and Ancona, Italy, and the Alpide belt," Bull. Seism. Soc. Am., 71:1993-2009.

Crouse, C. B. (1978), "Prediction of Free-Field Earthquake Ground Motions," Proceedings of Specialty Conference on Earthquake Engineering and Soil Dynamics, ASCE, Pasadena, California, Vol. 1, pp. 359-379.

Crouse, C. B. (1983), "Soil-Structure Interaction Effects at Accelerograph Stations," Proc. Workshop on Site-Specific Effects of Soil and Rock on Ground Motion and their Implications for Earthquake Resistant Design, Held July 26-28, 1983 in Santa Fe, New Mexico, U.S. Geological Survey Open File Report (in press).

Darragh, R. B., and K. W. Campbell (1981), "Empirical Assessment of the Reduction in Free Field Ground Motion Due to the Presence of Structures," (Abstract), Earthquake Notes, 52:18-19.

Esteva, L. (1970), "Seismic Risk and Seismic Design Criteria for Nuclear Power Plants," Edited by R. J. Hansen, The MIT Press, Cambridge, Massachusetts, pp. 142-182

Faccioli, E. (1981), "The Use of the RMS Acceleration as a Measure of Soil Amplification in Strong Earthquakes," in State-of-the-Art in Earthquake Engineering 1981, edited by O. Ergunay and M. Erdik, Turkish Natl. Comm. on Earthq. Engr, Ankara, Turkey.

Gallant, A. R. (1975), "Nonlinear Regression," The American Statistician, 29:73-81.

Hadley, D. M. and D. V. Helmberger (1980), "Simulation of Strong Ground Motions," Bull. Seism. Soc. Am., 70:617-630.

Hadley, D. M., D. V. Helmberger, and J. A. Orcutt (1982), "Peak Acceleration Scaling Studies," Bull. Seism. Soc. Am., 72:959-979.

Joyner, W. B. and D. M. Boore (1981), "Peak Horizontal Acceleration and Velocity from Strong-Motion Records Including Records from the 1979 Imperial Valley, California, Earthquake," Bull. Seism. Soc. Am., 71:2011-2038.

McCann, M. W. and D. M. Boore (1983), "Variability in Ground Motions: Root Mean Square Acceleration and Peak Acceleration for the 1971 San Fernando, California, Earthquake," Bull. Seism. Soc. Am., 73:615-632.

McGarr, A., (1982), "Upper Bounds on Near-Source Peak Ground Motion Based on a Model of Inhomogeneous Faulting," Bull. Seism. Soc. Am., 72:1825-1841.

McNeill, R. L. (1983), "Some Possible Errors in Recorded Free-Field Ground Motions," Proc. Workshop on Site-Specific Effects of Soil and Rock on Ground Motion and their Implications for Earthquake Resistant Design, Held July 26-28, 1983 in Santa Fe, New Mexico, U.S. Geological Survey Open-File Report (in press).

Mickey, W. V., V. Perez and W. K. Cloud (1973), "Response of Pacoima Dam to Aftershocks of San Fernando Earthquake," in the San Fernando, California, Earthquake of February 9, 1971, EERI/NOAA, Vol. II, pp. 403-415.

Reimer, R. B., R. W. Clough and J. M. Raphael (1973), "Evaluation of the Pacoima Dam Accelerogram," Proc. Fifth World Conf. Earthquake Engr., Rome, Italy, Paper 293.

TERA Corporation (1980), "Reduction in Free Field Ground Motion Due to the Presence of Structures," Report to Southern California Edison Company, TERA Corporation, Berkeley, California.

TERA Corporation (1982), "Estimation of Selected Response Spectral Values at San Onofre Nuclear Generating Station," Report to Southern California Edison Company, TERA Corporation, Berkeley, California.

ACKNOWLEDGEMENTS

This work was performed at TERA Corporation with funding from Southern California Edison Company and Pacific Gas and Electric Company. I wish to express my appreciation to the staff of the Lawrence Livermore National Laboratory for their support in the writing of this manuscript.

Predicting Site-Specific Attenuation of Ground Motion

Comments, Concerns, and Controversy

by

Joseph A. Fischer
Geoscience Associates, Inc.
Millington, New Jersey

Introduction

It would appear from this panel's assignment that we have been requested to discuss the theme of the conference, synthesize the results, define the applications, and point out some of the possible measures of reliability or Coefficients of Correlation that might be useful in testing the statistical suitability of the procedures recommended.

Fortunately, the panel has only one and one-half hours to accomplish our task so it will be much easier than if we were allotted, say a week, for the assignment.

The Problem

Before attempting to provide answers it may behoove us to examine the problem with which we are most concerned, that is the prevention, or amelioration, of damage to man's works and the safety of those that could be influenced by such damage, or even failure.

In the U. S. one of the earliest concerns regarding the relationship of site effects and the destructiveness of earthquakes was raised by Martin Duke. Much of his sources of data came from discussions with, and studies conducted by, Japanese investigators (Duke, 1958). The original studies, all empirical in nature, indicated that generalized conclusions could be drawn concerning the nature and degree of structural damage and the types of subsurface materials in particular locales. As time progressed, tremendous strides have been made in our overall scientific understanding of the problem and our analytic ability to format the problem in quantifiable terms.

Unfortunately it is to sometimes easy to miss the forest for the trees. To put this workshop's discussions in context we must rememember we are dealing with a multi-discipline problem, and an involved interelationship between the source mechanism, the travel path geometry and geology, the site geologic conditions (geometry and physical characteristics), and the structure(s) at the site, (see Figure 1, on the following page).

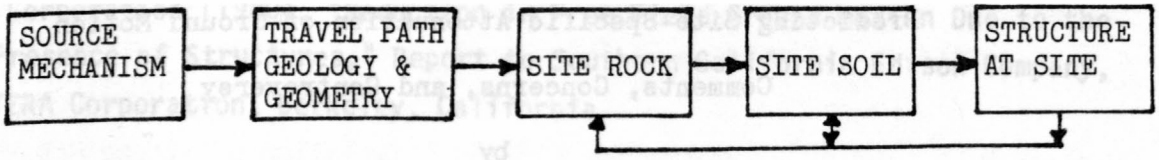

FIGURE 1

The first question is, do we truly have an understanding of the complexity of the problem and do we have enough mathematical sophistication to solve the entire interaction problem? While it may be easy to ask such these motherhood questions, there appeared little in the workshop to indicate we were cognizant of this broad interaction in designing our experiments. The authors in this workshop have, in the main, addressed only portions of the whole picture (with a notable lack of consistency in terminology).

From just the papers prepared for this meeting it appears that even if we deal solely with California earthquakes our source mechanism term creates a number of variations in recorded acceleration levels and/or local attenuation. As earthquakes from different regions of the world are believed to have different signatures this problem grows as we attempt to extrapolate our data base to areas where it was not gathered.

Other presentations in the workshop have shown how geometrical relationships between the recording instrument and the source influence the records. In addition it is a relatively well accepted fact that "Q" varies from region to region.

We also have a unanimity of opinion that site soils conditions and topography influence ground response. There is less unanimity in how they may affect ground response in an earthquake.

And finally there was data presented in the workshop in relationship to how the interaction between a structure and the site geology and topography can influence building performance and seismograph records.

Thus we are certainly progressing on the pieces, but seem to need coordination, and overall direction to ongoing and future research.

Comments

Rather than echo what a number of the other panelists may wish to say in regard to our assignment, I would like to suggest consideration be given to an alternate approach to the overall problem posed to our group, perhaps in somewhat of a devil's advocate position.

Much has been written in recent years in relation to; the attenuation of ground motion with distance, magnitude saturation (in which the writer is a believer), near field motions and the differences that seem to be found between different earthquakes; as well as the differences of opinion between different users of the same data base. Unfortunately, only a small number of

attempts have been made to correlate the data and evaluate the results, in light of the outer portions of Figure 1, the source mechanism, the travel path(s) and structural performance. (See Campbell, this workshop.)

We also have a rich supply of information relating various ground motion parameters, whether it be acceleration or velocity, to structural design, although the data is not necessarily correlative to how much damage a structure will suffer in an earthquake. Without developing an overall viewpoint of the problem, is it possible to provide a complete answer?

The response is probably yes, if we all do our homework and correctly understand the task assigned by our client, supervisor, or research granter. For the moment, however let us consider whether a very gross overview of the problem may be useful to us in any assignment that requires making a site dependent prediction of hazard. It might even be useful if the concept could be used in areas of lower seismicity where the data base was sparse and the funding was even sparser.

Variations in Source Mechanism and Travel Path

It is recognized that the "signature" of an earthquake differs in different tectonic settings. The type of faulting, the strength of the rocks, the magnitude and orientation of insitu stresses, etc. can all affect the pattern of "free-field" motion that might be recorded on our ideal rock site. The variation in "Q" with the tectonic setting is also well recognized.

Therefore if we hope to use any attenuation relationship for our site of interest we will need a data base consistent with our tectonic conditions, and our design earthquake size and location.

An example of the variations in attenuation of ground motion effects, perhaps indicating variations in source mechanisms and/or travel path attenuation with distance is presented on Figure 2. The format follows that of Gupta and Nuttli, 1976.

There can easily be many arguments concerning the use of the data on Figure 2. However, would it be any worse than using an acceleration/distance attenuation curve predicated upon a statistical analysis of world wide data for site studies in both Madrid, Spain and Oslo, Norway?

Site Effects/Structural Response

A session in this workshop addresses amplification models. Currently there are numerous one-dimensional mathematical models designed to handle simplifed earthquake wave motion input. Two-dimensional models that handle simplified wave trains are also readily available, although somewhat expensive in their application. However, no matter how advanced our mathematical capabilities are, can we economically and adequately define the variations in subsurface geometry and physical properties at our site in a manner that is consistent with our analytical strengths?

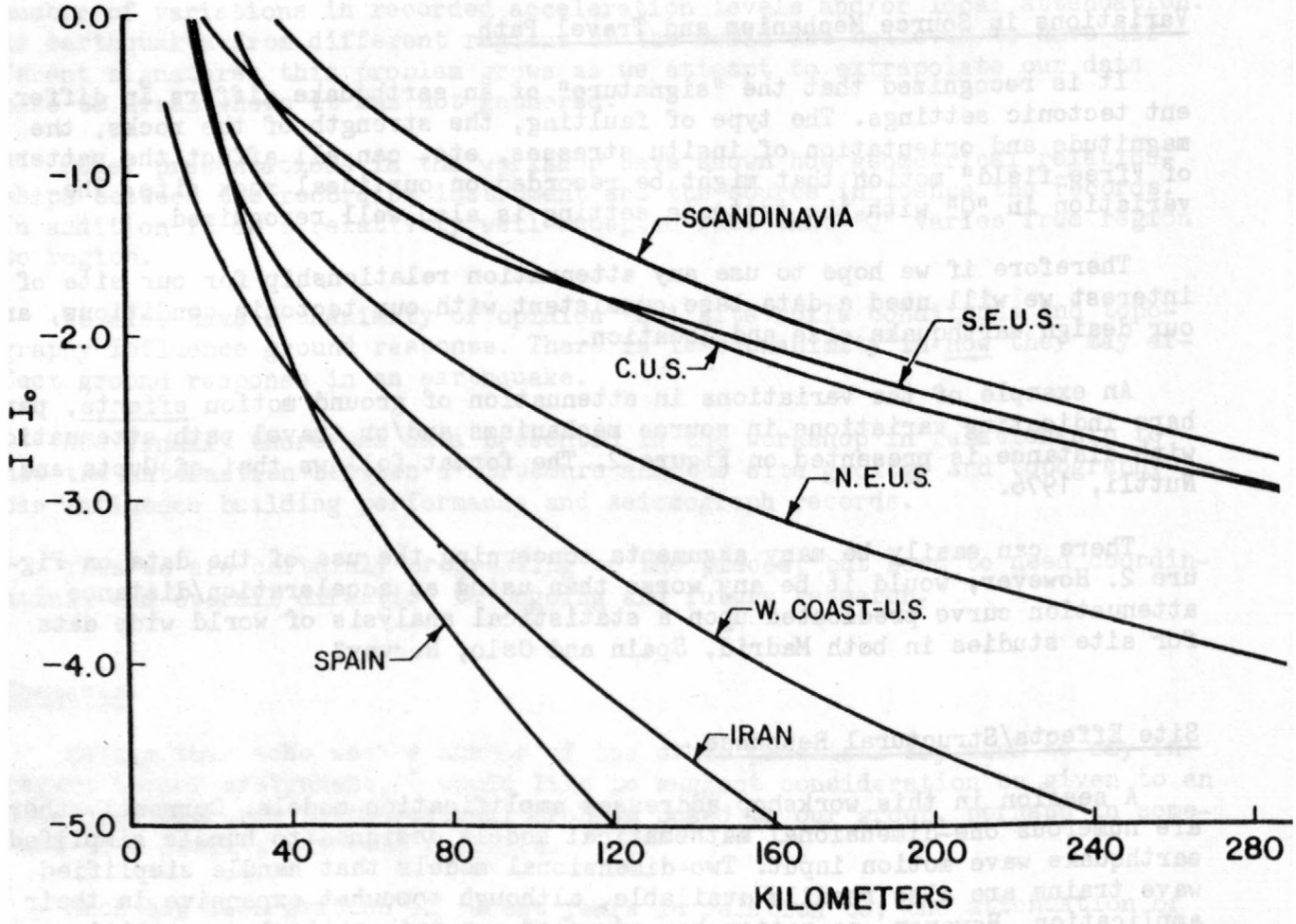

Figure 2.--Comparison of some World-wide attenuation relations (after Fischer and Spiker, 1979). The relations are given in terms of $I-I_0$ as a function of distance, where I_0 is the epicentral intensity.

The difficulties become compounded when one must incorporate the structure or facility of interest into the analysis. For design purposes the author once provided response spectra from an actual earthquake, recorded on subsurface conditions that were quite similiar to the client's site, at the same distance from the motion source as the site in question. He was later told that the design motion was too high because all the buildings that lived through the prototype earthquake were shown to be destroyed when the design spectrum was used to analyse their seismic capability. There may never be a situation where the recorded "free-field" motion, and the site motion experienced by a number of structures that were subsequently analysed will be closer, yet our analytical procedures produced results which were incompatible with the real world.

Therefore we must never lose sight of the many unknowns that we deal with in transforming our analytic capabilities and our experience into rational results. Duke's original work correlated structural damage statistics with soil conditions for a suite of earthquakes. The Intensity decay plots on Figure 2 perform essentially the same process for a variety of levels of ground motion. Could an approach similiar to Duke's be used with descriptors as crude as Intensity? Perhaps, if we knew more about structural design, site conditions, and ground motion parameters recorded for a large variety of earthquakes.

Intensity

Figure 3 represents an isosesmal map of a 1925 St. Lawrence Valley earthquake, prepared by Canadian Government sources. If one were to compare this shock with other regional earthquakes, see Figure 4, again in Gupta-Nuttli format, would it be possible to develop useful engineering information? The answer is yes, with a number of qualifiers.

One might develop a better understanding of the geometry of the source and azimuthal variations in attenuation, if fault plane solutions were calculated for the same shocks, or later, well recorded shocks from the same source zone. Local travel path parameters might be sorted out if instrumental variations in travel times were evaluated in concert with structural geologic patterns, generalized regional subsurface conditions, structural types versus damage, and unfortunately, to some extent, the population distribution of the region. Even more valuable would be the incorporation of strong motion data in any evaluation of intensity effects.

In support of "Intensities", the study of historical events and their distribution of damage does represent the "real world". Until such time as our technological understanding and analytic capability can account for the many variables of Figure 1, the historical decay of damage characteristics, in a particular tectonic setting, remains a useful diagnostic tool. It can be an important aspect of risk analyses for engineered structures, particularly in areas of lower rates of seismic activity.

To have a look at the other side of the coin however, Figure 5 represents the isoseismals from the 1904 Oslofjord earthquake. Oslofjord is the surface expression of a major northerly trending graben structure. The population parallels the fjord axis. The poorest soils also lie along the fjord shoreline.

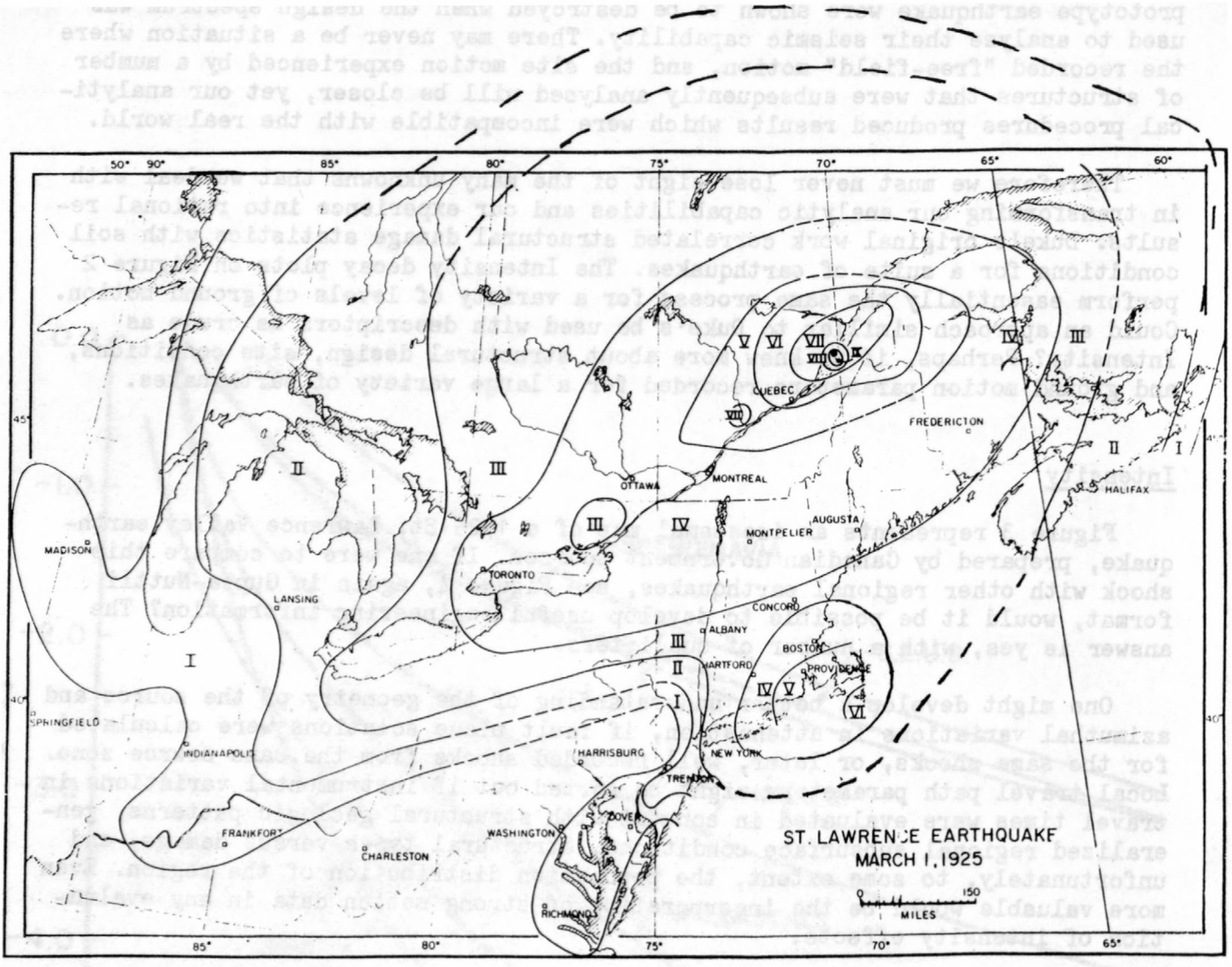

Figure 3.--Isoseismal map for the St. Lawrence earthquake of March 1, 1925, (after Smith, 1966).

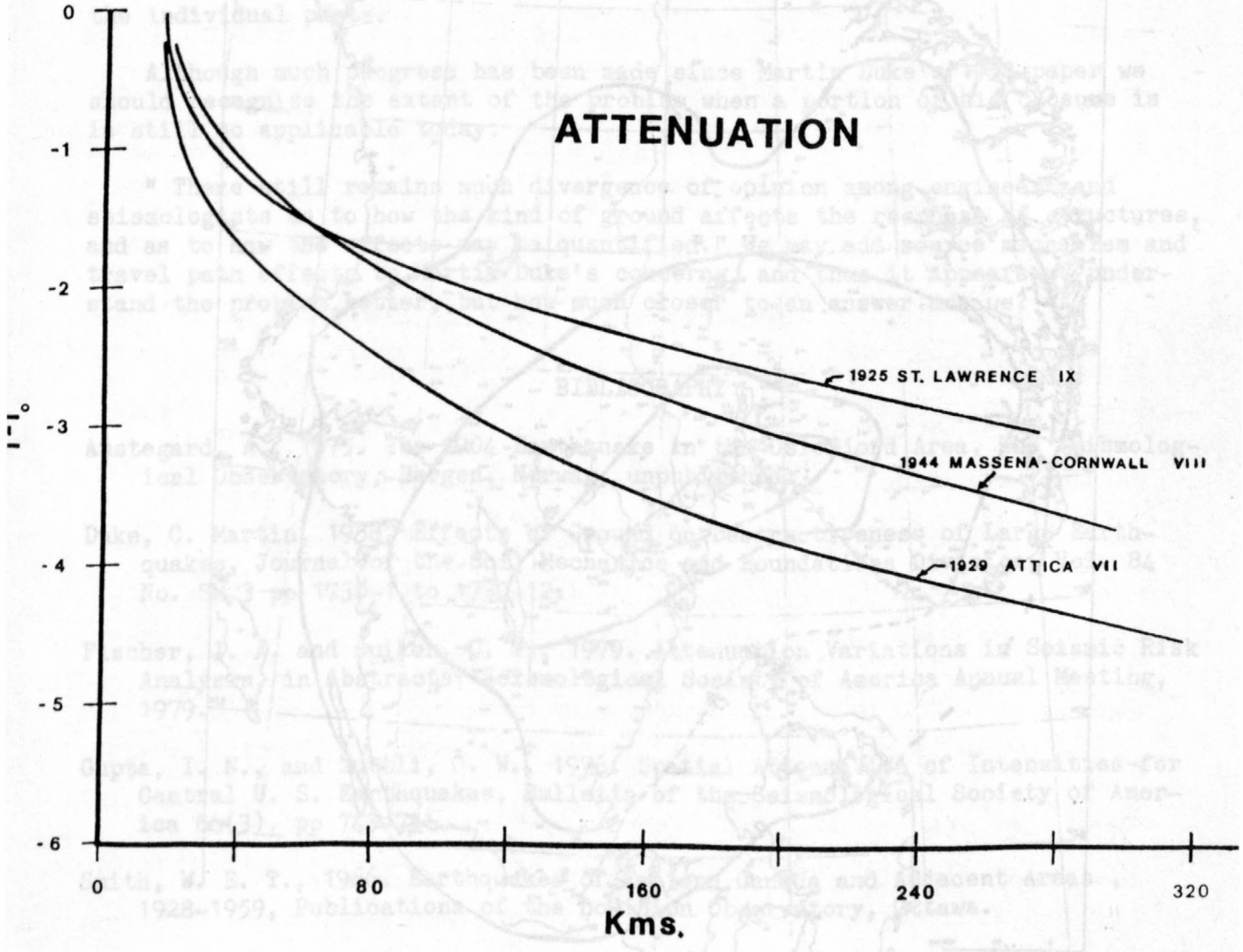

Figure 4.--Comparison of attenuation relations for three earthquakes in the Northeastern United States. The value of epicentral intensity (I_0) is shown for each curve.

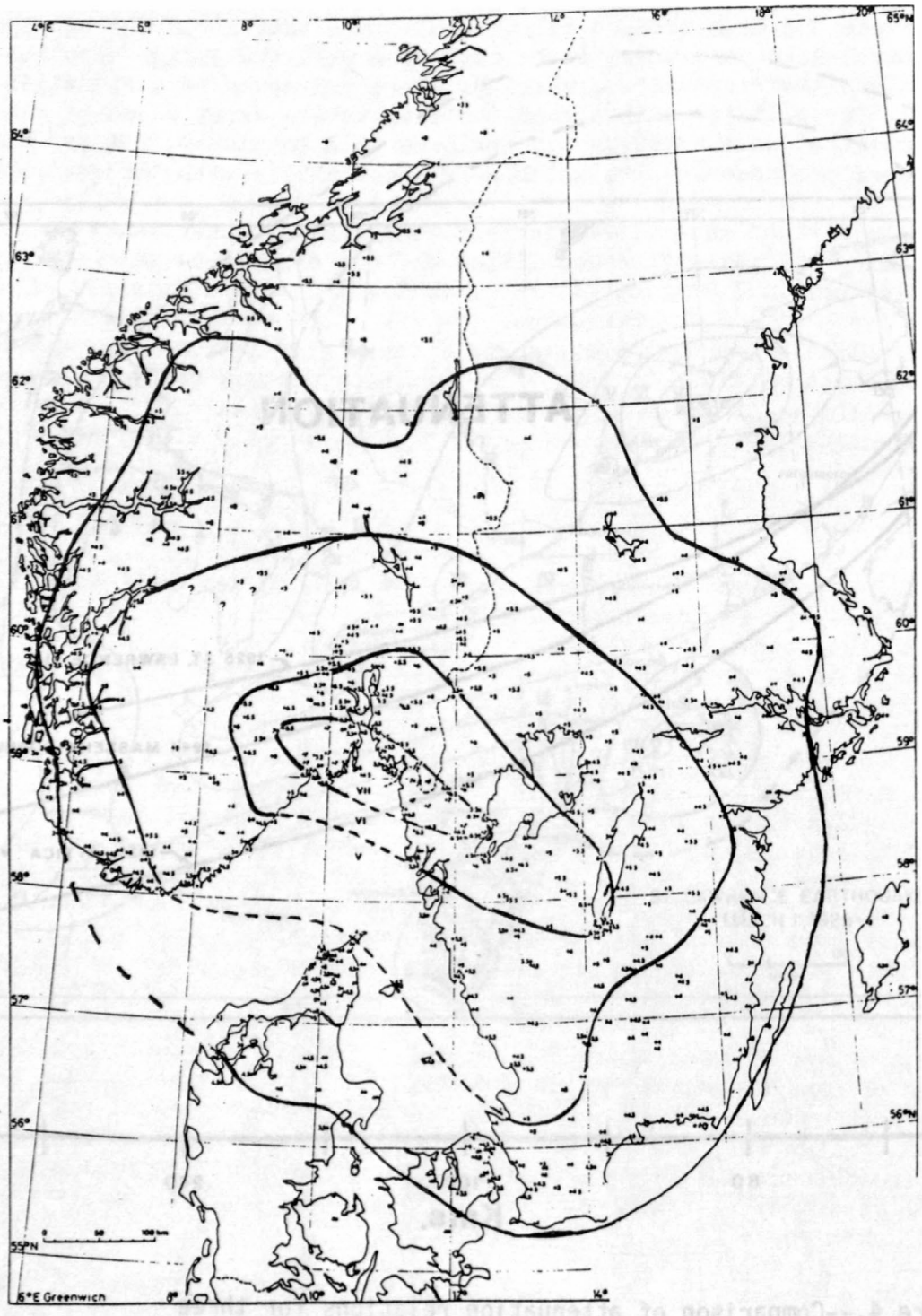

Figure 5.--Isoseismal map for the 1904 Oslofjord earthquake. Intensities are based on the Modified Mercalli scale (after Austegard, 1975).

The isoseismals are telling us something, but what it is, is not clear.

Controversy

There is no doubt that we must continue to pursue the current areas of research and practice in our attempts to understand site effects and their relation to earthquake induced damage. However, the need for a more consistent terminology and better communication is evident. We must also realize it's a complex problem and not allow the end product to be obscured by over emphasis on the fragments, without a realization of the whole. Perhaps a simple-minded approach such as analyzing MM Intensities (after disregarding geological descriptors of intensity) may be a helpful tool in defining the level of risk to structures and humanity. In effect, Intensity patterns treat the system, not the individual parts.

Although much progress has been made since Martin Duke's 1958 paper we should recognize the extent of the problem when a portion of his closure is is still so applicable today:

" There still remains much divergence of opinion among engineers and seismologists as to how the kind of ground affects the response of structures, and as to how the effects may be quantified." We may add source mechanism and travel path effects to Martin Duke's concerns, and thus it appears we understand the problem better, but how much closer to an answer are we?

BIBLIOGRAPHY

Austegard, A., 1975. The 1904 Earthquake in the Oslofjord Area, The Seismological Observatory, Bergen, Norway, unpublished.

Duke, C. Martin, 1958. Effects of Ground on Destructiveness of Large Earthquakes, Journal of the Soil Mechanics and Foundations Division, Vol. 84 No. SM 3 pp 1730-1 to 1730-12.

Fischer, J. A. and Spiker, C. T., 1979. Attenuation Variations in Seismic Risk Analysis, in Abstracts, Seismological Society of America Annual Meeting, 1979.

Gupta, I. N., and Nuttli, O. W., 1976. Spatial Attenuation of Intensities for Central U. S. Earthquakes, Bulletin of the Seismological Society of America 66(3), pp 743-751.

Smith, W. E. T., 1966. Earthquakes of Eastern Canada and Adjacent Areas , 1928-1959, Publications of the Dominion Observatory, Ottawa.

PERSPECTIVES ON PROPERTIES OF ATTENUATION FUNCTION VARIABILITIES USING A NAIVE RUPTURE MODEL

by

David M. Perkins
U.S. Geological Survey
Golden, Colorado

Our interest in attenuation function variability derives from its role in the calculation of probabilistic ground motion. For modest return periods, the effect of this variability is to increase probabilistic ground motions by 15 to 40%. At very long return periods, the calculated ground motions appear to be determined more by the properties of the attenuation variability than the underlying seismicity parameters of sources (Perkins, 1982).

Assessments of attenuation variability are usually derived from regressions of peak accelerations on simple functional forms. The attenuation variability is obtained from the residuals of the regression, assuming the variability to be independent of magnitude and distance. In this paper, a simple heuristic model is considered which predicts that an important proportion of the variability is magnitude- and distance-dependent. The model is crude, but leads to interesting predictions which can be tested in the data. In critiquing the model, we are led to some general conclusions which point up issues of importance even to more realistic models.

In the model, the earthquake is considered as a rupture consisting of a succession of N subruptures of a characteristic length, and for which the only variable is stress drop (fig. 1). At a site, the peak ground motion due to a subrupture is proportional to the stress drop on that subrupture. The probabilistic distribution of stress drops is assumed to be the same for each subrupture.

We consider two sites, one close to the rupture and one far from the rupture. For the near site, the peak ground motion experienced is likely to be due to the stress drop on the nearest subrupture. The variability of that peak ground motion is the same as that of the stress-drop distribution. The far site is nearly equidistant to all subruptures; and, hence, the peak ground motion experienced comes from that subrupture with the largest stress drop. The variability of that peak ground motion is the variability of the distribution function of the largest of a sample of size N from the stress-drop distribution function. The expected peak stress drop of the largest of N stress drops is near the (1-1/N) x 100 percentile of the stress-drop distribution (see Bury, 1975 p. 369-387). If the stress-drop distribution is bounded, this peak stress drop approaches the bound and its variability quickly becomes small (fig. 2). If the stress-drop distribution is exponential (and hence unbounded), the variability of the peak stress drop is the same as that of the

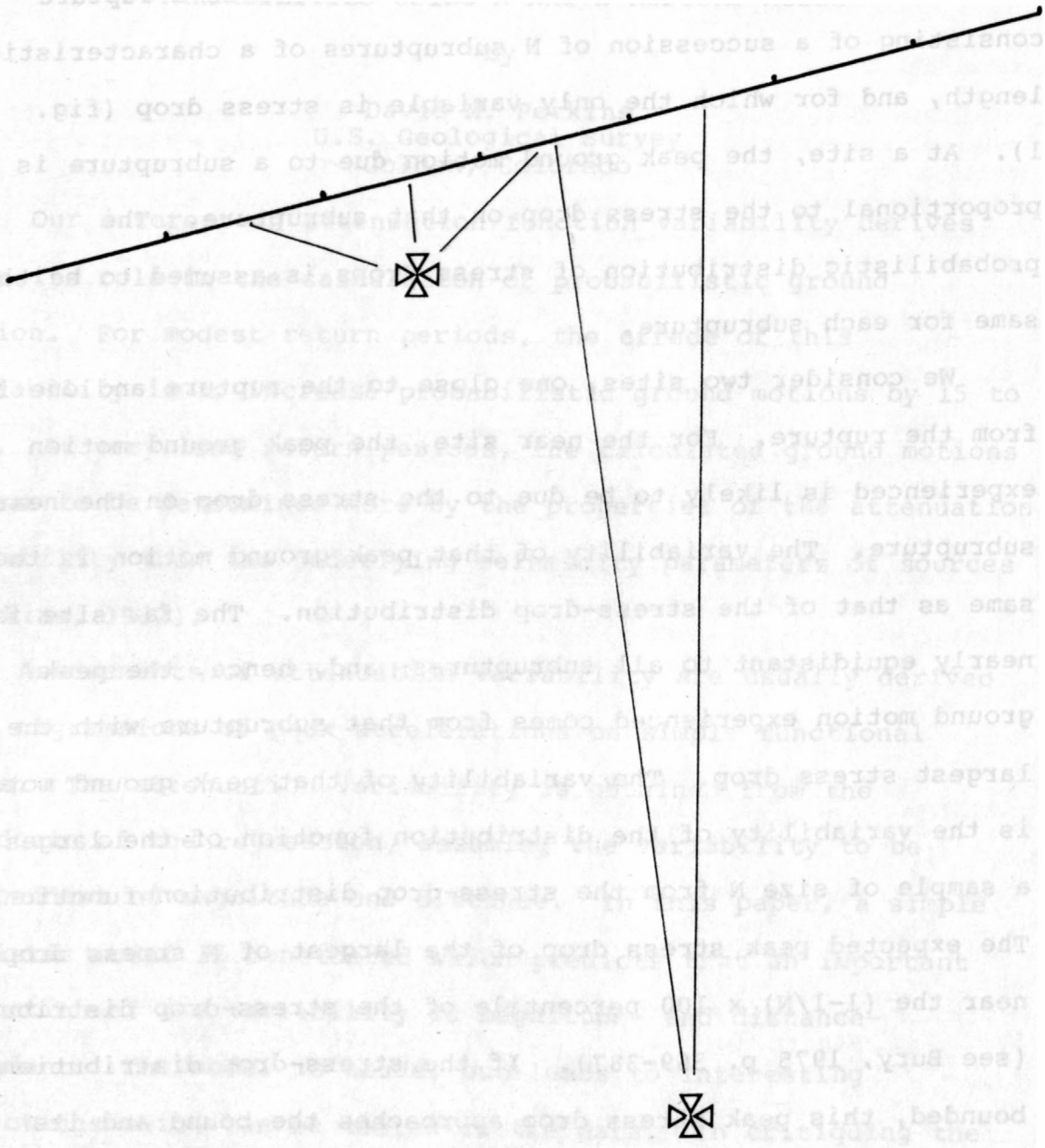

Figure 1.--The model: linear rupture with subruptures of equal length. Two sites, near and far, showing relative distance to subruptures.

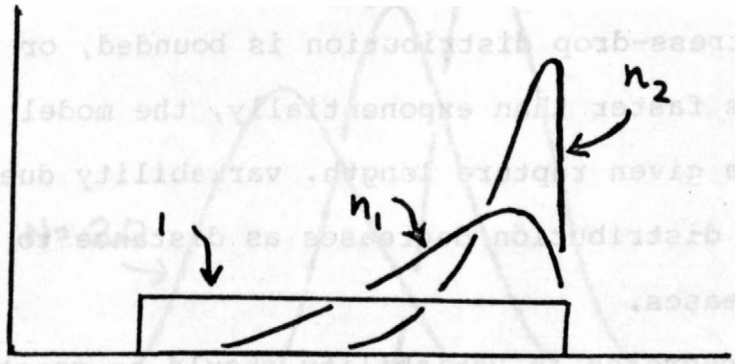

Figure 2.--Extreme distributions for a bounded distribution.

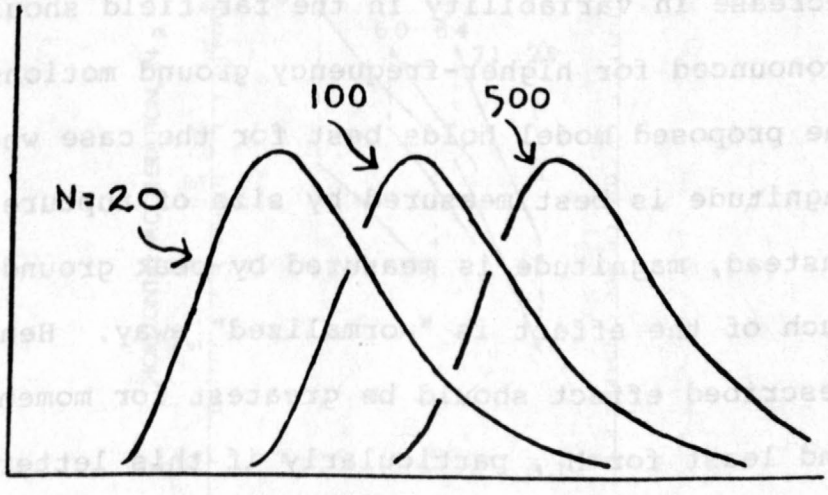

Figure 3.--Extreme distributions from exponential distribution (from Bury, 1975).

underlying stress-drop distribution (fig. 3). If the stress-drop distribution is normal, the result is intermediate to the above: the peak stress drop of N stress drops is unbounded, but its variability gets smaller as N increases (fig. 4).

If the stress-drop distribution is bounded, or if its upper tail decreases faster than exponentially, the model predicts:

1. For a given rupture length, variability due to stress-drop distribution decreases as distance to the site increases.
2. The decrease in variability should be greater for larger ruptures, if you are sufficiently far from the source.
3. For sites sufficiently close to the source, the variability due to stress-drop distribution should be independent of magnitude.
4. If it is appropriate to consider higher-frequency ground motions as representable by smaller subruptures, the decrease in variability in the far field should be more pronounced for higher-frequency ground motions.
5. The proposed model holds best for the case where magnitude is best measured by size of rupture. If, instead, magnitude is measured by peak ground motions, much of the effect is "normalized" away. Hence, the described effect should be greatest for moment magnitude and least for M_L, particularly if this letter is defined by strong ground motion peaks themselves (as with Espinosa, 1980).

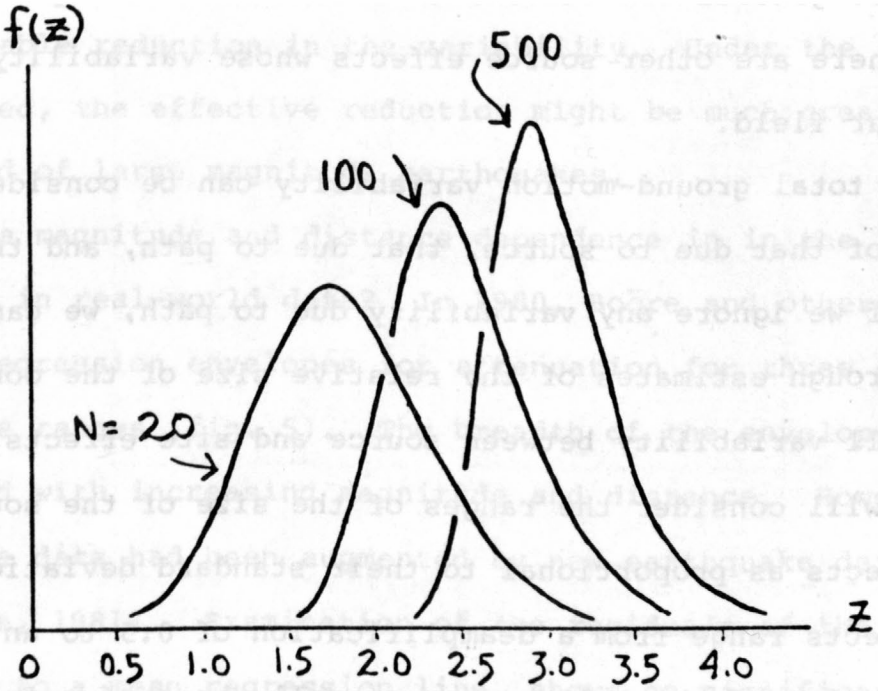

Figure 4.--Extreme distributions from normal distribution (from Bury, 1975).

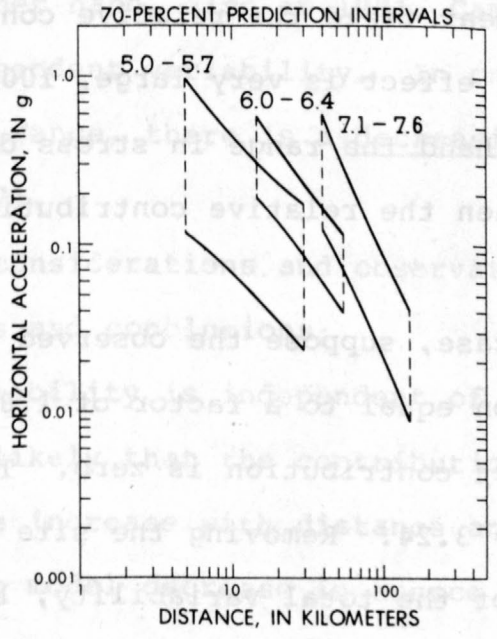

Figure 5.--Confidence intervals (70 percent) for three magnitude ranges. Note decreasing intervals with increasing magnitude and distance (Boore and others, 1980).

These general conclusions on source variability should hold unless there are other source effects whose variability increases in the far field.

The total ground-motion variability can be considered to be made up of that due to source, that due to path, and that due to site. If we ignore any variability due to path, we can make several rough estimates of the relative size of the contribution to overall variability between source and site effects.

We will consider the ranges of the size of the source and site effects as proportional to their standard deviations. The site effects range from a deamplification of 0.5 to an amplification of about 10, or an overall range of a factor of 20 (Rogers, oral communication). What is the range of stress drops?

If moment magnitude is independent of stress drop and the range of stress drops is from 1 to 100 bars, or an overall factor of 100, then in the near field the relative contribution of source effect to site effect is very large, 100^2 to 20^2, or 25 to 1. If, on the other hand the range in stress drop for any moment is a factor of 10, then the relative contribution is 10^2 to 20^2 or 1 to 4.

In this latter case, suppose the observed total variability has standard deviation equal to a factor of 1.8. Suppose the near-field path effect contribution is zero. The overall variability is $1.8^2 = 3.24$. Removing the site variability, which is a fraction $4/_{1+4}$ of the total variability, leaves us with a variability of $0.2 \times 3.24 = .648$, corresponding to a standard

deviation equal to a factor of $\sqrt{.648}$ = .8. This is a considerable reduction in the variability. Under the assumptions considered, the effective reduction might be much greater in the far field of large magnitude earthquakes.

Is a magnitude and distance dependence in in the variability observed in real-world data? In 1980, Boore and others showed linear regression envelopes for attenuation for three different magnitude ranges (fig. 5). The breadth of the envelopes decreased with increasing magnitude and distance. However by 1981, the data had been augmented by new earthquake data (Joyner and Boore, 1981). Examination of the residuals of the data, referred to a mean regression line, shows no significant difference in standard deviation (a factor of 1.8) between the two larger-magnitude categories, and a slightly larger value (2.0) for the smallest-magnitude category (fig. 6).

One the other hand, also in 1981, Campbell shows magnitude- and distance-dependent variability. In one illustration, for a given magnitude range, there is a <u>decreasing</u> variability with distance (fig. 7).

The above considerations and observations suggest the following issues and conclusions:

1. If variability is independent of magnitude and distance, it is likely that the contribution of path/transmission effects increase with distance and magnitude, making up for the model decrease in source contribution.

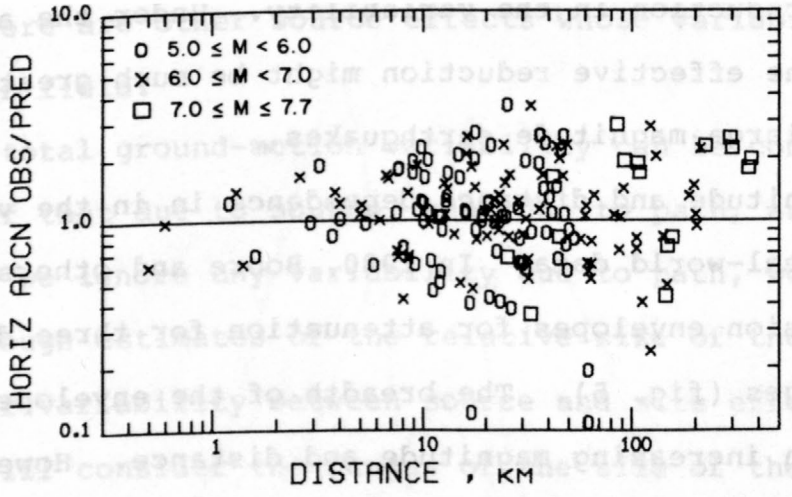

Figure 6.--Residuals of peak horizontal acceleration with respect to predicted values (Joyner and Boore, 1981).

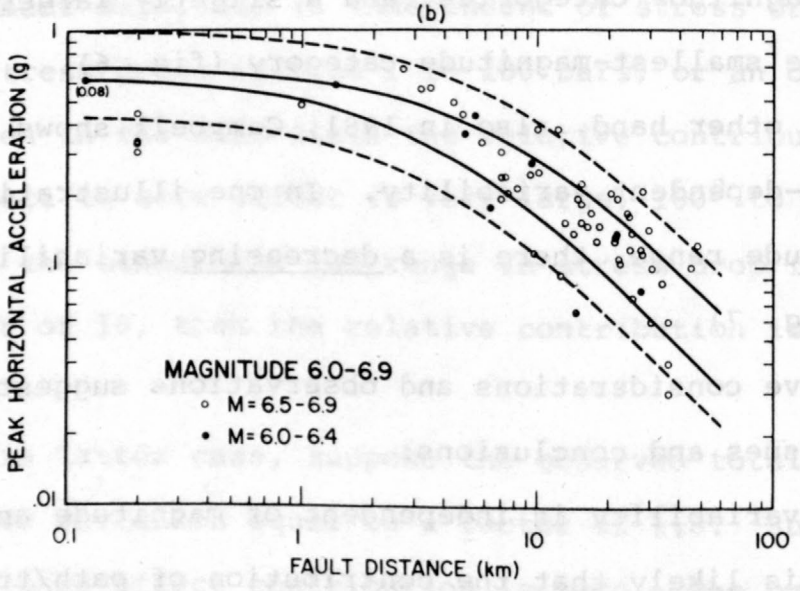

Figure 7.--Comparison of observed values of peak ground acceleration with predicted values for magnitude interval 6.0 to 6.9. The lines are not confidence intervals, but rather median predictions for the interval bounding magnitudes (solid), 84th percentile for upper bound (upper dashed), 16th percentile for lower bound (lower dashed) (Campbell, 1981). Data scatter appears to decrease with decreasing distance to fault.

2. Proof of the alleged dependence of variability on magnitude and distance may require a suitable set of attenuation functions with which to compare observed data. The shapes of the attenuation functions may have to be guided by physical models rather than the data themselves.
3. It should be expected that the relative proportion of the source contribution to overall variability may depend on the definition of magnitude used.
4. If the magnitude and distance variability suggested by the model is in fact present, there are excellent prospects for reducing the effect of variability on probabilistic ground motions for specific sites in the far field of earthquakes. This will be important for areas of broad source zones or sites at great distances from concentrated sources, as in the eastern United States.
5. However for very long return periods, probabilistic ground motion results may depend upon the probability distribution of stress drops and the shape of the upper tail of this distribution.

BIBLIOGRAPHY

Boore, D. M., Joyner, W. B., Oliver, A. A. III, and Page, R. A., 1980, Peak Acceleration, Velocity, and Displacement from Strong-Motion Records, Bulletin of the Seismological Society of America, v. 70, no. 1, p. 305-321.

Bury, K. V., 1975, Statistical models in applied science, John Wiley and Sons, Inc., New York.

Campbell, K. W. 1981, Near-Source Attenuation of Peak Horizontal Acceleration, Bulletin of the Seismological Society of America, v. 71, no. 6, p. 2039-2070.

Espinosa, A. F., 1980, Attenuation of Strong Horizontal Ground Accelerations in the Western United States and their relation to M_L, Bulletin of the Seismological Society of America, v. 70, no. 2, p. 583-616.

Joyner, W. B., and Boore, D. M., 1981, Peak Horizontal Acceleration and Velocity from Strong-Motion Records including Records from the 1979 Imperial Valley, California, Earthquake, Bulletin of the Seismological Society of America, v. 71, no. 6, p. 2011-2038, December, 1981.

Perkins, D. M., 1982, Effect of Changing Return Periods on Probabilistic Ground Motion: Proceedings of the Workshop on Seismic Performance of Underground Facilities, Augusta, Georgia, February 11-13, 1981, DP-1623, DuPont, Aiken, SC, p. 183-205.

UNCERTAINTY IN GROUND MOTION PREDICTIONS

by
Martin W. McCann, Jr.
Jack R. Benjamin & Associates, Inc.
Mountain View, California

INTRODUCTION

The basis for strong ground motion predictions made by engineers in selecting design criteria and by risk analysts in the probabilistic description of seismic hazards is for the most part empirical models. A matter of some concern in these applications is the uncertainty in predicted motions. With the continued use of probabilistic seismic hazard analysis, interest has focused on making complete assessments of the uncertainty in hazard evaluations (Cornell, 1982). This would include taking account of the inherent randomness of the attenuation process, statistical variability in parameter estimates and modeling uncertainty. Of interest then is the assessment of seismic hazards such that each type of uncertainty is incorporated in a probabilistic analysis. Bayesian methods are used to evaluate as well as combine the different types of uncertainty in the eventual prediction.

Statistical studies indicate that the variation in ground motion amplitudes ranges from a factor of 1.45 to 1.9 times the median at the one standard deviation level. At two standard deviations these factors are 2.1 and 3.6. For the most part,

this variability was considered irreducible. With the increased disbursement of strong motion recording instruments and the significant acquisition of recordings near large and moderate size earthquakes, the expanded data base presents an opportunity to isolate in statistical studies the various factors that contribute to the scatter in ground motions.

The focus of this paper is to discuss the sources of uncertainty in ground motion prediction. Results of recent work that have isolated various contributors to the variability in strong motion data and investigated some of the modeling uncertainties in ground motion predictions are presented. A comprehensive review of past work in these areas is not presented. Previous papers have presented detailed reviews of empirical ground motion prediction methods (Idriss, 1978); discussed matters of topical interest (Boore and Joyner, 1982), and summarized the general matter of recent developments in strong motion seismology (Boore, 1983). Our comments are based on analyses of strong ground motion in the Western U.S. and therefore in a strict sense do not apply to the difficult problem of attenuation in the eastern part of the country.

In the next section, a brief summary of the types of uncertainty is given. This is followed by a description of a general ground motion prediction model wherein each type of uncertainty is accounted for.

The results of recent ground motion studies that have isolated the contributions of individual factors to the scatter in ground motions are described next. Also, results of a study are presented where the degree of variability associated with the assumed mathematical form of the attenuation function can be inferred. The discussion herein will concentrate on peak ground (PGA) and the root mean square (RMS_a) acceleration. The question of the relative variability in the peak vs. root mean square acceleration is also considered.

We conclude that randomness in ground motions is a composite of individual contributions of source effects, propagation, local geologic influences and building effects. We find that influences near to the site (including building effects) contribute as much as a factor of 1.3 to the scatter in PGA attenuation. From similar estimates for other effects we infer that a reduction in the scatter in ground motion data can be achieved and suggest that detailed analysis of variance studies should be undertaken to further explain the scatter. The preliminary studies that have been conducted so far suggest strongly that local site effects are a major contributor to the scatter in ground motions.

With regard to modeling variability, we find the greatest uncertainty is at short distances (less than a few kilometers) from large events, as expected, for both PGA and RMS_a. Beyond ten kilometers median ground motion estimates vary by ±20% or

less. And from our study of PGA and RMS_a attenuation, we find in comparing four attenuation models and three measures of the root mean square, that peak acceleration has less variability in all cases.

ELEMENTS OF UNCERTAINTY

The development of strong ground motion prediction models is a complex process involving data set selection, parameter preference, amount of data, complexity of the physical process and our mathematical model of it, and the subjective bias of the analyst. Sources of uncertainty in ground motion predictions include:

- Inherent randomness - this source of uncertainty is the natural or irreducible variation. It is the residual that cannot be explained or otherwise predicted. It is interesting to recognize however, that our concept of what is irreducible can change. What was once considered irreducible may no longer be, as newly discovered facets of seismic sources, wave propagation or attenuation become part of our general understanding. This leads us to redefine what randomness is, as the variability associated with these or other factors is reduced or eliminated.
- Statistical variability - that component of uncertainty due to a limited sample size that precludes the exact evaluation of model parameters. This source of uncertainty can be eliminated if a much expanded data base were available.

- Model uncertainty - is attributed to the mathematical model of the earthquake process and in principle can be eliminated with sufficient data.

- In attenuation studies, uncertainty in independent parameters (i.e. magnitude and distance) also contribute to the uncertainty in prediction models. The independent parameters may be susceptible to each of the above sources of uncertainty.

For the most part interest in ground motion uncertainty has focussed on the scatter about a prediction curve, which is essentially accepted as the inherent randomness. Other sources of uncertainty have not been as fully investigated. However, with the major additions to the strong motion data base and the interest in probabilistic hazard predictions, a more complete accounting of each type of uncertainty is preferred.

PREDICTION MODELS

The prediction of ground motion amplitudes (i.e. PGA or RMS_a) can be expressed as,

$$F_X(x|\bar{g}) = g\ F(\varepsilon)$$

$$\bar{g} = g(x|M,R,S,\underline{C}) \qquad (1)$$

where $F_X(x|\bar{g})$ is the cumulative lognormal distribution function of X, the ground motion parameter, given the median, $\bar{g}$. Ground motion amplitudes are expressed in g in terms of magnitude, M; distance, R; site conditions, S; and a vector of empirically derived parameters, $\underline{C}$. The term ε is a lognormal random variable with a median of one and a logarithmic standard deviation, σ_{log}, derived from the residuals of the data about the function g( ). F( ) is the cumulative lognormal distribution function. Equation 1 is the form generally used to predict the probability of non-exceedance of ground motion amplitudes.

As expressed in equation 1, only one measure of uncertainty is taken into account. That is, ε is a measure of the randomness in ground motion amplitudes, with respect to the function g( ). However, it is generally recognized that ε is really a composite of many influences that contribute to the variability in ground motions (McCann and Boore, 1983). It could, for example, be a function of transmission, azimuth, gross geologic differences, local geologic variations, and building effects. Furthermore, each of these elements may in themselves be composites of factors on a more reduced scale. These effects may introduce a bias, towards higher or lower ground motions, as well as contribute to the scatter in the data. This suggests a modification to equation 1 of the form,

$$F_X(x|\bar{g}) = \bar{g}\, F(\underline{\varepsilon}) \qquad (2)$$

$$\bar{g} = g(x|M,R,\underline{Z},\underline{\Theta})$$

where $\underline{Z}$ is a vector of additional independent variables incorporated to account for factors other than magnitude and distance in the wave propagation process (i.e. transmission, azimuth, local geology, etc). The vector $\underline{\Theta}$ consists of the empirically derived coefficients of the model. In equation 2, $\underline{\varepsilon}$ is a vector of lognormal random variables that are a measure of the variability associated with each element of the wave propagation process accounted for in the model, the lack of fit to the data and of the inherent randomness of X, with respect to the model g( ).

In equation 2, the distribution on X is expressed given knowledge of the median. However, as described in the previous section, there are a number of uncertainties in g( ). Among them; statistical variability due to the limited number of data points; uncertainty that the functional form of g( ) is the true model; and variability in the independent variables (i.e. M, R, and $\underline{Z}$). Taking into account each source of uncertainty, (i.e. statistical, model, etc.), the unconditional distribution of the prediction of X is,

$$F_X(x) = \int F_X(x|\bar{g})\, f(\bar{g})\, d\bar{g} \qquad (3)$$

where f(g) is the probability density function on the median, $\bar{g}$. As there are a number of contributors to the uncertainty in $\bar{g}$, $f(\bar{g})$ is actually a joint distribution

$$f(\bar{g}) = f(\underline{\Theta}|\bar{g}_j)P(g_j) \quad (4)$$

where f ( ) accounts for the sources of uncertainty in the set of model coefficients $\underline{\Theta}$, and $P(\bar{g}_j)$ is a discrete probability that defines the likelihood that an assumed function, $\bar{g}_j$, is the "true" median. Values of $P(\bar{g}_j)$ are typically based on subjective opinion.

In some cases it is preferred to express the uncertainty in ground motion attenuations in the following format:

$$\{F_X(x|\bar{g}_j),\ P(\bar{g}_j)\} \quad (5)$$

where the randomness in ground motion predictions is expressed in $F_X(x|\bar{g}_j)$ and the modeling uncertainty is incorporated in $P(\bar{g}_j)$.

GROUND MOTION VARIABILITY

The previous section outlined in principal, an approach to predict ground motions. Although there are no studies that have conducted such an analysis, recent investigations provide an insight into some of the components of uncertainty described above. In this section we summarize results of studies that have attempted to isolate the contribution of individual elements of the earthquake process to the scatter in ground motions. Because of recent seismological and engineering interest in the root mean square acceleration (Hanks and McGuire, 1981; McCann and Boore,

1983; Kennedy et al., 1983), results for PGA and RMS_a are reported.

As indicated in equation 1, empirical studies have typically summarized the scatter in ground motions in a single term. The logarithmic standard deviation represented a measure of the inherent variability and the lack of fit to the data. Estimates of the scatter in ground motion residuals have ranged from a factor of 1.45 (Campbell, 1981) to 1.9 (McGuire, 1978), at the one standard deviation level. The relatively low value estimated by Campbell (1981) is attributed in part to the data selection criteria used in the study. An effort was made to eliminate factors considered to bias or otherwise contribute to the scatter in ground motions. In a study to be described more fully in the next section, results for peak acceleration attenuation using four different mathematical functions, produced similar results (McCann, et al., 1983). The factor at the one standard deviation level ranged from 1.43 to 1.50. In the same study, results for RMS_a ranged from 1.52 to 1.82. Most studies in the past have not had the opportunity to be as discriminating in the selection of data and thus have estimated the scatter in ground motions to be closer to the 1.9 value quoted above.

The analysis of the variance in ground motion residuals is a subject not often addressed in attenuation studies. However, two recent studies provide estimates of the variability that can be

associated with; source effects, propagation path, local site and building effects.

In their study of peak accelerations, Joyner and Boore (1981) conducted a two-step regression analysis that provided estimates of the intra-earthquake and propagation variability. From their regression analysis they estimate the base 10 logarithmic standard deviation associated with intra-earthquake variability to be, $\sigma_{log} = 0.13$, which corresponds to a factor of 1.35 at the one standard deviation level. This value was combined with a value of $\sigma_{log} = 0.22$ attributed to propagation effects to give an estimate of $\sigma_{log} = 0.26$ or a factor of 1.8 for the total variability. This is a value typical of those estimated in most attenuation studies.

In a relative sense, these results suggest that source effects contribute approximately 26% to the scatter, while propagation and other influences provide the remaining 74%. A variety of individual factors may contribute to the variability associated with sources effects, including differences in the patterns of stress release and faulting type (Campbell, 1981). Similarly, the variability associated with propagation is a composite of a number of factors. Some of which are discussed next.

In a study of the strong motion data recorded during the 1971 San Fernando earthquake, we attempted to isolate the

variability attributed to building embedment depth, local site response and propagation path (McCann and Boore, 1983). To do this, two independent data sets were used; an attenuation data subset and a local area data group where there were groups of strong motion stations in areas of approximately 1/2 km radius. Figure 1 shows the distribution of stations in the three area groups. This collection of stations presented a situation where source and propagation path effects could be assumed constant, allowing an evaluation of the variability due to local site effects. We concluded that geologic and other influences near to the site, including building effects, contribute a significant component to the scatter in attenuation, as much as a factor of 1.3 for peak acceleration. The scatter of PGA in the area data groups can be seen in Figure 2. Alone, building effects were estimated to account for a factor of 1.2, while the scatter due to propagation path influences was also a factor of 1.3. These results can be summarized by giving the per cent contribution of each source of uncertainty to the total variance. For peak acceleration, we observe that building effects contribute approximately 20 per cent, while local geology accounts for 40 per cent of the total variance, and propagation path effects also contribute a 40 per cent share. For the RMS_a using a constant duration measure, we found that propagation path effects contribute 60 per cent to the total variance, and building effects and local geology each contributed a 20 per cent share.

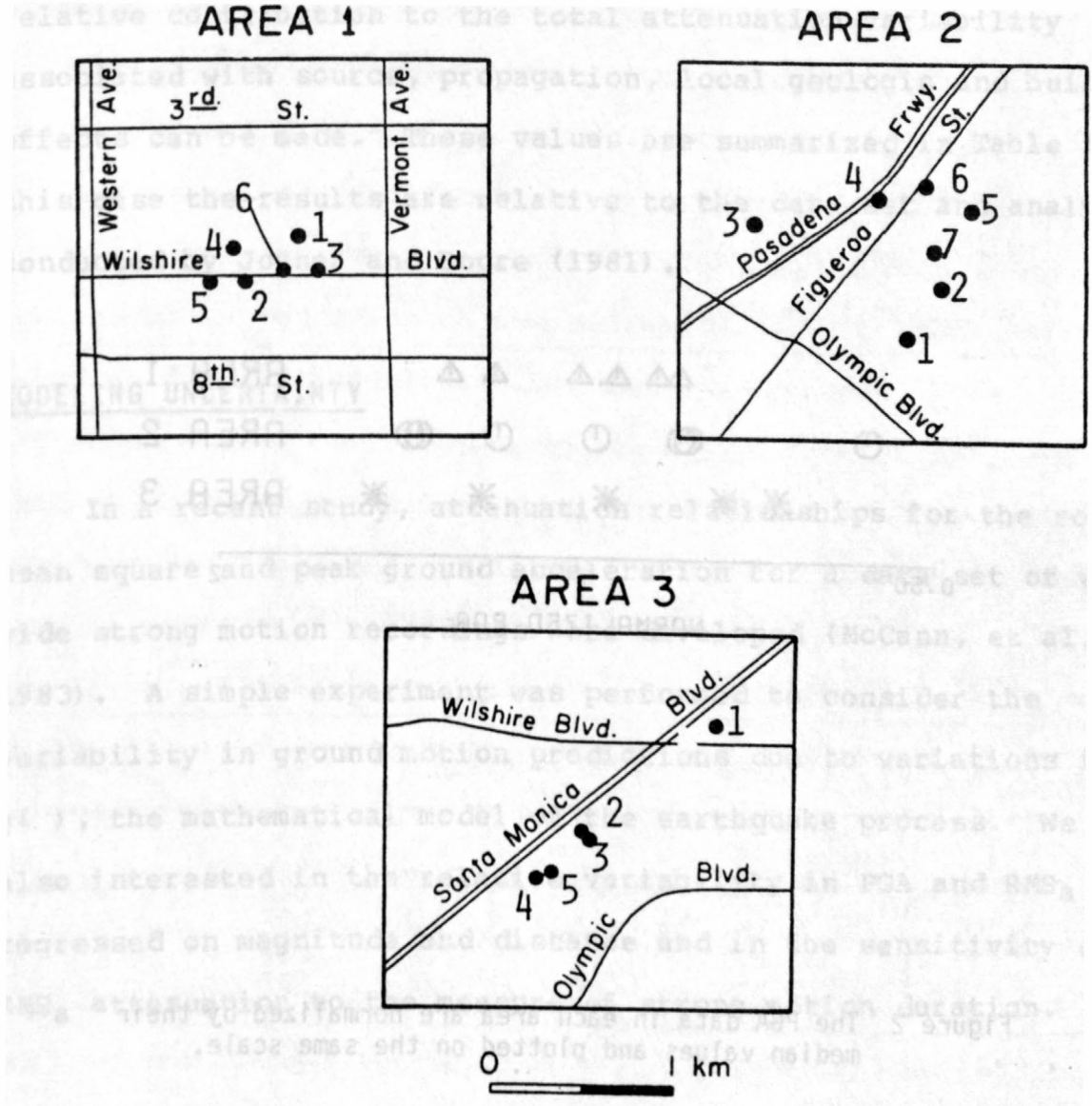

Figure 1 The locations of the recording stations in Areas 1, 2, and 3 in the Los Angeles area (modified from Hanks, 1975).

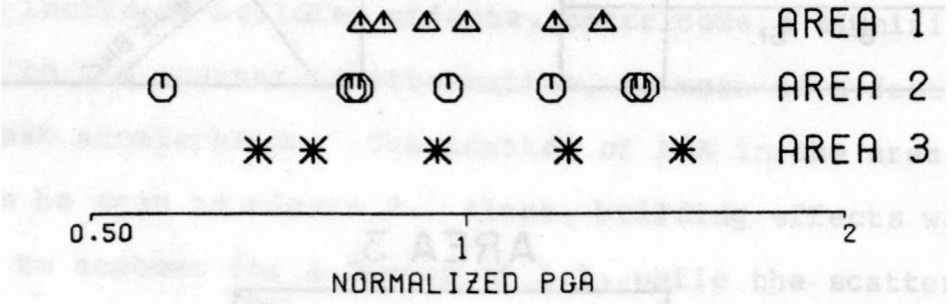

Figure 2 The PGA data in each area are normalized by their median values and plotted on the same scale.

These estimates are relative to the total variance in the attenuation data set used in the study.

If we combine the PGA results of the two studies, the relative contribution to the total attenuation variability associated with source, propagation, local geologic and building effects can be made. These values are summarized in Table 1. In this case the results are relative to the data set and analysis conducted by Joyner and Boore (1981).

MODELING UNCERTAINTY

In a recent study, attenuation relationships for the root mean square and peak ground acceleration for a data set of world-wide strong motion recordings were developed (McCann, et al., 1983). A simple experiment was performed to consider the variability in ground motion predictions due to variations in g( ), the mathematical model of the earthquake process. We were also interested in the relative variability in PGA and RMS_a when regressed on magnitude and distance and in the sensitivity of RMS_a attenuation to the measure of strong motion duration.

To carry out the analysis a data base of strong ground motion records from eighteen earthquakes were used. The data base was established according to criteria that was a composite of the selection processes used by Campbell (1981) and Joyner and Boore (1981). The data base included both North American and

Table 1

Relative Contribution to Ground Motion Variability for Peak Ground Acceleration

Effect	Contribution (%)
Source	26
Propagation	29.5
Local Geology	29.5
Building Effects	15

Table 2

Summary of PGA and RMS_a Statistics

	Peak Acceleration			RMS_a (VL)		
Model	r^2	σ	10^{σ}	r^2	σ	10^{σ}
M1	0.84	0.158	1.44	0.80	0.182	1.52
M2	0.85	0.154	1.43	0.80	0.181	1.52
M3	0.81	0.175	1.50	0.75	0.207	1.61
M4	0.76	0.174	1.49	0.75	0.188	1.54

foreign events. The maximum horizontal value at a recording station was used. The source-site distance was measured from the recording station to the closest point of rupture on the fault. The characterization of earthquake size was expressed in terms of moment-magnitude (Hanks and Kanamori, 1979). The data base was fixed throughout the study and is summarized in McCann et al. (1983). To avoid possible bias, estimates of the RMS_a were obtained using the strong motion duration measures of Vanmarcke and Lai (1980), Trifunac and Brady (1975), and McCann (1980). To describe the attenuation of the PGA and RMS_a with magnitude and distance, four mathematical relationships are used. The selection of the four relationships was not made strictly on the basis of which were the four most appropriate models. Rather, consideration was given to making selections that represented a range of reasonable possibilities. The first model, M1, is similar to the relationship recently used by Joyner and Boore (1981), which is expressed by the following equation,

$$\log_{10} Y = a + bM + d \log_{10}(R^2 + h^2)^c \qquad (6)$$

where Y is the ground motion parameter and c is taken as 1/2. Equation 6 differs slightly from the relation used by Joyner and Boore (1981) in two main respects; first the coefficient on the geometric spreading term is allowed to vary, whereas Joyner and Boore (1981) had set d = -1; and a term to account for anelastic attenuation is not included.

Model M2 corresponds to the functional form described by Campbell (1981) which can be expressed as

$$\log_{10} Y = a + bM + d \log_{10} (R + c_1 \exp c_2 M)) \qquad (7)$$

The significant feature of this equation is the magnitude dependent term, c1 exp c2M, which describes the transition from near-field to far-field attenuation. As implied here, and rejected in equation 6 is a distance saturation that depends on the extent of the fault rupture zone.

The third model, M3, was developed from consideration of the expression for the near-field response of an elastic whole space (Aki and Richards, 1980). From this expression, the attenuation of ground motion amplitudes was inferred to obtain the following general form,

$$\log_{10} Y = a + bM + d \log_{10} \left(\frac{c_1}{R^2} + \frac{c_2}{R}\right) + eR \qquad (8)$$

The significant feature here is the incorporation of the first and second order geometric spreading terms, R^{-1} and R^{-2}, respectively. Also, the term eR is included to account for anelastic attenuation. With respect to the objectives of this study, model three provides a unique variation in functional form that will further test the impact of modeling assumptions on attenuation.

The fourth model, M4, is a linear relationship of the form,

$$\log_{10} Y = a + bM + d \log_{10} (R + h) \qquad (9)$$

Equation 9 is a relationship that has been used in a number of studies in the last twenty years (Esteva and Rosenblueth, 1964; McGuire, 1978; among others). The constant term h is arbitrarily taken as 25, a value typically used. Clearly, a best fit of the data would be better achieved had h been a value derived in the regression analysis. Recall this was the case in equation 6. However, in order to investigate the potential variability in prediction equations, the simplicity of eq. 9 and its historical perspective provide the principal motivation for its selection. In an approach similar to that used by Campbell (1981), a weighting scheme was used in the regression analysis.

Thus, for PGA four attenuation relationships were derived and for RMS_a a total of twelve were developed. From these results the influence of functional form on ground motion predictions (i.e., PGA or RMS_a) and RMS_a measure on predicted values were considered. A summary of these results are given below.

In Figure 3, the four models for PGA for magnitudes 5.5, 6.5 and 7.5 are shown. Table 2 summarizes the statistics of the regression analysis in terms of r^2, the goodness-of-fit

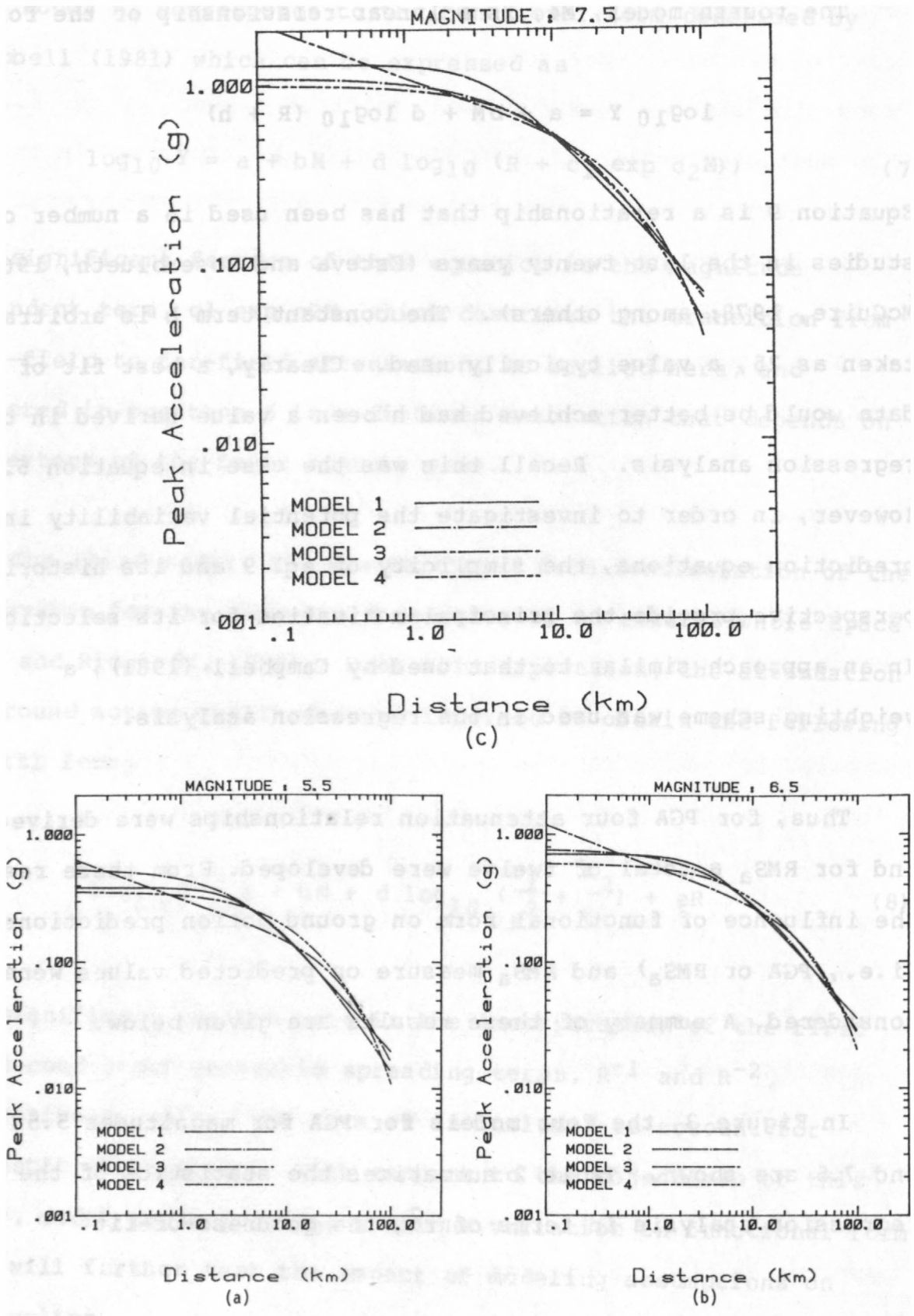

Figure 3. Comparison of the four attenuation models for peak acceleration for magnitudes, (a) 5.5, (b) 6.5, and (c) 7.5.

measure, σ_{log} the logarithmic standard deviation and the factor 10^{σ}.

We find the largest variation in the median PGA estimates for the four models is ±50%. As might be anticipated this difference occurs at very short distances (<1 km). Beyond this distance variations are typically ± 20% or less. As noted previously, the scatter in the data corresponds to a factor that ranges from 1.43 to 1.50.

For RMS_a similar comparisons can be made for the three duration measures. We report here only the results for the Vanmarcke and Lai method since it gave the best results. Results using the Trifunac and Brady duration were for the most part equivalent in terms of r^2 and σ_{log} comparisons, while the duration measure of McCann had greater scatter. Figure 4 shows the results for $RMS_a(VL)$ for the four models and magnitudes 5.5, 6.5, and 7.5. Table 2 also summarizes the $RMS_a(VL)$ statistics. A principal observation was that in all cases, peak acceleration has lower variability for all four models. As in the case of PGA, the greatest variation in the median RMS_a curves is at short distances.

The sensitivity of the median RMS_a attenuation to the measure of duration is shown in Figure 5 for Model 2 at magnitudes 5.5, 6.5 and 7.5. We observe that the variability is greatest at short distances and low magnitudes where the largest

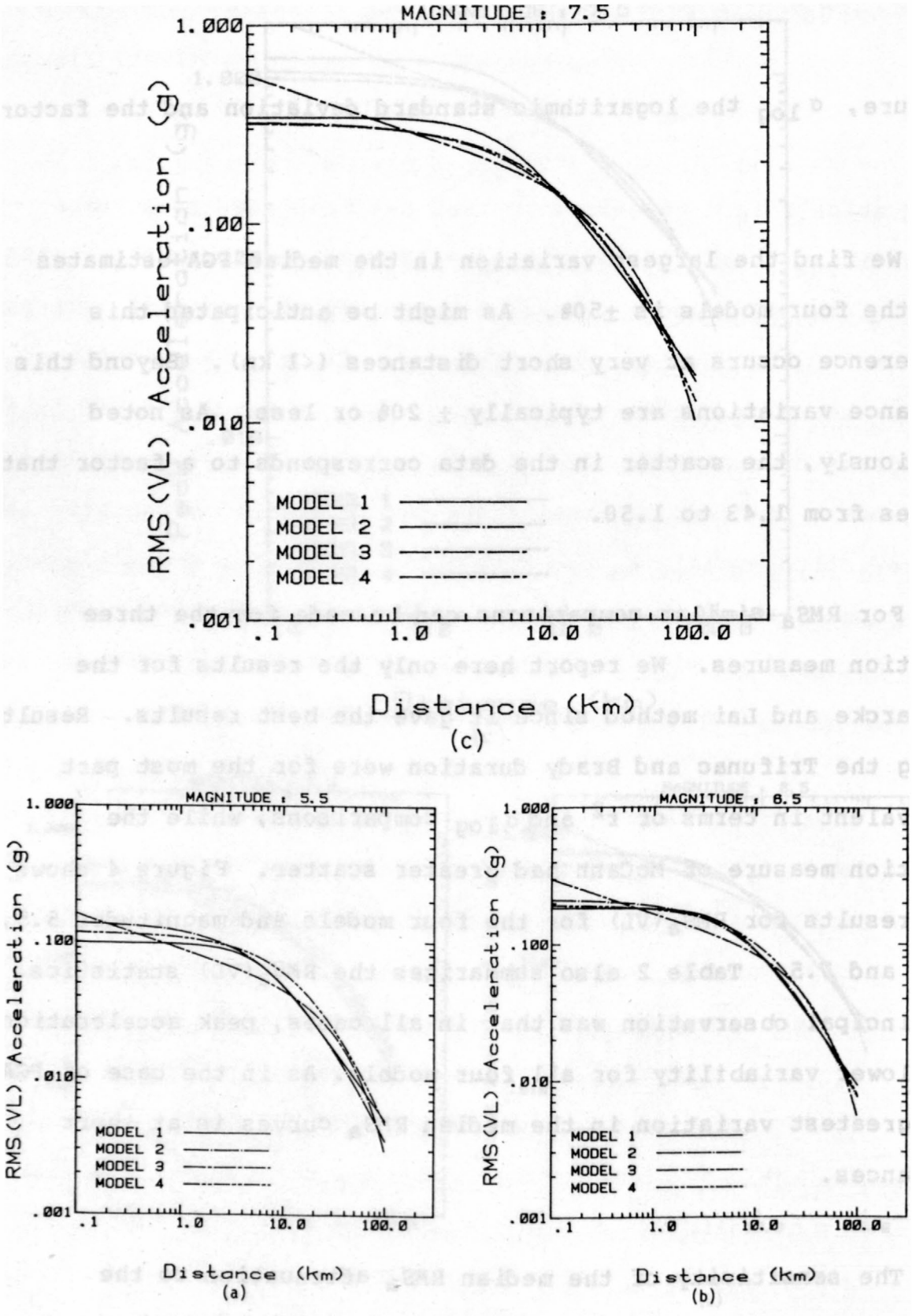

Figure 4. Comparison of the four RMS_a(VL) attenuation models for magnitudes, (a) 5.5, (b) 6.5, and (c) 7.5.

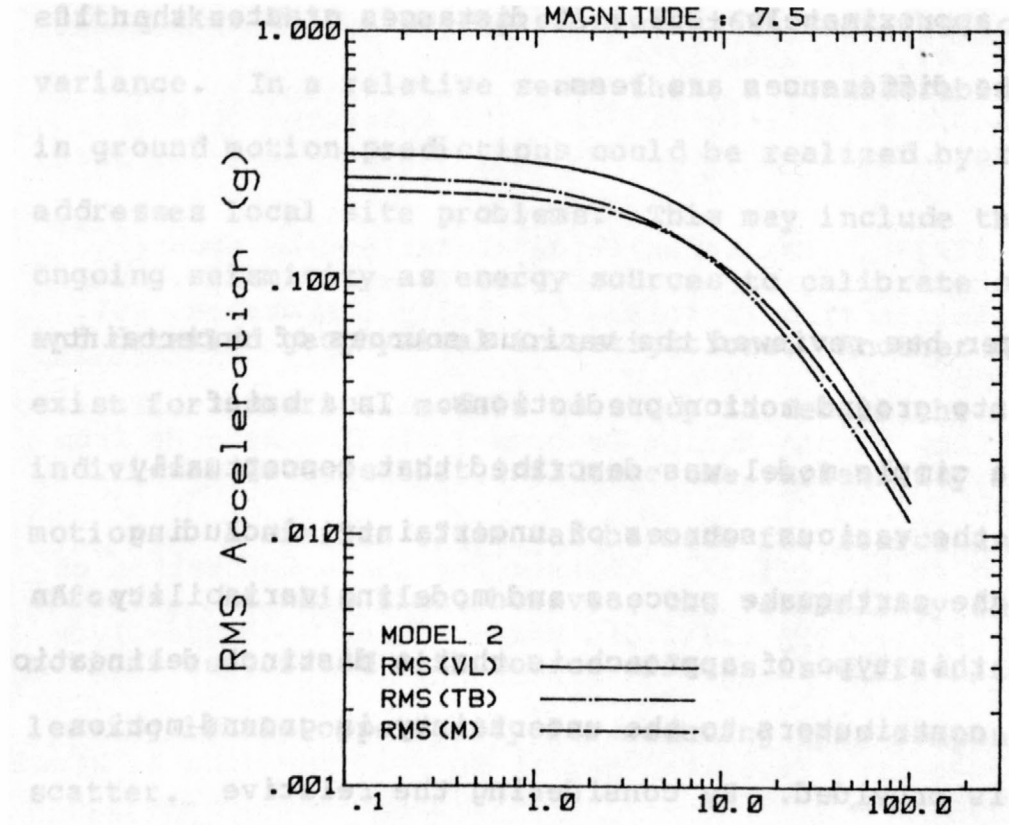

(c)

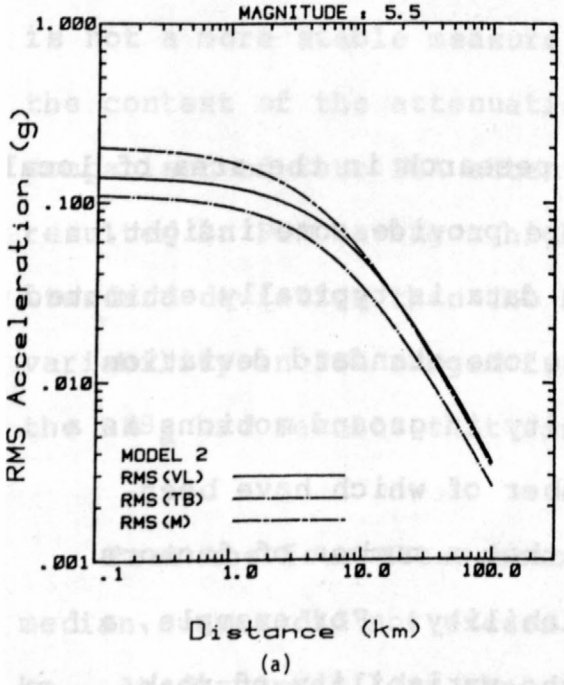

(a)

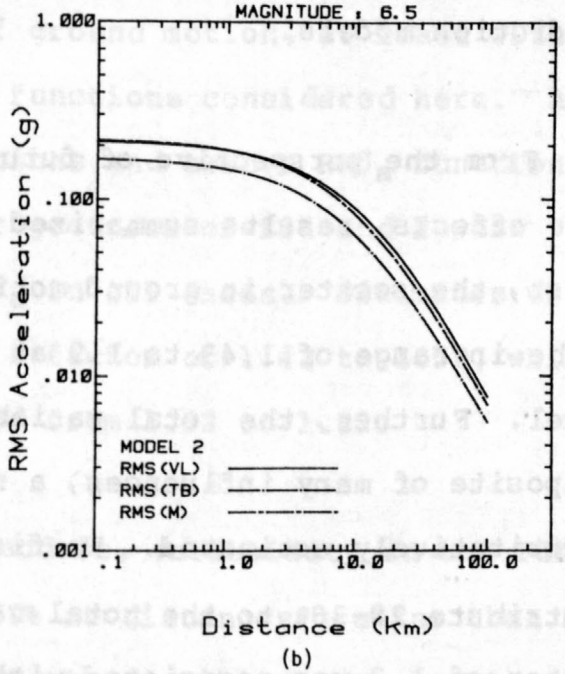

(b)

Figure 5. A comparison of RMS_a attenuation results for Model 2 for the 3 strong motion duration measures for magnitudes (a) 5.5, (b) 6.5, and (c) 7.5.

variation is approximately ±35%. At distances greater than 10 kilometers the differences are less.

DISCUSSION

This paper has reviewed the various sources of uncertainty that enter into ground motion predictions. In a brief discussion, a simple model was described that conceptually accounts for the various sources of uncertainty, including elements of the earthquake process and modeling variability. An advantage of this type of approach is that a distinct delineation of the major contributors to the uncertainty in ground motion predictions is provided. By considering the relative contribution of each element, it is possible to speculate where future research will provide for increased reliability in prediction models.

From the perspective of future research in the area of local site effects, results summarized here provide some insight. First, the scatter in ground motion data is typically estimated to be in range of 1.43 to 1.9 at the one standard deviation level. Further, the total variability in ground motions is a composite of many influences, a number of which have been quantitatively estimated. We find that a number of factors contribute 20-30% to the total variability. For example, a factor of 1.3 was associated with the variability of peak acceleration due to local site effects for the San Fernando

earthquake. This also represented a 60% contribution to the total variance. In a relative sense then, a considerable improvement in ground motion predictions could be realized by research that addresses local site problems. This may include the use of ongoing seismicity as energy sources to calibrate site response and detailed geophysical investigations. Another opportunity may exist for numerical models to study in detail the influence of individual factors that influence the variability in ground motions. A similar claim can be made for source and propagation effects. At this time, however, the variability in ground motions associated with source effects is difficult to analyze, leaving little opportunity for reducing this component of scatter.

From a study of PGA and RMS_a attenuation we find that RMS_a is not a more stable measure of ground motion, at least within the context of the attenuation functions considered here. A comparison of four PGA attenuations and twelve RMS_a functions resulted in PGA having a higher goodness-of-fit and lower standard deviation than the RMS_a in all cases. Estimates of the variability in PGA ranged from a factor of 1.43 to 1.50, while the RMS_a had results that ranged from 1.52 to 1.82.

From the four attenuation models, variability in the PGA median curves did not exceed ±20% at distances greater than 10 km. At distances less then 1 km, the variation was greater, as much as ±50%. For RMS_a, similar observations were made. A

Hanks, T.C. and H. Kanamori (1979). A Moment-Magnitude Scale, J. Geophys. Res. 84, pp. 2348-2350.

Hanks, T.C. and R.K. McGuire (1981). The Character of High Frequency Strong Ground Motion, Bull. Seism. Soc. Am. 71, pp. 655-670.

Idriss, I.M. (1978). Characteristics of Earthquake Ground Motions, Earthquake Engineering and Soil Dynamics, Proc. ASCE Geotechnical Engineering Division, Specialty Conference, Vol. III, pp. 1151-1265.

Joyner, W.B. and D.M. Boore (1981). Peak Horizontal Acceleration and Velocity from Strong-Motion Records Including Records from the 1979 Imperial Valley, Earthquake, Bull. Seism. Soc. Am. 71, pp. 2011-2038.

Kennedy, R.P., et al. (1983). Engineering Characterization of Ground Motion Effects of Characteristics of Free-Field Motion on Structural Response, SMA 12702.01, prepared for Woodward-Clyde Consultants.

McCann, Jr., M.W. (1980). RMS Acceleration and Duration of Strong Ground Motion, Technical Report No. 46, The John A. Blume Earthquake Engineering Center, Stanford University.

McCann, Jr., M.W. and D.M. Boore (1983). Variability in Ground Motions: Root Mean Square Acceleration and Peak Acceleration for the 1971 San Fernando, California Earthquake, Bull. Seism. Soc. Am. 73, pp. 615-632.

McCann, Jr., M.W., H. Echezuria, and E. Kavazanjian, Jr. (1983). RMS and Peak Ground Acceleratlon Attenuation, JBA 139-010-01, prepared for the U.S. Geological Survey (in preparation).

McGuire, R.K. (1978). Seismic Ground Motion Parameter Relations, Proc. Am. Soc. Civil Eng., J. Geotech. Eng. Div. 104, pp. 481-490.

Trifunac, M.D. and A.G. Brady (1975). A Study of the Duration of Strong Earthquake Ground Motion, Bull. Seism. Soc. Am. 65, pp. 581-626.

Vanmarcke, E. H. and S.P. Lai (1980). Strong Motion Duration and RMS Amplitude of Earthquake Records, Bull. Seism. Soc. Am. 70, pp. 1293-1307.

comparison of RMS_a attenuations for different measures of duration indicated that the largest variation did not exceed ±35%, again at short distances. Beyond 10 km this difference was less.

ACKNOWLEDGEMENTS

The partial support of the U.S. Geological Survey under contracts USGS-14-08-0001-20528 and USGS-14-08-0001-2059 is gratefully acknowledged. The findings and opinions expressed are those of the author and do not represent the official policies, either expressed or implied, of the United States Government.

REFERENCES

Aki, K. and P.G. Richards (1980). Quantitative Seismology, Theory and Methods, W. H. Freeman and Company.

Boore, D.M. and W.B. Joyner (1982). The Empirical Prediction of Ground Motion, Bull. Seism. Soc. Am. 72, pp. S43-S60.

Boore, D.M. (1983). Strong Motion Seismology - 1979 Through 1982, in U.S. National Report to International Union of Geodesy and Geophysics 1979-1982, American Geophysical Union.

Campbell, K.W. (1981). Near-Source Attenuation of Peak Horizontal Acceleration, Bull. Seism. Soc. Am. 71, pp. 2039-2070.

Cornell, C.A. (1982). Sources and Uncertainty in Treatment of Ground Motion Prediction (Abstract), Earthquake Notes 53, p. 45.

Esteva, L. and E. Rosenblueth (1964), Espectros de Temblores a Distancias Moeradeas y Grandes, Soc. Mexicana de Ingenienaia Sismica Bol., v. 2, pp. 1-18.

Hanks, T.C. (1975). Strong Ground Motion of the San Fernando, Calif. Earthquake; Ground Displacements, Bull. Seism. Soc. Am. 64, pp. 193-225.

SOIL-STRUCTURE INTERACTION EFFECTS AT ACCELEROGRAPH STATIONS

by

C. B. Crouse
Ertec, Inc.
3777 Long Beach Boulevard
Long Beach, California 90807

INTRODUCTION

Theoretical studies (Bycroft, 1978; McNeil, 1982) and recent experimental investigations (Crouse and Liang, 1983) suggest that soil-structure interation has influenced the ground motions recorded at some accelerograph stations that were originally thought to be immune from these interaction effects. These studies, as well as comparisons of ground motions recorded on a concrete pad and in the adjacent free-field (Haar et al, 1982), indicate that motions recorded at accelerograph stations can be amplified. The purpose of this paper is to discuss the conditions under which amplications may occur at accelerograph stations and to suggest methods to avoid the problem when constructing future stations.

DESCRIPTION OF ACCELEROGRAPH STATIONS

A schematic of a typical, "free-field" accelerograph station found in the U.S., Italy, China, and Japan is shown in Figure 1. The station consists of a rectangular concrete pad partially embedded in the ground. In some cases the pad will be anchored by means of a small cylindrical concrete pier that may extend as much as 1m deep into the ground. The plan dimension of the pad is generally between 1-2m and the thickness varies between about 0.2-0.6m. The strong motion instrument is bolted directly to the top of the pad, or in the case of some stations, to the top of a cylindrical pedestal, which serves to protect the instrument from potential flooding. Shelter is provided by a housing structure 1-2m tall that is made of plywood, brick, concrete, fiberglass, or aluminum siding.

SOIL-STRUCTURE INTERACTION EFFECTS

Based on the theory of soil-structure interaction, the factors that can influence the motions recorded at an accelerograph station include:

- size of the concrete pad
- amount of embedment of the concrete pad
- location of instrument on pad
- size and stiffness of the shelter and its attachment to the pad
- properties of the foundation medium
- frequency content of earthquake ground motions.

Because of their relatively small size, and because they are generally constructed on stiff soil or rock, existing accelerograph stations will not appreciably influence the motions recorded during earthquakes unless the earthquakes are located close to the stations. High frequency motions generated during nearby earthquakes can be amplified by the accelerograph station due to soil-structure interaction (Bycroft, 1978; McNeil, 1982; Crouse and Liang, 1983). The response spectra of the recorded motions at the lower frequencies could also be amplified due to the amplification of the higher frequencies.

An example of the theoretical amplification that could occur at a typical installation is shown in Figure 2, which is a corrected version of Figure 8 from Bycroft (1978). The peak in the amplification curve at approximately $a_o = 2\pi fa/\beta = 1.2$ would occur at a frequency of f = 25 Hz for an equivalent radius of the pad, a = 1.2m, and a shear-wave velocity for the foundation soil, β = 160m/s. Larger or smaller amplifications are possible depending on the various factors influencing the soil-structure interaction listed above.

To reduce possible amplification effects at accelerograph stations, the installations should be as small as possible. Some minimum size is required to adequately house the instrument and other supporting equipment, but for most stations a 1-m square concrete pad about 0.2m thick would be sufficient. The pad should be embedded or anchored in the ground to increase the foundation stiffness or impedence. The instrument should be mounted at the center of the pad close to the ground surface. This will minimize the translational components of the pad's rocking and torsional motions that the instrument would record

during an earthquake. Thus, pedestals that substantially elevate the instrument should be avoided.

The shelter design should not be overlooked either. Lightweight fiberglass or aluminum construction is ideal. Tall and heavy shelters, such as those made of thick plywood, brick or concrete, could affect the response of the pad. The connection between the larger shelters and the pad is also important. For example, if the shelter is extremely stiff and is rigidly attached to the pad, the fundamental natural frequency of the system would decrease and the rocking response of the pad would tend to increase, which in turn could further amplify the recorded motions. On the other hand, if the connection is flexible, an extra degree of freedom and, hence, natural frequency will be introduced to the system, which could result in significant amplification in one more frequency band.

As the stiffness or shear-wave velocity of the ground medium supporting the pad decreases, the natural frequency of the station decreases. Thus, if motions on relatively soft alluvial deposits are not the motivating factor in site selection for a particular accelerograph station, then the station should be located on the stiffest material in the region of interest to minimize any potential amplification in the lower frequencies.

REFERENCES

Bycroft, G.N., 1978, The effect of soil-structure interaction on seismometer readings: Bull. Seism. Soc. Am., Vol. 68, No. 3, p. 823-843.

Crouse, C.B. and Liang, G.L., 1983, Experimental study of soil-structure interaction at an accelerograph station: Earthquake Notes, Eastern Section SSA, Vol. 54, No. 1, p. 56.

Haar, L.C., Fletcher, J.B., and Semberra, E., 1982, A preliminary analysis of digital seismograms from the Arkansas earthquake swarm of 1982: EOS, Vol. 63, No. 45, p. 1024.

McNeil, R.L., 1982, Some possible errors in recorded free-field ground motions: Earthquake Notes, Eastern Section SSA, Vol. 53, No. 1, p. 90.

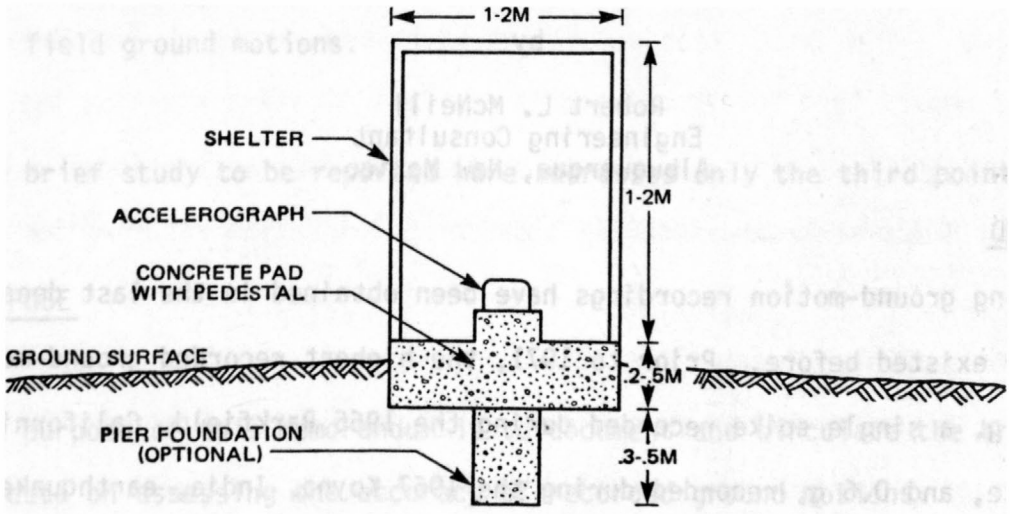

FIGURE 1. TYPICAL ACCELEROGRAPH STATION

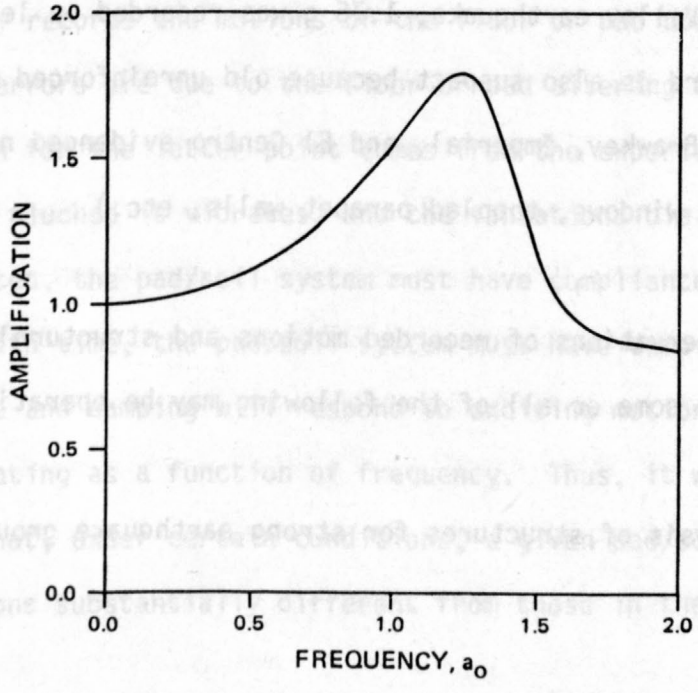

FIGURE 2. AMPLIFICATION VERSUS DIMENSIONLESS FREQUENCY (MODIFIED FROM BYCROFT, 1978)

Some Possible Errors in Recorded Free-Field Ground Motions

by

Robert L. McNeill
Engineering Consultant
Albuquerque, New Mexico

BACKGROUND

More strong ground-motion recordings have been obtained in the last decade than ever existed before. Prior to 1971, the highest recorded ground motions were 0.5 g, a single spike recorded during the 1966 Parkfield, California, earthquake, and 0.6 g, recorded during the 1967 Koyna, India, earthquake. In the 1971 San Fernando, California, earthquake, 1.24 g was recorded on the abutment of Pacoima Dam. That record is suspect in an engineering sense because the masonry chimney on the nearby caretaker's house did not fall, whereas experience in that earthquake indicates that masonry chimneys in the area toppled at accelerations considerably smaller than the recorded 1.24 g. In the 1979 Imperial Valley earthquake, 1.75 g was recorded on level ground at Station 6. That record is also suspect because old unreinforced masonry structures in nearby Brawley, Imperial, and El Centro evidenced no or only slight damage (broken windows, toppled parapet walls, etc.).

These comparative observations of recorded motions and structural behavior seem to indicate that some or all of the following may be operative:

1. The dynamic analysis of structures for strong earthquake ground motions is inaccurate.

2. Structures respond with motions different from those recorded on small instruments in the free field.

3. Seismographs placed in the free field do not faithfully record the free-field ground motions.

The brief study to be reported here addresses only the third point.

PURPOSE

The purpose of this memorandum is to document and circulate the brief studies to date on assessing the accuracy of recorded ground motions.

INTRODUCTION

Free-field instruments are normally located on the floor of a small building or on small concrete pads. The present study will assume that the instrument faithfully records the motions of the floor or pad upon which it rests; and that any errors are due to the floor or pad altering the ground motions. The motivation for the latter point comes from the experience that if such a floor or pad is plucked it vibrates, and the vibrations die out with time. If the pad vibrates, the pad/soil system must have compliance; and if the vibrations die out with time, the pad/soil system must have damping. Any system with compliance and damping will respond to exciting motions by either amplifying or attenuating as a function of frequency. Thus, it would not be surprising to find that, under certain conditions, a given pad/soil system could respond with motions substantially different from those in the adjacent free field.

LITERATURE REVIEW

A number of papers have been published in the last 40 years alerting the profession to the possibility of errors in free-field ground-motion recordings. A landmark experimental study for its time was reported by Washburn and Wiley (1941). For these experiments two vertical seismometers were bonded together one above the other, and were circuited so that one could act as a driver and the other as a pickup. The resulting seismometer pair was then exercised on various soils, with and without bases, and with and without weights. The resulting data, which are analyzed in detail in the next section, clearly show that the seismometer pair exhibited strong response, and would be expected to modify free-field motions to an appreciable degree (e.g., amplications by as much as 6 1/2, attenuation to as much as 0.2).

Washburn and Wiley had no theoretical basis upon which to analyze their results, but Wolf (1944) published on approximate theory based on an ideally elastic earth. Wolf's derivation was based on the widely shared position at the time that some effective mass of soil participated in the motion. The operating mass was therefore taken to be the mass of the seismometer plus the effective mass of the participating soil. The problem, of course, is to formulate the effective mass and the compliance and damping of the soil. Wolf mentioned the Washburn and Wiley experiments, but chose to analyze them in the paper in only the most cursory fashion. The approximate derivation clearly showed that ground-emplaced seismometers could distort free-field motion.

The problem was also studied in Russia, Pasecnik (1952), where experiments were performed using the scheme of Washburn and Wiley, and analyzing the

results of Wolf's approximate method. The results clearly demonstrated that a seismometer can alter free-field ground motions.

A complete and exact formulation of the response of a rigid circular plate vibrating at the surface of an elastic half-space was presented by Bycroft (1956). The theoretical results are somewhat tedious to use, involving reference to influence charts for some functional relationships needed in calculations.

All of the above experimental and theoretical studies address the problem of response of a seismometer: that is, if the seismometer is vibrated (from above), how does the seismometer/soil system respond? The problem which needs to be addressed is transmissibility: that is, if the seismometer/soil system is vibrated (from below), how does the seismometer/soil system transmit the motion to the seismometer? The two problems are quite different. Figure 1 shows the response curves for constant-force excitation, Figure 1(a), and the transmissibility curves for ground excitation, Figure 1(b). Reference to the applicable transmissibility curve of Figure 1(b) shows that ground motions will be least distorted (i.e., transmissibility 1) at frequencies less than the natural frequency if the natural frequency and/or the damping are high. Thus soft (low frequency) and/or lightly damped systems are expected to distort ground motions.

These facts were recognized by Bycroft (1957), who extended his earlier work to the transmissibility case. It was concluded that, "The mass of a ground measuring instrument will substantially alter the motion of the pick-up point and radically alter the shape of any complex train of waves it is receiving

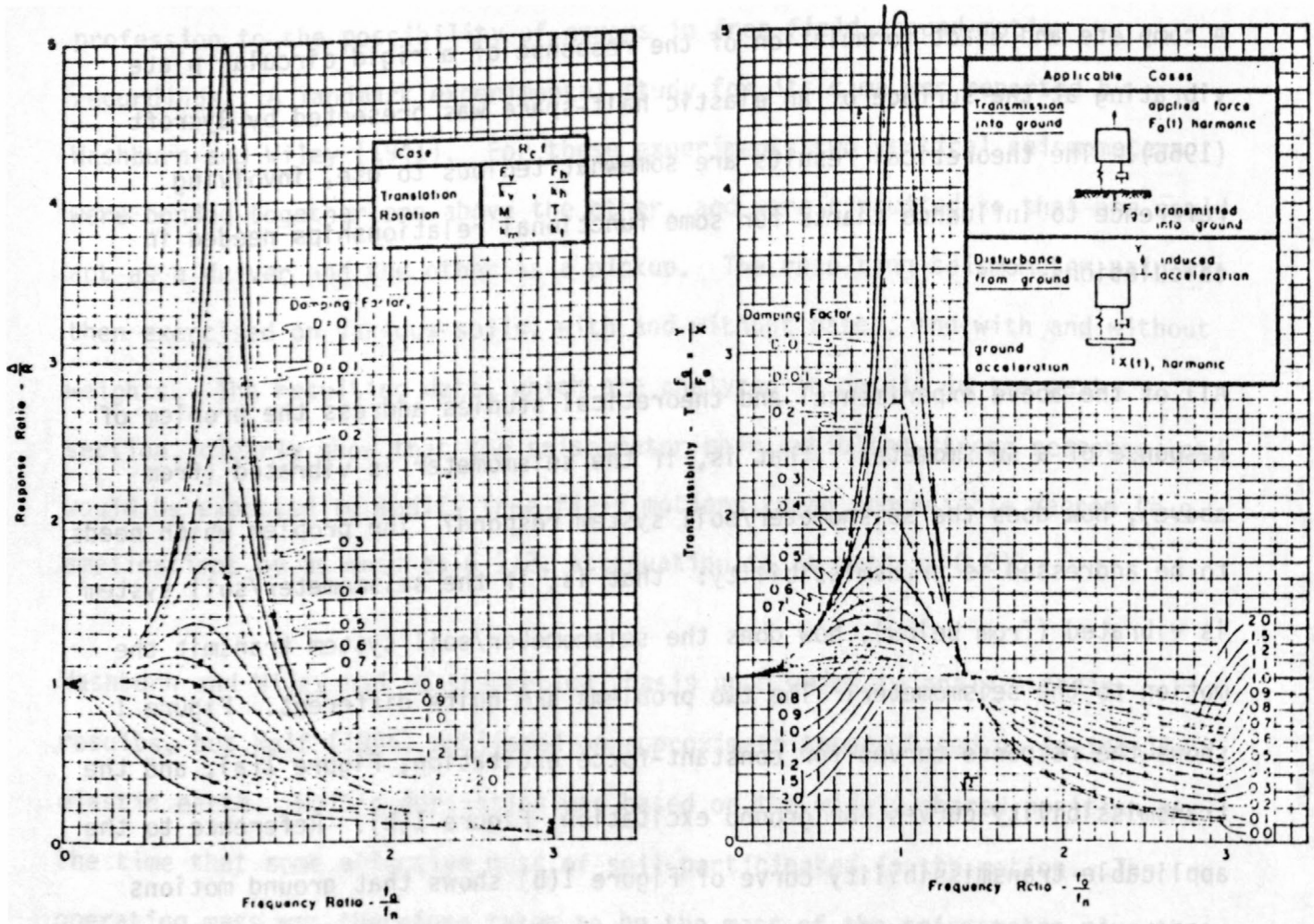

Constant-Force Response Curve

Transmissibility Curve

Figure 1. Vibration Curves, McNeill (1969).

both by amplitude and phase changes." That statement seems clear, and it was published in the Transactions of the American Geophysical Union in 1957.

Later, the French, Fail et al (1963), published the results of over 1,250 seismograph-coupling experiments, in the laboratory and in the field. They used the experimental methods of Washburn and Wiley (1940), coupling two seismographs so that one was the driver and the other the pickup. They confirmed that the Bycroft (1957) approach gives correct orders of magnitude of the amplification of a seismograph. They recommended that small devices for geophysical prospecting be tightly anchored to the ground. They also demonstrated that the response of a seismograph is a close function of the properties of very-near-surface soils.

It has often been observed that rocks, benches, gravestones and other unsecured objects are thrown up and displaced from their original positions after an earthquake. These occurrences have sometimes been used to deduce that the sustained vertical acceleration must have been greater than 1 g in that earthquake. The situation was treated by Newmark (1973) and by Bolt, et al (1977). Both used discrete-particle mechanics, which is admittedly a gross simplification of the situation. Nevertheless, both studies showed that flat objects founded on soft ground could amplify ground motions. Newmark concluded that "rocks of 2 to 3 ft. in height might be possible candidates for upthrow under vertical earthquake ground acceleration of the order of about 0.5 g". Bolt, et al analyzed the excursions of a fire truck, which was in gear with the brakes set, during the 1971 San Fernando Earthquake: "A 20-ton fire truck enclosed in the garage moved 6 to 8 ft. fore and aft, 2 to 3 ft. sideways, without leaving visible skid marks on the garage floor. . . . Marks

which appear to have been made by the right rear tire were found on the door frame, 3 ft. above the floor, while the metal fender was not damaged."

Bolt calculates that the truck would have lifted off the garage floor at a vertical minimum ground acceleration of 0.1 g (a correction to his theoretical derivation yields a value of 0.22 g, RLM). Although the derivations in these works are approximate, they indicate that the response of ground-founded objects can exceed the free-field ground vibrations.

An attempt to minimize the distortion (amplification) of ground motions has been presented by Safar (1978). The geophone-soil system damping can be increased by installing an array of closely spaced geophones and processing the results properly. Reference to Figure 1(b) shows that increasing the damping lowers the amplification factor for lower frequencies (i.e., less than 1.4 times the natural frequency), and raises the attenuation factor for higher frequencies. Safar also recognized that the. distortion problem is in general greatest on softer soils. The array idea seems to be the first attempt to do something about the problem, but it probably is not practical for earthquake seismometry because of the number of instrument installations required.

Another effort to quantify the situation and to present a solution has been presented by Bycroft (1978). He extended his earlier work (1957) to include a solution for coupled horizontal translation and rocking motions of a typical modern (USGS) seismometer installation. He presented several examples to show that, for a seismometer mounted on a small flat slab, the soil/slab system could easily multiply the free-field motions by factors of more than two. He then suggested that seismometers might under certain conditions better be

buried, and proceeded to demonstrate theoretically that a small buried seismometer will trivially distort the free-field motions. (Note, Sandia buries the seismometers at NTS-RLMc.) Finally, Bycroft derived the form of a transfer function which might be used to convert the motions of a seismometer-slab-soil system to free-field motions.

Graphic evidence of the amplification phenomenom has been provided by McJunkin (1979). In 1972, California initiated a Strong-Motion Instrumentation Program (SMIP). The standard SMIP installation chosen is a 3-ft. square concrete pad, about 5 in. thick, supporting a 16-in. cube of concrete upon which the seismometer is placed. To protect the seismometer, a 0.4-in. thick iron dome is placed over the concrete cube. The dome is larger than the cube, so that the installation resembles a stubby inverted pendulum. These installations have been producing accelerograms for almost a decade. In mid 1978, a seismometer installation similar to many USGS installations was placed about 20 ft. away from a SMIP installation. A magnitude of 4.9 earthquake occurred about 6 mi. from the site, and both installations produced high-quality records. The results are as follows:

	Peak Acceleration at Installation	
Component	USGS	SMIP
Horizontal-T	0.11g	0.22g
Horizontal-L	0.10g	0.16g
Vertical	0.04g	0.05g

The SMIP installation amplified the horiziontal components by 1.6 and 2.0, and the vertical component by 1.25, compared to the USGS installation. No information was offered on the distortion of the free-field motions by the USGS installation. California no longer publishes records from the SMIP installations, McJunkin (1981).

Finally, analysis of the main shock and the well recorded strong aftershocks of the 15 October 1979 Imperial Valley earthquake (magnitude 6.9) indicate that some installations systematically recorded more than and less than other installations. For the main shock, and for aftershocks located north, south, and west of the seismometer array, there is, with but few exceptions, a hierarchy of recorded values. For example, during the main shock and four large aftershocks, Station 6 recorded average horizontal motions which were 1.42 and 2.65 times the nearest stations (5 and 7, each 1 km) away, and average vertical motions which were 1.58 and 3.25 times those stations. Those are not trivial factors. In fact, the performances of the seismometers are so consistent that it is possible to identify a predictable hierarchy for their relative responses when the hypocentral distances are the same for the small ($M \approx 3$, aftershocks or when distances to the fault are the same for the larger ($M \approx 6$) aftershocks:

$$6 > 5 > 7 > 8 > 4$$

The theoretical and experimental results presented above seem to make clear the conclusion that seismometer installations can, under some conditions, record motions different from those in the free field, and by substantial factors. It is not presently clear, however, what the conditions are for

distorted records, and what corrections should be applied to derive usable information. Some suggestions for pursuing these lines will be made in the following sections. In the meantime, it would be difficult to assign any quantitative engineering value to any recorded instrumental free-field strong motion record.

ANALYSIS

The elastic half-space derivation of Bycroft (1956, 1957, 1978) offers a method for analyzing the situation to provide tentative answsers to the questions:

1. Under what conditions do seismometer installations distort free-field motions?

2. What corrections should be applied to seismograph records to obtain usable information?

It is expected that those tentative answers will be used to plan definitive experiments to provide firm answers, if such exist.

The half-space calculational methods have been simplified as reported by McNeill (1969) and by Luco and Westmann (1971). The method has enjoyed wide engineering use, and many case histories are reported in the literature, McNeill, et al (1965; 1967a, b; 1968), Margason, et al (1969). The case histories clearly show that, when applied properly, the method yields good engineering results. Controlled vibration, Anandakrishnan (1973) and impact,

Barneich, et al (1974), experiments have been reported on small (3- to 6-ft. diameters) concrete foundations, indicating excellent agreement between theory and experiment for such controlled conditions. The case histories and experiments reported are mostly for response, where the excitation is on the slab, rather than for transmissibility, which is the present case; and all of them dealt with competent soils. Thus there is a need to verify the theory for the case of ground-motion excitation, and for all soil stiffnesses. That will be partially done in this section using results from the literature. The following section will then outline some proposed controlled experiments.

The literature data to be analyzed are taken from Washburn and Wiley (1941). They reported the appropriate sizes and weights for each experiment, the response of the seismometer pair as a function of frequency, and a verbal description of the surface-soil conditions. They did not report any measure of the stiffness of the soil, such as the shear-wave velocity.

The shear-wave velocity can, however, be backcalculated by the half-space theory, as will now be developed.

Table 1 gives the pertinent simplified equations. In the usual case, where the foundation and soil properties are known and the response is desired, the given radius, r, and loaded weight, W, of the foundation, along with the unit weight, and Poisson's ratio, , for the soil, are used to compute a convenient mass ratio, B (Eqn 1), for the appropriate direction of vibration. The ratio B is then used to compute the damping ratio, D (Eqn 2), as a proportion of critical damping for the system; and, along with the soil shear-wave velocity, Cs, the ratio B is used to compute the natural frequency,

f (Eqn 3). The natural frequency and damping are then used with Figure 1(a) or 1(b), depending upon the nature of the problem, to select the proper curve, for which response or transmissibility ratio can be calculated for any excitation frequency.

In the present case, the foundation (seismometer) properties and the response as a function of frequency are given, and the soil-properties are backcalculated. Before explaining how this is done, it is necessary to explain from experience that it is in general not reasonable to assume that the rigid base of a small, light seismometer will be always in complete contact with the ground unless that ground is very soft or unless some unusual precautions have been taken. Thus any calculation should start by calculating the effective area or radius actually in contact with ground for that experiment. That is done by first measuring the reported response ratio and peak frequency from the experimental response curve. For example in Figure 2, from Washburn and Wiley (1941), the response ratio for Case A is about 2.2; and the peak frequency is about 65 cps. Referring to Figure 1(a), a response ratio of 2.2 corresponds to a damping ratio of about 0.24. When Eqn 1 and 2 in Table 1 are combined to solve for the effective radius, the result in terms of the experimental damping and weight of seismometer is given in En 4. It is necessary to choose values of unit weight and Poisson's ratio for the soil; but because these vary but little for all soils, this is not a serious choice (values of 110 pcf and 0.25 were assumed for these calculations). The effective radius is then used in all further calculations. The mass ratio is calculated from Eqn 1. The shear-wave velocity is then calculated for that particular experiment by Eqn 5 (which follows from Eqn 3), using the measured peak frequency. Some examples will now be presented.

The experiments of Figure 2 involved: case A, seismometer radius 0.18 ft.; case B, seismometer mounted on base of radius 0.42 ft. It is assumed that both experiments were carried out at the same site at about the same time. Using the response ratio from Figure 2, reference to Figure 1a yields damping ratios of 0.24 and 0.35 for A and B, respectively. Application of Eqn 4 for Case A yields r = 0.18 ft.; indicating that A was in 100 percent contact. This is not surprising: application of Eqn 5 yields a shear-wave velocity of 135 fps, indicating a very soft soil. Thus even the most cursory pressure would probably have seated the small seismometer. Case B is somewhat different, however. The radius is given as 0.42 ft., and the added weight of the base is about 1 lb. Thus if the base were steel, it would only be about 1/16 in. thick; and if of wood, about 1/2 in. Either of these might be somewhat flexible, depending upon the amplitude of the excitations; and the larger size would lessen the chances of complete contact over a perfectly plane surface. It is encouraging then to calculate an effective radius of 0.25 ft. in support of the physical expectation. It is further encouragement to calculate a shear-wave velocity of 125 fps, compared to 135 fps calculated for case A.

Figure 3 shows three experiments, assumed to be at the same site and at about the same time, where the seismometer base area was held constant, but the seismometers were weighted. The base area of the seismometer was not given. It was therefore assumed that the heaviest, 27 lb, was the most likely to be in full contact. The calculated radius was 0.21 ft. The same calculation for case B, 16 lb, was 0.18 ft. Therefore, recalling the experiment of Figure 2 where the radius was reported as

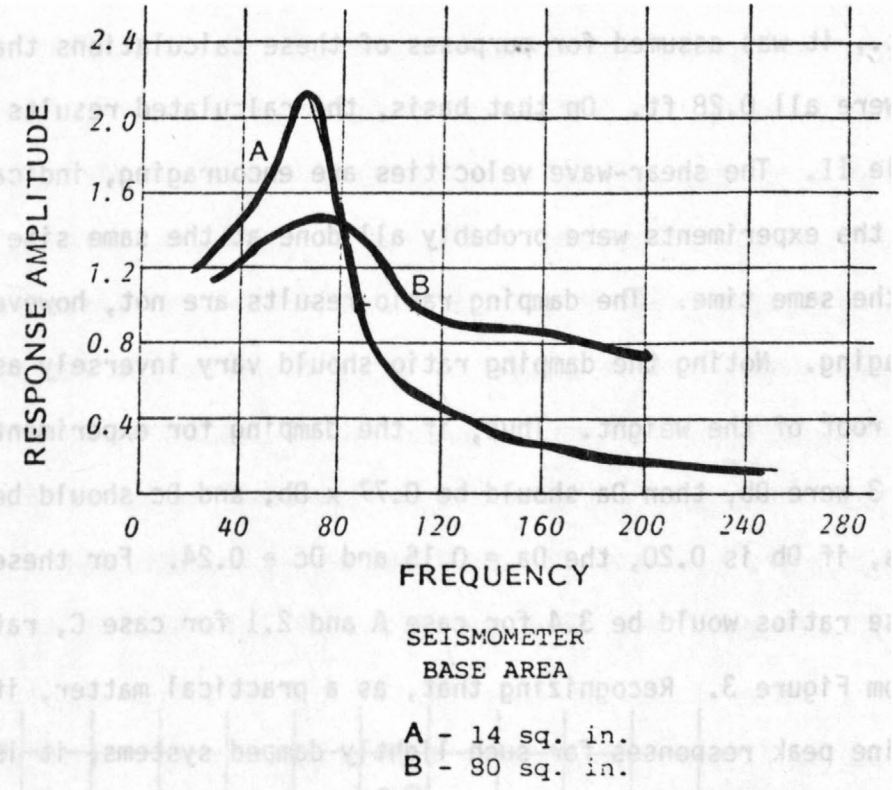

Figure 2. Seismometer response for two base areas.

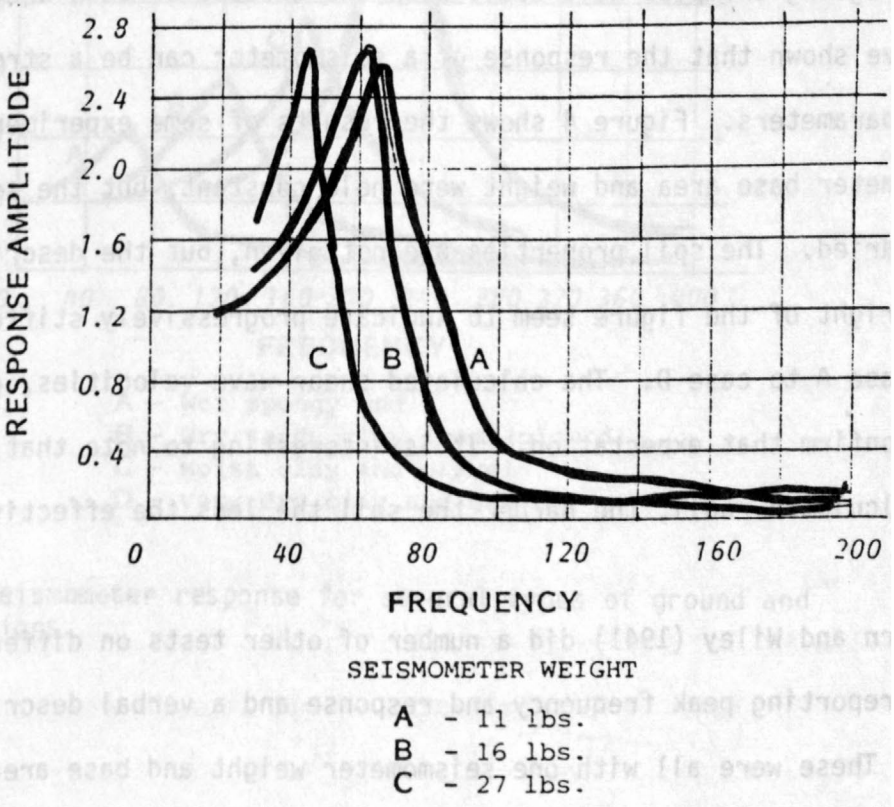

Figure 3. Response for three seismometer weights.

0.25 ft., it was assumed for purposes of these calculations that the radii were all 0.28 ft. On that basis, the calculated results are given in Table II. The shear-wave velocities are encouraging, indicating that indeed the experiments were probably all done at the same site and at about the same time. The damping ratio results are not, however, so encouraging. Noting the damping ratio should vary inversely as the square root of the weight. Thus, if the damping for experimental case B in Figure 3 were Db, then Da should be 0.77 x Db, and Dc should be 1.21 x Db. That is, if Db is 0.20, the Da = 0.15 and Dc = 0.24. For these values the response ratios would be 3.4 for case A and 2.1 for case C, rather than the 2.6 from Figure 3. Recognizing that, as a practical matter, it is difficult to define peak responses for such lightly damped systems, it is assumed for this study that the experimental data are slightly in error.

The foregoing examples have dealt with the effects of base area and weight, and have shown that the response of a seismometer can be a strong function of these parameters. Figure 4 shows the results of some experiments in which the seismometer base area and weight were held constant, but the soil conditions were varied. The soil properties are not given, but the descriptions in the upper right of the figure seem to indicate progressively stiffer soils going from case A to case D. The calculated shear-wave velocities, given in Table III, confirm that expectation. It is interesting to note that, according to the calculated radii, the harder the soil the less the effective contact area.

Washburn and Wiley (1941) did a number of other tests on different types of soil, reporting peak frequency and response and a verbal description of the soil. These were all with one seismometer weight and base area. The

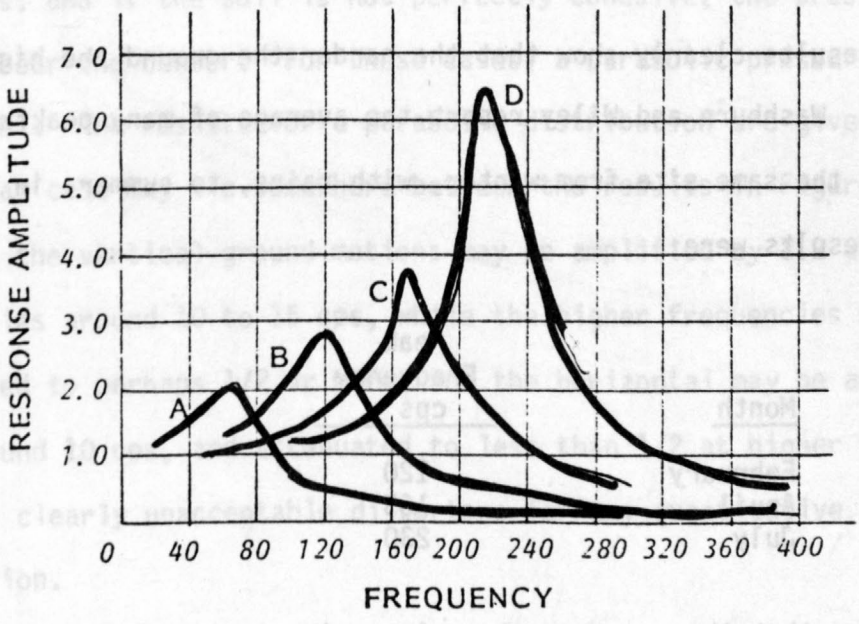

A - Wet spongy mud
B - Dry sandy clay loam (plowed)
C - Moist clay and gravel
D - Very dry clay and gravel

Figure 4. Seismometer response for several types of ground and surface conditions.

calculated radii and shear-wave velocoties are given in Table IV. Of curious interest are cases 2, 6, and 10, where the calculated radii are greater than the 0.18 ft. reported. Such a result would come about if the seismometer were pushed into the soil, but were analyzed as if it were on the surface (which is assumed in these calculations). This is plausible for cases 2 and 6, where the "gumbo" description may refer to the black expansive clays commonly found in southern California where the experiments were apparently done (Pasadena). That explanation would probably only apply to case 10, asphalt, if it were postulated that the seismometers were placed upon a bleed area of asphalt, which could be the case in the summer in California.

The foregoing results clearly show that the harder the ground the higher the peak frequency. Washburn and Wiley report the average of many peakfrequency measurements at the same site from winter, with rains, to summer, in drought. The results were:

Month	Peak Frequency cps
February	120
April	165
July	230

This demonstrates that the response at a given site may not be a constant, if environmental conditions are allowed to affect the soils under the seismometer.

The experiments analyzed were for a very small, light seismometer founded directly on the ground. Thus the peak frequencies were rather high (40 to 200 cps), compared to the frequencies of interest to earthquake engineers (e.g., 0

to 50 cps). to investigate the effects in the frequency range of interest, the transmissibility for case A, Figure 2 was calculated, and is presented in Figure 5. The amplification exceeds 10 percent for frequencies above about 12 cps, and is about 2 for the higher frequencies. For contrast, Figure 6 shows the transmissibility typical of a typical USGS installation as described by Bycroft (1978). the site conditions are the same as for Figure 5. The calculations in Figures 5 and 6 assume that the soil pressure is uniformly distributed over the base. This seems to be a fair assumption in some cases for the small, rigid seismometer case, but it perhaps is not a good assumption for a slab. When undergoing strong ground motion, a slab probably flexes near its edges; and if the soil is not perfectly cohesive, the pressure will be greater near the center. For these cases, a parabolic pressure distribution is assumed. The results for a parabolic distribution are given in Figure 6. The actual case may lie somewhere between the results in Figures 5 and 6. That is, the vertical ground motions may be amplified by 1.2 and 1.5 at frequencies around 10 to 15 cps, while the higher frequencies may be attenuated to perhaps 1/2 or more; and the horizontal may be amplified by 1.4 to 2 around 10 cps, and attenuated to less than 1/2 at higher frequencies. Such are clearly unacceptable distortons for any quantitative engineering application.

To study the matter further, calculations were performed for the standard USGS installation, Bycroft (1978), varying the stiffness of the soil. The results are given in Figures 8 and 9. As the ground becomes stiffer, as measured by the shear-wave velocity, the effect is to increase the peak frequency, which as the effect of flattening the transmissibility curve and stretching it to the higher-frequency end. Based on these

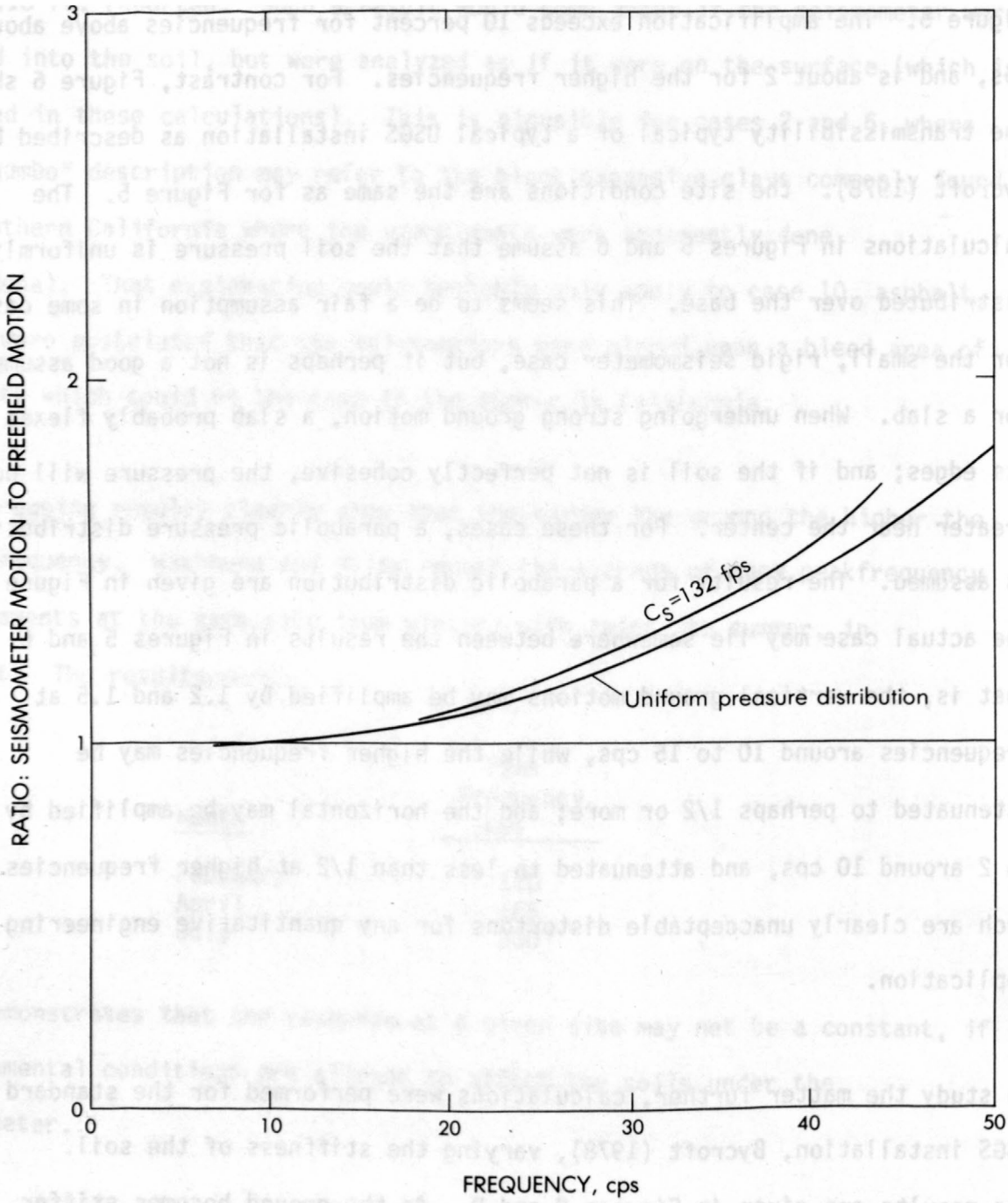

Figure 5.--Transmissibility of Washburn and Wiley Seismomenter, using response-calculated shear-wave velocity, C_s = 132 fps and assuming uniform pressure distribution under seismometer case.

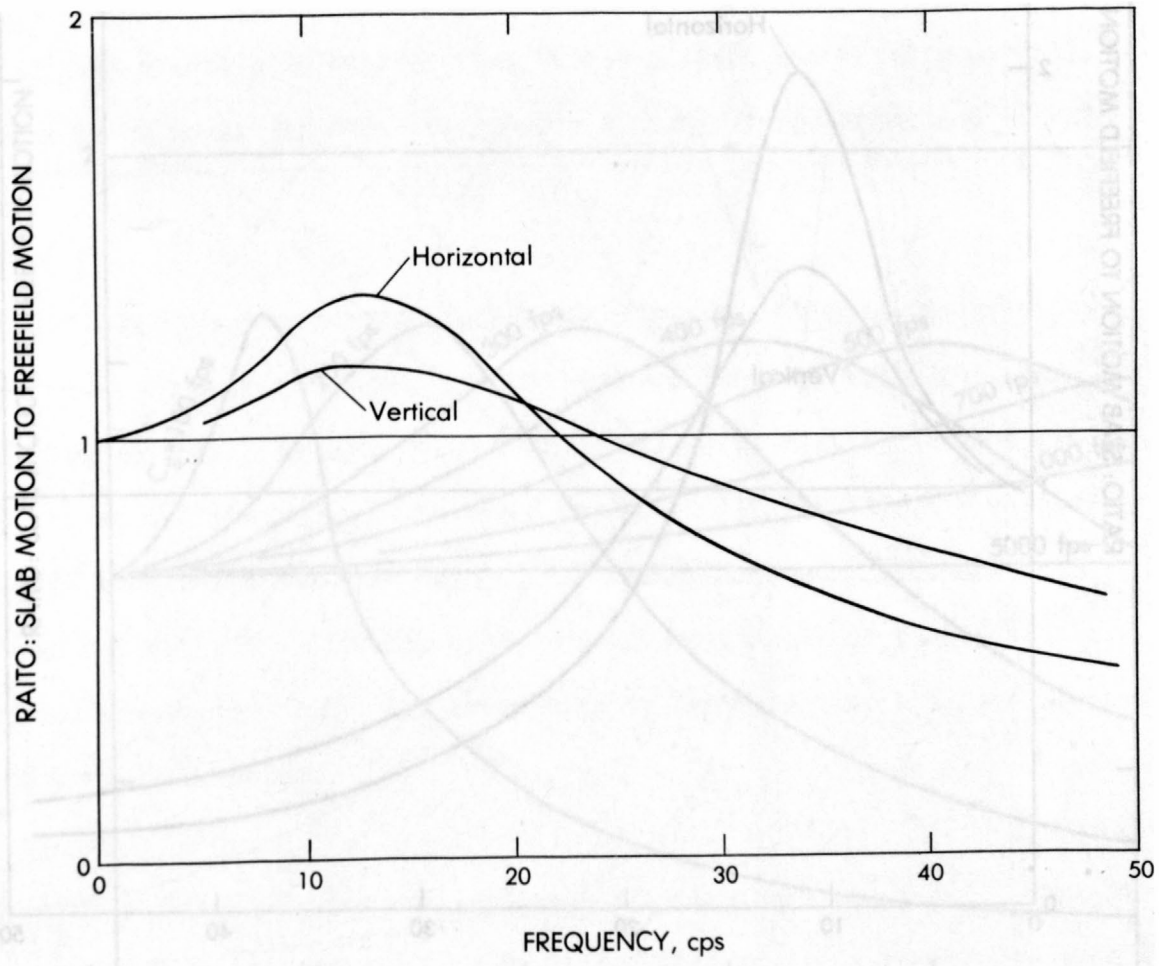

Figure 6.--Transmissibility of Small Slab. Based on standard USGS deployment (after Bycroft (1973)), with shear-wave velocity, C_s = 132 fps and assuming uniform pressure distribution under slab.

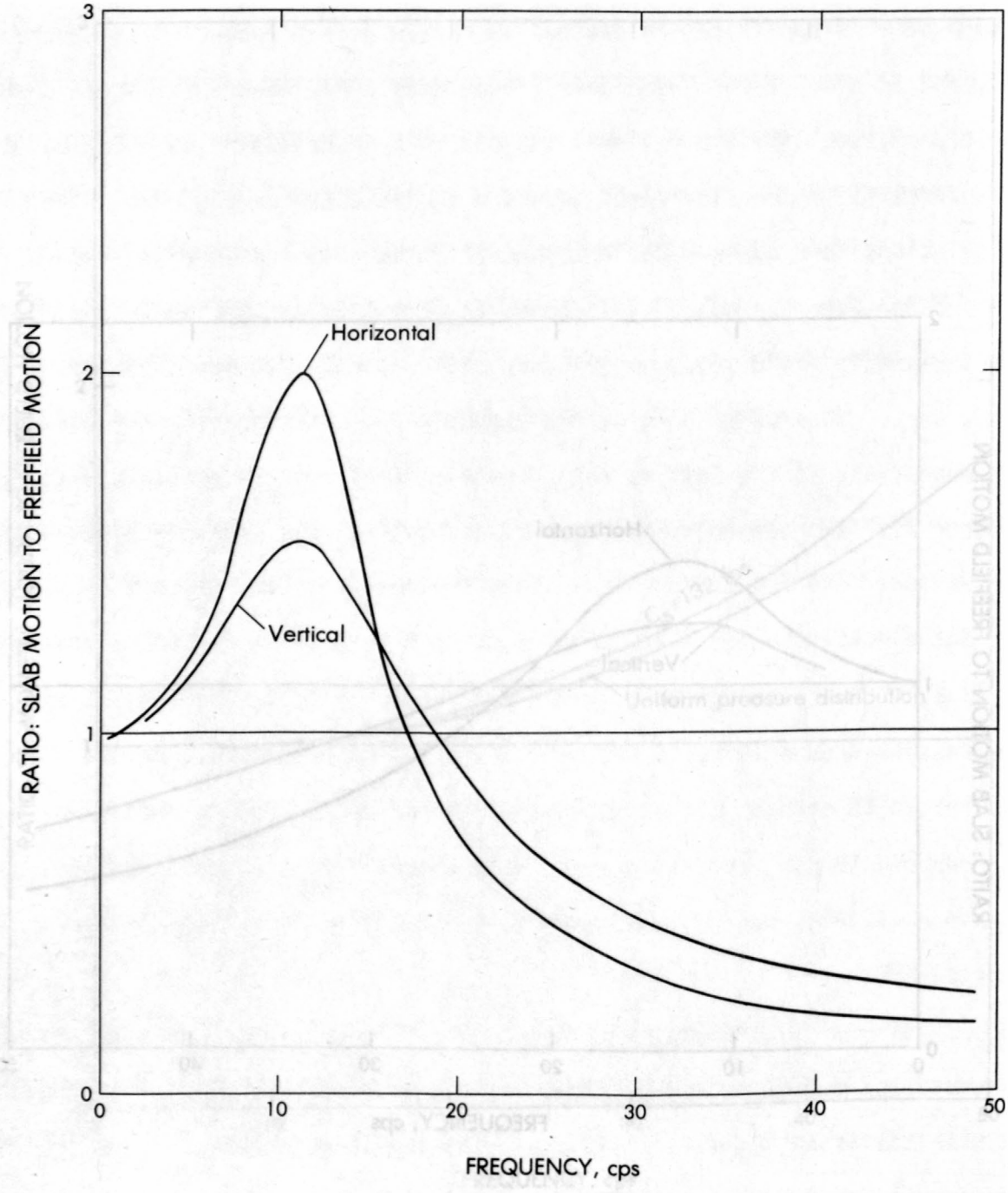

Figure 7.--Transmissibility of Small Slab. Based on standard USGS deployment (after Bycroft (1973)), with shear-wave velocity, C_s = 132 fps and assuming parabolic pressure distribution under slab.

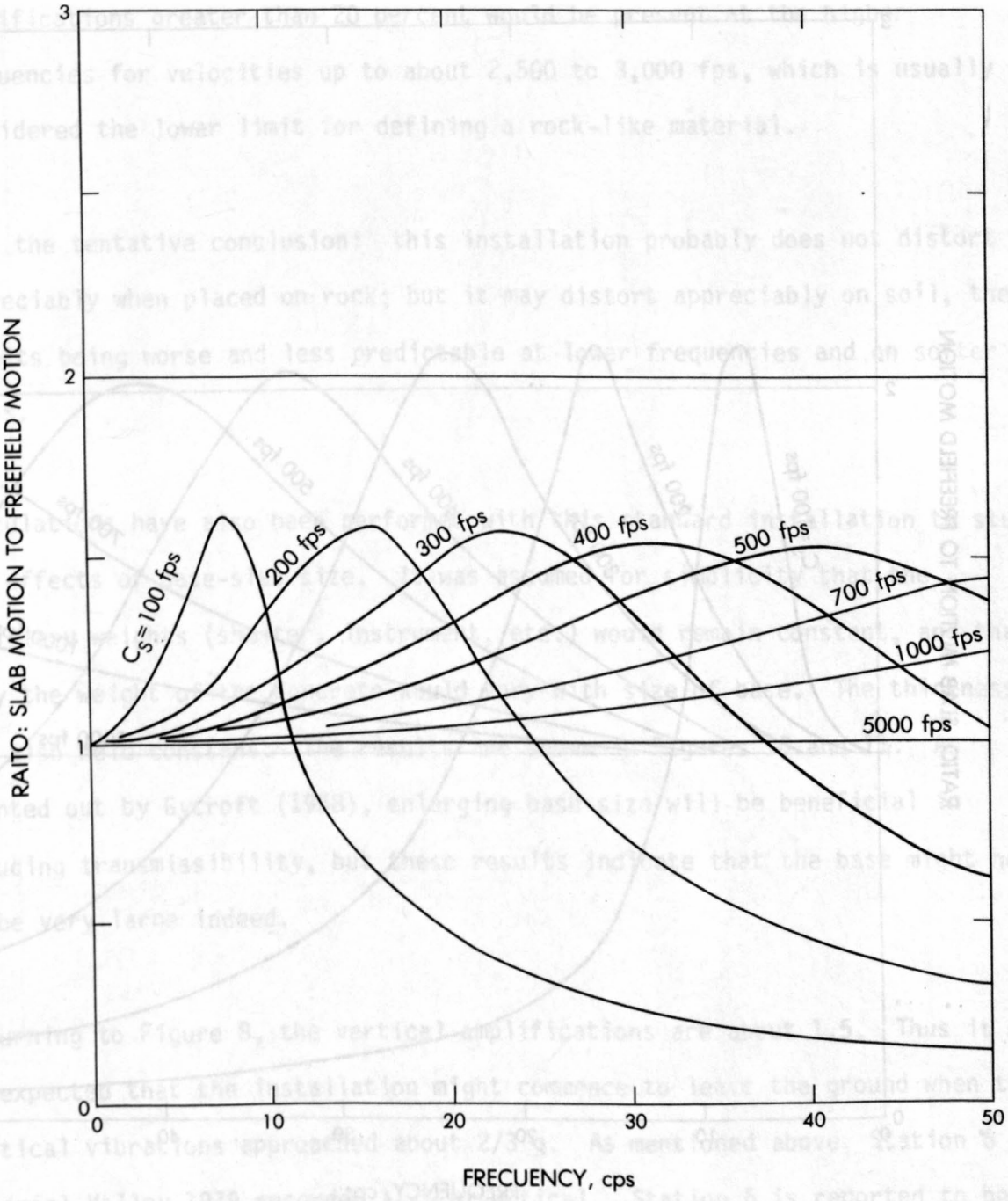

Figure 8.--Vertical transmissibility of standard insulation, as a function of shear-wave velocity.

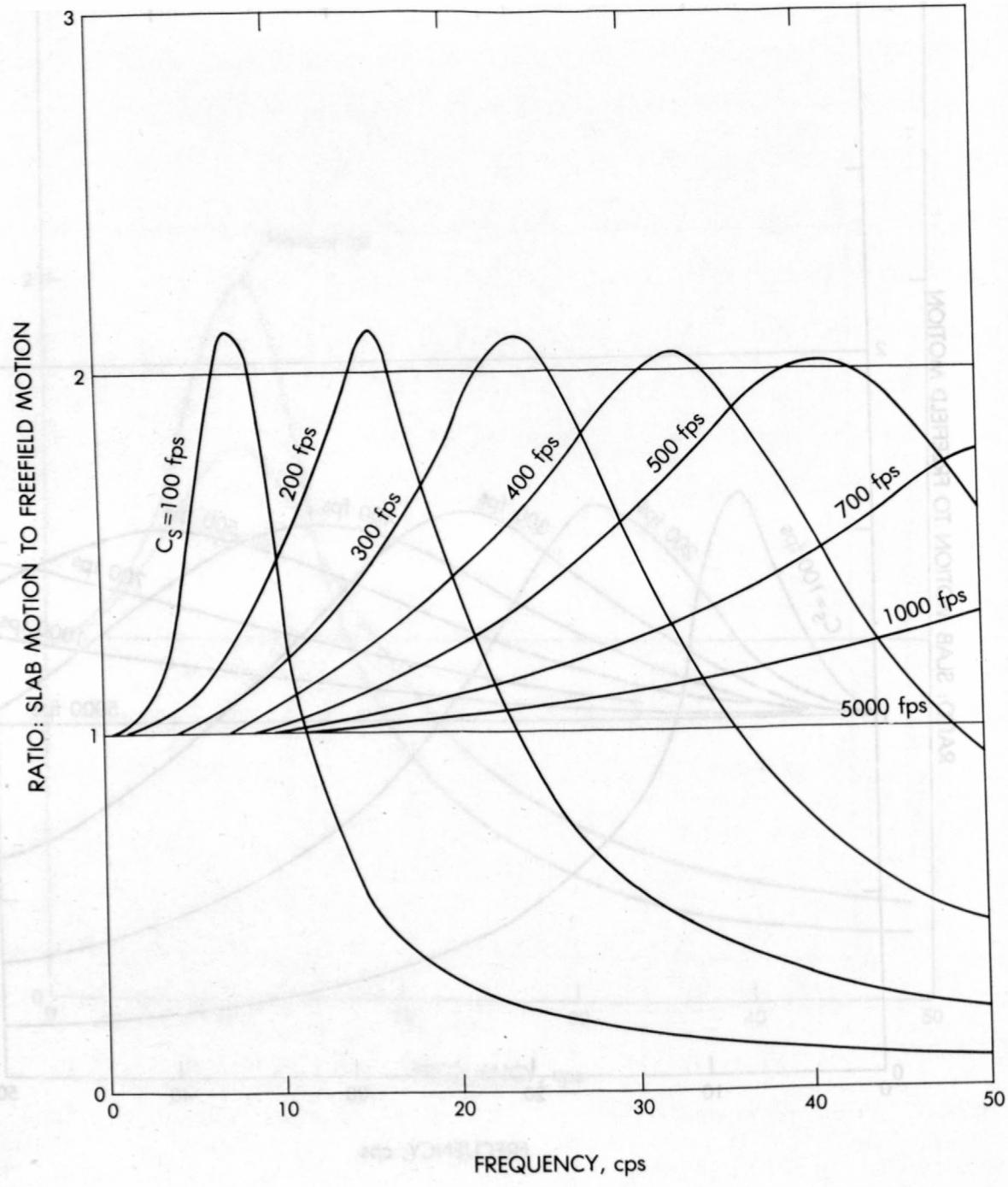

Figure 9.--Horizontal transmissibility of standard installation as a function of shear-wave velocity.

simple calculations, it would be expected that, for this particular installation, there would be only amplification, with no attenuation, in the periods of interest for soils with shear-wave velocities above 400 fps. Amplifications greater than 20 percent would be present at the higher frequencies for velocities up to about 2,500 to 3,000 fps, which is usually considered the lower limit for defining a rock-like material.

Thus the tentative conclusion: this installation probably does not distort appreciably when placed on rock; but it may distort appreciably on soil, the effects being worse and less predictable at lower frequencies and on softer soils.

Calculations have also been performed with this standard installation to study the effects of base-slab size. It was assumed for simplicity that the ancillary weights (shelter, instrument, etc.) would remain constant, and that only the weight of the concrete would vary with size of base. The thickness was also held constant. The results are shown in Figures 10 and 11. As pointed out by Bycroft (1958), enlarging base size will be beneficial in reducing transmissibility, but these results indicate that the base might have to be very large indeed.

Returning to Figure 8, the vertical amplifications are about 1.5. Thus it may be expected that the installation might commence to leave the ground when the vertical vibrations approached about 2/3 g. As mentioned above, Station 6 at Imperial Valley 1979 recorded 1.75 g vertical. Station 6 is reported to be a typical USGS instrument shelter, and presumably is not very different from that analyzed here. Thus, it would seem prudent to anchor such an

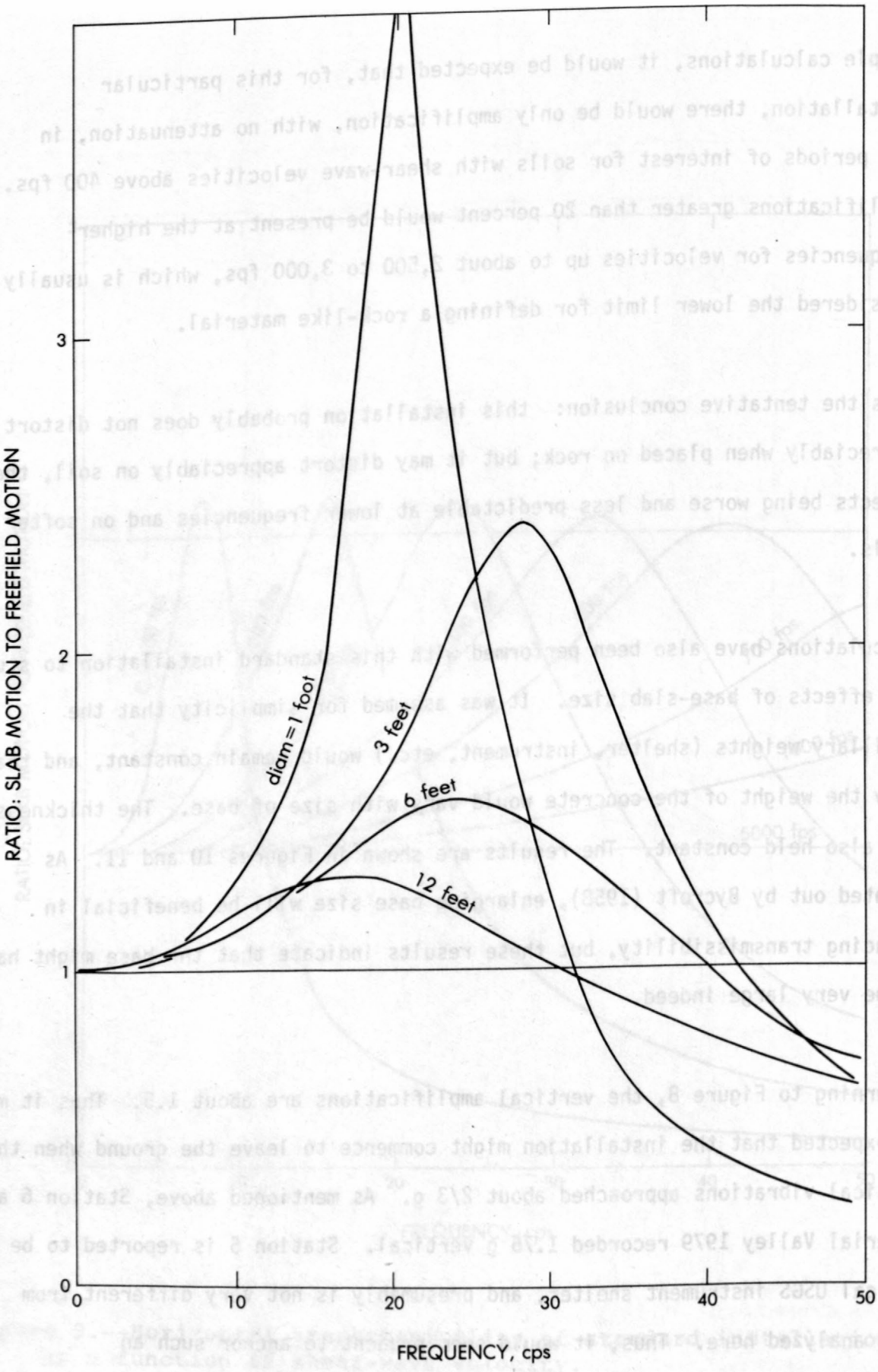

Figure 10.--Vertical transmissibility of standard installation as a function slab size. Shear wave velocity, C_s = 300 fps.

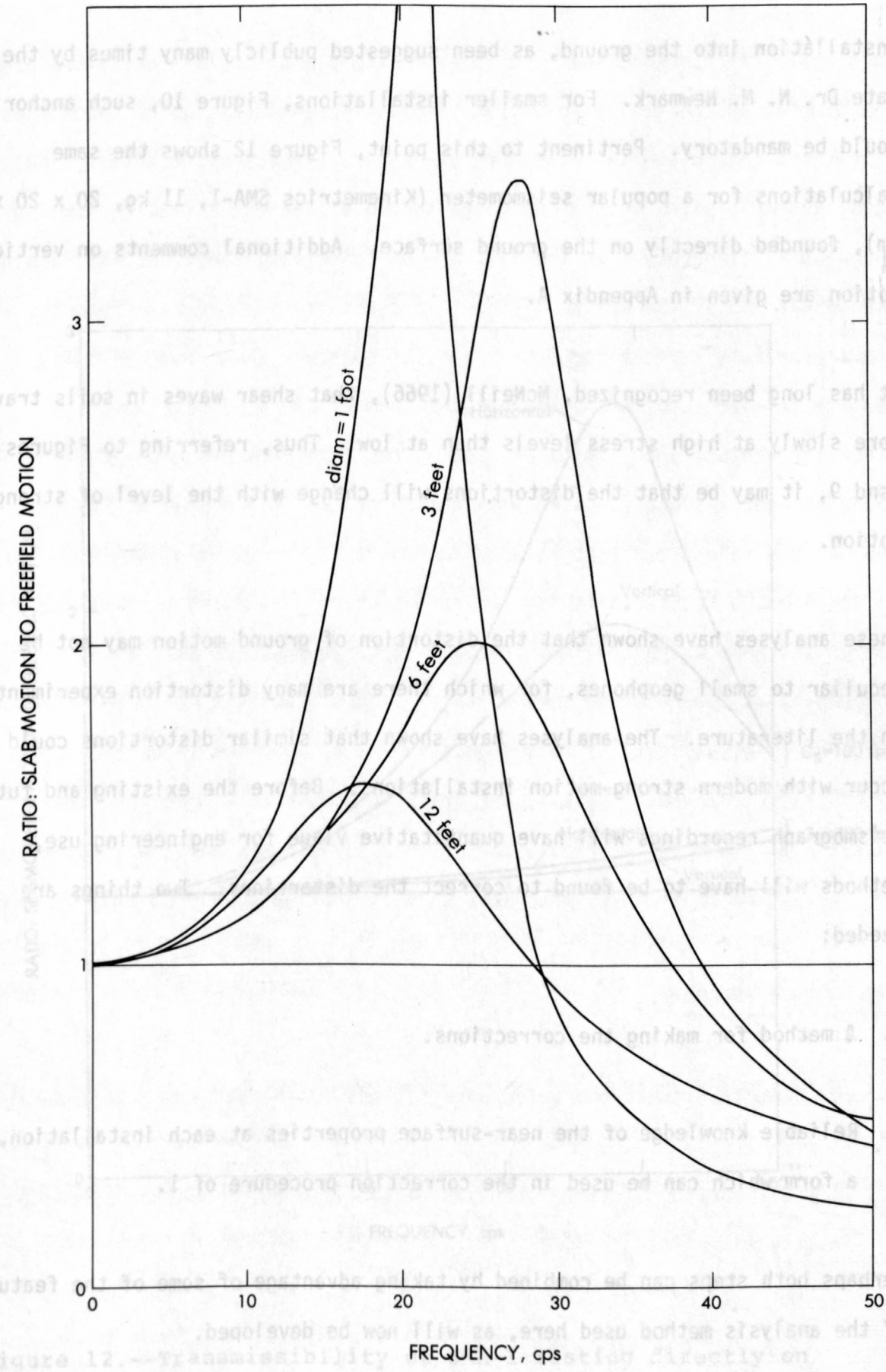

Figure 11.--Horizontal transmissibility of standard installation as a function of slab size. Shear-wave velocity C_s = 300 fps.

installation into the ground, as been suggested publicly many times by the late Dr. N. M. Newmark. For smaller installations, Figure 10, such anchoring would be mandatory. Pertinent to this point, Figure 12 shows the same calculations for a popular seismometer (Kinemetrics SMA-1, 11 kg, 20 x 20 x 31 cm), founded directly on the ground surface. Additional comments on vertical motion are given in Appendix A.

It has long been recognized, McNeill (1966), that shear waves in soils travel more slowly at high stress levels than at low. Thus, referring to Figures 8 asnd 9, it may be that the distortions will change with the level of strong motion.

These analyses have shown that the distortion of ground motion may not be peculiar to small geophones, for which there are many distortion experiments in the literature. The analyses have shown that similar distortions could occur with modern strong-motion installations. Before the existing and future seismograph recordings will have quantitative vlaue for engineering use, methods will have to be found to correct the distortions. Two things are needed:

1. A method for making the corrections.

2. Reliable knowledge of the near-surface properties at each installation, in a form which can be used in the correction procedure of 1.

Perhaps both steps can be combined by taking advantage of some of the features of the analysis method used here, as will now be developed.

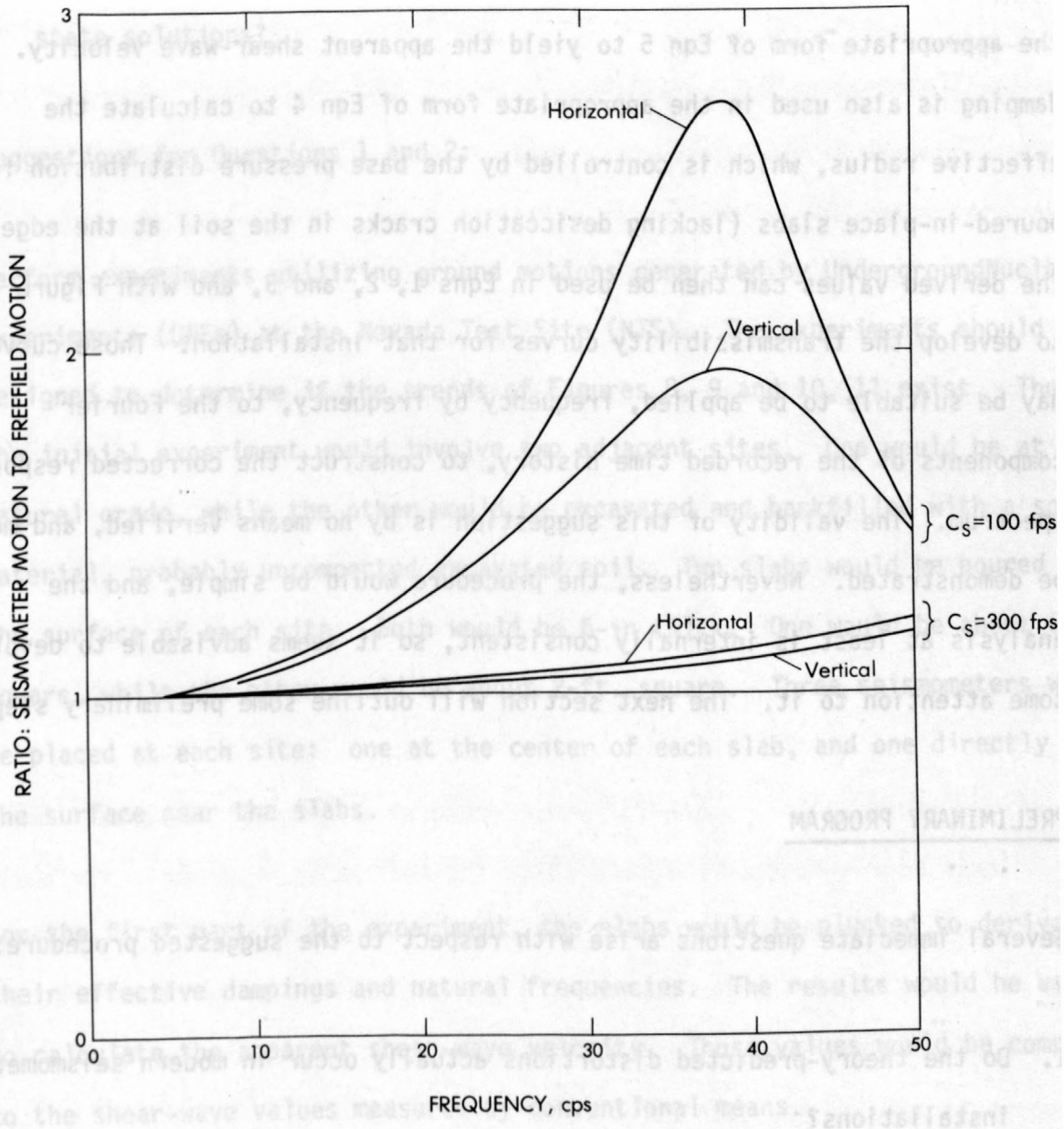

Figure 12.--Transmissibility of SMA-1 resting directly on surface.

When a slab is plucked, the rate at which the vibrations die out is related to the damping of the soil-slab system; and the frequency at which those free vibrations take place is related to the natural frequency, McNeill (1969). Thus, a simple pluck test at an installation yields the effective damping and the natural frequency. In Table I, use of Eqn 2 with the effective damping yields the mass ratio which, in turn, is used with the natural frequency as the appropriate form of Eqn 5 to yield the apparent shear-wave velocity. The damping is also used in the appropriate form of Eqn 4 to calculate the effective radius, which is controlled by the base pressure distribution for poured-in-place slabs (lacking desiccation cracks in the soil at the edge). The derived values can then be used in Eqns 1, 2, and 3, and with Figure 1(a) to develop the transmissibility curves for that installation. Those curves may be suitable to be applied, frequency by frequency, to the Fourier components of the recorded time history, to construct the corrected response spectrum. The validity of this suggestion is by no means verified, and must be demonstrated. Nevertheless, the procedure would be simple, and the analysis at least is internally consistent, so it seems advisable to devote some attention to it. The next section will outline some preliminary steps.

PRELIMINARY PROGRAM

Several immediate questions arise with respect to the suggested procedure:

1. Do the theory-predicted distortions actually occur in modern seismometer installations?

2. Do the parameters derived from a simple pluck test allow adequate predictions of the response and transmissibility characteristics of an installation?

3. Are there enough repetitions of the Fourier components in actual earthquake records to allow application of corrections based on steady-state solutions?

Suggestions for Questions 1 and 2:

Perform experiments utilizing ground motions generated by UndergroundNuclear Experiments (UNEs) at the Nevada Test Site (NTS). The experiments should be designed to determine if the trends of Figures 8, 9 and 10, 11 exist. Thus the initial experiment would involve two adjacent sites. One would be at natural grade, while the other would be excavated and backfilled with a soft material, probably uncompacted excavated soil. Two slabs would be poured at the surface of each site. Both would be 6-in thick. One would be about 6-ft. square, while the other would be about 2-ft. square. Three seismometers would be placed at each site: one at the center of each slab, and one directly on the surface near the slabs.

For the first part of the experiment, the slabs would be plucked to derive their effective dampings and natural frequencies. The results would be used to calculate the apparent shear-wave velocity. Those values would be compared to the shear-wave values measured by conventional means.

For the second part of the experiment, the slabs would be subjected to forced vibrations over a spectrum of frequencies to derive their response curves. Those would be compared to the response curves calculated from the parameters derived from the first part. If those comparisons were poor, the suggested method would have to be thoroughly reinspected, but the third part of the experiment would probably be undertaken anyway.

The third part of the experiment would be the UNE. The resulting time histories would be decomposed into their Fourier components, which would be corrected according to the transmissibility curves calculated from the parameters derived from the first part. The results would be used to calculate response spectra which would be compared to each other and to the spectra of the raw time histories from the ground-founded seismographs.

The results of the second and third part would be used to revise the analysis procedures, and to design further experiments as appropriate.

Suggestions for question 3:

Obtain a representative number of uncorrected seismograms. Decompose them into their Fourier components, and calculate the response spectrum for each at the calculated or measured dmaping for that seismometer installatin. Compare the resulting amplification ratios with theoretical values for that frequency and damping. Review the oscillator time histories to deduce how the components tend to approach steady state (or not).

The results of this work would be used to revise the analysis procedures, and to design further experiments as appropriate.

CONCLUSIONS

The literature survey and analyses have demonstrated that modern seismometer installations may distort free-field ground motions. The effects are expected to include distortions in both amplitude and phase, and are generally expected to be greatest on softer soils.

A simple method for correcting existing and future seismograms is suggested. A first-step experimental program to evaluate the suggestion is outlined.

REFERENCES

Anandakrishnan, B. M. and N. R. Krishnaswamy: "Response of Embedded Footings to Vertical Vibrations," J., SM & FE Div, SM10 American Society Civil Engineers, Oct. 1973.

Barneich, J. A., R. L. McNeill, and D. H. Johns: "Soil Structure Interaction Parameters for Seismic Design of Nuclear Power Stations," Preprint 2182, American Society Civil Engrs, New York, 1974.

Bolt, B. A., and R. A. Hansen: "The Upthrow of Objects in Earthquakes," vol. 67, no. 5, Bull. Seis. Soc. of america, 1977.

Bycroft, G. N.: "Forced Vibrations of a Rigid Circular Plate on a Semi-Infinite Elastic Half Space and on an Elastic Stratum," Phil. Trans. Roy. Soc. London, 1956.

Bycroft, G. N.: "The Magnification Caused by Partial Resonance of the Foundations of a Ground Vibration Detector," Trans. Amer. Geophysical Union, vol. 38, no. 6, 1957.

Bycroft, G. N.: "The Effect of Soil Structure Interaction on Seismometer Readings," vol. 68, no. 3, Bull. Seis. Soc. of america, 1978.

Fail, J. P., G. Grau, and M. LaVergne: "Coupling of Seismographs to Soil (in French)," Vol X, Geophysical Propsecting, 1962.

Luco, J. E., and R. A. Westmann: "Dynamic Response of Circular Footings," J. of E.M. Div. EM5, Amer. Soc. Civ. Engrs., Oct., 1971.

Margason, B. E., R. L. McNeill, and F. M. Babcock: "Case Histories in Foundation Vibrations," STP 450, ASTM, 1969.

McJunkin, R. D.: "Strong-Motion Free-Field Site Design Characteristics," California Geology, Calif. Div. Mines and Geology, Aug, 1979.

McJunkin, R. D.: Telephone communication, 12 Aug 1981.

McNeill, R. L., B. E. Margason, and F. M. Babcock: "The Role of Soil Dynamics in the Design of Stable Test pads," Proc. Paper 10N-65, AIAA, 1965.

McNeill, R. L., B. E. Margason, and J. A. Barneich: "Design of Test Pads for Transient Loadings," Proc. paper 67-550, AIAA, 1967(a).

McNeill, R. L., and B. E. Margason: "Modern Foundation Design for Dynamic Loadings," Proceedings SEATA Conf. on Soil Engineering, Bangkok, 1967(b).

McNeill, R. L., B. E. Margason, F. M. Babcock, and J. A. Barneich: "Design Methods for Transient Response and Isolation of Ground-Founded Microprecision.

Slabs," J. Spacecraft and Rockets, vol. 5, no. 11, AIAA, 1968.

McNeill, R. L.: "Machine Foundations: The State of the ARt," Invited paper, Proc. Spec. Session 2. Seventh Annual Int'l Cnference on Soil Mech. and Fndtn. Energy, Mexico City, 1969.

McNeill, R. L.: "The Propagation of Stress Waves in Sand," AWFL-TR-65-180, USAF, Kirtland AFB, 1966.

Newmark, N. M.: "Interpretation of Apparent Upthrow of Objects in Earthquakes," Proc., Fifth World Conference on Earthquake Engineering, Rome, 1973.

Pasecnik, P.: "Theoretical and Experimental Study of the Resonance of a Seismometer System (in Russian)," Izv. Akad, Nauk SSSR, ser. geofiz., 1952.

Safar, M. H.: "On the Minimization of the Distortion Caused by the Geophone-Ground Coupling," vol. 26, Geophysical Prospecting, 1978.

Washburn, H., and H. Wiley: "The Effect of the Placement of a Seismometer on its Response Characteristics," vol. VI, Geophysics, 1941.

Wolf, A.: "The Equation of Motion of a Geophone on the surface of an Elastic Earth," vol. IX, Geophysics, 1944.

APPENDIX A

UPTHROWN OBJECTS

There are many post-earthquake reports of objects being displaced from their pre-earthquake positions. Some of the reports contain information indicating that some of the objects must have departed the earth with a near-vertical velocity. For example, many reports of displaced boulders emphasize the apparently intact condition of the hole in which the boulder sat. Bolt, et al (1977) present a good review of some cases since 1897.

The analysis method of this report has been applied to some cases to study the phenomenon. For example, Fig. A-1 shows the calculated motions of a rock whose dimensions are shown in the sketch. Newmark (1973) suggests that such rocks woud be candidates for upthrow at about 1/2 g. If this analysis method is approximately correct for such situations, Newmark's statement might be modified to include the range from 1/3 to 1/2 g.

Often mentioned is the behavior of the concrete benches on the north side of Olive View Hospital in the 09 Feb 71 San Fernando Earthquake. The benches were made of precast concrete, with oversize holes at the bottom of the legs to receive bolts that had been precast into the patio slab. After the earthquake, most of the benches were upside down in the vicinity of their original location. To do this, they would have to rise vertically several inches. The hospital was probably directly over the upward-progressing thrust type rupture, and may have been focused in high-frequency energy. Fig. A-2 shows the

calculated behavior of the benches. Those results indicate that, at the higher frequencies, the benches could lift off at fairly modest free-field acceleration.

Many observers report that gravestones are displaced after an earthquake. This is not necessarily surprising, because the back-filling of a grave is hardly a quality-control process. Thus it seems reasonable to assume that the soil supporting gravestones in many cases could be rather soft. Using that assumption, and applying the apparent shear-wave velocity for soft soil from Washburn and Wiley (1941), Fig. A-3 has been prepared to show the response of a small gravestone. The effects of the depth of burial were not considered in the calculations. The effects of considering depth of burial would be to lower the peak and move the curve to the right slightly. Nevertheless, the results show that movements of small gravestones in soft soils should be expected; and occassional overturned stones should not be surprising.

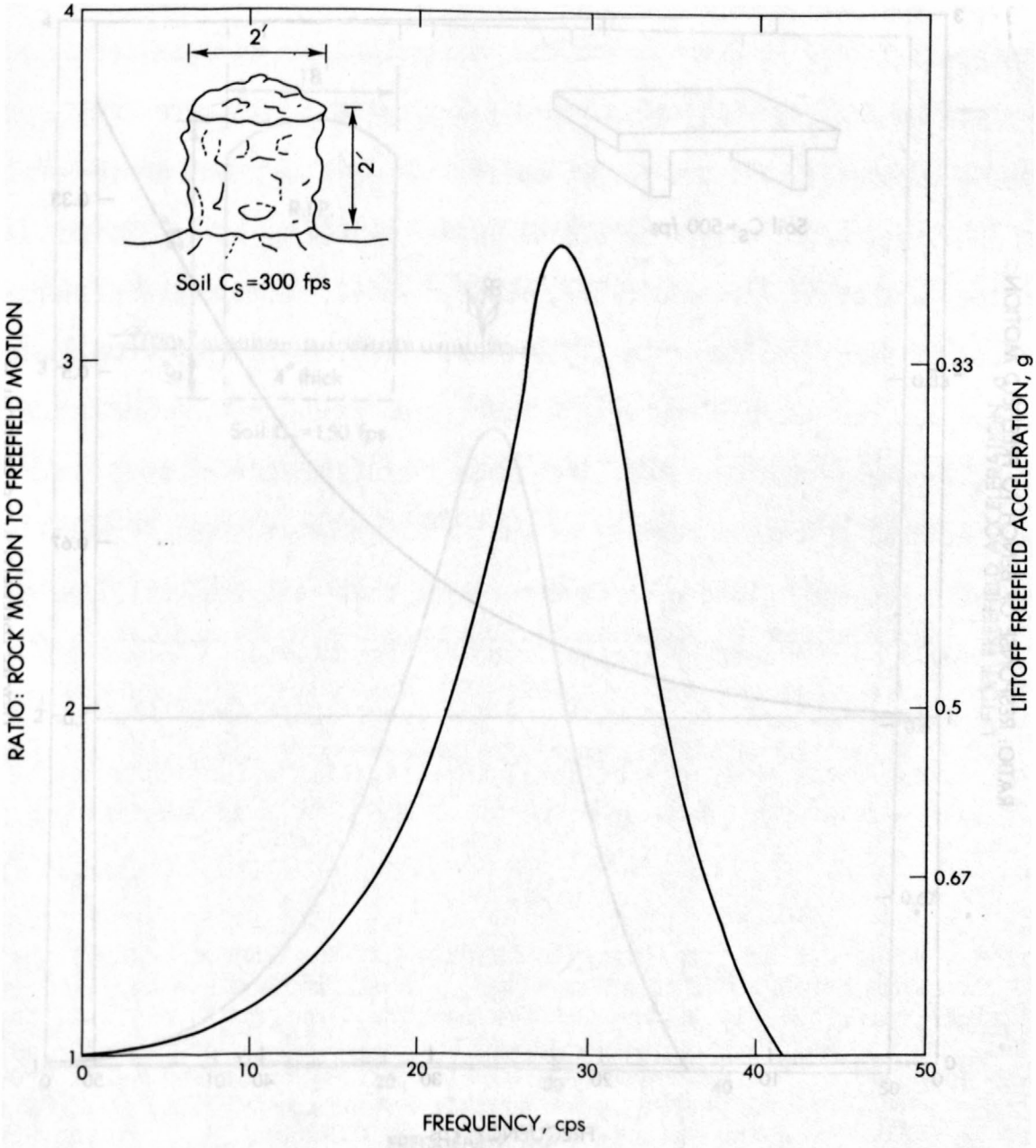

Figure A-1.--Vertical response of a rock.

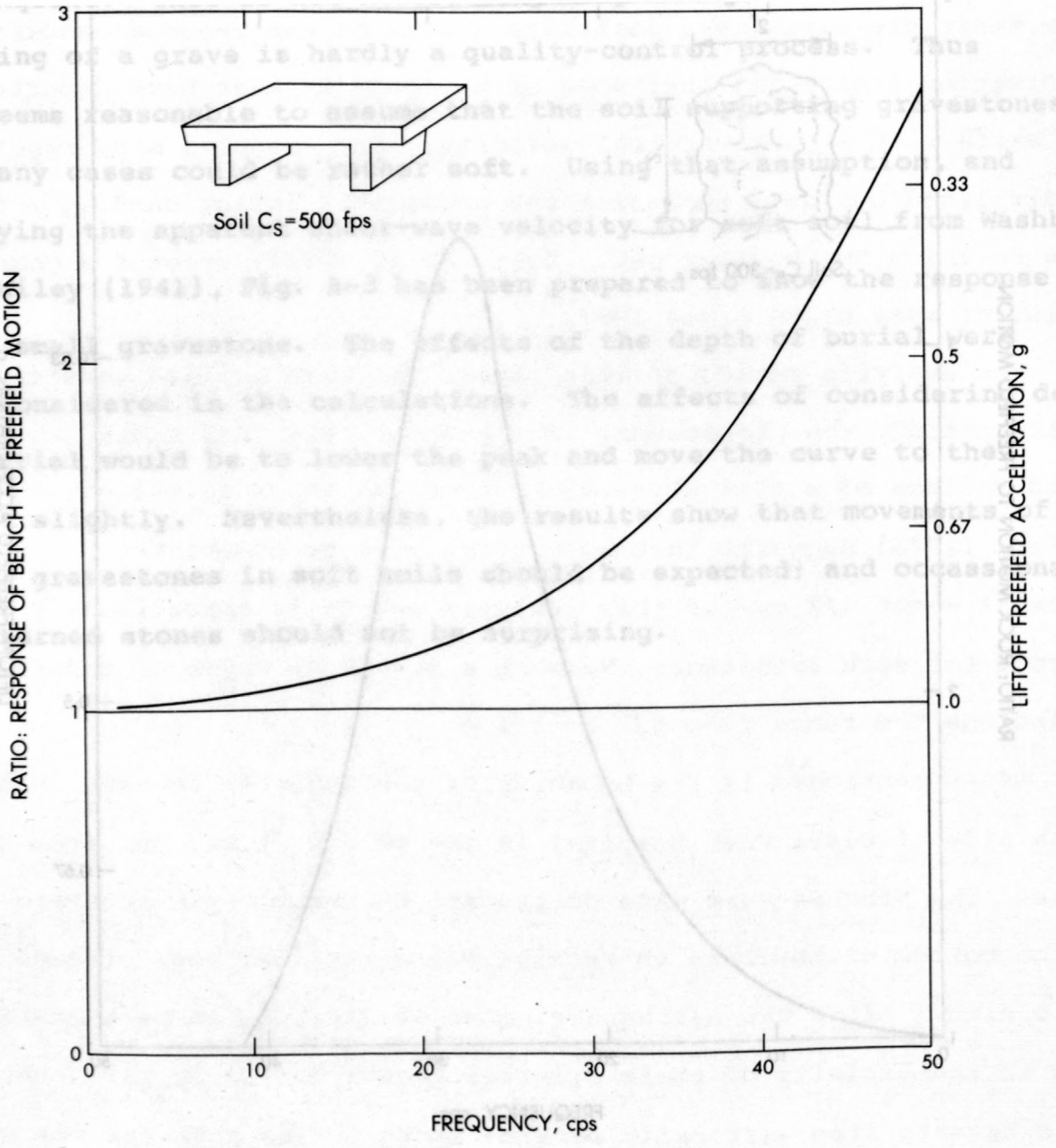

Figure A-2.--Vertical response of benches at Olive View Hospital.

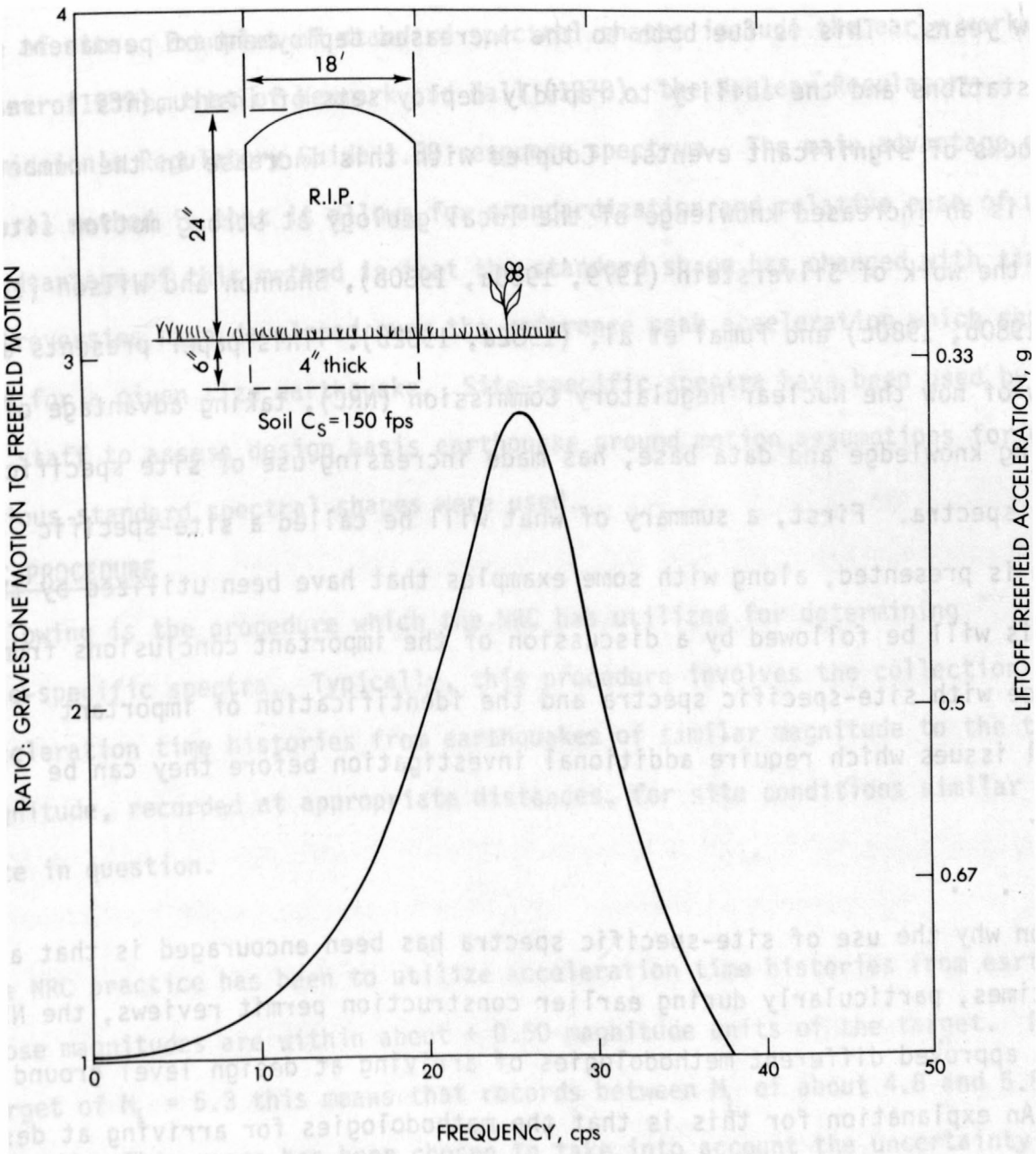

Figure A-3.--Vertical response of gravestone.

The Use of site Dependent Spectra

by

Jeffrey K. Kimball
U.S. nuclear Regulatory Commission
Washington, D.C. 20555

INTRODUCTION

The catalog of strong motion accelerograms has been increasing rapidly during the past few years. This is due both to the increased deployment of permanent strong motion stations and the ability to rapidly deploy sets of instruments to record aftershocks of significant events. Coupled with this increase in the number of records is an increased knowledge of the local geology at strong motion sites through the work of Silverstein (1979, 1980a, 1980b), Shannon and Wilson (1978, 1980a, 1980b, 1980c) and Fumal et al. (1982a, 1982b). This paper presents an overview of how the Nuclear Regulatory Commission (NRC), taking advantage of this increasing knowledge and data base, has made increasing use of site specific response spectra. First, a summary of what will be called a site-specific spectrum is presented, along with some examples that have been utilized by the NRC. This will be followed by a discussion of the important conclusions from our experience with site-specific spectra and the identification of important technical issues which require additional investigation before they can be resolved.

One reason why the use of site-specific spectra has been encouraged is that at various times, particularly during earlier construction permit reviews, the NRC staff has approved different methodologies of arriving at design level ground motion. An explanation for this is that the methodologies for arriving at design level ground motion has evolved with time as more data has been recorded and we have gained more knowledge of the effects of earthquake source, propagation path, and local site conditions upon strong ground motion. The past practice can generally be classified as a site independent approach, which typically uses a

standardized response spectrum and a reference peak acceleration. The resulting spectral amplification factors from a standardized response spectrum are typically developed by using strong motion records recorded from earthquakes of a wide range of magnitudes, at widely recorded distances, and site conditions. They are therefore, by definition, not specifically designed for use on any one type of site. Examples of standard spectral shapes include the early work of Housner (1959), that of Newmark and Hall (1978), the Nuclear Regulatory Commission's Regulatory Guide 1.60 response spectrum. The main advantage of this general method is that it allows for standardization and relative ease of use. A disadvantage of this method is that the standard shape has changed with time and controversies have developed over the reference peak acceleration which should be used for a given size earthquake. Site-specific spectra have been used by the NRC staff to assess design basis earthquake ground motion assumptions for which various standard spectral shapes were used.

NRC PROCEDURE

Following is the procedure which the NRC has utilized for determining site-specific spectra. Typically, this procedure involves the collection of acceleration time histories from earthquakes of similar magnitude to the target magnitude, recorded at appropriate distances, for site conditions similar to the site in question.

The NRC practice has been to utilize acceleration time histories from earthquakes whose magnitudes are within about + 0.50 magnitude units of the target. For a target of M_L = 5.3 this means that records between M_L of about 4.8 and 5.8 could be used. This range has been chosen to take into account the uncertainty of the assumed magnitude and more importantly, to ensure that a large enough, yet reasonable, data sample can be collected. In terms of the target distance, we

have generally utilized acceleration times histories recorded within about 25 kilometers of the source, with the average distance being about 15 kilometers. The matching of site conditions is usually accomplished by comparing the shear wave velocity profile at the target site with whatever shear wave velocity information may be available for the strong motion recording stations. Important information in matching site conditions is not only the value of the shear wave velocity, but also the layer thicknesses and impedance contrasts.

Following, are a few examples of site specific spectra that have been developed by both consultants to applicants and the NRC staff. Figure 1 shows the shear wave velocity profile of a soil site in Michigan where the target magnitude was an M_L of 5.3. Figure 2 shows the shear wave velocity profiles of the strong motion recording stations that were used by the applicant to develop the spectrum. As can be observed, the match is not perfect, and in fact the decision of whether to include or exclude records requires care and judgement. Figure 3 is a plot of the response spectra (5% damping) of all the horizontal components collected by the applicant, listed in Table 1, that were used in developing this spectrum. Once this collection is accomplished, a specific fractile can be determined for use in the analysis or comparison. In the examples in this paper the 84th percentile is used.

At the particular site in Michigan, there was some controversy over one particular set of records, as to whether or not they should be included. Figure 4 shows the effect of adding three sets of records from the 1966 Parkfield earthquake, with the original collection of twenty-one sets of records. These results demonstrate that care must be exercised when choosing strong motion

records because the inclusion or exclusion of specific data can have a significant effect on the spectrum. However, the advantages of using site specific spectra outweigh the precautions which must be observed. These advantages will be shown in the following figures.

One sensitivity test that was performed by the applicant, using the site specific spectrum that included the Parkfield records, was examining the impact of systematically restricting the source distance of the strong motion data collected. This test was undertaken to help assess the statistical completeness of the data set collected. Figure 5 shows the effects of changing the average distance of the collected data set from 14.6 kilometers to 11.4 kilometers. The 84th percentile spectrum increases at a rate roughly equivalent to the ratio of the decreasing distance.

At this same site in Michigan, a portion of the facility was founded on about 40 feet of soft fill material on top of the stiff soil. A second suite of strong motion records was collected by the applicant matching the same target magnitude and distance but for strong motion sites with slightly deeper soil profiles then those originally selected. In this case some of the same records fit both the soil and the soil-plus-the-fill profile equally well. Figure 6 compares the 84th percentile of these two sets of data. As expected, the deeper soil site spectrum is "richer" in low frequencies while it is approximately the same as the shallower soil site-specific spectrum at frequencies of 4 hertz and greater.

The applicant in the above case, had also calculated theoretical amplification of the soft fill on top of the stiff soil using the SHAKE computer code. Figure 7

shows the ratio of soil-plus-fill over soil from both the site-specific response spectra and the SHAKE calculations. The shape (peaks and valleys) of the amplification curve is roughly the same for both methods, however, the magnitude of the amplification appears to be underestimated by about a factor of 2, using the theoretical technique. In this case the empirical results were directly used to evaluate the site, while the theoretical results verified the shape of the amplification of ground motion through the fill material.

Figures 8 and 9 show the 84th percentile spectra in a comparison of rock sites (100's of feet of still soil) for target magnitudes of 5.3 and 5.8 completed by the applicant and NRC staff's consultant, respectively. In thse examples, the rock spectra are more deficient in the lower frequencies. In the above examples the higher frequency spectral values are roughly equivalent. Figure 10 compares a rock spectrum and a shallow soil (10's of feet) site-specific spectrum completed by the NRC staff's consultant, again for a target magnitude of about 5.3. In this example the shallow-soil spectrum is very much richer in the higher frequencies compared to the rock case.

The above examples show one advantage of site specific spectra, that is, the ability to model a difference in the predominant frequency content of the ground motion for different site conditions. Use of a standard spectral shape would not reproduce the above variations observed in site specific spectral shapes and would require assumptions regarding the choice of peak acceleration and/or velocity. These assumptions are unnecessary if site specific spectra is calculated.

In the above cases, the target magnitude and recorded distance of records collected was kept roughly constant and different site conditions were compared. The next examples show what happens when the site conditions and distance are held roughly constant, and the target magnitude is varied. Figure 11 contains the the 84th percentile level spectra collected by consultants to applicants and the NRC staff, for rock sites, with the average magnitudes of the 3 curves being 5.3, 5.7 and 6.0. Figure 12 shows the 84th percentile spectra collected by consultants to applicants for deep stiff soil sites with the average magnitudes of about 5.4 and 6.1. These two cases suggest that, in this magnitude range, the lower frequency ground motion increases at a faster rate compared to the high frequencies for a given increase in magnitude. The log of spectral acceleration (measured at 25 Hz on response spectrum to roughly correspond with peak acceleration frequency) roughly scales at 0.20 to 0.25 times the magnitude whereas the log of spectral velocity (measured at 1 to 2 Hz on response spectrum to roughly correspond to peak velocity frequencies) roughly scales at 0.45 to 0.50 times the magnitude. The scaling of spectral acceleration and spectral velocity, in these two examples is very close to the scaling of peak acceleration and peak velocity estimated by Joyner and Boore (1981). Thus, the above observations using site specific spectra demonstrates a way of accounting for the change in the frequency content of ground motion as the size of the earthquake changes.

The above cases show two of the advantages of the use of site-specific spectra. However, there are still limitations to this method including technical issues that need to be investigated, and the limited size of existing data base. These technical issues include attenuation, source characteristics and the scaling of

data to match the conditions of interest. Many critical facilities are located in regions of the United States where the attenuation characteristics are very different than those in California, where most of the strong ground motion data has been recorded. The examples in this paper have utilized strong motion recordings at distances of less than about 25 kilometers where these attenuation differences are minimized, yet there may be cases where the controlling earthquake will be at a greater distance such that attenuation differences are much more important. One key technical issue is, whether scaling of records in the western United States can be utilized to take into account attenuation differences for different regions of the country. In addition to attenuation differences, there also may exist source characteristic differences between various regions of the United States. Research into quantifying these potential source differences is an area which requires work. Once this is quantified, Western United States strong motion records may again need some type of scaling to be utilized in other regions of the United States, particularly if there continues to be a lack of strong motion data in the East.

Although the general shift in the frequency content for differing site conditions has been observed, as shown in the present paper, more research is needed to document the effect that local site conditions have on modifying strong motion. This includes a better documentation of which specific subsurface properties should be used to better model potential amplification effects. In addition, care needs to be exercised in deploying strong motion instruments, both permanent and portable, in areas where the site conditions have been, or could be, easily documented. As an example, there appear to be no rock recordings, which do not have at least some thin soil cover, from the Mammoth Lakes strong motion data

set. In addition, the current data base, although rapidly expanding, is still limited particularly for magnitudes greater than about 6.5 at small source distances.

CONCLUSION

In conclusion, the NRC has utilized site specific spectra in an attempt to mor realistically account for both the spectral level and frequency content of str motion at different sites. However, this use is limited by both the extent of the existing data base, and regional differences in attenuation and uncertaint of source characteristics. With additional research an expanded use of the existing data may be possible.

TABLE 1

Date	M_L	Location	Stations Used
3/22/57	5.3	San Francisco, CA	Southern Pacific Bldg. Alexander Bldg. Golden Gate Park
6/28/66	5.6	Parkfield, CA	Cholame 5 Cholame 8 Cholame 12
9/12/70	5.4	Lytle Creek, CA	Cedar Springs Pump House San Bernardino Hall of Records Colton Wrightwood
11/28/74	5.2	Gilroy, CA	Gavilan College
1/12/75	5.2	Cape Mendocino, CA	Petrolia Gen. Store
6/7/75	5.2	Cape Mendocino, CA	Petrolia Gen. Store
5/7/76	4.9	Friuli, Italy	Tolmezzo
5/9/76	5.5	Friuli, Italy	Forgaria Maiano Tolmezzo
5/11/76	5.3	Friuli, Italy	Forgaria Maiano Tolmezzo Torcento
9/11/76	5.5		Forgaria Tarcento
9/15/76	5.0		Forgaria

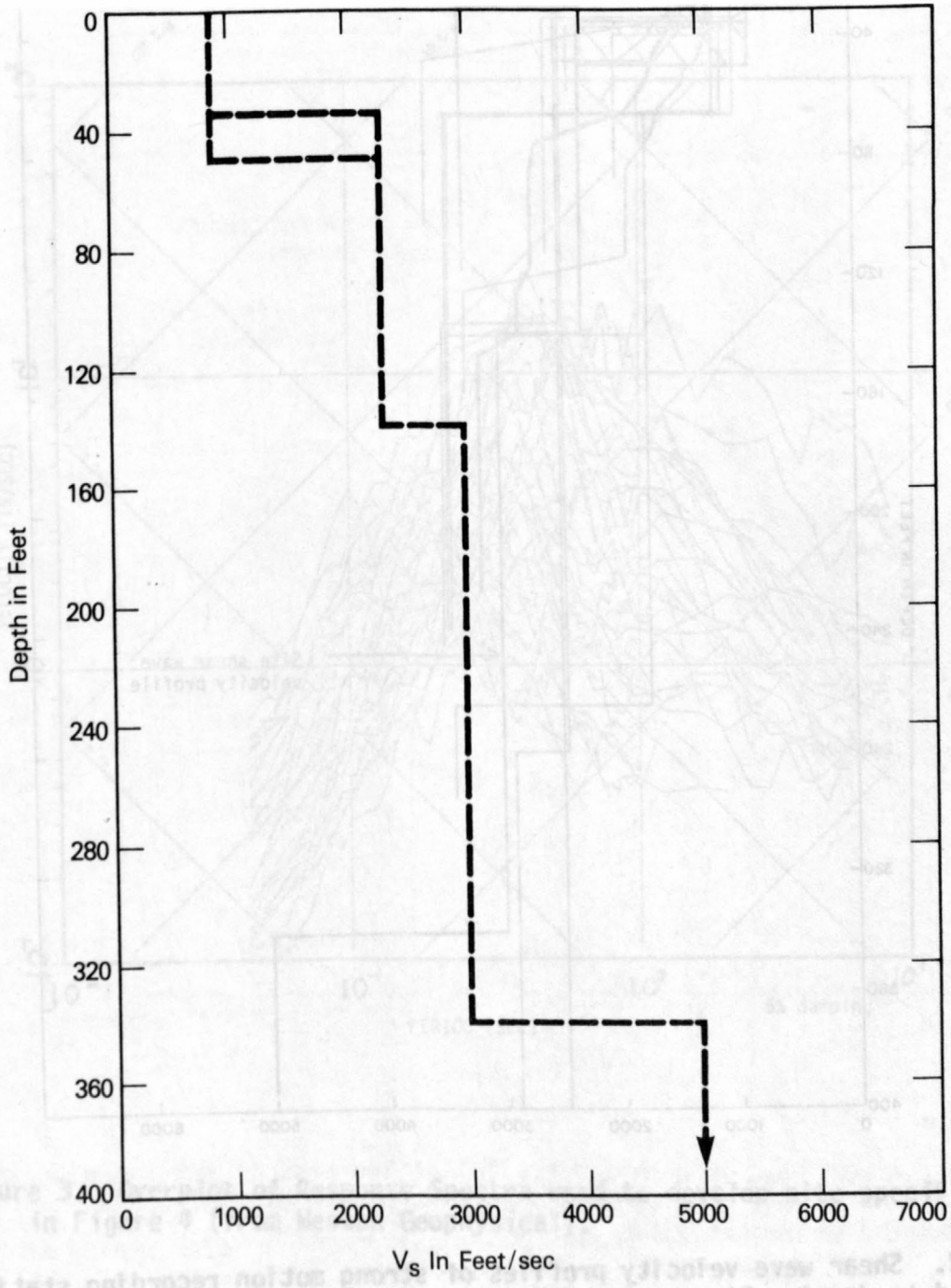

Figure 1. Shear wave (V_S) velocity profile of soil site in Michigan (from Weston Geophysical).

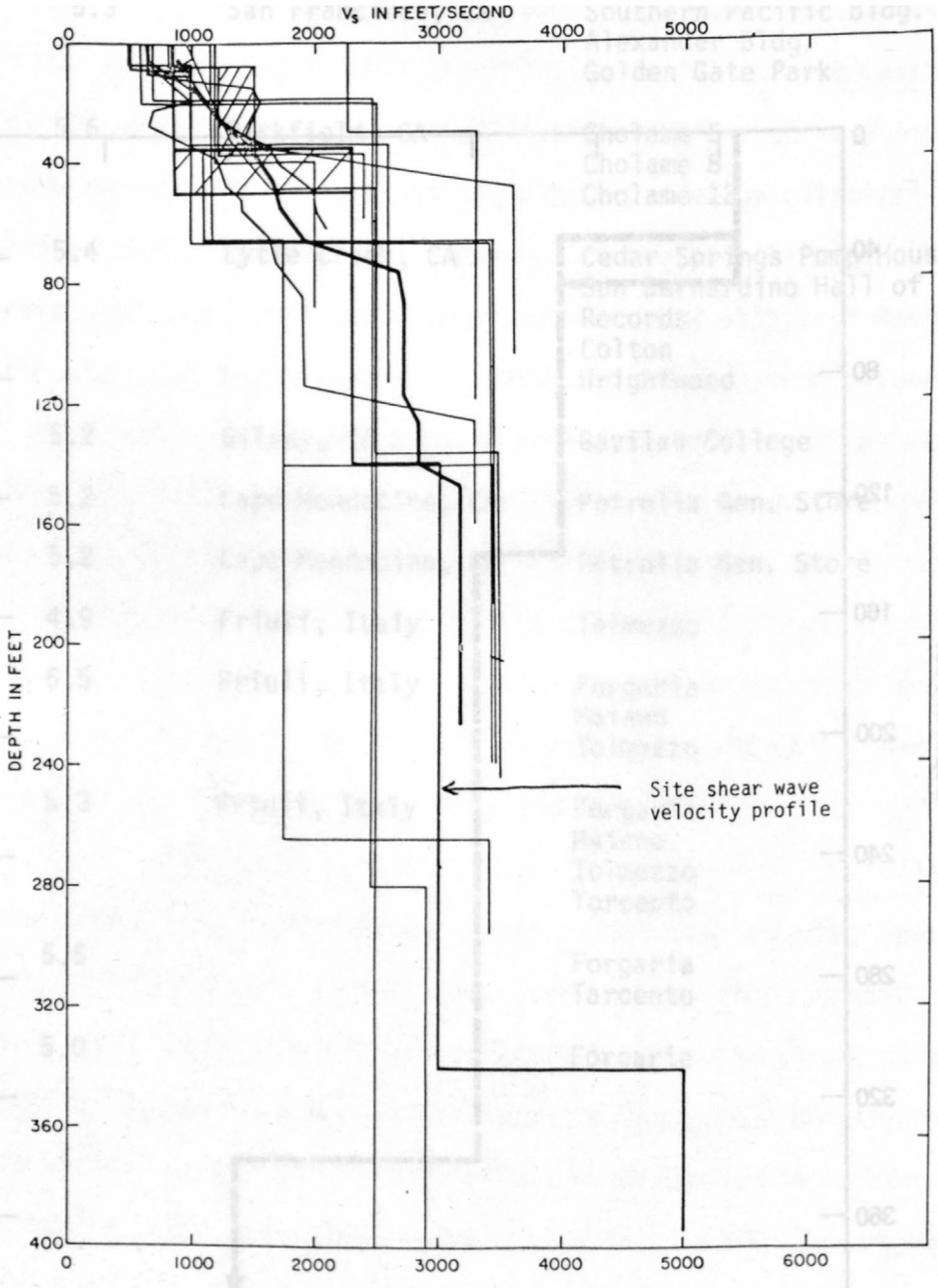

Figure 2. Shear wave velocity profiles of strong motion recording stations used to develop Figures 3 and 4 (from Weston Geophysical).

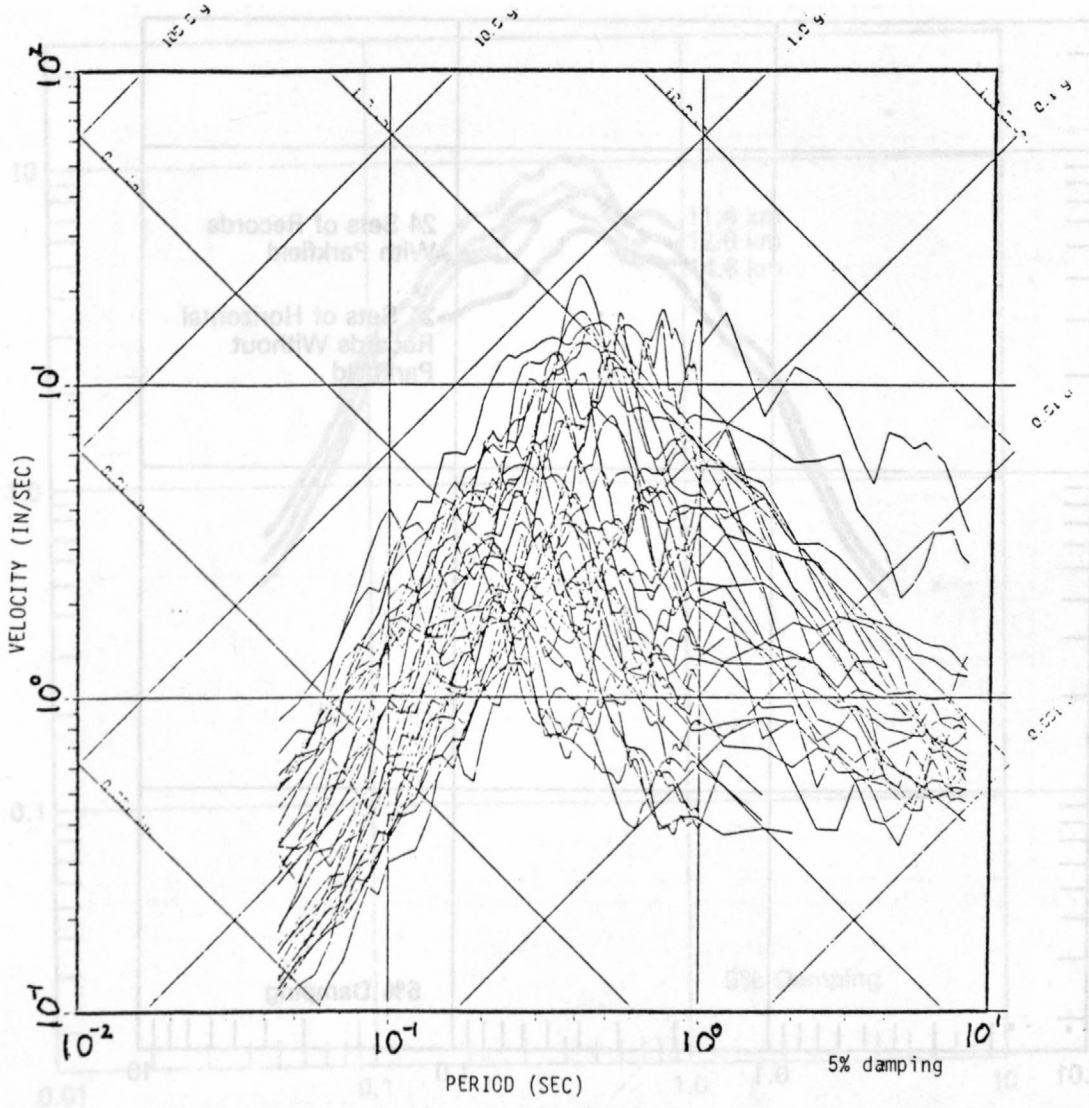

Figure 3. Overplot of Response Spectra used to develop site specific spectrum in Figure 4 (from Weston Geophysical).

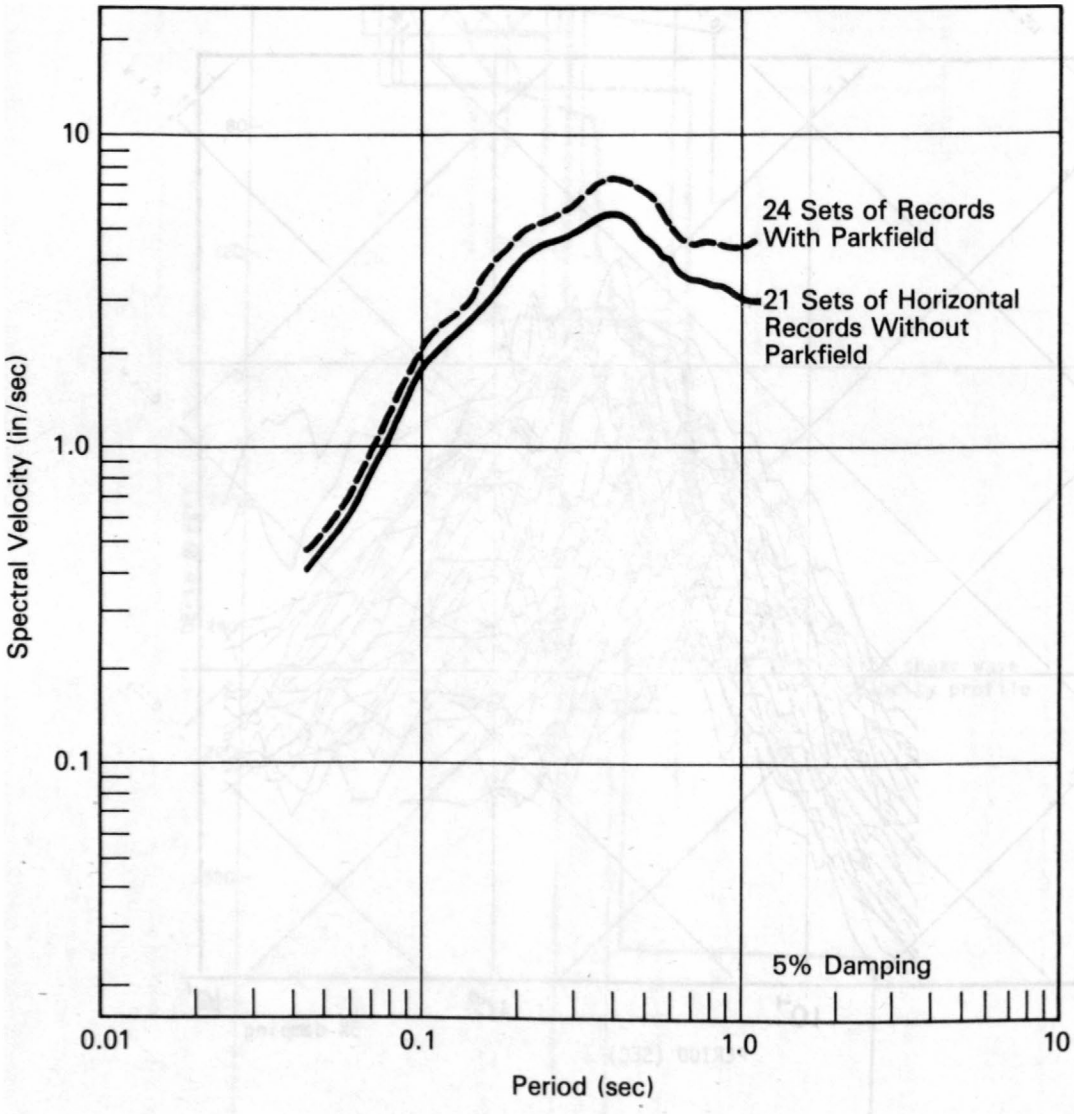

Figure 4. Comparison of 84th percentiles of two sets of data showing the effect of adding records from the 1966 Parkfield, California, earthquake (from Weston Geophysical).

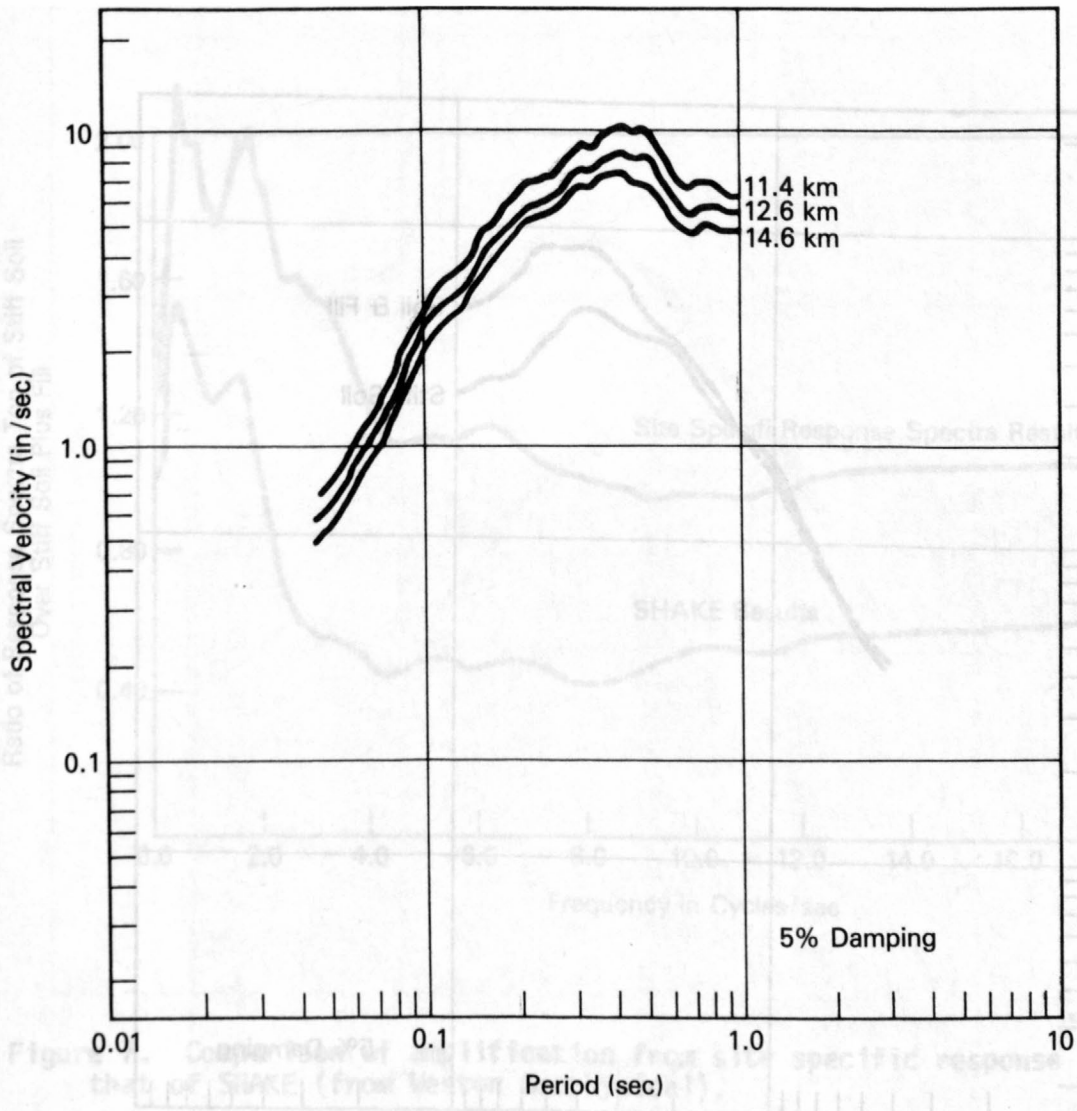

Figure 5. Comparison of 84th percentiles of the site specific spectra with Parkfield data in Figure 4, as the source distance of the strong motion data is systematically restricted (from Weston Geophysical).

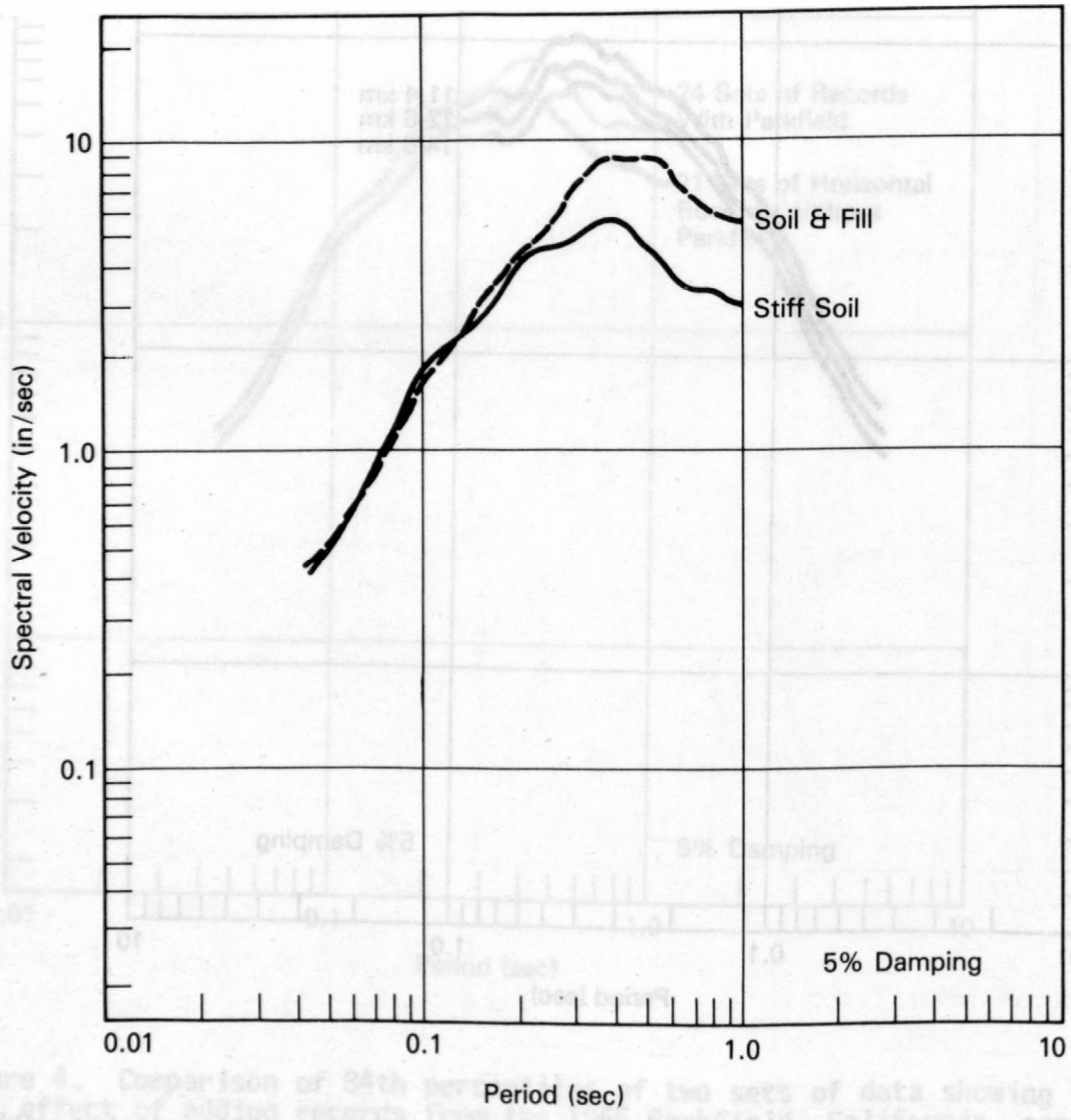

Figure 6. Comparison of 84th percentile of site specific spectra on top of stiff soil and on top of stiff soil plus fill material (from Weston Geophysical).

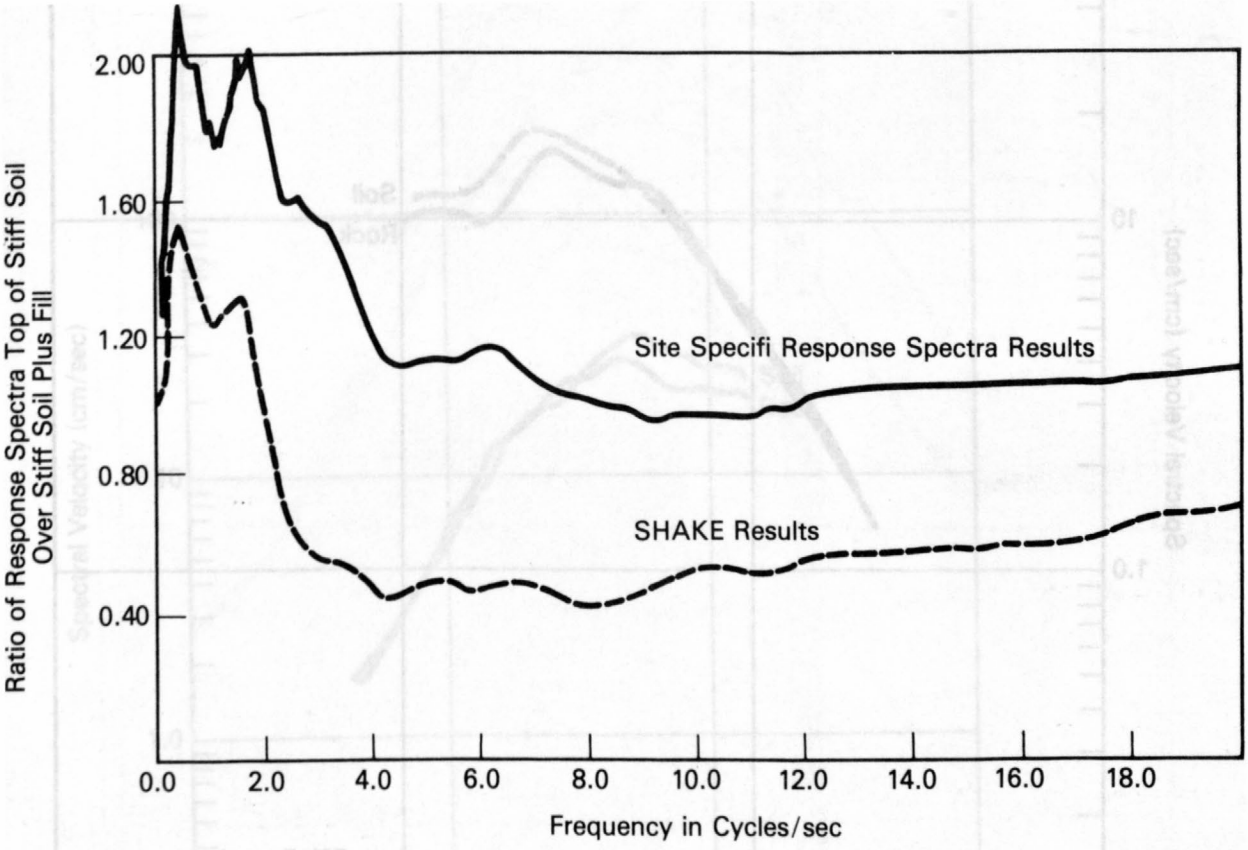

Figure 7. Comparison of amplification from site specific response spectra to that of SHAKE (from Weston Geophysical).

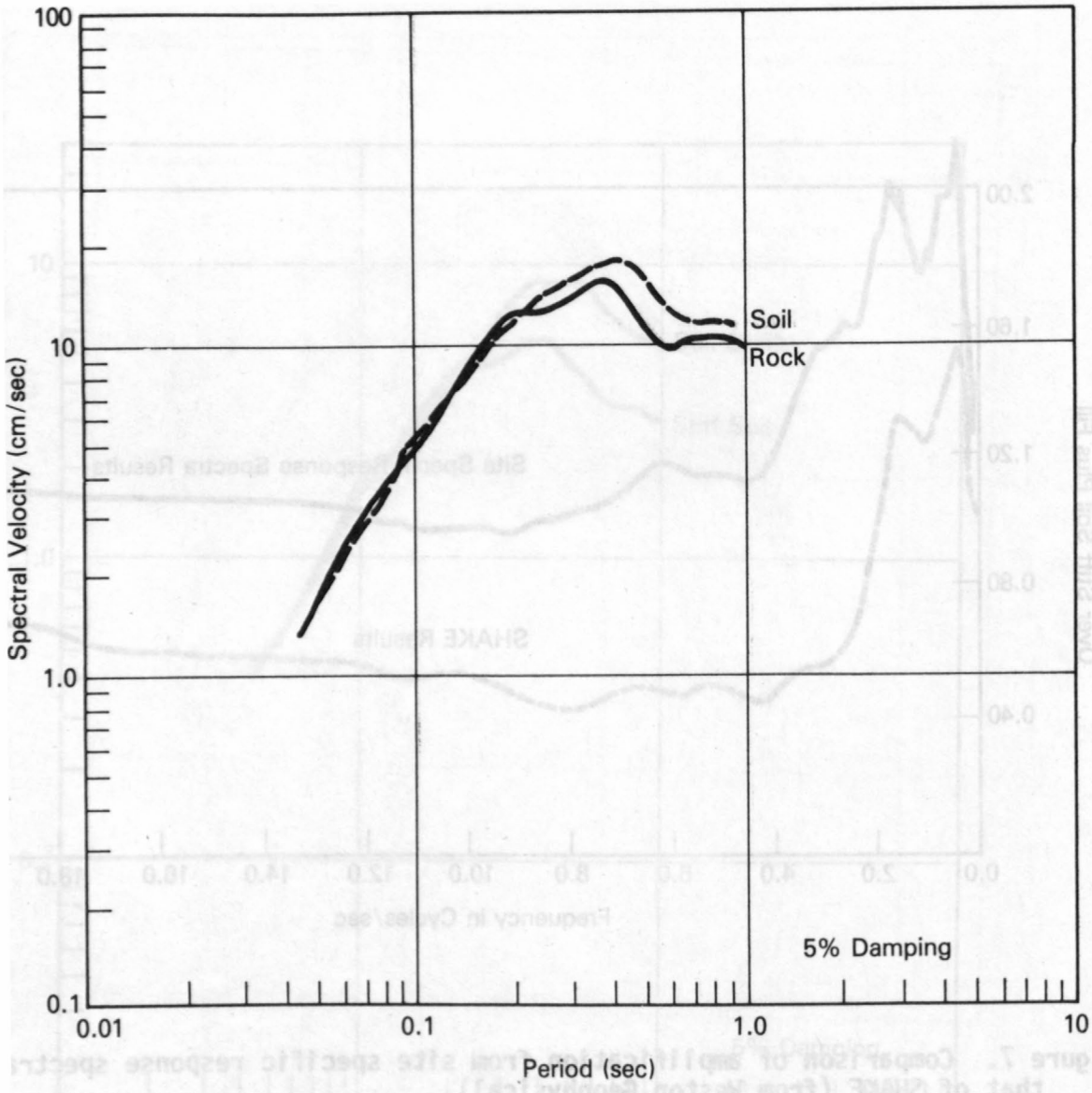

Figure 8. Comparison of 84th percentile of M_L = 5.3 soil and rock site specific spectra (from Weston Geophysical).

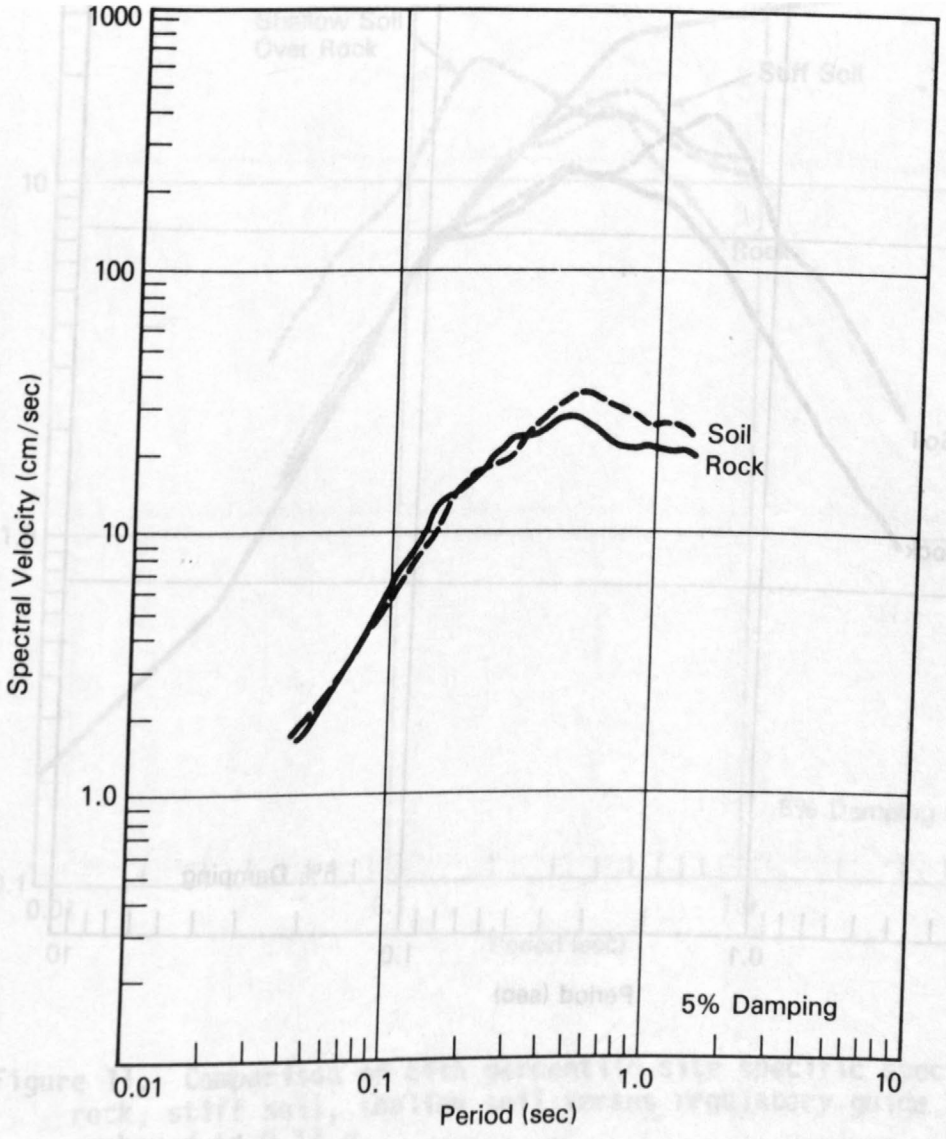

Figure 9. Comparison of 84th percentile of M_L = 5.8 soil and rock site specific spectra (from Lawrence Livermore National Laboratory).

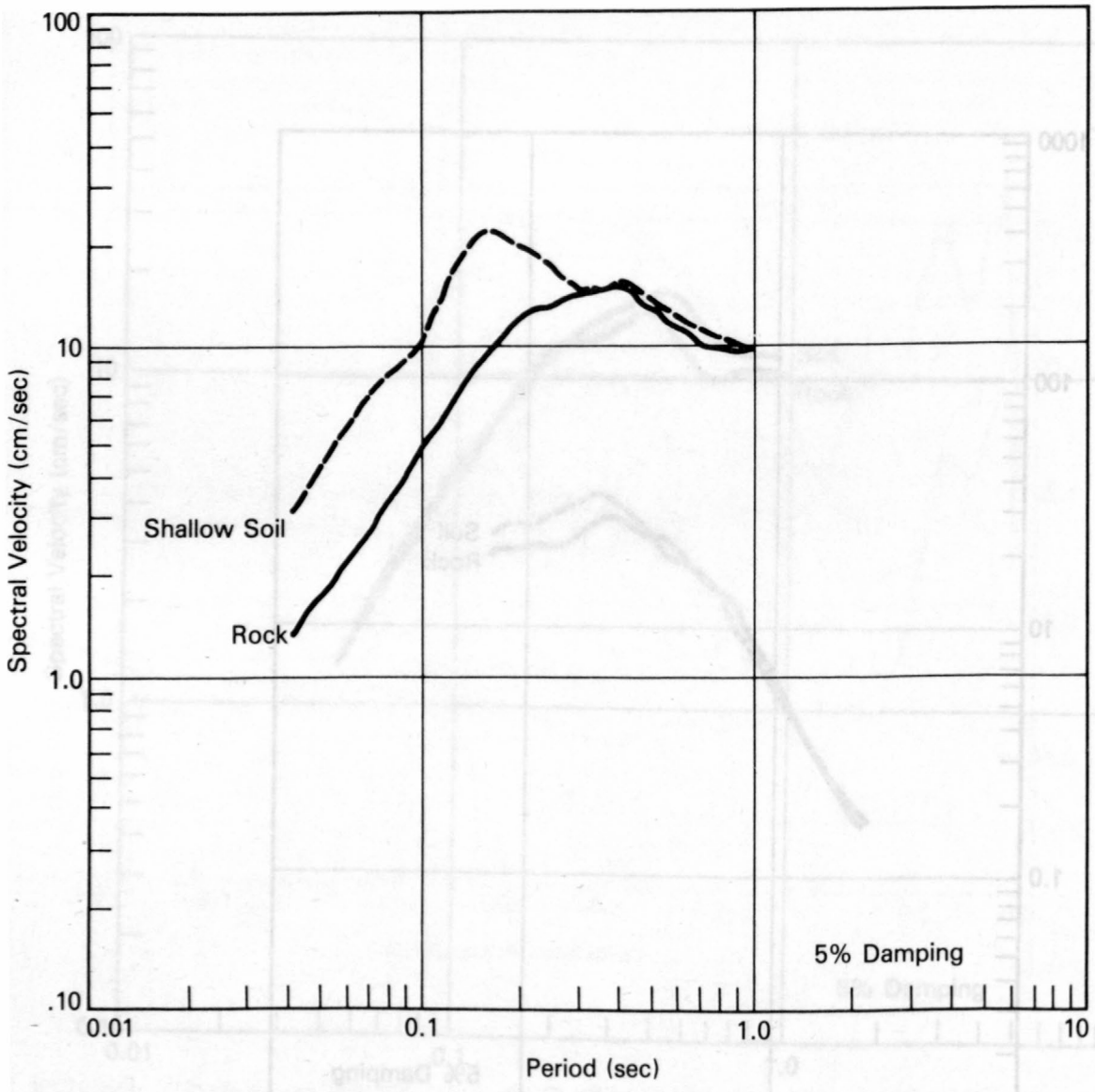

Figure 10. Comparison of 84th percentiles of M_L = 5.3 shallow soil and rock site specific spectra (from Lawrence Livermore National Laboratory).

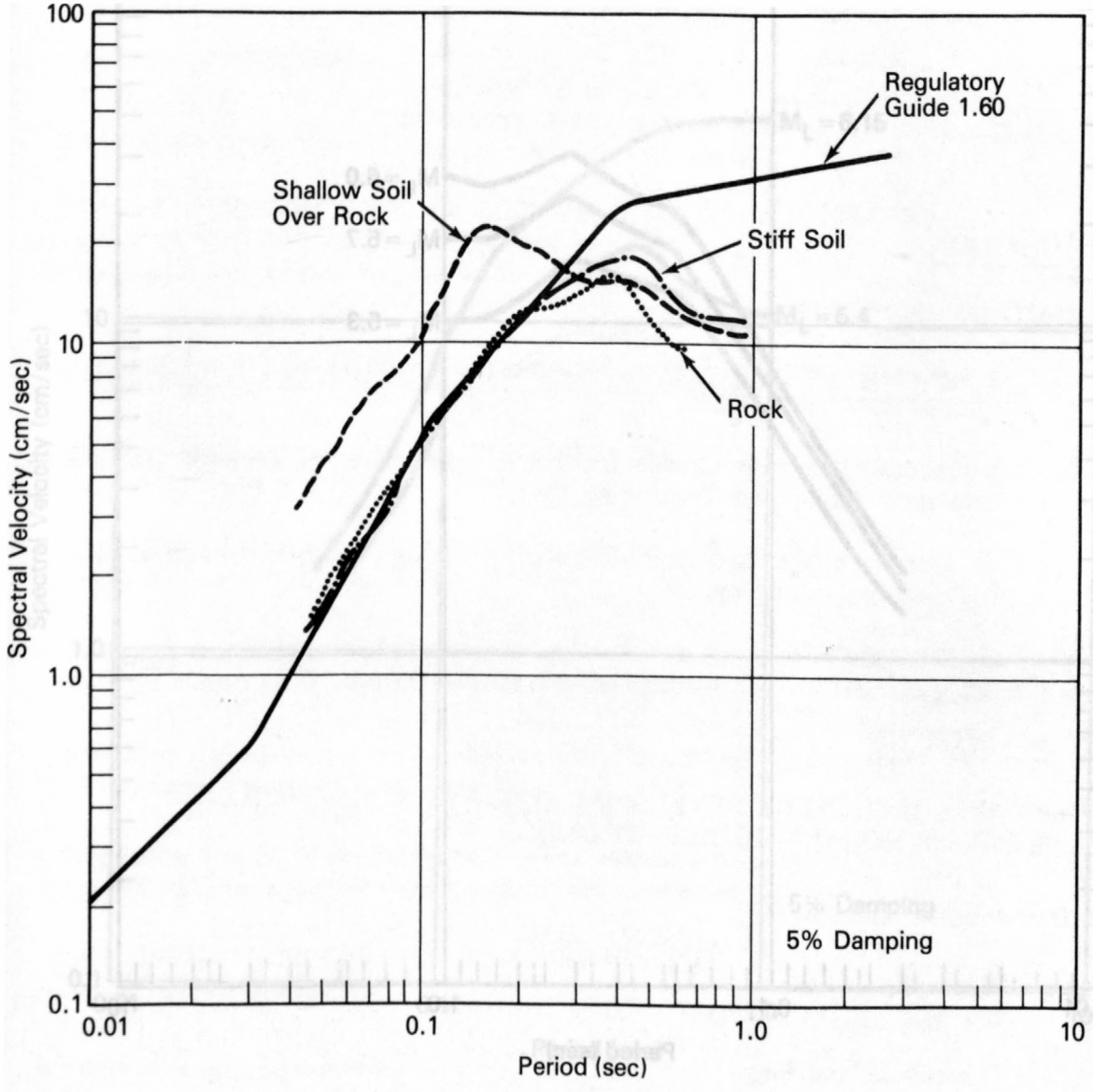

Figure 11. Comparison of 84th percentile site specific spectra, M = 5.3, rock, stiff soil, shallow soil versus regulatory guide 1.60 spectrum anchored to 0.13 g.

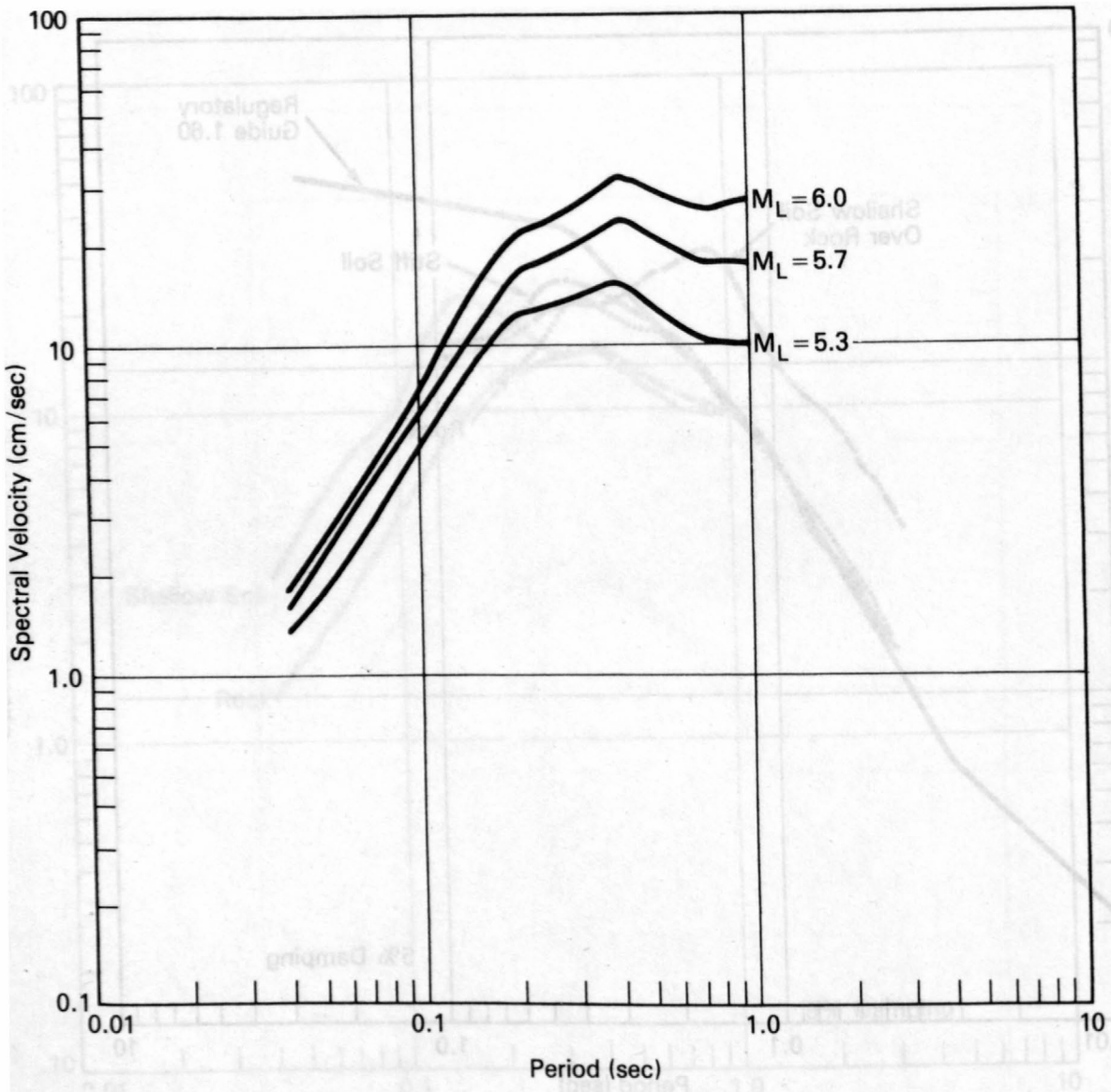

Figure 12. Comparison of 84th percentile of M_L = 5.3, 5.7, 6.0 rock site specific spectra (from Lawrence Livermore National Laboratory, Weston Geophysical, and Tennessee Valley Authority).

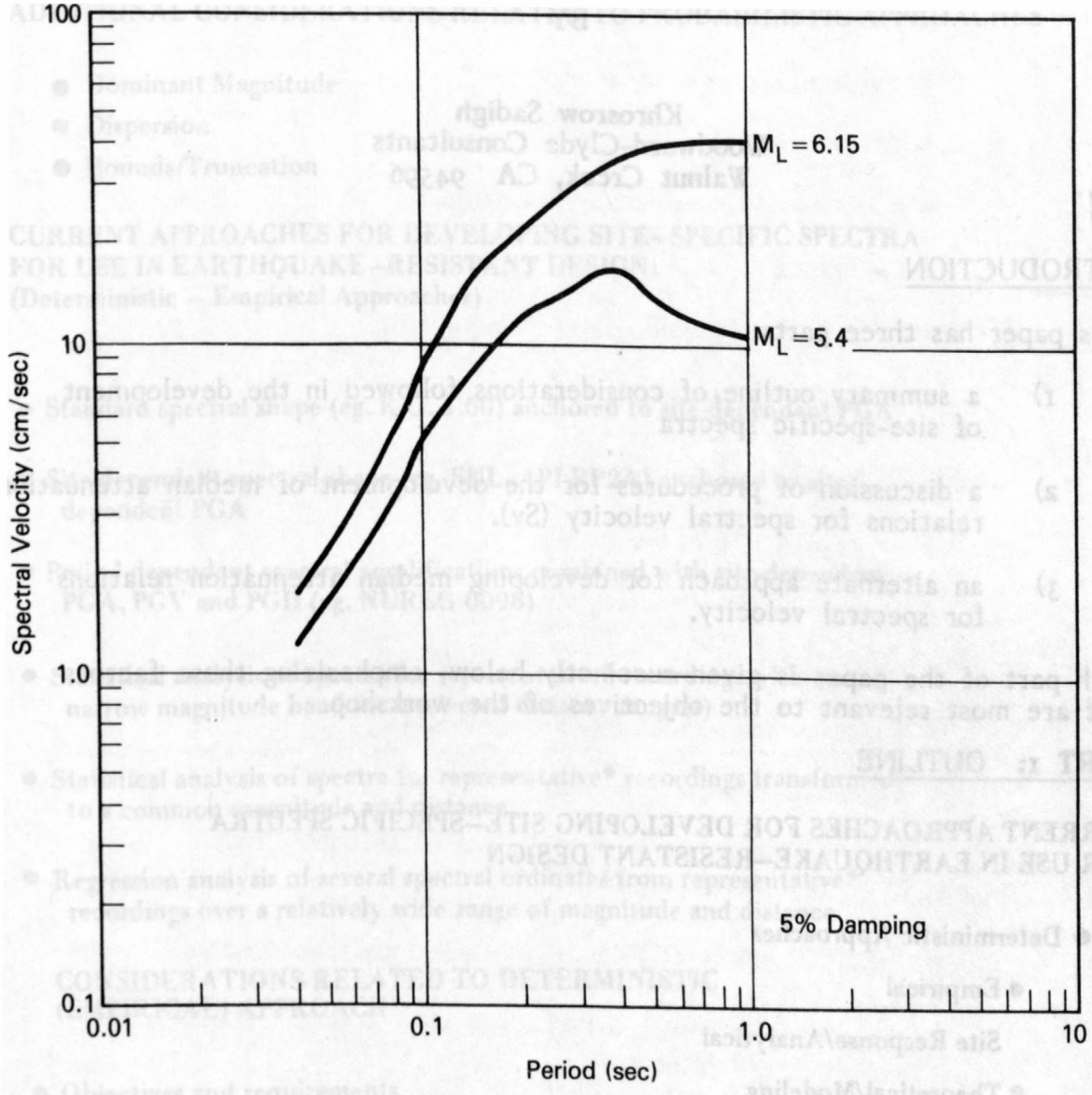

Figure 13. Comparison of the 84th percentile of M_L = 6.15, 5.4 soil site specific spectra (from Woodward-Clyde and Weston Geophysical).

CONSIDERATIONS IN THE DEVELOPMENT OF SITE-SPECIFIC SPECTRA

BY

Khrosrow Sadigh
Woodward-Clyde Consultants
Walnut Creek, CA 94596

INTRODUCTION

This paper has three parts:

1) a summary outline of considerations followed in the development of site-specific spectra

2) a discussion of procedures for the development of median attenuation relations for spectral velocity (Sv).

3) an alternate approach for developing median attenuation relations for spectral velocity.

Each part of the paper is given succinctly below, emphasizing those factors that are most relevant to the objectives of the workshop.

PART 1: OUTLINE

CURRENT APPROACHES FOR DEVELOPING SITE–SPECIFIC SPECTRA FOR USE IN EARTHQUAKE–RESISTANT DESIGN

- Deterministic Approaches
  - Empirical

    Site Response/Analytical
  - Theoretical/Modeling
- Probabilistic Approaches
  - ZPA (probabilistic) x Spectral Shape
  - Response Spectral Ordinates (several periods)

CONSIDERATIONS RELATED TO DETERMINISTIC (EMPIRICAL) APPROACHES

- Source/path effects
- Scaling for distance and magnitude
- Quantification of effects of local soil conditions
- Quantification of dispersion

CONSIDERATIONS RELATED TO DETERMINISTIC (Site Response/Analytical) APPROACH

CONSIDERATIONS RELATED TO DETERMINISTIC
(Thoretical/Modeling) APPROACH

ADDITIONAL CONSIDERATIONS RELATED TO PROBABILISTIC APPROACHES

- Dominant Magnitude
- Dispersion
- Bounds/Truncation

CURRENT APPROACHES FOR DEVELOPING SITE–SPECIFIC SPECTRA FOR USE IN EARTHQUAKE–RESISTANT DESIGN:
(Deterministic – Empirical Approaches)

- Standard spectral shape (eg. R.G. 1.60) anchored to site-dependent PGA
- Site-dependent spectral shape (eg. SUL, API RP2A) anchored to site-dependent PGA
- Period-dependent spectral amplifications combined with site-dependent PGA, PGV and PGD (eg. NUREG 0098)
- Statistical analysis of spectra for representative* recordings within a narrow magnitude band for a selected distance range(s)
- Statistical analysis of spectra for representative* recordings transformed to a common magnitude and distance
- Regression analysis of several spectral ordinates from representative* recordings over a relatively wide range of magnitude and distance

CONSIDERATIONS RELATED TO DETERMINISTIC
(EMPIRICAL) APPROACH

- Objectives and requirements
- Availability of representative recordings
- Scaling for source, distance and magnitude
- Quantification of dispersion
- Quantification of effects of local soil conditions
(Guidelines from other procedures)
- Over-sensitivity due to limited size of data base
- Examination of consistency of individual/isolated cases with the overall trends from world-wide data base

*To the extent possible, representative of tectonic environment and local soil conditions

CURRENT APPROACHES FOR DEVELOPING SITE–SPECIFIC SPECTRA FOR USE IN EARTHQUAKE–RESISTANT DESIGN

- SITE RESPONSE/ANALYTICAL PROCEDURE
  - Appropriateness of the model
  - Characterization of material properties
  - Selection of appropriate input motion
  - Calibration
  - Wave type and period range accommodated
  - Absolute or relative indication ?
- THEORETICAL/MODELING PROCEDURE
  - Appropriateness of the model
  - Charaterization of source-path-site conditions
  - Calibration
  - Wave type and period range accommodated
  - Absolute or relative indication ?

CURRENT APPROACHES FOR DEVELOPING SITE–SPECIFIC SPECTRA FOR USE IN EARTHQUAKE–RESISTANT DESIGN

PROBABILISTIC APPROACHES: Requirements and Considerstions

- Attenuation relationship for PGA over wide range of magnitudes and distances
- Attenuation relationships of spectral ordinates over a wide range of magnitudes and distances
- Identification of the dominant source, dominant magnitude and dominant distance
- Considerations related to ground motion dispersion
- Considerations related to ground motion truncation
- Considerations related to ground motion bounds
- Considerations related to weighting with magnitude
- Validity of results viz a viz the rate of seismic activity
- Considerations related to deterministic constraints

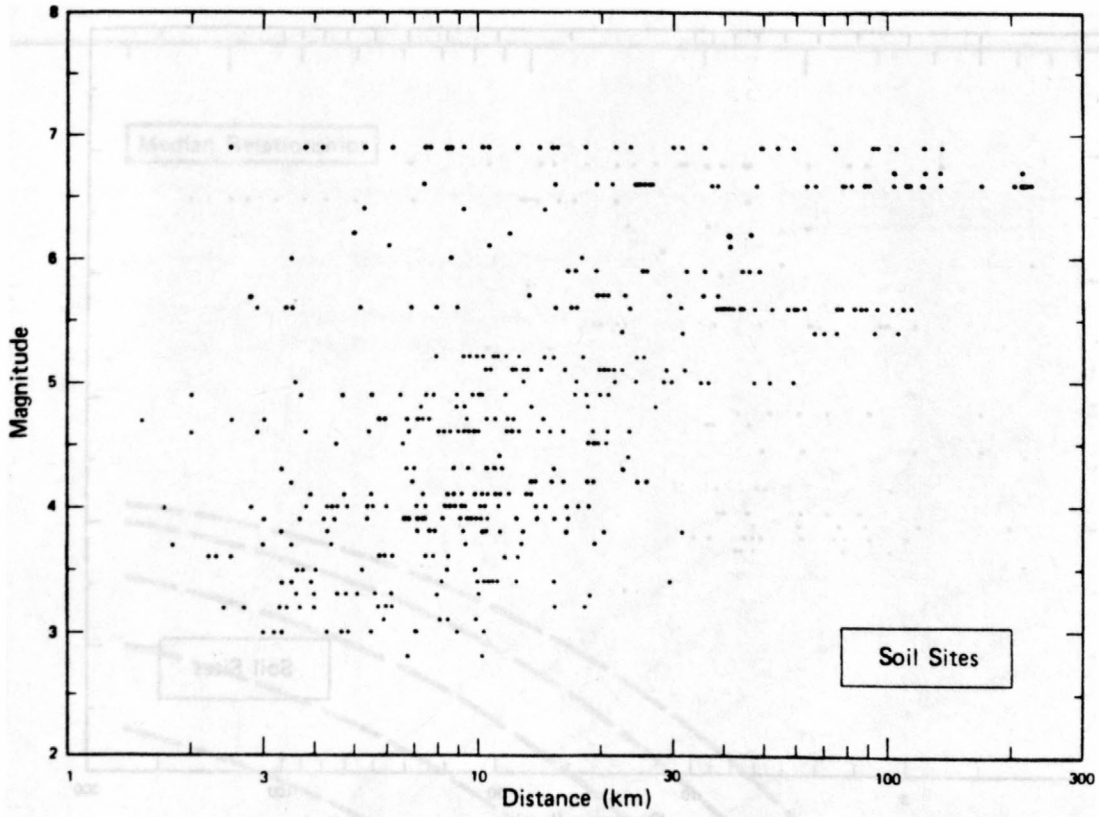

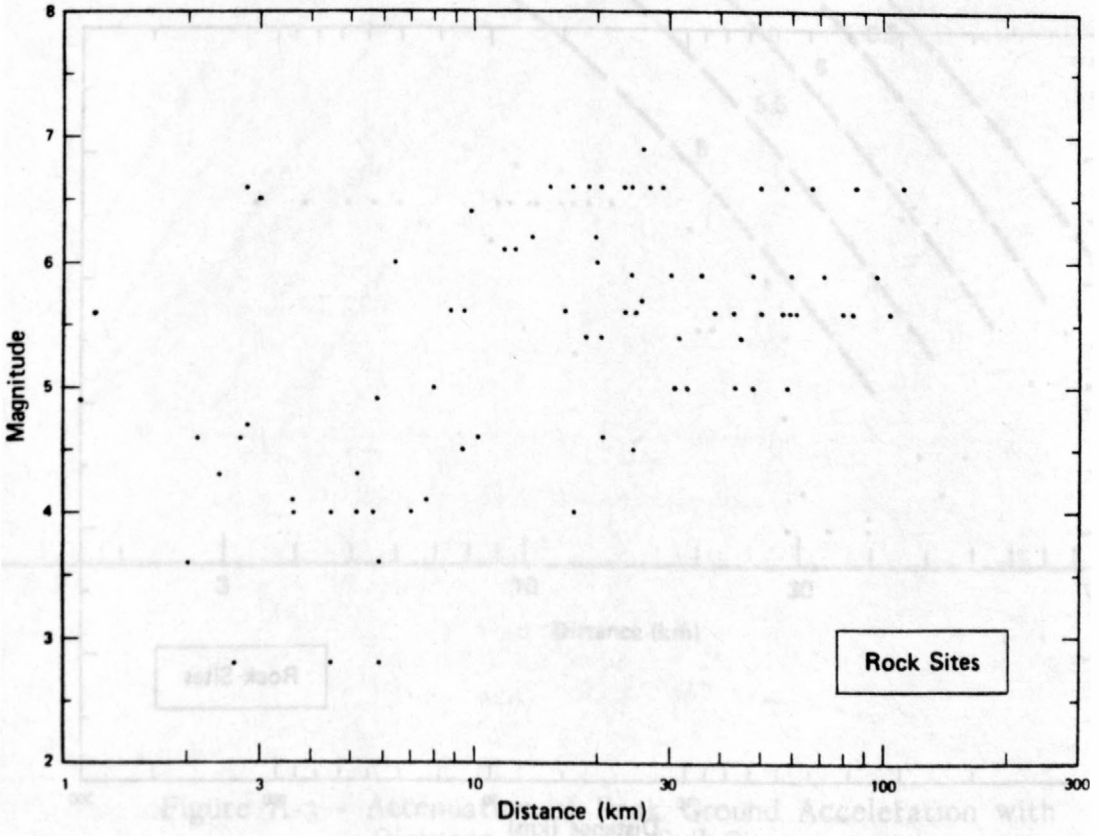

Figure A-1 - Distribution of PGA Data

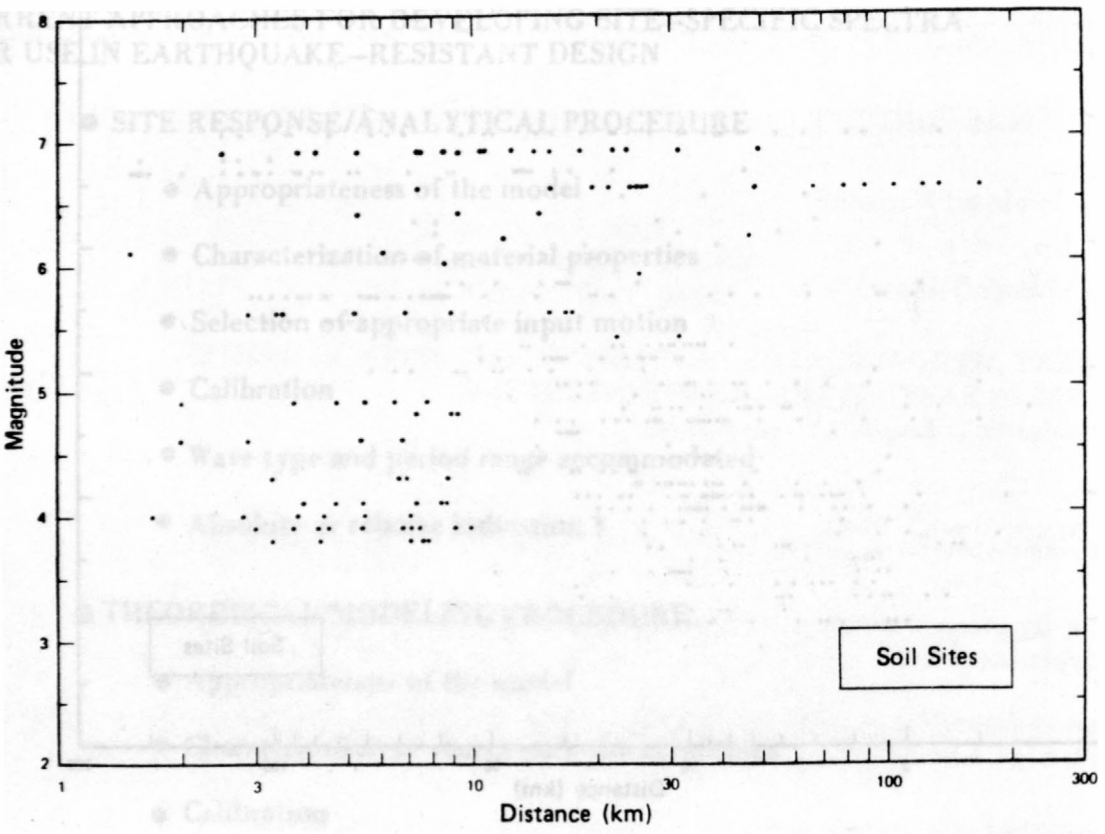

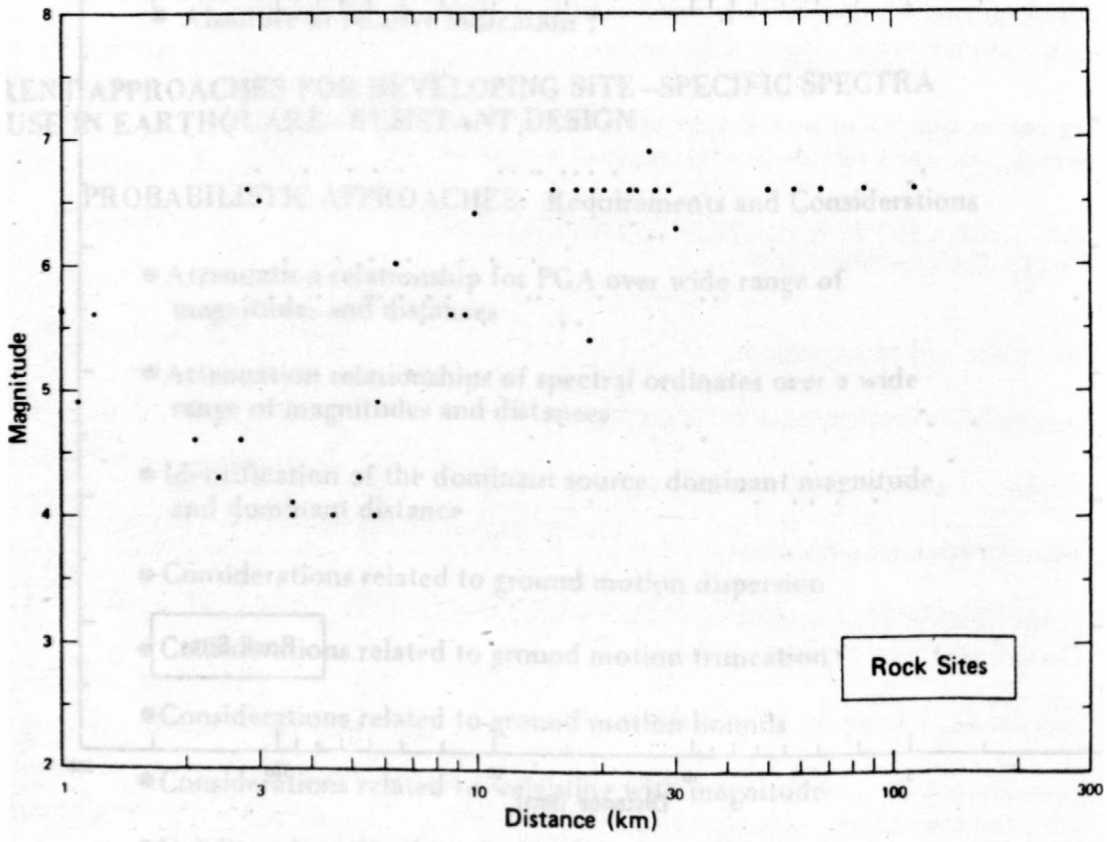

Figure A-2 - Distribution of Response Spectra Data

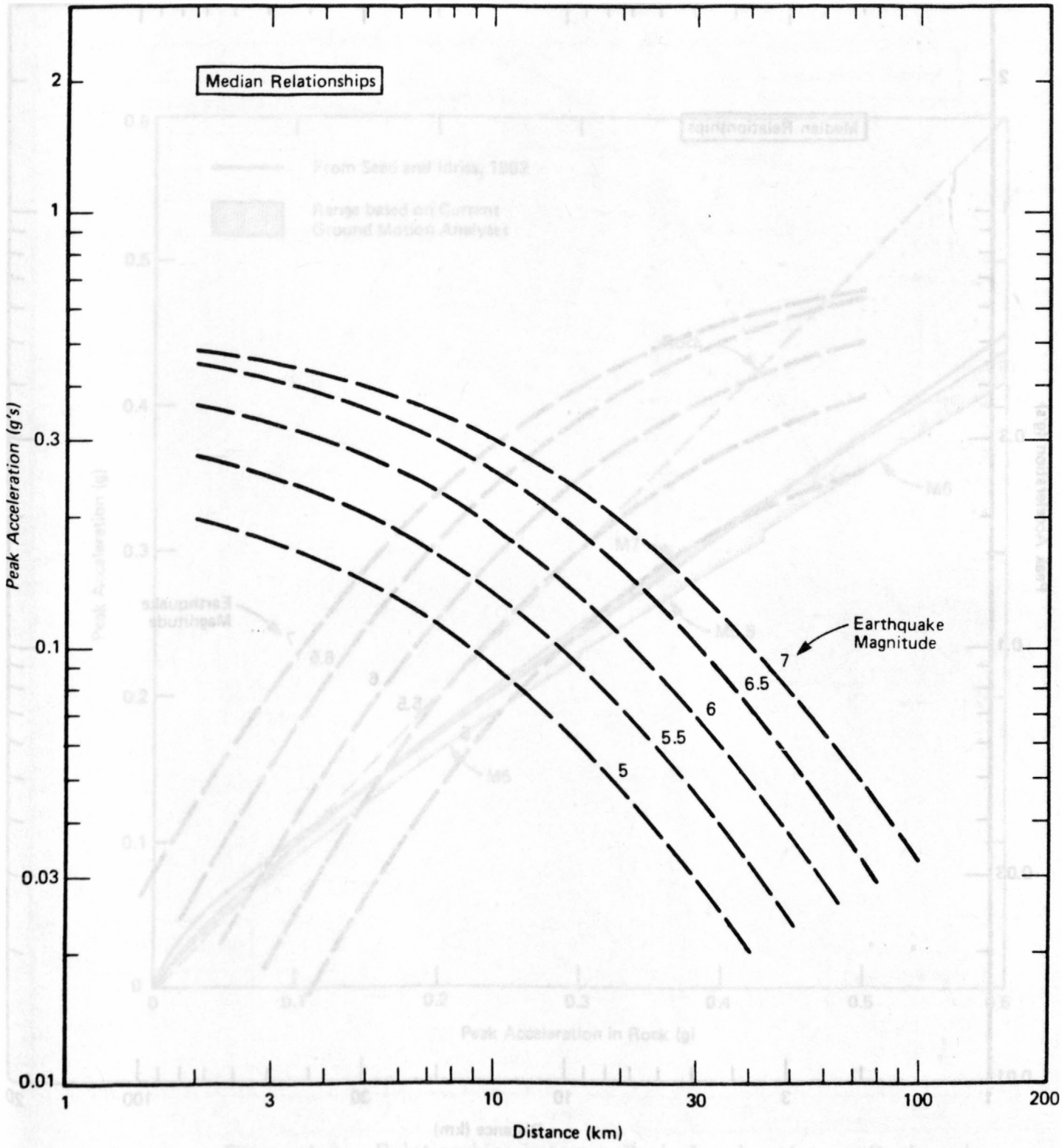

Figure A-3 - Attenuation of Peak Ground Acceleration with Distance for Deep Soil Sites

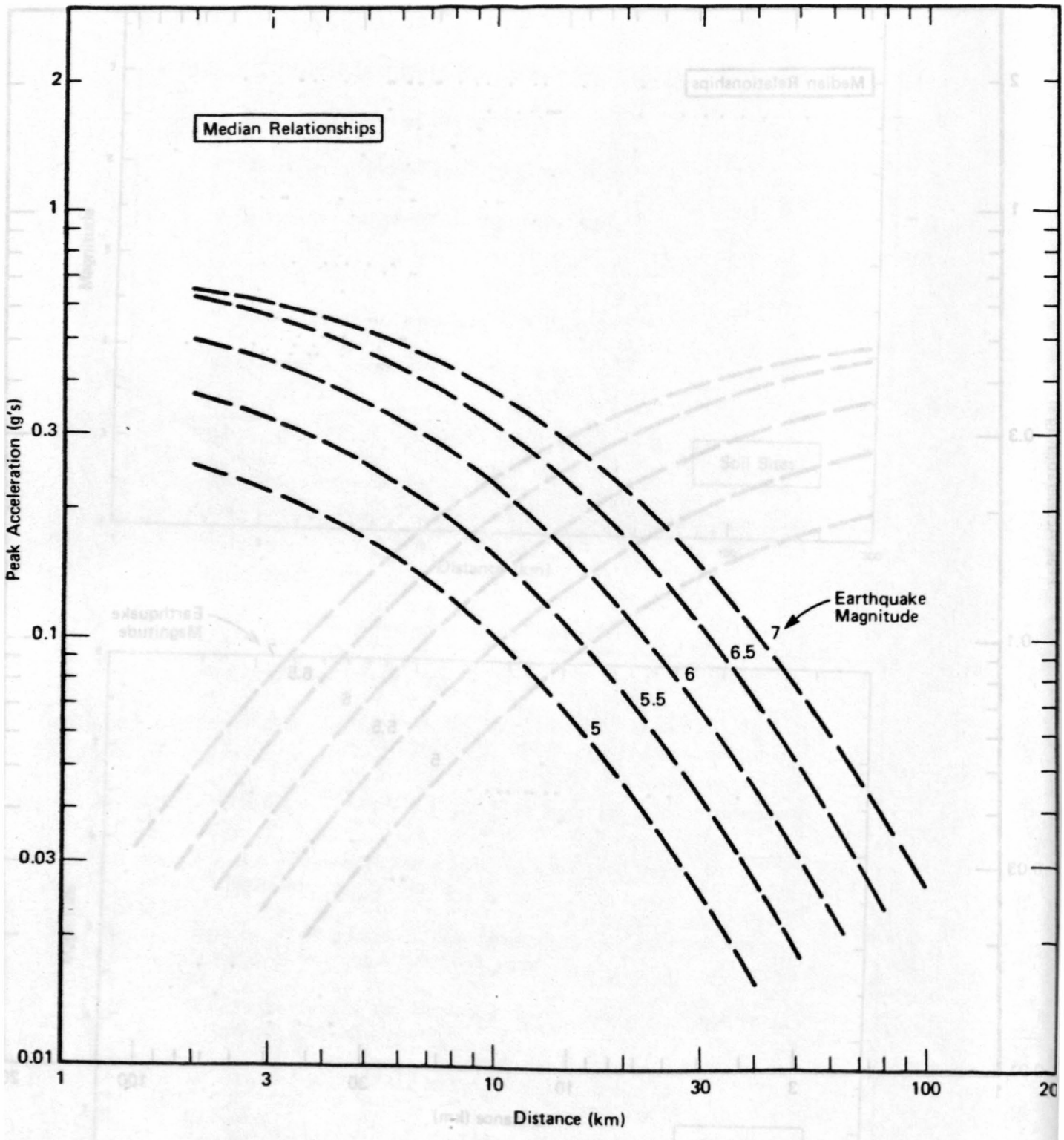

Figure A-4 - Attenuation of Peak Ground Acceleration with Distance for Rock Sites

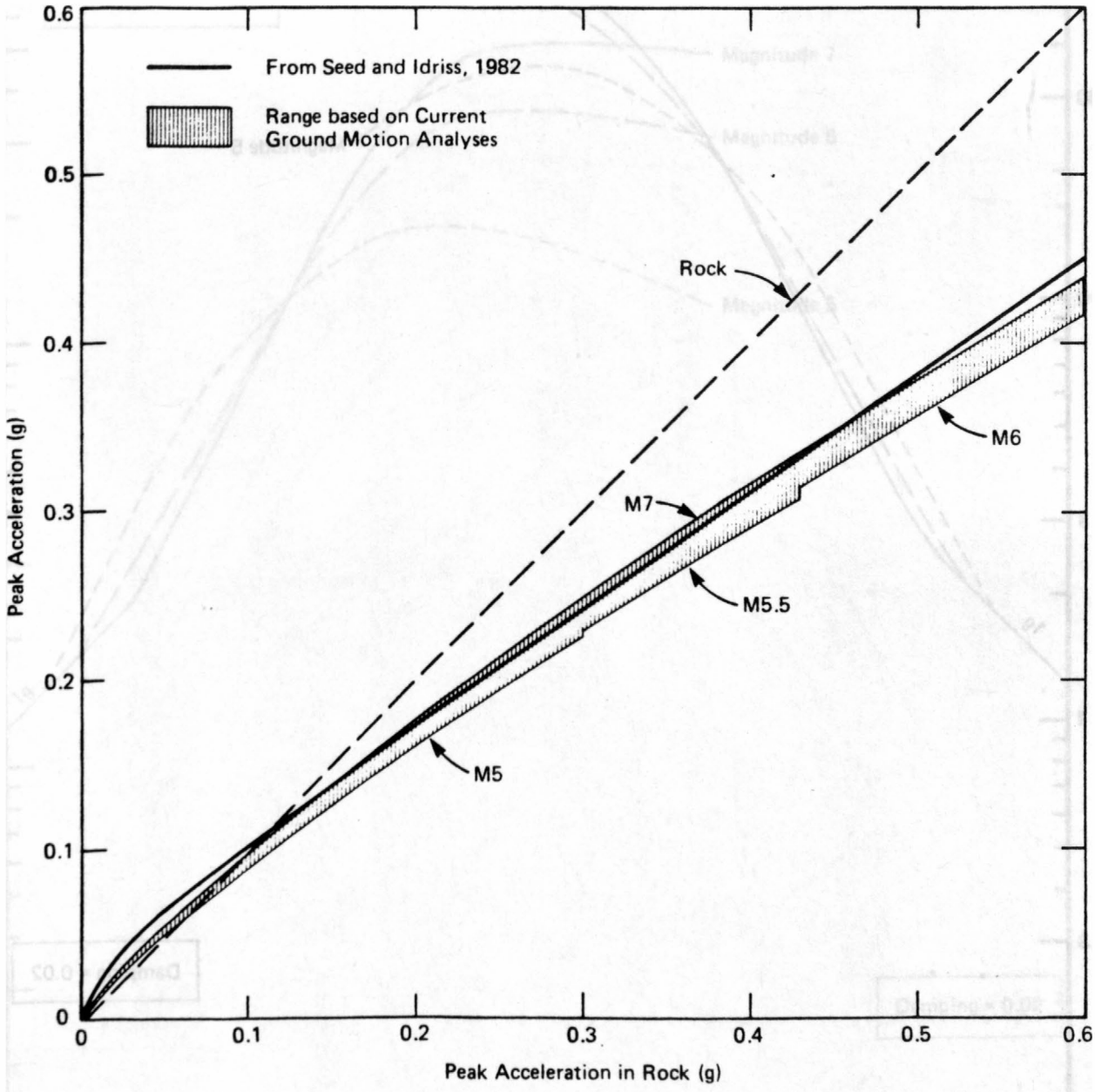

Figure A-5 - Relationships between Peak Acceleration on Rock and Deep Cohesionless Soil

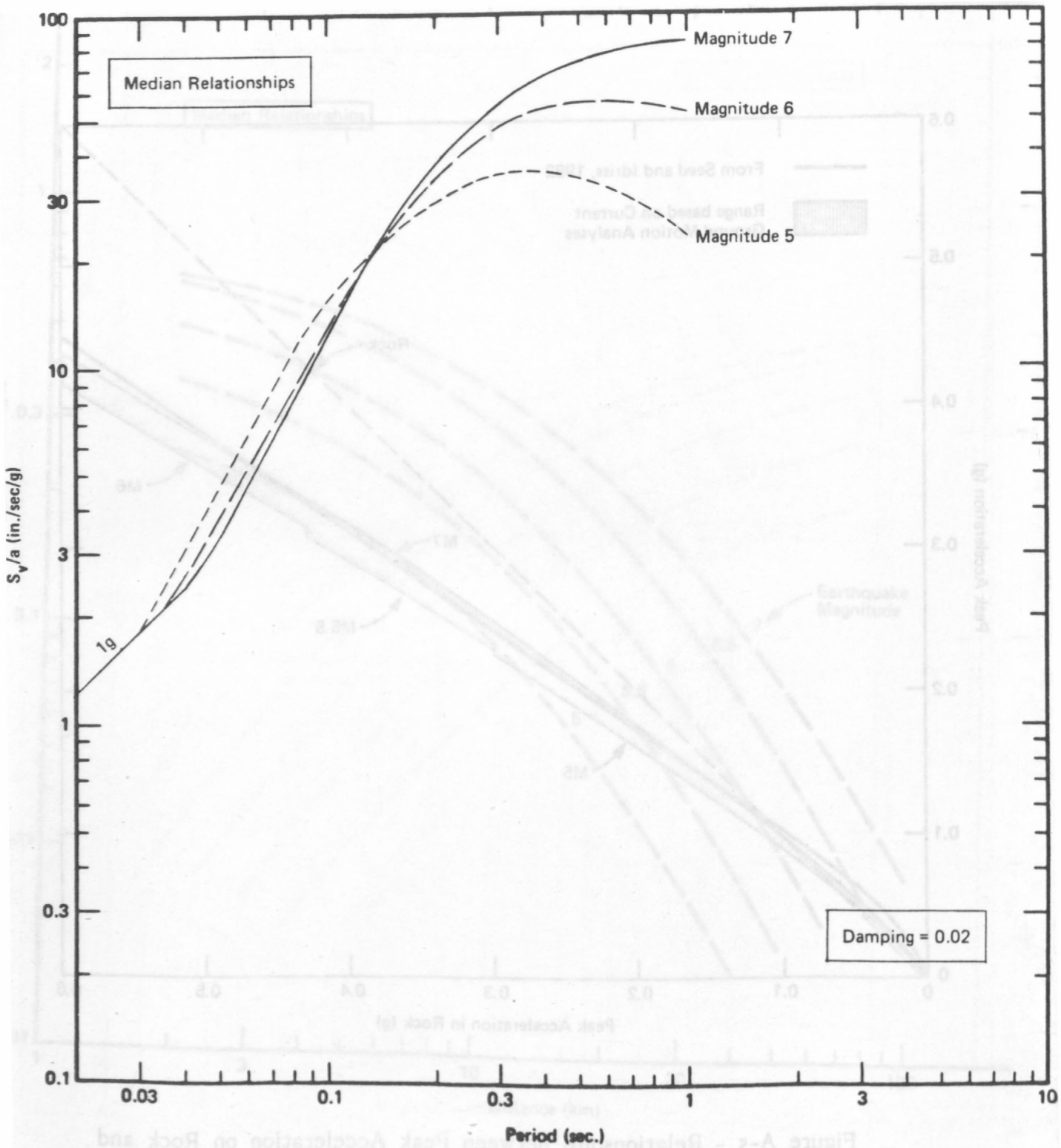

Figure A-6 - Summary of S_V/a versus T for M 5, 6, and 7 for Soil Sites at R = 8 km

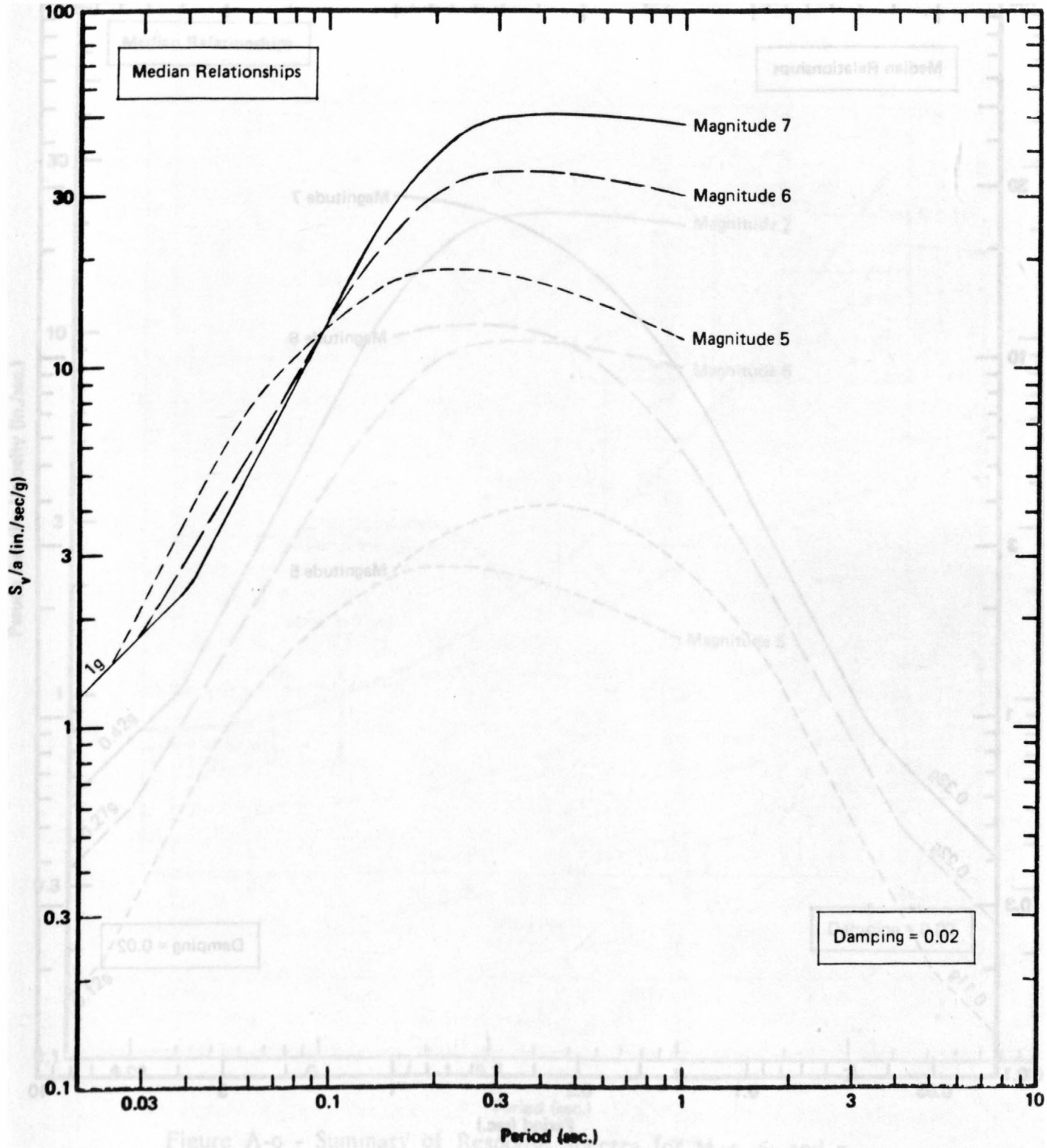

Figure A-7 - Summary of S_V/a versus T for M 5, 6, and 7 for Rock Sites at R = 8 km

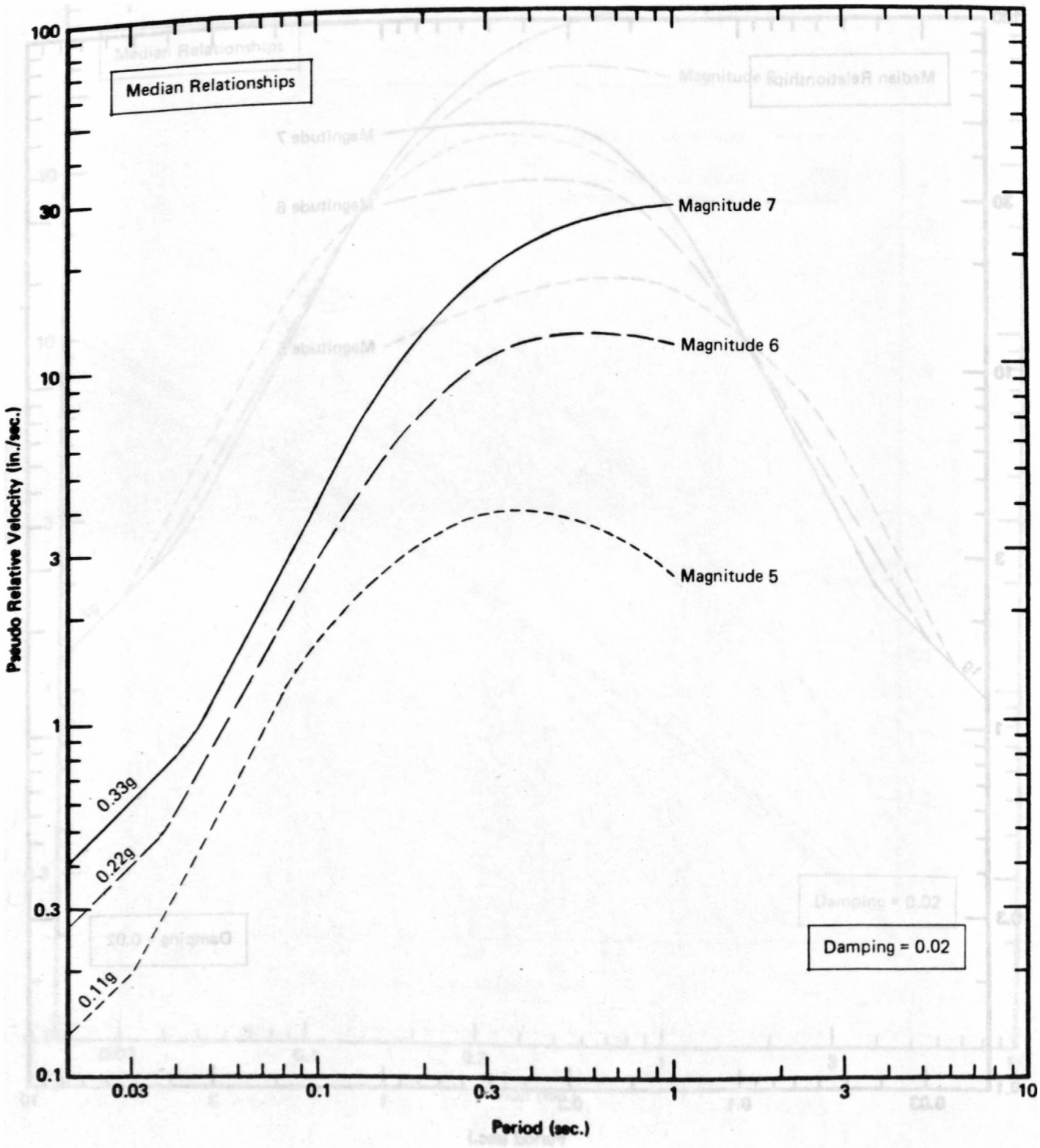

Figure A-8 - Summary of Response Spectra for M 5, 6, and 7 for Soil Sites at R = 8 km

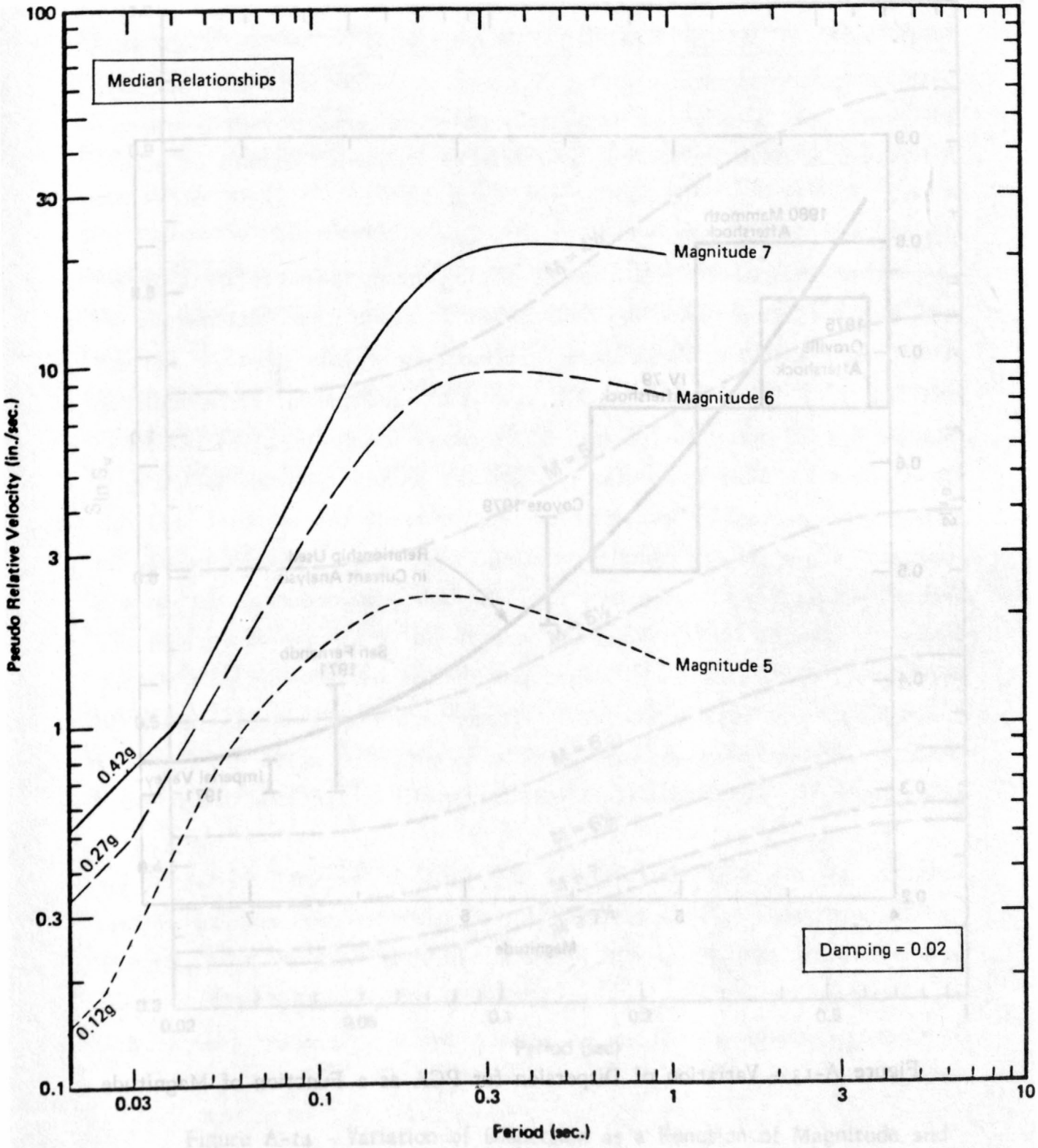

Figure A-9 - Summary of Response Spectra for M 5, 6, and 7 for Rock Sites at R = 8 km

Editor's note: Figures 10, 11, and 12 were not provided.

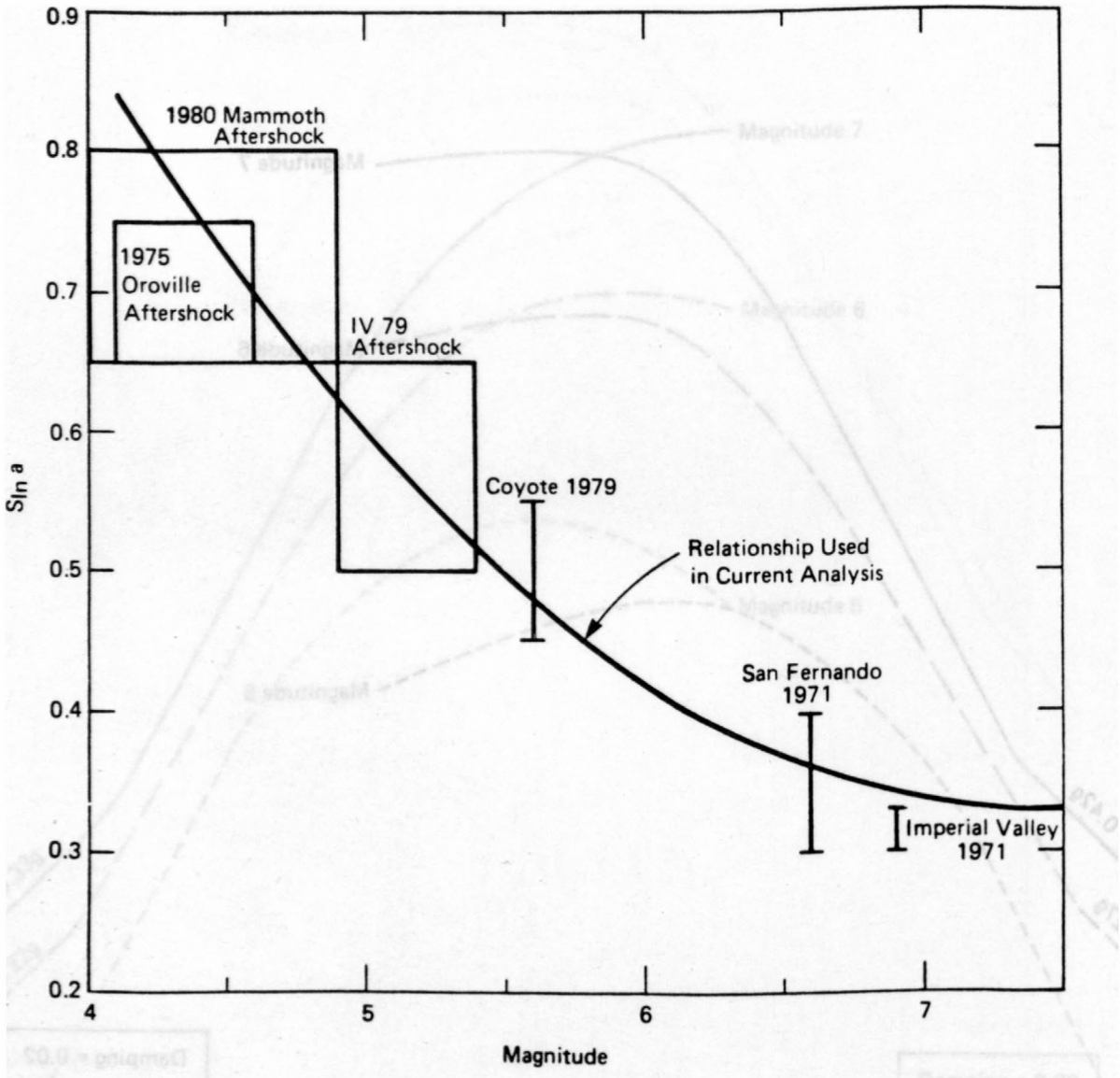

Figure A-13 - Variation of Dispersion for PGA as a Function of Magnitude

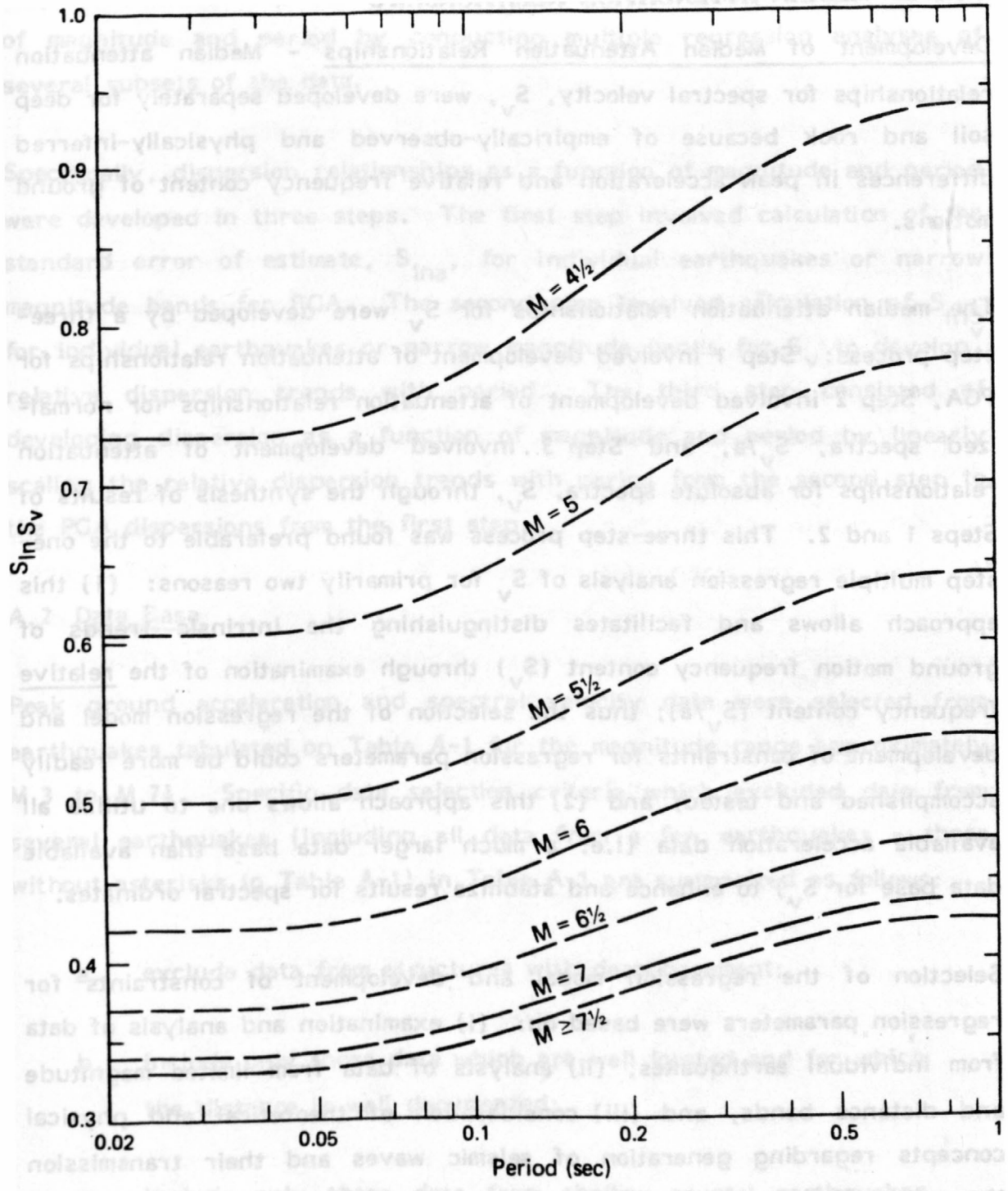

Figure A-14 - Variation of Dispersion as a Function of Magnitude and Period

PART 2: MEDIAN ATTENUATION RELATIONSHIPS

Development of Median Attenuation Relationships - Median attenuation relationships for spectral velocity, S_v, were developed separately for deep soil and rock because of empirically-observed and physically-inferred differences in peak acceleration and relative frequency content of ground motions.

The median attenuation relationships for S_v were developed by a three-step process: Step 1 involved development of attenuation relationships for PGA, Step 2 involved development of attenuation relationships for normalized spectra, S_v/a, and Step 3 involved development of attenuation relationships for absolute spectra, S_v, through the synthesis of results of Steps 1 and 2. This three-step process was found preferable to the one-step multiple regression analysis of S_v for primarily two reasons: (1) this approach allows and facilitates distinguishing the intrinsic trends of ground motion frequency content (S_v) through examination of the relative frequency content (S_v/a); thus the selection of the regression model and development of constraints for regression parameters could be more readily accomplished and tested; and (2) this approach allows one to utilize all available acceleration data (i.e. a much larger data base than available data base for S_v) to enhance and stabilize results for spectral ordinates.

Selection of the regression model and development of constraints for regression parameters were based on: (i) examination and analysis of data from individual earthquakes, (ii) analysis of data from limited magnitude and distance bands, and (iii) consideration of theoretical and physical concepts regarding generation of seismic waves and their transmission through earth materials.

Development of Relationships for Dispersion - One of the limitations of least-squares regression analysis is that the variation of dispersion as a function of magnitude cannot be directly obtained from the multiple regression analysis results. In the current ground motion analyses,

dispersion relationships for spectral ordinates were developed as a function of magnitude and period by conducting multiple regression analyses of several subsets of the data.

Specifically, dispersion relationships as a function of magnitude and period were developed in three steps. The first step involved calculation of the standard error of estimate, S_{lna}, for individual earthquakes or narrow magnitude bands for PGA. The second step involved calculation of S_{lnS_v} for individual earthquakes or narrow magnitude bands for S_v to develop relative dispersion trends with period. The third step consisted of developing dispersion as a function of magnitude and period by linearly scaling the relative dispersion trends with period from the second step to the PGA dispersions from the first step.

A.2 Data Base

Peak ground acceleration and spectral velocity data were selected from earthquakes tabulated on Table A-1 for the magnitude range approximately M 3 to M 7½. Specific data selection criteria which excluded data from several earthquakes (including all data from a few earthquakes - those without asterisks in Table A-1) in Table A-1 are summarized as follows:

a. exclude data from structures with deep basement;

b. include only those data which are well located and for which the distance is well documented;

c. include only those data from shallow crustal earthquakes typical of California; and

d. include only those data for deep soil and rock excluding shallow soil over rock or very soft soil sites.

Based on the analysis format (Table 2-1), the data were separated by site classification to fall under two general classifications: deep soil sites and rock sites. For peak acceleration, applying the selection criteria to the recordings from earthquakes shown in Table A-1 yielded 1,053 Volume I PGA values of which 892 were from deep soil sites and 161 were from rock sites. The data set for response spectra are subsets of the deep soil and rock PGA data set and are comprised of the digitized and processed accelerograms. The spectral data subsets represent approximately one-third of the main PGA data set. Specifically, the spectral subset is comprised of 292 spectra (224 for soil and 68 for rock) defined by 68 periods between 0.04 and 10 seconds at 2% damping.

The distribution of data for each earthquake as a function of distance for rock and soil are summarized in Tables A-2 through A-5. Specifically, Tables A-2 and A-3 show the number of PGA data points, in various distance ranges, for soil and rock sites, respectively. Similarly, Tables A-4 and A-5 show the number of spectra in various distance ranges from soil and rock sites, respectively. The overall distribution of PGA data as a function of magnitude and distance is summarized for soil sites as follows:

	NO. OF DATA POINTS MAGNITUDE RANGE			
R (km)	2.8 - 3.9	4.0 - 4.9	5.0 - 5.9	6.0 - 6.9
0 - 10	170	150	27	55
10 - 25	56	112	87	42
25 - 50	4	4	55	34
50 - 100	0	0	29	22
>100	0	0	5	40

and for rock sites:

R (km)	NO. OF DATA POINTS MAGNITUDE RANGE 2.8 - 3.9	4.0 - 4.9	5.0 - 5.9	6.0 - 6.9
0 - 10	10	30	10	8
10 - 25	0	6	15	22
25 - 50	0	2	26	6
50 - 100	0	0	15	8
>100	0	0	1	2

Similarly, the overall distribution of spectral data as a function of magnitude and distance is summarized for soil sites as follows:

R (km)	NO. OF SPECTRA MAGNITUDE RANGE 2.8 - 3.9	4.0 - 4.9	5.0 - 5.9	6.0 - 6.9
0 - 10	32	62	13	37
10 - 25	0	0	10	34
25 - 50	0	0	4	18
50 - 100	0	0	0	6
>100	0	0	0	8

and for rock sites:

R (km)	NO. OF SPECTRA MAGNITUDE RANGE 2.8 - 3.9	4.0 - 4.9	5.0 - 5.9	6.0 - 6.9
0 - 10	0	20	8	8
10 - 25	0	0	2	12
25 - 50	0	0	0	8
50 - 100	0	0	0	8
>100	0	0	0	2

The various distributions of data presented above for PGA for soil sites, PGA for rock sites, spectra for soil sites and spectra for rock sites are plotted as points of M vs. R on Figures A-1 and A-2. In general, these graphs show that the PGA data sets are more complete than for spectra

(Figure A-1 vs. Figure A-2), and that the soil data sets are more complete than the rock data sets (Figure A-1 for PGA and Figure A-2 for S_v). For these reasons, spectra shapes S_v/a were analyzed and augmented by the more extensive PGA data base. Also, the analysis of rock data required careful extrapolation of the regression into close distances taking into account the relative trends of soil and rock data with distance and acknowledgement of physical principles.

A.3 Attenuation Relationships for Peak Ground Acceleration

The soil and rock PGA data sets described in Section A.2 were analyzed by multiple regression using the following relationship:

$$\ln a = b_1 + b_2 M + b_3 \ln [R + C(M)]$$

Constraints on parameter b_3 (far field slope) and C (distance normalizing parameter) were developed based on: (i) examination and analysis of data from individual earthquakes, (ii) analysis of data from limited magnitude and distance bands, and (iii) consideration of theoretical and physical concepts regarding generation of seismic waves and their transmission through earth materials.

These multiple regression analyses resulted in the development of median attenuation curves of PGA as a function of distance for M 5 to 7 as shown in Figure A-3 for deep soil sites and Figure A-4 for rock sites. By cross plotting PGA values for deep soil site from Figure A-3 versus PGA values for rock from Figure A-4, the range of values shown in Figure A-5 was developed. As can be noted from Figure A-5, this range of value is in good agreement with the curve developed by Seed and Idriss (1982) for deep soil sites.

A.4 Attenuation Relationships for Response Spectra

The soil and rock spectra data sets described in Section A.2 were normalized by their corresponding PGA values and analyzed period by period by multiple regression using the following relationship:

$$\ln S_v/a = b_1' + b_2' (8.5 - M)^n + b_3' \ln [R + C(M)]$$

Use of the term $b_2' (8.5 - M)^n$ instead of the more common $b_2 M$ term in the above equation was found to better represent the effect of magnitude on the normalized spectral ordinates. It also provides for saturation of normalized spectral ordinates at a magnitude of 8.5.

Parameters b_3' and C were constrained for each period considered in much the same manner as for PGA. The results of the S_v/a analyses were then augmented by the PGA results to develop attenuation relationships for S_v having the following form:

$$\ln S_v = b_1'' + b_2 M + b_2' (8.5 - M)^n + b_3'' \ln [R + C(M)]$$

The attenuation relationship developed for PGA in Figures A-3 and A-4, together with the spectral ordinate attenuation relationship described above, were used to develop the spectral shapes and absolute response spectra for a distance of 8 km appropriate to the SONGS site. The results for soil and rock for S_v/a (spectral shapes) for M 5 to 7 are presented in Figures A-6 and A-7, respectively. The corresponding median response spectra for soil and rock are presented in Figures A-8 and A-9, respectively. For comparison purposes, Figure A-10 shows the spectra for M_s 7 at 8 km for soil and rock. As indicated in Figure A-10, the rock spectrum is higher than the soil spectrum in the period range below about

PART 3: AN ALTERNATE APPROACH FOR DEVELOPING MEDIAN ATTENUATION RELATIONS

As descrbied in the June 1982 WCC report (see Appendix A), attenuation relationships for S_v were developed by a three-step process: Step 1 involved development of attenuation relationships for PGA, Step 2 involved development of attenuation relationships for normalized spectra, S_v/a, and Step 3 involved development of attenuation for absolute spectra, S_v, through the synthesis of results of Steps 1 and 2.

Attenuation relationships for PGA were developed by multiple-regression using the general form:

$$\ln a = b_1 + b_2 M + b_3 \ln[R + C(M)]$$

The resulting equations are plotted on the data for various magnitude bands in Figures 4-1 through 4-4. Note that the relationships shown in Figures 4-1 through 4-4 are best regression fits to the data for the selected form.

Selection of the form of the attenuation relationships for S_v could be more readily accomplished and tested by examining and analyzing the relative frequency content, S_v/a, rather than directly analyzing S_v. This approach allows and facilitates distinguishing the intrinsic trends of ground motion frequency content. After examination and analysis of S_v/a data subsets* using commonly used linear form, it was found that the nonlinear form:

* Subsets for magnitudes 4 to 5, 5 to 6.9 and 4 to 6.9.

$$\ln S_v/a = b_1 + b_2(8.5 - M)^n + b_3 \ln[R + C(M)]$$

provides a better basis (both observationally and from physical considerations) for prediction of relative frequency content of the ground motion than the linear form. This is illustrated in Figures 4-5 through 4-14 which compare the relationships derived from the multiple-regression analyses of S_v/a data for ten selected periods (in the range 0.07 to 1 sec) with the corresponding S_v/a data. To facilitate inspection of the trends for each earthquake, the average S_v/a values are shown in these figures. Inspection of Figures 4-6 through 4-14 shows that the selected form captures well the general trends of data, namely the trends toward saturation with magnitude.

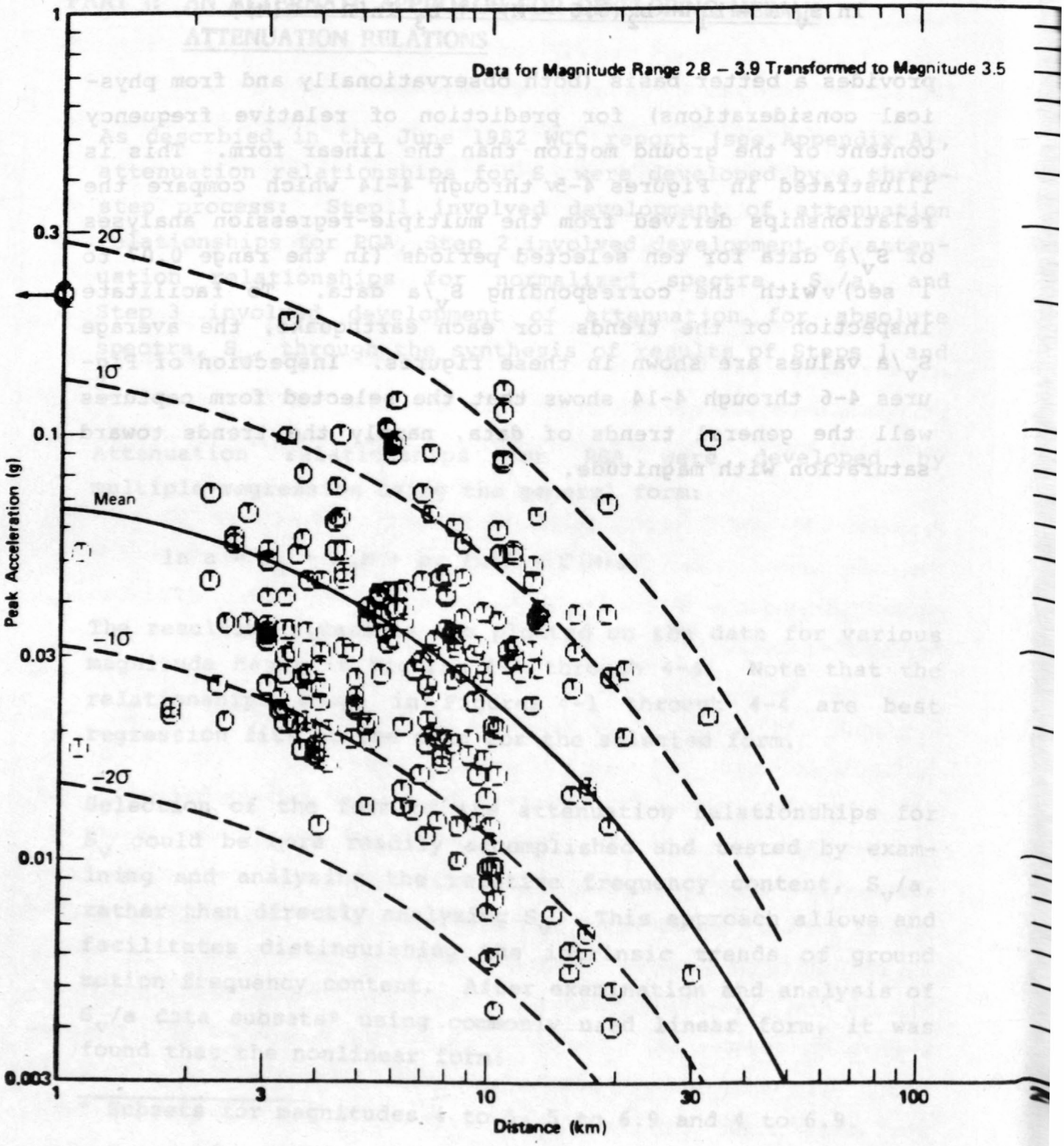

Figure 4-1 – Comparison of Regression Results with Magnitude 2.8 – 3.9 Data Transformed to Magnitude 3.5

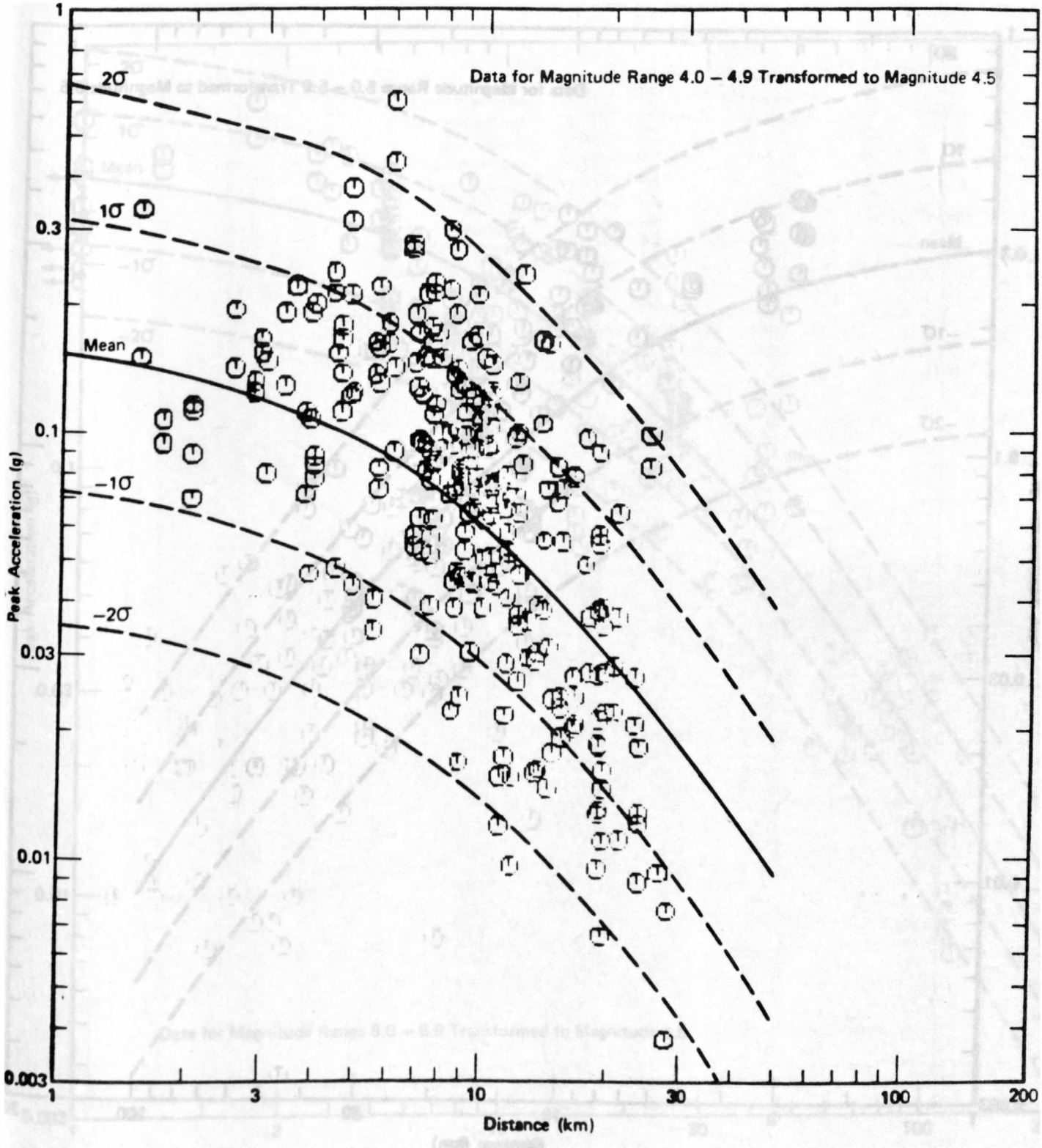

Figure 4-2 – Comparison of Regression Results with Magnitude 4.0 – 4.9 Data Transformed to Magnitude 4.5

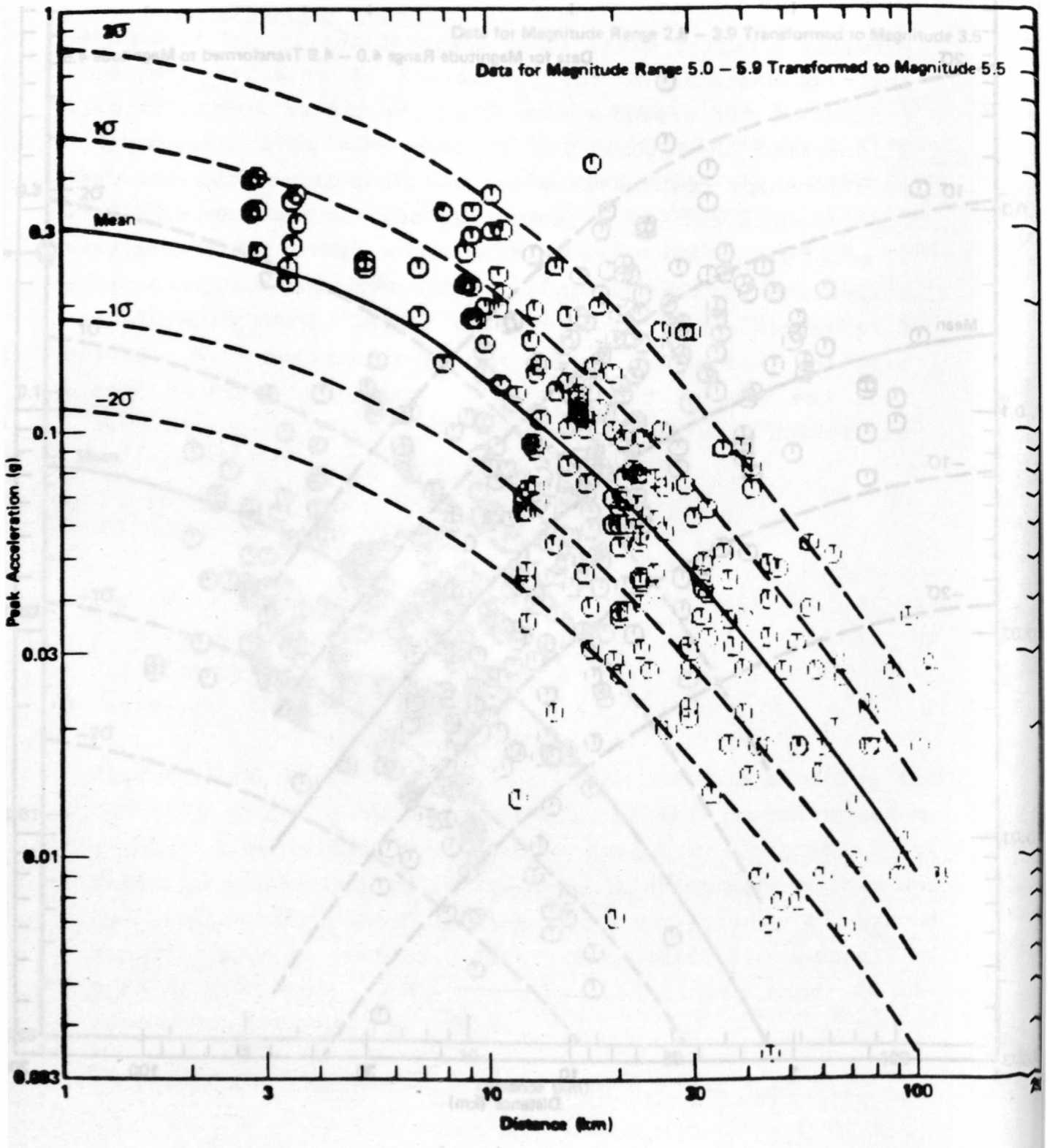

Figure 4-3 – Comparison of Regression Results with Magnitude 5.0 – 5.9 Data Transformed to Magnitude 5.5

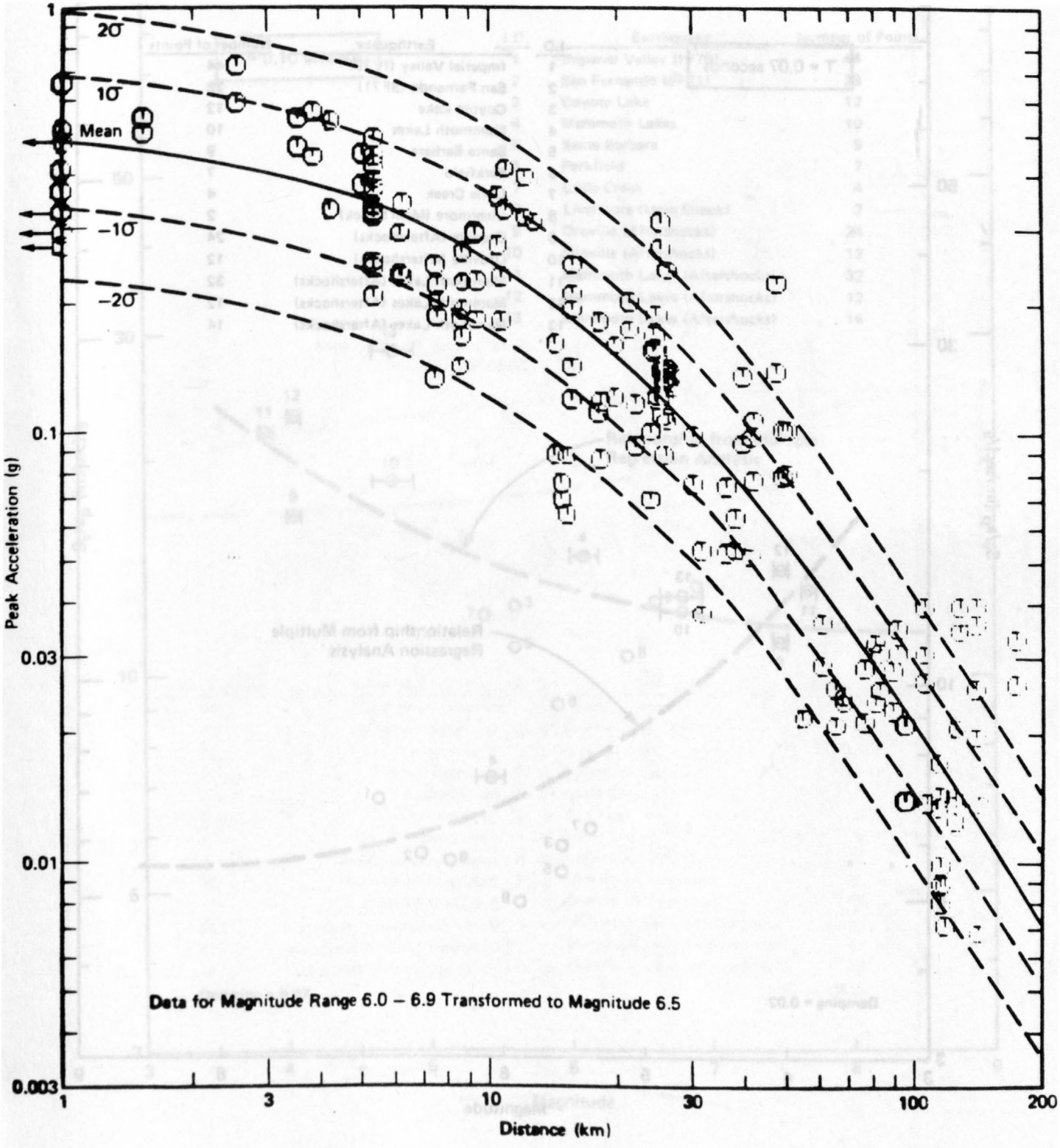

Figure 4-4 – Comparison of Regression Results with Magnitude 6.0 – 6.9 Data Transformed to Magnitude 6.5

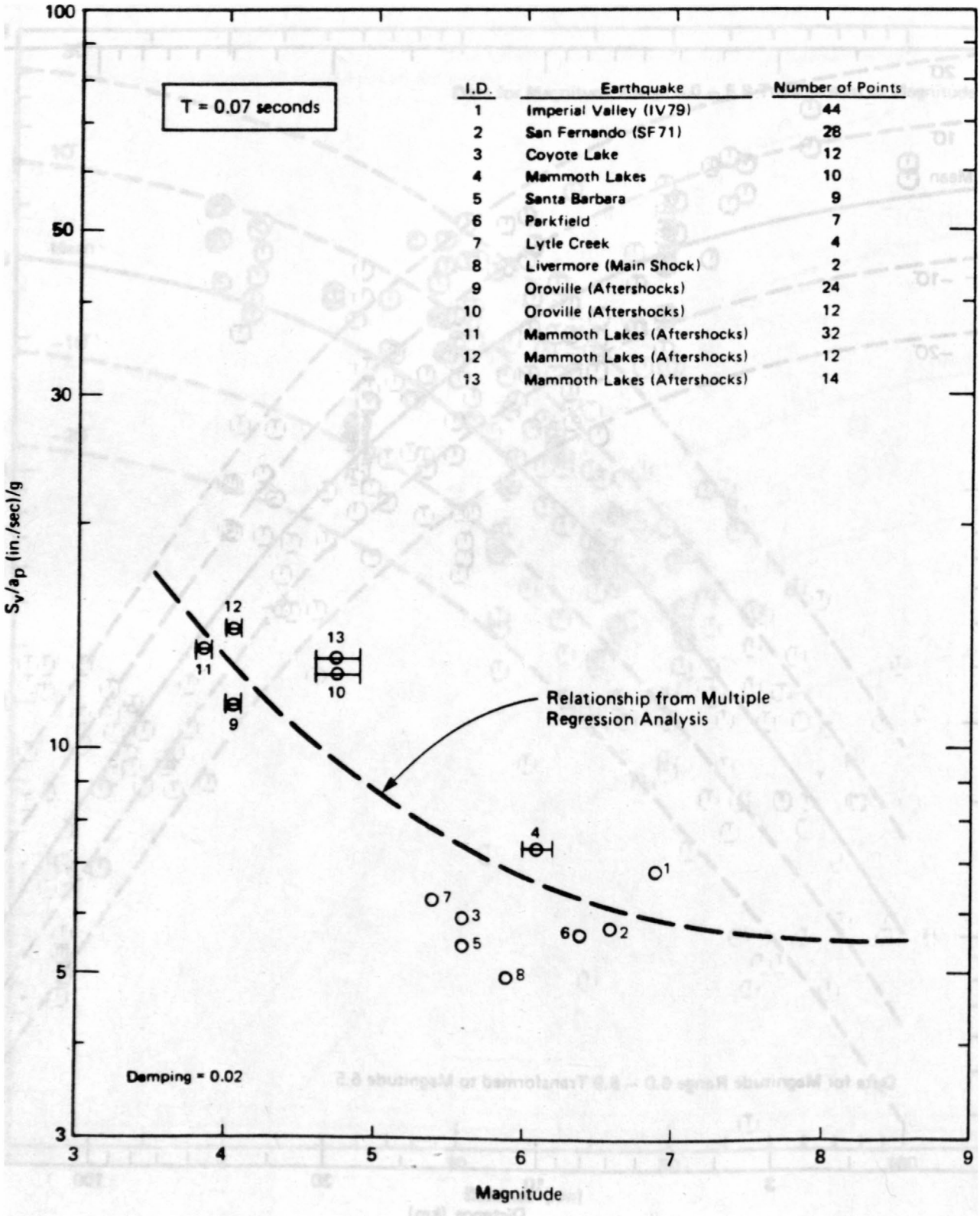

Figure 4-5 – Comparison of Regression Results with S_v/a_p Data for T = 0.07

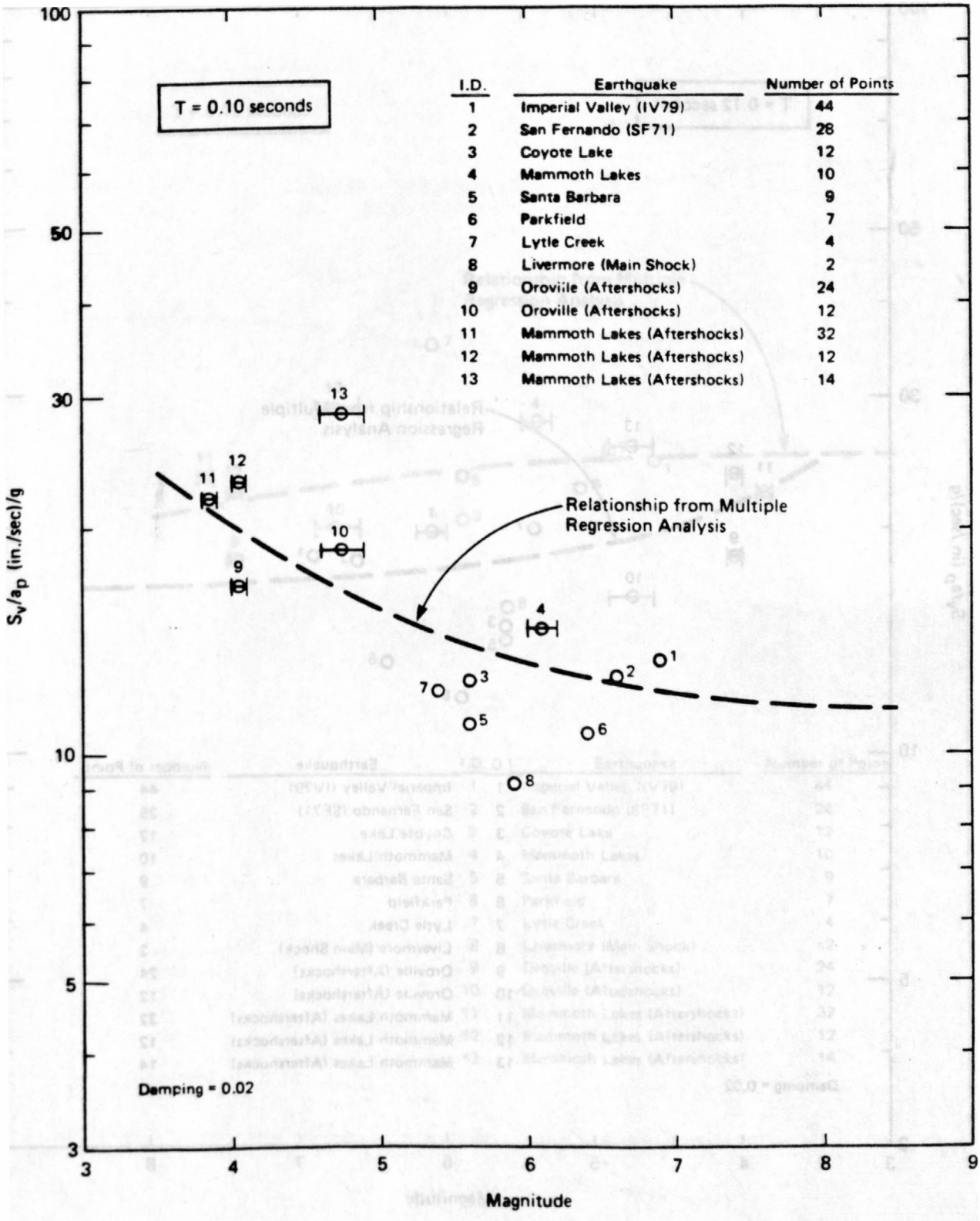

Figure 4-6 – Comparison of Regression Results with S_v/a_p Data for T = 0.10

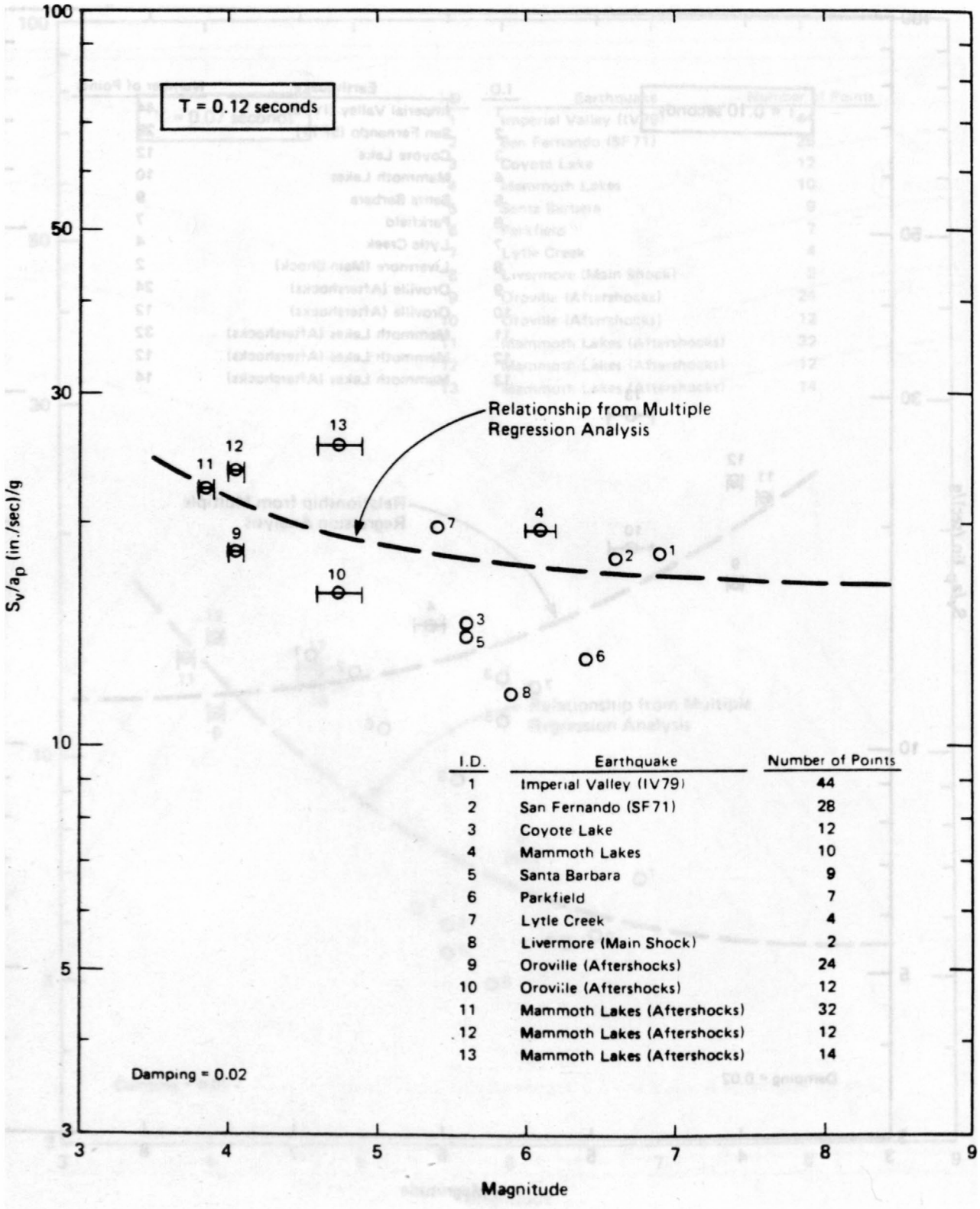

I.D.	Earthquake	Number of Points
1	Imperial Valley (IV79)	44
2	San Fernando (SF71)	28
3	Coyote Lake	12
4	Mammoth Lakes	10
5	Santa Barbara	9
6	Parkfield	7
7	Lytle Creek	4
8	Livermore (Main Shock)	2
9	Oroville (Aftershocks)	24
10	Oroville (Aftershocks)	12
11	Mammoth Lakes (Aftershocks)	32
12	Mammoth Lakes (Aftershocks)	12
13	Mammoth Lakes (Aftershocks)	14

Figure 4-7 – Comparison of Regression Results with S_v/a_p Data for T = 0.12

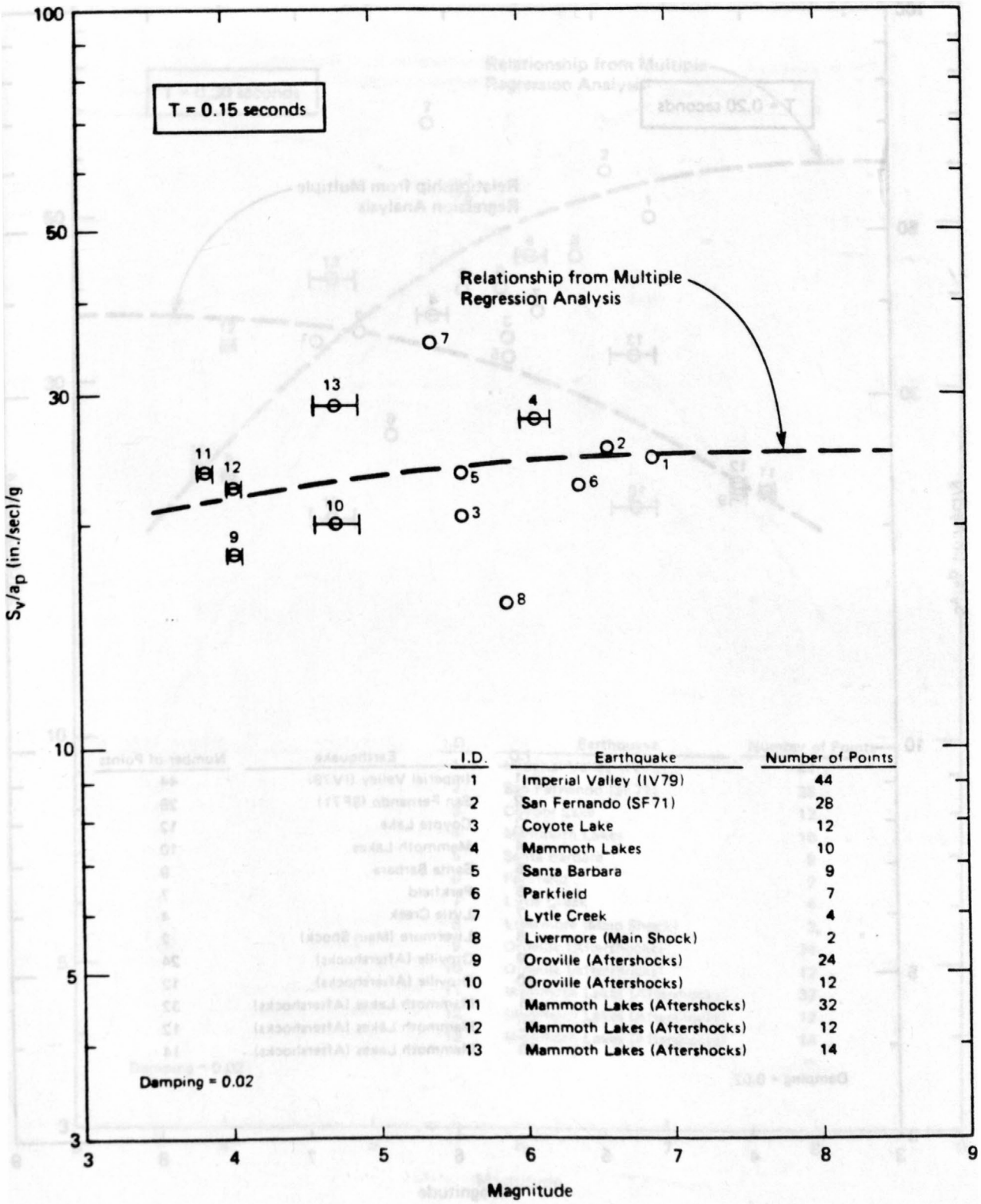

I.D.	Earthquake	Number of Points
1	Imperial Valley (IV79)	44
2	San Fernando (SF71)	28
3	Coyote Lake	12
4	Mammoth Lakes	10
5	Santa Barbara	9
6	Parkfield	7
7	Lytle Creek	4
8	Livermore (Main Shock)	2
9	Oroville (Aftershocks)	24
10	Oroville (Aftershocks)	12
11	Mammoth Lakes (Aftershocks)	32
12	Mammoth Lakes (Aftershocks)	12
13	Mammoth Lakes (Aftershocks)	14

Figure 4-8 – Comparison of Regression Results with S_v/a_p Data for T = 0.15

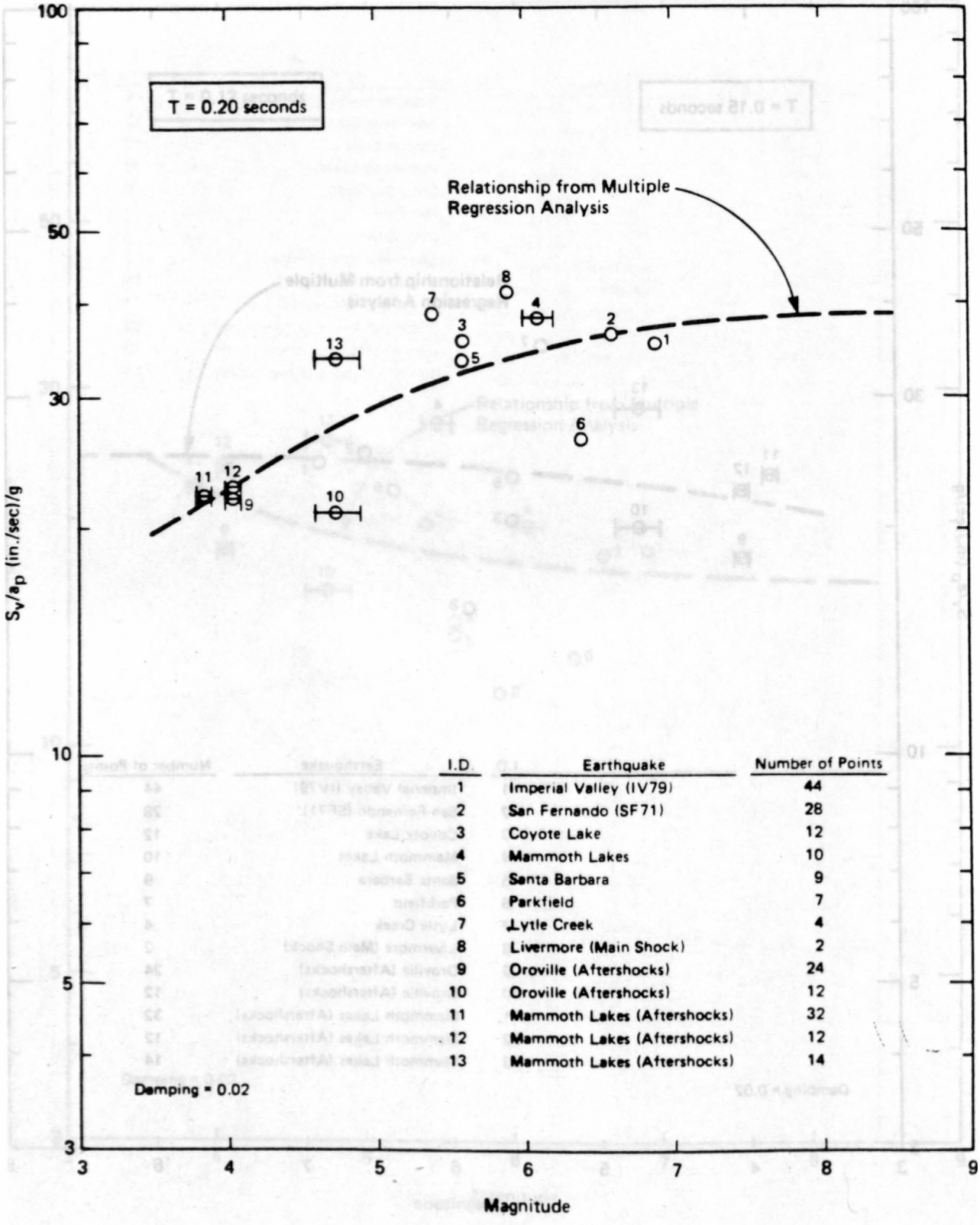

Figure 4-9 – Comparison of Regression Results with S_v/a_p Data for T = 0.20

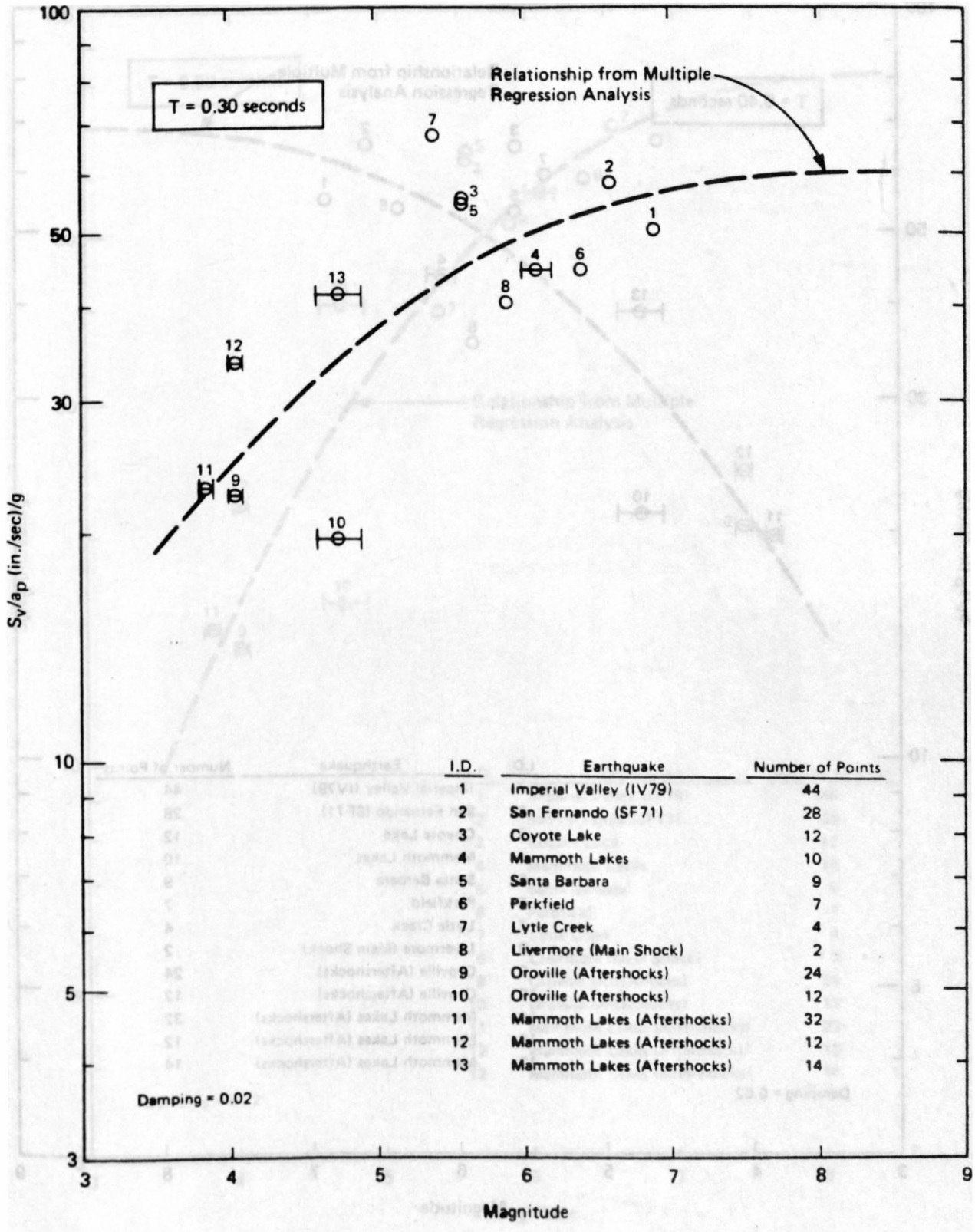

I.D.	Earthquake	Number of Points
1	Imperial Valley (IV79)	44
2	San Fernando (SF71)	28
3	Coyote Lake	12
4	Mammoth Lakes	10
5	Santa Barbara	9
6	Parkfield	7
7	Lytle Creek	4
8	Livermore (Main Shock)	2
9	Oroville (Aftershocks)	24
10	Oroville (Aftershocks)	12
11	Mammoth Lakes (Aftershocks)	32
12	Mammoth Lakes (Aftershocks)	12
13	Mammoth Lakes (Aftershocks)	14

Figure 4-10 – Comparison of Regression Results with S_v/a_p Data for T = 0.30

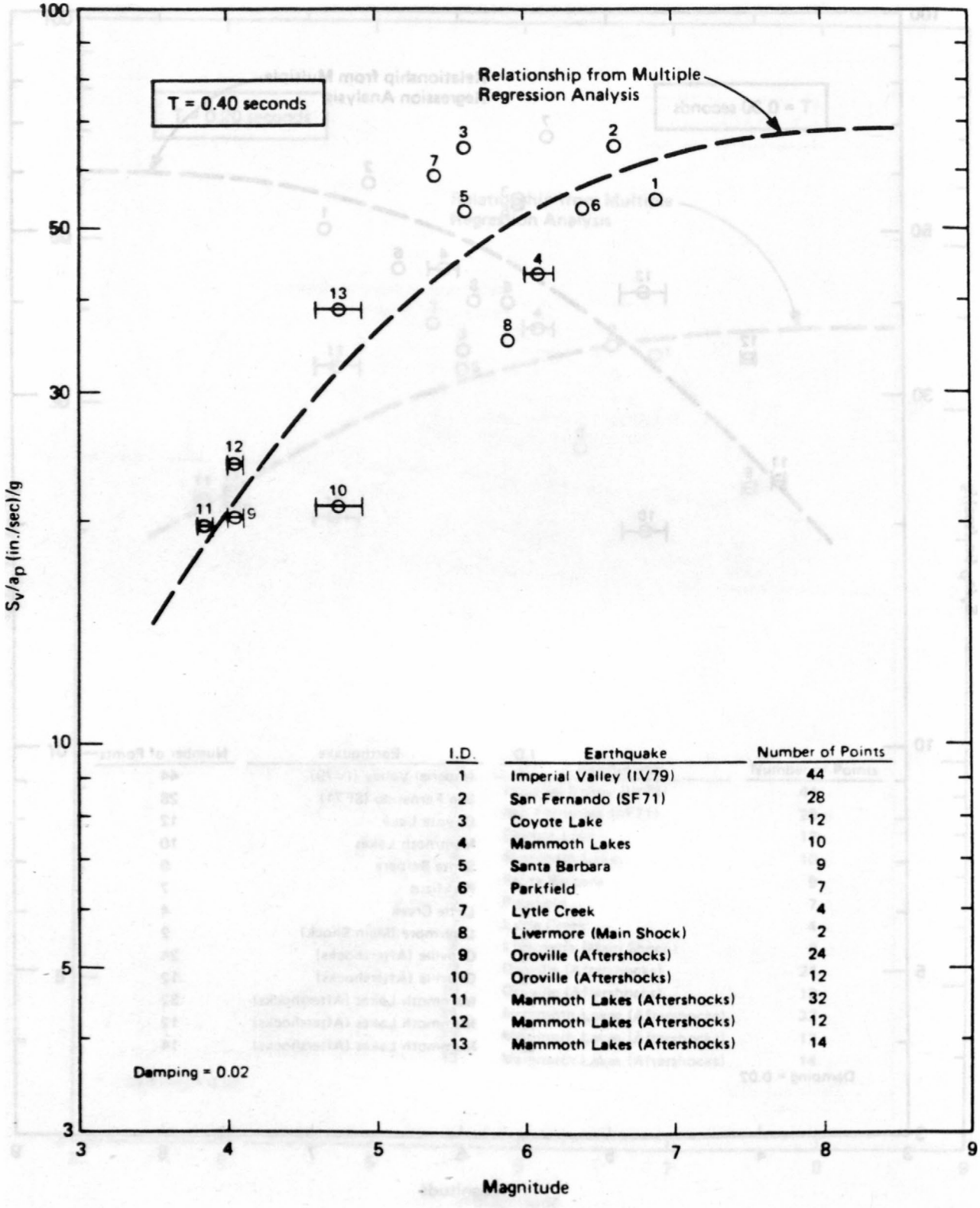

Figure 4-11 – Comparison of Regression Results with S_v/a_p Data for T = 0.40

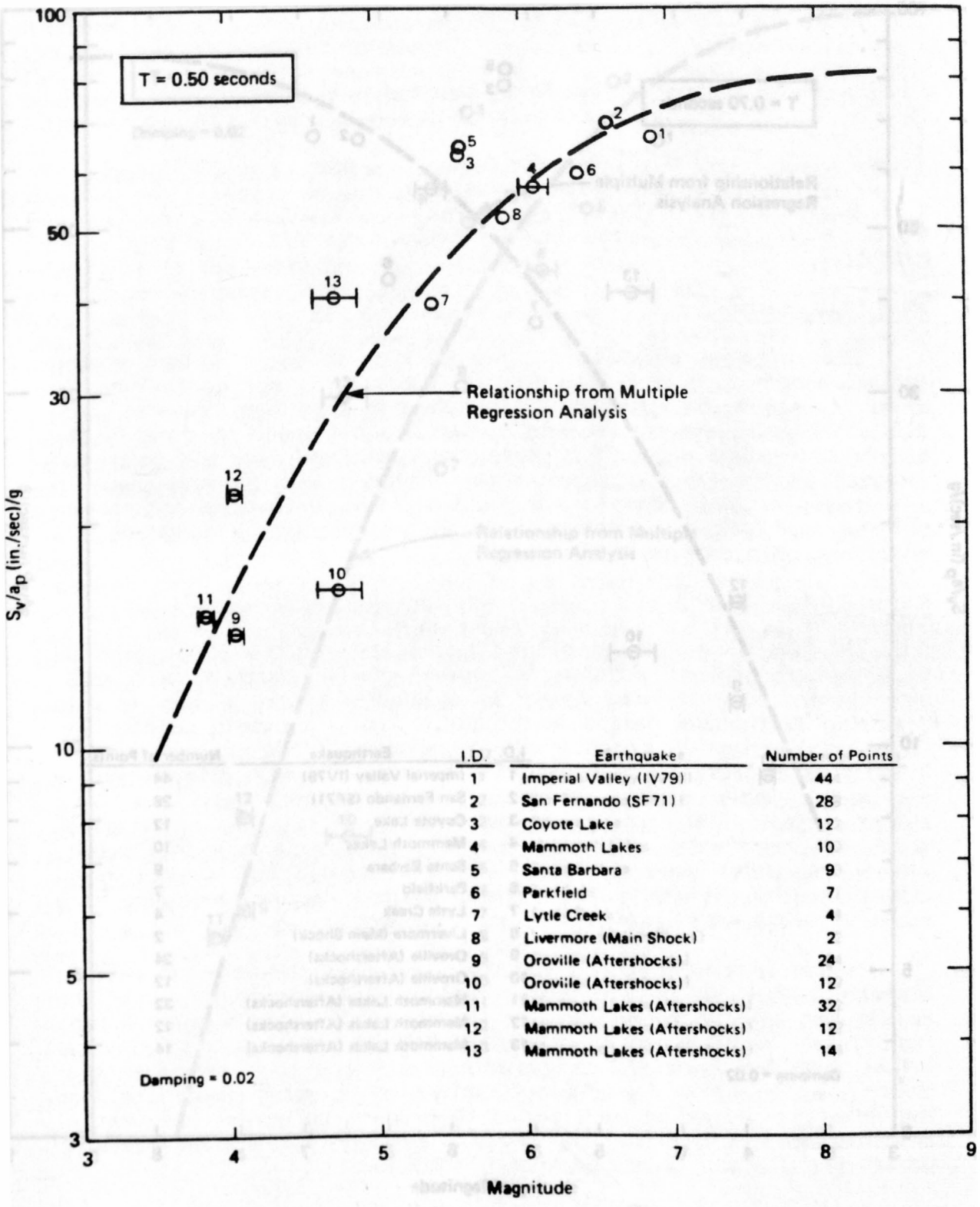

I.D.	Earthquake	Number of Points
1	Imperial Valley (IV79)	44
2	San Fernando (SF71)	28
3	Coyote Lake	12
4	Mammoth Lakes	10
5	Santa Barbara	9
6	Parkfield	7
7	Lytle Creek	4
8	Livermore (Main Shock)	2
9	Oroville (Aftershocks)	24
10	Oroville (Aftershocks)	12
11	Mammoth Lakes (Aftershocks)	32
12	Mammoth Lakes (Aftershocks)	12
13	Mammoth Lakes (Aftershocks)	14

Figure 4-12 – Comparison of Regression Results with S_v/a_p Data for T = 0.50

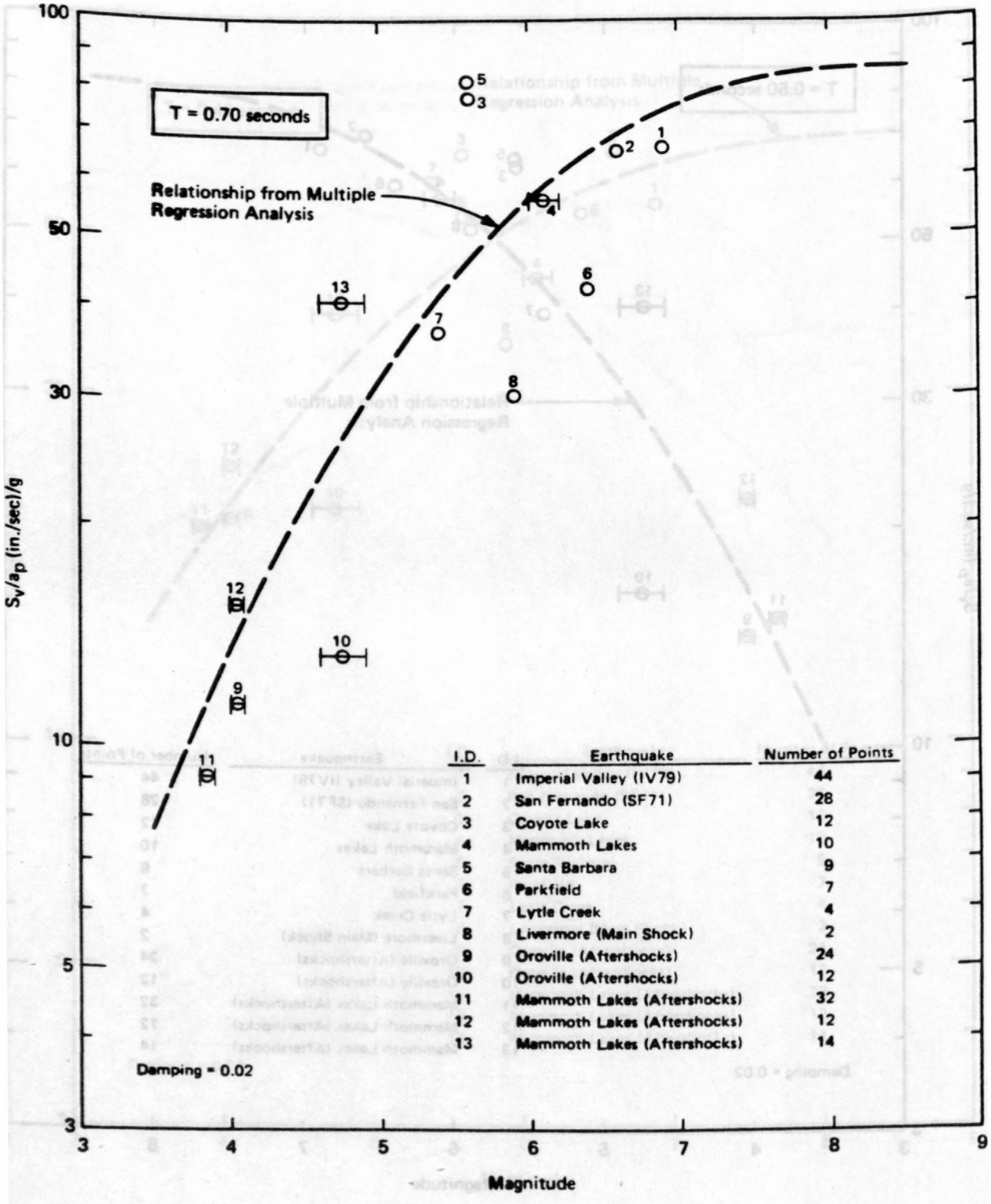

I.D.	Earthquake	Number of Points
1	Imperial Valley (IV79)	44
2	San Fernando (SF71)	28
3	Coyote Lake	12
4	Mammoth Lakes	10
5	Santa Barbara	9
6	Parkfield	7
7	Lytle Creek	4
8	Livermore (Main Shock)	2
9	Oroville (Aftershocks)	24
10	Oroville (Aftershocks)	12
11	Mammoth Lakes (Aftershocks)	32
12	Mammoth Lakes (Aftershocks)	12
13	Mammoth Lakes (Aftershocks)	14

Figure 4-13 – Comparison of Regression Results with S_v/a_p Data for T = 0.70

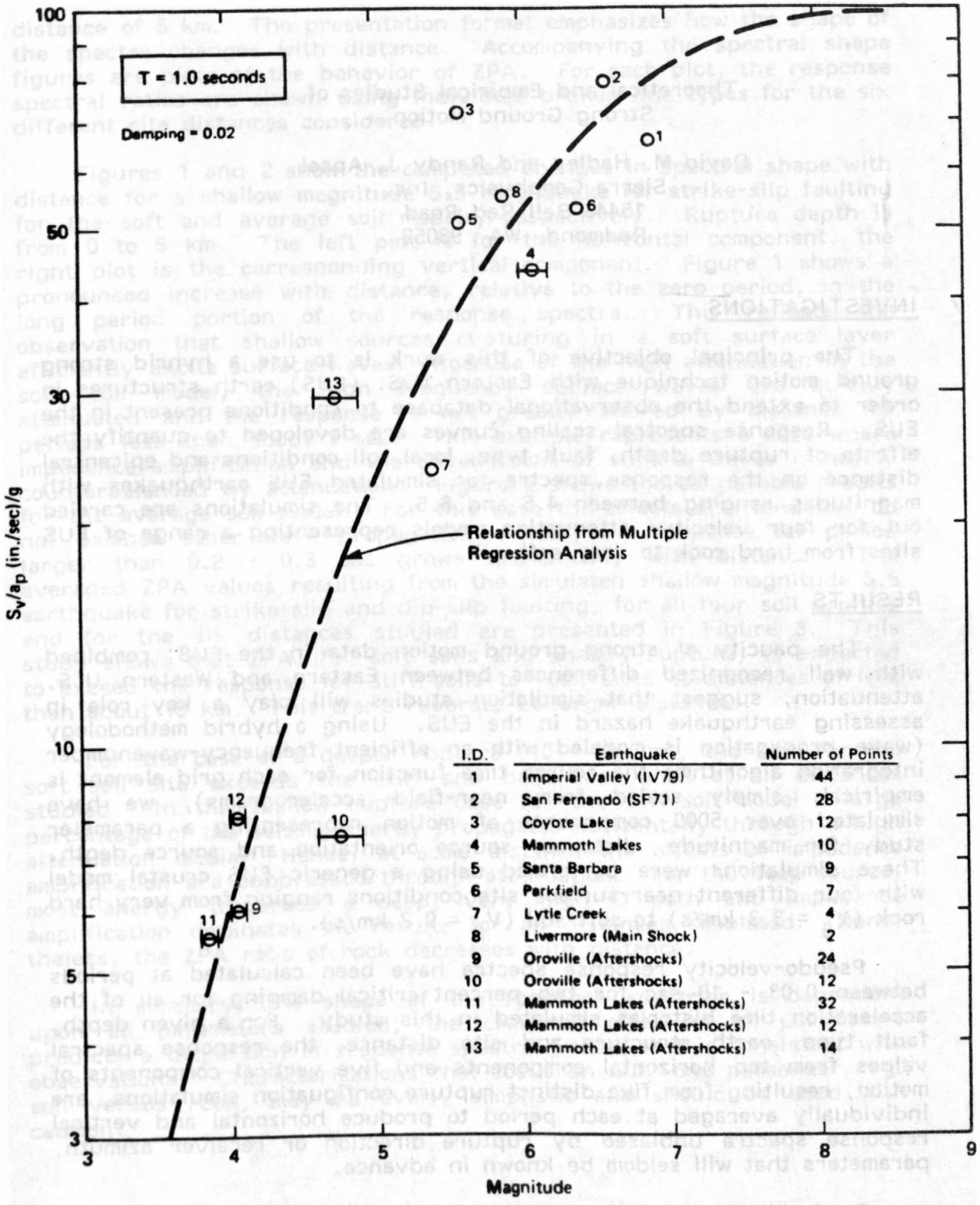

I.D.	Earthquake	Number of Points
1	Imperial Valley (IV79)	44
2	San Fernando (SF71)	28
3	Coyote Lake	12
4	Mammoth Lakes	10
5	Santa Barbara	9
6	Parkfield	7
7	Lytle Creek	4
8	Livermore (Main Shock)	2
9	Oroville (Aftershocks)	24
10	Oroville (Aftershocks)	12
11	Mammoth Lakes (Aftershocks)	32
12	Mammoth Lakes (Aftershocks)	12
13	Mammoth Lakes (Aftershocks)	14

Figure 4-14 – Comparison of Regression Results with S_V/a_p Data for T = 1.0

Theoretical and Empirical Studies of Strong Ground Motion

David M. Hadley and Randy J. Apsel
Sierra Geophysics, Inc.
15446 Bell-Red Road
Redmond, WA 98052

INVESTIGATIONS

The principal objective of this work is to use a hybrid strong ground motion technique with Eastern U.S. (EUS) earth structures in order to extend the observational database to conditions present in the EUS. Response spectral scaling curves are developed to quantify the effects of rupture depth, fault type, local soil conditions and epicentral distance on the response spectra for simulated EUS earthquakes with magnitudes ranging between 4.5 and 6.5. The simulations are carried out for four velocity/ attenuation models representing a range of EUS sites from hard rock to very soft soil.

RESULTS

The paucity of strong ground motion data in the EUS, combined with well recognized differences between Eastern and Western U.S. attenuation, suggest that simulation studies will play a key role in assessing earthquake hazard in the EUS. Using a hybrid methodology (wave propagation is modeled with an efficient frequency-wavenumber integration algorithm; the source time function for each grid element is empirical, simply scaled from near-field accelerograms), we have simulated over 5000 components of motion representing a parameter study for magnitude, distance, source orientation and source depth. These simulations were performed using a generic EUS crustal model with four different near-surface site conditions ranging from very hard rock (V_β = 3.3 km/s) to soft soil (V_β = 0.2 km/s).

Pseudo-velocity response spectra have been calculated at periods between 0.03 - 10 sec for two percent critical damping for all of the acceleration time histories simulated in this study. For a given depth, fault type, earth structure and site distance, the response spectral values from ten horizontal components and five vertical components of motion, resulting from five distinct rupture configuation simulations, are individually averaged at each period to produce horizontal and vertical response spectra unbiased by rupture direction or receiver azimuth, parameters that will seldom be known in advance.

To facilitate using the results of this study for scaling response spectra for distance, all response spectra are presented in a normalized format. The normalized shapes are calculated by adjusting all response to a common zero period acceleration (ZPA) and then by dividing each adjusted spectra by the corresponding spectra calculated for the

distance of 5 km. The presentation format emphasizes how the shape of the spectra changes with distance. Accompanying the spectral shape figures are plots of the behavior of ZPA. For each plot, the response spectral ratios are shown using individual broken line types for the six different site distances considered.

Figures 1 and 2 show the computed changes in spectral shape with distance for a shallow magnitude 5.5 earthquake for strike-slip faulting for the soft and average soil models, respectively. Rupture depth is from 0 to 5 km. The left plot is for the horizontal component, the right plot is the corresponding vertical component. Figure 1 shows a pronounced increase with distance, relative to the zero period, in the long period portion of the response spectra. This reflects the observation that shallow sources rupturing in a soft surface layer efficiently excite surface waves. Because of the high attenuation in the soft soil model, the high frequency surface waves are quickly attenuated and the response is not greatly altered by distance for periods less than about 1 sec. This example represents a case where impedance amplification and the development of surface waves is nearly counterbalanced by attenuation. Figure 2 shows the comparable results for the average soil model. For this case the effects of attenuation do not balance other wave propagation effects; the response for period larger than 0.2 - 0.3 sec grows dramatically with distance. The averaged ZPA values resulting from the simulated shallow magnitude 5.5 earthquake for strike-slip and dip-slip faulting, for all four soil profiles and for the six distances studied are presented in Figure 3. This study shows that ZPA, for soft soils and shallow rupture, is expected to exceed the response for stiff soils to rock sites at distances of less than about 15 km. This trend reverses at larger distances.

For the case of a deeper rupture (10 - 15 km), the ZPA for the soft soil site exceeds the stiff and hard rock sites at all distances studied. In the shallow rupture case for the soft-soil model a large percentage of the seismic energy propagates horizontally through a high attenuation media. Hence, at some distance the effects of impedance amplification are suppressed through attenuation. For the deep source, most energy traverses a deep, very high Q path and impedance amplification dominates the results for all distances simulated. Nonetheless, the ZPA ratio of rock decreases with distance.

In summary, the shape of the response spectrum is dependent upon all parameters studied; the combined effect of all parameters predicts a dispersion of response spectral values that is consistent with observations. Characterizations that focus on only one parameter, eg. soil versus rock, may be overly simplistic and should be used with caution.

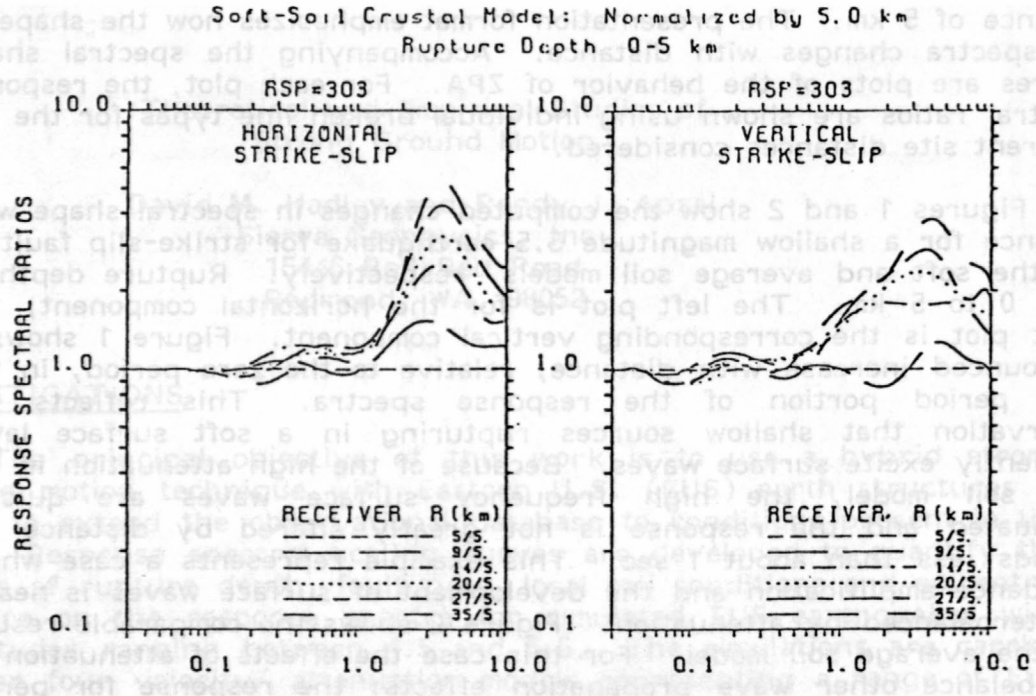

Figure 1. Variation of response spectra shape with distance for strike-slip faulting, soft-soil model. The normalized shapes are calculated by adjusting all response to a common zero period acceleration and then by dividing each adjusted spectra by the spectra calculated for the distance of 5 km. Each broken line type corresponds to the response at a particular distance (range 5-35 km).

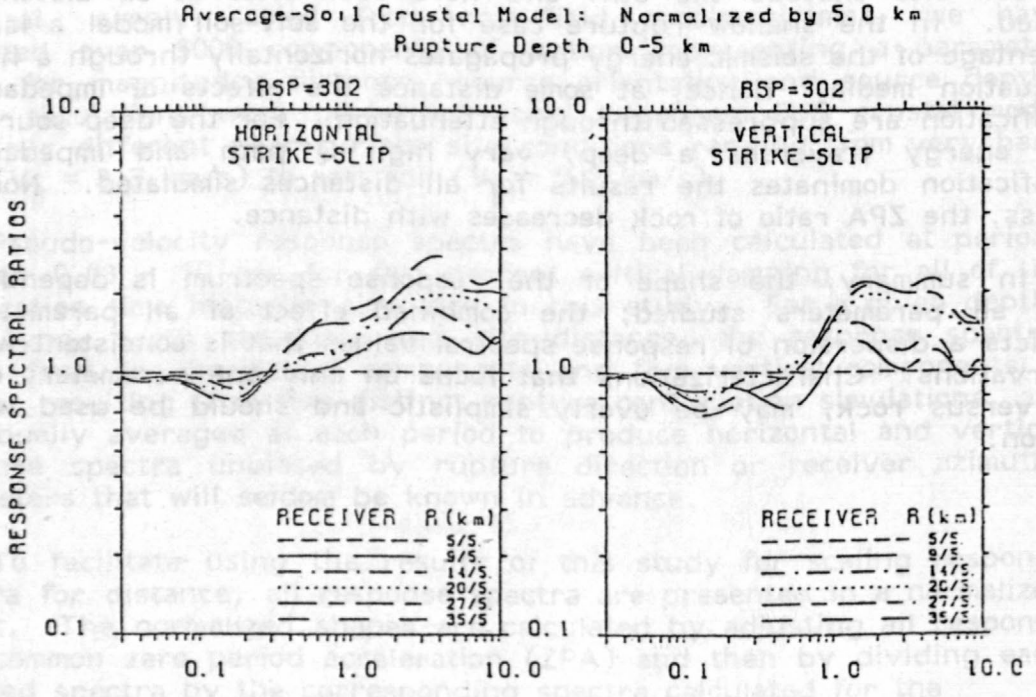

Figure 2. Variation of response spectra shape with distance for strike-slip faulting, average soil model.

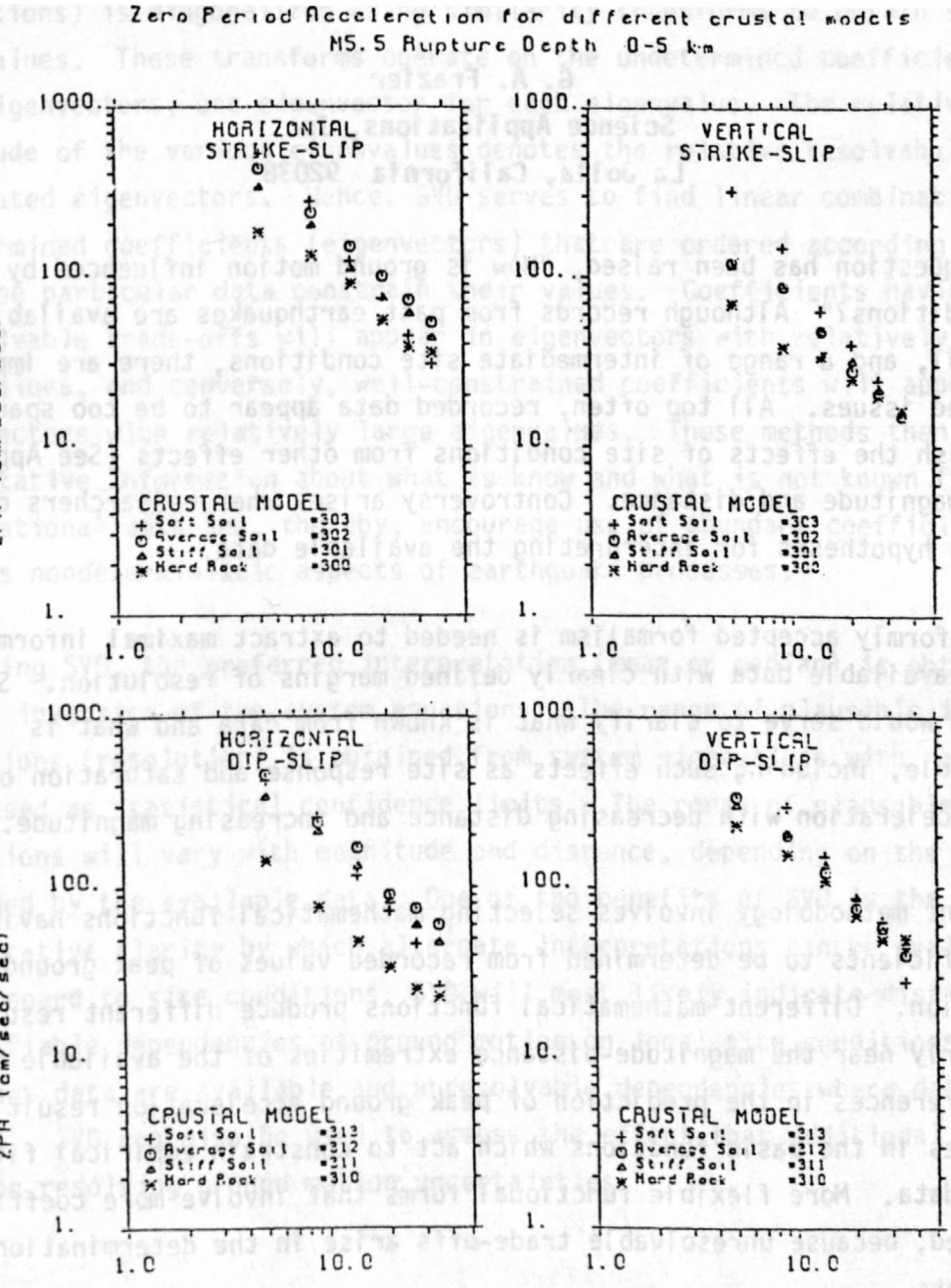

Figure 3. Simulated zero period accelerations for shallow strike-slip and dip-slip faulting for four soil profiles.

EMPIRICAL RESOLUTION OF GROUND MOTION EFFECTS

by

G. A. Frazier
Science Applications, Inc.
La Jolla, California 92038

The question has been raised, "How is ground motion influenced by local site conditions?" Although records from past earthquakes are available for rock, soil, and a range of intermediate site conditions, there are important unresolved issues. All too often, recorded data appear to be too sparse to distinguish the effects of site conditions from other effects (See Appendix 1) such as magnitude and distance. Controversy arises when researchers develop alternate hypotheses for interpreting the available data.

A uniformly accepted formalism is needed to extract maximal information from the available data with clearly defined margins of resolution. Such a formalism would serve to clarify what is known from data and what is unresolvable, including such effects as site response and saturation of peak ground acceleration with decreasing distance and increasing magnitude.

Current methodology involves selecting mathematical functions having about four coefficients to be determined from recorded values of peak ground acceleration. Different mathematical functions produce different results, particularly near the magnitude-distance extremities of the available data. These differences in the prediction of peak ground acceleration result from differences in the basic functions which act to constrain empirical fits with observed data. More flexible functional forms that involve more coefficients are avoided, because unresolvable trade-offs arise in the determination of coefficients.

This troublesome problem can be turned into an asset using procedures common to the class of methods known as generalized inverse. In particular,

an algebraic method known as singular value decomposition (SVD) can be used to order and assign significance to system parameters. Using SVD, the influence matrix (the matrix that transforms coefficients into observational predictions) is diagonalized using similarity transforms to obtain system eigenvalues. These transforms operate on the undetermined coefficients to form eigenvectors, one eigenvector for each eigenvalue. The relative amplitude of the various eigenvalues denotes the relative resolvability of the associated eigenvectors. Hence, SVD serves to find linear combinations of the undetermined coefficients (eigenvectors) that are ordered according to how well the particular data constrain their values. Coefficients having unresolvable trade-offs will appear in eigenvectors with relatively small eigenvalues, and conversely, well-constrained coefficients will appear in eigenvectors with relatively large eigenvalues. These methods then provide quantitative information about what is know and what is not known from observational data and, thereby, encourage use of abundant coefficients to express nondeterministic aspects of earthquake processes.

Using SVD, the preferred interpretation (mean or median) is obtained by direct inversion of the system equations. The range of plausible interpretations (resolution) is obtained from system eigenvalues with results expressed as statistical confidence limits. The range of plausible interpretations will vary with magnitude and distance, depending on the constraints provided by the available data. One of the benefits of SVD is the quantitative clarity by which alternate interpretations can be evaluated. With regard to site conditions, SVD will most likely indicate distinct and identifiable dependencies of ground motion on local site conditions where abundant data are available and unresolvable dependencies where data are sparse. SVD can also be used to assess the effect that additional data will have on resolving ground motion uncertainties.

APPENDIX 1

List of Parameters Affecting the Interpretation of Ground Motion Records

1. SOURCE PRESCRIPTION

a. Gross Properties
   - o Magnitude (M_S, m_b, M_L), moment (M_O)
   - o Epicenter, Depth
   - o Mechanism (reverse, strike-slip, etc.)

b. Fracture Parameters
   - o Hypocenter, Rupture Velocity
   - o Slip Characteristics (dynamic stress drop, offset, etc.)
   - o Fracture Orientation and Extent

c. Fracture Irregularities
   - o Variations in Slip (Fracture Asperities)
   - o Multiple Fracture and Associated Creep

2. EARTH PROPERTIES

a. Geologic Layering
   - o Geometric Boundaries

b. Seismic Velocities
   - o P and S Wave

c. Material Attenuation
   - o Amplitude and Frequency Dependence

d. Geologic Asperities
   - o Wave Guides and Scattering

3. SITE PROPERTIES

(same as for Earth Properties)

A MODEL FOR THE SHAPE OF THE FOURIER AMPLITUDE SPECTRUM OF ACCELERATION AT HIGH FREQUENCIES

by

John G. Anderson and Sue Hough

Institute of Geophysics and Planetary Physics

Scripps Institution of Oceanography

La Jolla, California

ABSTRACT

At frequencies, f, higher than the earthquake corner frequency, the spectrum of S-wave accelerations is characterized by a trend of exponential decay, $e^{-\pi \kappa f}$. The spectral decay parameter, κ shows little variation at a single station for multiple earthquakes at the same distances, but it increases gradually as the epicentral distance increases. For multiple recordings of the San Fernando earthquake, κ increases slowly with distance, and κ is systematically smaller for sites on rock than for sites on alluvium. Under the assumption that the Fourier spectrum of acceleration at the source is constant above the corner frequency (an ω^{-2} source model), the exponential decay is consistent with frequency-independent attenuation, in which Q increases rapidly with depth in the shallow crustal layers.

INTRODUCTION

The shape and amplitude of the Fourier amplitude spectrum of strong ground acceleration is recognized as useful for various applications to earthquake engineering (McGuire, 1978). This acceleration spectrum also

TABLE 1 - SPECTRAL DECAY PARAMETERS FOR ACCELEROGRAMS RECORDED AT HOLLISTER, FERNDALE, AND EL CENTRO.

HOLLISTER

DATE	REC	DIST	M	KAPPA1
Ø3/Ø9/49	U3Ø1	19.9	5.3	Ø.Ø85Ø
Ø4/25/54	U3Ø5	29.1	5.3	Ø.Ø828
Ø1/19/6Ø	U3Ø7	8.5	5.Ø	Ø.Ø865
Ø4/Ø8/61	U3Ø9	19.8	5.6	Ø.Ø667
12/18/67	U313	39.Ø	5.8	Ø.Ø88Ø

FERNDALE

DATE	REC	DIST	M	KAPPA1
1Ø/Ø7/51	AØØ2	56.3	5.8	Ø.Ø858
12/21/54	AØØ9	4Ø.4	6.5	Ø.Ø821
Ø9/11/38	BØ26	55.3	5.5	Ø.Ø9Ø9
Ø2/Ø9/41	BØ27	98.4	6.4	Ø.Ø9Ø9
Ø9/22/52	BØ3Ø	45.2	5.5	Ø.Ø887
Ø7/Ø6/34	U294	128.9	6.Ø	Ø.Ø923
Ø2/Ø6/37	U298	85.1	5.8	Ø.1Ø19
1Ø/Ø3/41	U3ØØ	29.8	6.4	Ø.1114
Ø6/Ø5/6Ø	U3Ø8	6Ø.3	5.7	Ø.Ø667
12/1Ø/67	U312	3Ø.6	5.6	Ø.Ø447

EL CENTRO

DATE	REC	DIST	M	KAPPA1	KAPPA2
Ø5/19/4Ø	AØØ1	9.3	6.7	Ø.Ø6Ø8	Ø.Ø8Ø6
Ø2/Ø9/56	AØ11	126.9	6.8	Ø.Ø945	Ø.1Ø77
Ø4/Ø8/68	AØ19	69.8	6.4	Ø.1Ø11	Ø.Ø938
12/3Ø/34	BØ24	6Ø.8	6.5	Ø.Ø682	Ø.Ø711
1Ø/21/42	T286	46.5	6.5	Ø.Ø645	Ø.Ø645
Ø1/23/51	T287	27.5	5.6	Ø.Ø77Ø	Ø.Ø63Ø
Ø6/13/53	T288	23.6	5.5	Ø.Ø591	Ø.Ø751
11/12/54	T289	119.8	6.3	Ø.Ø923	Ø.Ø975
12/16/55	T292	23.5	5.4	Ø.Ø452	Ø.Ø369
Ø8/Ø7/66	T293	148.1	6.3	Ø.1Ø48	Ø.1217

contains fundamental information about physical processes at the earthquake source and wave propagation in the crust of the earth. Yet at high frequencies we still do not have a satisfactory model for the shape of the acceleration spectrum. By the shape of a spectrum we refer to a smooth trend through the spectrum; the fine structure which is superimposed on this trend is not meant to be included.

At low frequencies and sufficiently far from the fault, the inevitable result of an elastic rebound source model is that the acceleration spectrum increases as ω^2, where $\omega = 2\pi f$ and f is the frequency of ground motion. For example, a widely employed model by Brune (1970) relates the coefficient of this ω^2 trend to the seismic moment, M_0, and relates the corner frequency (f_0) where this ω^2 trend terminates to a stress drop parameter at the source. Above the corner frequency, Trifunac (1976) and McGuire (1978) have carried out empirical regressions for the shape of the acceleration spectrum but these regressions do not yield much insight into the physical processes which are involved. Hanks (1982) suggests that in general the acceleration spectrum is flat above the corner frequency to a second corner frequency (f_{max}) above which the spectrum decays rapidly.

In the next section we propose a parametric shape for the acceleration spectrum above the corner frequency which differs from the Hanks (1982) model. Our model is characterized by just one parameter, which we designate as the spectral decay parameter, κ. Subsequent sections explore the systematic behavior of κ for the S-wave portion of the accelerogram. We also recognize a plausible attenuation model to explain the observations but intentionally avoid introducing the termi-

nology and notation of that model into the observation sections of this paper.

SPECTRAL SHAPE AT HIGH FREQUENCIES

Figure 1 shows the Fourier amplitude spectrum of acceleration for the S16°E component of the Pacoima Dam accelerogram from the 1971 San Fernando, California earthquake. Figure 1A shows the spectrum plotted on log - log axes. Based on a figure of this type, Hanks (1982, Fig. 2) selects f_{max} for this record to be near 10 Hz. In Figure 1B, the frequency axis is linear. On these axes, it appears that the log of the spectral amplitude decreases linearly with frequency, and there is no apparent additional slope break in the vicinity of 10 Hz.

Figure 2 is the equivalent of Figure 1, but for the spectrum of an accelerogram recorded at Cucapah, Baja California, Mexico from the June 1980 earthquake (M_L = 6.1) in the Mexicali Valley, across the international border from the Imperial Valley, California. This data is described by Anderson et al. (1982). The accelerograph in this case is a digital recorder (Kinemetrics DSA-1) which samples the output of a force-balance accelerometer (natural frequency 50 Hz) at a rate of 200 samples per second, so that the Nyquist frequency is 100 Hz. The least count is about 0.5 cm/sec^2. Because the response of the force-balance sensor is flat to 50 Hz, no instrument correction has been applied to this record. Because of the highly accurate digital recording, there is no uncertainty about the reliability of the digitization on this record as there might be for hand-digitized data (e.g. Cormier, 1982; Sacks, 1980).

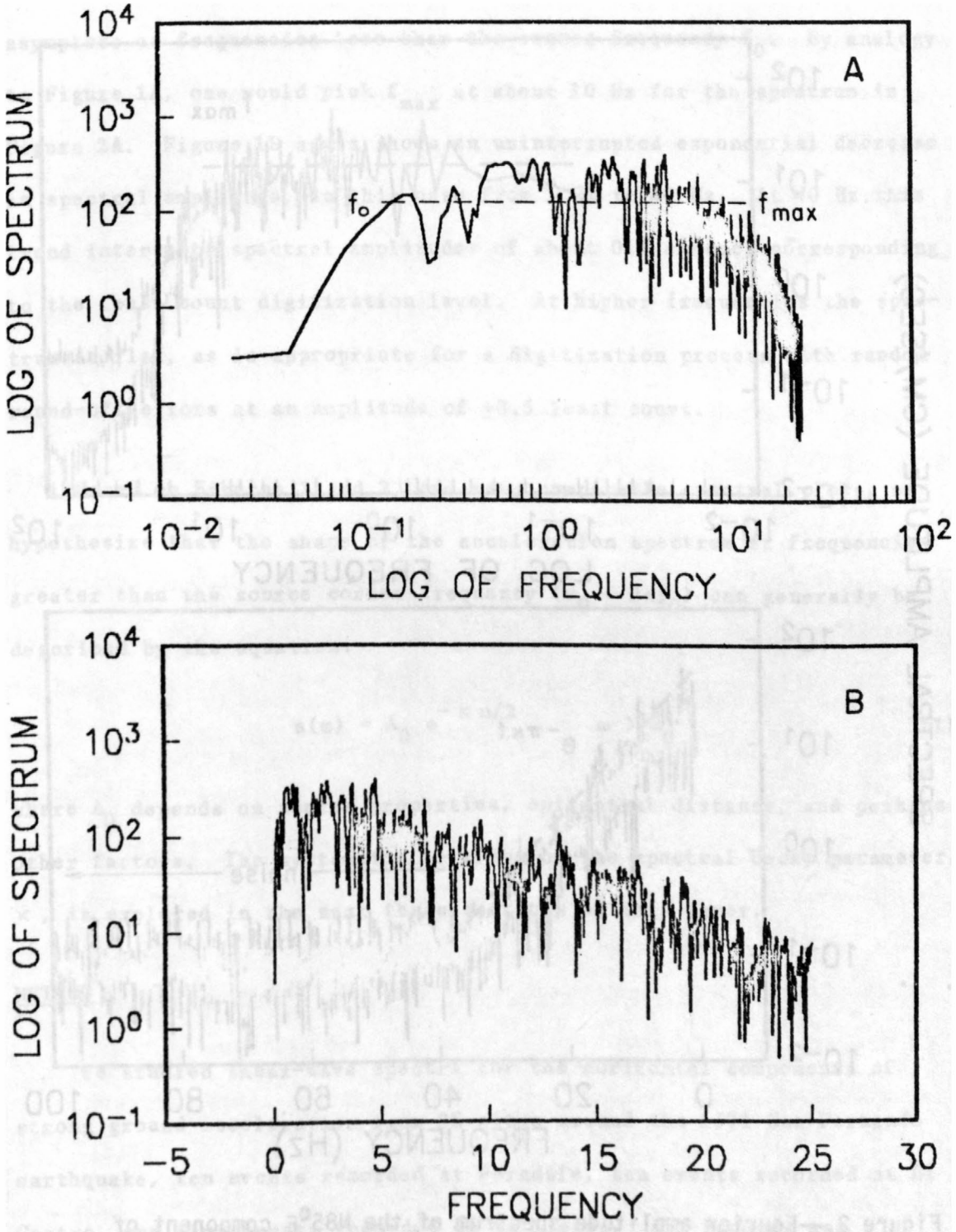

Figure 1.--Fourier amplitude spectrum of acceleration for the S16°E component of the Pacoima Dam accelerogram, San Fernando, California, earthquake of February 9, 1971. Accelerogram was digitized by hand. 1A. Log - log axes. 1B. Linear - log axes.

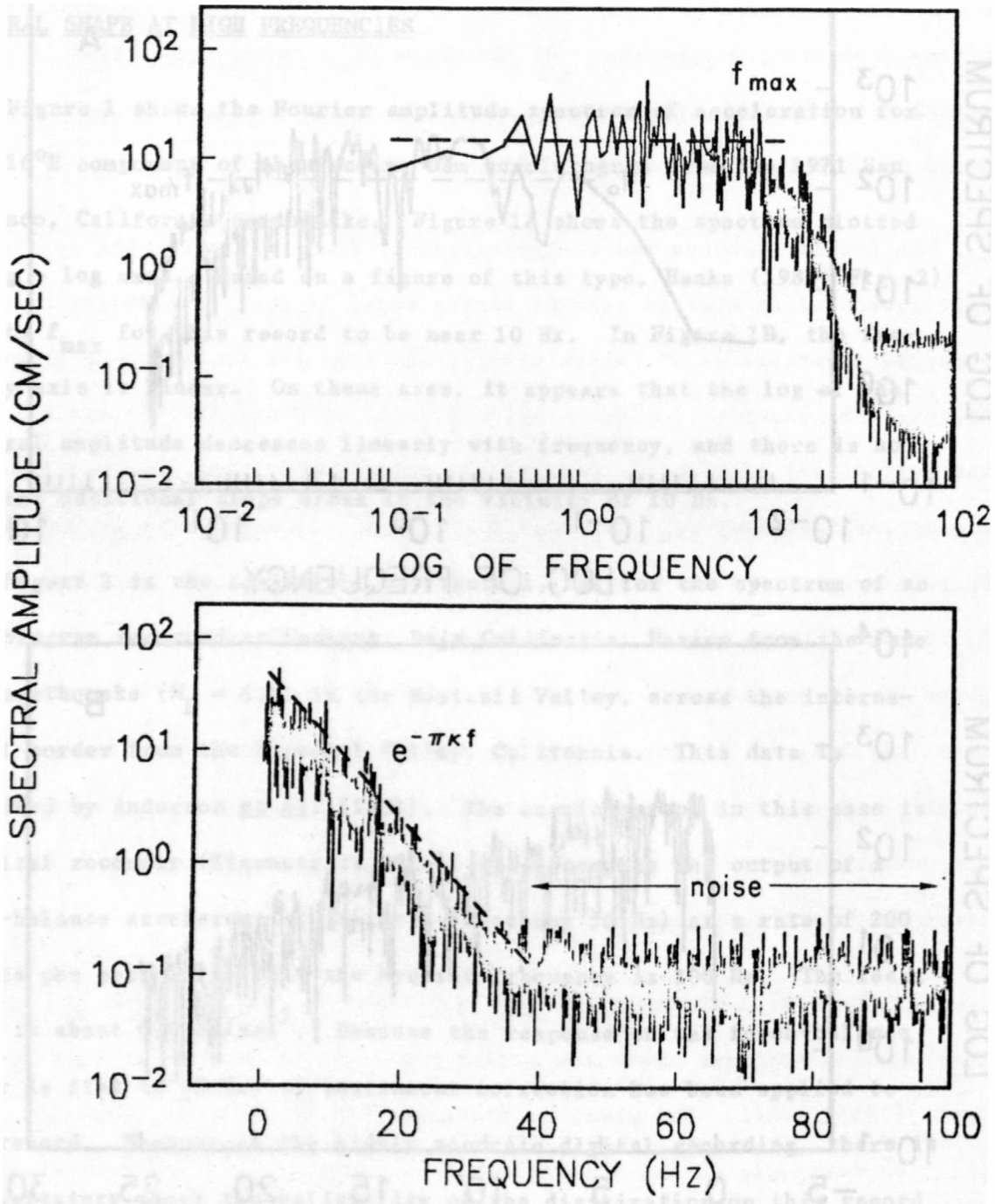

Figure 2.--Fourier amplitude spectrum of the N85^{o}E component of strong ground acceleration recorded at Cucapah during the Mexicali Valley earthquake of June 9, 1980, (m_L = 6.2). Accelerograph was a digital recorder which sampled at a rate of 200 per second. 2A. Log - log axes. 2B. Linear - log axes.

Figure 2A shows the same general properties as Figure 1A, although the window in this case was not long enough to establish a low frequency asymptote at frequencies less than the corner frequency f_0. By analogy to Figure 1A, one would pick f_{max} at about 10 Hz for the spectrum in Figure 2A. Figure 1B again shows an uninterrupted exponential decrease in spectral amplitude, in this case from 1 Hz to 40 Hz. At 40 Hz this trend intersects spectral amplitudes of about 0.1 cm/sec, corresponding to the least count digitization level. At higher frequencies the spectrum is flat, as is appropriate for a digitization process with random round-off errors at an amplitude of ± 0.5 least count.

Based on Figures 1 and 2, and many comparable spectral plots, we hypothesize that the shape of the acceleration spectrum at frequencies greater than the source corner-frequency ($\omega_0 = 2\pi f_0$) can generally be described by the equation:

$$a(\omega) = A_0 \, e^{-\kappa \omega/2} \qquad \omega > \omega_0 \tag{1}$$

where A_0 depends on source properties, epicentral distance, and perhaps other factors. The systematic behavior of the spectral decay parameter, κ, is explored in the next three sections of this paper.

METHOD

We studied shear-wave spectra for the horizontal components of strong ground acceleration from 98 sites around the 1971 San Fernando earthquake, ten events recorded at Ferndale, ten events recorded at El Centro, and five events recorded at Hollister. All records are corrected accelerograms from the Volume II data tape prepared by the Earthquake Engineering Research Laboratory of California Institute of Technology (EERL, 1971).

Fourier transforms of the shear waves were computed from accelerograms. The time window was chosen to include only direct S-wave arrivals. In cases where the transition from direct S-wave arrivals to coda was not readily apparent, our choice for the time window favored including coda rather than possibly eliminating direct arrivals. Spectral shape was found to be fairly insensitive to the time window length as long as it was reasonably chosen. The value of κ at stations ~40 km from the epicenter of the San Fernando earthquake showed no correlations with time window length. The transforms were computed with a standard fast Fourier transform routine after a cosine taper was applied to the raw data and the time series were padded out to powers of two with zeroes. The spectra were plotted from 0-25 Hz (Nyquist frequency = 25 Hz).

To obtain the spectral decay parameter, linear least-squares fits to the spectra were obtained. A 2-12 Hz interval was used for the El Centro, Ferndale and Hollister records. Higher frequencies were considered potentially unreliable on some of these records in these data sets. For the San Fernando records, the interval used for regression was 2-18 Hz.

Values of the slopes were converted to the spectral decay parameter, κ, and subsequently plotted against epicentral distance to evaluate distance-dependence. To quantize trends we found a linear regression between κ and distance, R, even though we do not believe a linear relationship is the definitive dependence of κ on R. For the multiple event data, these straight lines were fit directly. The San Fernando data were averaged within 10 km distance bands and then fit with

straight lines. This latter procedure reduces the weight of the distance ranges which are represented by large numbers of stations. Regression done on the complete data sets yielded similar results.

RESULTS: SINGLE STATION AND MULTIPLE EVENTS

Figures 3 through 9 illustrate results for records of earthquakes at multiple distances from a single station. Figure 3 is a map of the vicinity of the El Centro accelerograph, showing locations of the station, epicenters of ten earthquakes which were recorded on the accelerograph, and generalized surficial geology. Corresponding S-wave spectra and least-squares fits are shown in Figure 4. Figure 5 is a map of the Ferndale vicinity, and Figure 6 shows corresponding spectra for ten earthquakes which have been recorded there. Locations of the earlier earthquakes recorded at El Centro and Ferndale may have substantial errors. The 1934 and 1954 earthquakes at El Centro are shown at the relocated epicenters of Leeds (1979). These epicenters may be more reliable than others among the earlier earthquakes on these maps. Figure 7 is a map of the Hollister vicinity and Figure 8 shows corresponding spectra for five earthquakes recorded at Hollister. Finally, Figure 9 shows measured values of κ as a function of distance for all three stations.

Figure 4 shows spectra for both components of the El Centro station. On these spectra, for frequencies between 2 Hz and 12 Hz, a linear trend dominates the spectral shapes. Spectra for the 1934, 1940, and 1942 earthquakes (records B024, A001, and T286 respectively) have a nearly constant trend starting at frequencies between 12 Hz and 15 Hz.

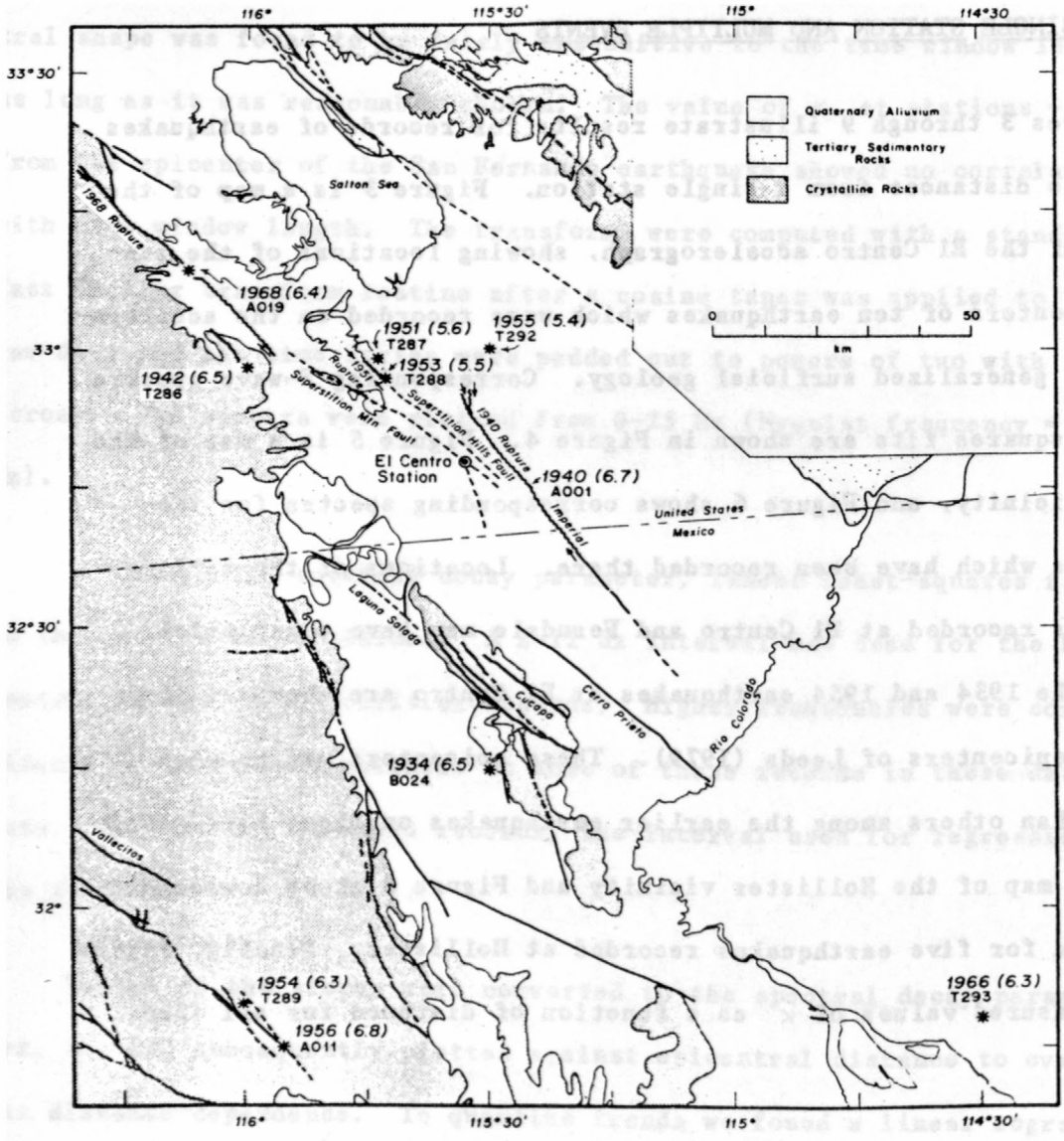

Figure 3.--Map of Imperial Valley, California - Mexico showing generalized geological features. Epicenters (asterick) from Leeds (1979) or Hileman et al., (1973) are shown with year and magnitudes of earthquakes which have generated accelerograms at the El Centro station. Accelerogram number on the Caltech tapes is given below year. The 1940 and 1968 ruptures are from Jennings (1975).

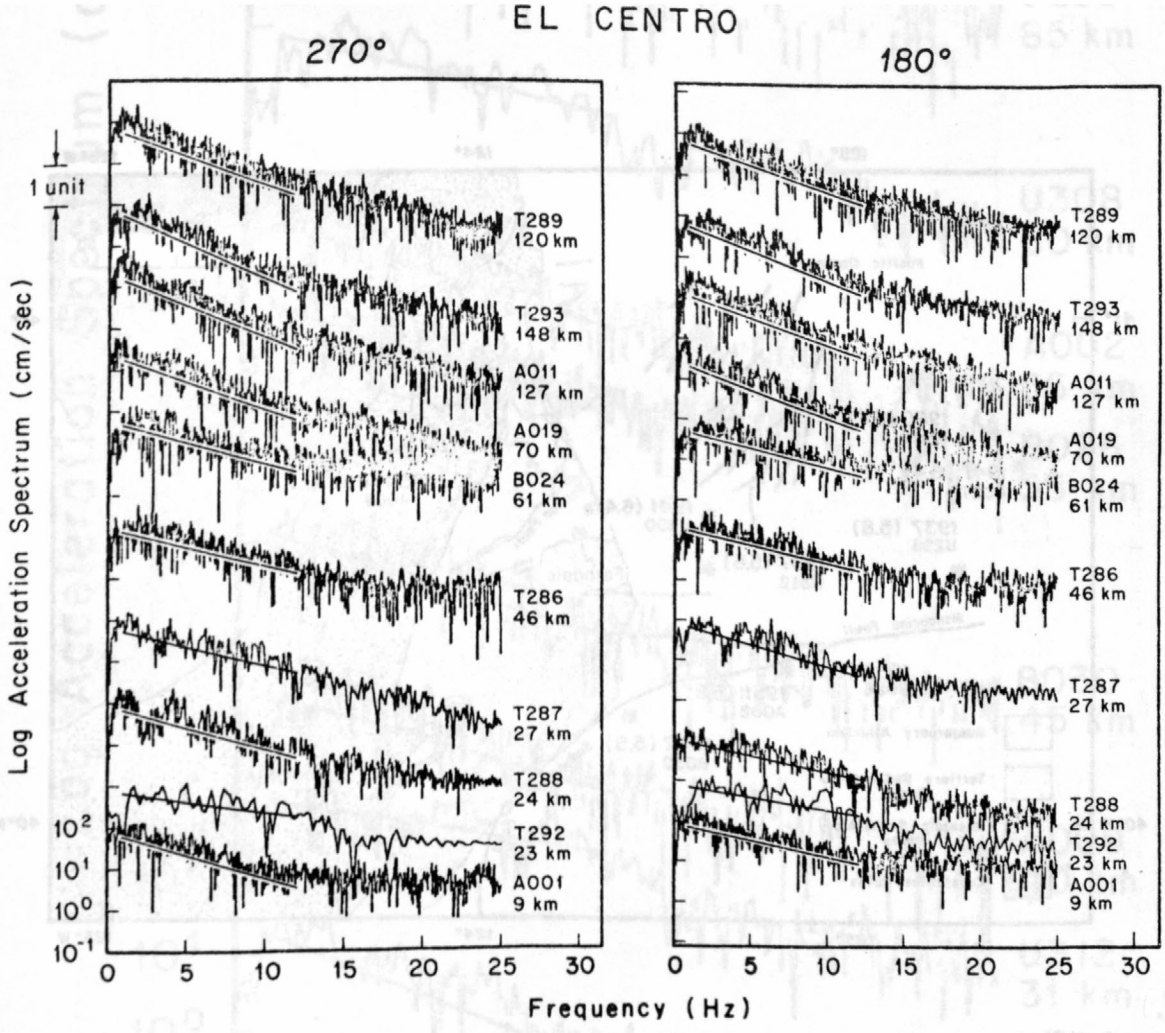

Figure 4.--Fourier amplitude spectra of S-wave accelerograms corresponding to epicenters from Figure 3. Record number and distance from the accelerograph are indicated to right of each spectrum. Each spectrum is offset by two logarithmic units from the spectrum immediately below. Superimposed on each spectrum is a linear, least-squares fit over the frequency band 2 Hz to 12 Hz.

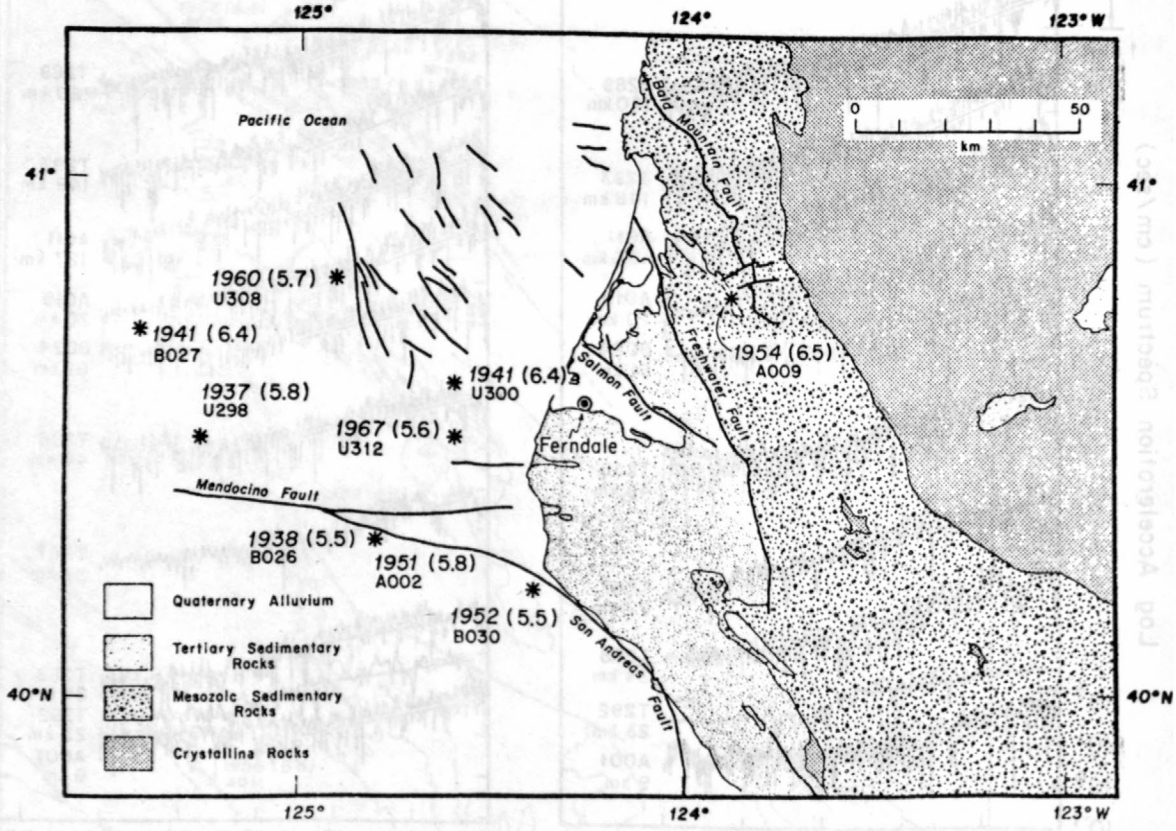

Figure 5.--Map of Cape Mendocino, California, showing generalized geological features. Epicenters from Trifunac and Lee (1978) are identified with the same notation as in Figure 3, and represent earthquakes which have produced accelerograms on the Ferndale accelerograph. The 1934, M = 6.0 earthquake (Record U294) was located off map at 41.7°N, 124.6°W. Real et al., (1978) location for the 1938 earthquake is 40°N, 124°W, about 75 km from the epicenter shown here.

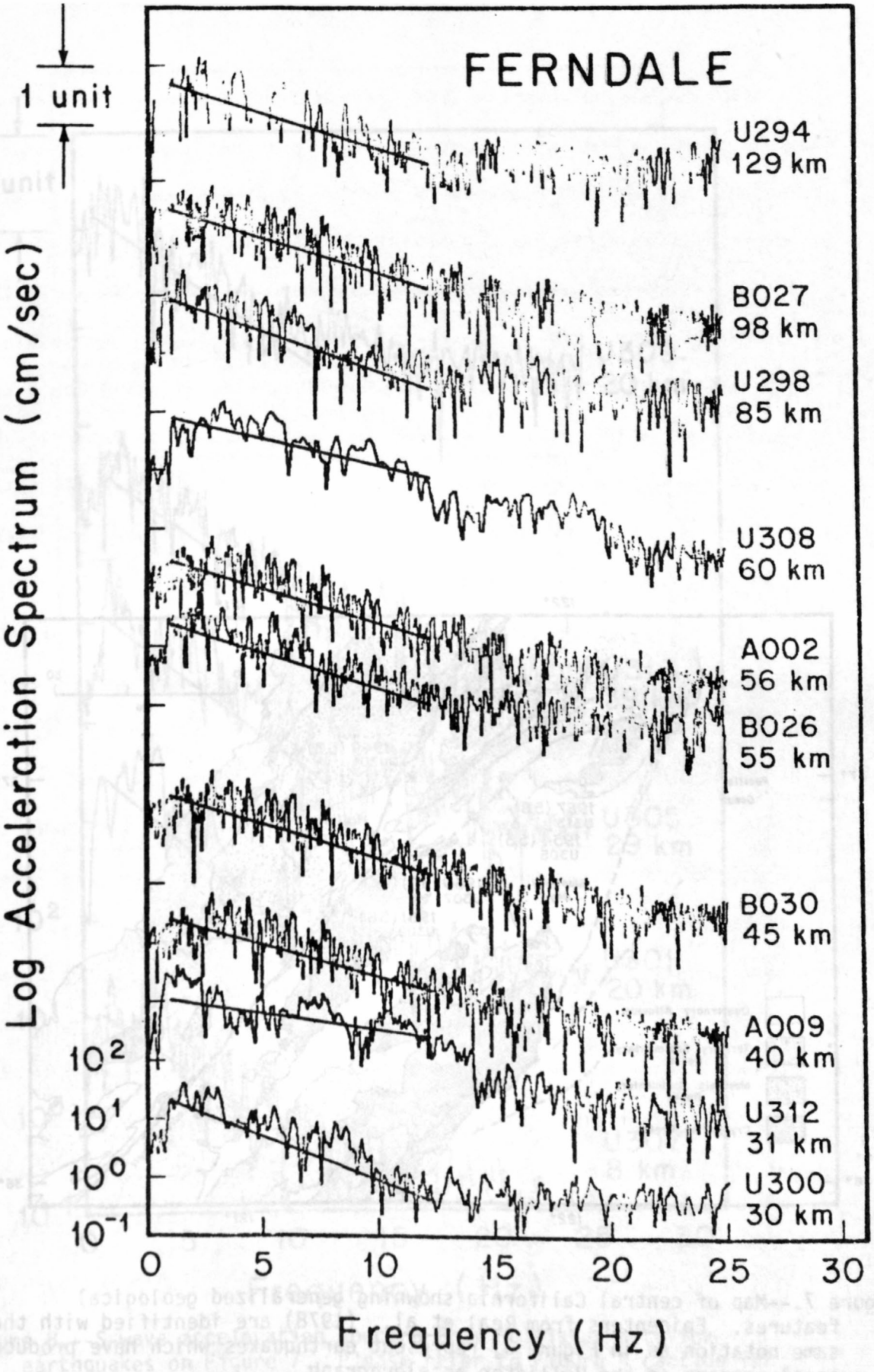

Figure 6.--S-wave acceleration spectra from Ferndale site for earthquakes on Figure 5. Please refer to Figure 4 caption for other notation.

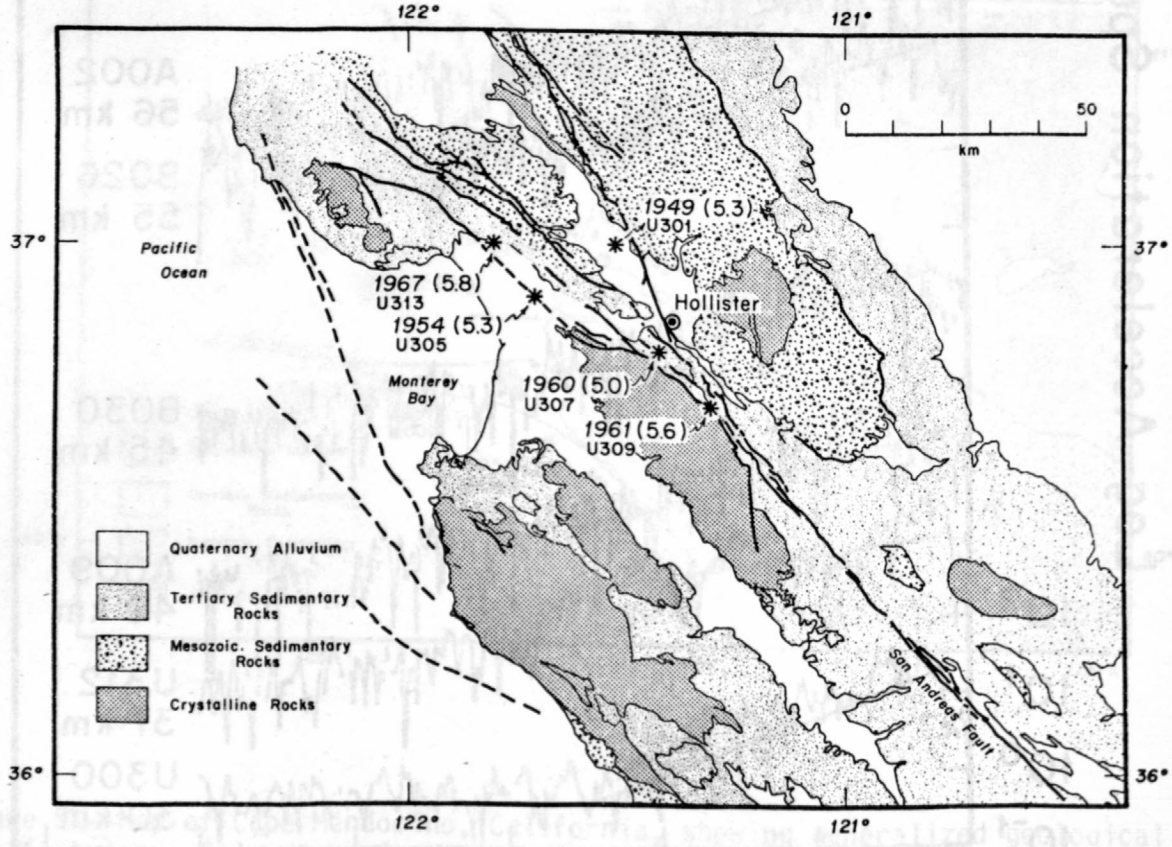

Figure 7.--Map of central California showning generalized geological features. Epicenters from Real et al., (1978) are identified with the same notation as in Figure 3, represent earthquakes which have produced accelerograms on the Hollister accelerograph.

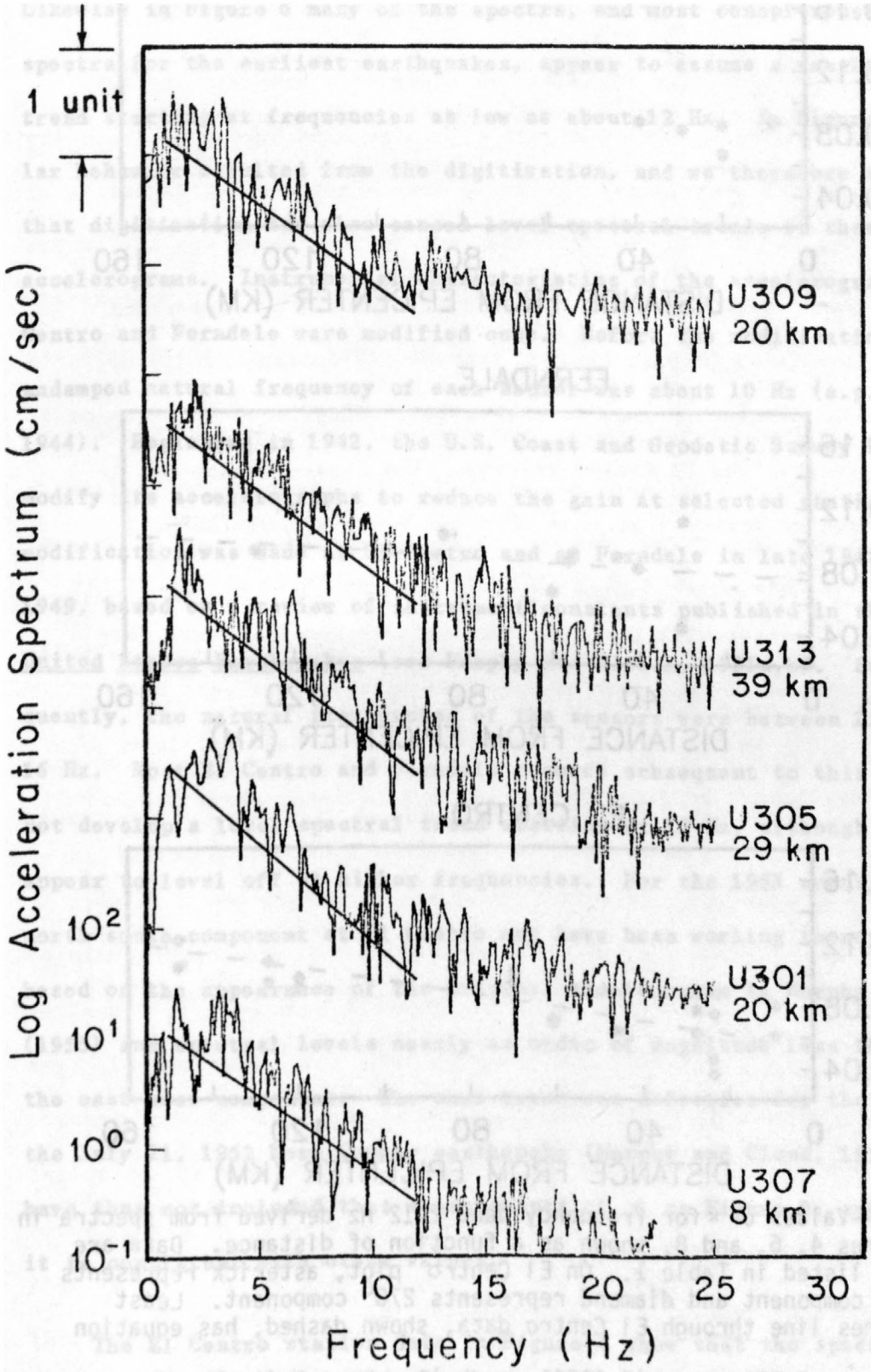

Figure 8.--S-wave acceleration spectra from Hollister site for earthquakes on Figure 7. Please refer to Figure 4 caption for other notation.

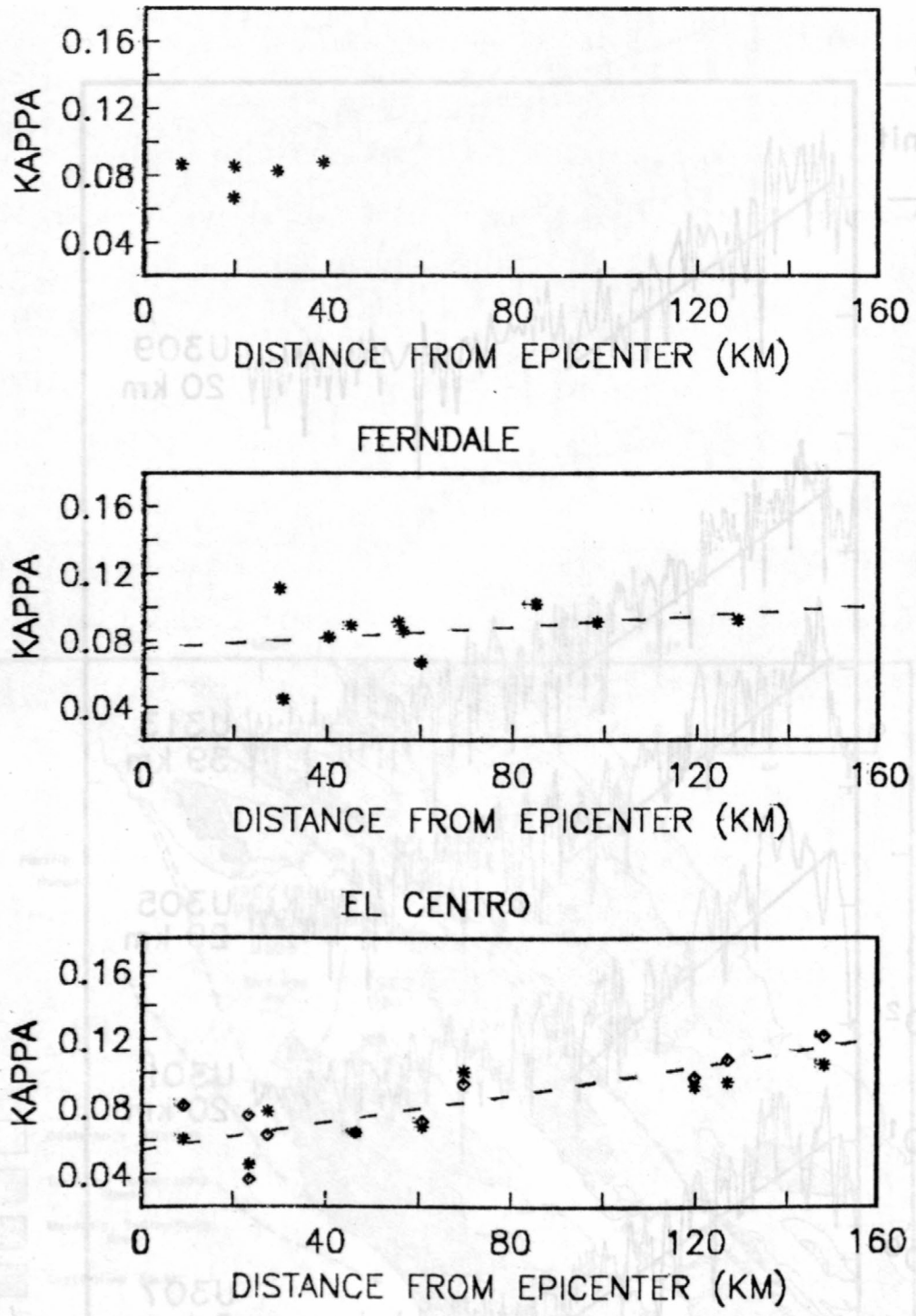

Figure 9.--Values of κ for frequency band 2-12 Hz derived from spectra in Figures 4, 6, and 8, shown as a function of distance. Data are also listed in Table 1. On El Centro plot, asterick represents 180^{0} component and diamond represents 270^{0} component. Least squares line through El Centro data, shown dashed, has equation

$\kappa = 0.054$ sec + (0.00041 sec/km)R, where R is the distance from epicenter. Least squares line through Ferndale data has the equation $\kappa = 0.075$ sec + (0.00016sec/km)R.

Likewise in Figure 6 many of the spectra, and most conspicuously the spectra for the earliest earthquakes, appear to assume a nearly constant trend starting at frequencies as low as about 12 Hz. In Figure 2, similar behavior resulted from the digitization, and we therefore suspect that digitization has also caused level spectral trends on these accelerograms. Instrumental characteristics of the accelerographs at El Centro and Ferndale were modified once. Before the modification, the undamped natural frequency of each sensor was about 10 Hz (e.g. Bodle, 1944). Beginning in 1942, the U.S. Coast and Geodetic Survey began to modify its accelerographs to reduce the gain at selected stations. This modification was made at El Centro and at Ferndale in late 1948 or early 1949, based on a review of instrument constants published in the series United States Earthquakes (see Murphy and Ulrich, 1951a,b). Subsequently, the natural frequencies of the sensors were between 15 Hz and 16 Hz. Most El Centro and Ferndale records subsequent to this change do not develop a level spectral trend starting at 12 Hz, although some appear to level off at higher frequencies. For the 1953 event, the north-south component at El Centro may have been working improperly based on the appearance of the original accelerogram in Murphy and Cloud (1955) and spectral levels nearly an order of magnitude less than for the east-west component. The same trace was defective for the record of the July 21, 1952 Kern County earthquake (Murphy and Cloud, 1954). We have thus not included that measurements of κ on Figure 9, even though it is consistent with other values.

The El Centro station data in Figure 4 show that the spectral slopes of the two horizontal components of S-waves from an earthquake are similar. Spectra in Figure 4, generally arranged from farthest to

nearest, show a weak but clear distance dependence of the spectral shape, which is confirmed on Figure 9 by the numerical values of the spectral decay parameters. The least-squares line through these data on Figure 9 has the equation κ = .054 sec +(0.00041 sec/km)R, where R is the source-to-station distance.

Accelerograms which have been recorded at Ferndale are primarily from offshore locations (Figure 5), and many of the epicenters are not well controlled. Spectra (Figure 6) show a less conspicuous increase of κ with distance than for El Centro records. The least-squares fit to the Ferndale data on Figure 9 is κ = .075 sec +(0.00016 sec/km)R. Spectra from Hollister (Figure 8) do not show a conclusive change in the spectral decay parameter with distance, but all the accelerograms were obtained at distances of less than 40 km. The spectra on Figure 8 conform to Equation (1) in the 2 to 12 Hz frequency band; they all level off in the manner caused by digitization noise at a level about two orders of magnitude below the peak but at an absolute level which varies from one record to the next.

Figure 9 summarizes the three studies of multiple recordings at a single station. At El Centro, Ferndale, and Hollister the spectral decay parameter exhibits a common type of behavior. Within the resolution of the data, κ tends toward a finite value as epicentral distance approaches zero; we interpret this finite value as a site characteristic. Furthermore, a path-distance effect also seems to be present, and causes κ to increase gradually with distance. The existence of this systematic behavior suggests that the source spectral shapes of the several earthquakes probably had identical trends between the frequencies of 2 Hz and 12 Hz.

RESULTS: SAN FERNANDO EARTHQUAKE

The San Fernando earthquake represents a situation in which multiple recordings have been made of a single event. Azimuthal variations in κ resulting from the source function were assumed negligible. This earthquake was used to study the effect of variable local geology and distance on κ. A map showing station locations and generalized geology has been prepared by Hanks (1975).

About 90 percent of the spectra from the San Fernando records have an average trend which is modeled well by Equation (1). The other ten percent of the records appear to follow the same trend, except for a superimposed bulge which we tentatively identify as a site amplification effect. Figure 10 shows an example of one Fourier spectrum which shows a relatively large apparent amplification of this type. Smaller broad-band resonances may be unrecognized, and we conjecture that such resonances may add noise to determinations of κ.

Table 2 and Figure 11 summarize values of κ obtained from the San Fernando earthquake. Table 2 also lists the distance, the window length employed (T), and site classification, S. In Figure 11, the stations were grouped into three categories: alluvium (S = 0), consolidated sedimentary rock (S = 1), and hard (igneous or metamorphic) rock (S = 2), following the site classification of Trifunac and Brady (1975). Stations listed as being on sedimentary rocks actually include sites on shallow alluvium as well as those on consolidated sediments. However, there were not enough stations in either of these sub-types to distinguish any reliable differences.

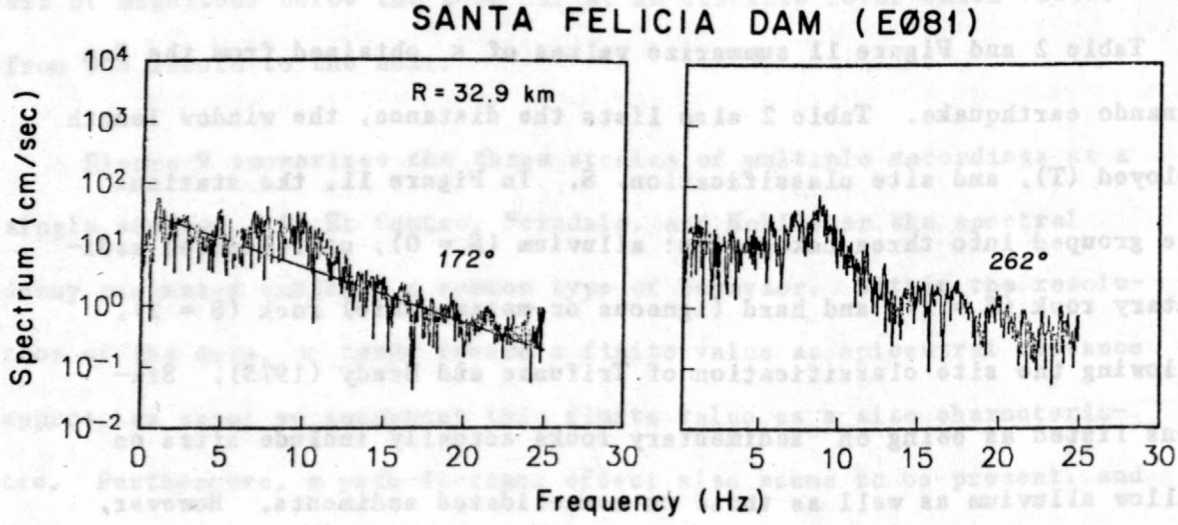

Figure 10.--S-wave acceleration spectra from Santa Felicia Dam for the San Fernando earthquake, showing a conspicuous site resonance superimposed on average linear trend.

TABLE 2 – SPECTRAL DECAY PARAMETERS FOR ACCELEROGRAMS OF THE FEBRUARY 9, 1971 SAN FERNANDO, CALIFORNIA EARTHQUAKE

REC	DIST (KM)	T	S	KAPPA1	PEAK ACCEL1	KAPPA2	PEAK ACCEL2
Ø41	9.1	1Ø	2	Ø.Ø4779	1Ø54.9	Ø.Ø4675	1148.1
Ø48	22.4	15	Ø	Ø.Ø8971	25Ø.Ø	Ø.Ø8817	131.7
Ø51	42.8	8	Ø	Ø.Ø5699	97.8	Ø.Ø4631	122.7
Ø54	41.9	8	Ø	Ø.Ø6874	147.1	Ø.Ø7277	117.Ø
Ø56	28.6	8	1	Ø.Ø7872	3Ø9.4	Ø.Ø7Ø11	265.4
Ø57	37.1	9	Ø	Ø.Ø9294	1Ø3.8	Ø.Ø9Ø59	148.2
Ø58	37.1	9	Ø	Ø.Ø6295	167.3	Ø.Ø7219	2Ø7.Ø
Ø59	39.8	8	Ø	Ø.Ø7439	133.8	Ø.Ø8Ø4Ø	147.1
Ø62	42.8	13	Ø	Ø.Ø6945	118.Ø	Ø.Ø8282	13Ø.3
Ø65	4Ø.Ø	8	1	Ø.Ø9Ø59	146.7	Ø.Ø914Ø	155.7
Ø68	35.Ø	9	Ø	Ø.Ø7Ø79	81.2	Ø.Ø6168	98.Ø
Ø71	86.Ø	12	Ø	Ø.Ø3Ø4	26.9	Ø.Ø4829	25.5
Ø72	39.5	8	1	Ø.Ø5829	82.2	Ø.Ø6585	115.Ø
Ø75	4Ø.1	9	Ø	Ø.Ø8253	133.8	Ø.Ø9279	111.8
Ø78	42.5	9	1	Ø.Ø5721	12Ø.5	Ø.Ø5418	189.2
Ø81	32.9	14	1	Ø.Ø6929	213.Ø	Ø.Ø5894	198.3
Ø83	4Ø.Ø	1Ø	Ø	Ø.Ø7754	158.2	Ø.Ø6231	161.9
Ø86	49.4	1Ø	Ø	Ø.Ø7681	1Ø4.6	Ø.Ø88Ø3	8Ø.5
Ø87	88.5	15	Ø	Ø.Ø8839	26.8	Ø.Ø9448	28.2
Ø88	34.1	8	1	Ø.Ø7989	265.7	Ø.Ø8978	2Ø9.1
Ø89	44.Ø	13	Ø	Ø.Ø6279	139.9	Ø.Ø583Ø	139.Ø
Ø92	43.1	9	1	Ø.Ø5726	64.2	Ø.Ø5475	79.1
Ø95	37.4	13	Ø	Ø.Ø6588	96.2	Ø.Ø729Ø	83.9
Ø98	42.7	12	Ø	Ø.Ø5991	236.4	Ø.Ø5312	192.Ø
1Ø1	1Ø7.6	1Ø	Ø	Ø.Ø9Ø88	36.5	Ø.Ø8744	29.6
1Ø2	68.5	1Ø	2	Ø.Ø582Ø	25.4	Ø.Ø6617	21.8
1Ø3	45.4	12	Ø	Ø.Ø4756	91.5	Ø.Ø5441	12Ø.5
1Ø4	52.2	1Ø	1	Ø.Ø7579	85.1	Ø.Ø7952	1Ø3.1
1Ø5	38.7	12	Ø	Ø.Ø7762	83.1	Ø.Ø6872	77.6
1Ø6	36.1	12	2	Ø.Ø56Ø5	87.4	Ø.Ø7842	188.7
1Ø7	39.8	14	Ø	Ø.Ø5Ø36	93.5	Ø.Ø715Ø	1Ø7.1
1Ø8	39.8	15	Ø	Ø.Ø8341	198.1	Ø.Ø9623	181.4
11Ø	31.5	13	1	Ø.Ø5216	2Ø7.9	Ø.Ø3243	138.9
112	42.5	1Ø	Ø	Ø.Ø4682	78.7	Ø.Ø4438	1Ø1.9
114	32.3	13	Ø	Ø.Ø699Ø	11Ø.8	Ø.Ø7417	136.1
115	29.3	12	Ø	Ø.Ø7373	22Ø.5	Ø.Ø86Ø5	145.Ø
118	5Ø.2	17	Ø	Ø.Ø8Ø48	33.7	Ø.Ø7432	32.6
121	43.1	13	Ø	Ø.Ø5157	119.5	Ø.Ø45Ø9	112.2
124	76.2	16	Ø	Ø.Ø9689	35.2	Ø.Ø8517	34.5
128	37.1	13	Ø	Ø.Ø5878	6Ø.9	Ø.Ø6735	91.6
131	38.2	14	Ø	Ø.Ø7476	184.3	Ø.Ø9228	16Ø.5
134	38.9	13	Ø	Ø.Ø6123	97.8	Ø.Ø56Ø4	82.1
137	29.Ø	13	Ø	Ø.Ø475Ø	14Ø.2	Ø.Ø4Ø27	128.9
141	29.6	8	2	Ø.Ø72ØØ	145.5	Ø.Ø5393	1Ø8.6
142	26.8	7	2	Ø.Ø3432	168.1	Ø.Ø4Ø46	143.5
143	26.6	6	2	Ø.Ø2957	119.3	Ø.Ø1954	1Ø9.4
144	23.3	7	1	Ø.Ø6374	346.2	Ø.Ø5216	277.9
145	24.9	12	Ø	Ø.Ø8Ø11	113.9	Ø.Ø7637	1Ø3.5
148	39.9	12	1	Ø.Ø6ØØ3	1Ø7.5	Ø.Ø6183	112.1
157	42.5	12	Ø	Ø.Ø6392	168.2	Ø.Ø6ØØ8	116.1
166	3Ø.8	9	1	Ø.Ø5897	164.2	Ø.Ø6264	147.6
171	139.8	17	1	Ø.Ø8Ø33	11.8	Ø.Ø9143	16.2
176	42.9	12	Ø	Ø.Ø5869	83.4	Ø.Ø6363	115.7
179	7Ø.7	4	1	Ø.Ø3292	19.7	Ø.Ø41Ø8	49.1
18Ø	84.3	2Ø	Ø	Ø.Ø8663	23.8	Ø.Ø9352	29.7
183	7Ø.8	15	1	Ø.Ø5593	43.2	Ø.Ø5558	56.5
184	7Ø.8	16	1	Ø.Ø6284	43.1	Ø.Ø5887	57.2
185	75.6	13	1	Ø.Ø8348	67.3	Ø.Ø8348	67.3
186	54.1	15	Ø	Ø.Ø82Ø2	95.7	Ø.Ø7542	96.8
187	72.1	14	Ø	Ø.Ø6144	75.8	Ø.Ø7842	56.2
188	38.9	13	Ø	Ø.Ø6968	114.4	Ø.Ø9352	126.8
191	67.8	19	1	Ø.1Ø598	24.8	Ø.Ø9711	4Ø.1
192	4Ø.7	12	1	Ø.Ø4946	96.6	Ø.Ø4525	98.7
195	122.6	32	Ø	Ø.Ø8Ø5	41.Ø	Ø.Ø7996	3Ø.9
196	75.4	17	Ø	Ø.Ø9396	35.1	Ø.Ø9873	31.2
197	185.7	2Ø	Ø	Ø.Ø8678	24.9	Ø.Ø9462	34.8
198	34.Ø	12	2	Ø.Ø5185	176.9	Ø.Ø5Ø22	167.4
199	42.Ø	15	Ø	Ø.Ø5691	137.8	Ø.Ø7Ø81	238.6
2Ø4	73.8	23	Ø	Ø.Ø88Ø3	26.Ø	Ø.Ø9242	2Ø.8
2Ø5	73.6	28	Ø	Ø.Ø9799	28.4	Ø.Ø6ØØ9	28.1
2Ø6	1Ø8.2	2Ø	Ø	Ø.Ø8964	37.4	Ø.Ø9389	44.1
2Ø7	32.8	15	2	Ø.Ø6582	65.1	Ø.Ø5861	97.1
2Ø8	133.4	23	1	Ø.Ø8385	16.5	Ø.Ø7659	17.1
21Ø	151.4	13	Ø	Ø.Ø6873	35.Ø	Ø.Ø7356	39.2
214	36.2	1Ø	1	Ø.Ø7142	154.1	Ø.Ø7251	156.3
217	4Ø.Ø	12	Ø	Ø.Ø8231	1Ø8.3	Ø.Ø73Ø7	88.2
22Ø	95.8	17	1	Ø.Ø9462	24.2	Ø.Ø8869	34.3
221	43.3	13	2	Ø.Ø4982	137.7	Ø.Ø3745	165.8
222	79.3	2Ø	Ø	Ø.Ø9132	25.9	Ø.Ø9792	25.2
223	65.Ø	15	2	Ø.Ø8436	69.7	Ø.Ø7586	53.9
231	51.7	16	Ø	Ø.Ø6543	41.2	Ø.Ø66Ø7	37.9
233	29.3	13	Ø	Ø.Ø669Ø	243.3	Ø.Ø4534	197.3
236	34.9	14	Ø	Ø.Ø6931	122.4	Ø.Ø5461	167.1
239	38.4	15	Ø	Ø.Ø618Ø	119.4	Ø.Ø7469	161.6
241	41.8	15	1	Ø.Ø5381	86.9	Ø.Ø66Ø7	137.8
244	41.9	15	1	Ø.Ø724Ø	149.1	Ø.Ø7886	126.9
246	35.7	13	Ø	Ø.Ø5526	115.9	Ø.Ø6757	1Ø7.1
248	35.7	13	Ø	Ø.Ø6393	184.Ø	Ø.Ø6155	174.2
249	39.2	15	Ø	Ø.Ø5755	8Ø.Ø	Ø.Ø6Ø29	84.1
251	41.8	12	1	Ø.Ø796Ø	195.7	Ø.Ø8319	188.2
253	42.Ø	15	Ø	Ø.Ø6888	22Ø.8	Ø.Ø6Ø31	242.Ø
255	38.9	12	1	Ø.Ø8Ø18	124.1	Ø.Ø75Ø5	128.4
258	44.6	16	Ø	Ø.Ø6178	56.1	Ø.Ø54Ø8	83.1
261	39.6	1Ø	Ø	Ø.Ø5781	98.Ø	Ø.Ø6Ø25	1Ø7.9
262	39.Ø	14	1	Ø.Ø9ØØØ	68.5	Ø.Ø8231	93.9
265	39.9	15	1	Ø.Ø655Ø	1Ø4.2	Ø.Ø5625	125.3
266	4Ø.Ø	15	Ø	Ø.Ø5469	153.5	Ø.Ø6297	129.8
267	52.Ø	18	Ø	Ø.Ø5696	55.4	Ø.Ø6615	61.5

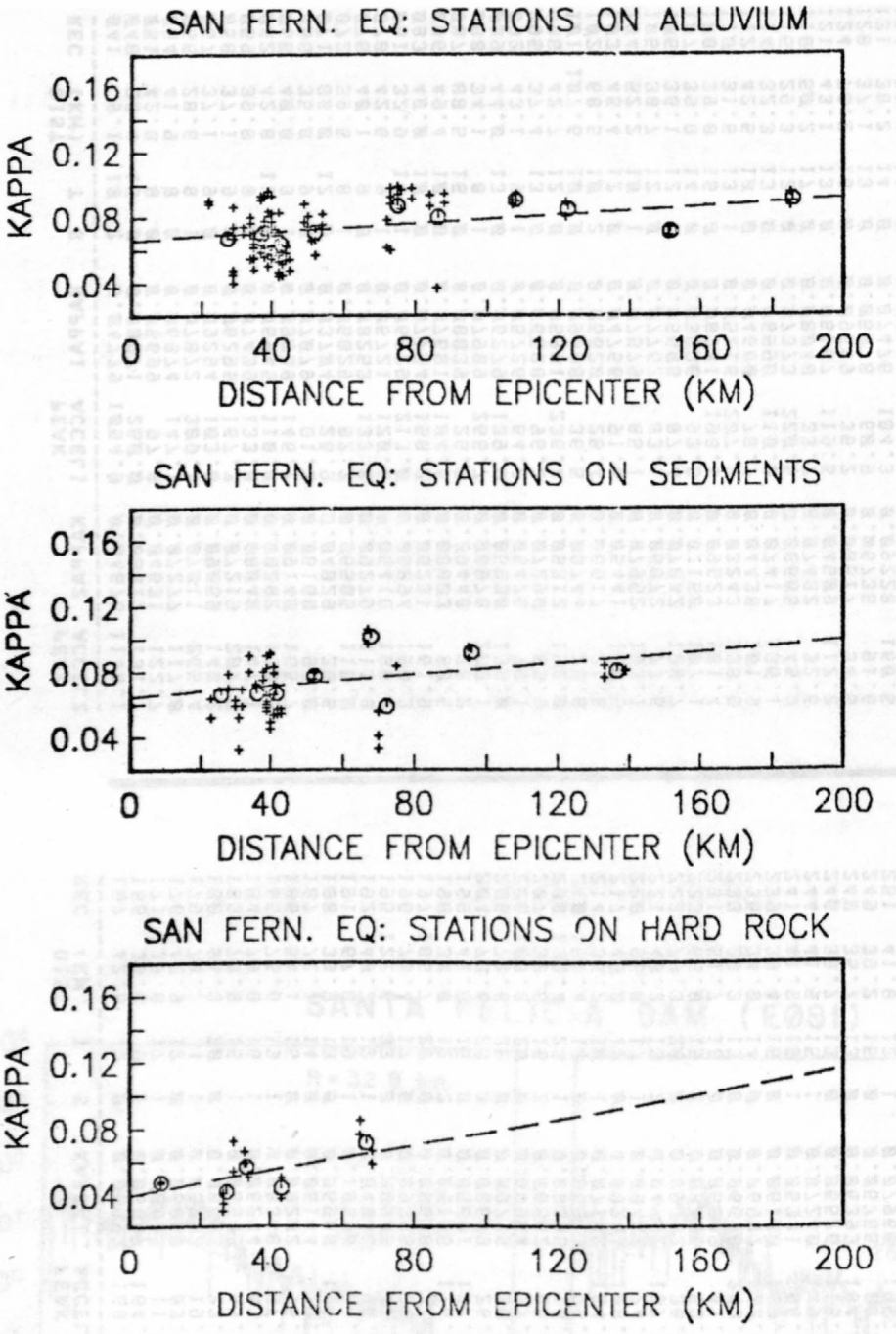

Figure 11.--Value of κ (small "+") for the frequency band 2-18 Hz derived from both components of San Fernando earthquake accelerograms. Data are listed in Table 2. Stations are classified as alluvium, consolidated sediments, or hard rock as in Trifunac and Brady (1975). Larger circles are at average values of both and distance (R) for 10 km intervals. Least squares lines (dashed) have the following equations:

alluvium	$\kappa = 0.066 \text{ sec} + (0.000126 \text{ sec/km}^{-1})R$
consolidated sediments	$\kappa = 0.065 \text{ sec} + (0.000172 \text{ sec/km}^{-1})R$
rock	$\kappa = 0.040 \text{ sec} + (0.000380 \text{ sec/km}^{-1})R$

Trends in the raw data on Figure 11 resemble trends on Figure 9, except for a larger amount of scatter: κ tends toward a finite intercept and increases slowly with distance. The larger amount of scatter is predictable from the interpretation of Figure 9 which says a major contribution to κ results from a site effect. Figure 11 also shows average values of κ over 10 km intervals and least-square linear regression through these averages. Numerical values of the regression lines between κ and R are in the figure captions. There is a factor of three difference between the slopes of these regressions for stations on alluvium and on rock. These differences result in part from different distance ranges involved in the regressions. Considering this and the scatter in the data it is doubtful that the slope differences are significant. An observation which may be significant is that the values of κ for hard rock sites average about 25 percent lower than values for the other two conditions over the distance range to 70 km.

DISCUSSION

This section presents a plausible model to explain the observations which are described above. We first hypothesize that the S-wave displacement spectrum at the earthquake source has an ω^{-2} behavior at frequencies higher than the corner frequency. Hanks (1979) has reviewed some of the evidence for such behavior and argues that the strong motion spectra generally supports this hypothesis. Modiano and Hatzfeld (1982) and Sipkin and Jordan (1980) have previously used these assumptions to study attenuation. In particular, we hypothesize that the spatial quality factor of shear wave attenuation, Q_β, is independent of frequency, but a strong function of depth. If this is a valid hypothesis, one can

define an attenuation time, t*, for seismic phases which are modeled by rays as (Cormier, 1982)

$$t^* = \int \frac{dr}{Q_\beta(r)\beta(r)} \quad , \tag{2}$$

and the spectrum of that phase is multiplied by the factor $e^{-\pi f t^*}$. The integral in Equation (2) is along the ray path. When Q_β is independent of frequency, then t* also is independent of frequency. Converting the source spectral behavior to acceleration and incorporating the effect of attenuation leads to a spectral shape above the corner frequency of

$$a(\omega) = A_0 \, e^{-\pi f t^*} \quad . \tag{3}$$

The quantity t* is then exactly equivalent to the quantity κ as defined in Figure 2. The finite intercept of the trends of κ with distance (Figures 9,11) then corresponds to the attenuation which the S-waves all encounter in traveling through shallow layers to the surface of the earth, while the slope of the mean trend corresponds to the incremental attenuation due to predominantly horizontal propagation of S-waves through the crust. By this model, one might expect complications in the dependence of κ on distance at distances greater than 100 km, which cannot be resolved from the data employed here, to result from interference from the phase S_n which travels along the Mohorovicic discontinuity. S_n becomes the first arrival at the distance of about 150 km in our region (Richter, 1958).

Figure 12 illustrates several alternative source spectral shapes and Q models. Figure 12A illustrates the ω^{-2} displacement spectrum behavior with four models for Q: $Q = \infty$, $Q = Q_0$, $Q = Q_1 f^1$, and $Q = Q_2 f^{0.5}$. The constants Q_1 and Q_2 are chosen so that for these two

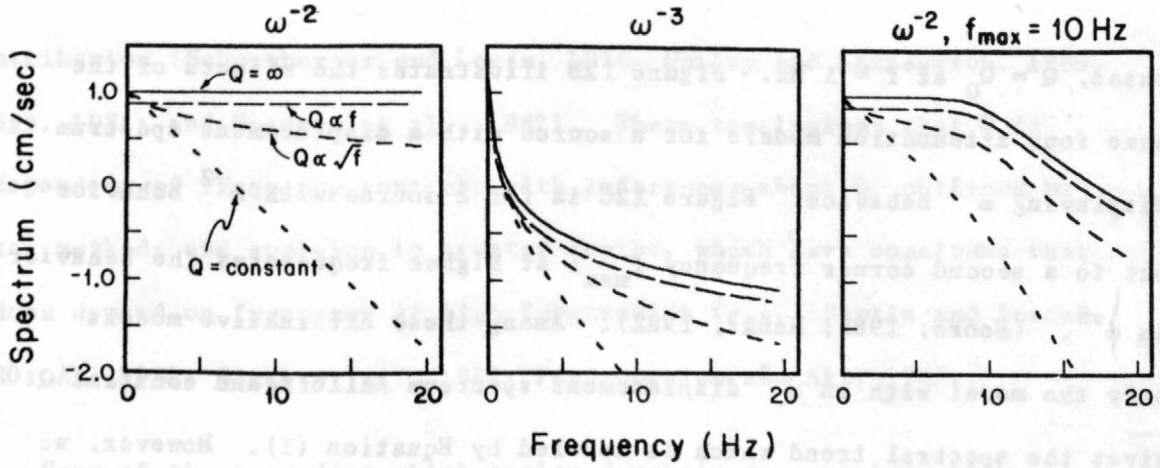

Figure 12.--Idealized acceleration spectral shapes at an accelerograph site for three source-spectral models and various attenuation models. The source spectra are described, following tradition, by falloff at high frequencies on a displacement spectrum. The following ω^{-2} models yield a constant acceleration spectrum (left and ω^{-3} models yield an acceleration spectrum with ω^{-1} falloff (center). Source model on right consists of ω^{-2} model, but with a second corner at 10 Hz, and ω^{-4} falloff in acceleration at frequencies higher than the second corner. Attenuation models are no attenuation ($Q = \infty$), constant Q attenuation, attenuation with $Q \propto f$, and with $Q \propto f^{1/2}$.

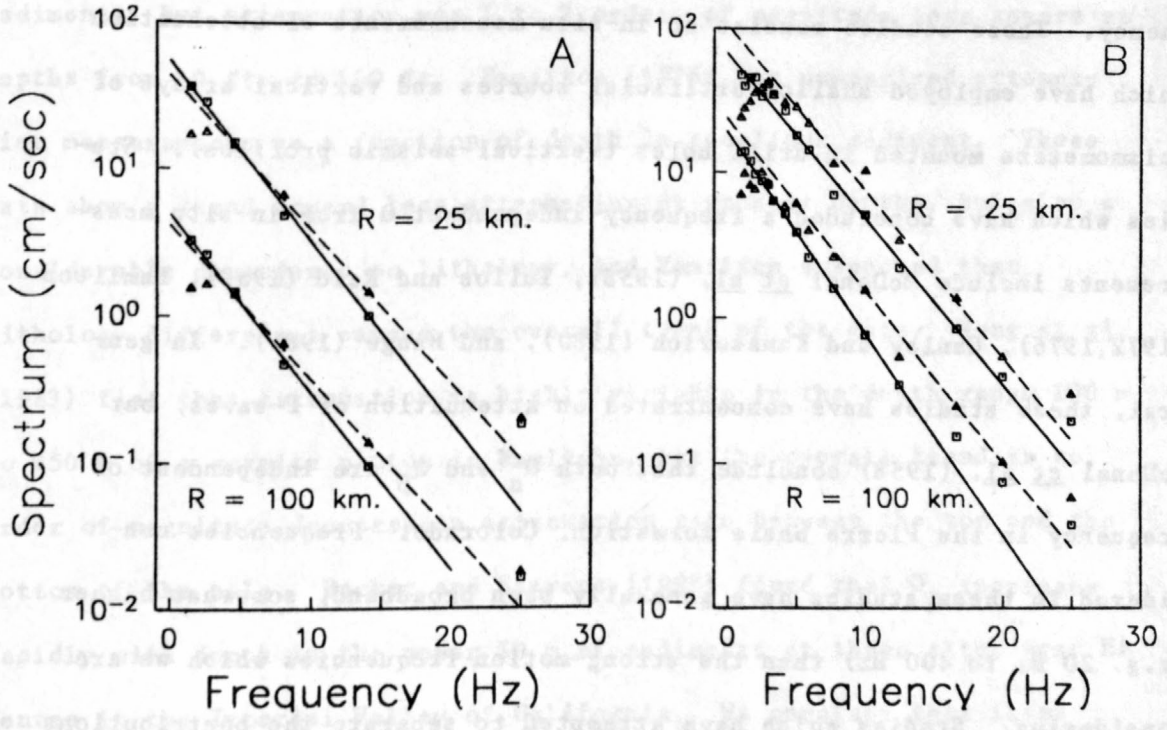

Figure 13.--A) Discrete points are mean Fourier spectral amplitudes for a magnitdue 6.5 earthquake from the regression of Trifunac (1976) at frequencies greater than 1 Hz. Lines are shown to illustrate the extent of agreement of regression points with exponential decay of the spectrum with frequency. Squares and solid lines apply to soil sites; triangles and dashed lines apply to rock sites. B) Equivalent of 13 A for the regression of McGuire (1978).

cases, $Q = Q_0$ at f = 1 Hz. Figure 12B illustrates the effects of the same four attenuation models for a source with a displacement spectrum displaying ω^{-3} behavior. Figure 12C is for a source with ω^{-2} behavior out to a second corner frequency f_{max}; at higher frequencies the behavior is ω^{-6}. (Boore, 1983; Hanks, 1982). Among these alternative models only the model with an ω^{-2} displacement spectrum falloff and constant Q gives the spectral trend which is modeled by Equation (1). However, we cannot yet rule out the possibility that other phenomena conspire to give the same spectral shape, or that the curvature associated with a different model is slight in reality.

There is some independent evidence, obtained in conjunction with seismic exploration techniques, indicating that Q is independent of frequency. These studies consist of in-situ measurements of attenuation which have employed shallow artificial sources and vertical arrays of seismometers mounted in drill holes (vertical-seismic profiles). Studies which have concluded a frequency-independent Q from in-situ measurements include McDonal *et al*. (1958), Tullos and Reid (1969), Hamilton (1972,1976), Ganley and Kanasewich (1980), and Hauge (1981). In general, these studies have concentrated on attenuation of P-waves, but McDonal *et al*. (1958) conclude that both Q_α and Q_β are independent of frequency in the Pierre Shale formation, Colorado. Frequencies considered in these studies have generally been broadband, somewhat higher (e.g. 20 Hz to 400 Hz) than the strong-motion frequencies which we are considering. Studies which have attempted to separate the contributions from dissipation and from dispersion due to layering have concluded that dispersion is variable and sometimes important (e.g. Schoenberger and Levin, 1978), but that dissipation always makes a significant

contribution (Schoenberger and Levin, 1978; Ganley and Kanasewich, 1980; Hauge, 1981; and Spencer et al., 1982). These conclusions that Q is independent of frequency contrast with inferences about Q, obtained by other methods and applying to greater depths, which have concluded that Q does depend on frequency at high frequencies (e.g. Sipkin and Jordan, 1980; Aki 1980; Singh et al., 1982; Papageorgiou and Aki, 1983).

Some of these studies which employ downhole sensors have also obtained results for the attenuation as a function of depth. McDonal et al. (1958) estimated that attenuation between the depths of 250 feet to 750 feet was three times as rapid as the average over the entire depth range to 4000 feet. Tullos and Reid (1969) found severe attenuation (corresponding to Q_α ~2) over the depth range 1 to 10 feet in Gulf Coast sediments, but attenuation was 1 to 2 orders of magnitude less severe at depths from 10 ft. to 100 ft. Hamilton (1976) has summarized attenuation measurements as a function of depth in sea-floor sediment. These data show a trend toward less attenuation at greater depths, but also a considerable dependence on lithology, and Hamilton suspected that lithology differences caused the overall trend of the data. Wong et al. (1983) find that attenuation is highly variable in the depth range 100 m to 350 m of a granite pluton in Manitoba, but the overall trend is an order of magnitude decrease in attenuation rate between the top and the bottom of the hole. Barker and Stevens (1983) found that Q_β increases rapidly with depth in the upper 50 m of sediments at three sites near El Centro in the Imperial Valley of California. We conclude that these studies provide evidence of a low Q surface layer for both P-waves and S-waves.

In summary, the seismic exploration results are consistent with our model which hypothesizes that κ is t*, and that the intercept of the trend of κ with distance is a result of relatively intense attenuation experienced by the propagation of seismic waves through shallow layers below each station. At El Centro, the intercept (Figure 9) gives t* = 0.054 sec. This corresponds to an average $Q_\beta \simeq 50$ distributed over a sediment thickness of 3.50 km. The slope of the least-squares line with distance, 0.00041 sec/km, corresponds to an average $Q_\beta \simeq 800$ below the sediments. The slope of the least-squares line through the Ferndale data (0.00016 sec/km) suggests an average $Q_\beta \simeq 2000$ below the high attenuation zone near the surface.

The values of κ derived for San Fernando accelerograms might suggest that the picture is not quite so simple. We observe first that if the dominant contribution to t* is from near-surface geology, and if the slope of t* with distance is a result of propagation at depth, then one would not expect the near-surface geology to affect the slope of the relationship between κ and R. By this inference, the possibly different slopes which were derived for different types of surface conditions would have to result from sample differences. It was pointed out previously that this may be the case. We notice that the slope is greatest for rock sites which are only represented at relatively short distances, while the slope is smallest for alluvium sites which are represented to the greatest distances. These observations suggest the possibility that the slope, $\frac{d\kappa}{dR}$, is a decreasing function of distance. There is no theoretical reason for $\frac{d\kappa}{dR}$ to be independent of distance and our linear regressions were intended only to illustrate general trends. It may be possible to invert κ and $\frac{d\kappa}{dR}$ as a function of distance to derive Q as a function of depth.

The median spectral shapes which were obtained by the regressions of Trifunac (1976) and McGuire (1978) also show exponential decay with frequency. Discrete points at frequencies greater than 1 Hz from both regressions are illustrated in Figure 13 for a magnitude 6.5 earthquake at 25 km and 100 km. For the Trifunac (1976) regression, the mean predicted spectra on soil conditions agree with exponential decay for frequencies from 2 Hz to 15 Hz and mean predicted spectra on rock conditions agree with exponential decay for frequencies from 5 Hz to 15 Hz. The points at 25 Hz fall above the level consistent with exponential decay, but this may result from noise, as in some of the spectra shown in previous figures. The results from McGuire (1978), shown in Figure 13B, confirm this result. This regression indicates that exponential decay persists to frequencies of 20 Hz at 25 km, and for rock sites at 100 km. The results by Trifunac (1976) at 25 km and at 100 km, and results of McGuire (1978) at 100 km anticipate the lower values of the spectral decay parameter on rock sites, as found in our study. The McGuire results for soil sites anticipate the observed increase of the spectral decay parameter with distance. Numerical values of spectral decay parameters for all lines on Figure 13 are between 0.077 sec and 0.090 sec, and are slightly higher than values which would have been anticipated based on our results. However, spectra studied by Trifunac and by McGuire were whole record spectra, while we used S-wave spectra; this might account for some of the discrepancies.

CONCLUSIONS

At high frequencies the Fourier acceleration spectrum of S-waves decays exponentially in a majority of existing California accelerograms. The spectral decay parameter, κ, was defined in Equation (1), and a study of its properties was pursued in this paper. The spectral decay parameter plays a role similar to f_{max} (Hanks, 1982) in describing the phenomenon that the acceleration spectrum is curtailed at high frequency. However, the spectral decay parameter can be measured more quantitatively than f_{max}. In light of results such as Figures 1 and 2, which show that high frequency energy above the recording noise level exists at frequencies greater than f_{max}, we question whether the terminology "f_{max}" might be somewhat misleading. The interpretation that the spectral decay parameter is primarily controlled by local site conditions is consistent with the origin for f_{max} favored by Hanks (1982).

We have attributed deviations from a trend of exponential decay to two sources, broadband site resonances and noise. The obvious site resonances, such as in Figure 10, appear on about 10 percent of the San Fernando accelerograms. Weaker resonances may add some noise to determinations of κ. Figure 2 shows a clear example of the effect of digitization noise on the spectrum, and by analogy we have interpreted observations that spectra in Figures 4, 6, and 8 approach a level trend as evidence for digitization or instrumental noise. However, it is clear that such an interpretation is not unique, and the problem needs to be studied in detail.

The spectral decay parameter seems to depend primarily on physical conditions near the accelerograph site because it is only a weak

function of distance. The interpretation that it is exactly t*, the attenuation parameter, then implies that attenuation to distances from 100 to 200 km is dominated by shallow structure below the site, and that Q is very high at the depth of propagation of the S_g phase. To the extent that we can resolve attenuation at depth from the more important shallow contribution, our interpretation is that Q is independent of frequency, which contradicts a considerable body of seismology literature. For example, Papageorgiou and Aki (1983) have concluded that the decrease in the Fourier acceleration spectrum at high frequencies is a property of the seismic source, and that Q is proportional to frequency allowing the source spectrum to be transmitted essentially unmodified to the receiver. Our observation of a subtle, but measurable, increase in the spectral decay parameter with distance is not consistent with this hypothesis, but does not necessarily rule out a hybrid model in which the spectrum falls off due to both source and attenuation effects. Below a low-Q surface zone, the results of Papageorgiou and Aki (1983) agree with our conclusion that Q is high at high frequency; it is at low frequency (~1 Hz) where resolution is not as good in either study and that the conclusions differ.

If further evidence supports the conclusion that the spectral decay parameter is a single station measure of average attenuation encountered by S-waves, then a number of research topics might be addressed. Topics might include studies of the relationship of κ to site geology including research into non-linear effects, studies to reduce scatter about attenuation equations, inversion of κ - distance observations for attenuation as a function of depth, and investigation of high quality data to search for frequency dependence in attenuation.

ACKNOWLEDGEMENTS

J.E. Luco and M. Reichle provided helpful critical reviews of this manuscript. P. Bodin provided much assistance in gathering information for this study. This research was supported by National Science Foundation grant CEE 81-20096.

REFERENCES

Aki, K. (1980). Attenuation of shear-waves in the lithosphere for frequencies from 0.05 to 25 Hz, Physics of the Earth and Planetary Interiors, 21, 50-60.

Anderson, J.G., J. Prince, J.N. Brune, and R.S. Simons (1982). Strong motion accelerograms, in J.G. Anderson and R.S. Simons, eds., The Mexicali Valley Earthquake of 9 June 1980, Newsletter Earthquake Eng. Res. Inst., 16, 79-83.

Barker, T.G. and J.L. Stevens (1983). Shallow shear wave velocity and Q structures at the El Centro strong motion accelerograph array, Geophys. Res. Lttrs., 10, 853-856.

Bodle, R.R. (1944). United States Earthquakes 1942, Serial 662, U.S. Dept. of Commerce, Coast and Geodetic Survey, Washington, D.C.

Boore, D.M. (1983). Stochastic simulation of high frequency ground motions based on seismological models of the radiated spectra (abstract), Earthquake Notes, 54, 70.

Brune, J.N. (1970). Tectonic stress and the spectra of seismic shear waves from earthquakes, J. Geophys. Res., 75, 4997-5009.

Cormier, V.F. (1982). The effect of attenuation on seismic body waves, Bull. Seism. Soc. Am., 72 S169-S200.

Earthquake Engineering Research Laboratory (1971). Strong Motion Earthquake Accelerograms Volume II - corrected accelerograms and integrated ground velocity and displacement curves, Report EERL 71-50, California Institute of Technology, Pasadena.

Ganley, D.C. and E.R. Kanasewich (1980). Measurement of absorption and dispersion from check shot surveys, J. Geophys. Res., 85:B10, 5219-5226.

Hamilton, E.L. (1972). Compressional-wave attenuation in marine sediments, Geophysics, 37:4, 620-646.

Hamilton, E.L. (1976). Sound attenuation as a function of depth in the sea floor, J. Acoust. Soc. Am., 59:3, 528-535.

Hanks, T.C. (1975). Strong ground motion of the San Fernando, California, earthquake: ground displacements,

Hanks, T.C. (1979). b-values and $\omega^{-\gamma}$ seismic source models: implications for tectonic stress variations along active crustal fault zones and the estimation of high-frequency strong ground motion, J. Geophys. Res., 84, 2235-2242.

Hanks, T.C. (1982). f_{max}, Bull. Seism. Soc. Am., 72A, 1867-1880.

Hanks, T.C. and R.K. McGuire (1981). The character of high-frequency strong ground motion, Bull. Seism. Soc. Am., 71, 2071-2096.

Hauge, P.S. (1981). Measurements of attenuation from vertical seismic profiles, Geophysics, 46:11, 1548-1558.

Hileman, J.A., C.R. Allen and J.M. Nordquist (1973). Seismicity of the southern California region. 1 January 1932 to 31 December 1972, Seismological Laboratory, Calif. Inst. of Technology, Pasadena.

Jennings, C.W. (1975). Fault Map of California, Map No. 1, Faults, Volcanos, Thermal Springs and Wells, Calif. Div. of Mines and Geology, Sacramento, CA.

Leeds, A. (1979). The locations of the 1954 northern Baja California earthquake, Masters Thesis, UC San Diego, La Jolla, Calif.

McDonal, F.J., F.A. Angona, R.L. Mills, R.L. Sengbush, R.G. Van Nostrand, and J.E. White (1958). Attenuation of shear and compressional waves in Pierre Shale, Geophysics, 23:3, 421-439.

McGuire, R.K. (1978). A simple model for estimating Fourier amplitude spectra of horizontal ground acceleration, Bull. Seism. Soc. Am., 68, 803-822.

Modiano and Hatzfeld (1982). Experimental study of the spectra content for shallow earthquakes, Bull. Seism. Soc. Am., 72, 1739-1758.

Murphy, L.M. and F.P. Ulrich (1951a). United States Earthquakes 1948, U.S. Dept. of Commerce, Serial 746, Coast and Geodetic Survey, Washington, D.C.

Murphy, L.M. and F.P. Ulrich (1951b). United States Earthquakes 1949, Serial 748, U.S. Dept. of Commerce, Coast and Geodetic Survey, Washington, D.C.

Murphy, L.M. and W.K. Cloud (1954). United States Earthquakes 1952, Serial 773, U.S. Dept. of Commerce, Coast and Geodetic Survey, Washington, D.C.

Murphy, L.M. and W.K. Cloud (1955). United States Earthquakes 1953, U.S. Dept. of Commerce, Coast and Geodetic Survey, Washington, D.C.

Papageorgiou, A.S. and K. Aki (1983). A specific barrier model for the quantitative description of inhomogenous faulting and the prediction of strong ground motion. Part II. Applications of the model, Bull. Seism. Soc. Am., 73, 953-978.

Real, C.R., T.R. Toppozada, and D.L. Parke (1978). Earthquake Epicenter Map of California, Map Sheet 39, Calif. Div. of Mines and Geology, Sacramento, Ca.

Richter, C.F. (1958). Elementary Seismology, W.F. Freeman and Co., San Francisco, Ca.

Sachs, I.S. (1980). Mantle Q from body waves - difficulties in determining frequency dependence, (abstract), Transactions Am. Geophys. Union, EOS, 61, 299.

Schoenberger, M. and F.K. Levin (1978). Apparent attenuation due to intrabed multiples, II, Geophysics, 43:4, 730-737.

Singh, S.K., R.J. Apsel, J. Fried, and J.N. Brune (1982). Spectral attenuation of SH waves along the Imperial fault, Bull. Seism. Soc. Am., 72, 2003-2016.

Sipkin, S.A. and T.H. Jordan (1980). Regional variation of Q_{scs}, Bull. Seism. Soc. Am., 70, 1071-1102.

Spencer, T.W., J.R. Sonnad, and T.M. Butler (1982). Seismic Q - Stratigraphy or dissipation, Geophysics, 47:1, 16-24.

Trifunac, M.D. and Brady, A.C. (1975). On the correlation of seismic intensity scales with peaks of recorded strong ground motion, Bull. Seism. Soc. Am., 65, 139-162.

Trifunac, M.D. (1976). Preliminary empirical model for scaling Fourier amplitude spectra of strong ground accelerations in terms of earthquake magnitude, source to station distance, and recording site conditions, Bull. Seism. Soc. Am., 66, 1343-1373.

Trifunac, M.D. (1978). Uniformly processed strong earthquake ground accelerations in the western United States of America for the period from 1933 to 1971: corrected acceleration, velocity and displacement curves, Report CE 78-01, Dept. of Civil Engineering, Univ. of Southern California, Los Angeles, Calif.

Tullos, F.N. and A.C. Reed (1969). Seismic attenuation of Gulf Coast sediments, Geophysics, 34:4, 516-528.

Wong, J., P. Hurley, and G.F. West (1983). Crosshole seismology and seismic imaging in crystalline rocks, Geophys. Res. Lttrs, 10:8, 686-689.

USGS LIBRARY-RESTON
3 1818 00071075 4